

Aerobic Methylophilic Microorganisms in an Acidic Deciduous Forest Soil: Substrate Range and Effect of pH

Dissertation

To obtain the Academic Degree

Doctor rerum naturalium

(Dr. rer. nat.)

Submitted to the Faculty of Biology, Chemistry, and Geosciences
of the University of Bayreuth

by

Mareen Morawe

Bayreuth, March 2017

This doctoral thesis was prepared at the Department of Ecological Microbiology at the University of Bayreuth from April 2012 until March 2017 and was supervised by PD Dr. Steffen Kolb.

This is a full reprint of the dissertation submitted to obtain the academic degree of Doctor of Natural Sciences (Dr. rer. nat.) approved by the Faculty of Biology, Chemistry and Geosciences of the University of Bayreuth.

Date of submission: 09.03.2017

Date of defence: 20.06.2017

Acting dean:

Prof. Dr. Stefan Schuster

Doctoral committee:

PD Dr. Steffen Kolb (1st reviewer)

Prof. Dr. Dirk Schüler (2nd reviewer)

Prof. Dr. Bettina Engelbrecht (chairman)

Prof. Dr. Egbert Matzner

*Once upon a time there was a lonely methylotroph called *Bacillus methanicus*^{*},
sole representative in the literature of a metabolic type of microorganism
capable of growth on methane or methanol as sole source of carbon and energy"*

C. Anthony, 1982 in "The Biochemistry of Methylotrophs"

^{*} *Bacillus methanolicus* was posterior determined as *Methylomonas methanica*

See the microcosm in macro vision...

M.L.Gore, 2005, "Macro"

∞ Dedicated to all my magnificent Ms ∞

CONTENTS

CONTENTS	I
FIGURES	VI
TABLES	IX
APPENDIX	XI
EQUATIONS	XIII
ABBREVIATIONS	XIV
SUMMARY	XV
ZUSAMMENFASSUNG	XVII
1. INTRODUCTION	1
1.1. The representative C1 compounds methane, methanol and chloromethane and their climatic relevance	1
1.1.1. Methane – climatic relevance, sources and sinks.....	2
1.1.2. Methanol – climatic relevance, sources and sinks.....	4
1.1.3. Chloromethane – climatic relevance, sources and sinks.....	7
1.2. The microbial sink – methylotrophic microorganisms	8
1.3. Metabolic features of methylotrophy	9
1.4. Dissimilatory pathways in methylotrophs – from methane, methanol and chloromethane to CO₂	11
1.5. Assimilatory pathways of C1 compounds in <i>Bacteria</i>	12
1.5.1. Ribulose monophosphate (RuMP) cycle.....	12
1.5.2. Ribulose biphosphate (RuBP) cycle.....	12
1.5.3. Serine cycle und glyoxylate regeneration	13
1.6. Methylotrophic varieties in <i>Bacteria</i>	14
1.6.1. Aerobic methanotrophs, methane-utilisation, and methane monooxygenases (MMO).....	14
1.6.2. High-affinity methanotrophs	17
1.6.3. Methanol-utilising methylotrophs and methanol oxidation	18
1.6.4. Facultatively methylotrophic <i>Bacteria</i>	22
1.6.5. Chloromethane-utilising methylotrophs and the <i>cmu</i> -pathway	26
1.7. Fungal methylotrophs and the MUT	28
1.8. Ecological niche-defining factors of methylotrophs	31
1.9. Hypothesis and objectives of the current study	31
2. MATERIALS AND METHODS	34
2.1. Sampling sites and sampling	34
2.1.1. The main sampling site <i>Steinkreuz</i> in the area <i>Steigerwald</i>	34
2.1.2. Further terrestrial sampling sites.....	36
2.1.3. Sampling sites associated with aquatic environments.....	39
2.2. Chemicals, gases, solutions, growth media and labware	42
2.2.1. Trace element solution.....	42
2.2.2. Substrate solutions for incubations concentrating on methane	42
2.2.3. [¹³ C _u]-Substrates for SIP incubations concentrating on methanol	43
2.2.4. KCN solutions	44
2.2.5. Toluene solutions	44
2.2.6. Solutions for DNA SIP.....	44
2.2.7. Cloning (SOC and LB agar plates)	46

CONTENTS

2.3. Incubations and microcosm experiments	46
2.3.1. Long-term incubation under mixed substrate conditions with methane and alternative substrates	47
2.3.1.1. Methane degradation potential after mixed substrate incubation under solely methanotrophic conditions	48
2.3.1.2. Methane degradation potential after mixed substrate incubation under methanotrophic and mixed substrate conditions	49
2.3.2. Methane degradation potential of fresh forest soil under changed substrate availabilities	49
2.3.3. Oxic soil slurry incubations of the substrate SIP experiment under mixed substrate conditions	51
2.3.4. Oxic soil slurry incubations of the pH shift SIP experiment under methylotrophic conditions	53
2.3.5. Oxic soil slurry incubations of different soil environments to assess the abundance of methylotrophs	54
2.3.6. Chloromethane degradation in different forest-derived compartments	55
2.3.7. Chloromethane degradation in forest soil	57
2.3.8. Inhibitory effects of toluene on the chloromethane degradation in forest soil	58
2.3.9. Chloromethane degradation potential of terrestrial and aquatic environments and the putative inhibition by toluene	59
2.3.10. Oxic incubations of the methanol/chloromethane SIP experiment with sieved soil	60
2.4. Analytical methods	62
2.4.1. Determination of pH values	62
2.4.2. Dry weight and water content of environmental samples	62
2.4.3. Gas chromatography (GC)	62
2.4.4. Gas chromatography–mass spectrometry (GC-MS)	66
2.4.5. High performance liquid chromatography (HPLC)	66
2.5. Molecular methods	68
2.5.1. Co-extraction of nucleic acids	68
2.5.2. Enzymatic digestion of RNA and DNA after extraction	69
2.5.3. Purification and precipitation of nucleic acids	69
2.5.3.1. Approach with polyethylene glycol and glycogen	69
2.5.3.2. Approach with isopropyl alcohol and sodium chloride	69
2.5.4. Quantification of nucleic acids	70
2.5.4.1. Spectrophotometry (via NanoDrop™)	70
2.5.4.2. Fluorescence-based quantification (via PicoGreen®)	70
2.5.5. Agarose gel electrophoresis	70
2.5.6. 16S rRNA-based stable isotope probing with DNA	71
2.5.6.1. Density gradient centrifugation of DNA and fractionating of the gradient	72
2.5.6.2. Separation of ‘heavy’ (H), ‘middle’ (M) and ‘light’ (L) DNA by fractionation	73
2.5.7. Polymerase chain reaction (PCR)	74
2.5.7.1. Primers	75
2.5.7.2. PCR approaches to amplify <i>pmoA</i>	78
2.5.7.3. PCR approaches to amplify <i>mmoX</i>	79
2.5.7.4. PCR approaches to amplify <i>pxmA</i>	81
2.5.7.5. PCR approaches to amplify <i>cmuA</i>	83
2.5.7.6. 2-step approach PCRs for pyrosequencing	84
2.5.7.7. PCR approaches to amplify 16S rRNA and <i>mxnF/xoxF II</i> for ‘ILLUMINA’ sequencing	89
2.5.7.8. PCR approaches to amplify 16S rRNA gene sequences for T-RFLP	90
2.5.8. Quantitative polymerase chain reaction (qPCR)	91
2.5.8.1. qPCR primers	92
2.5.8.2. Preparation of qPCR standards	92

CONTENTS

2.5.8.3. qPCR assay to evaluate gene copy numbers	95
2.5.8.4. Evaluation of a putative qPCR inhibition	97
2.5.8.5. Calculation of transcript numbers	97
2.5.9. Purification of PCR products	97
2.5.9.1. Gel extraction.....	97
2.5.9.2. Purification with columns	98
2.5.10. Cloning	98
2.5.10.1. Ligation	98
2.5.10.2. Transformation.....	98
2.5.10.3. Screening for successful cloning	99
2.5.11. Terminal restriction fragment length polymorphism (T-RFLP) analysis.....	99
2.5.11.1. Amplification with fluorescence-dye tagged primers	100
2.5.11.2. Mung bean endonuclease digestion.....	100
2.5.11.3. Restriction enzyme digestion.....	100
2.5.11.4. Denaturing Polyacrylamide Gel Electrophoresis (PAGE).....	101
2.5.11.5. Analysis of T-RF profiles	101
2.5.12. Sequencing	102
2.5.12.1. Sequencing by chain-termination ('Sanger sequencing').....	102
2.5.12.2. Pyrosequencing with barcoded amplicons	102
2.5.12.3. Sequencing by synthesis ('ILLUMINA sequencing').....	103
2.5.13. Sequence analyses (filtering and clustering of raw reads)	103
2.5.13.1. Analyses of sequences derived from pyrosequencing	103
2.5.13.2. Analyses of sequences derived from synthesis-sequencing.....	105
2.5.14. Identification of ¹³ C-labelled' phylotypes	106
2.5.15. Calculation of phylogenetic trees	108
2.5.16. Nucleotide sequence accession numbers	110
2.5.17. Statistical analyses and calculations.....	110
2.5.17.1. Arithmetic mean, standard deviation, standard error, error propagation.....	110
2.5.17.2. Calculation of the methane degradation rate ' <i>R_{ACH4}</i> '.....	111
2.5.17.3. Coverage	111
2.5.17.4. Community analyses (diversity indices, ANOSIM, NPMANOVA, SIMPER)	111
2.5.17.5. Visualisation by NMDS plots and heatmaps	112
3. RESULTS	113
3.1. Methane degradation and abundance of 'high-affinity' USCα methanotrophs in an acidic forest soil	113
3.2. Effects on the methane degradation by the simultaneous supplementation of methane and alternative substrates	115
3.2.1. Effects of acetate and n-alkanes.....	115
3.2.2. Effects of sugars: cellobiose and xylose	118
3.2.3. Effects of other C1 compounds: methylamine and methanol	120
3.2.4. Effects of aromatic compounds: vanillic acid and guaiacol.....	123
3.2.5. Long-term effects on the methane degradation potential caused by alternative substrates under solely methanotrophic conditions	125
3.2.6. Long-term effects on the methane degradation potential caused by alternative substrates under methanotrophic and mixed substrate conditions.....	127
3.2.7. Effects of alternative substrates on the methane degradation potential in fresh forest soil under changed substrate availabilities	130
3.3. Multi-carbon compound assimilation by methanol-utilising microorganisms in an acidic forest soil	132
3.3.1. Conversion of methanol and multi-carbon substrates and the formation of [¹³ C]-CO ₂ as evidence for substrate dissimilation	132
3.3.2. Influence of the soil pH on methanol utilisation and the [¹³ C]-CO ₂ formation.....	134

3.4. Pyrosequencing read yield of 16S rRNA gene, ITS gene sequences and <i>mxoF</i> gene sequences	135
3.5. The impact of methanol, multi-carbon substrates and pH on the microbial community in an acidic forest soil.....	136
3.5.1. The impact of substrates and pH on <i>Bacteria</i>	136
3.5.1.1. Comparison of t_0 and t_{End} of the substrate-treated samples	139
3.5.1.2. Comparison of the methanol-treated samples and multi-carbon-treated samples	141
3.5.1.3. Comparison of samples incubated under different pH conditions	141
3.5.2. The impact of substrates and pH on methylotrophs	142
3.5.2.1. Comparison of the methanol treated samples and multi-carbon treated samples	145
3.5.2.2. Low abundant <i>mxoF</i> phylotypes in the substrate SIP experiment	147
3.5.2.3. Comparison of the <i>mxoF</i> -possessing methylotrophic community incubated under different pH conditions.....	148
3.5.2.4. The effect of the pH on <i>mxoF</i> - and <i>mmoX</i> -possessing methylotrophs	149
3.5.3. The impact of substrates and pH on Fungi in an acidic soil	150
3.5.3.1. Comparison of t_0 and t_{End} of the samples treated with different substrates.....	154
3.5.3.2. Comparison of the methanol-treated samples and multi-carbon-treated samples	155
3.5.3.3. Comparison of samples incubated under different pH conditions	156
3.6. Identification of methylotrophic microorganisms assimilating methanol or alternative substrates in an acidic forest soil by DNA-SIP	156
3.6.1. Separation of DNA and distribution of nucleic acids along the gradient	157
3.6.2. Determination of heavy (H), middle (M) and light (L) fractions	158
3.6.3. Identification of labelled taxa	161
3.7. Methanol-utilising microorganisms and their multi-carbon substrate range	162
3.7.1. Bacterial methylotrophs.....	163
3.7.1.1. Methanol assimilating <i>Bacteria</i>	164
3.7.1.2. Multi-carbon substrate assimilating <i>Bacteria</i>	166
3.7.1.3. Methanol-assimilating <i>Bacteria</i> under shifted pH conditions.....	167
3.7.1.4. Comparative analysis and identification of putative facultatively methylotrophic bacteria	168
3.7.2. <i>mxoF</i> -possessing methylotrophs	171
3.7.2.1. Methanol-assimilating methylotrophs	171
3.7.2.2. Multi-carbon substrate-assimilating methylotrophs	172
3.7.2.3. Methanol-assimilating methylotrophs under shifted pH conditions	174
3.7.2.4. Comparative analysis and identification of facultative methylotrophs	174
3.7.3. Fungal methylotrophs.....	176
3.7.3.1. Methanol-assimilating fungi	177
3.7.3.2. Multi-carbon substrate-assimilating fungi	178
3.7.3.3. Methanol-assimilating methylotrophic fungi under shifted pH conditions.....	180
3.7.3.4. Comparative analysis and assessment of the substrate range of methylotrophic fungi	182
3.8. Methanol-utilisers in further soil environments	183
3.9. Forest soil – a microbial sink of chloromethane	186
3.10. Utilisation of methanol or chloromethane by methylotrophic organisms in an acidic soil	189
3.10.1. Conversion of methanol and chloromethane and the formation of [^{13}C]-CO ₂ as evidence for substrate dissimilation	190
3.10.2. The influence of methanol and chloromethane on <i>Bacteria</i> in an acidic soil.....	192
3.10.3. The influence of methanol and chloromethane on <i>mxoF/xoxF</i> -type MDH and <i>cmuA</i> phylotypes in an acidic soil.....	195
3.11. Microorganisms assimilating methanol and chloromethane	199
3.11.1. Identification of <i>Bacteria</i> assimilating methanol and chloromethane	199

3.11.2. Identification of <i>mxoF/xoxF</i> -type MDH-possessing methylotrophs assimilating methanol and chloromethane	202
3.11.3. Identification of <i>cmuA</i> -possessing methylotrophs assimilating methanol and chloromethane	206
3.12. Chloromethane degradation in different ecosystem types – a comparison of terrestrial and aquatic environments	207
3.13. Halocarbons and aromatic compounds – the impact of toluene on chloromethane degradation	210
4. DISCUSSION	213
4.1. The methanotrophic community and their alternative substrate range in an acidic forest soil.....	213
4.1.1. The methane degradation potential by USC α and the presence of other methanotrophs	213
4.1.2. Alternative substrates of USC α methanotrophs.....	218
4.1.2.1. Acetate.....	219
4.1.2.2. n-Alkanes.....	222
4.1.2.3. Sugars (D-cellobiose and D-xylose).....	222
4.1.2.4. Other C1 compounds (methanol and methylamine).....	223
4.1.2.5. Aromatic compounds (vanillic acid and guaiacol)	226
4.1.3. Concluding remarks on the substrate range of 'high-affinity' methanotrophs (USC α)	227
4.2. The substrate range of methanol-utilising methylotrophs and methanol-derived carbon-utilising microorganisms in the acidic soil	229
4.2.1. Methanol-utilising <i>Bacteria</i> and their multi-carbon substrate range.....	230
4.2.2. Putative fungal methanol-utilisers in the forest soil.....	233
4.2.3. Methanol-derived carbon assimilating <i>Bacteria</i>	235
4.2.3.1. <i>Acidobacteria</i>	236
4.2.3.2. <i>Planctomycetes</i>	236
4.2.3.3. <i>Verrucomicrobia</i>	238
4.2.3.4. <i>Actinobacteria</i>	241
4.2.4. Hypothetical methanol-driven food web and ecological niches of associated microorganisms in the acidic soil	243
4.3. The influence of an elevated pH on the indigenous methanol-derived carbon-utilising microbiome.....	245
4.4. The chloromethane-utilising guild of methylotrophs	246
4.4.1. Forest soils as chloromethane-sink	247
4.4.2. (Co)utilisers of methanol and chloromethane in the acidic forest soil	249
4.4.3. Striking differences between chloromethane-utilisers of different soil environments confirming their underestimation <i>in situ</i>	256
4.4.4. Variety of trophic types of methanol- and chloromethane-utilising methylotrophs	257
4.4.5. Existing co-utilisation of aromatic compounds and chloromethane in soils?	260
4.5. Addressing the hypotheses and future perspectives.....	261
5. REFERENCES	265
6. ACKNOWLEDGMENTS.....	289
7. PUBLICATIONS.....	290
8. APPENDICES	291
9. (EIDESSTATTLICHE) VERSICHERUNGEN UND ERKLÄRUNGEN	375

FIGURES

Figure 1	Reactions of methane, methanol and chloromethane and their contribution to ozone depletion.....	2
Figure 2	Global sources and sinks for atmospheric methane, methanol and chloromethane.	6
Figure 3	Simplified overview on methylotrophic modules and some examples of their combination in methylotrophic organisms.....	10
Figure 4	Dissimilatory oxidation of methane, methanol and chloromethane to CO ₂	11
Figure 5	Assimilation cycles in methylotrophic Bacteria.	14
Figure 6	Diversity of known enzymes facilitating the oxidation of methanol in different methylotrophic organisms (A) and the crystal structure of a PQQ-MDH (B).	19
Figure 7	Interactions of metabolic pathways and entry points of multi-carbon compounds in facultatively methylotrophic bacteria.	24
Figure 8	Metabolic diversity covered by members of the <i>Beijerinckiaceae</i>	25
Figure 9	Three C1 compound oxidising pterin-dependent pathways in <i>Methylobacterium extorquens</i> CM4.....	27
Figure 10	Methanol metabolism in methylotrophic yeasts (A) and the crystal structure of a FAD AOx (B).	29
Figure 11	Localisation of the exploration area <i>Steinkreuz</i> in the <i>Steigerwald</i> forest.	34
Figure 12	Soil profile from cambisol at the sampling area <i>Steinkreuz</i>	35
Figure 13	Images of the sampling site ' <i>Steinkreuz</i> ' in the deciduous forest area <i>Steigerwald</i>	36
Figure 14	Further terrestrial sampling sites covering different soil environments.....	38
Figure 15	Sampling sites covering different aquatic environments.....	40
Figure 16	Compounds tested as putative alternative substrates for ambient methane-utilisers.	43
Figure 17	Compounds tested as putative multi-carbon substrates for methanol-utilisers in the substrate SIP experiment.....	44
Figure 18	Experimental set-up of the long-term incubations under methanotrophic and mixed substrate conditions (see 2.3.1) and following experiments (see 2.3.1.1, 2.3.1.2).	48
Figure 19	Experimental set-up to evaluate the methane degradation potential under changed substrate availabilities of fresh soil.	50
Figure 20	Experimental set-up of the Substrate SIP experiments.	52
Figure 21	Experimental set-up of the pH shifted SIP experiments.....	54
Figure 22	Experimental set-up to evaluate the chloromethane degradation potential of different forest-derived compartments.	56
Figure 23	Experimental set-up to evaluate inhibitory effects of toluene to CH ₃ Cl degradation in a forest soil.	58
Figure 24	Experimental set-up to evaluate the chloromethane degradation potential of different ecosystem types and assessing the putative inhibition by toluene.	60
Figure 25	Experimental set-up of the methanol / chloromethane SIP experiment.	61
Figure 26	Absorption spectrum of vanillic acid in the sample and from the standard detected by HPLC with a DAD.....	67
Figure 27	Schematic overview of SIP experiment procedures.	72
Figure 28	Fractionation of a gradient.	73
Figure 29	Humic acids contamination.	85
Figure 30	Schematic overview on the operating principle of qPCR analysis.....	92
Figure 31	Restriction sites of the applied restriction enzymes <i>MspI</i> and <i>RsaI</i>	100
Figure 32	Correlation between the number of detected phylotypes and the nucleotide sequence similarities of <i>mxoF</i> gene sequences.	104
Figure 33	Identification of labelled phylotypes.	107
Figure 34	Methane degradation (A) and corresponding gene copy numbers of 16S rRNA and <i>pmoA</i> (USCα) (B) in soil slurry treatments during the long-term incubation.....	114
Figure 35	Effect of acetate and n-alkanes (butane & dodecane) on CH ₄ degradation in soil slurry treatments.	116

FIGURES

Figure 36	Influence of acetate and n-alkanes on gene copy numbers of 16S rRNA and <i>pmoA</i> (USCα) in soil slurry treatments.	117
Figure 37	Effect of sugars (glucose & xylose) on CH ₄ degradation in soil slurry treatments.....	119
Figure 38	Influence of sugars (glucose and xylose) on gene copy numbers of 16S rRNA and <i>pmoA</i> (USCα) in soil slurry treatments.	120
Figure 39	Effect of C1 compounds (methylamine & methanol) on CH ₄ degradation in soil slurry treatments.	121
Figure 40	Influence of C1 compounds (methylamine and methanol) on gene copy numbers of 16S rRNA and <i>pmoA</i> (USCα) in soil slurry treatments.	122
Figure 41	Effect of aromatic compounds (vanillic acid & guaiacol) on CH ₄ degradation in soil slurry treatments.	124
Figure 42	Influence of aromatic compounds (vanillic acid and guaiacol) on gene copy numbers of 16S rRNA and <i>pmoA</i> (USCα) in soil slurry treatments.	125
Figure 43	Long-term effect of alternative substrates on CH ₄ degradation.....	126
Figure 44	Long-term effect of alternative substrates on CH ₄ degradation.....	129
Figure 45	Effect of acetate and vanillic acid supplementation on CH ₄ degradation in fresh soil samples.....	131
Figure 46	CO ₂ formation and conversion of different multi-carbon substrates in soil slurry treatments.	133
Figure 47	Diversity and richness estimators of 16S rRNA gene sequences from pyrosequencing amplicon pools at similarity level 90.1% (family level).	137
Figure 48	nMDS analyses (A) and the phylogenetic compositions (B) of the bacterial community after different substrate or pH treatments.....	138
Figure 49	Bacterial taxa responsible for dissimilarity in substrate treatments.	140
Figure 50	Diversity and richness estimators of <i>mxoF</i> gene sequences from pyrosequencing amplicon pools at similarity level 90%.	143
Figure 51	nMDS analyses of the <i>mxoF</i> -possessing bacterial community after different substrate or pH treatments.	144
Figure 52	Composition of various <i>mxoF</i> genotypes after different substrate or pH treatments.	146
Figure 53	Influence of different pH conditions on 16S rRNA, <i>mxoF</i> and <i>mmoX</i> gene numbers in soil slurry treatments.	150
Figure 54	Diversity and richness estimators of ITS gene sequences from pyrosequencing amplicon pools at similarity level of 97% (species level).	151
Figure 55	nMDS analyses (A) and the phylogenetic compositions (B) of the fungal community after different substrate or pH treatments.	152
Figure 56	Fungal taxa responsible for dissimilarity in substrate treatments.	154
Figure 57	Distribution of DNA in the gradients of t ₀ , [¹² C]- and [¹³ C]-methanol treatments of Substrate SIP experiment and determination of 'heavy' (H), 'middle' (M) and 'light' (L) fractions.	158
Figure 58	T-RF patterns of 16S rRNA gene sequences from methanol treatment of Substrate SIP experiments after digestion with RsaI (A) and MspI (B).	159
Figure 59	Bacterial phyla composition in 'heavy' fractions after different substrate or pH treatments based on all detected phylotypes.	162
Figure 60	nMDS analyses of bacterial communities in 'heavy' and 'middle' fractions of both SIP experiments.....	163
Figure 61	Labelled 16S rRNA phylotypes in 'heavy' and 'middle' fractions of different [¹³ C]-isotopologues treatments.....	165
Figure 62	Congruently labelled bacterial phylotypes in treatments of both SIP experiments.....	169
Figure 63	Labelled <i>mxoF</i> phylotypes in 'heavy' and 'middle' fractions of different [¹³ C]-isotopologues treatments.....	173
Figure 64	nMDS analyses of fungal communities in 'heavy' and 'middle' fractions of both SIP experiments.....	177
Figure 65	Labelled ITS phylotypes in 'heavy' and 'middle' fractions of different [¹³ C]-isotopologue treatments.....	181

FIGURES

Figure 66	Congruently labelled fungal phylotypes in treatments of both SIP experiments.	183
Figure 67	Comparison of different soil environments with a focus on methylotrophs.....	184
Figure 68	Influence of methanol on the <i>in situ</i> <i>mxoF</i> -possessing methylotrophs in different soil environments.	185
Figure 69	Degradation of low amounts of chloromethane in different forest-derived compartments.	187
Figure 70	Degradation of low amounts (i.e., 100 ppb) of chloromethane of a forest soil.	188
Figure 71	Degradation of high amounts (i.e., 1 %) of chloromethane of a forest soil.....	189
Figure 72	Degradation of CH ₃ Cl (A) and formation of CO ₂ (B) in the methanol/chloromethane SIP experiment.....	191
Figure 73	Diversity and richness estimators of 16S rRNA gene sequences of the methanol/chloromethane SIP experiment.....	193
Figure 74	nMDS analyses (A) and the phylogenetic compositions (B) of the bacterial community after treatments with methanol or/and chloromethane.....	194
Figure 75	Diversity and richness estimators of <i>mxoF/xoxF</i> -type MDH and <i>cmuA</i> gene sequences of the methanol/chloromethane SIP experiment.	196
Figure 76	nMDS analyses of the <i>mxoF/xoxF</i> -type MDH and <i>cmuA</i> sequences (A) and the corresponding phylogenetic compositions (B) after treatments with methanol or/and chloromethane.	198
Figure 77	nMDS analyses of 16S rRNA gene sequences from the 'heavy' and 'middle' fractions of the methanol/chloromethane SIP experiment.	200
Figure 78	Phylotypes of 16S rRNA gene sequences in the 'heavy' and 'middle' fractions of the methanol/chloromethane SIP.....	201
Figure 79	nMDS analyses of <i>mxoF/xoxF</i> -type MDH sequences from the 'heavy' and 'middle' fractions of the methanol/chloromethane SIP experiment.	203
Figure 80	Phylotypes of <i>mxoF/xoxF</i> -type MDH and <i>cmuA</i> gene sequences in the 'heavy' and 'middle' fractions of the methanol/chloromethane SIP.....	204
Figure 81	nMDS analyses of <i>cmuA</i> sequences from the 'heavy' and 'middle' fractions of the methanol/chloromethane SIP experiment.....	206
Figure 82	Comparison of endogenously formed chloromethane in different terrestrial and aquatic ecosystem type samples.	208
Figure 83	Initial chloromethane degradation potential of different terrestrial and aquatic ecosystem type samples.....	209
Figure 84	Chloromethane degradation potential of forest soil in the presence of toluene.	211
Figure 85	Degradation of chloromethane in different terrestrial and aquatic ecosystem type samples.....	212
Figure 86	Substrate range of 'high-affinity' methanotrophs in an acidic soil of a temperate deciduous forest.....	228
Figure 87	The central role of <i>Beijerinckiaceae</i> in a methanol-driven food web in a temperate deciduous forest with acidic soil.....	244
Figure 88	Variety of metabolic profiles of methanol- and chloromethane-utilising methylotrophs in a temperate deciduous forest with acidic soil.....	260

TABLES

Table 1	Comparison of both methane monooxygenases (MMO).....	16
Table 2	Overview on the different sampling sites.	41
Table 3	Components of the trace element solution after Whittenbury <i>et al.</i> , 1970a.....	42
Table 4	Composition of the gradient buffer used for DNA SIP.	45
Table 5	Parameters of GC analyses with Hewlett-Packard 5890 Series II gas chromatographs.	63
Table 6	Calculation basis values for a solubility coefficient value for CH ₃ Cl.	66
Table 7	Parameters of HPLC analyses.....	67
Table 8	Composition of the enzymatic digestion reactions after coextraction.	69
Table 9	Amount of applied DNA of different SIP experiments to separate unlabelled and labelled DNA in isopycnic centrifugation.	72
Table 10	Structure of the barcoded fusion primers used for amplicon pyrosequencing.	76
Table 11	Primer sequences of 'conventional' primers used to amplify 16S rRNA, <i>mxoF/xoxF</i> , <i>cmuA</i> , <i>pmoA</i> , and ITS gene fragments.....	77
Table 12	Composition of reagents for PCR reactions of the assays for <i>pmoA</i>	78
Table 13	PCR programs to amplify <i>pmoA</i>	79
Table 14	Composition of reagents for PCR reactions of the assays for <i>mmoX</i>	80
Table 15	Different PCR programs to amplify <i>mmoX</i>	80
Table 16	Different PCR programs to amplify <i>pxmA</i>	81
Table 17	Composition of reagents for PCR reactions of the assays for <i>pxmA</i>	82
Table 18	PCR programs to amplify <i>cmuA</i>	83
Table 19	Composition of reagents for PCR reactions of the assays for <i>cmuA</i>	84
Table 20	Composition of reagents for PCR reactions in the 2-step approach PCR of barcoded amplification for bacterial gene fragments (16S rRNA, <i>mxoF/xoxF I</i>)	86
Table 21	Composition of reagents for PCR reactions in the two-step approach PCR of barcoded amplification for fungal gene fragments (ITS).....	87
Table 22	PCR programs to amplify 16S rRNA, <i>mxoF/xoxF I</i> and ITS gene fragments in step-1-PCR and step-2-PCR of barcoded amplification.	88
Table 23	Composition of reagents for PCR reactions of the assays for 16S rRNA and <i>mxoF/xoxF II</i> for 'ILUMINA' sequencing.	89
Table 24	PCR programs to amplify 16S rRNA and <i>mxoF/xoxF II</i> for 'ILUMINA' sequencing.	90
Table 25	Composition of reagents for PCR reactions for amplifying 16S rRNA gene fragments with fluorescent dye labelled primer.	90
Table 26	PCR programs to amplify 16S rRNA and <i>mxoF/xoxF II</i> for 'ILUMINA' sequencing.	91
Table 27	Primer sequences of primers used for qPCR and to prepare qPCR standards.	93
Table 28	Composition of reagents for PCR reactions of qPCR standard preparation (16S rRNA, <i>mxoF</i> , <i>mmoX</i> , M13) and cloning (pJET).	93
Table 29	Composition of reagents for PCR reactions of qPCR standard preparation of <i>pmoA</i> -USC α	94
Table 30	PCR programs to amplify gene fragments for qPCR standards.	94
Table 31	Composition of reagents for PCR reactions of the qPCR assays.	95
Table 32	Modified qPCR programs to amplify 16S rRNA, <i>pmoA</i> -USC α , <i>mxoF</i> , <i>mmoX</i> and artificial DNA (Inhibit).	96
Table 33	Composition of the reactions with PreCR Repair Mix.....	102
Table 34	Percentage of USC α methanotrophs on total bacterial cell numbers in different treatments with alternative substrates over time.	115
Table 35	Potential T-RFs (based on 16S rRNA gene sequences) of known methylotrophic bacteria as a result of virtual digestion with <i>MspI</i> and <i>RsaI</i>	160
Table 36	Putative trophic types comprised by the <i>Beijerinckiaceae</i> -phylogroup.	170
Table 37	Amounts of supplemented [¹³ C _w]-isotopologues, ¹³ CO ₂ and the resulting C-recoveries of carbon per substrate pulse.	192

TABLES

Table 38	Substrate spectrum of known facultatively methanotrophic representatives.....	218
Table 39	Methylamine utilisation by methano- and methylotrophs.....	225
Table 40	Buoyant densities according to the GC-mol% content of microbial species.....	240

APPENDIX

APPENDIX TABLES

Table A 1	Sequences of the barcodes for 16S rRNA and <i>mxoF</i> sequence classification of PYRO-sequencing derived sequences.	291
Table A 2	Sequences of the barcodes for ITS sequence classification of PYRO-sequencing derived sequences.	293
Table A 3	Sequences of the barcodes used to identify individual samples in ILLUMINA amplicon libraries (methanol/chloromethane SIP experiment).	294
Table A 4	Number of all sequences obtained from pyrosequencing amplicon libraries.	295
Table A 5	Number of all 16S rRNA gene sequences obtained from ILLUMINA amplicon libraries.	298
Table A 6	Number of all <i>mxoF/xoxF</i> -type MDH and <i>cmuA</i> gene sequences obtained from ILLUMINA sequencing amplicon libraries.	299
Table A 7	ANOSIM and NPMANOVA of microbial communities (substrate SIP and pH shift SIP experiments).	300
Table A 8	ANOSIM and NPMANOVA of microbial communities (methanol/chloromethane SIP experiments).	302
Table A 9	Relative abundance of bacterial taxa (16S rRNA gene sequences) in the substrate and pH shift SIP experiment.	303
Table A 10	Relative abundance of methylotrophic taxa (<i>mxoF</i> gene sequences) in the substrate and pH shift SIP experiment.	306
Table A 11	Relative abundance of fungal taxa (ITS gene sequences) in the substrate and pH shift SIP experiment.	309
Table A 12	Phylogenetic affiliation of bacterial taxa in the substrate and pH shift SIP experiment.	311
Table A 13	Phylogenetic affiliation of fungal taxa in the substrate and pH shift SIP experiment.	332
Table A 14	Labelled bacterial taxa in the treatments with methanol.	337
Table A 15	Labelled bacterial taxa in the treatments with acetate.	338
Table A 16	Labelled bacterial taxa in the treatments with glucose.	339
Table A 17	Labelled bacterial taxa in the treatments with xylose.	340
Table A 18	Labelled bacterial taxa in the treatments with vanillic acid.	341
Table A 19	Labelled bacterial taxa in the treatments with CO ₂ and additional methanol.	342
Table A 20	Labelled bacterial taxa in the treatments with CO ₂	343
Table A 21	Labelled bacterial taxa in the treatments with methanol at <i>in situ</i> pH.	344
Table A 22	Labelled bacterial taxa in the treatments with methanol at pH 7.	344
Table A 23	Labelled methylotrophic taxa in the treatments with methanol.	345
Table A 24	Labelled methylotrophic taxa in the treatments with acetate.	346
Table A 25	Labelled methylotrophic taxa in the treatments with glucose.	347
Table A 26	Labelled methylotrophic taxa in the treatments with xylose.	348
Table A 27	Labelled methylotrophic taxa in the treatments with vanillic acid.	349
Table A 28	Labelled methylotrophic taxa in the treatments with CO ₂ and additional methanol.	350
Table A 29	Labelled methylotrophic taxa in the treatments with carbon dioxide.	351
Table A 30	Labelled methylotrophic taxa in the treatments with methanol at <i>in situ</i> pH.	352
Table A 31	Labelled methylotrophic taxa in the treatments with methanol at pH 7.	353
Table A 32	Labelled fungal taxa in the treatments with methanol.	354
Table A 33	Labelled fungal taxa in the treatments with acetate.	355
Table A 34	Labelled fungal taxa in the treatments with glucose.	356
Table A 35	Labelled fungal taxa in the treatments with xylose.	356
Table A 36	Labelled fungal taxa in the treatments with vanillic acid.	357
Table A 37	Labelled fungal taxa in the treatments with CO ₂ and additional methanol.	358
Table A 38	Labelled fungal taxa in the treatments with CO ₂	359

Table A 39	Labelled fungal taxa in the treatments with methanol at <i>in situ</i> pH.	360
Table A 40	Labelled fungal taxa in the treatments with methanol at pH 7.	361
Table A 41	Calculated ratios based on quantified gene numbers of <i>mxoF</i> and 16S rRNA genes in different soil ecosystem types <i>in situ</i> and after methanol supplementation.	362
Table A 42	Relative abundance of bacterial taxa (16S rRNA gene sequences) of the methanol/chloromethane SIP experiment.	363
Table A 43	Relative abundance of methylotrophic taxa (<i>mxoF/xoxF</i> -type MDH gene sequences) of the methanol/chloromethane SIP experiment.	365
Table A 44	Relative abundance of methylotrophic taxa (<i>cmuA</i> gene sequences) of the methanol/chloromethane SIP experiment.	367
Table A 45	Phylogenetic affiliation of bacterial taxa (16S rRNA gene sequences) of the methanol/chloromethane SIP experiment.	368
Table A 46	Labelled bacterial taxa in all treatments of the methanol/chloromethane SIP experiment.	372
Table A 47	Labelled methylotrophic taxa (<i>mxoF/xoxF</i> -type MDH gene sequences) in all treatments of the methanol/chloromethane SIP experiment.	373
Table A 48	Labelled methylotrophic taxa (<i>cmuA</i> gene sequences) in all treatments of the methanol/chloromethane SIP experiment.	374

APPENDIX FIGURES

Figure A 1	Phylogenetic tree of <i>Alphaproteobacteria</i> -affiliated phylotypes.	317
Figure A 2	Resolution of the <i>Beijerinckiaceae</i> -affiliated phylotype OTU _{16S} 438.	318
Figure A 3	Phylogenetic tree of <i>Betaproteobacteria</i> -affiliated phylotypes.	319
Figure A 4	Phylogenetic tree of <i>Gammaproteobacteria</i> -affiliated phylotypes.	320
Figure A 5	Phylogenetic tree of <i>Actinobacteria</i> -affiliated phylotypes.	321
Figure A 6	Phylogenetic tree of <i>Acidobacteria</i> -affiliated phylotypes.	322
Figure A 7	Phylogenetic tree of <i>Bacteroidetes</i> -affiliated phylotypes.	323
Figure A 8	Phylogenetic tree of <i>Firmicutes</i> -affiliated phylotypes.	324
Figure A 9	Phylogenetic tree of <i>Verrucomicrobia</i> -affiliated phylotypes.	325
Figure A 10	Phylogenetic tree of <i>Planctomycetes</i> -affiliated phylotypes.	326
Figure A 11	Phylogenetic tree of phylotypes affiliated to <i>Parcubacteria</i> , <i>Armatimonadetes</i> , <i>Chlamydia</i> , and “ <i>Candidatus</i> Saccharibacteria”.	327
Figure A 12	Phylogenetic tree of all <i>mxoF</i> and <i>xoxF</i> phylotypes obtained in all SIP experiments.	330
Figure A 13	Phylogenetic tree of all labelled bacterial phylotypes obtained in the methanol/chloromethane SIP experiment.	369
Figure A 14	Phylogenetic affiliation of the putative CH ₃ Cl-utilizing taxon (OTU _{16S} 6) within the <i>Actinomycetales</i>	370
Figure A 15	Phylogenetic tree of all <i>cmuA</i> phylotypes detected in the methanol/chloromethane SIP experiment.	371

EQUATIONS

Equation 1	Density adjustment of the gradient buffer used for separation of DNA.	45
Equation 2	Gravimetric water content Wg [%].....	62
Equation 3	Volumetric water content Wv [%]	62
Equation 4	Ideal gas law	64
Equation 5	Total amount of gases nt [mmol].....	64
Equation 6	Amount of gases in the gas phase ng [mmol].....	64
Equation 7	Molar volume $Vmol$ of the gas under current conditions [ml/mmol].....	65
Equation 8	Amount of gases np physically dissolved in the liquid phase [mmol].....	65
Equation 9	Amount of gases nc chemically dissolved in the liquid phase [mmol]	65
Equation 10	Bunsen solubility coefficient α at standard conditions*.....	65
Equation 11	Number of molecules Ms in qPCR standard solutions [molecules μl^{-1}].....	95
Equation 12	Calculation of corrected gene copy numbers $lgSQcor$ including putative qPCR inhibition	97
Equation 13	Individual threshold Tx calculated for the methanol/chloromethane SIP experiment....	108
Equation 14	Relative error REx	108
Equation 15	Labelling proportion LPx	108
Equation 16	Arithmetic mean x	110
Equation 17	Standard deviation SDi	110
Equation 18	Standard error SEi	110
Equation 19	Error propagation EP	111
Equation 20	Methane degradation rate $R\Delta CH_4$	111
Equation 21	Coverage C [%] of a sequence database.	111

ABBREVIATIONS

^{12}C	^{12}C -isotopologue or ^{12}C -isotope	NAD	nicotinamide adenine dinucleotide
^{13}C	^{13}C -isotopologue or ^{13}C -isotope	NAD ⁺	nicotinamide adenine dinucleotide (oxidized)
AOx	alcohol oxidase	NADH	nicotinamide adenine dinucleotide (reduced)
ANOSIM	analysis of similarities	nMDS	Non-metric multidimensional scaling
BD	buoyant density	NPMANOVA	non-parametric multivariate analysis of variance
BLAST	basic local alignment search tool	OTU	operational taxonomic unit
bp	base pairs	PCR	polymerase chain reaction
BSA	bovine serum albumin	PCR-H ₂ O	autoclaved, sterile filtered ddH ₂ O
C1	one-carbon (no carbon- carbon bound)	PHB	polyhydroxybutyrate
CH ₄	methane	pMMO	particulate methane monooxygenase
CH ₃ OH	methanol	ppb	parts per billion (10 ⁻⁹)
CH ₃ Cl	chloromethane	ppm	parts per million (10 ⁻⁶)
cmu	chloromethane utilising	ppt	parts per trillion (10 ⁻¹²)
CoA	coenzyme A	PQQ	pyrroloquinoline quinone
CO ₂	carbon dioxide	qPCR	quantitative polymerase chain reaction
CsCl	cesium chloride	REM	rare earth metals
DAD	diode array detector	RID	refractive index detector
ddH ₂ O	deionized double distilled water	rRNA	ribosomal ribonucleic acid
DNA	deoxyribonucleic acid	SIMPER	similarity percentage analysis
ECD	electron capture detector	SIP	stable isotope probing
ECMP	ethylmalonyl-CoA-pathway	sp.	species
EDTA	ethylenediaminetetraacetate	sMMO	soluble methane monooxygenase
EPS	Extracellular polymeric substance	t ₀	starting time point (i.e., untreated samples)
FAD	flavin adenine dinucleotide	t _{END}	end-time point (i.e., after a treatment)
FID	flame ionisation detector	TAE	tris - acetate – EDTA
GC	gas chromatography	TCA	tricarboxylic acid cycle
H ₄ F	tetrahydrofolate	TCD	thermal conductivity detector
H ₄ MPT	tetrahydromethanopterin	TRFLP	terminal restriction length polymorphism
HGT	horizontal gene transfer	USC	upland soil cluster
HPLC	high performance liquid chromatography	VOC	volatile organic compounds
ITS	internal transcribed spacer		
KCN	potassium cyanide		
LP	labelling proportion		
MeOH	methanol		
MDH	methanol dehydrogenase		
MDO	methanol oxidoreductase		
MMO	methane monooxygenase		
MUT	methanol utilisation pathway		

SUMMARY

Methylotrophic microorganisms possess a unique metabolism that enables them to utilize one-carbon (C1) compounds as a sole source of carbon and energy rendering methylotrophs important sinks of atmosphere-relevant compounds such as methane, methanol and chloromethane. These volatile organic compounds (VOCs) affect the climate and the atmospheric chemistry. Although methylotrophic microorganisms are an object of research since the 19th century, the environmental factors that drive their biodiversity in soils have been hardly resolved. Most soil-derived methylotrophic isolates are neutrophilic and facultatively methylotrophic, which means that they are capable of utilising multi-carbon compounds. Thus, the substrate range as well as the pH might be important ecological niche-defining factors for methylotrophs in a complex microbial community.

The current study analysed aerobic methylotrophs in an acidic deciduous forest soil regarding their diversity, their substrate range in terms of utilisation of different C1 compounds and the capability to assimilate multi-carbon compounds, as well as the effect of the pH of soil. Therefore, different incubation experiments mimicking *in situ* conditions were applied targeting 'high-affinity' methanotrophs, methanol-utilisers, and chloromethane-utilisers.

Long-term incubations of soil slurries under methanotrophic and mixed substrate conditions focussing on the methane degradation potential of the forest soil, the abundance of 'high-affinity' USC α (upland soil cluster α) methanotrophs (based on qPCR analyses targeting the *pmoA* gene of USC α) and their substrate range revealed a very restricted substrate range comprising apparently solely methane. Therefore, the assumption that 'high-affinity' methanotrophs such as USC α might utilise alternative substrates besides methane could not be verified.

Insights into the metabolic behaviour and substrate range of soil-derived methanol-utilising methylotrophs was enabled by slurry incubations, which were treated under methylotrophic and mixed substrate conditions. The studies combined comparative stable isotope probing (SIP) experiments and next generation sequencing (NGS) techniques with general (16S rRNA, ITS) and methylotrophic specific (*mxoF/xoxF*, *cmuA*) marker genes. In this way, members of the *Rhizobiales* were identified as methanol-utilisers of which *Beijerinckiaceae* were the main methanol-utilisers. *Beijerinckiaceae* occupied a central role in a methanol-dependent food web including other non-methylotrophic *Bacteria* (i.e., *Acidobacteria*, *Actinobacteria*, *Planctomycetes* and *Verrucomicrobia*) as well as fungi (*Trichosporon*, *Cryptococcus*, *Mortierella*). The identified substrate range of methylotrophic *Beijerinckiaceae* was restricted to C1 compounds rather than multi-carbon compounds. Other methanol-utilisers, such as *Methylobacteriaceae* and *Hyphomicrobiaceae*, likely possessed a larger substrate range including acetate, sugars, and aromatic compounds.

Moreover, an unexpected diversity of chloromethane utilisers was uncovered comprising taxa affiliated to *Alphaproteobacteria* (i.e., *Beijerinckiaceae*, *Methylobacteriaceae*, *Hyphomicrobiaceae*, and *Bradyrhizobiaceae*) as well as *Actinobacteria* (i.e., *Actinomycetales*, *Pseudonocardiaceae*, and *Microbacteriaceae*). These chloromethane-utilising taxa were further classified as different 'trophic types', regarding to the utilisation of methanol and chloromethane as carbon and/or energy sources.

Furthermore, an experimentally induced pH shift was associated with substantial changes in the active methylotrophic community, suggesting that the soil pH was a crucial niche-defining factor of the detectable methanol utilisers. Under neutral but still methylotrophic conditions *Bacteroidetes* (*Flavobacteriaceae*), *Actinobacteria* (*Microbacteriaceae*), and *Beta-proteobacteria* (*Methylophiliaceae*) as well as the yeast *Trichosporon* were identified as methanol utilisers.

The conclusions of the current work are therefore (i) that acidotolerant methylotrophic *Rhizobiales*, especially *Beijerinckiaceae*, contribute to the main methanol sink in an acidic forest soil, (ii) that soil-derived methylotrophs seem to possess a limited substrate range including methane, methanol, and chloromethane regarding carbon assimilation under environmental conditions, (iii) that the soil's pH is a crucial ecological niche-defining factor, and (iv) that saprotrophic fungi and further soil *Bacteria* are tightly trophically linked to methylotrophs in a complex microbial community in the investigated forest soil.

ZUSAMMENFASSUNG

Methylotrophe Mikroorganismen besitzen einen einzigartigen Metabolismus, der es ihnen ermöglicht, C1-Verbindungen als einzige Kohlenstoff- und Energiequelle zu nutzen. Deshalb sind Methylotrophe eine wichtige Senke für gasförmige C1-Verbindungen wie Methan, Methanol und Chlormethan, die für die Atmosphärenchemie relevant sind. Diese flüchtigen organischen Verbindungen (VOC, volatile organic compounds) beeinflussen das Klima und die Chemie der Atmosphäre. Obwohl methylotrophe Mikroorganismen seit dem letzten Jahrhundert Forschungsgegenstand sind, ist das Wissen über die Umweltfaktoren, die deren Biodiversität steuern, begrenzt. Die meisten aus dem Boden gewonnenen Isolate sind neutrophil und fakultativ methylotroph, was bedeutet, dass sie in der Lage sind Mehrfachkohlenstoffverbindungen zu nutzen. Aus diesem Grund könnten das Substratspektrum sowie der pH-Wert wichtige Faktoren sein, die die ökologische Nische von Methylotrophen in einer komplexen mikrobiellen Gemeinschaft bestimmen.

In der vorliegenden Arbeit wurden aerobe Methylotrophe in einem sauren Laubwaldboden bezogen auf ihre Diversität, ihr Substratspektrum hinsichtlich verschiedener C1-Verbindungen und ihrer Fähigkeit Mehrfachkohlenstoffverbindungen zu assimilieren, sowie den Effekt des pH-Wertes im Boden analysiert.

Langzeitinkubationen unter methanotrophen und gemischten Substratbedingungen, die sich auf das Methanabbaupotenzial eines Waldbodens, die Abundanz der „hochaffinen“ USC α Methanotrophen (basierend auf qPCR Analysen des *pmoA*-Gens von USC α) und deren Substratspektrum konzentrierten, ergaben ein sehr eingegrenztes Substratspektrum, das sich scheinbar nur auf Methan beschränkt. Aus diesem Grund konnte die Vorstellung, dass „hochaffine“ Methanotrophe wie USC α alternative kohlenstoffhaltige Substrate außer Methan nutzen können, nicht bestätigt werden.

Einblicke in das Stoffwechselverhalten und das Substratspektrum bodenbürtiger Methylotrophen, die Methanol nutzen können, wurden durch Inkubationsstudien unter methylotrophen und gemischten Substratbedingungen ermöglicht. Diese Experimente kombinierten vergleichende stabile Isotopensondierungsexperimente (SIP, stable isotope probing) und Hochdurchsatz-Sequenzierungstechniken (NGS) auf Grundlage allgemeiner (16S rRNA, ITS) und methylotroph-spezifischer (*mxoF/xoxF*, *cmuA*) Genmarker. So wurden Angehörige der *Rhizobiales* als Methanolnutzer identifiziert, wobei *Beijerinckiaceae* die Hauptnutzer von Methanol waren. *Beijerinckiaceae* nahmen dabei eine zentrale Rolle in einem methanol-abhängigen Nahrungsnetz ein, das andere Bakterien (*Acidobacteria*, *Actinobacteria*, *Planctomycetes* und *Verrucomicrobia*) sowie Pilze (*Trichosporon*, *Cryptococcus*, *Mortierella*) umfasste. Die als assimiliert identifizierten Substrate der methylotrophen *Beijerinckiaceae* waren ausschließlich C1-Verbindungen und keine Mehrfachkohlenstoffverbindungen. Bei anderen Methanolnutzern wie z.B.

Methylobacteriaceae und *Hyphomicrobiaceae* wurde ein breiteres Substratspektrum detektiert, welches Acetat, Zucker und Aromaten einschloss.

Außerdem wurde eine unerwartete hohe Diversität chlormethannutzender Taxa identifiziert, die den *Alphaproteobacteria* (*Beijerinckiaceae*, *Methylobacteriaceae*, *Hyphomicrobiaceae* und *Bradyrhizobiaceae*) sowie *Actinobacteria* (*Actinomycetales*, *Pseudonocardiaceae* und *Microbacteriaceae*) zuzuordnen sind. Diese chlormethannutzenden Taxa konnten zudem in verschiedene „trophische Typen“ hinsichtlich der Nutzung von Methanol und Chlormethan als Kohlenstoff- und/oder Energiequelle eingeteilt werden.

Darüber hinaus führte eine experimentell induzierte Verschiebung des pH-Wertes zu erheblichen Änderungen der aktiven methylo-trophen Gemeinschaft, was darauf hindeutet, dass der pH-Wert des Bodens ein entscheidender nischenbestimmender Faktor für die detektierten Methanolnutzer ist. Unter pH-neutralen, aber dennoch methylo-trophen Bedingungen wurden *Bacteroidetes* (*Flavobacteriaceae*), *Actinobacteria* (*Microbacteriaceae*) und *Betaproteobacteria* (*Methylophilaceae*) sowie die Hefe *Trichosporon* als Methanolnutzer identifiziert.

Aus den dargestellten Ergebnisse lässt sich schlussfolgern, (i) dass acidotolerante methylo-trophe *Rhizobiales*, vor allem *Beijerinckiaceae*, die Hauptsenke von Methanol in dem untersuchten sauren Waldboden waren; (ii) dass Methylo-trophen des untersuchten Waldbodens nur ein limitiertes Substratspektrum besitzen, das Methan, Methanol und Chlormethan umfasst; (iii) dass der pH-Wert des Bodens ein entscheidender Faktor ist, der die ökologische Nische dieser Mikroorganismen bestimmt; und (iv) dass saprotrophe Pilze und andere Bakterien in dem untersuchten Waldboden trophisch eng mit Methylo-trophen verbunden sind.

1. INTRODUCTION

Methylotrophs were discovered more than 100 years ago and possess a unique metabolism that enables them to utilise C1 compounds as sole source of carbon and energy, rendering methylotrophs important sinks for atmospheric relevant compounds such as methane, methanol and chloromethane (see 1.1 - 1.7). These volatile organic compounds (VOC) contribute to the greenhouse effect and the depletion of ozone having great implications on the climate (see 1.1). Methylotrophs are further important microorganisms in the global cycling of carbon, nitrogen, sulphur and halogens since they are physiologically and phylogenetically diverse and occur ubiquitously in different, even contrasting environments (see 1.2). Methylotrophs were also the first microorganisms targeted by molecular tools in environmental studies, and with the emergence of comprehensive sequencing studies the world of methylotrophs expanded since methylotrophic capabilities were recognized in chemoorganotrophs hitherto not known as methylotrophs (see 1.2 & 1.3). However, the knowledge on methylotrophs in terrestrial environments such as forest soils and their interaction with the existing microbial community as well as their ecological niche-defining parameters, such as alternatively utilised multi-carbon substrate or the pH, are not well understood.

Thus, the focus of this doctoral thesis was (i) to uncover methylotrophic organisms, i.e., methane-, methanol- and chloromethane-utilisers in a forest soil, (ii) to assess metabolic behaviours of 'high-affinity' methanotrophs (see 3.1, 3.2 & 4.1), (iii) to evaluate ecological niche-defining parameters such as the multi-carbon substrate range and the pH (see 3.3 - 3.7 & 4.2), and (iv) to unravel the metabolic capacity to co-utilise C1 compounds such as methanol and chloromethane simultaneously (see 3.9 - 3.11 & 4.4).

1.1. The representative C1 compounds methane, methanol and chloromethane and their climatic relevance

The atmospheric concentrations of methane, methanol and chloromethane are only marginal with 1.8 ppm (methane), 0.1 - 10 ppb (methanol), and 600 ppt (chloromethane), but their local concentrations at the earth's surface such as in soils, in litter, at plant surfaces (i.e., leaves and the phyllosphere) in aquatic environments are often not known and might reach dramatically higher concentrations. Nevertheless, these compounds are the most abundant organic and halogenated compounds in the atmosphere with high impacts on the concentration of tropospheric radicals. Thus, methane, methanol and chloromethane can cause a domino effect, based on photon-triggered or radical-triggered reactions resulting in the formation of further highly reactive radicals (Figure 1 and 1.1.1 - 1.1.3).

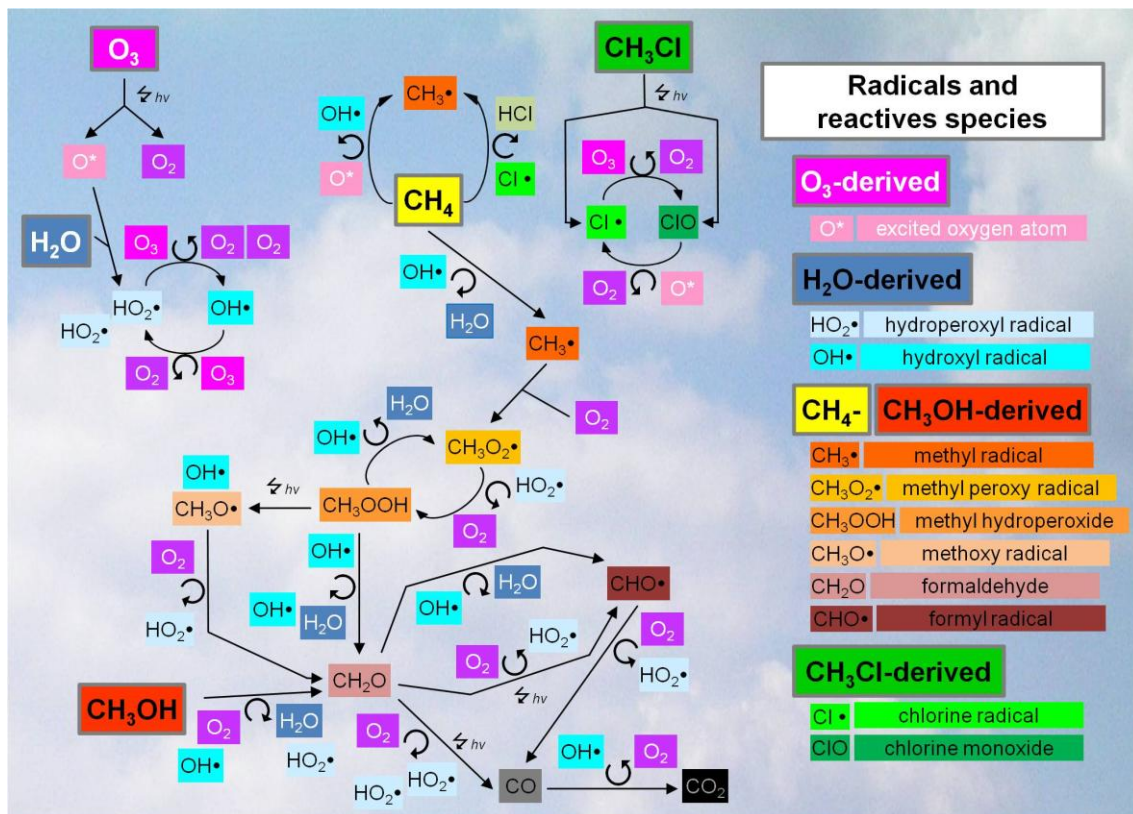


Figure 1 Reactions of methane, methanol and chloromethane and their contribution to ozone depletion.

Methane, methanol and chloromethane affect the formation of highly reactive radicals, the formation of CO and CO₂ as well as the ozone depletion in the atmosphere by abiotic photon-triggered ($\nabla h\nu$) or radical-triggered (X•) reactions. Colours indicate the origin of compounds (purplish, oxygen-derived; bluish, water derived; yellowish to reddish, methane- and methanol-derived; greenish, chloromethane-derived). The figure is based on Cicerone & Oremland, 1988; Jacob, 1999; and Keene *et al.*, 1999.

1.1.1. Methane – climatic relevance, sources and sinks

Methane is the simplest hydrocarbon compound, a biogenic volatile organic compound (bVOC) and the most prominent C1-substrate. It is the second most important greenhouse gas after CO₂ with a high impact on radiative forcing (difference between absorbed and emitted sunlight) [Myhre *et al.*, 2013]. Methane contributes to the tropospheric water vapour concentration that is important for the global climate, Earth’s radiative balance, and ozone loss [Hartmann *et al.*, 2013]. Moreover, methane is chemically coupled to hydroxyl radicals (OH•) in the atmosphere, and an increase in methane emissions leads to decreased concentrations of tropospheric hydroxyl radicals (OH•), which in turn increases the lifetime of methane [Myhre *et al.*, 2013]. Although nowadays the atmospheric concentration of methane seems to be low (i.e., 1.8 ppm) the tropospheric mixing ratio has increased by 150 % since 1750 (pre-industrial time), and is presumed for a further doubling by 2100 [Myhre *et al.*, 2013]. Sources and sinks of methane are mainly known, but reasons for the recent increase of methane emission since 2007 are not uncovered yet. It might be possible that ‘global

warming' effects, such as longer periods of thawed permafrost regions (i.e., a longer activity phase of these wetlands producing methane by methanogenesis) or extreme weather events (such as heavy rain falls, floodings, pronounced El Niño phenomena), contribute to this increase as well as anthropogenic intrusions such as the re-rise of coal mining (China) and fracking (USA) [Nisbet *et al.*, 2014].

The formation of methane can be of biogenic, thermogenic or pyrogenic origin. Thermogenic sources include natural emissions from geological sources (such as seepages, geothermal vents and mud volcanos) or anthropogenic emissions by the leakage of natural gas during the extraction of fossil fuel (oil industry, coal mines, fracking) [Cias *et al.*, 2013]. The pyrogenic sources are also of natural and anthropogenic origin, and comprise the incomplete burning of plant biomass (natural fires, fire clearance) and fossil fuels [Cias *et al.*, 2013]. The same is true for all biogenic sources (mainly wetlands, wild and livestock ruminants, rice paddy fields, waste water treatments) [Cias *et al.*, 2013], in which the sum of all biogenic sources reveals that more than 60 % are of anthropogenic origin, which is in accordance to the reported increase of atmospheric methane concentrations during the industrial time (since 1750) (Figure 2) [Neef *et al.*, 2010; Cias *et al.*, 2013]. 'Wetlands' comprise the main natural source for methane emissions including several ecosystems such as (temporary) wet soils, swamps, bogs, and peatlands, where the methane production is caused by the activity of methanogenic microorganisms that convert organic matter under oxygen-limited up to anoxic conditions into methane [Conrad, 1996]. Apart from wetlands also herbaceous and woody plants can be a source of methane. Keppler and colleagues reported the emission of methane by plant-derived material and they assumed pectin as main source, since this heteropolysaccharide represents the major C1-pool (based on methoxyl groups) in plants [Keppler *et al.*, 2006]. In addition, plants might also transport methane from methanogenic regions within the rhizosphere or from the inside of tree stems (methane can be produced by the anaerobic decomposition of wetwood) to the leaves and thus, emit methane acting as a 'source' [Zeikus & Ward, 1974; Rusch & Rennenberg, 1998; Terazawa *et al.*, 2007; Conrad, 2009]. Further, the fungal degradation of complex plant-derived material like wood can result in methane directly or indirectly (i.e., the stimulation of methanogens by providing nutrients) [Muhkin & Voronin, 2009; Lenhart *et al.*, 2012].

The main sink (it contributes more than 80 %) for the atmospheric methane is the atmosphere itself (troposphere and stratosphere), and therein the photochemical oxidation of methane enabled by hydroxyl radicals (OH•) as already mentioned (Figure 1, Figure 2) [Cias *et al.*, 2013]. Further, but minor sinks are reactions with excited oxygen atoms (O*) or chloride radicals (Cl•) in the stratosphere and the reaction with chlorine in the marine boundary layer resulting in chloromethane [Dlugokencky *et al.*, 2011; Allan *et al.*, 2007; Neef *et al.*, 2010]. Nevertheless, biotic sinks also exist including oceans and terrestrial soils. Their role should not be underestimated, since only a minor fraction of formed or released methane enters the atmosphere. Methanotrophs in the oceans are crucial, since they consume most of the marine-derived methane before it is emitted into the atmosphere

[Dlugokencky *et al.*, 2011]. The same is true for soils, although they contribute only up to 5 % of the global atmospheric methane sinks [Conrad, 2009]. However, between 50 % and 95 % of the belowground produced methane is consumed by methanotrophs before it reaches the atmosphere emphasizing the importance of methanotrophic bacteria in soils [Kuivila *et al.*, 1988; Reeburgh, 2003; Kvenvolden & Rogers, 2005; Le Mer & Roger, 2011; Chistoserdova & Lidstrom, 2013; Nazaries *et al.*, 2013].

1.1.2. Methanol – climatic relevance, sources and sinks

Another bVOC is methanol that is after methane the second most abundant organic gas in the atmosphere, but its chemical reactivity is greater [Jacob *et al.*, 2005; Seco *et al.*, 2011; Wohlfahrt *et al.*, 2015]. In the troposphere a methanol loop occurs. Methanol can be formed through the reaction of methylperoxy radicals ($\text{CH}_3\text{O}_2\bullet$) with itself or higher peroxy radicals ($\text{RO}_2\bullet$), and the oxidation of methanol or other VOCs leads in turn to the formation of peroxy radicals ($\text{RO}_2\bullet$) [Jacob *et al.*, 2005]. In the atmosphere methanol reacts with hydroxyl radicals ($\text{OH}\bullet$) leading to the formation of formaldehyde, hydrogen radicals ($\text{H}\bullet$) and ozone (O_3) [Heikes *et al.*, 2002] (Figure 1).

The average atmospheric concentration of methanol is estimated to range from 0.1 ppb up to 10 ppb [Jacob *et al.*, 2005; Seco *et al.*, 2011; Wohlfahrt *et al.*, 2015]. However, on a regional scale the methanol concentrations can differ by a multiple, rendering the assessment of the global methanol budget more difficult [Wohlfahrt *et al.*, 2015]. For example, the lowest mixing ratios were measured in the troposphere ranging from 0.2 - 1 ppb (average 0.6 ppb), followed by 0.9 ppb over the open ocean, 2 ppb for continental background (i.e., no impact of humans), 6 ppb for grasslands and 10 ppb for forests, and highest concentrations with more than 20 ppb for urban areas [Heikes *et al.*, 2002]. Moreover, the atmospheric methanol concentrations vary depending on the latitude, hemisphere, seasonality, temperature, or even humidity which is in accordance with the reported sources and sinks [Millet *et al.*, 2008].

The main sources of atmospheric methanol are of natural origin (biogenic), comprising marine systems (ocean) and terrestrial systems (plants) (Figure 2). Minor sources are anthropogenic activities such as solvent use, vehicle exhaust, industrial processes, and biomass burning, where wood pyrolysis (meaning the decomposition of wood at elevated temperatures in the absence of oxygen) of plant fibres (e.g. cellulose, hemicelluloses, lignin) is the reason of methanol formation and emission [Howard *et al.*, 1990; Medeiros *et al.*, 2008; Maleknia *et al.*, 2009; Goepfert *et al.*, 2014; Woolf *et al.*, 2014]. In terrestrial environments methanol is mainly released by plant material as already mentioned. It is assumed that 40 - 80 % (large range due to the different models of methanol budget) of the annually arising methanol is originated from plant growth [Singh *et al.*, 2000; Galbally & Kristine, 2002; Heikes *et al.*, 2002; Tie *et al.*, 2003; Jacob *et al.*, 2005; Millet *et al.*, 2008], but also dead and decaying plant material provides remarkable amounts of methanol [Warneke

et al., 1999; Schade & Cluster, 2004; Karl *et al.*, 2005a]. In growing plant biomass methanol is formed during demethylation processes of compounds rich in methoxy groups such as pectin and lignin [Schink & Zeikus, 1980; Fall & Benson, 1996; Warneke *et al.*, 1999; Millet *et al.*, 2008]. It was assumed that especially during plant or leaf growth methanol productions are high (up to 75 % of the emitted methanol is assumed as leaf-derived) [Fall & Benson, 1996; Nemecek-Marshall *et al.*, 1995; Hüve *et al.*, 2007], but also during the abscission of plant leaves methanol is released [Willats *et al.*, 2001]. In addition, methanol emissions depend on diurnal variations. For example, amounts of leaf-emitted methanol vary between night and day (especially in the morning) up to 18fold, which is correlated with stomata conductance, and a higher transpiration of plants also increases the amount of emitted methanol [Nemecek-Marshall *et al.*, 1995; Hüve *et al.*, 2007; Dorokhov *et al.*, 2015]. In addition, methanol flux studies revealed seasonality for methanol concentrations according to plant growth behaviour with highest measured amounts in spring and fall [Tie *et al.*, 2003]. Further, damaged plants release substantial amounts of methanol caused by cutting, mowing, or animal feeding (herbivore insects up to herbivore animals) [Karl *et al.*, 2001; Peñuelas *et al.*, 2005; Von Dahl *et al.*, 2006; Brilli *et al.*, 2011]. These emissions can be high for several days as it was reported for a lucerne-covered meadow [Warneke *et al.*, 2002]. Also plant stress causes enhanced methanol emissions [Seco *et al.*, 2007]. In dead or decaying plant material methanol can be released from residual in-leaf methanol, or it can be formed biotically by the activity of microorganisms degrading the plant fibers, or abiotically by physico-chemical degradation processes [Warneke *et al.*, 1999; Galbally & Kirstine, 2002; Schade & Custer, 2004; Millet *et al.*, 2008]. Thus, the role of plants in terms of methanol emission is crucial, and plants are the main providers of this C1 compound for methanol-utilising organisms.

The two major sinks for methanol are atmospheric reactions with hydroxyl radicals (OH•) in the troposphere and clouds, as well as oceanic uptake, in which the role of the ocean is a net sink including gross methanol emission and uptake in the ocean mixed layer (OML) (Figure 2) [Millet *et al.*, 2008]. Phytoplankton (i.e., unicellular algae, diatoms, dinoflagellates and bacteria) is a major source of methanol emission in the ocean, which is depending on several other factors (such as temperature, oxygen, nutrients, and light) [Heikes *et al.*, 2002]. The major oceanic sink is likely caused by photochemical destruction and the high water solubility of methanol, as well as by the activity of marine methylotrophic microorganisms [Heikes *et al.*, 2002; Millet *et al.*, 2008]. Methanol-utilising microorganisms are also the main sink of methanol in terrestrial environments and are included in the term 'dry deposition' (Figure 2) [King, 1992; Oremland & Culbertson, 1992; Jacob *et al.*, 2005; Dunfield, 2007; Trotsenko & Murrell, 2008; Conrad, 2009; Kolb, 2009a; Vorholt, 2012; Knief, 2015]. Methylotrophic organisms in the phyllosphere are well known and well studied [Omer *et al.*, 2004; Anda *et al.*, 2011; Wellner *et al.*, 2011; Madhaiyan *et al.*, 2012; Meena *et al.*, 2012]. They can even comprise up to 16 % of the total leaf microbiome [Vorholt, 2012]. However, the important role of methanol-utilising microorganisms in the soil has hardly been investigated in the last decades, and the main knowledge is based on pure cultures and artificial laboratory

experiments [Radajewski *et al.*, 2000; Radajewski *et al.*, 2002; Morris *et al.*, 2002; Kolb, 2009a; Stacheter *et al.*, 2013]. Thus, it is easily conceivable that for methanol-utilising organisms the same scenario like for methanotrophic organisms in terrestrial environments is likely – they might consume the highest proportion of produced methanol before it can reach the atmosphere acting as an important regulating agent in terms of methanol emissions.

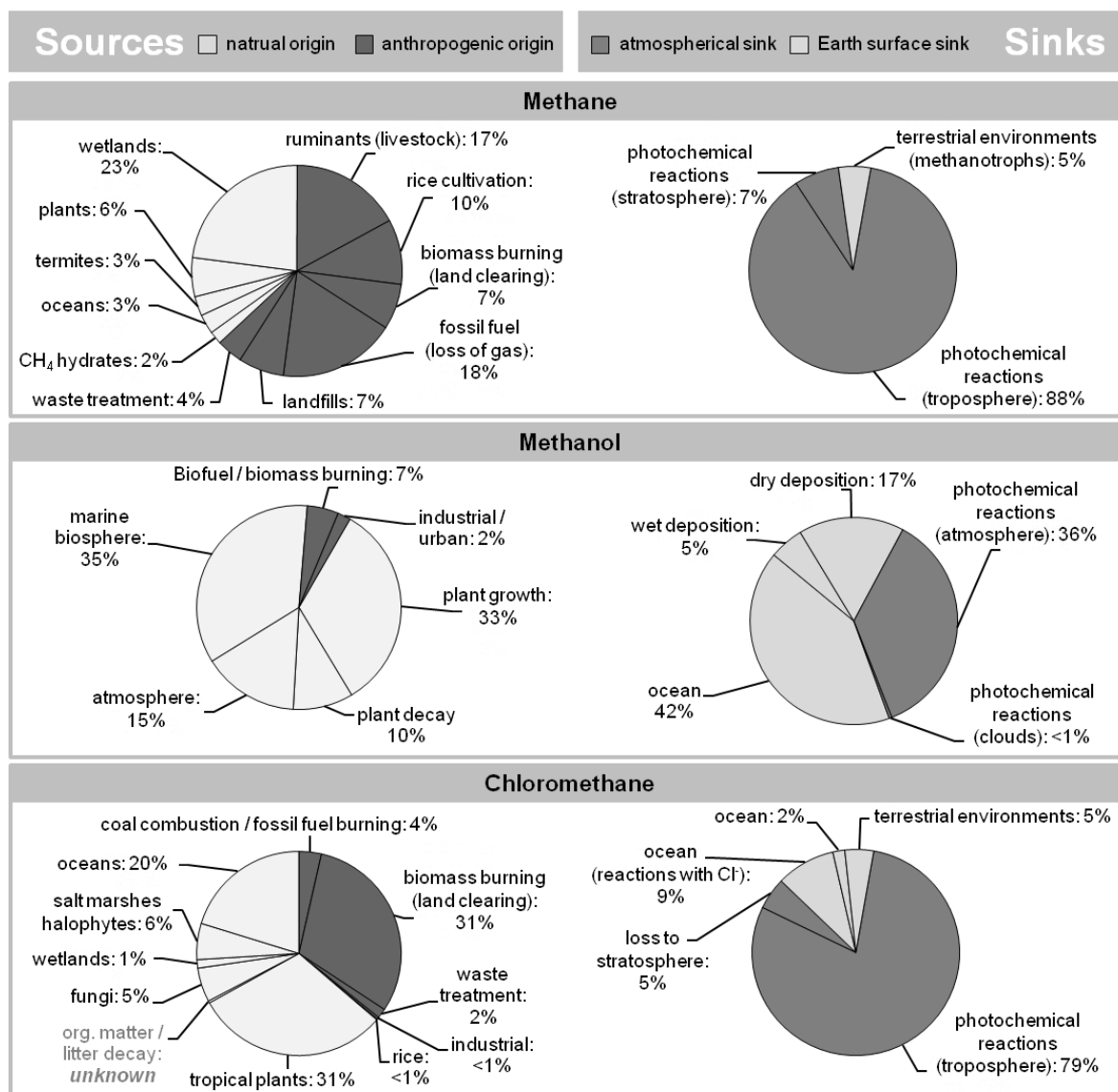


Figure 2 Global sources and sinks for atmospheric methane, methanol and chloromethane.

The contribution of sources (left side) and sinks (right side) of atmospheric methane, methanol and chloromethane are already known, but the local amounts of formed gases or the local contribution of microbial degradation are not assessed and might be substantially higher. Sources are divided into their natural (light grey) and anthropogenic (dark grey) origin and sinks are divided based on their localisation in the atmosphere (dark grey) and on the Earth surface (light grey) in which 'Earth surface sinks' include deposition, ocean uptake, and microbial degradation. For detailed information please refer to the text in 1.1.1, 1.1.2, and 1.1.3. All charts are based on values mentioned in Nazaries *et al.*, 2013 for methane, Millet *et al.*, 2008 for methanol, and Keppler *et al.*, 2005 for chloromethane.

1.1.3. Chloromethane – climatic relevance, sources and sinks

The monohalomethane chloromethane (CH_3Cl ; synonym: methyl chloride) is one of the structurally simplest representative of halomethanes. Halomethanes are derivatives of methane where at least one hydrogen atoms is replaced by a halogen 'X' (i.e., chlorine Cl, bromine Br, iodine I, and fluorine F) resulting in molecular formulas like CH_3X to CX_4 . Within these halogenated compounds CH_3Cl and chlorofluoromethane (CH_2ClF) are most important regarding to their usage and environmental impact [Wackett *et al.*, 1992]. CH_3Cl and other monohalomethanes are mainly of natural origin and contribute substantially to the ozone layer depletion. Although the atmospheric concentration of CH_3Cl is only about 600 ppt, it is the most abundant halocarbon in the atmosphere, can cause 15 % - 20 % of the chlorine-derived ozone destruction in the stratosphere, and seems to be the most abundant source of atmospheric chlorine [Harper, 2000; Coulter *et al.*, 1999; Khalil & Rasmussen, 1999; Montzka *et al.*, 2011]. Tropospheric CH_3Cl that reaches the stratosphere is one source of free chloride radicals ($\text{Cl}\bullet$), which are a result of the photolytically destruction of CH_3Cl [Keene *et al.*, 1999]. These $\text{Cl}\bullet$ react with ozone forming chlorine monoxide (ClO), which reacts again with ozone or free oxygen (O^*) atoms releasing molecular oxygen and $\text{Cl}\bullet$ again (Figure 1). In this way a chlorine based cycle of ozone destruction is initiated and one CH_3Cl molecule (i.e., one $\text{Cl}\bullet$) can destroy 100 000 ozone molecules until chlorine radicals will be bound (for example in compounds such as HCl or ClONO_2) [www.theozonehole.com/ozonedestruction.htm].

Analogous to methanol, CH_3Cl is mainly formed and emitted in terrestrial environments by plants (Figure 2). In aqueous environments nucleophilic substitution processes (i.e., halide exchange or hydrolysis) contribute to the formation of CH_3Cl [Lovelock, 1975; Elliott & Rowland, 1995; Schäfer *et al.*, 2007]. In marine environments CH_3Cl can also be produced by phytoplankton and algae [Moore *et al.*, 1995; Tait & Moore, 1995; Scarrat & Moore, 1996; Scarratt *et al.*, 1998; Manley & Dastoor, 1987; Wuosmaa & Hager, 1990]. Further biological sources of CH_3Cl are halophytes growing in salt marshes [Rhew *et al.*, 2000], fungi involved in plant material degradation [Cowan *et al.*, 1973; Turner *et al.*, 1975; Waitling *et al.*, 1998; Harper, 2000], and plants producing CH_3Cl as side reaction during defence response caused by tissue cutting [Rhew *et al.*, 2003; Nagatoshi & Nakamura, 2007]. In terrestrial environments the abiotic methylation of chloride is a large source of CH_3Cl [Keppler *et al.*, 2005]. Such processes can occur in plants, when methoxy groups of pectin-components react with chloride ions [Hamilton *et al.*, 2003], or during the oxidation of soil organic matter (such as humus) in the presence of ferric iron and halides [Keppler *et al.*, 2000]. However, the extent of decaying plant material, such as litter and rotten wood, as a CH_3Cl source is not resolved yet, but might be substantial when considering that (i) pectin is one of the major plant cell wall components (i.e., pectin contributes around 35 % of the primary cell wall of dicotyledonous plants, 1 - 10 % of the cell wall in grasses and 5 % in wood tissue [Voragen

et al., 2009]) and (ii) that a large amount of the global carbon (i.e., 1500 ± 2200 Gt) is stored as methoxy group-possessing components in the organic layer of soils [Post *et al.*, 1982].

In addition to the uncertainties of the CH₃Cl sources, also the sinks and their general contribution are not fully resolved (Figure 2). Analogous to methanol and methane photochemical reactions with radicals in the atmosphere are the major sink for atmospheric CH₃Cl [Harper, 2000; Schäfer *et al.*, 2007; Keppler *et al.*, 2005]. Minor, but important sinks are of biotic origin. Several methyl halide-degrading bacterial isolates were obtained from marine environments [Goodwin *et al.*, 1998; Schäfer *et al.*, 2002; Schäfer *et al.*, 2005]. The significance of marine CH₃Cl-consumers might be emphasised by the isolation of the methylotrophic CH₃Cl-utilising isolate 'HTCC2181' that is phylogenetically affiliated to the very abundant coastal bacterioplanktonic clade OM43 [Giovannoni *et al.*, 2008; Halsey *et al.*, 2012]. Thus, CH₃Cl-utilising bacteria seem to be widespread and abundant in marine environments and contribute to the oceanic sink. Several studies on the biotic CH₃Cl degradation facilitated by microbes in soils from pristine and polluted sites accentuate the relevance of soils as large sink for CH₃Cl [Doronina *et al.*, 1996; Harper, 2000; McAnulla *et al.*, 2001a; Miller *et al.*, 2004]. Thus, the microbial degradation might be an underestimated sink with great importance in terms of the global CH₃Cl budget. Regarding the plant-associated sources, it is also easily conceivable that – like previously assumed for methane and methanol – the CH₃Cl-utilising microorganisms consume the majority of the locally produced CH₃Cl before it can reach the atmosphere acting as a regulative force.

1.2. The microbial sink – methylotrophic microorganisms

Methylotrophic microorganisms comprise the specific metabolic capability to utilise reduced carbon substrates without carbon-carbon bonds as their sole source of carbon and energy and therefore creating every carbon-carbon bond 'de novo' [Anthony, 1982; Chistoserdova & Lidstrom 2013; Chistoserdova, 2015]. Thus, these microorganisms can grow on substrates such as methane, methanol, halogenated methanes, methylated amines, and methylated sulphur species. Some methylotrophs also possess the ability to fix nitrogen and/or denitrify [Chistoserdova & Lidstrom, 2013]. In addition, methylotrophs are widespread in nature detectable in aquatic and terrestrial environments including even extreme environments such as acidic volcanic muds (pH 1) or alkaline lake sediments (pH 10) [King, 1992; Dunfield *et al.*, 2007; Pol *et al.* 2007; Islam *et al.* 2008; Trotsenko & Murrell, 2008; Antony *et al.*, 2010; Chistoserdova & Lidstrom, 2013]. Based on the ubiquity and the high activity in the transformation of a variety of C1 compounds methylotrophs are important in the global cycling of materials such as carbon, sulphur, nitrogen, and halogens [Kolb, 2009a; Chistoserdova, 2015]. Further – as already mentioned (see 1.1) – methylotrophs are important as a biological sink for greenhouse gases and VOCs emphasizing their crucial role in terms of the climate [Chistoserdova & Lidstrom, 2013].

Methylotrophs are diverse. They can be aerobic or anaerobic, autotrophic (i.e., they dissimilate the C1 compound to CO₂ and assimilate this formed CO₂ again) or heterotrophic, obligately or facultatively methylotrophic [Anthony, 1982; Hanson & Hanson, 1996; Lidstrom, 2006; Trotsenko & Murrell, 2008; Chistoserdova & Lidstrom, 2013]. Aerobic methylotrophy is also not restricted to a distinct clade of microorganisms and can be found within the *Alpha*-, *Beta*-, *Gammaproteobacteria*, *Actinobacteria*, *Firmicutes*, *Verrucomicrobia*, and within fungi (ascomyceteous yeasts and mould fungi) [Anthony, 1982; Kolb, 2009a; Chistoserdova & Lidstrom 2013; Kolb & Stacheter, 2013]. Anaerobic methylotrophy is found within *Archaea* (anaerobic methanotrophic archaeae 'ANME' and methylotrophic methanogens) and *Clostridia* (methylotrophic acetogens) [Zinder, 1993; Cheng *et al.*, 2007; Knittel & Boetius, 2009; Penger *et al.*, 2012; Drake *et al.*, 2013; Oren, 2013].

Methylotrophs have been known since the first isolation of methylotrophic bacteria more than 100 years ago [Loew, 1892; Kaserer, 1905; Söhngen, 1906], but it is only since the 1970s that the knowledge on these bacteria increased by the isolation of further methylotrophs (mainly methanotrophs) [Whittenbury *et al.*, 1970a]. However, only with the effort of studies mimicking *in situ* conditions as well as molecular based environmental studies the view on methylotrophs was dramatically expanded raising the question on the abundance and ubiquity of methylotrophy [Chistoserdova *et al.*, 2009; Kolb & Stacheter, 2013]. Additionally, the increased knowledge on methylotrophs and the recognition of methylotrophic capacities by culture-independent surveys query the laboratory model methylotrophs and how well they might reflect methylotrophy in terms of *in situ* relevant conditions.

1.3. Metabolic features of methylotrophy

Based on the previous knowledge on methylotrophs the C1-based metabolism can be partitioned into three major metabolic modules: (i) an 'initial activation' of the C1-substrate (oxidation, demethylation or dehalogenation) resulting in intermediate compounds, (ii) oxidation of these intermediate C1 compounds to CO₂ (includes formaldehyde oxidation / detoxification or methylene-tetrahydrofolate (CH₂=H₄F) oxidation, and the oxidation of formate to CO₂), and (iii) the assimilation of the C1-units to gain biomass [Chistoserdova *et al.*, 2003; 2009; Chistoserdova, 2011]. All these three modules are enabled by different pathways and enzymes that are characteristic for some groups of methylotrophs (Figure 3). For example, the assimilation of carbon in alphaproteobacterial methylotrophs is enabled by the serine cycle, whereas in methanotrophic *Verrucomicrobia* the assimilation is enabled by the ribulose biphosphate cycle (RuBP) [Trotsenko & Murrell, 2008; Op den Camp *et al.*, 2009; Chistoserdova, 2011]. These findings led to the assumption of 'methylotrophic modularity', in which methylotrophy is enabled by the combination of all three modules leading to 'classical combinations' detectable in well studied model methylotrophs such as *Methylococcus capsulatus*, *Methyosinus trichosporium*, and *Methylobacterium extorquens*,

as well as more recently discovered combinations as found in verrucomicrobial *Methylacidiphilum inferorum* for example (Figure 3) [Chistoserdova, 2011].

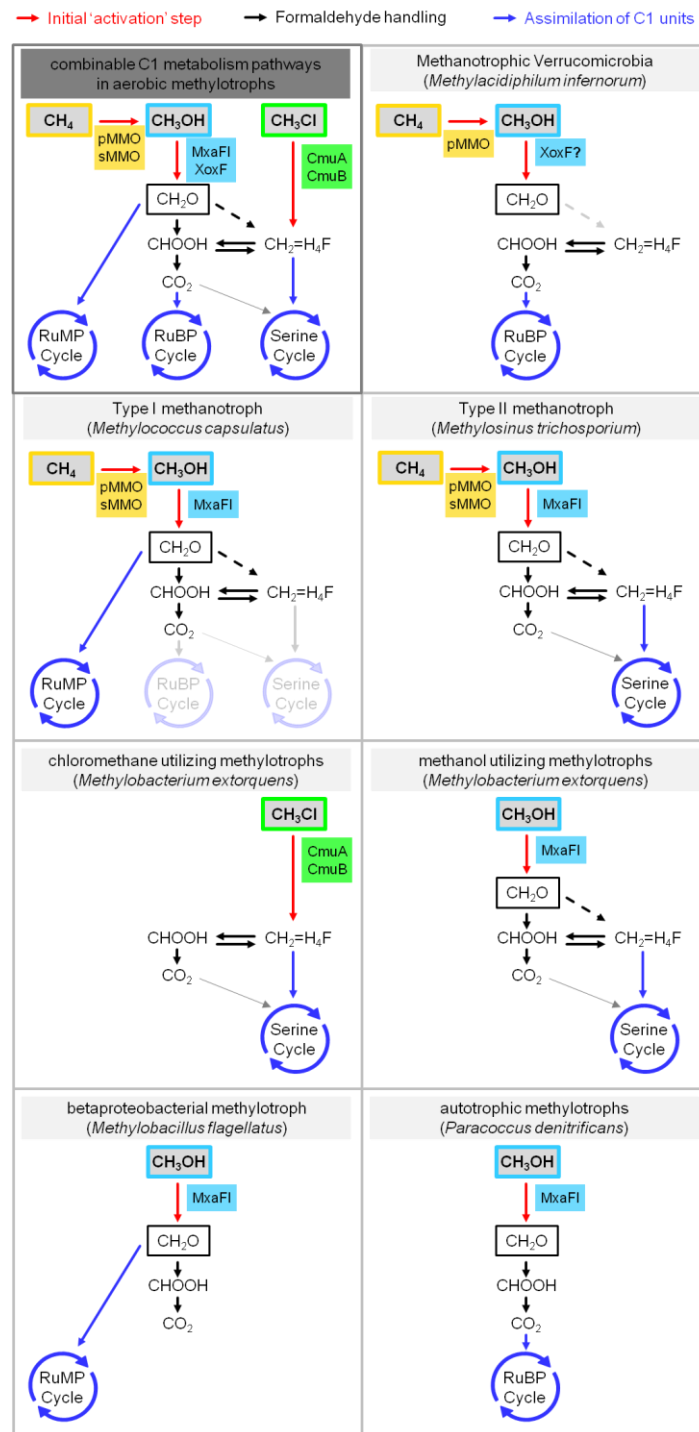


Figure 3 Simplified overview on methylotrophic modules and some examples of their combination in methylotrophic organisms.

The combination of possible pathway modules required in methylotrophic organisms (top left, 'combinable C1-metabolism pathways in aerobic methylotrophs') leads to different metabolic variations of methylotrophs in terms of methane-, methanol- and chloromethane-utilisation. Marker enzymes: pMMO and sMMO, methane monooxygenase (see 1.6.1); MxaFI and XoxF, PQQ-methanol dehydrogenase (see 1.6.3); CmuA and CmuB, methyltransferases (see 1.6.5). Module colour code: red arrows, initial 'activation' step modules by marker enzymes; blue arrows, assimilation modules (see 1.5); black arrows, formaldehyde oxidation (detoxification) modules. The figure is based on Chistoserdova, 2011.

1.4. Dissimilatory pathways in methylotrophs – from methane, methanol and chloromethane to CO₂

Aerobic bacterial methylotrophs possess specific pathways for the dissimilation of C1 compounds. This section concentrates briefly on the dissimilatory pathways from methane, methanol, and chloromethane to CO₂, but does not go into further details of the dissimilation of other C1 compounds such as methylated amines or methylated sulphur species, since these substrates were not in the focus of the present study. In addition, this section summarises the different pathways reviewed in Chistoserdova & Lidstrom, 2013.

In general, the initial C1 compound is oxidised, demethylated or dehalogenated to obtain formaldehyde or methylene-tetrahydrofolate (methylene-H₄F; CH₂=H₄F) by specific oxidases (e.g. MMO, see 1.6.1), dehydrogenases (e.g. PQQ-MDH, see 1.6.3), methyltransferases (e.g. CmuAB, see 1.6.5), or dehalogenases. Dehydrogenases are coupled to the energy metabolism at the cytochrome-level, whereas oxidases, methyltransferases, and dehalogenases are not providing energy. Formaldehyde is further oxidised to formate via a linear pathway (facilitated by formaldehyde dehydrogenases) or via pterin-dependent pathways enabled by several enzymes and the pterin-cofactors tetrahydrofolate (H₄F) or tetrahydromethanopterin (H₄MPT) [Trotsenko & Murrell, 2008]. The last step of the complete dissimilation is the oxidation of formate to CO₂ facilitated by formate dehydrogenases resulting in reducing equivalents or free electrons (Figure 4).

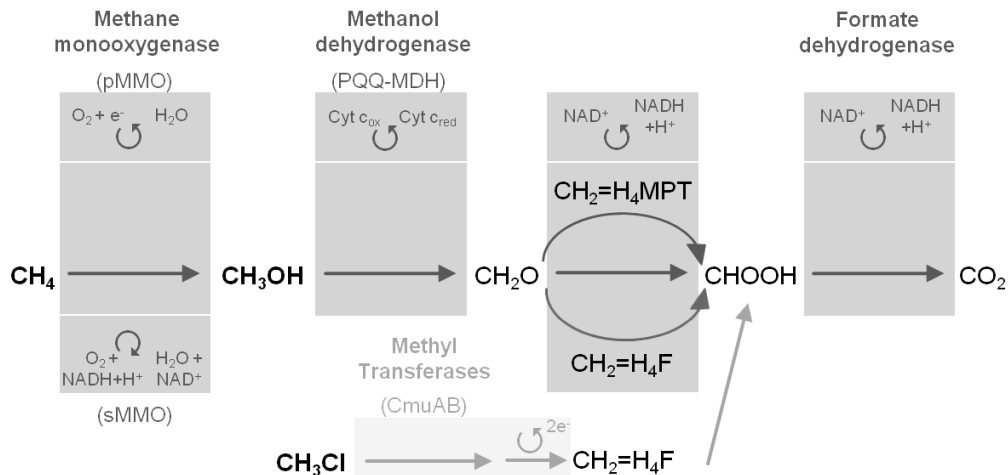


Figure 4 Dissimilatory oxidation of methane, methanol and chloromethane to CO₂.

The utilisation of methane, methanol and chloromethane to CO₂ is facilitated by the initial oxidation steps and necessary enzymes. The conversion of formaldehyde to formate can be facilitated by three different pathways (see text for short details) wherefore enzymes are not mentioned. The figure is based on Anthony, 1982; Trotsenko & Murrell, 2008; Chistoserdova & Lidstrom, 2013; Studer *et al.*, 2002.

1.5. Assimilatory pathways of C1 compounds in *Bacteria*

In methylotrophic bacteria the assimilation of C1 compound-derived carbon can occur at three different levels (formaldehyde, formate, and CO₂), which is in accordance with the three known assimilation pathways: (i) ribulose monophosphate (RuMP) cycle (see 1.5.1), (ii) ribulose bisphosphate (RuBP) cycle, or Calvin Besson Bassham (CBB) cycle (see 1.5.2), and (iii) the serine cycle (see 1.5.3) [Anthony, 1982; Chistoserdova, 2011; Chistoserdova & Lidstrom, 2013].

1.5.1. Ribulose monophosphate (RuMP) cycle

Carbon assimilation at the level of formaldehyde is facilitated by the RuMP cycle providing carbohydrates as intermediates [Anthony, 1982]. The general principle is that a C1-unit (formaldehyde) is added onto a C5-acceptor sugar molecule (RuMP, ribulose monophosphate or ribulose-5-phosphate) to create a C6-sugar molecule (hexulose-6-phosphate), which is metabolically widespread in the cellular metabolism. This C6-sugar phosphate is further converted into C3-molecules, which are used for cell biomass synthesis, generation of reducing equivalents, and the regeneration of C5-acceptor sugar molecules [Anthony, 1982]. In total four different variants of the RuMP exist, differing in sugar cleavage scenarios and acceptor regeneration pathways [Anthony, 1982]a (Figure 5).

The RuMP cycle is not restricted to methylotrophs only and can be used by other bacteria in terms of formaldehyde detoxification [Yasueda *et al.*, 1999; Chistoserdova & Lidstrom, 2013]. Methylotrophs possessing the RuMP cycle are often type I methanotrophs (*Methylococcaceae*) and some beta- or gammaproteobacterial and gram-positive methylotrophs [Chistoserdova, 2011].

1.5.2. Ribulose bisphosphate (RuBP) cycle

The RuBP cycle is well known for autotrophic microorganisms assimilating carbon at the level of CO₂. Thus, this assimilatory pathway is no unique feature of methylotrophs and some methylotrophs possess other carbon assimilation pathways besides the RuBP cycle, questioning the contribution of the RuBP in terms of carbon assimilation [Chistoserdova *et al.*, 2005; Chistoserdova, 2011]. Acquisition of key genes of the RuBP cycle by lateral gene transfer events is further assumed [Chistoserdova *et al.*, 2005]. The RuBP cycle can be found in all autotrophic methylotrophs: (i) methanotrophic *Verrucomicrobia* (*Methylacidiphilaceae*), (ii) methanotrophs of the anaerobic NC10 phylum (*Methylomirabilis oxyfera*), and (iii) autotrophic alphaproteobacterial methylotrophs (e.g. *Paracoccus denitrificans*) [Chistoserdova, 2011; Chistoserdova & Lidstrom, 2013].

The RuBP can be divided into three major parts and is somehow comparable with the RuMP cycle. In the first part – (*fixation*) – the C1-unit (CO₂) is added to a C5-acceptor sugar (RuBP, ribulose-1.5-bisphosphate) yielding two C3-molecules (3-phosphoglycerate, PGA). The C3-molecule PGA is further reduced in the second part of the cycle (*reduction*) to another C3-molecule (glyceraldehyde-3-phosphate, GAP) that is used for cell biomass synthesis and the third (*rearrangement*) part of the cycle. Two variations of the *rearrangement* part (i.e., regeneration of C1 acceptor molecule RuBP) are possible, but all result in the formation of a new C5-acceptor sugar. [Anthony, 1982]

1.5.3. Serine cycle und glyoxylate regeneration

The serine cycle is one of the specific assimilatory pathways of methylootrophy and is mainly attributed to type II methanotrophs and non-methane-utilising methylootrophs not possessing the RuBP cycle [Chistoserdova, 2011]. Contrary to the RuBP cycle and the RuMP cycle, the serine cycle provides carboxylic acids and amino acids as intermediates [Anthony, 1982]. In the serine cycle carbon is assimilated at the level of CH₂=H₄F [Anthony, 1982; Hanson & Hanson, 1996; Chistoserdova, 2011; Chistoserdova & Lidstrom, 2013] generated from formaldehyde by a non-enzymatic reaction or from formate by an enzymatic reaction (methylene-H₄F-dehydrogenase) [Trotsenko & Murrell, 2008; Chistoserdova, 2011; Chistoserdova & Lidstrom, 2013]. CH₂=H₄F is further added to glycine (C2), which represents the acceptor molecule for the C1-unit, resulting in the formation of serine (C3). Based on serine, several C3 and C4 molecules are generated such as hydroxypyruvate (C3), pyruvate (C3), oxalacetate (C4), malate (C4) and acetyl-CoA (C2), which are all usable for cell biomass synthesis [Anthony, 1982; Hanson & Hanson, 1996; Trotsenko & Murrell, 2008; Peyraud *et al.*, 2009]. Interestingly the serine cycle comprises some reactions of other metabolic pathways like the tricarboxylic acid cycle (TCA) [Trotsenko & Murrell, 2008; Chistoserdova, 2011; Chistoserdova & Lidstrom, 2013] representing a metabolic connection of C1 compound and alternative substrate utilisation (Figure 5).

Methylootrophs harbouring the serine cycle must also possess regeneration reactions for glyoxylate (C2), which is necessary for the formation of the C1-acceptor molecule glycine (C2) [Hanson & Hanson, 1996; Trotsenko & Murrell, 2008; Peyraud *et al.*, 2009]. Therefore different pathways are known such as the glyoxylate shunt and the ethylmalonyl-CoA pathway (EMCP), in which the majority of serine cycle methylootrophs employ the EMCP [Anthony, 1982; Chistoserdova & Lidstrom, 2013]. The EMCP shares also reactions with several other metabolic pathways (e.g. serine cycle, TCA, and polyhydroxybutyrate (PHB) cycle) (Figure 5) [Chistoserdova, 2011]. However, EMCP is not restricted to methylootrophs, and serves in non-methylootrophic organisms as C2-assimilation pathway [Alber, 2010; Okubo *et al.*, 2010; Schneider *et al.*, 2011] emphasizing a metabolic connection of alternative substrate utilisation by methylootrophs. However, some serine cycle-possessing methylootrophs such as *Methylibium petrophilum* and *Methylocella silvestris* use the

glyoxylate shunt and lack EMCP genes [Kane *et al.*, 2007; Chen *et al.*, 2010a]; some methylotrophs such as *Hyphomicrobium denitrificans* encodes for both pathways [Chistoserdova, 2011]; and in the genome of *Methylococcus capsulatus* neither EMCP nor glyoxylate shunt genes were detected [Chistoserdova *et al.*, 2005].

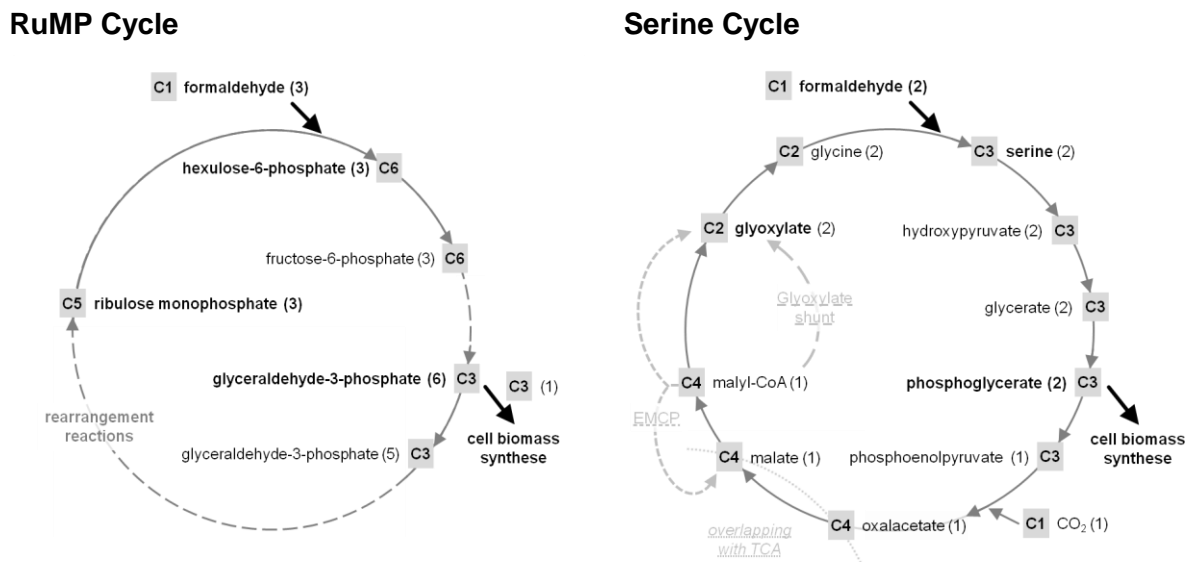


Figure 5 Assimilation cycles in methylotrophic Bacteria.

A comparison of the two common carbon assimilation pathways in bacterial methylotrophs – the RuMP and serine cycle – regarding formed molecules (carbon atoms per molecule in grey boxes and amount of formed molecules in brackets) and specific characteristics such as the different multistep pathway variations of sugar cleavage and acceptor regeneration scenarios in the RuBP cycle (dashed lines) as well as the interconnection between the serine cycle and the TCA (overlapping lines) and the glyoxylate regeneration pathways (EMCP and glyoxylate shunt; dashed lines). For further information see the text and the references listed therein. The figure is based on Anthony, 1982; Hanson & Hanson, 1996; Trotsenko & Murrell, 2008; Peyraud *et al.*, 2009.

1.6. Methylotrophic varieties in *Bacteria*

Methylotrophs are metabolically diverse; however, the main focus was in the past mainly on methanotrophic organisms (see 1.6.1, 1.6.2). Since the majority of methylotrophs are not capable of oxidizing methane, and methanol serves as common intermediate in methylotrophic organisms, the diversity of methanol-utilising methylotrophs is much higher (see 1.6.3, 1.6.4). Further, methylotrophic organisms are also able to utilise other C1 compounds such as CH₃Cl, expanding again the variety of methylotrophs (see 1.6.5).

1.6.1. Aerobic methanotrophs, methane-utilisation, and methane monooxygenases (MMO)

Methanotrophs are those methylotrophs, which can use solely methane as carbon and energy source [Anthony, 1982; Hanson & Hanson, 1996]. Methane utilisation is enabled by the oxidation of methane under oxic conditions (electron acceptor is oxygen) and anoxic

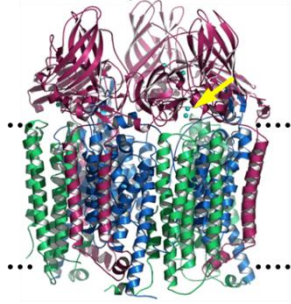
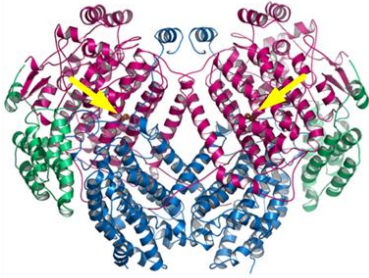
conditions (electron acceptors sulphate, nitrate, nitrite, iron) [Anthony, 1982; Ettwig *et al.*, 2008; 2010; 2016]. The anaerobic oxidation of methane (AOM) is a metabolic feature of anaerobic methanotrophic euryarcheota (ANME) and is limited to anoxic habitats [Knittel & Boetius, 2009], wherefore this group of methanotrophic microorganisms is no further subject of the present work of this thesis. The aerobic counterpart of the ANME are aerobic methanotrophs that are found within the *Alphaproteobacteria* (*Methylocystaceae*, *Beijerinckiaceae*), *Gammaproteobacteria* (*Methylococcaceae*), and *Verrucomicrobia* (*Methylacidiphilaceae*), and are often detectable at anoxic/oxic interfaces in various environments [Hanson & Hanson, 1996; Trotsenko & Murrell, 2008; Nazaries *et al.*, 2013; Knief, 2015]. Traditionally, methanotrophs were primarily divided into type I (*Gammaproteobacteria*) and type II (*Alphaproteobacteria*) methanotrophs based on morphological, physiological and genetic characteristics [Hanson & Hanson, 1996]. With the description of type X methanotrophs (i.e., *Methylococcus*, *Methylocaldum*) [Trotsenko & Murrell, 2008], the blurring of typical characteristics, and the discovery of methanotrophic *Verrucomicrobia* this classification is nowadays not applicable anymore [Nazaries *et al.*, 2013; Knief, 2015].

However, all aerobic methanotrophs depend on a methane monooxygenase (MMO) enabling the initial step of methane oxidation [Anthony, 1982; Hanson & Hanson, 1996; Trotsenko & Murrell, 2008]. In general, methane is further oxidised to methanol, formaldehyde, formate and CO₂, and carbon will be assimilated at the level of formaldehyde or formate depending on the assimilation pathway of the methanotrophic organism (see 1.4 & Figure 4, 1.5 & Figure 5) [Anthony, 1982; Hanson & Hanson, 1996; Trotsenko & Murrell, 2008].

Two different types of the marker enzyme MMO exist – the membrane-bound particulate type (pMMO, marker gene is *pmoA*) and the cytoplasmatic soluble type (sMMO, marker gene is *mmoX*) [Hanson & Hanson, 1996; Trotsenko & Murrell, 2008; Semrau *et al.*, 2010]. The pMMO is more widespread among methanotrophs and the associated *pmoA* gene (encoding the β -subunit) exists in almost all known members of methanotrophs [Zahn & DiSpirito, 1996; McDonald *et al.*, 1997; Murrell *et al.*, 2000; Knief *et al.*, 2015]. The *pmoA* is also a well established marker gene, reflecting also congruent 16S rRNA phylogenies [Knief, 2015]. The same is also true for *mmoX* encoding the hydroxylase subunit of the sMMO [Murrell *et al.*, 2000; Horz *et al.*, 2001; Leahy *et al.*, 2003; Knief, 2015]. However, the distribution of the sMMO and thus, *mmoX* as marker gene is restricted to alphaproteobacterial methanotrophs (*Methylocystis*, *Methylosinus*, *Methylovulum*, *Methylorosula*) and gammaproteobacterial methanotrophs (*Methylococcus*, *Methylomicrobium*, *Methylomonas*, *Methylovulum*) [Nazaries *et al.*, 2013]. Although most sMMO-possessing methanotrophs also possess a pMMO, some methanotrophs such as *Methylocella* species and *Methyloferula stellata* only possess the sMMO [Dunfield *et al.*, 2003; Theisen & Murrell, 2005; Vorobev *et al.*, 2011].

Apart from the phylogenetic distribution both MMO enzymes have several differences that are briefly listed in Table 1.

Table 1 Comparison of both methane monooxygenases (MMO).

pMMO (particulate MMO)	sMMO (soluble MMO)
<p>Membrane bound copper-containing trimeric enzyme with three subunits each, where PmoA and PmoC are primarily transmembrane helices and PmoB contains transmembrane and periplasmic domains.</p>	<p>Cytoplasmatic hexameric enzyme comprising three components (i) hydroxylase component (MmoX, MmoY, MmoZ) with di-iron in the active center of the α-subunit (MmoX), (ii) reductase component (MmoC) with FAD and [Fe₂S₂] cluster, and (iii) regulatory component (MmoB) [Lee <i>et al.</i>, 2013]</p>
	
<p>Overall protein structure of the pMMO trimer (PmoA, PmoB, PmoC; yellow arrow: di-copper atoms in one active center; dotted line indicates cell membrane).</p>	<p>Overall protein structure of the sMMO dimer (MmoX, MmoY, MmoZ; yellow arrow di-iron atoms in the active center)</p>
<p>Coding genes: <i>pmoCAB</i></p>	<p>Coding genes: <i>mmoXYBZDC</i></p>
<p>Marker gene applied in environmental studies: <i>pmoA</i></p>	<p>Marker gene applied in environmental studies: <i>mmoX</i></p>
<p>Substrate affinity ($K_M = 1 - 2 \mu\text{M}$)</p>	<p>substrate affinity ($K_M = 3 \mu\text{M}$)</p>
<p>narrow substrate range</p>	<p>broad substrate spectrum</p>
<p>Reaction:</p>	<p>Reaction:</p>
<p>$\text{CH}_4 + \text{O}_2 + \text{Cyt}_{\text{red}} \rightarrow \text{CH}_3\text{OH} + \text{H}_2\text{O} + \text{Cyt}_{\text{ox}}$</p>	<p>$\text{CH}_4 + \text{O}_2 + \text{NAD(P)H} + \text{H}^+ \rightarrow \text{CH}_3\text{OH} + \text{H}_2\text{O} + \text{NAD(P)}^+$</p>
<p><u>Cyt_{red}</u> / <u>Cyt_{ox}</u>: cytochrome b_{559/569} or C₅₅₃</p>	

All information are taken from Hanson & Hanson, 1996; Trotsenko & Murrell, 2008; Hakemian & Rosenzweig, 2007; Liebermann & Rosenzweig, 2005; Myronova *et al.*, 2006. Images of the protein structures are taken from <http://www.methanotroph.org/wiki/biochemistry/>.

If a methanotroph possess both MMOs, the MMO expression is depending on the concentration of copper, which means for example that under copper starving conditions the sMMO is expressed (known as ‘copper switch’) [Murrell *et al.*, 2000; Semrau *et al.*, 2010]. The pMMO is evolutionary related to the ammonium monooxygenase (AMO) of ammonia-oxidising bacteria (AOB), wherefore these bacteria can fortuitously oxidise methane, but AOBs cannot assimilate methane-derived carbon [Holmes *et al.*, 1995; Hanson & Hanson, 1996]. In addition, some type II methanotrophs (such as *Methylocystis* and *Methylosinus*) encode for a divergent type of pMMO (PmoCAB2), which has a higher substrate affinity and might be responsible for the methane oxidation capacity of ‘high-affinity’ methanotrophs [Baani & Liesack, 2008; Chistoserdova *et al.*, 2009] (see 1.6.2).

1.6.2. High-affinity methanotrophs

The first hints for methanotrophs that are able to utilise atmospheric methane concentrations were obtained by Bender and Conrad, who observed two different enzyme kinetics depending on the surrounding methane concentrations in different soil samples, which indicated 'low-affinity' and 'high-affinity' enzymes [Bender & Conrad, 1992]. Further studies in various oxic soils confirmed the existence of 'high-affinity' methanotrophs [Roslev *et al.*, 1997; Kähkönen *et al.*, 2002; Saari *et al.*, 2004]. Studies concerning the adaption to low methane concentrations (i.e., < 1000 ppm or even < 100 ppm) revealed that type II methanotrophs such as *Methylocystis* have a high potential to remain active [Knief & Dunfield, 2005]. Nevertheless, all 'low-affinity' methanotrophs, which are represented by the known cultured strains, are only able to grow with methane concentrations higher than 100 ppm [Nazaries *et al.*, 2013]. The highly specialised methanotrophs belonging to 'upland soil cluster' (USC) groups were shown to be capable to utilise atmospheric methane [Holmes *et al.*, 1999; Knief *et al.*, 2003; Jaatinen *et al.*, 2004; Kolb *et al.*, 2005, Dunfield, 2007; Lau *et al.*, 2007; Kolb, 2009b; Degelmann *et al.*, 2010; Pratscher *et al.*, 2011]. These 'high-affinity' methanotrophs have not been cultivated yet, but several studies based on molecular and biochemical methods were conducted to target them [Holmes *et al.*, 1999; Henckel *et al.*, 2000; Knief *et al.*, 2003]. In aerated soils from different environments the 'high-affinity' methanotrophs were classified as 'upland soil cluster' (USC), in which two distinct phylogenetic clades exist, USC α and USC γ [Holmes *et al.*, 1999; Knief *et al.*, 2003; Kolb *et al.*, 2005; Dunfield, 2007; Lau *et al.*, 2007; Degelmann *et al.*, 2010]. USC γ is detectable in soils with a more neutral pH and is distantly related to type I methanotrophs of the *Methylococcaceae* and therefore affiliated to *Gammaproteobacteria*, whereas USC α is abundant in acidic soils and is distantly related to the type II methanotrophs of the acidophilic representatives belonging to the *Beijerinckiaceae* and *Methylocystaceae*, wherefore it is affiliated to *Alphaproteobacteria* [Dedysh *et al.*, 2002, Ricke *et al.*, 2005, Kolb *et al.*, 2005, Knief, 2015]. USC methanotrophs are enigmatic, since the low atmospheric methane concentrations (1.8 ppm) raise the question how these bacteria maintain or even grow in their habitats, and several possible survival scenarios are assumed [Dunfield, 2007]: (i) they are genuine oligotrophs living solely on atmospheric methane, (ii) they are 'flush feeders' of occasionally produced methane and endure unfavourable methane-low conditions, (iii) the utilise other substrates besides methane, or (iv) methane is fortuitously oxidised by another enzyme, wherefore 'true' methanotrophy would be queried. However, all of these scenarios might be true. It might be possible that the amount of methane is sufficient for growth [Kolb *et al.*, 2005], but further calculations also contradict this assumption [Degelmann *et al.*, 2010]. It might be further possible that methanogenic organisms sporadically supply enough methane for the methanotrophs increasing the local methane concentration [Megraw & Knowles, 1987; Dunfield *et al.*, 1995; Yavitt *et al.*, 1995; Andersen *et al.*, 1998; Horz *et al.*, 2002; Knief & Dunfield, 2005]. It might be also possible that alternative substrates are indeed utilised by

these 'high-affinity' methanotrophs leading to a pronounced facultatively methanotrophic metabolism. Such facultative methanotrophs exist among the genera *Methylocella*, *Methyloferula*, *Methylocapsa*, and *Methylocystis*, which can grow on acetate (C₂) and several other organic acids (up to C₄) and possess the serine cycle for carbon assimilation [Dedysh *et al.*, 2005a; Theisen & Murrell, 2005; Semrau *et al.*, 2011; Belova *et al.*, 2013]. Acetate assimilation was also revealed for USC α methanotrophs, but with no effect on methane degradation [Pratscher *et al.*, 2011]. However, since no cultured members of the 'high-affinity' methanotrophs are available, they remain enigmatic and present a great research gap in terms of methanotrophy.

1.6.3. Methanol-utilising methylotrophs and methanol oxidation

The majority of soil-derived methylotrophic isolates is non-methanotrophic and utilise methanol as preferred C₁ compound [Kolb, 2009a]. However, most studies on methylotrophs in terrestrial environments were focussing mainly on methanotrophs [Dunfield, 2007; Trotsenko & Murrell, 2008; Conrad, 2009; Kolb, 2009a; Degelmann *et al.*, 2010; Stolaroff *et al.*, 2012; Chistoserdova, 2015], and only a handful of studies giving insights to methylotrophs in aerated soil environments were conducted [Radajewski *et al.*, 2000; Radajewski *et al.*, 2002; Lueders *et al.*, 2004; Stacheter *et al.*, 2013]. Further, the limited molecular detection based on gene markers in most of the previous studies on soil methylotrophs might have led to an underestimation of their taxonomic biodiversity.

The initial enzymatic step in terms of methanol utilisation is the oxidation of methanol to formaldehyde. For this reaction at least three different enzymes are known in *Bacteria*: (i) a pyrrolo-quinoline quinone (PQQ)-dependent methanoldehydrogenase (PQQ-MDH), occurring in gram-negative *Proteobacteria* and *Verrucomicrobia*; (ii) a nicotinamide adenine dinucleotide (NAD)-dependent nicotinoprotein MDH (NAD-MDH), occurring in gram-positive *Bacillus* strains [Arfman *et al.*, 1989; de Vries *et al.*, 1992; McDonald & Murrell, 1997; Chistoserdova *et al.*, 2009; Krog *et al.*, 2013; Keltjens *et al.*, 2014]; and (iii) a methanol:NDMA (N,N'-dimethyl-4-nitrosoaniline) oxidoreductase (MDO, synonym MNO), occurring in gram-positive *Actinobacteria* [Bystrykh *et al.*, 1993; van Ophem *et al.*, 1993; Park *et al.*, 2010] (Figure 6). Additionally, in methylotrophic *Eukaryotes* another enzyme facilitates the first step of methanol oxidation [Hartner & Glieder, 2006; Gvozdev *et al.*, 2012] (see 1.7). With this spectrum of different enzymes several marker genes could be addressed, but genetic and molecular information for most of them are rare [Kolb, 2009a; Kolb & Stacheter, 2013]. Only genes encoding a part of the α -subunit of the PQQ-MDH of *Proteobacteria*, are well-characterized marker genes with suitable primers available for environmental surveys [McDonald & Murrell, 1997; Dumont *et al.*, 2005; Moosvi *et al.*, 2005; Neufeld *et al.*, 2007; Stacheter *et al.*, 2013; Taubert *et al.*, 2015].

The protein structure of the PQQ-MDH was resolved for *Methylobacterium extorquens*, *Methylophilus* sp., and the methanotroph *Methylococcus capsulatus* [Anthony & Williams,

2002; Culpepper & Rosenzweig, 2014]. In terms of the methanotrophs the PQQ-MDH and the MMO are assumed to form a supercomplex that facilitates the electron transfer without any requirement for NADH [Myronova *et al.*, 2006; Culpepper & Rosenzweig 2014]. In general for all methanol-utilisers, the PQQ-MDH is a soluble quinoprotein tetramer ($\alpha_2\beta_2$) located in the periplasm and possessing calcium ions and pyrrolo-quinoline quinone (PQQ) as prosthetic group that passes electrons to a soluble cytochrome C_L [Gosh *et al.*, 1995; Anthony & Williams, 2002; Gvozdev *et al.*, 2012] (Figure 6B). The PQQ and the Ca^{2+} are located in the catalytic α -subunit, which shows a characteristic 'propeller blade' structure forming a superbarrel [Gosh *et al.*, 1995; Anthony & Williams, 2002; Gvozdev *et al.*, 2012; Culpepper & Rosenzweig, 2014] (Figure 6B). The exact function of the smaller β -subunit is not resolved yet, but other quinoproteins lack this subunit indicating a specific function [Gvozdev *et al.*, 2012].

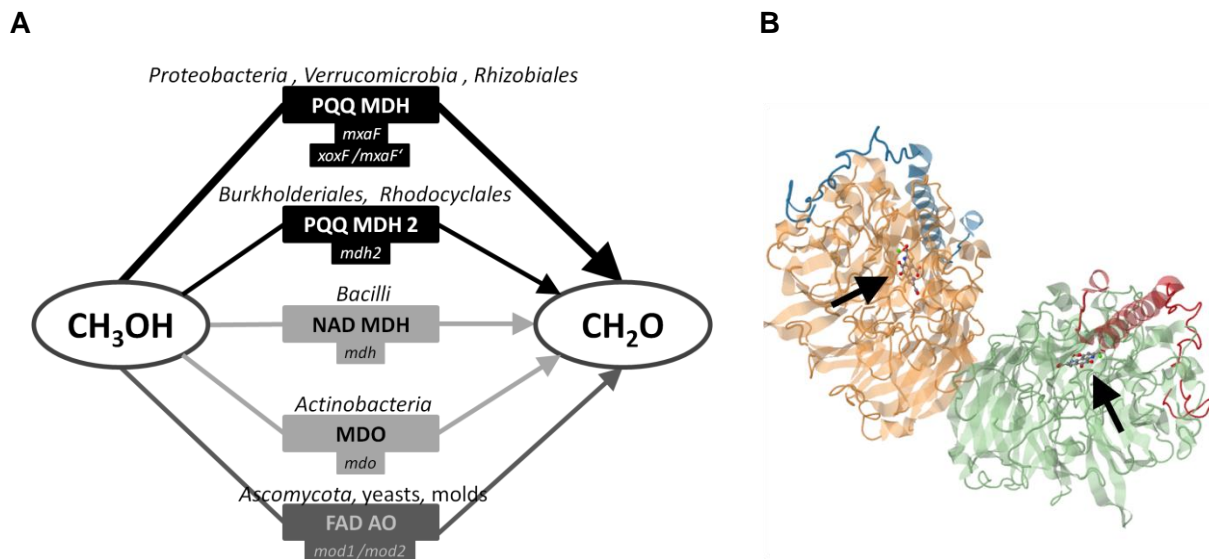


Figure 6 Diversity of known enzymes facilitating the oxidation of methanol in different methylotrophic organisms (A) and the crystal structure of a PQQ-MDH (B).

Panel A summarizes briefly the known diversity of enzymes and the corresponding encoding marker genes for the initial oxidation of methanol to formaldehyde as well as their phylogenetic distribution along **gram-negative methylotrophs**, **gram-positive methylotrophs**, and **eukaryotic methylotrophs** and emphasizes the PQQ-MDH as well-characterized marker enzyme with suitable primers available. For more details and abbreviations refer to the text. The figure is based on Kolb & Stacheter, 2013.

Panel B shows the tetrameric ($\alpha_2\beta_2$) crystal structure of the PQQ-MDH of *Methylococcus capsulatus* BATH. The subunits are indicated with different colours (large α -subunits in orange and green, small β -subunits in blue and red) and arrows point at the pyrrolo-quinoline quinones located the active centre. Image: <http://www.rcsb.org> (PDB ID: 4TQO).

The molecular marker genes for a PQQ-MDH are *mxoF* and *xoxF* (synonymous to *mxoF*), since they are highly conserved among proteobacterial methylotrophs [Lidstrom *et al.*, 1994; Kalyuzhnaya *et al.*, 2008a]. Primarily, *mxoF* was used as universal marker gene, since the enzymatic role of *xoxF*-encoded PQQ-MDH enzymes remained unclear, was highly

ambiguous and therefore underestimated [McDonald & Murrell, 1997; McDonald *et al.*, 2008; Kolb 2009a, Kolb & Stacheter, 2013]. However, within the last years the importance, high frequency and ubiquity of *xoxF*-type PQQ-MDHs were recognized [Keltjens *et al.*, 2014; Taubert *et al.*, 2015]. The initial underestimation of *xoxF* could be due to the fact that *XoxF*-type MDHs depend on lanthanide ions (Ln^{3+} , such as La^{3+} and Ce^{3+}) to be functional, which was not considered under laboratory conditions previously [Chistoserdova & Lidstrom, 2013; Keltjens *et al.*, 2014]. Although the chemical similarities between Ca^{2+} (necessary for functional *MxaF*-type MDH) and Ln^{3+} are significant, there is a dissimilarity, proposing Ln^{3+} to be catalytically more efficient [Chistoserdova, 2016]. Thus, it is assumed that the presence of Ln^{3+} at the active site of an enzyme turns *XoxF*-type MDH to more efficient enzymes being also functional at low methanol concentrations [Schmidt *et al.*, 2010; Skovran *et al.*, 2011; Keltjens *et al.*, 2014]. Genomic studies revealed that several *xoxF* copies – paralogs and orthologs – can be present in only one single bacterial genome, while only one *mxoF* copy is present [Keltjens *et al.*, 2014]. In addition, phylogenetic trees covering known sequences of PQQ-dehydrogenase enzymes indicate that the *MxaF*-type MDHs represent only a minor fraction in comparison to *XoxF*-type MDHs, which emphasise the minority of *mxoF* in relation to their *xoxF* counterparts [Kalyuzhnaya *et al.* 2008b; Bosch *et al.* 2009; Sowell *et al.* 2011; Chistoserdova, 2011; Keltjens *et al.*, 2014; Taubert *et al.*, 2015]. Currently, five distinct clades of *xoxF* (*xoxF1* to *xoxF5*) genes are known [Chistoserdova, 2011; Keltjens *et al.*, 2014; Taubert *et al.*, 2015]. The *xoxF1* clade includes sequences of *Xanthomonadales*, *Methylocella* and *Methyloferula* and the methanotrophic species “*Candidatus* *Methylomirabilis oxyfera*”, thus covering methanotrophic and non-methylotrophic species [Keltjens *et al.*, 2014; Taubert *et al.*, 2015]. The *xoxF2* clade seems restricted to the methanotrophic *Methylacidiphilum* species (*Verrucomicrobia*) and enzymes have been shown to catalyse the direct oxidation of methanol to formate [Keltjens *et al.*, 2014; Pol *et al.*, 2014; Taubert *et al.*, 2015]. The deepest branching *xoxF3* clade includes several methylotrophic species affiliated to *Rhizobiales*, *Methylococcales*, *Methylophiliales*, *Burkholderiales*, and “*Candidatus* *Solibacter usitanicus*” (*Acidobacteria*) [Keltjens *et al.*, 2014]. Interestingly, most of the members of this clade are also harbouring *xoxF* genes from the clades 4 and 5 [Taubert *et al.*, 2015]. The *xoxF4* clade includes exclusively *Methylophilales* species, in which the enzyme is for some members the only functional MDH (such as the isolate HTCC2181), and seems also restricted to freshwater and coastal environments [Giovannoni *et al.*, 2008; Kalyuzhnaya *et al.*, 2009; Taubert *et al.*, 2015]. The *xoxF5* clade is the largest clade so far, includes methylotrophs as well as non-methylotrophs of *Alpha*-, *Beta*- and *Gammaproteobacteria*, and the existing subgroups within the clade are in agreement with the taxonomy of their members [Keltjens *et al.*, 2014; Taubert *et al.*, 2015]. Thus, the main differences between both MDHs encoded by *mxoF* and *xoxF* genes are: (i) the enzymatic function (i.e., *xoxF* might be both: an active MDH and/or regulatory unit for the *MxaF* enzyme), (ii) the presence of Ca^{2+} or Ln^{3+} at the active side, (iii) the amount of gene copies within a bacterial genome (one copy of *mxoF* vs. several copies of *xoxF*), and (iv) the

phylogenetic distribution among proteobacterial methylotrophs [Schmidt *et al.*, 2010; Fitriyanto *et al.*, 2011; Skovran *et al.*, 2011; Nakagawa *et al.*, 2012; Keltjens *et al.*, 2014; Chistoserdova, 2016]. However, molecular analyses based on *xoxF* must be interpreted with caution, since also non-methylotrophs possess these genes [Keltjens *et al.*, 2014; Taubert *et al.*, 2015]. In turn, in some methylotrophic species that are affiliated to *Methylophilales* and are mainly restricted to aquatic environments, *xoxF* is the only gene encoding for a functional PQQ-MDH [Giovannoni *et al.*, 2008; Kalyuzhnaya *et al.*, 2009; Chistoserdova, 2015; Taubert *et al.*, 2015].

Although the PQQ-MDHs are encoded by *mxoF* and *xoxF*, some methylotrophic isolates such as the betaproteobacterial methylotrophs *Methylibium petroleiphilum* and *Methyloversatilis universalis* lacking these genes. They possess an alternative PQQ-MDH (PQQ-MDH2), which seems widespread among *Burkholderiales*, reveals a low similarity to the 'notorious' PQQ-MDH (35 %) and is encoded by the *mdh2* gene, indicating a convergent evolution of PQQ-MDHs [Kalyuzhnaya *et al.*, 2008a]. Further, as for some *xoxF* genes also *mdh2* genes seem to dominate marine habitats indicating the presence of habitat specific methanol oxidative systems [Rusch *et al.*, 2007; Kalyuzhnaya *et al.*, 2008a].

Gram-positive methylotrophs (*Bacilli* and *Actinobacteria*) possess NAD(P)-dependent type III alcoholdehydrogenases facilitating the oxidation of methanol (i.e., the NAD-MDH and the MDO or MNO) [de Vries *et al.*, 1992; Bystrykh *et al.*, 1993]. Both cytoplasmatic enzymes are induced by methanol and share similar structural characteristics such as a homo-decameric structure, the non-covalently bound NAD(H) cofactor molecules, as well as Zn²⁺ and Mg²⁺ associated with the subunits [Vonck *et al.*, 1991; Arfman *et al.*, 1991; de Vries, 1992; Bystrykh, 1993; Park *et al.*, 2010]. In addition, the MDO of *Actinobacteria* is *in vivo* associated with two further components building a multi-enzymatic system [van Ophem *et al.*, 1991; Bystrykh *et al.*, 1993; Bystrykh *et al.*, 1997]. The NAD-MDH of *Bacillus* does not form such an enzymatic system, but can be stimulated (up to 40-fold increase [Arfman *et al.*, 1991; Krog *et al.*, 2013]) by an activator protein (ACT) that catalyses a 'ping-pong reaction' of electron transport from methanol to NAD⁺ [Hektor *et al.*, 2002]. Among *Bacillus* strains plasmid-dependent methylotrophy is widespread [Brautaset *et al.*, 2004; 2007; Krog *et al.*, 2013], but genomic analyses of *Bacillus* strains revealed that in total 3 different NAD-MDHs are encoded (two MDHs are chromosomal and one is plasmid-borne) [Krog *et al.*, 2013]. These NAD-MDHs are transcribed at different levels depending on substrate conditions (methylotrophic vs. non-methylotrophic), and revealed a broad substrate spectrum with different preferences for alcohols, in which methanol appears to be not the preferred substrate [Krog *et al.*, 2013]. Further, in several enzymatic tests all MDHs revealed higher affinities to other alcohols and even to formaldehyde than to methanol, indicating an additional role of formaldehyde detoxification *in situ* [Krog *et al.*, 2013]. Thus, thermotolerant bacilli possess a larger repertoire of methanol-oxidizing enzymes with a more complex regulation than previously thought [Krog *et al.*, 2013].

In summary, the broad spectrum of several methanol converting enzymes and the increasing recognition of them among methylotrophs, especially in the case of the PQQ-MDHs (i.e., *xoxF* and the PQQ-MDH2), emphasises the need for molecular detection tools targeting the methanol-utilising methylotrophic capacity in environments to gain a more comprehensive and detailed assessment of the methylotrophic diversity.

1.6.4. Facultatively methylotrophic *Bacteria*

The majority of methylotrophic organisms are facultatively methylotrophic and are thus capable of utilising multi-carbon compounds [Kolb, 2009a]. The substrate spectrum of these methylotrophs includes several soluble compounds such as mono-, di-, and polysaccharides (e.g. inulin, dextrin), sugar acids and polyols, primary alcohols (ethanol, butanol, and isopropanol), glycerol, amino acids, mono-, di-, tricarboxylic acids, aromatic compounds, and various other nitrogen- and sulfur-containing carbon compounds [Kolb, 2009a]. Even recalcitrant polymers might be utilised, since one cellulolytic methylotrophic representative (*Sagittula stellata*) is reported that also grows on aromatic compounds and exhibits lignin transformation capabilities [Gonzalez *et al.*, 1997]. Facultatively methylotrophic taxa are for example members of the alphaproteobacterial families *Methylobacteriaceae*, *Hyphomicrobiaceae*, *Beijerinckiaceae*, *Methylocystaceae*, *Bradyrhizobiaceae*, *Rhodobacteraceae*, and *Xanthobacteraceae* [Kolb, 2009a]. Within the *Betaproteobacteria* facultatively methylotrophic genera are for instance *Methylophilus*, *Methylovorus*, *Methyloversatiles*, and *Methylibium* [Kalyuzhnaya *et al.*, 2006; Nakatsu *et al.*, 2006; Yoon *et al.*, 2007; Doronina *et al.*, 2013]. Also some gammaproteobacterial facultative methylotrophs are reported in genera such as *Methylohalomonas* or *Methylonatronum*, but the majority of methylotrophic *Gammaproteobacteria* seems to be obligately methylotrophic within the methanotrophic representatives (e.g. *Methylococcaceae*) [Sorokin *et al.*, 2007; Kolb, 2009a; Bowman, 2013]. Additionally, among the methylotrophic (methanotrophic) *Verrucomicrobia* also no facultatively methylotrophic metabolism in terms of alternative carbon sources is reported up to date [Op den Camp *et al.*, 2009; Van Teeseling *et al.*, 2014], but *Verrucomicrobia* are capable of mixotrophic growth on methane and H₂, utilising H₂ as electron donor for respiration and carbon assimilation [Carere *et al.*, 2016]. Among the actinobacterial methylotrophic taxa such as *Mycobacterium*, *Brevibacterium* or *Arthrobacter*, no obligately methylotrophic taxa are reported [Kolb, 2009a]. It is in general worthy to mention here, that not all taxa in these mentioned families are mandatory methylotrophic. Nevertheless, from a phylogenetic perspective facultatively methylotrophic organisms are quite diverse. Further, due to emerging genomic and metagenomic studies, methylotrophic capabilities were predicted in species that were initially not known to be methylotrophic such as *Granulibacter bethesdensis*, *Bradyrhizobium japonicum* or *Variovorax paradoxus* [Kaneko *et al.*, 2002; Anesti *et al.*, 2005; Greenberg *et al.*, 2006; Chistoserdova *et al.*, 2009]. Additionally, methylotrophic capabilities might also be often overlooked, since C1 compounds

are often not tested during species characterisation (if the species was not isolated on C1 compounds), wherefore several heterotrophic organisms might be undiscovered methylotrophs. Thus, in the last years the field of methylotrophy expanded regarding novel methylotrophic representatives and methylotrophic pathways (see 1.3).

Among the facultative methylotrophs a further distinction can be made between 'restricted' and 'non-restricted' facultatively methylotrophic organisms in terms of their substrate ranges. 'Non-restricted' facultatively methylotrophic organisms can utilise carbonic acids, sugars, and even aromatic compounds, whereas 'restricted' facultative methylotrophs are only able to grow on a small range of substrates such as carbonic acids (such as acetate, malate, pyruvate or succinate), alcohols (such as ethanol, propanol, glycerol) or some short chain alkanes (such as ethane, propane). The utilisation of these substrates might be possible due to already existing enzymes and metabolic pathways. Comparative studies revealed that the ability of being facultatively methano- or methylotrophic depends more probably on the substrate transport into the cytoplasm than on the presence of metabolic pathways [Eccleston & Kelly, 1973; Shishkina & Trotsenko, 1982; Chain *et al.*, 2003; Ward *et al.*, 2004; Tamas *et al.*, 2014]. This assumption is further emphasised by the fact that the obligately methanotrophic *Methylococcus capsulatus* possesses indeed sugar metabolism genes (e.g. alpha-ketoglutarate dehydrogenase), although it cannot grow on multi-carbon compounds [Ward *et al.*, 2004; Kelly *et al.*, 2005; Tamas *et al.*, 2014].

The growth on C1- and multi-carbon substrates is assumed to require different central metabolic pathways [Skovran *et al.*, 2010]. Thus, the central metabolism of a facultatively methylotrophic organism is an elegant interaction of common heterotrophic and C1-specific pathways (Figure 7) [Skovran *et al.*, 2010; Peyraud *et al.*, 2011; Peyraud *et al.*, 2012].

However, the general metabolic behaviour or the carbon flux in facultative methylotrophs under *in situ* conditions have been not revealed, since multi-carbon utilisation studies are often conducted as a comparison between methylotrophic (only C₁-compounds supplemented) and multi-carbotrophic (only multi-carbon compounds supplemented) conditions. Moreover, such studies are mainly limited, since they are conducted under laboratory conditions and often concentrating on pure cultures of well studied model organisms such as facultatively methylotrophic *Methylobacterium extorquens* strains, which are in the laboratory focus for more than 50 years [Ochsner *et al.*, 2015]. A critical parameter for growth is also the amount of energy that is available for assimilatory processes [Peyraud *et al.*, 2011]. Growth studies with the well established facultatively methylotrophic model organism *M. extorquens* AM1 revealed that under strictly methylotrophic conditions more than 80 % of the methanol is directly used for energy conservation [Peyraud *et al.*, 2011]. Nevertheless, the endogenously formed CO₂ is subsequently used for assimilation processes [Large *et al.*, 1961; Crowther *et al.*, 2008; Peyraud *et al.*, 2011]. Under multi-carbotrophic substrate conditions a permanent high methanol oxidation capacity is still maintained, enabling a quick response to methanol [Bosch *et al.*, 2008; Skovran *et al.*, 2010; Peyraud *et*

al., 2011]. Thus, altering substrate availabilities (e.g. primarily multi-carbon followed by C1-substrates) led to an effective and flexible switch of metabolic pathways within minutes. In this ‘switching phase’ methanol will be immediately used to gain energy and allows the organism being highly competitive [Skovran *et al.*, 2011]. Under mixed substrate conditions methanol is still used as main energy source, and the multi-carbon substrate (e.g. succinate) is the main carbon source [Peyraud *et al.*, 2012]. This partitioning is facilitated by the repression of C1-derived carbon entering the serine cycle, but a small amount of methanol can be still converted into biomass (i.e., in purine syntheses pathways) [Peyraud *et al.*, 2012]. However, this knowledge is mainly based on the model organism *Methylobacterium extorquens* AM1. Carbon flux or other metabolic studies are not available for facultatively methylotrophic organisms possessing not the serine cycle for carbon assimilation or lacking the EMCP in which the interaction of the different metabolic pathways might be different.

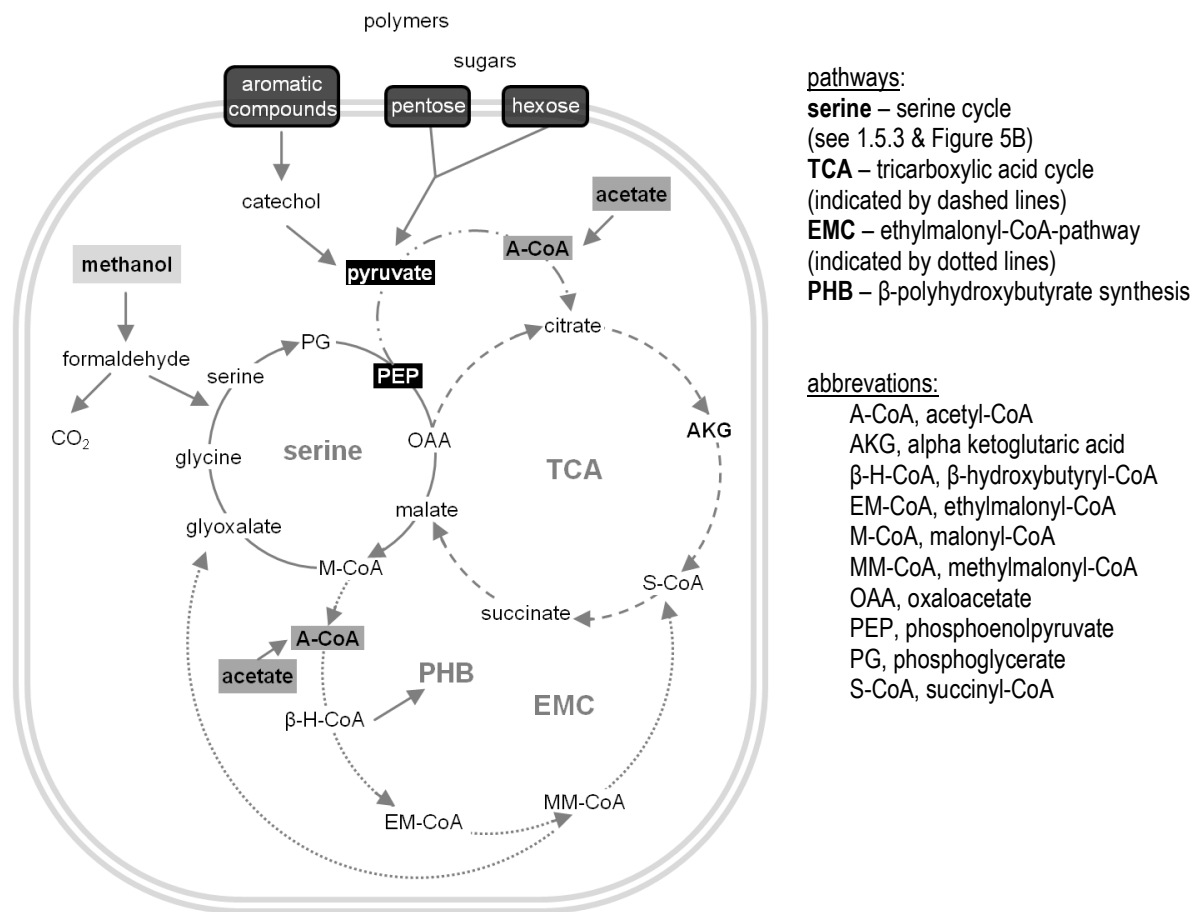


Figure 7 Interactions of metabolic pathways and entry points of multi-carbon compounds in facultatively methylotrophic bacteria.

Schematic overview of metabolic pathways and their interconnections in a facultatively methylotrophic metabolism exemplified on serine-cycle possessing methylotrophs (*Methylobacterium extorquens* AM1, *Methylocystis* strain SB2). Acetate can enter the cell's metabolism as acetyl-CoA, sugars and aromatic compounds must be metabolised to central intermediates such as pyruvate. Substrate uptake via transporter proteins is indicated by black boxes. The figure is based on Anthony, 1982; Anthony, 2011; Peyraud *et al.*, 2012; Vorobev *et al.*, 2014; and the KEGG PATHWAY database (<http://www.genome.jp/kegg/pathway.html>).

Also the substrate preference by facultative methylotrophs towards C1- and multi-carbon compounds might be different, possibly revealing a preference for one substrate over the other. Within some 'restricted' facultative methanotrophs able to utilise methane and acetate, methane is preferred by *Methylocapsa* and *Methylocystis*, whereas *Methylocella* prefers acetate as substrate [Dunfield et al., 2010; Belova et al., 2011; Im et al., 2011; Semrau et al., 2011; Dunfield & Dedysh, 2014]. However, there are rarely been studies available targeting a putative preferred substrate utilisation if both substrates are available at the same time, still questioning the *in situ* behaviour of facultative methylotrophs.

Evolutionary reasons for the metabolic phenomenon of obligate methylotrophy (especially methanotrophy) are also not well understood, but were tried to be unravel in the metabolic versatile family of *Beijerinckiaceae* [Tamas et al., 2014]. This family comprises specialists and generalists: obligate methanotrophs, 'restricted' facultative methanotrophs, 'non-restricted' facultative methylotrophs, and non-methylotrophic chemoorganotrophs [Dedysh et al., 2005a, 2005b; Dunfield et al., 2010; Marín & Arahal, 2013; Tamas et al., 2014; Dedysh et al., 2015] (Figure 8).

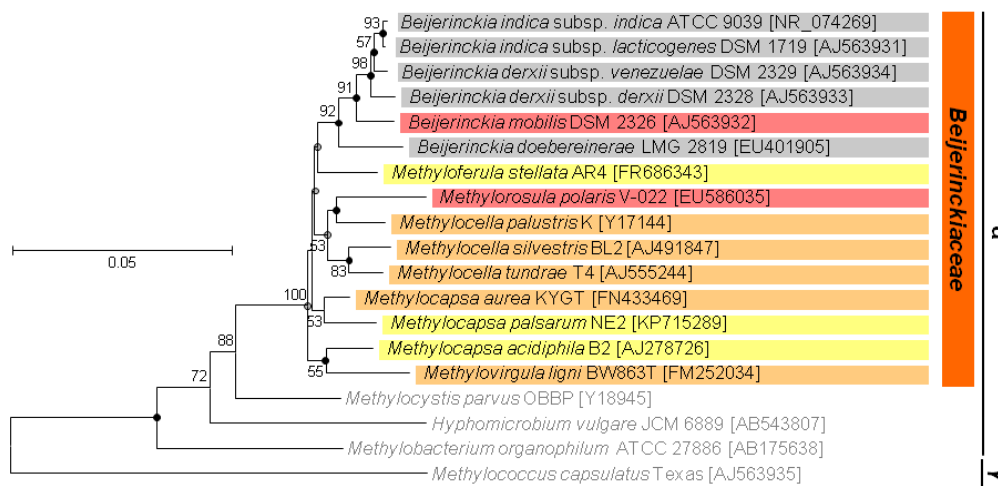


Figure 8 Metabolic diversity covered by members of the *Beijerinckiaceae*.

Phylogenetic reconstruction of *Beijerinckiaceae*-affiliated species based on 16S rRNA gene sequences (fragment length ≥ 1380 bp) and their metabolic diversity covering obligately methylotrophic (methanotrophic, ■), 'restricted' facultatively methylotrophic (methanotrophic, ■), 'non-restricted' facultatively methylotrophic (non-methanotrophic, ■), and non-methylotrophic (chemoorganotrophic, ■) species. The shown neighbour joining tree is based on 19 nucleotide sequences in total including further alphaproteobacterial methylotrophic representatives and the gammaproteobacterial *Methylococcus capsulatus* serving as outgroup. Bootstrap values were calculated from 1000 replicates and are shown for values ≥ 50 . Dots at the nodes indicate congruent nodes with trees based on the maximum likelihood and maximum parsimony method (●, true for both phylogenetic trees; ●, only true for one phylogenetic tree). Accession numbers are given in squared brackets. The bar indicates 0.05 change per nucleotide.

Despite of their metabolic diversity these species are evolutionarily close (≤ 3.8 % dissimilarity based on whole 16S rRNA gene analyses) and the most parsimonious scenario suggests that a methylotrophic ancestor (together with other methylotrophs like *Methylobacteriaceae*) acquired methanotrophic capabilities [Tamas et al., 2014]. This ancient methanotroph might also acquired organotrophic capabilities over time by gene transfer

events and finally even discarded methylotrophic metabolism [Tamas *et al.*, 2014]. Thus, both, the utilisation of C1 compounds as well as the utilisation of alternative multi-carbon substrates, might have been and still is an ecological niche-defining parameter in general, allowing the organisms to establish in a complex microbial community.

1.6.5. Chloromethane-utilising methylotrophs and the *cmu*-pathway

First reports of the utilisation of CH₃Cl were based on observations of the co-metabolic oxidation by the MMO of methanotrophs that were, however, unable to grow on methyl halides [Stirling & Dalton, 1979]. The first isolate growing on CH₃Cl as sole source of carbon and energy was *Hyphomicrobium* sp. MC1 isolated from an industrial sewage plant [Hartmans *et al.*, 1986]. Regrettably, this strain was lost, but within the last years several other isolates growing on CH₃Cl were obtained including anaerobically growing ones such as *Acetobacterium dehalogenans* MC [Traunecker *et al.*, 1991] and aerobically growing ones affiliated to *Alphaproteobacteria* (*Hyphomicrobium*, *Aminobacter*, *Leisingeria*, *Methylobacterium*, and the *Roseobacter* group) [Miller *et al.*, 2004; Borodina *et al.*, 2005; Schäfer *et al.*, 2005; Nadalig *et al.*, 2011] and *Actinobacteria* (i.e., *Nocardioides* sp. strain SAC-4) [McAnulla *et al.*, 2001a]. Aerobic CH₃Cl utilisers were detected in several environments including polluted and pristine soils and marine habitats indicating a ubiquity of CH₃Cl-utilisers in nature [McAnulla *et al.*, 2001a; Schäfer *et al.*, 2007].

Insights into the CH₃Cl utilisation were obtained by studying the model organism *Methylobacterium extorquens* CM4 (formerly *M. chloromethanicum* CM4 [Doronina *et al.*, 1996]) and revealed that CH₃Cl utilisation is distinct from methanol utilisation [Vannelli *et al.*, 1998; 1999; Studer *et al.*, 1999; 2001; 2002]. The initial utilisation of CH₃Cl is catalysed by two interdependent methyltransferases, CmuA and CmuB (*cmu*: chloromethane-utilisation) [Vannelli *et al.*, 1999]. The methyltransferase I 'CmuA' (i.e., chloromethane:halide methyltransferase) transfers the methyl group of CH₃Cl onto a corrinoid (cobalamin, Co(I)) and the methyltransferase II 'CmuB' (i.e., methylcobalamin:H₄folate methyltransferase) transfers the methyl group further onto H₄F resulting in CH₃-H₄F and subsequently CH₂=H₄F (Figure 9) [Studer *et al.*, 1999; 2001]. CmuA (marker gene *cmuA*) is a bifunctional (i.e., N-terminal methyltransferase domain and C-terminal corrinoid-binding domain) monomeric enzyme containing cobalt, zinc, and vitamin B₁₂ bound as cofactor, whereas CmuB (marker gene *cmuB*) is a homodimeric enzyme and is rate-limiting during CH₃Cl utilisation, since it depends on the intermediate methylcobalamin [Studer *et al.*, 1999; 2001].

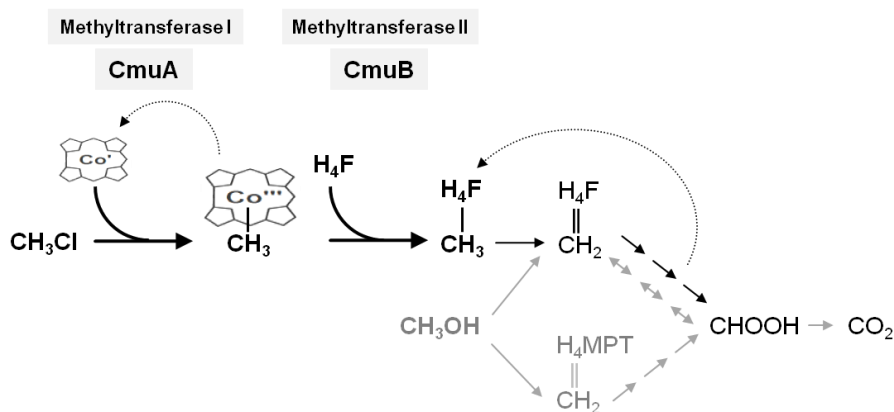


Figure 9 Three C1 compound oxidising pterin-dependent pathways in *Methylobacterium extorquens* CM4.

The CH_3Cl -specific *cmu* pathway (black arrows) focussing on both methyl group transferring steps (methyltransfer onto corrinoid (cobalamin, Co(I)) and methyltransfer onto tetrahydrofolate (H_4F); thick arrows) facilitated by the methyltransferases CmuA and CmuB and both possible pathways for methanol utilisation (pterin dependent pathways with pterin-cofactors tetrahydrofolate (H_4F) or tetrahydromethanopterin (H_4MPT) [Trotsenko & Murrell, 2008]; grey arrows). Each arrow indicates an independent enzymatic reaction and multi-step enzymatic pathways are indicated by sequential arrows. The scheme was simplified after Studer *et al.*, 2001; 2002.

Interestingly, such reactions based on a cobalamin-dependent methyltransferase had been described for strict anaerobic organisms [Ludwig & Matthews, 1997; Wohlfahrt & Diekert, 1997]. Additionally, CmuA and CmuB exhibit sequence similarities to methyltransferases of methanogens assuming a common origin of some methylotrophic genes of methylotrophs and methanogens [Vannelli *et al.*, 1999]. Interestingly, comparative genomic analyses of several *Bacteria* exhibited the presence of *cmu* genes in obligate anaerobes such as *Desulfotomaculum alcoholivorax* or *Thermosediminibacter oceani*. These anaerobes are not known for CH_3Cl -utilisation, and *cmu* genes show on protein level high similarities to the *cmu* homologs of *M. extorquens* CM4 [Nadalig *et al.*, 2014]. Therefore a common evolutionary origin of *cmu* genes and their distribution via HGT events is assumed.

In total, the growth of *M. extorquens* CM4 on CH_3Cl depends also on 4 genes: *cmuA*, *cmuB*, *cmuC*, and *purU* [McAnulla *et al.*, 2001b]. The gene *purU* encodes for a putative formyl- H_4F hydrolase catalysing the formation of formate [McAnulla *et al.*, 2001b], wherefore in CH_3Cl -utilisers another H_4F -dependent C1-metabolism pathway is further present than in methanol-utilisers [Studer *et al.*, 2002]. The *in vivo* function of CmuC remains unresolved yet, but it is assumed that *cmuC* encodes for a further methyltransferase that might be facilitated a H_4MPT -dependent *cmu*-pathway expanding the capabilities for CH_3Cl -utilising organisms [McAnulla *et al.*, 2001b; Studer, 2001]. Moreover, the *cmu*-pathway genes are plasmid-born in *M. extorquens* CM4 facilitating the chance for HGT of CH_3Cl utilisation capabilities [Chaignaud, 2016]. Apart from the uncovered *cmu*-pathway some CH_3Cl -utilising bacteria such as the marine strains *Leisingera methylohalidovorans* MB2 and *Roseovarius* sp. 217 lack *cmuA* genes, but can grow on CH_3Cl indicating another *cmu*-pathway not yet resolved [Schäfer *et al.*, 2007].

Another pathway, that is not resolved in detail yet, is the anaerobic degradation of CH₃Cl by the strictly anaerobic methylotrophic homoacetogenic *Acetobacterium dehalogenans* MC, mediating the formation of acetate from CO₂ or reduced C1 compounds [Traunecker *et al.*, 1991]. The utilisation of CH₃Cl is facilitated by a methyl chloride dehalogenase, initially transferring the methyl group to the central metabolic intermediate H₄F. The resulting CH₃-H₄F is further oxidized to CO₂, gaining reducing equivalents, or is used for acetate formation by the subsequently carbonylation reaction, where acetate is formed from the methyl group, coenzyme A and CO [Meßmer *et al.*, 1993; 1996]. However, whether a corrinoid protein is involved in the carbonyl reaction is not resolved yet, as well as more details on the dehalogenase (i.e., marker gene or enzyme structure) are lacking [Meßmer *et al.*, 1996]. Another still completely unknown *cmu* pathway exists in *Pseudomonas aeruginosa* NB1 that can utilise CH₃Cl under aerobic and nitrate-reducing conditions [Freedman *et al.*, 2004].

Taken together, the knowledge on CH₃Cl utilisation has grown over the last 30 years. In terrestrial environments the phyllosphere was recognized as a suitable habitat for CH₃Cl-utilisers [Nadalig *et al.*, 2011; Bringel & Couée, 2015]. Considering the existence of soil-derived *cmu*-sequences and plants / plant material as a great source of CH₃Cl (see 1.1.3 & Figure 2), also soils should be more studied in terms of CH₃Cl-utilising methylotrophs uncovering the putative importance and metabolism of soil-dwelled CH₃Cl-utilisers.

1.7. Fungal methylotrophs and the MUT

Methylotrophic fungi are known since their first isolation in 1969 [Ogata *et al.*, 1969], and several representatives are well established in biotechnological applications (e.g. single cell protein production, recombinant protein production [Wegner, 1990; Gellissen & Hollenberg, 1997; Gellissen, 2000]). They are abundant in nature and are often associated with pectin-rich (methoxy group-rich) plant compounds such as fruits, litter and wood [Craveri *et al.*, 1976; Negruță *et al.*, 2010]. It seems that methylotrophic yeast can only use methanol-derived compounds as energy and carbon source whereas methylamine might be a nitrogen source [Yurimoto *et al.*, 2011]. Methane utilisation by some yeast strains was reported in the 1980s, but no further reports on methanotrophic fungi or putative pathways and enzymes are available [Wolf & Hanson, 1980; Anthony, 1982; Hanson & Hanson, 1996].

Most prominent are methylotrophic yeasts belonging to several genera such as *Candida*, *Hansenula*, *Torulopsis*, *Trichosporon*, *Pichia*, *Polyporus*, *Poria*, and *Radulum*, as well as the recently from *Pichia* separated genera *Ogataea*, *Kuraishia*, and *Komagataella* [Hartner & Glieder, 2006; Kaszycki *et al.*, 2006; Kondo *et al.*, 2008; Limtong *et al.*, 2008; Negruță *et al.*, 2010; Yurimoto *et al.*, 2011]. Within mould fungi methylotrophic representatives are more limited, and although some representatives possess genetic hints, methylotrophy is physiologically not proven [Kondo *et al.*, 2008; Gvozdev *et al.*, 2012; Kolb & Stacheter, 2013]. However, the classification and assignment of methylotrophic fungi is complicated.

For example the yeast *Pichia angusta* has several synonyms such as *Hansenula angusta*, *Hansenula polymorpha*, and *Ogataea polymorpha* [Negruță *et al.*, 2010].

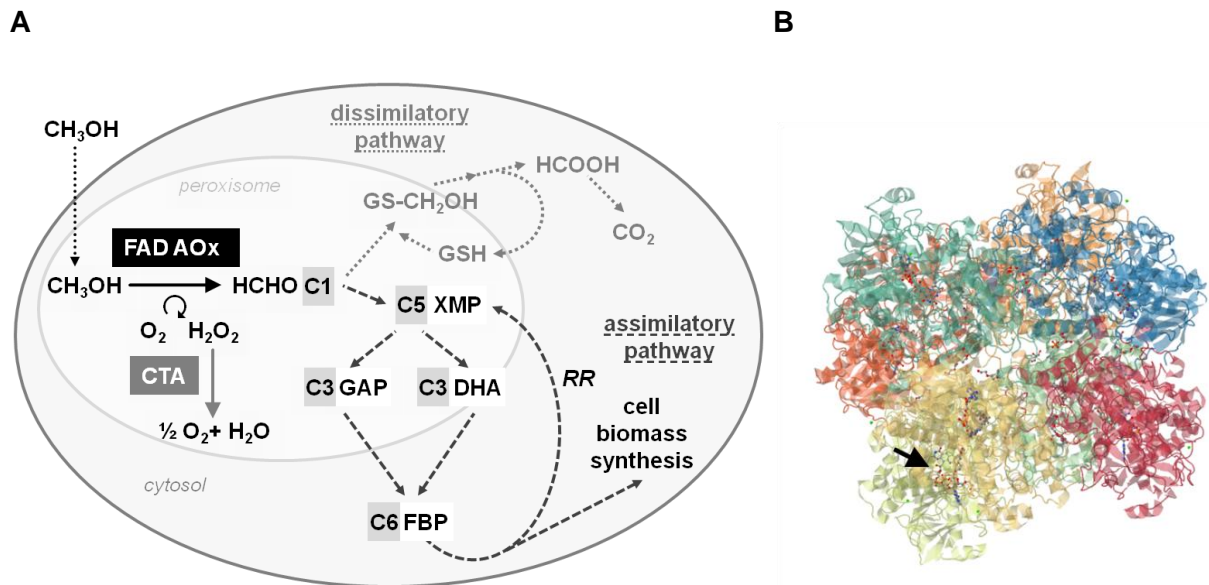


Figure 10 Methanol metabolism in methylotrophic yeasts (A) and the crystal structure of a FAD AOx (B).

Panel A shows details of the MUT in yeast cells focussing on the peroxisomal oxidation of methanol (black lines) and the cytosolic assimilatory (dark grey dashed lines) and dissimilatory pathways (light grey dotted lines). For more details refer to the text. The amount of carbon atoms per molecule in the assimilatory pathway are indicated in grey boxes. Abbreviations: FAD AOx, FAD dependent alcohol oxidase; CTA, catalase; RR, rearrangement reactions. Molecule abbreviations: DHA, dihydroxyacetone; FBP, fructose 1,6-bisphosphate; GAP, glyceraldehyde 3-phosphate; GSH, reduced form of glutathione; GS-CH₂OH, S-hydroxymethyl glutathione; XMP, xylulose 5-phosphate. The figure is based on Yurimoto *et al.*, 2011.

Panel B shows the homo-octameric crystal structure of the FAD AOx of the methylotrophic yeast *Pichia pastoris*. Each subunit is indicated with different colours and the arrow point at one non-covalently bound FAD as prosthetic group (in total 10 FAD molecules are present). Image: <http://www.rcsb.org> (PDB ID: 5HSA).

All methylotrophic yeasts employ a common methanol utilisation pathway (MUT, Figure 10A) that was mainly characterized in *Hansenula polymorpha* (*Pichia angusta*) and *Candida boidinii* [Veenhuis *et al.*, 1983; Tani, 1984; Large & Bamforth, 1988; Yurimoto *et al.*, 2011]. This MUT is transcriptionally repressed by glucose and ethanol, but can be highly induced by methanol resulting in large amounts of necessary enzymes and peroxisomes [Hartner & Glieder, 2006; Nakawaga *et al.*, 2006; Yurimoto *et al.*, 2011; Koch *et al.*, 2016]. The MUT pathway is in many ways different from the pathways described for methylotrophic bacteria (see 1.4, 1.5) with the main differences being (i) the nature of the key enzyme and (ii) the compartmentation of the pathway in peroxisomes [Anthony, 1982]. Initially in peroxisomes methanol is oxidised to formaldehyde resulting in the formation of hydrogen peroxide (H₂O₂) that is subsequently removed by catalase activity [Anthony, 1982; Hartner & Glieder, 2006; Yurimoto *et al.*, 2011]. As for methylotrophic *Bacteria* formaldehyde is the branching point for dissimilation and assimilation. The cytosolic assimilatory pathway – dihydroxyacetone cycle

(DHA) or xylulose monophosphate pathway – is somehow similar to the RuMP cycle of methylotrophic *Bacteria* (see 1.5.1). The C1-unit (formaldehyde) is transferred to a C5-acceptor (xylulose monophosphate) resulting in the C3-units dihydroxyacetone (DHA) and glyceraldehyde phosphate (GAP) used for the biosynthesis of cell material and the rearrangement of the C5-acceptor [Anthony, 1982; Hartner & Glieder, 2006; Yurimoto *et al.*, 2011]. The cytosolic dissimilatory pathway plays a crucial role in detoxification [Sakai *et al.*, 1997; Lee *et al.*, 2002; Hartner & Glieder, 2006], and formaldehyde reacts non-enzymatically with reduced glutathione (GSH) generating S-hydroxymethyl glutathione (S-HMG) that is further oxidised to CO₂ by a omnipresent GSH-dependent pathway [Harms *et al.*, 1996; Hartner & Glieder, 2006; Yurimoto *et al.*, 2011].

One key enzyme for methylotrophic fungi facilitating the initial oxidation step of methanol is a flavin adenine nucleotide dependent alcohol oxidase (FAD AOx) [Hartner & Glieder, 2006; Gvozdev *et al.*, 2012; Koch *et al.*, 2016], which was primarily described in a *Basidiomycetes* [Janssen *et al.*, 1965; Gvozdev *et al.*, 2012]. The FAD AOx is a homo-octameric enzyme possessing one non-covalently bound FAD as prosthetic group per monomer and is formed of two facing tetramers (Figure 10B) [Koch *et al.*, 2016]. The FAD AOx is not restricted to methanol only, but can also oxidise other short aliphatic alcohols such as ethanol and 1-propanol [Koch *et al.*, 2016]. Enzymatic and molecular studies have revealed two subunits of the FAD AOx differing in their amino acid residues, encoding genes (i.e., α -subunit is encoded by MOD1 (synonyms: AOX1, AUG1) and β -subunit is encoded by MOD2 (synonyms: AOX2, AUG2)) and synthesis conditions (e.g. α -subunit at low methanol concentrations; β -subunit at high (>3%) methanol concentrations) [Hartner & Glieder, 2006; Gvozdev *et al.*, 2012]. Thus, both subunits are active under different conditions enabling an elegant fine-tuning of the methylotrophic fungi in response to environmental conditions and resulting in up to nine different FAD AOx isoenzymes consisting of a combination of both subunits [Ito *et al.*, 2007; Gvozdev *et al.*, 2012]. Such FAD AOx isoenzymes are widespread among the methylotrophic yeasts, but some representatives such as the well established model yeast strain *Candida boidinii* and *Hansenula polymorpha* possess only one gene (i.e., MOD1) encoding for the FAD AOx [Hartner & Glieder, 2006; Ito *et al.*, 2007; Negruță *et al.*, 2010].

However, although methylotrophic yeast, the MUT pathway and its regulation are well understood, the role and diversity of methylotrophic fungi in the environment and especially inside microbial communities in terrestrial habitats is hardly resolved. Based on the knowledge of the methylotrophic capabilities and the metabolic versatility of fungi they might be underestimated and represent another large microbial sink of methanol besides methanol-utilising bacterial methylotrophs in forest soils.

1.8. Ecological niche-defining factors of methylotrophs

Several biotic and abiotic factors define the ecological niche of organisms allowing them to permanently establish in a complex community [Hutchinson, 1957; Kolb, 2009a]. Such factors can be biotic or abiotic, such as the substrate range that comprises for example narrow and wide substrate ranges (i.e., obligately methylotrophic vs. facultatively methylotrophic, see 1.6.4), the utilisation of specific substrates such as specific C1 compounds (e.g. methanotrophs or CH₃Cl-utilising methylotrophs), as well as the concentration of available substrates (e.g. 'low-affinity' and 'high-affinity' methanotrophs, see 1.6.1 & 1.6.2). Further abiotic factors include the availability of oxygen or alternative electron acceptors, the availability of nitrogen or the ability to fix nitrogen, the soil temperature, the concentration of salts and the osmotic stress tolerance of an organism as well as the tolerable pH-range [Kolb, 2009a]. Microorganisms can tolerate pH values below and above their pH optima, and soils exhibit pH buffer capacities preventing dramatic pH shifts. However, soil is not homogeneous and within microhabitats the pH can differ up to one pH unit [Or *et al.*, 2007].

Along the soil-derived aerobic methylotrophs the majority is neutrophilic and is *inter alia* affiliated to alphaproteobacterial methylotrophs such as *Methylobacteriaceae* or *Hyphomicrobiaceae*, gammaproteobacterial methanotrophs, betaproteobacterial methylotrophs, and *Actinobacteria* [Kolb, 2009a]. Acidotolerant and acidophilic aerobic methylotrophs are affiliated to *Beijerinckiaceae* and *Methylocystaceae* for example and the methanotrophic *Verrucomicrobia*, in which these microorganisms are highly acidophilic [Kolb, 2009a; Marín & Arahal, 2013; van Teeseling *et al.*, 2014; Knief, 2015]. The minority of aerobic methylotrophs is alkaliphilic such as some *Methylomicrobium* species, *Methyloarcula terricola*, or *Paracoccus alcaliphilus* [Kolb, 2009a; Knief, 2015].

In addition, the occurrence of some methylotrophic guilds such as the 'high-affinity' methanotrophs of the USC α and USC γ group and the community structure of methanol-utilisers in soils is also pH-correlated [Kolb *et al.*, 2005; Kolb, 2009a; Stacheter *et al.*, 2013]. Thus, the endogenous pH and shifts in the pH can dramatically affect microbial communities and the associated methylotrophs.

1.9. Hypothesis and objectives of the current study

Methylotrophs are widespread in nature being important regulators of the emission of VOCs like methane, methanol and chloromethane (see 1.2, 1.6) [Hanson & Hanson, 1996; Kolb, 2009a; Schäfer *et al.*, 2007; Chistoserdova & Lidstrom, 2013; Chistoserdova 2015]. These compounds are produced in natural environments, and the contribution of the terrestrial sources can reach high amounts (see 1.1 & Figure 2) [Keppler *et al.*, 2005; Millet *et al.*, 2008; Nazaries *et al.*, 2013]. Methane is in nature mainly produced in anoxic soil environments and

methanol and chloromethane are mainly derived from plants or degraded pectin-rich plant-derived material (i.e., litter, wood, humus) (see 1.1 & Figure 2) [Keppler *et al.*, 2005; Millet *et al.*, 2008; Nazaries *et al.*, 2013]. Therefore, forest soil environments are perfect habitats for methylotrophic organisms utilising methane, methanol and/or CH₃Cl.

The role of methylotrophic microorganisms in terrestrial ecosystems as global sinks of C1 compounds is undisputed [Kolb, 2009a; Degelmann *et al.*, 2010; Stacheter *et al.*, 2013; Wohlfahrt *et al.*, 2015], but their environmental controls, their distribution in the phyllo- and rhizosphere, and their diversity in different climate zones are largely unresolved [Kolb, 2009a; Stacheter *et al.*, 2013; Kolb & Stacheter, 2013; Wohlfahrt *et al.*, 2015]. The taxonomic diversity of methylotrophs in temperate forest soils is affected by soil pH and the vegetation, but a detailed understanding of driving factors in these ecosystems is lacking [Kolb, 2009a; Degelmann *et al.*, 2010; Stacheter *et al.*, 2013]. Several studies were carried out to gain a better understanding of methylotrophic taxa in soil environments [Radajewski *et al.*, 2000; Radajewski *et al.*, 2002; Stacheter *et al.*, 2013], but the actual knowledge is mainly based on pure cultures and artificial laboratory experiments [Radajewski *et al.*, 2002; Kolb, 2009a] or concentrates on methanotrophs [Dunfield *et al.*, 1999; Knief *et al.*, 2003; Degelmann *et al.*, 2010; Liebner *et al.*, 2011; Gupta *et al.*, 2012; Knief, 2015]. Further, it is likely that the limited molecular view by marker gene-based studies leads to an underestimation of methylotrophic taxa due to the poor availability of suitable molecular tools as well as the recognized 'modularity of methylotrophy', which revealed a methylotrophic versatility and the modularity of methylotrophic pathways (see 1.3, 1.6).

Since the majority of soil-derived methylotrophic isolates are facultatively methylotrophic, they can utilise also other multi-carbon substrates common in soil environments [Kolb, 2009a]. Thus, methylotrophs occupy different ecological niches *in situ* probably defined by their substrate range, which enables them to permanently establish in a complex soil community along with other methanol-utilisers and non-methylotrophic heterotrophs [Hutchinson, 1957].

Based on this knowledge and the still open questions the following central hypothesis was proposed for this doctoral thesis:

The substrate spectrum of methylotrophs including one-carbon compounds and multi-carbon compounds as well as the soil pH are important ecological niche-defining parameters in a forest soil.

Since three different C1 compounds were the focus of this doctoral thesis – methane, methanol and chloromethane – the following text is subdivided based on the addressed C1 compounds.

Methane – In order to address methanotrophic organisms the following sub-hypothesis was proposed based on the current knowledge on ‘high-affinity’ methanotrophs facilitating the oxidation of low methane concentrations in the investigated *Steigerwald* soil:

Alternative substrates support ‘high-affinity’ methanotrophs in soil.

Thus, the following objectives were formulated:

- (i) Evaluation of the response of ‘high-affinity’ methanotrophs on putative alternative substrates besides CH₄.
- (ii) Identification of alternative substrates of ‘high-affinity’ methanotrophs in an acidic forest soil.
- (iii) Enrichment of ‘high-affinity’ methanotrophs.

Methanol – In order to address methanol-utilising organisms the following sub-hypothesis was proposed based on the current knowledge on facultatively methanol-utilisers and the assumed underestimation of methylotrophic diversity in forest soils:

The multi-carbon substrate spectrum of methylotrophs and the soil pH are important ecological niche-defining parameters in soil.

Thus, the following objectives were formulated:

- (i) Identification of bacterial and fungal key methanol-utilising taxa in an acidic forest soil.
- (ii) Determination of facultatively methylotrophic organisms assimilating also alternative multi-carbon substrate besides methanol.
- (iii) Identification of hitherto unknown facultatively methylotrophic organisms.
- (iv) Assessment of the influence of a shifted pH on the indigenous soil methylotrophs.

Chloromethane – In order to address CH₃Cl-utilising organisms the following sub-hypothesis was proposed based on the current knowledge on soil-derived CH₃Cl-utilising taxa:

The co-utilisation of chloromethane by methanol-utilisers is an ecological niche-defining parameter in soil.

Thus, the following objectives were formulated:

- (i) Identification of bacterial methanol- or CH₃Cl-utilising taxa in an acidic forest soil.
- (ii) Determination of methylotrophs co-utilising methanol and CH₃Cl in an acidic forest soil.
- (iii) Assessment of partitioned C1 compound utilisation.
- (iv) Identification of hitherto unknown methanol-utilisers and CH₃Cl-utilisers in an acidic forest soil.

2. MATERIALS AND METHODS

2.1. Sampling sites and sampling

2.1.1. The main sampling site *Steinkreuz* in the area *Steigerwald*

The approx. 1000 km² comprising area of the *Steigerwald* is one of the largest deciduous forest sides in Germany [Müller *et al.*, 2008]. The area is located in the North of *Bavaria* between *Nürnberg*, *Bamberg* and *Würzburg*. Dominant deciduous tree types are beeches (*Fagus L.*) and oaks (*Quercus L.*) [Ellerbrock *et al.*, 2005]. The sampling site was at the exploration area *Steinkreuz*, which is located near *Ebrach* (Figure 11). The area *Steinkreuz* is located 400 – 460 m above sea level and was a research topic of several ecological system studies.

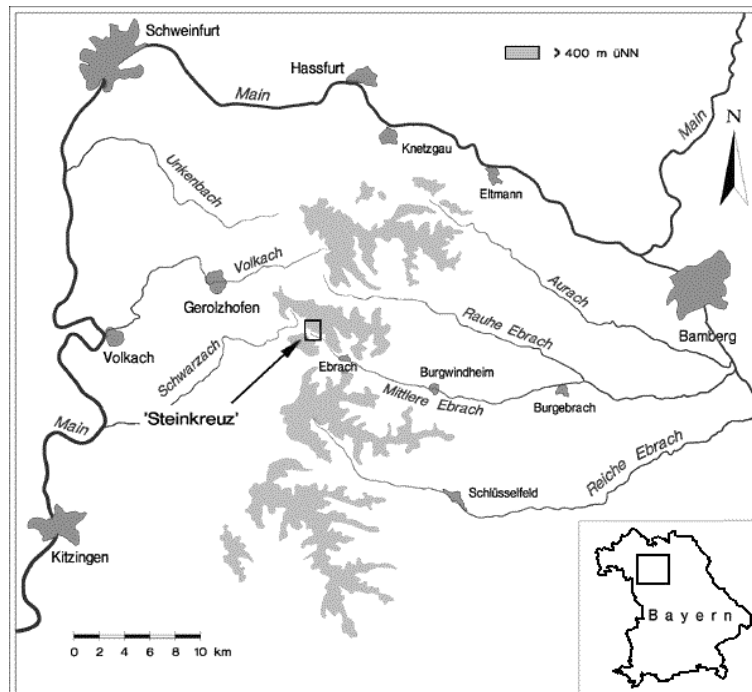


Figure 11 Localisation of the exploration area *Steinkreuz* in the *Steigerwald* forest.

Image was taken from <http://www.bayceer.uni-bayreuth.de/bitoe/de/forschung/5429/standorte/steinkreuz.php>.

The soil is classified as a cambisol and presents a sandy or sandy-loamy texture with partially clay. The upper part of this soil (i.e., first 5 cm corresponding to the A horizon) was used in all experiments (Figure 12). The A horizon is enriched with humus (Ah). The rock strata at the *Steinkreuz* belong to the sediments of the middle Keuper alternating with sandy and clayey layers. The soil pH of the A horizon is acidic (i.e., 4.75 - 5.00). (data reference: <http://www.bayceer.uni-bayreuth.de/bitoe/de/forschung/5429/standorte/steinkreuz.php>)

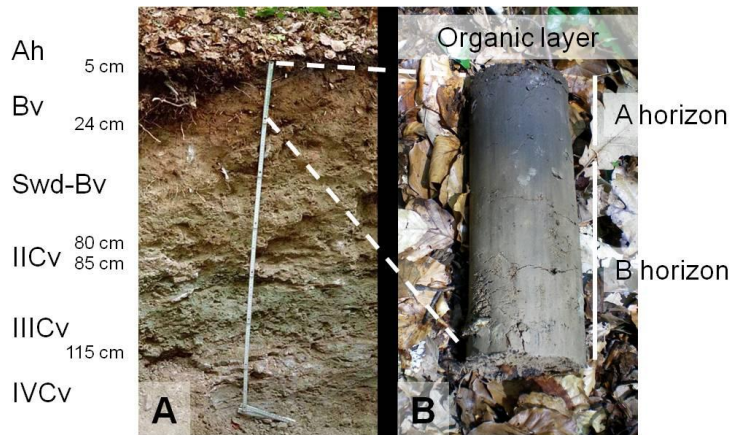


Figure 12 Soil profile from cambisol at the sampling area *Steinkreuz*.

The image of the soil profile (A) was taken from http://www.bayceer.uni-bayreuth.de/bitoeck/de/forschung/5429/standorte/Steinkreuz_Bodenprofil.jpg and the image of the soil core of the upper soil layer (B) was taken during the first sampling survey in May 2012.

The vegetation at *Steinkreuz* is dominated by beeches (mainly European beech *Fagus sylvatica*, at different ages) and young oaks (*Quercus petraea*) (Figure 13). The top soil is completely covered by litter (mainly beech leaves) and partially dead wood in different rotting stages (small branches and trunks). Since the area is ring-fenced, an undisturbed soil environment is assumed, i.e., no impact of hoofed game (such as deer and boar) or humans.

Additionally, the sampling area was a previous research object of studies on methanotrophic microorganism in forest soils [Degelmann *et al.*, 2009; 2010; Degelmann, 2010].

Further information and a comparison to the other sampling sites of this thesis are listed in Table 2 at the end of the section 'Sampling sites'.

All samples were taken from the upper layer of soil corresponding to the A horizon (Figure 12). For every time point of sampling (in total 6; Table 2, see 2.3.1, 2.3.2, 2.3.3, 2.3.4, 2.3.6, 2.3.7, 2.3.8, and 2.3.10) different sides (at least 5 m distance to each other) were chosen reflecting the general characteristics of the total sampling area (saplings, dead wood, clearing, shady, old beeches). The litter layer was always manually removed with a spade before soil sampling. Loose soil of each sampling point containing roots, wood and other particles was separately stored in plastic bags covered with litter on the top in order to prevent desiccation. Plastic bags were not sealed to maintain oxic conditions. Soil samples were always stored at 20°C in the dark (maximal storage of 3 days).



Figure 13 Images of the sampling site '*Steinkreuz*' in the deciduous forest area *Steigerwald*.

The sampling site at different sampling time points in early and late summer between 2012 and 2014. The snapshots reflect the characteristics of the sampling site, i.e., an unmanaged forest with beech stand, saplings, dead wood, clearing, shady, and old beeches.

2.1.2. Further terrestrial sampling sites

Apart from the main sampling site concentrating on a temperate forest soil, several different other soils were analysed in different experiments (see 2.3.5, 2.3.9). These sampling sites include other forest soils, meadow soils, field soils, and compost soil (Figure 14). All samples were taken from the uppermost layer of each soil according to the sampling of forest soil, i.e., soil was taken with a spade or shovel and loose soil was stored in plastic bags (see 2.1.1).

The soil sample of the 'compost soil' was taken from garden compost that was filled with plant waste (leaves, flowers, fruits, lawn cuttings) at the top and underlies the normal composting processes (no drum composting) (Figure 14A). Soil was taken in between the concrete units and was already decomposed, i.e., no unrotten plant material was included. The compost soil was dark brownish and also partially loamy.

The sampling sites 'canola', 'meadow 1', 'mixed forest', 'herbs', and 'beech' are located in the area of the *Landeskrone*, the local mountain of *Görlitz* (eastern Saxony). The *Landeskrone* is of volcanic origin, the bed rock is mainly basalt and granite. The area of the *Landeskrone* is mainly under natural protection and a local recreation area.

The agricultural field sampling site 'canola' is subjected to crop rotation preventing lacking of nutrient. At the time of sampling the crop was canola that already bloomed (Figure 14B). Soil samples were taken directly next to the plants including roots and were characterised as very loamy.

The sampling site 'meadow 1' was dominated by grasses herbage (species of *Poales*, not further classified) and clover (*Trifolium* sp.) (Figure 14C). The soil samples taken were intensively permeated by roots and were also characterised as very loamy.

The vegetation at the 'mixed forest' site was characterised by trees of different ages (shoots and old trees) of beech (*Fagus* sp.), birch (*Betula* sp.), lime (*Tilia* sp.) and maple (*Acer* sp.) *inter alia* (Figure 14K). The herb layer was only small; instead a litter layer was present. Soil samples were taken below the litter layer and were not intensively permeated by roots. The soil was dark brownish and not very loamy.

The sampling site 'herbs' was a small clearing with a very pronounced herb layer including common herbs such as nettles (*Urtica* sp.), deadnettles (*Lamium* sp.), bedstraw (*Galium* sp.), lesser celandine (*Ficaria* sp.), chickweed or stichwort (*Stellaria* sp.), and wild arum (*Arum* sp.) (Figure 14F). The clearing was bordered with several tree species such as maple (*Acer* sp.) and beech (*Fagus* sp.). The soil samples taken were dark brownish to black indicating high amount of humus.

The sampling site 'beech' is a more than 90 years old European beech stand (*Fagus sylvatica*) with old beeches dominating the vegetation and a pronounced litter layer of beech leaves (Figure 14J). The soil samples were taken next to beeches below the litter layer. The soil samples were not permeated by roots and the soil colour (i.e., dark brownish to black) was again indicative for a higher amount of humus.

The sampling sites 'syringa', 'meadow 2', 'birch', 'pine', and 'blueberry' are located in the area of *Bayreuth*, whereas the sampling sites of 'birch', 'pine' and 'blueberry' are all located in the same area (small forest area near *Bayreuth Wolfsbach*).

The soil samples of 'syringa' were taken from the soil directly below the plant bush parts. Although syringa is a deep-root plant the upper soil was permeated with several roots and the soil was highly condensed. No further vegetation was below the bush at the sampling site (Figure 14G).

The sampling site 'meadow 2' was located near *Bayreuth*. The soil texture is characterised as sandy clay loam [Horn *et al.*, 2003]. The vegetation of 'meadow 2' is dominated by grass herbage (species of *Poales*, not further classified) and flowering plants such as common

dandelion (*Taraxacum officinale*), hawkbits (*Leontodon* sp.), daisy (*Bellis perennis*), tufted vetch (*Vicia* sp.), and crowfoots (*Ranunculaceae*) (Figure 14D).

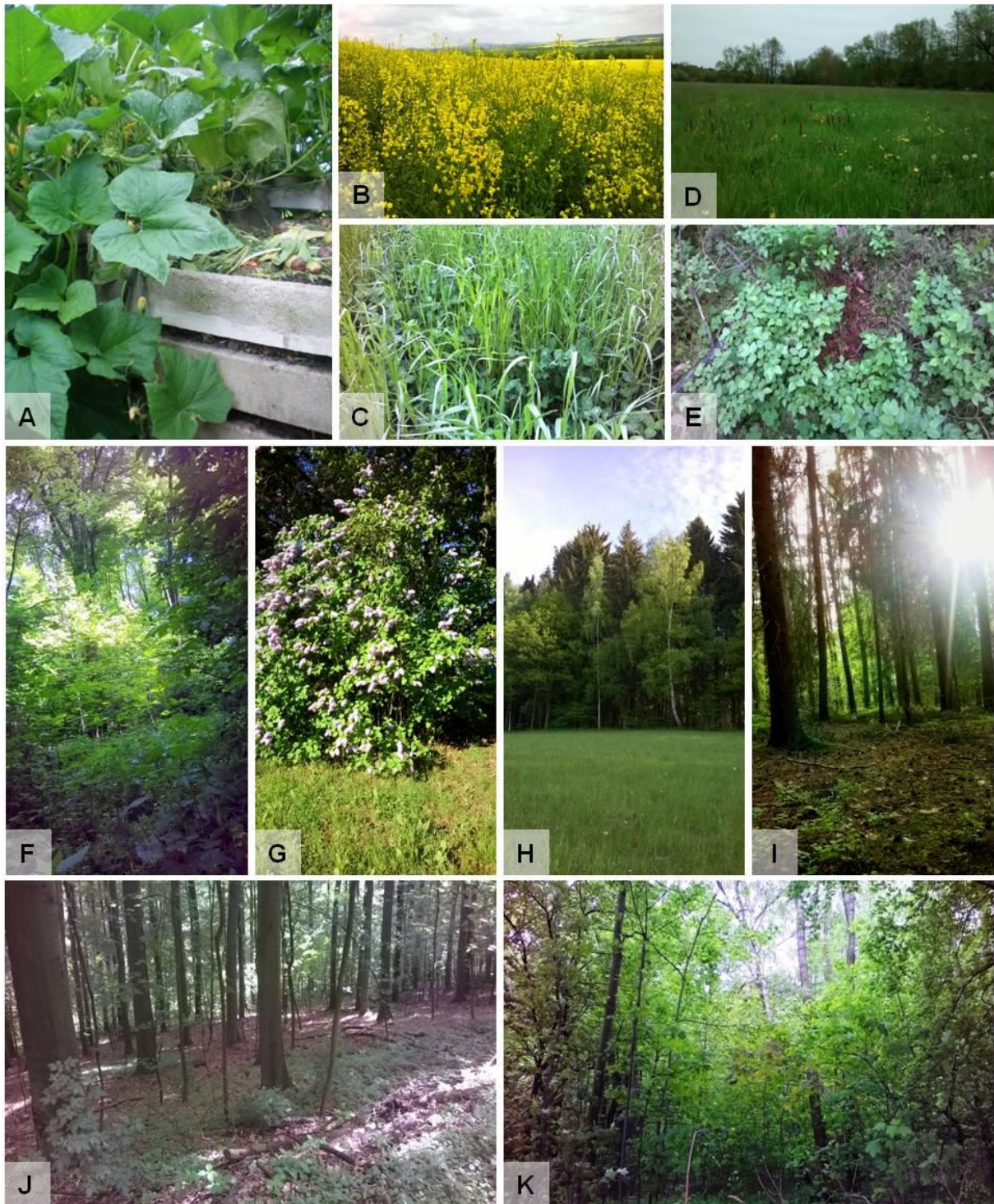


Figure 14 Further terrestrial sampling sites covering different soil environments.

Pictures of further different soil ecosystem types at the time of their sampling: compost soil (A), canola (B), meadow 1 (C), meadow 2 (D), blueberry (E), herbs (F), syringe (G), birch (H), pine (I), beech (J), and mixed forest (K). Sampling site descriptions are given in the text.

The sampling site at the 'pine' site was characterised by a pine (*Pinus* sp.) stand with a litter layer comprised of pine needles and cones. The forest floor was partially covered with moss (specis of *Bryophyta*, not further classified), cowberry and blueberry (*Vaccinium* sp.) (Figure 14I). In order to take soil samples next to a pine tree from the uppermost part of soil, the litter layer was removed until soil was apparent. However, a huge amount of pine needles was still in this soil samples. The soil was very dry and sandy.

The sampling site 'blueberry' was near the 'pine' site and was characterised by an extensive stand of blueberry plants (*Vaccinium myrtillus*) and moss (specis of *Bryophyta*, not further classified) (Figure 14E). The soil was taken below the moss layer and included pine needles. Soil samples from these two sampling sites were acidic in pH.

Soil samples taken from the sampling site 'birch' were taken directly from a birch tree (*Betula* sp.) at the edge of the forest. The vegetation around the birch was dominated by grasses (species of *Poales*, not further classified) (Figure 14H). The soil sample was very sandy and of reddish colour indicating a higher amount of iron oxides.

2.1.3. Sampling sites associated with aquatic environments

Apart from terrestrial ecosystems two different aquatic systems were additionally targeted (see 2.3.9). One was a freshwater system (*Berzdorfer See*) and the other was a marine system (*Baltic Sea*).

The samples 'lakewater' and 'lakeshore' were taken from the *Berzdorfer See* (see Figure 15). The lake is located near *Görlitz* (eastern Saxony) and is an artificial lake created out of a former brown coal (lignite) mine. The flooding process was finished in 2013 and the area of the lake is now 9.6 km². The lake is partially protected by nature conservation and a local recreation area. The lake has an excellent water quality with a neutral pH (pH value 7.6). Samples were taken at the eastern shore site. 'Lakeshore' samples were taken from a depth of approximately 30 cm. The texture of the shore was sandy to gravelly (small stones up to a length of 1 cm). 'Lakewater' was taken from the surface. The vegetation at the shore site included rushes (*Juncus* sp.), sedges (*Carex* sp.), reed (*Phragmites* sp.), and bulrush (*Typha* sp.). (Reference: <https://www.lmbv.de>, key word 'Berzdorfer See'; <http://www.berzdorfer-see.eu/> – all references are in German)

The samples 'seashore', 'seawater' and 'sea sediment' were taken from the *Baltic Sea*. The 'seashore' samples were taken from the northern shore of *Strande* that is located at the entrance of the *Kieler Förde*. Samples of 'seawater' and 'sea sediment' were taken at *Boknis Eck* that is located at the entrance of the *Eckernförde* Bucht. *Boknis Eck* is one of the oldest time series stations (since 1957) and is mainly characterised by the regular inflow of *North Sea* water instead of riverine inflow. Hypoxia and sporadically anoxia at the sea floor arise caused by seasonal stratification occurring from March to September. 'Seawater' was taken from the surface water at *Boknis Eck* and 'sea sediment' was taken from the uppermost

sediment layer from the sea floor at a depth of 28 m. The sediment sample was of dark black colour and muddy with only small particles in texture. All marine environmental samples were kindly provided by Dr. Sonja Endres. (Reference: <https://www.bokniseck.de/de>)

All aquatic samples were taken and stored in glass bottles with a large oxic phase to ensure oxic conditions. Shore samples were always covered by water. The 'sea sediment' was stored in a glass bottle closed with a cotton plug. Samples were always stored at 4°C in the dark.



Figure 15 Sampling sites covering different aquatic environments.

Pictures of freshwater and marine ecosystem types: 'lakewater' and the *Berzdorfer See* (A), 'lakeshore' of *Berzdorfer See* (B), 'seashore' at *Strande* beach (C), 'seashore' (close-up) (D), 'sea sediment' of *Boknis Eck* (close-up) (E), and 'seawater' at *Boknis Eck* (F). Sampling site descriptions are given in the text.

MATERIALS AND METHODS

Table 2 Overview on the different sampling sites.

Location	geographic location	altitude [m] ^a	temp [°C] ^b	precipitation [mm] ^c	pH	experiment (link)	Sampling date	
Forest soil	<i>Steigerwald</i>	49°52'N / 10°28'E	400 – 460	7 - 8	700 - 800	acidic	2.3.1	01.05.2012
							2.3.2	21.05.2013
							2.3.3	12.08.2013
							2.3.6	20.08.2013
							2.3.7 / 2.3.8	18.06.2014
2.3.4 / 2.3.10	29.09.2014							
Compost soil	<i>Görlitz</i>	51°09'N / 14°57'E	200	4 – 11	655	neutral	2.3.9	12.10.2014
Lakewater Lakeshore	<i>Görlitz</i> (<i>Berzdorfer See</i>)	51°5'N / 14°58'E	186	4 – 11	655	neutral neutral	2.3.9	12.10.2014
Seawater Sea sediment	<i>Boknis Eck</i> (<i>Baltic Sea</i>)	54°31'N / 10°01'E	-28 – 0	6 - 12	778	neutral neutral	2.3.9	28.09.2014 17.09.2014
Seashore	<i>Strande Beach</i> (<i>Baltic Sea</i>)	54°27'N / 10°11'E	0	6 - 12	778	neutral neutral	2.3.9	01.10.2014
herbs, mixed forest, beech, meadow 1, canola	<i>Görlitz</i> (<i>Landeskrone</i>)	51°08'N / 14°56'E	200 – 420	4 – 11	655	n.a. ^d n.a. ^d n.a. ^d n.a. ^d	2.3.5	14.05.2015
pine, blueberry, birch	<i>Bayreuth</i>	49°54'N / 11°37'E	340	3 – 12	594	n.a. ^d n.a. ^d n.a. ^d	2.3.5	11.05.2015
meadow 2	<i>Bayreuth</i> (<i>Trafowiese</i>)	49°55'N / 11°32'E	340	3 – 12	594	neutral	2.3.5	18.05.2015
syringa	<i>Bayreuth</i>	49°57'N / 11°36'E	340	3 – 12	594	neutral	2.3.5	13.05.2015

^a above sea level

^b mean annual temperature

^c mean annual precipitation

^d not analysed

2.2. Chemicals, gases, solutions, growth media and labware

All chemicals, gases and labware were obtained from Sigma Aldrich (Steinheim, Germany), Fluka (Buchs, Switzerland), Applichem (Darmstadt, Germany), Rießner (Lichtenfels, Germany), Eppendorf (Hamburg, Germany), BioRad (Hercules, USA), and Carl Roth (Karlsruhe, Germany), unless otherwise indicated. Sterile syringes and needles (BD Biosciences, Heidelberg, Germany) were used to take gas samples or for the fractionation of SIP gradients.

All solutions and media were prepared with deionised double distilled water ('ddH₂O'; Seralpur Pro CN, Seral Erich Alhauser, Ransbach-Baumbach, Germany) and set-up in sterile glass ware or tubes (VWR International, Darmstadt, Germany). Sterilisation of solutions and media was done either via autoclaving (Sanoclav, Wolf, Geislingen, Germany) or filtration (0.2 µm pore size, cellulose acetate membrane, Schleicher & Schuell MicroScience GmbH, Dassel, Germany).

2.2.1. Trace element solution

The trace element solution was prepared according to Whittenbury *et al.*, 1970a (trace element solution of the NMS medium). In short, a trace element stock solution (1000x) was prepared, filter-sterilized and stored frozen at -20°C (1 ml aliquots). For the trace element solution used to prepare soil slurries the stock solution was diluted (1x; i.e., 1 mL in 1L).

Table 3 Components of the trace element solution after Whittenbury *et al.*, 1970a.

Component	Concentration in stock solution (1000x)	Final concentration (1x)
37% HCl	50 mM	50 µM
FeCl ₂ x 4 H ₂ O	5 mM	5 µM
ZnCl ₂	0.50 mM	0.50 µM
MnCl ₂ x 2 H ₂ O	0.50 mM	0.50 µM
CoCl ₂ x 6 H ₂ O	0.50 mM	0.50 µM
Na ₂ MoO ₄ x 2 H ₂ O	0.15 mM	0.15 µM
H ₃ BO ₃	0.10 mM	0.10 µM
NiCl ₂ x 6 H ₂ O	0.10 mM	0.10 µM
CuCl ₂ x 2 H ₂ O	0.01 mM	0.01 µM

2.2.2. Substrate solutions for incubations concentrating on methane

Filter-sterilized 50 mM and 250 mM stock solutions of each alternative substrate were prepared. Alternative substrates were acetate (as sodium acetate), cellobiose, D-xylose, methanol, methylamine, n-dodecan, vanillic acid (4-Hydroxy-3-methoxybenzoic acid), and guaiacol (2-methoxyphenol).

Vanillic acid was only soluble at an alkaline pH. Thus, filter-sterilized NaOH was supplemented stepwise to the stock solution till crystalline vanillic acid was solved.

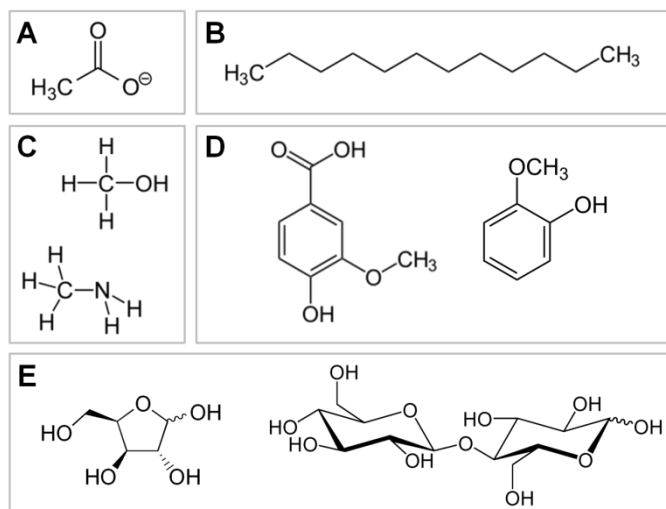


Figure 16 Compounds tested as putative alternative substrates for ambient methane-utilisers.

The alternative substrates tested were grouped into five different categories covering carboxylic acids (acetate, A), n-alkanes (n-dodecane, B), C1 compounds (methanol & methylamine, C), aromatic compounds (vanillic acid & guaiacol, D), and sugars (xylose & cellobiose, E).

Filter-sterilized 250 mM stock solutions of acetate (as sodium acetate) and vanillic acid (4-Hydroxy-3-methoxybenzoic acid) were used to obtain substrate solutions that were applied to coarse-grained soil by spraying in order to analyse the methane degradation potential of fresh forest soil under changed substrate availabilities (see 2.3.2). In total three different concentrated solutions were prepared to obtain the required final concentrations (i.e., 0.5 mM, 2.5 mM, 5 mM) by supplementing 1 mL substrate solution.

2.2.3. [¹³C_u]-Substrates for SIP incubations concentrating on methanol

For the alternative substrate SIP experiment (see 2.3.3) and pH shift SIP experiment (see 2.3.4) stock solutions had a concentration of 40 mM. Stock solutions of methanol and multi-carbon substrates (i.e., acetate, glucose, xylose and vanillic acid) were prepared with either the [¹³C]-isotopologue ('labelled', 99atom% C) or the [¹²C]-isotopologue (i.e., 'unlabelled', natural abundance of ¹³C). All multi-carbon substrate stock solutions also included 40 mM [¹²C]-methanol. All ¹³C-isotopologues were fully labelled (i.e., [¹³C_u]), excepting vanillic acid, where only the aromatic ring carbon was [¹³C]-labelled (i.e., [¹³C₁₋₆]), methyl and carboxyl groups possessed [¹²C]-carbon. For CO₂ incubations either gaseous [¹³C]-CO₂ ('labelled', 99atom% C; <3atom% ¹⁸O) or [¹²C]-CO₂ was used. [¹³C]-isotopologues were purchased from Campro Scientific (Berlin, Germany) and Sigma-Aldrich (Steinheim, Germany), [¹²C]-isotopologues were purchased from Roth (Karlsruhe, Germany), Sigma-Aldrich (Steinheim,

Germany), PanReac Applichem (Darmstadt, Germany), Merck (Darmstadt, Germany) and Rießner (Lichtenfels, Germany).

For the methanol/chloromethane SIP experiment (see 2.3.10) the stock solution of methanol was 216 mM, but was prepared as the methanol stock solutions of the other SIP experiments.

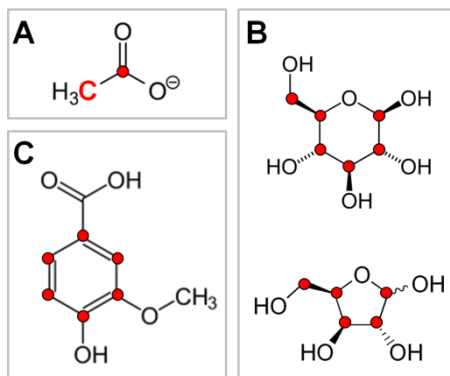


Figure 17 Compounds tested as putative multi-carbon substrates for methanol-utilisers in the substrate SIP experiment.

The multi-carbon substrates tested were grouped into three different categories covering carboxylic acids (acetate, A), sugars (glucose & xylose, B), and aromatic compounds (vanillic acid, C). All ^{13}C isotopes of the used ^{13}C isotopologues are highlighted in red.

2.2.4. KCN solutions

For all incubations were KCN (Sigma-Aldrich, Steinheim, Germany) was applied appropriate stock solutions were prepared in order to obtain the required final concentrations (i.e., 20 mM) by supplementing 0.5 mL KCN stock solution.

2.2.5. Toluene solutions

For all incubations where toluene (purity $\geq 99.9\%$; Sigma-Aldrich, Steinheim, Germany) was applied, appropriate stock solutions were prepared in order to obtain the required final concentrations (i.e., 0.2 μM , 1 μM , and 50 μM or 0.5 μM) by supplementing 0.5 mL toluene stock solution. Stock solutions were obtained by preparing a 1 M solution that was diluted accordingly.

2.2.6. Solutions for DNA SIP

The DNA SIP was performed according to the protocol of Neufeld *et al.*, 2007. The CsCl solution was prepared by dissolving CsCl salt in ddH₂O to obtain a final concentration of approximately 8 M. After autoclaving the density of the solution was determined by weighing at 20°C. Typically, the density of the CsCl solution ranged between 1.72 to 1.90 g ml⁻¹. The gradient buffer was prepared by mixing 100 mM Tris, 100 mM KCl and 1mM EDTA. The pH

was adjusted to pH 8 and after autoclaving the density of the solution was determined by weighing at 20°C. Typically, the density of the gradient buffer was about 1.00 g ml⁻¹.

Table 4 Composition of the gradient buffer used for DNA SIP.

Component	each stock solution		gradient buffer	
	Composition	Final concentr.	Component	Final concentr.
Tris	3.03 g Tris 50 ml ddH ₂ O (pH 7.8)	500 mM	20 ml Tris (500mM)	100 mM
KCl	1.49 g KCl 20 ml ddH ₂ O	1 M	20 ml KCL (500mM)	100 mM
EDTA ^a	0.291 g 10 ml ddH ₂ O	100 mM	10 ml EDTA (100 mM)	1 mM
			up to 100 ml (pH 8)	

^a alkaline pH necessary to dissolve EDTA (supplementation of NaOH)

The gradient solution with a defined buoyant density was prepared by mixing a CsCl solution with gradient buffer. Since the buoyant density of the gradient solution is crucial for the successful separation of ‘heavy’ and ‘light’ DNA, it was necessary to adjust the density using Equation 1.

Equation 1 Density adjustment of the gradient buffer used for separation of DNA.

$$V_S = V_{GS} \times \frac{(\rho_{GS} - \rho_R)}{(\rho_R - \rho_S)}$$

V_S , volume of the solution (CsCl solution^a or gradient buffer^b) [ml]

ρ_S , density of the solution (CsCl solution^a or gradient buffer^b) [g ml⁻¹]

V_{GS} , volume of the gradient solution [ml]

ρ_{GS} , density of the gradient solution [g ml⁻¹]

ρ_R , required density for separation of DNA (i.e., 1.732 g ml⁻¹)

^a necessary if the density is lower than required (< 1.732 g ml⁻¹)

^b necessary if the density was higher than required (> 1.732 g ml⁻¹)

The ‘overlying solution’ used during fractionation was prepared by dissolving 5 g ml⁻¹ coomassie brilliant blue in sterile ddH₂O (5 g ml⁻¹) and was stored at room temperature.

The PEG solution necessary to precipitate fractionated DNA was prepared by mixing 150 g of PEG 6000 (polyethylene glycol) with 46.8 g NaCl in a total volume of 500 ml ddH₂O. The solution was filter-sterilized and autoclaved. The solution is 30% PEG 6000 and 1.6 M NaCl.

2.2.7. Cloning (SOC and LB agar plates)

For the SOC-medium, prepared after Green & Sambrook, 2012 and used during cloning (see 2.5.10), 2 g tryptone, 0.5 g yeast extract, 1 ml NaCl solution (1 M), and 0.25 ml KCl solution (1 M) were mixed with approximately 95 ml ddH₂O and autoclaved. Subsequently, sterile filtered 1 ml MgCl₂ solution (2 M) and 1 ml glucose solutions (2 M) were added, the pH was adjusted to pH 7 (using sterile filtered solutions), the volume was filled up to 100 ml and the SOC-medium was stored frozen at -20°C until further use.

For the LB (lysogeny broth) agar plates with ampicillin after Green & Sambrook, 2012 used during cloning (see 2.5.10) 10 g tryptone, 5 g yeast extract, 5 g NaCl, and 15 g agar were mixed with 980 mL ddH₂O, the pH was adjusted to pH 7, the volume was filled up to 1 L, and the medium was autoclaved. 1 ml of filter-sterilized ampicillin solution (100 mg ml⁻¹) was added to the medium after cooling down to 60°C. The medium was poured into sterile plastic Petri dishes. LB agar plates were stored at 4°C for maximal 7 days.

2.3. Incubations and microcosm experiments

In general three different C1 compounds were addressed in this thesis: methane, methanol and chloromethane. Needless to say, that all performed incubations are somehow overlapping in terms of methylotrophs, since methanotrophs are also able to utilise methanol for example. However, for better understandings of the main intensions of the different experiments, all incubations and microcosm experiments are grouped to the C1 compound that was mainly addressed in the individual experiments. Additionally, the thesis was concentrating on a forest soil, but also addressed other environments (other soils and aquatic environments) in side experiments in order to gain a more global reflection on methylotrophic microorganisms.

<u>Addressed C1 compound</u>	<u>Main intension</u>
Methane	Assessing alternative substrates of methanotrophic microorganisms
Methanol	Assessing alternative substrates of methanol-utilising methylotrophic microorganisms
Chloromethane	CH ₃ Cl degradation studies and assessing a congruence of CH ₃ Cl-utilisers and methanol-utilisers

All experiments were conducted with fresh samples. Roots, dead wood, stones, plant debris, beechnuts and acorns were manually removed from soil samples before further preparation. In the case of the forest soil samples, fresh soil of different sampling points (see 2.1.1) was sieved (mesh size 2 mm) and equally pooled to further prepare the soil slurries. Most incubations were conducted as soil slurries (see 2.3.1, 2.3.3, 2.3.4, and 2.3.5) to achieve a

homogenous environment that provides a sufficient distribution of supplemented substrates as well as a balanced distribution of microorganisms (i.e., no formation of microscale hot-spots).

2.3.1. Long-term incubation under mixed substrate conditions with methane and alternative substrates

'High-affinity' methanotrophs are able to oxidise methane at atmospheric concentrations, but these low concentrations might be too low to maintain cell metabolism only by methane oxidation [Degelmann *et al.*, 2010]. Therefore it might be conceivable that 'high-affinity' methanotrophs are utilising other substrates than methane and thus, exhibit a broader substrate spectrum than previously assumed. In soil environments the simultaneously availability of methane and other substrates might affect the methane oxidation in an inhibitory or stimulating manner. Thus, the impact of alternative substrates on the methane degradation and the abundance of methanotrophs might provide first hints to putative alternative substrates.

In order to enrich 'high-affinity' methanotrophs only low concentrations of substrates were supplemented to soil slurry treatments of forest soil over a long incubation period, since low methane concentrations might delay cell growth. Soil slurries consisted of forest soil from 5 different sampling points reflecting the general characteristics of the total sampling area (see 2.1.1). For each sampling point 1.4 kg of sieved soil was equally mixed resulting in a total of 7 kg sieved soil. The sieved soil was mixed with 7 l sterile water in 5 l glass flasks (DURAN) and the preliminary slurry was mixed for 3 h on a shaker at 5°C in the dark. Subsequently 250 ml of slurry was filled in sterile screw-capped natural-rubber-stopped 1L flask (Glasgerätebau Ochs, Bovenden, Germany; Müller + Krempel, Bülach, Switzerland). In total 27 1L flasks containing soil slurry were prepared (Figure 18). Methane was weekly supplemented in the headspace to a final concentration of 200 ppm. Alternative substrates (i.e., acetate, sugars, n-alkanes, methanol, methylamine, aromatic compounds; 0.5 ml of a 50 mM stock solution, see 2.2.2) were weekly supplemented to a final concentration of 100 µM over 14 weeks of incubation (15x 100 µM supplemented). Since after 14 weeks of incubation no clear impact of alternative substrates on methanotrophs was obvious (see 3.2), the concentration of the weekly pulsed supplemented alternative substrates was raised per pulse to 500 µM (5x 500 µM supplemented; 0.5 ml of a 250 mM stock solution, see 2.2.2). The long-term incubation was finished after 18 weeks of incubation.

All soil slurry incubations were performed in triplicates for each approach (controls and alternative substrate treatments) on a horizontal shaker (Gallenkamp Orbital Incubator INR-401, London, UK) at 200 rpm at 20°C in the dark. Oxidic conditions were offered by a large gas phase inside the flasks (i.e., ration slurry to gas phase was 1:4) and by weekly opening allowing acclimatising before re-sealing. CO₂ and O₂ concentrations were measured before the weekly re-opening of the flasks and CH₄ was measured before re-opening and after

repeated supplementation. Several slurry aliquots (0.5 ml - 1 ml each) for analytical and molecular analysis (see 2.4, 2.5.8) were taken before and after supplementation and were kept at -20°C or -80°C, respectively. In addition, pH was monitored to prevent an impact of shifted pH conditions.

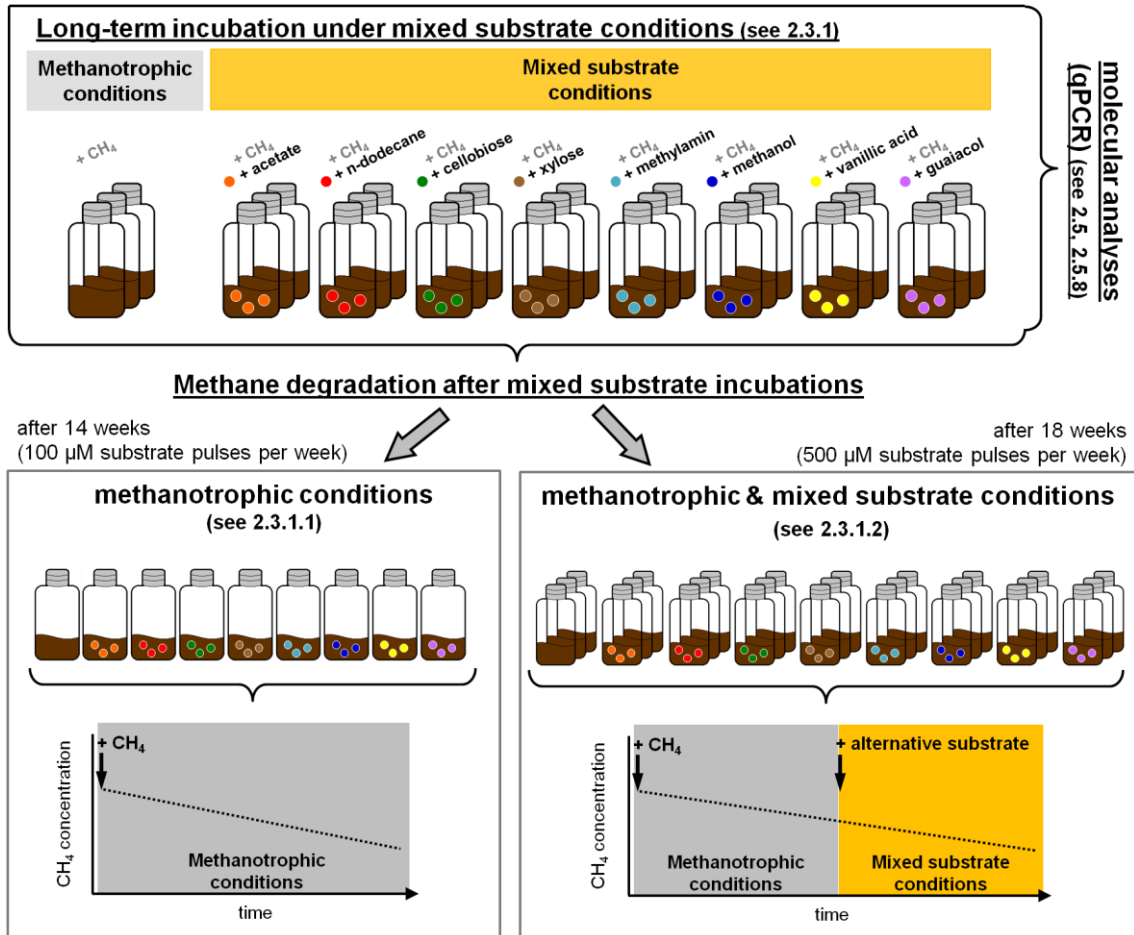


Figure 18 Experimental set-up of the long-term incubations under methanotrophic and mixed substrate conditions (see 2.3.1) and following experiments (see 2.3.1.1, 2.3.1.2).

Soil slurries were supplemented with CH₄ and alternative substrates (i.e., acetate, n-alkanes, cellobiose, xylose, methylamine, methanol, vanillic acid, and guaiacol; see 2.2.2) in order to obtain methanotrophic (grey box) or mixed substrate conditions (orange box). Incubated slurry aliquots were evaluated for their methane degradation potential after the incubation and under different conditions.

2.3.1.1. Methane degradation potential after mixed substrate incubation under solely methanotrophic conditions

If the ‘high-affinity’ methanotrophs are facultatively methylotrophic and utilise other substrates, it is conceivable that the long-term incubation had an effect on these methanotrophs and the resulting methane degradation potential.

In order to analyse the impact of alternative substrates on the methane degradation during the long-term incubation under mixed substrate conditions (see 2.3.1) 15 ml slurry were taken from one replicate of each treatment (Figure 18). Slurry aliquots were taken after 14

weeks of incubation and were filled in sterile screw-capped natural-rubber-stopped 125 mL flask (Glasgerätebau Ochs, Bovenden, Germany; Müller + Krempel, Bülach, Switzerland). Solely methane was supplemented to a final concentration of 20 ppm to the gas phase (consisting of sterile air) and the methane degradation was monitored. No further substrates were supplemented. Thus, aliquots were kept solely under methanotrophic conditions (Figure 18). Between the different measurement time points treatments were kept on an end-over-end shaker at 20°C in the dark.

2.3.1.2. Methane degradation potential after mixed substrate incubation under methanotrophic and mixed substrate conditions

Since the co-presence of different substrates might lead to a co-consumption of substrates or even a preferred consumption of the alternative substrate, the methane degradation might be highly influenced by this co-presence. In order to analyse immediate changes in the methane degradation between methanotrophic and mixed substrate conditions slurry aliquots of the long-term incubation under mixed substrate conditions (see 2.3.1) were taken after 18 weeks. Samples were taken from each replicate (i.e., 3x 8 different substrate treatments and 3 controls) of each treatment (Figure 18). 15 ml of slurry aliquots were filled in sterile screw-capped natural-rubber-stopped 125 mL flask (Glasgerätebau Ochs, Bovenden, Germany; Müller + Krempel, Bülach, Switzerland). Solely methane was supplemented to the gas phase to a final concentration of 20 ppm and thus, methane degradation was evaluated under strictly methanotrophic conditions (Figure 18). After one week 500 µM of the corresponding alternative substrates were supplemented to the existing slurry approaches, changing methanotrophic conditions to mixed substrate conditions (Figure 18). The methane degradation was now evaluated under changed substrate availabilities for one week and both methane degradation potentials under strictly methanotrophic and mixed substrate conditions were subsequently compared.

2.3.2. Methane degradation potential of fresh forest soil under changed substrate availabilities

The results of the long-term incubation were not clear in terms of the impact of alternative substrates on methanotrophic activity (see 3.2.1 - 3.2.4). In addition, the incubation manner as soil slurry appeared as inhibitory in terms of the methane degradation even on control treatments (i.e., solely methanotrophic conditions) (see 3.1). Regrettably, such an inhibitory effect on the methane degradation was previously mentioned by Pratscher and colleagues [Pratscher *et al.*, 2011]. For that reason the effect of two selected alternative substrates on the methane degradation in fresh soil without long-term incubation was analysed (Figure 19). Soil was taken from 5 different sampling points and crushed manually to obtain coarse-grained soil. Equal amounts of soil were mixed and each replicate was set-up with 20 g of

fresh soil in sterile screw-capped natural-rubber-stopped 125 mL flask (Glasgerätebau Ochs, Bovenden, Germany; Müller + Krempel, Bülach, Switzerland). The experiment on methane degradation comprised in total 18 replicates. Each soil approach was performed in triplicates with 3 different substrate concentrations tested (i.e., 0.5 mM, 2.5 mM and 5 mM) resulting in 9 replicates per alternative substrate (i.e., acetate or vanillic acid) (Figure 19). The first time point of methane degradation was always measured 30 min after the supplementation of substrate(s) (i.e., methane or alternative substrates) and was recorded hourly. Before each supplementation the flasks were opened allowing the gas phase to acclimatise before re-sealing. Between the different measurement days the flasks were kept in the dark at 20°C.

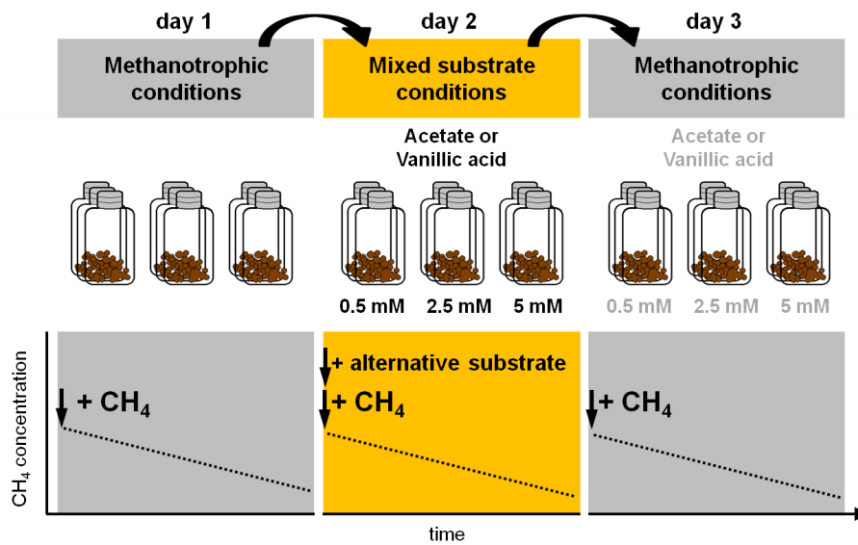


Figure 19 Experimental set-up to evaluate the methane degradation potential under changed substrate availabilities of fresh soil.

Fresh soil was coarse-grained and methane degradation was successively evaluated under changed substrate conditions (i.e., methanotrophic or mixed substrate conditions) in the same treatments. Day 1: Methane degradation under methanotrophic conditions (= native methane degradation). Day 2: Methane degradation under mixed substrate conditions (= immediately impact of alternative substrates). The alternative substrates were supplemented in different concentrations. Day 3: Methane degradation under methanotrophic conditions (= delayed impact of alternative substrates).

The methane degradation potential was evaluated in three approaches. At the first day solely methane was supplemented in the gas phase to a concentration of 30 ppm in order to determine the native methane degradation of each replicate. At the second day methane (30 ppm) and the alternative substrates were supplemented. The alternative substrates were supplemented by spraying. The corresponding stock solutions revealed different concentrations in order to supplement the same volume to each replicate (see 2.2.2). After each spray the flasks were vigorously turned by hand in order to moisten soil particles and the flask wall more effective. In total 5 sprays were supplemented per replicate corresponding to a volume of 1 ml supplemented. At the third day again solely methane was

supplemented in the gas phase to a concentration of 30 ppm. For an overview on the experimental set-up see Figure 19.

Moreover, for each alternative substrate and each concentration additional replicates (in total 6) were conducted to evaluate the potential of methanogenesis. These approaches were handled in the same manner as the other replicates with the exception that only the alternative substrates were supplemented at the second day of measurements (methane was never supplemented).

2.3.3. Oxic soil slurry incubations of the substrate SIP experiment under mixed substrate conditions

Most soil-derived methylotrophic microorganisms are facultatively methylotrophic organisms utilising also multi-carbon compounds [Kolb, 2009a]. The majority of methylotrophs possess C1-pathways that covers methanol – as initial substrate or as intermediate (e.g. methanotrophs) [Anthony, 1982]. Thus, the majority of methylotrophs are methanol-utilising. The co-consumption of methanol and multi-carbon substrates is already known [McNerny & O'Connor, 1980; Peyraud *et al.*, 2012; Nayak *et al.*, 2014], but most studies on the substrate range of methylotrophs are conducted mainly with model organisms such as *Methylobacterium extorquens* AM1, and as comparison studies between methylotrophic (only C1 compounds supplemented) and multi-carbotrophic (only multi-carbon compounds supplemented) conditions [Bosch *et al.*, 2008; Skovran *et al.*, 2010; Smejkalova *et al.*, 2010; Peyraud *et al.*, 2011]. An advantage of the experimental design of the substrate SIP experiment was the simultaneously supplementation of C1 compounds and alternative substrates that might provide insights into the consumption habits of methylotrophs.

For each sampling point (5 points in total) 500 g soil was sieved and equally mixed resulting in a total of 2'500 g sieved soil. In total 35 soil slurries were prepared. Each soil slurry was prepared individually by mixing 50 g sieved soil (mesh size 2 mm, fresh weight) with 40 ml trace element solution (see 2.2.1). All slurries were initially homogenised by hand shaking. Soil slurry incubations were performed in duplicates for each approach (controls, ¹²C- or ¹³C-isotopologue supplemented treatments) in sterile screw-capped natural-rubber-stopped 0.5 L flask (Glasgerätebau Ochs, Bovenden, Germany; Müller + Krempel, Bülach, Switzerland) on an end-over-end shaker at 20°C in the dark. Substrates (i.e., methanol, acetate, sugars; 1 ml) and CH₄ were supplemented daily to a final concentration of 1 mM and 200 ppm, respectively. Vanillic acid was supplemented, if it was no longer detectable, to a final concentration of 1 mM. For an overview on the experimental set-up see Figure 20.

The time points for molecular analyses of each substrate differed and were based on the time points of ¹³CO₂, i.e., when a comparable similar amount of ¹³CO₂ was formed. Thus, the time points for molecular analyses were conducted after different amounts of substrate pulses, i.e., methanol after 18 pulses (\triangleq 18 mM), acetate after 12 pulses (\triangleq 12 mM), glucose

after 12 pulses (\cong 12 mM), xylose after 10 pulses (\cong 10 mM), and vanillic acid after 5 pulses (\cong 5 mM).

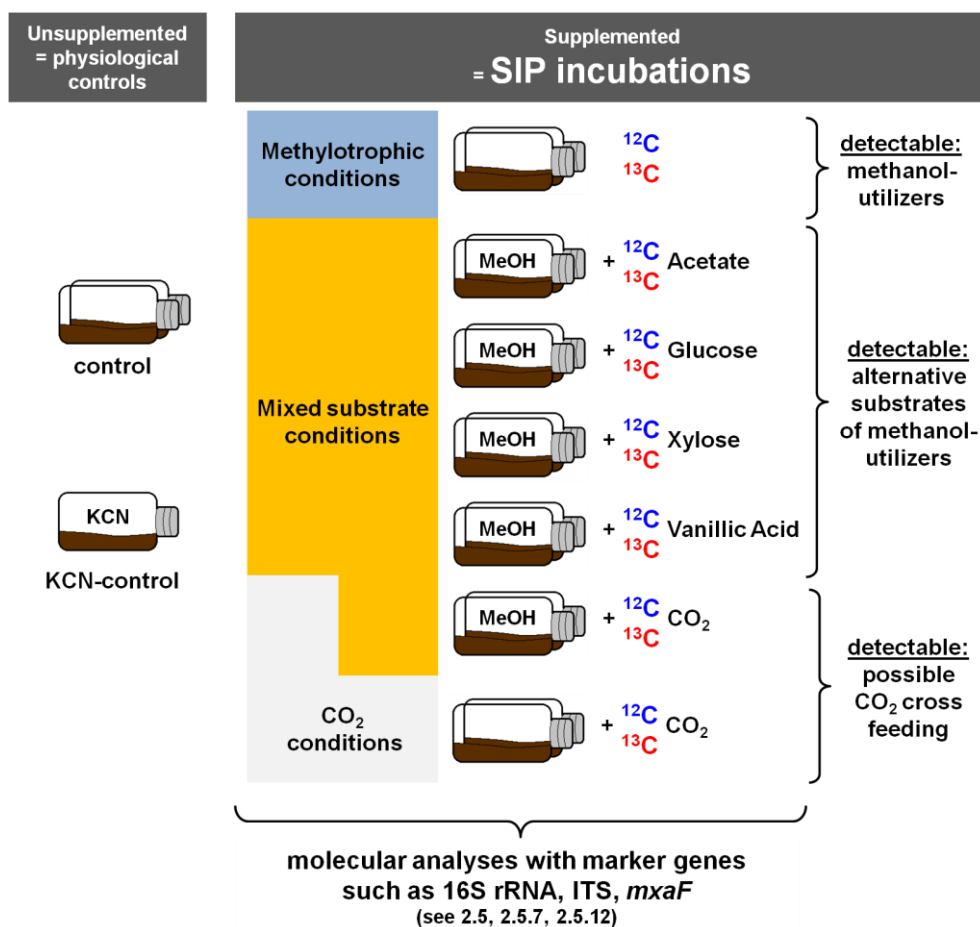


Figure 20 Experimental set-up of the Substrate SIP experiments.

Different SIP incubations supplemented with ^{12}C - or ^{13}C -isotopologues were set up under methylotrophic (i.e., solely methanol supplemented, blue box) or mixed substrate (i.e., methanol and alternative substrate supplemented, orange boxes) conditions. Incubations under CO₂ conditions served as cross feeding controls (grey boxes). Unsupplemented incubations served as physiological controls (formation of CO₂). SIP incubations were further molecularly analysed (see 2.5, 2.5.7, 2.5.12). All incubations were supplemented with methane in the headspace (not shown).

Unsupplemented control slurry incubations served as methanol control treatments and lacked any substrate treatment besides CH₄. The additional supplemented aqueous volume per substrate pulse in substrate treatments (i.e., 1 ml) was compensated by the supplementation of the same volume of trace element solution (i.e., 1 ml) to the control. Since multi-carbon substrate treatments were additionally supplemented with methanol (1 mM, final concentration), methanol treatments served as substrate control treatments. CO₂ incubations were supplemented with 10% CO₂ in the headspace (approx. 7 mM total amount) and opened if the O₂ concentration was below 10%. The purpose of CO₂ treatments was (i) to analyse cross feeding effects and (ii) to address potential CO₂-assimilating taxa as well.

An oxic atmosphere was offered by a large gas phase inside the flasks (i.e., the ratio of gas phase to slurry volume was 12:1) and by daily opening allowing acclimatising before re-sealing. CO₂ and O₂ concentrations were measured before each re-opening and CH₄ was measured before re-opening and after repeated CH₄ supplementation. In addition, before each substrate supplementation 5 ml of the gas phases of the [¹³C]-isotopologue treatments (i.e., [¹³C₁]-methanol and [¹³C_u]-substrates) were stored in 3 ml exetainer vials (Labco Ltd., High Wycombe, England) for subsequent analysis of ¹³CO₂ formation (see 2.4.4).

Several slurry aliquots (0.5 ml - 1 ml each) for analytical and molecular analyses (see 2.4, 2.5.6, 2.5.11, 2.5.12.2) were taken before and after supplementation and were kept at -20°C or -80°C, respectively. The pH was immediately determined in order to adjust the pH.

2.3.4. Oxic soil slurry incubations of the pH shift SIP experiment under methylo-trophic conditions

The investigated soil was determined as acidic with a soil pH around 3.5 to 4. Most methylo-trophic isolates are known to possess growth optima at a more neutral pH, but also acidophilic and acidotolerant methylo-trophs are known [Kolb, 2009a]. Thus, pH is undisputable an ecological niche-defining parameter for soil methylo-trophs. In addition, soil is not homogeneous and thus, microscale areas exist with different conditions such as elevated pH values. For example, within 2 mm of soil the pH can differ up to one pH unit [Allredge & Cohen, 1987; Or *et al.*, 2007]. Thus, the impulse to conduct the pH shift SIP experiment was to address if/how the indigenous methanol-utilisers might be affected to elevated pH values.

The pH shift SIP experiment was conducted according to the substrate SIP experiment (see 2.3.3) in order to maintain comparability. However, only methanol was supplemented as ¹²C- or ¹³C-isotopologue and the headspace was not supplemented with CH₄ in order to evaluate and compare the impact of CH₄ on the methylo-trophic organisms in the soil. For an overview on the experimental set-up see Figure 21.

Two different slurry preparations were conducted in accordance with pH conditions. For each sampling point (5 points in total) 150 g soil was sieved and equally mixed resulting in a total of 750 g sieved soil. In total 12 soil slurries were prepared – 6 soil slurries with the *in situ* pH (pH 4) and 6 slurries with an elevated pH (pH 7).

Each soil slurry of the treatment with *in situ* pH was prepared individually by mixing 50 g sieved soil with 40 ml trace element solution (see 2.2.1) in sterile screw-capped natural-rubber-stopped 0.5 L flask (Glasgerätebau Ochs, Bovenden, Germany; Müller + Krempel, Bülach, Switzerland). All slurries were initially homogenised by hand shaking.

Adjustment of pH was necessary for elevated pH treatments. Thus, 300 g freshly sieved soil was mixed with 240 ml trace element solution (see 2.2.1) in a beaker and mixed using a magnetic stirrer till the slurry was homogenous. The pH was adjusted to 7 (6.8) with filter-

sterilized NaOH (10 M and 0.5 M) and mixed till the pH remained constant. 90 ml of pH adjusted slurry were filled into sterile screw-capped natural-rubber-stopped 0.5 L flask (Glasgerätebau Ochs, Bovenden, Germany; Müller + Krempel, Bülach, Switzerland).

[^{12}C]- or [$^{13}\text{C}_1$]-methanol was supplemented daily to a final concentration of 1 mM per pulse corresponding to substrate SIP experiments (see 2.3.3). Unsupplemented control slurry incubations for each pH approach were added with the same volume of trace element solution (1 ml). Soil slurry incubations were performed in duplicates for each approach (controls, ^{12}C - or ^{13}C - isotopologue treatment; pH 4 and pH 7) on an end-over-end shaker at 20°C in the dark.

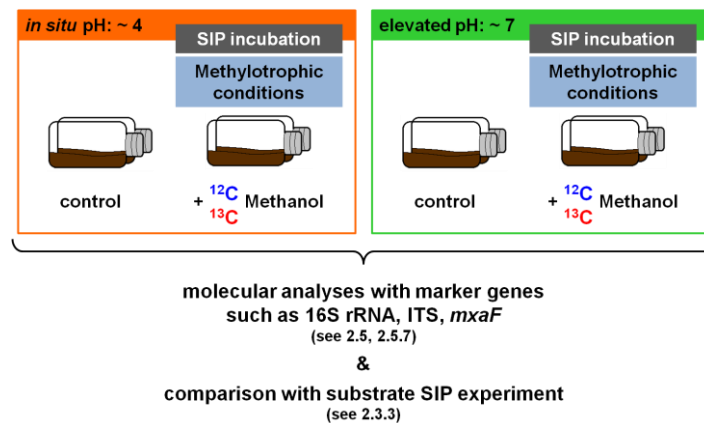


Figure 21 Experimental set-up of the pH shifted SIP experiments.

Two SIP incubations supplemented with ^{12}C - or [$^{13}\text{C}_1$]-methanol were set up under *in situ* (orange frame) and elevated pH (green frame) conditions. SIP incubations were further molecular analysed (see 2.5, 2.5.7, 2.5.12). The pH shift SIP experiment was in accordance to the substrate SIP experiment (see 2.3.3), with the exception that no methane was supplemented.

An oxic atmosphere was offered by a large gas phase inside the flasks (i.e., the ratio of gas phase to slurry volume was 12:1) and by daily opening allowing acclimatising before re-sealing. CO_2 and O_2 concentrations were measured before each re-opening. In addition, before each substrate supplementation 5 ml of the gas phases of the [$^{13}\text{C}_1$]-methanol treatments were stored in 3 ml exetainer vials (Labco Ltd., High Wycombe, England) for subsequent analysis of $^{13}\text{CO}_2$ formation (see 2.4.4).

Several slurry aliquots (0.5 ml - 1 ml each) for analytical and molecular analyses (see 2.4, 2.5.6, 2.5.12.2, 2.5.8) were taken before and after supplementation and were kept at -20°C or -80°C, respectively. The pH was immediately determined in order to adjust the pH if necessary.

2.3.5. Oxic soil slurry incubations of different soil environments to assess the abundance of methylotrophs

The main focus of the work was on forest soils, but methylotrophic microorganisms were shown to be ubiquitous and playing a crucial role in global C1-metabolism of volatile organic

compounds such as methane and methanol [King, 1992; Kolb, 2009a; Chistoserdova & Lidstrom, 2013]. Since most methylotrophic organisms use methanol [Lidstrom, 2006; Chistoserdova *et al.*, 2009; Kolb, 2009a], and different soils were already shown to exhibit specific affinities to methanol [Stacheter *et al.*, 2013], the *in situ* abundance and the impact of enhanced methanol concentrations and availabilities on methylotrophs in different terrestrial environments covering forest-related and meadow-related sites was assessed. In order to cover a wide range of soil samples from different ecosystem types the vegetation was also considered.

In total 8 different soil environments were analysed in terms of methylotrophic abundances in these environments (see 2.1.2). Of each environment soil was sieved (mesh size 2 mm) and soil slurries were prepared by mixing 15 g soil with 5 ml of trace element solution (see 2.2.1) in sterile screw-capped natural-rubber-stopped 125 mL flask (Glasgerätebau Ochs, Bovenden, Germany; Müller + Krempel, Bülach, Switzerland). All soil slurry incubations were performed in duplicates for each approach on an end-over-end shaker at 20°C in the dark. Methanol was supplemented 4 times as a 1 ml pulse of 5 mM (final concentration) resulting in a total amount of 20 mM methanol over the incubation time of 20 days. Methanol was supplemented at the beginning and at the days 7, 12, and 16. Oxidic conditions were offered by a large gas phase inside the flasks (i.e., the ratio of gas phase to slurry volume was 12:1) and by opening the flasks at the time points of pulsing allowing acclimatising before re-sealing. CO₂ and O₂ concentrations were monitored by GC just before the methanol pulsing.

Soil aliquots (0.5 ml - 1 ml each) for molecular analyses (see 2.5, 2.5.8) were taken at the beginning and at end of the experiment of each individual replicate. The pH was monitored at the time points of pulsing.

2.3.6. Chloromethane degradation in different forest-derived compartments

Apart from the most prominent C1 compounds, i.e., methane and methanol, also halogenated hydrocarbon compound such as halomethanes can be utilised as sole source of energy and carbon by several methylotrophic microorganisms [McDonald *et al.*, 2002; Miller *et al.*, 2004; Schäfer *et al.*, 2007; Kolb, 2009a]. The source of chloromethane is mainly of natural origin including terrestrial and marine environments [Schäfer *et al.*, 2007], wherefore this great amount and diversity of natural sources might indicate a ubiquity of microorganisms capable of utilising these halogenated methanes. In addition, the role of forest soils as a biological sink of CH₃Cl is undisputed [Harper, 2000].

Leaves (= phyllosphere) produce CH₃Cl as a side reaction involved in plant defence mechanisms [Rhew *et al.*, 2003; Nagatoshi & Nakamura, 2007] and in decomposed plant material CH₃Cl is formed during demethylation processes of pectin [Hamilton *et al.*, 2003]. During fungal wood degradation CH₃Cl is formed in methylation processes during the

decomposition of aromatic structures derived from lignin [Keppler *et al.*, 2000]. Soil layers that are rich in organic matter (i.e., humus) might be another important source of CH₃Cl by the formation of CH₃Cl in abiotic reactions such as redox or substitution [Harper, 2000; Keppler *et al.*, 2000]. Although all these forest-related sources of CH₃Cl are known, it is not resolved yet which forest compartment might reveal the highest CH₃Cl degradation potential.

In total 5 different forest-derived compartments were analysed and samples were taken from different places of the sampling area 'Steinkreuz' (see 2.1.1). Soil-derived samples were taken from the organic layer soil (uppermost 5 to 10 cm, dark brown to blackish indicative for humic substances) and the subjacent mineral soil (maximal depth of 30 cm, grayish in colour and no visual evidenced for humic substances). Plant-derived samples were taken from the litter layer, fresh leaves and dead wood. Only litter that revealed no visual decomposition was taken directly from the soil surface. For samples of fresh leaves several branches of beeches (*Fagus sylvatica*) were cut from trees, put in water to keep leaves alive and were transferred to the laboratory. Just before incubation experiments the leaves were picked. The dead wood samples derived from branches or trunks of beeches (*Fagus sylvatica*) and revealed a partially spongy structure assuming beginning decomposition.

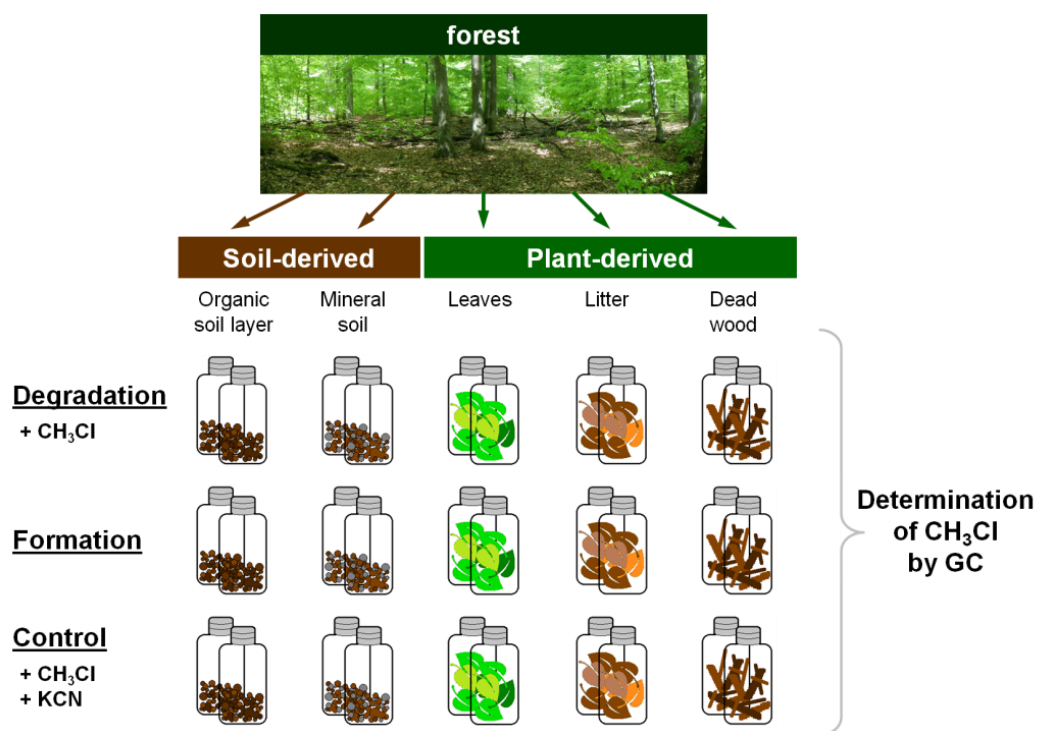


Figure 22 Experimental set-up to evaluate the chloromethane degradation potential of different forest-derived compartments.

Samples were derived from different forest-compartments of the same forest (see 2.1.1, Figure 13). From each compartment three different approaches were set-up as duplicates in order to evaluate the CH₃Cl degradation potential ('degradation'), the potential to form CH₃Cl endogenously ('formation'), and the biotic character of the CH₃Cl degradation ('control').

5 g of coarse-grained soil, litter, and wood as well as 25 fresh leaves were transferred into sterile screw-capped natural-rubber-stopped 125 mL flask (Glasgerätebau Ochs, Bovenden, Germany; Müller + Krempel, Bülach, Switzerland). For an overview on the experimental set-up see Figure 22. The biological control approaches were supplemented with KCN (final concentration 20 mM) and flasks were sealed and flushed with synthetic air (Rießner Gase GmbH, Deutschland). The KCN controls and the approaches to evaluate CH₃Cl degradation were supplemented with CH₃Cl to a final concentration of 100 ppb. All incubations were set-up as duplicates at 20°C. In total, eight 5 ml gas samples were taken over 180 minutes and stored in 3 ml exetainer vials (Labco Ltd., High Wycombe, England) for the subsequent analysis of CH₃Cl by GC (see 2.4.3).

2.3.7. Chloromethane degradation in forest soil

The atmospheric concentration of CH₃Cl is only 600 ppt, but isolates growing on CH₃Cl were isolated with much higher concentrations (%-range) [Doronina *et al.*, 1996; Borodina *et al.*, 2005]. Thus, the capacity of forest soil to degrade low and high amounts of CH₃Cl was evaluated. In addition, observations of these degradation analyses were pre-experiments of the methanol/chloromethane SIP experiment (see 2.3.10).

Forest soil samples (i.e., uppermost soil) were taken from different places, manually crushed and equally mixed. 50 g of coarse-grained soil were filled in sterile screw-capped natural-rubber-stopped 500 mL flask (Glasgerätebau Ochs, Bovenden, Germany; Müller + Krempel, Bülach, Switzerland) and supplemented with CH₃Cl to a final concentration of 100 ppb and 1%, respectively. The approaches with 100 ppb CH₃Cl were conducted in duplicates (at two consecutive days); the approach with 1 % CH₃Cl was conducted as one replicate. Additionally, one flask was free of soil and only supplemented with 1 % CH₃Cl in order to evaluate previously observed losses of CH₃Cl in incubation flask without soil (data not shown and not further discussed, flasks were gas tight). All replicates were supplemented with additional air to obtain overpressure in the flasks allowing gas sampling.

The CH₃Cl concentration in the approaches with 100 ppb was measured during the incubation every 15 min - 30 min over 180 min and 285 min, respectively. For the approach with 1 % CH₃Cl the degradation was evaluated in 4 consecutive cycles depending on CH₃Cl consumption over several days (i.e., 1st cycle over 16 days, 2nd cycle over 6 days, and 3rd and 4th cycle over 3 days). The 2nd, 3rd, and 4th cycle started only several hours after the previous cycle. Before each cycle the gas atmosphere was exchanged by opening the flask and CH₃Cl was again supplemented. Since the CH₃Cl degradation was highly increased (see 3.9) the 4th cycle was closely sampled and each 5 ml gas samples had to be stored in 3 ml exetainer vials (Labco Ltd., High Wycombe, England) for the subsequent analysis of CH₃Cl by GC (see 2.4.3).

2.3.8. Inhibitory effects of toluene on the chloromethane degradation in forest soil

CH₃Cl-utilisers were not only isolated from pristine environments [McAnulla *et al.*, 2001a; Schäfer *et al.*, 2005; Nadalig *et al.*, 2011]. The first isolated CH₃Cl-utilising bacteria were derived from petrochemical sites, where contaminated soil is assumed [Hartmanns *et al.*, 1986; Doronina *et al.*, 1996]. Aromatic compounds, such as benzene, toluene, ethylbenzene and xylene (BTEX), are associated with the petrolchemical industry; but they are also associated with natural gases and crude oil [Deeb *et al.*, 2001]. An inhibitory effect of toluene on the CH₃Br and CH₃Cl degradation in marine water samples was reported by Goodwin and colleagues and a widespread inhibitory effect was assumed [Goodwin *et al.*, 2005]. Since the authors focussed on seawater, the effect of toluene in terrestrial environments was unsolved. Forest soil samples (i.e., uppermost soil) were taken from different places, sieved and equally mixed. 10 g of sieved soil were filled in sterile butyl-rubber-stopped aluminium crimp-sealed 120 mL serum flask (Glasgerätebau Ochs, Bovenden, Germany; Müller + Krempel, Bülach, Switzerland). Before sealing, the approaches for toluene inhibition were supplemented with toluene solutions to 3 different final concentrations of 0.2 µM, 1 µM and 50 µM (in each case 1 ml of toluene solution). Samples were left to settle for 45 minutes. Subsequently CH₃Cl was supplemented to a final concentration of 100 ppb and 1 %, respectively.

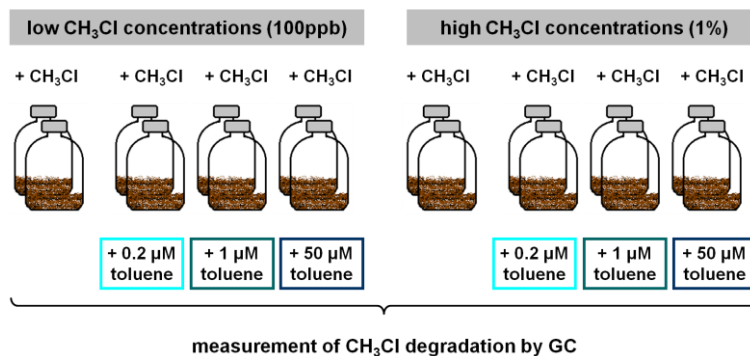


Figure 23 Experimental set-up to evaluate inhibitory effects of toluene to CH₃Cl degradation in a forest soil.

Sieved forest soil was supplemented with 2 different CH₃Cl concentrations (i.e., 100 ppb and 1 %) and three different toluene concentrations (i.e., 0.2 µM, 1 µM, and 50 µM) to evaluate the inhibitory effect of the aromatic compound.

All incubations were set-up in duplicates resulting in a total of 16. For an overview on the experimental set-up see Figure 23.

The first measuring time point was immediately after CH₃Cl supplementation. Approaches with 100 ppb CH₃Cl were sampled within 180 minutes and approaches with 1 % CH₃Cl were sampled over 48 hours. For all approaches all gas samples taken (6 ml) were stored in 3 ml exetainer vials (Labco Ltd., High Wycombe, England) for the subsequent analysis of CH₃Cl by GC (see 2.4.3).

2.3.9. Chloromethane degradation potential of terrestrial and aquatic environments and the putative inhibition by toluene

CH₃Cl-utilising microorganisms were detected and isolated from terrestrial and aquatic environments assuming an ubiquity of these specialised methylotrophs [Doronina *et al.*, 1996; Miller *et al.*, 1997; Coulter *et al.*, 1999; McAnulla *et al.*, 2001a; Borodina *et al.*, 2005; Schäfer *et al.*, 2005]. Within both environments important sinks for CH₃Cl are present. However, a direct comparison of terrestrial and aquatic environments was never conducted. In addition, toluene inhibition was only shown for seawater samples [Goodwin *et al.*, 2005]. Thus, the current experiment was conducted in order to evaluate the global role of the acidic forest soil as CH₃Cl sink in comparison with other partly completely soil samples of different ecosystem types.

In total 7 environments were analysed in terms of CH₃Cl degradation and the putative inhibition by toluene. These environments were classified as terrestrial and aquatic environments (see 2.1.2, 2.1.3, Table 2). From the terrestrial environments fresh soil samples were crushed manually to obtain coarse-grained soil and 15 g of soil were used per replicate (\cong ~ 15 ml volumes in the flask). From the shore sediment samples (i.e., lakeshore and seashore) 25 g of sediments were mixed with 5 ml of corresponding water per replicate (\cong ~15 ml volumes in the flask). From the sea sediment samples 11 g of sediments were mixed with 5 ml of corresponding water per replicate (\cong ~ 15 ml volumes in the flask). From the water samples (i.e., lakewater and seawater) 15 ml of unfiltered water were used per replicate. All incubations were performed in sterile screw-capped natural-rubber-stopped 125 mL flask (Glasgerätebau Ochs, Bovenden, Germany; Müller + Krempel, Bülach, Switzerland). Approaches to evaluate the endogenously amount of formed CH₃Cl were set-up in duplicates. Approaches to evaluate the CH₃Cl degradation were set-up as triplicates and 0.5 % CH₃Cl was initially supplemented. Approaches to evaluate the putative inhibition of toluene were set-up as triplicates and 0.5 % CH₃Cl and 0.5 ml toluene (final concentration 500 nM) were initially supplemented. Approaches to characterise the biotic character of the CH₃Cl degradation were set-up as one replicate per environment and 0.5 ml KCN (final concentration 20 mM) were initially supplemented. All replicates were supplemented with additional air (~ 100 ml) to obtain overpressure in the flasks allowing gas sampling. For an overview on the experimental set-up see Figure 24.

Oxic conditions were offered by a large gas phase inside the flasks (i.e., the ratio of gas phase to 'solid phase' was 8.5:1). During the whole incubation period the flasks were not opened. The O₂ concentrations were monitored by GC, but did not fall below 10 %. Gas samples of the head space were taken at several time points. Flasks were always swivelled before 5 ml of the gas phases were sampled and stored in 3 ml exetainer vials (Labco Ltd., High Wycombe, England) for the analysis of CH₃Cl and CO₂ and by GC (see 2.4.3).

Between the sampling time points the flasks were horizontally stored at 20°C in the dark and occasionally rotated by hand. The experiment was finished after 60 days of incubation.

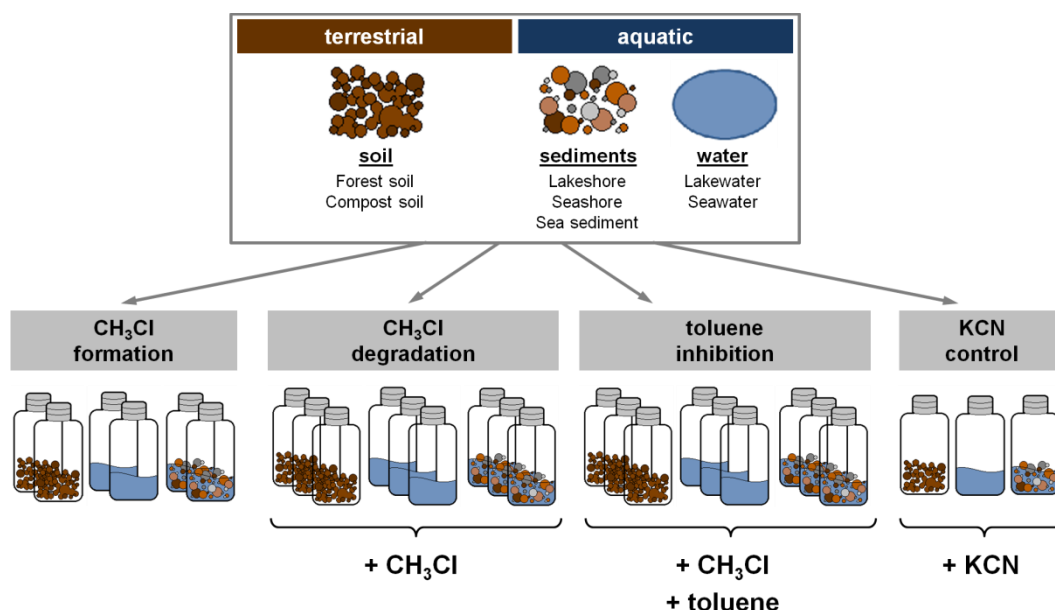


Figure 24 Experimental set-up to evaluate the chloromethane degradation potential of different ecosystem types and assessing the putative inhibition by toluene.

Samples were derived from different ecosystem types (see 2.1.2, 2.1.3, Table 2). From each ecosystem type four different approaches were set-up in order to evaluate the endogenously formed amount of CH₃Cl ('CH₃Cl formation'), the CH₃Cl degradation, the putative inhibition of CH₃Cl degradation by toluene, and the biotic character of the CH₃Cl degradation ('KCN control').

2.3.10. Oxic incubations of the methanol/chloromethane SIP experiment with sieved soil

The utilisation of methanol is often facilitated by its oxidation to formaldehyde [Anthony, 1982], in which the utilisation of CH₃Cl is initiated by a dehalogenation processes [Schäfer *et al.*, 2007]. Thus, different enzymes are necessary to utilise both C1 compounds. However, on the level of formaldehyde both pathways can be merged. In addition, the simultaneous utilisation of methanol and CH₃Cl seems to be common along alphaproteobacterial methylotrophs including the well-characterized *Hyphomicrobium* and *Methylobacterium* strains [McDonald *et al.*, 2001]. Whether methanol-utilising methylotrophs are also utilising CH₃Cl and vice versa was tested in the conducted SIP experiment.

The methanol/chloromethane SIP experiment was a cooperation project. Thus, the incubation of samples and sampling was primarily conducted by Pauline Chaignaud with my support.

For each sampling point (5 points in total) 300 g soil was sieved and equally mixed resulting in a total of 1'500 g sieved soil. The soil was filled into sterile screw-capped natural-rubber-stopped 1 L flask (Glasgerätebau Ochs, Bovenden, Germany; Müller + Krempel, Bülach, Switzerland) and the gas phase was supplemented with 1 % CH₃Cl to preincubate the soil

and activate CH_3Cl -utilising microorganisms in the soil. The preincubation was conducted on an end-over-end shaker at 20°C in the dark. The CH_3Cl concentration was monitored by GC and the preincubation was finished after 2 weeks when no CH_3Cl was detectable anymore.

The preincubated soil was subsequently split to set-up different treatments for the SIP incubation. For each treatment 70 g of activated soil (correspond to ~ 50 ml) was filled into sterile screw-capped natural-rubber-stopped 0.5 L flask (Glasgerätebau Ochs, Bovenden, Germany; Müller + Krempel, Bülach, Switzerland). In total, 8 different treatments were set-up in duplicates and were partly supplemented with ^{12}C - or ^{13}C -isotopologue of methanol or chloromethane in different mixtures (solely methanol, solely chloromethane or both substrates supplemented simultaneously). All treatments were placed on an end-over-end shaker at 20°C in the dark. For an overview on the experimental set-up see Figure 25.

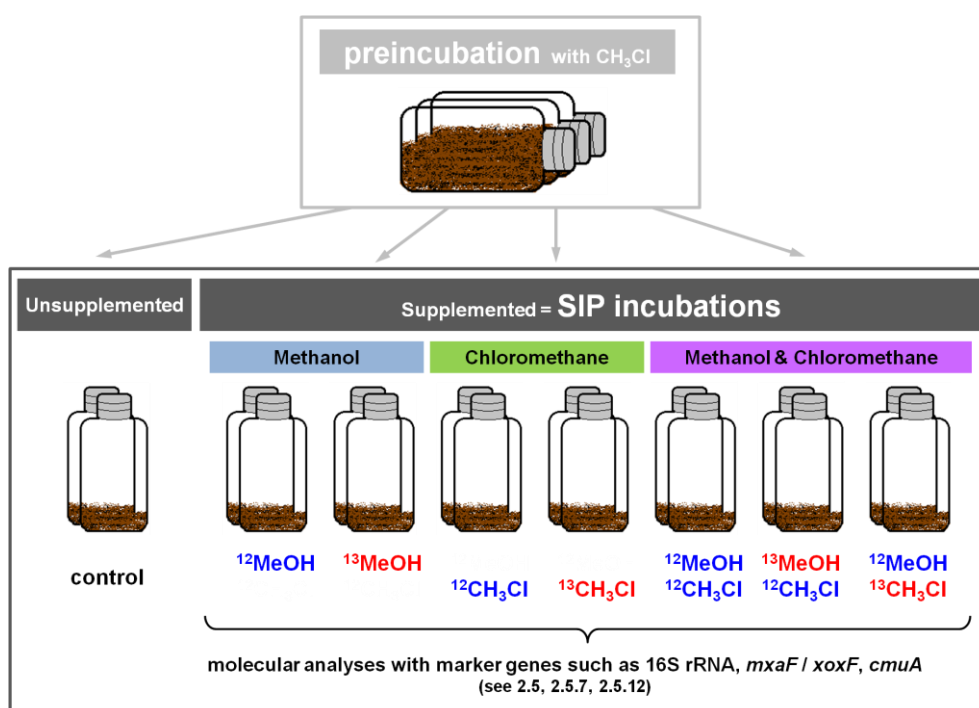


Figure 25 Experimental set-up of the methanol / chloromethane SIP experiment.

Soil was preincubated with CH_3Cl and subsequently split into treatments supplemented with solely methanol (blue box), solely chloromethane (green box) or both substrates simultaneously supplemented (purple box). SIP incubations were conducted with ^{12}C - or ^{13}C -isotopologues of the substrates in different combinations. SIP incubations were further molecular analysed (see 2.4, 2.5.6, 2.5.12.3).

In total, 5 substrate pulses were conducted over a time period of 23 days. Each substrate was pulsed at equal amounts of $216 \mu\text{mol}$ per treatment. Substrates were supplemented if CH_3Cl was no longer detectable in the corresponding approach with CH_3Cl , i.e., treatments with solely one substrate supplemented were processed together and treatments with simultaneously supplemented substrates were processed together. Thus, the time points of pulsing were sometimes divergent.

At each time point of pulsing incubation flasks were opened and allowing to acclimatise before re-sealing. CO_2 and O_2 concentrations were measured every 1 to 2 days to control

oxic conditions. Before each re-opening (= substrate pulse) 5 ml of the gas phases of the [¹³C₁]-methanol treatments were stored in 3 ml exetainer vials (Labco Ltd., High Wycombe, England) for subsequent analysis of ¹³CO₂ formation (see 2.4.3).

Several soil aliquots (0.5 g - 1 g each) for analytical and molecular analysis (see 2.4, 2.5.6, 2.5.12.3) were taken before and after the preincubation as well as before and after substrate supplementations and kept at -80°C. The pH was monitored in all treatments.

2.4. Analytical methods

2.4.1. Determination of pH values

The pH of soil and media was determined by using a pH electrode (U457-S7/110, Ingold, Steinbach, Germany) and a digital pH meter (WTW pH 330, Wissenschaftlich-Technische Werkstätten, Weilheim, Germany). The soil pH was determined in soil slurries.

2.4.2. Dry weight and water content of environmental samples

In order to determine the dry weight of soil samples the weight of sieved soil and dried soil was determined as triplicates. Samples were dried at 60°C for at least 24 h (sometimes several days). Dry weight was determined if the weight remained constant.

The gravimetric water content was determined using the determined fresh and dry weights of a sample. The volumetric water content of a sample was determined using a sampling ring with a defined volume of exact 100 cm³ (≅ total volume of the soil sample).

Equation 2 and Equation 3 were used to calculate the gravimetric and volumetric water contents, respectively.

Equation 2 **Gravimetric water content W_g [%]**

$$W_g = \frac{m_f - m_d}{m_d} \times 100$$

m_f , fresh weight
 m_d , dry weight

Equation 3 **Volumetric water content W_v [%]**

$$W_v = \frac{V_w}{V_t} \times 100$$

V_w , water volume
 V_t , total volume of soil sample (≅ 100 cm³)

2.4.3. Gas chromatography (GC)

The gases CH₄, CH₃Cl, CO₂, and O₂ were analysed via gas chromatography (GC) with Hewlett Packard 5890 Series II gas chromatographs (Hewlett Packard, Palo Alto, CA, USA) using the conditions listed in Table 5.

Table 5 Parameters of GC analyses with Hewlett-Packard 5890 Series II gas chromatographs.

gas	CH ₄	CH ₃ Cl	CO ₂	O ₂
Detector	FID	ECD	TCD	TCD
	Flame ionization detector	Electron capture detector	Thermal conductivity detector	Thermal conductivity detector
Column	Molecular Sieve, 2 m x 1/2''	Poropak Q (80/100), 4 m x 1/8''	Chromosorb 102, 2 m x 1/8''	Molecular Sieve, 2 m x 1/8''
	(Alltech, Unterhaching, Germany)	(Supelco Bellefonte, PA, USA)	(Alltech, Unterhaching, Germany)	(Alltech, Unterhaching, Germany)
Carrier gas	Ar (100%)	Ar : CH ₄ (95% : 5%)	He (100%)	Ar (100%)
<u>Settings:</u>				
Flow rate	40 ml / min	20 ml / min	15 ml / min	33 ml / min
Oven temperature	60°C	120°C	40°C	60°C
Injector temperature	120°C	250°C	150°C	150°C
Detector temperature	150°C	300°C	250°C	175°C
Injection volume	500 µl	500 µl	100 µl	100 µl
Retention time	1.7 min	8 min	2.3 min	1.1 min

The operating principle of the Flame ionization detector (FID) used for CH₄ determination is the detection of free electrons formed during combustion in a hydrogen flame.

The operating principle of the ECD (electron capture detector) used for CH₃Cl determination is based on the ionisation of the carrier gas (Ar) by a radioactive source (⁶³Ni) resulting in a base current. Analyte molecules with a high electron affinity (such as halogenated compounds) reduce this base current by capturing the electrons. These changes of the base current are detected by the ECD.

The operating principle of the TCD (thermal conductivity detector) used for CO₂ and O₂ determination is based on changes of the thermal conductivity between a measuring cell perfused by the pure carrier gas and a measuring cell perfused by the carrier gas mixed with the analyte molecules. Changes in the measuring gas composition cause temperature changes in the measuring cells.

All gas samples were taken with sterile syringes and flushed with 100 % argon before each measurement or sampling from the incubation treatments. Signals of the GC were transformed by Knauer IF2 (Knauer, Berlin, Germany) integrator and the gas concentrations were finally quantified using the software EuroChrom (Version V3.05, Knauer, Berlin, Germany) and external standards. The over pressure in each incubation flask was always measured directly before each sampling with a digital precision manometer (GHM 3111, GHM Messtechnik GmbH, Regenstauf, Germany). For gas samples stored in exetainer vials (Labco Ltd., High Wycombe, England) always the overpressure of the incubation flask and not of the vial was used for calculations of gas concentration.

The total concentration of gases was calculated in consideration of the concentrations of gases in the gas and in the liquid phase, the volume of the gas and the liquid phase in the incubation flasks, the ambient pressure (measured with a barometer (Barogeber, 946...1053 hPa, ThiesClima, Gottingen, Germany)), the overpressure in the incubation flasks, the temperature at the time of sampling, the pH and solubility coefficients of the gases. For the calculation of total gas amounts the following Equation 5 - Equation 9 were used based on the ideal gas law (Equation 4). The total concentration of gases is the sum of the amounts gases in the gas phase (n_g) and in the liquid phase (n_p , physically dissolved; n_c , chemically dissolved). Only for CO₂ the amount of chemically dissolved gas was calculated (Equation 9). The total amount of gases in the gas phase (n_g) was calculated using Equation 6. The total amount of gases physically dissolved in the liquid phase (n_p) was calculated using Equation 8, and the total amount of CO₂ chemically dissolved in the liquid phase (n_c) was calculated using Equation 9.

Equation 4 **Ideal gas law**

$$p \times V = n \times R \times T$$

p , pressure;
 V , volume;
 n , amount of substance;
 R , gas constant (83,145 (mbar·ml) x (mmol·K)⁻¹);
 T , absolute temperature

Equation 5 **Total amount of gases n_t [mmol]**

$$n_t = n_g + n_p (+ n_c)$$

Equation 6 **Amount of gases in the gas phase n_g [mmol]**

$$n_g = V_g \times \left(\frac{C}{V_{mol}} \right) \times \left(\frac{p_a + p_o}{p_a} \right)$$

V_g , volume of the gas phase in the incubation flask [ml]
 C , concentration of the gas referred to 1
 V_{mol} , molar volume of the gas under current conditions [ml/mmol] (see Equation 7)
 p_a , current atmospheric pressure [mbar]
 p_o , over pressure in the incubation flask [mbar]

Equation 7 Molar volume V_{mol} of the gas under current conditions [ml/mmol]

$$V_{mol} = R \times \frac{T}{p_a}$$

R , gas constant (83,145 (mbar·ml) x (mmol·K)⁻¹);
 T , absolute temperature [K]
 p_a , current atmospheric pressure [mbar]

Equation 8 Amount of gases n_p physically dissolved in the liquid phase [mmol]

$$n_p = V_l \times \left(\frac{C}{V_{mol}} \right) \times \left(\frac{p_a + p_o}{p_a} \right) \times \alpha$$

V_l , volume of the liquid phase in the incubation flask [ml]
 C , concentration of the gas referred to 1
 V_{mol} , molar volume of the gas under current conditions [ml/mmol] (→ see equation 6)
 p_a , current atmospheric pressure [mbar]
 p_o , over pressure in the incubation flask [mbar]
 α , solubility coefficients of the gases, see Table 6

Equation 9 Amount of gases n_c chemically dissolved in the liquid phase [mmol]

$$n_c = n_p \times 10^{(pH - pKa)}$$

n_p , amount of gases physically dissolved in the liquid phase [mmol]
 (→ see Equation 8)
 pH , pH of the liquid phase
 pKa , logarithmic acid dissociation constant for bicarbonate (6.37 at 25°C)

The solubility coefficients of the gases CH₄, CO₂ and O₂ are the dimensionless Bunsen solubility coefficients (α) taken from Blachnik, 1988. For CH₃Cl no α value was available, thus a comparable approximate value was calculated based on the equation for α (Equation 10) and the solubility of CH₃Cl in water (see Table 6).

Equation 10 Bunsen solubility coefficient α at standard conditions*

$$\alpha = \frac{V_G}{V_L}$$

V_G , volume of dissolved gas [ml]
 V_L , volume of the solution [ml]

*standard conditions: 273,15 K; 1,01325 bar

Table 6 Calculation basis values for a solubility coefficient value for CH₃Cl.

gas	CH ₃ Cl	CH ₄	CO ₂
Solubility in water ^a	5.32 g/L (25°C)	22 mg/L (25°C)	1.7 g/L (20°C)
Density at 0°C ^b	2.31 g/L	0.72 g/L	1.98 g/L
Calculated α	2.303	0.0307	0.8585
determined α (20°C)	-	0.032	0.85

[Blachnik, 1998]

^a Values taken from: <https://www.ncbi.nlm.nih.gov/pccompound>; applicable temperature in brackets^b Values taken from: <http://www.dguv.de/ifa/gestis/gestis-stoffdatenbank/index.jsp>

2.4.4. Gas chromatography–mass spectrometry (GC-MS)

For the determination of [¹³C]-CO₂ in the gas samples from all SIP incubations (see 2.3.3, 2.3.4, 2.3.10) gas samples were stored in exetainer vials (Labco Ltd., High Wycombe, England) and measured at the Department of Molecular Systems Biology, UFZ – Helmholtz Centre for Environmental Research in Leipzig (Germany).

The [¹³C]-CO₂ determination was performed using a Perkin–Elmer GC Clarus 600 system with an Rtx®-1 capillary column (60 m x 320 μ M). For GC-MS detection, an electron ionization system was operated with an ionization energy of 70 eV. Mass spectra were taken from 14 to 70 Da. Helium was used as carrier gas at a constant flow of 300 kPa, and an injection volume of 10 μ l (split ratio 10:1) was administered manually using a gastight syringe. Each sample was measured five times. The total amount of [¹²C]-CO₂ and [¹³C]-CO₂ was analysed by the extraction of m/z values 44 and 45 followed by peak integration. The peak areas were corrected with [¹²C]-CO₂ and [¹³C]-CO₂ indoor air values, and finally, the ratio of the m/z values 45/44 was calculated.

2.4.5. High performance liquid chromatography (HPLC)

The concentrations of acetate, sugars, and vanillic acid in the microcosm experiments were measured by high performance liquid chromatography (HPLC) under the conditions listed in Table 7. The operating principle of the universal RID (refractive index detector) is based on the comparison of the refractive index of the pure mobile phase with the refractive index of the mobile phase mixed with the investigated sample. The operating principle of the DAD (diode array detectors) is based on the absorption spectrum of the analyte molecule in the sample. The identity and purity of the substrate was additionally verified by the absorption spectrum ranging from 210 – 350 nm (see Figure 26). The absorption at 264 nm was used for the quantification of vanillic acid in the samples.

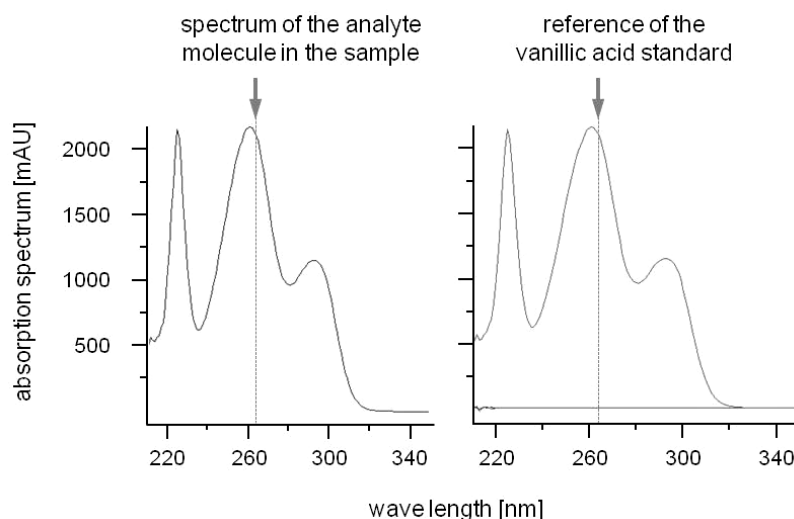


Figure 26 Absorption spectrum of vanillic acid in the sample and from the standard detected by HPLC with a DAD.

The absorption maximum at 264 nm (arrow) was used to quantify the concentration of vanillic acid in samples.

Table 7 Parameters of HPLC analyses.

Compounds	Acetate and Sugars	Vanillic acid
HPLC	Hewlett-Packard 1090 series II Hewlett Packard, Paola Alto, CA, USA	Agilent 1200 Series HPLC Agilent Technologies, Böblingen, Germany
Detector	RID Agilent 1200 Infinity Refractive Index Detector RID G1362A (Agilent Technologies, Böblingen, Germany)	DAD Agilent 1200 Infinity Diode Array Detectors DAD G1315D (Agilent Technologies, Böblingen, Germany)
Separation processes	ion exclusion	reverse phase
Pre-column	Security Guard Cartridge, suitable for 7.8 mm ID column, 50 x 7.8 mm	ZORBAX SB-C18, UHPLC guard column, 2.1 mm x 5 mm, 1.8 µm
Column	Rezex ROA Organic Acid H+ (8%), 300 x 7.8 mm (Phenomenex, Torrance, CA, USA)	ZORBAX Rapid Resolution HT SB-C18, 2.1 x 50mm, 1.8µm (Agilent Technologies, Böblingen, Germany)
Flow rate	0.8 ml / min	1 ml / min
Mobile phase	4 mM phosphoric acid solution	20 mM sodium acetate (pH 3) – 50% acetonitrile buffer
Oven temperature	60°C	30°C
Injection volume	20 µl	50 µl

Soil slurry samples used for HPLC analyses were always collected in sterile microcentrifuge tubes and kept at -20°C. Before the HPLC analyses were performed the frozen samples were prepared by centrifugation for 10 min at 13'000 × g (1-15K Sartorius microcentrifuge, Sigma Laborzentrifugen, Osterode am Harz, Germany). The aqueous supernatant was transferred into sterile tubes and diluted if necessary, i.e., slurry samples before the substrate pulses were assumed to show low substrate concentrations, and thus, these samples were not diluted. Subsequently samples were filtered (pore size 0.2 µM, nylon filter, Infocroma, Zug, Switzerland) into butyl rubber stopped aluminium crimp sealed HPLC glass vials. Samples were stored at 4°C for several days in order to repeat measurements. For all samples of vanillic acid treatments and corresponding standards vial, which are insensitive to light (brownish glass vials) were used.

External standards with known concentrations were used to identify and quantify the different compounds. Additionally, in each HPLC analytical run defined substrate standards were also measured in order to evaluate possible fluctuations of the retention time or concentration.

2.5. Molecular methods

2.5.1. Co-extraction of nucleic acids

Nucleic acids from soil slurry and sieved soil aliquots were extracted followed a modified protocol of Griffiths and colleagues [Griffiths *et al.*, 2000]. Each extraction was conducted in 2 ml screw-capped tubes (VWR International) with approximately 0.5 g of soil slurry / sieved soil. Equal amounts of extraction buffer (5% CTAB, 0.35 M NaCl, 120 mM potassium phosphate buffer, pH 8), phenol / chloroform / isoamyl alcohol (25:24:1), and zirconia/silica beads (0.5 g of Ø 0.5 mm beads and 0.5 g of Ø 0.1 mm beads; BioSpec, Bartlesville, OK, USA) were added and cells were disrupted by bead-beating (speed of 5.5 m s⁻¹ for 30 s in a FastPrep FP120 bead beater (Thermo Savant, Holbrook, NY, USA)). Immediately samples were chilled on ice for 2 minutes and subsequently centrifuged (5 min at 14'000 x g, 4°C, 1-15K Sartorius microcentrifuge) to separate liquid phase (containing nucleic acids) from the solid phase. The supernatant was carefully transferred without displacing the white interface onto the solid phase (containing fragmented cells and proteins) and mixed with the same amount of chloroform / isoamyl alcohol (24:1). Tubes were vigorously mixed several times over 5 minutes and subsequently centrifuged (5 min at 14'000 x g, 4°C) to separate the nucleic acids from residual proteins, humic acids and phenol. If the supernatant was still brownish, this washing step with chloroform / isoamyl alcohol was repeated. Nucleic acids in the supernatant were precipitated with the double volume of precipitation buffer (0.1 M HEPES pH 7 - 30% PEG; Fluka, Neu-Ulm, Germany) and mixed vigorously. Precipitation was done with clear solutions (i.e., no turbidity, colourless to brownish colour possible) for 2.5 h at room temperature. After a centrifugation step (15 min at 21'000 x g, 4°C) to pelletize nucleic acids, the supernatant was discarded and the pellet was washed 2 times with ice cold

ethanol (70 %) to remove salt residues. After washing the pellets were dried at room temperature and resuspended in 30 - 50 µl PCR-H₂O (distilled water (DNase/RNase free) from gibco (Paisley, United Kingdom)) by heating for 2 min at 65°C.

2.5.2. Enzymatic digestion of RNA and DNA after extraction

In order to separate DNA and RNA after coextraction (see 2.5.1) enzymatic digestions were conducted. RNA was removed with RNase A (10 µg µl⁻¹, Fermentas, St. Leon-Roth, Germany) and DNA was removed with DNase I (1 U µl⁻¹, Fermentas). The composition of both digestion approaches is listed in Table 8. Both enzymatic digestions were stopped by the precipitation with isopropyl alcohol of nucleic acids (see 2.5.3.2).

Table 8 Composition of the enzymatic digestion reactions after coextraction.

<u>RNA digestion</u>		<u>DNA digestion</u>	
1 Vol	extract of nucleic acids	1 Vol	extract of nucleic acids
0.05 Vol	RNase ^a	0.125 Vol	10x reaction buffer ^a
		0.033 Vol	DNase ^a

^a chemicals from Fermentas, St. Leon-Roth, Germany

2.5.3. Purification and precipitation of nucleic acids

2.5.3.1. Approach with polyethylene glycol and glycogen

This precipitation was mainly conducted after the fractionation of SIP gradients (see 2.5.6, 2.5.6.2). Mainly half of a fraction (i.e., 225 µl) was used for precipitation and the other half was stored as back-up. The precipitation was conducted by adding 2 volumes of 30 % PEG solution (see 2.2.6) and 0.02 volumes of glycogen (10 mg ml⁻¹; glycogen from bovine liver, Fluka, Steinheim, Germany) to the fraction. Glycogen acts as a carrier for small amounts of DNA and is necessary to ensure the almost complete recovery of DNA. The precipitation was incubated for 2.5 h at room temperature and DNA was pelletized by centrifugation (21'000 x g, 20 min, 4°C). Pellets were washed with ice cold ethanol (70 %), subsequently dried at room temperature, and dissolved in PCR-H₂O (distilled water (DNase/RNase free) from gibco (Paisley, United Kingdom)). In the case of 225 µl starting volume of a fraction, DNA was finally resolved in 10 µl PCR-H₂O.

2.5.3.2. Approach with isopropyl alcohol and sodium chloride

This precipitation was mainly conducted after enzymatic digestions (see 2.5.2, 2.5.11). The precipitation of 1 volume of nucleic acid extract was conducted with 0.7 volume of ice cold

isopropyl alcohol and 0.1 volume of sodium chloride (5 mM) at -20°C for at least 12 h [Green & Sambrook, 2012]. Nucleic acids were pelleted by centrifugation (60 min, 21'000 x g, 4°C). Pellets were washed with ice cold ethanol (70 %), subsequently dried at room temperature, and dissolved in 20 µl PCR-H₂O (distilled water (DNase/RNase free) from gibco (Paisley, United Kingdom)).

2.5.4. Quantification of nucleic acids

2.5.4.1. Spectrophotometry (via NanoDrop™)

The quantity and quality of extracted nucleic acids (see 2.5.1) and amplicons (see 2.5.7) was determined spectrophotometrically with a ND-1000 (NanoDrop Technology, Wilmington, NC, USA). 2 µl of extracts were used to measure the absorption 'A' at 230, 260, and 280 nm wavelength. Nucleic acids absorb mainly at 260 nm. Proteins, phenols or other contaminants absorb at 280 nm and humic acids may absorb at 230 nm [Tsutsuki & Kuwatsuka, 1979]. Assessing the purity of DNA and RNA the ratio A₂₆₀/A₂₈₀ is used. A ratio of 1.8 is indicative for pure DNA a ratio 2.0 is indicative for pure RNA extracts without massive contaminations of proteins or phenols [Sambrook & Russell, 2001]. The ratio A₂₆₀/A₂₃₀ is a secondary measure of purity and should be in a range of 2 - 2.2. Lower values are indicative for contaminations by humic acids.

Reference, if not clearly mentioned: <http://www.nanodrop.com>

2.5.4.2. Fluorescence-based quantification (via PicoGreen®)

A more sensitive quantification method that is less vulnerable to interferences by contaminants was used to quantify low amounts of DNA (see 2.5.6, 2.5.8.2, 2.5.11). The Quant-iT-PicoGreen dsDNA (Invitrogen, Carlsbad, CA, USA) reagent is an ultra sensitive fluorescent nucleic acid stain for double-stranded DNA (dsDNA) and might quantitate as little as 25 pg mL⁻¹ of dsDNA. The quantification was done followed by the manufacturer's protocol in microtiter plates. The fluorescence was measured with a FLx800 Microplate fluorimeter (BioTek, Bad Friedrichshall, Germany) and DNA concentrations were evaluated with external DNA standards delivered by the manufacturer and the software Gen5 (BioTek).

2.5.5. Agarose gel electrophoresis

Agarose gel electrophoresis was used to visualize nucleic acid extracts (see 2.5.1) and PCR products (see 2.5.7) and for the purification of PCR products by gel extraction (see 2.5.9.1).

For the visualization the gels were prepared with 1 % w/v low EEO standard agarose (AppliChem GmbH, Darmstadt, Germany) and 1 × TAE buffer (40 mM Tris-HCl, 20 mM acetate, 1 mM EDTA, pH 8). The mixture was heated (microwave) until the agarose was completely melted. After chilling to approximately 60°C the fluid mixture was supplemented with ethidium bromide (3,8-diamino-5-ethyl-6-phenyl-phenanthridium bromide, BioRad) to a

final concentration of 0.08 mg ml⁻¹ and poured into gel tray allowing to harden. Samples (3 - 10 µl) were prepared with 0.2 volumes 6x loading dye (0.05 % bromophenol blue, 0.05 % xylene cyanol, 55 % glycerin) and transferred into gel slots. Additionally, several slots were filled with molecular weight marker (MWM 1, Bilatec, Viernheim, Germany). Electrophoresis was performed in migration chambers (BioRad Mini- or Maxi-Sub cell, BioRad) filled with 1 × TAE buffer for 20 - 60 min at 80 - 120 V (Power-Pak 3000, BioRad). Gels were visualized by UV light (302 nm, Transilluminator UVT-20M, Herolab GmbH, Wiesloch, Germany) and photographed with a Canon PowerShot G5 camera (Canon, Krefeld, Germany).

Gel electrophoresis for purification was prepared in the same manner as for the visualization with the exception of lower concentrated gels, i.e., 0.8 % w/v low EEO standard agarose (AppliChem GmbH, Darmstadt, Germany) and 1 × TAE buffer (40 mM Tris-HCl, 20 mM acetate, 1 mM EDTA, pH 8) were mixed. The running buffer was 1 × TAE buffer (40 mM Tris-HCl, 20 mM acetate, 1 mM EDTA, pH 8) and the running time was always 60 min at 80 V.

2.5.6. 16S rRNA-based stable isotope probing with DNA

The stable isotope probing (SIP) technique is an elegant method to circumvent the focused enrichment, cultivation and isolation of microorganisms responsible for substrate turnovers in environments. The technique also enables the detection of uncultivable or low abundant organism by labelling them with stable isotopes. In general, each SIP starts with the incubation of a sample with a [¹³C_n]-substrate and relies on its assimilation and incorporation by subsets of microorganisms resulting in 'heavy' cell molecules such as nucleic acids. The buoyant density (BD) of DNA enriched by ¹³C-isotopes is higher than the BD of unlabelled DNA (contains only ¹²C-isotopes) enabling the separation of labelled and unlabelled DNA by density gradient centrifugation. Subsequently, the separated DNA is the basis of molecular analyses based on gene markers allowing the characterisation and phylogenetic affiliation. In addition, the comparison of labelled and unlabelled DNA as well as the comparison of ¹³C-incubations with ¹²C-incubations enables the detection of labelled organisms. A schematic overview of SIP is shown in

Figure 27, and for more information on SIP see also Radajewski *et al.*, 2000; Lueders *et al.*, 2004; Friedrich *et al.*, 2006; Neufeld *et al.*, 2006. In this work several DNA SIP experiments were performed with forest soil samples in order to estimate the multi-carbon substrate range of methanol-utilising methylotroph (see 2.3.3), the impact of pH on these methanol-utilising methylotrophs (see 2.3.4) and to reveal methanol- and chloromethane-utilisers and their congruent utilisation of these C1-substrates (see 2.3.10). All SIP experiments were performed after the SIP protocol of Neufeld *et al.*, 2007 (partly modified).

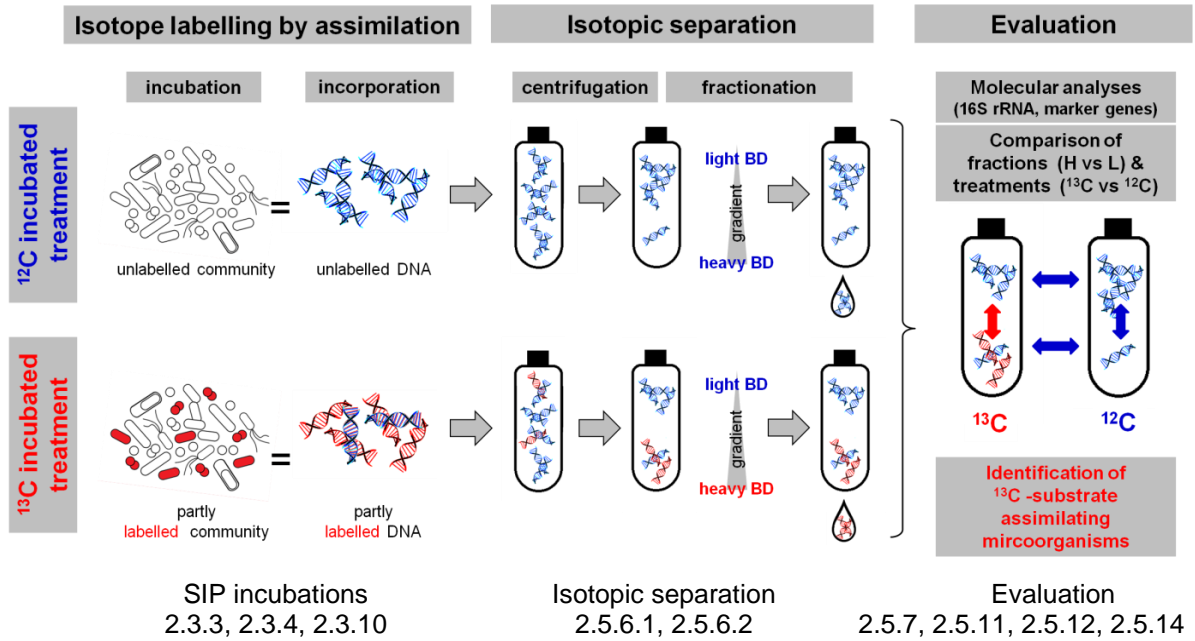


Figure 27 Schematic overview of SIP experiment procedures.

Environmental samples need to be incubated with ^{13}C -isotopologues finally enabling the identification of microorganism. The overview exemplified DNA SIP and was inspired by Friedrich *et al.*, 2006.

2.5.6.1. Density gradient centrifugation of DNA and fractionating of the gradient

Extracted and RNA-free (see 2.5.1, 2.5.2) DNA from the SIP experiment treatments (including ^{13}C - and corresponding ^{12}C -treatments, see 2.3.3, 2.3.4, 2.3.10) were used. In order to identify labelled phylotypes (see 2.5.14) and compare different treatments DNA samples from the beginning (t_0) and after incubation were used. DNA from each treatment replicate and each extraction replicate (i.e., duplicated treatments and duplicated extraction resulting in 4 DNA aliquots in total) was pooled in equal parts (see Table 9) to a final volume of 20 μl and was added to CsCl-containing gradient solutions (see 2.2.6).

Table 9 Amount of applied DNA of different SIP experiments to separate unlabelled and labelled DNA in isopycnic centrifugation.

SIP experiment	applied DNA	treatment (^{12}C - and ^{13}C -isotopologue)
Substrate SIP	5 μg	t_0 , glucose, xylose vanillic acid
	10 μg	methanol & acetate
pH shift SIP	10 μg	all
methanol/chloromethane SIP	5 μg	all

Independent centrifugation runs were conducted for substrate SIP, pH SIP and methanol/chloromethane SIP experiments. Comparability was still given due to gradient solutions (see 2.2.6) with a density of $1.732 \pm 0.0006 \text{ g ml}^{-1}$ used for all runs as well as the isopycnic centrifugation of corresponding DNA from ^{12}C - and ^{13}C -isotopologues treated samples of corresponding treatments (i.e., DNA derived from $[^{12}\text{C}]$ - and $[^{13}\text{C}_1]$ -methanol incubations were subjected to the same centrifugation run, and so forth). In each run an unloaded gradient was carried along for the determination of the buoyant densities of the resulting fractions (see 2.5.6.2).

2.5.6.2. Separation of 'heavy' (H), 'middle' (M) and 'light' (L) DNA by fractionation

After isopycnic centrifugation (see 2.5.6.1) each gradient was fixed vertically in a rag and separated into 11 fractions (450 μl each). The fractionation was performed using a low-flow peristaltic pump (Econo Pump 1, Biorad, Hercules, USA) generating a continuous flow. A sterile needle (23G \times 1") connected to the pump via a silicon tube (1.6 mm inner diameter) and already filled with 'overlying solution' (see 2.2.6) was pierced into the top of the tube underneath the black plug (see Figure 28), and a second needle (23G \times 1") was used to pierce a second hole into the bottom of the tube. Fractionation was done by pumping the 'overlay solution' at a flow rate of 0.45 ml min^{-1} through the tube and collecting the fractions drop-wise in separate tubes.

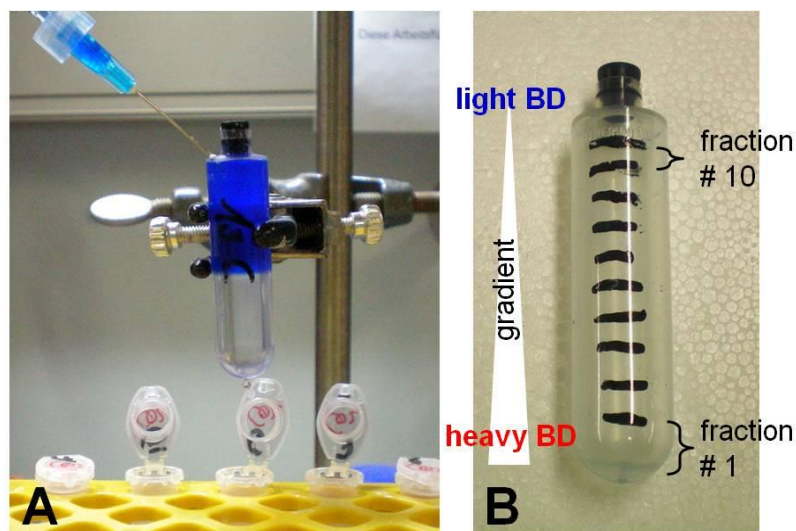


Figure 28 Fractionation of a gradient.

The fractionation of a gradient was done by pumping 'overlay solution' (blue) through the tube and collecting the fraction drop-wise in separate tube (A). In total 11 fractions a 450 μl were achieved, in which only fraction 1 – 10 were used for analyses and the uppermost fraction 11 was always rejected (B).

In order to determine the density gradient along the tube fractions the unloaded gradients were used. The buoyant density of each fraction was determined by repeated weighing of 100 μl per fraction at 20°C (at least 10 measured values). For the substrate SIP experiments gradients loaded with DNA for bacterial analyses (see 2.5.7.6, 2.5.12.2, 2.5.13.1) ranged in general from $1.750 \pm 0.003 \text{ g ml}^{-1}$ to $1.697 \pm 0.007 \text{ g ml}^{-1}$ and for fungal analyses (see 2.5.7.6, 2.5.12.2, 2.5.13.1) from $1.750 \pm 0.004 \text{ g ml}^{-1}$ to $1.696 \pm 0.004 \text{ g ml}^{-1}$. For the pH shift SIP experiment gradients ranged in general from $1.744 \pm 0.004 \text{ g ml}^{-1}$ to $1.699 \pm 0.004 \text{ g ml}^{-1}$. For the methanol/chloromethane SIP experiment gradients ranged in general from $1.747 \pm 0.004 \text{ g ml}^{-1}$ to $1.700 \pm 0.002 \text{ g ml}^{-1}$.

Fractions 1 to 10 were used for DNA precipitation and further analyses. The DNA was precipitated with glycogen (10 mg ml^{-1}) and polyethylenglycol (see 2.5.3.1) and quantified with Quant-iT-Pico Green (Invitrogen, Carlsbad, CA, USA) (see 2.5.4.2).

Fractions 1 to 10 were separately pooled into 'heavy' (i.e., all fractions with a buoyant density $\geq 1.730 \text{ g ml}^{-1}$), 'middle' (i.e., all fractions with a buoyant density between 1.730 and 1.715 g ml^{-1}), and 'light' (i.e., all fractions with a buoyant density $\leq 1.715 \text{ g ml}^{-1}$) fractions. This was in agreement with reported buoyant densities for non-labelled native DNA (i.e., $1.69 - 1.725 \text{ g ml}^{-1}$ [Carter *et al.*, 1983; Lueders *et al.*, 2004]) and the comparison of T-RFLP patterns of all fractions of [^{12}C]- and [$^{13}\text{C}_1$]-methanol treatments (see 3.6.2).

2.5.7. Polymerase chain reaction (PCR)

The polymerase chain reaction (PCR) is used to directly amplify DNA. By utilising specific primers DNA fragments of interest can be replicated and thus, even low amounts of DNA are analysable. Each PCR is structured in repeating cycles including denaturation of template DNA, annealing of primers and elongation by heat-stable DNA-polymerases [Chien *et al.* 1976, Saiki *et al.*, 1988, Lewin, 1998].

All PCR reactions were always set up on ice in either single or 8-stripes 0.2 ml PCR tubes or 96 well plates (all PCR clean; Eppendorf, Hamburg, Germany; AHN Biotechnology, Nordhausen, Germany; Sorenson Bioscience, Murray, USA). All PCRs performed at the University of Bayreuth were conducted in a SensoQuest labcycler (SensoQuest GmbH, Göttingen, Germany). Before each PCR started lids and heating blocks of the thermocyclers were preheated to 95°C to prevent unspecific reactions (= 'heat start PCR'). Several different PCR conditions for the different target gene fragments were tested, but only conditions that resulted in amplicons are mentioned here.

2.5.7.1. Primers

The total bacterial community was mainly analysed with a universal 16S rRNA-specific primer pair (341f and 785/805r) that was proposed to reveal the best overall coverage and phylum spectrum and is assumed to reduce the bias in diversity studies [Klindworth *et al.*, 2013]. For the T-RFLP analysis (see 2.5.11) longer amplicons were needed, wherefore another universal primer pair was used (27F and 907r). In addition, the forward primer was labelled with a fluorescent dye.

The methanol-utilising microorganisms were targeted by the amplification of the marker genes *mxoF* and *xoxF* that encodes for subunits of different types of PQQ-methanol dehydrogenases [Chistoserdova, 2011]. The primer pairs of *mxoF/xoxF I* were assumed to target both marker genes without any bias against one of these genes. However, a revision revealed that the primers bias against *xoxF* (pers. communication P. Chaignaud and F. Bringel). Thus, new designed primers targeting also *xoxF* were used in further study concerning methanol-utilisers (*mxoF/xoxF II*).

The chloromethane-utilising organisms were targeted by the amplification of the marker gene *cmuA* encoding for a subunit of the unusual bifunctional methyltransferase/corrinoid-binding enzyme catalysing the initial step of CH₃Cl utilisation [Studer *et al.*, 2001; McDonald *et al.*, 2002; Schäfer *et al.*, 2005].

Methanotrophic microorganisms were targeted by the amplification of the *pmoA* gene that encodes a region around the active site of the particulate methane monooxygenase (pMMO) [Holmes *et al.*, 1995; Costello & Lidstrom, 1999; Bourne *et al.*, 2001]. Although two distinct types of MMOs exist (i.e., pMMO and sMMO, soluble methane monooxygenase), the pMMO is present in almost all methanotrophs, wherefore targeting *pmoA* is assumed to cover a higher diversity of methanotrophs. However, the marker gene *mmoX* encoding for the active site of the subunit of the sMMO was also targeted, since some methanotrophs such as *Methylocella* or *Methyloferula* species only possess the sMMO [Dedysh *et al.*, 2000; Dunfield *et al.*, 2003; Dedysh *et al.*, 2004; Vorobev *et al.*, 2011]. Besides the well known methane monooxygenase marker genes *pmoA* and *mmoX*, the enigmatic gene *pxmA* was also targeted in this study. It is a homolog of *pmoA* and might play a role in methylotrophic metabolism. However, its function remains still unknown, but it seems to be widespread in nature contributing to a group of '*pmoA/amoA* like' gene sequences [Tavormina *et al.*, 2011; Knief, 2015].

The total fungal community was analysed by targeting the internal transcribed spacer region (ITS) within the rRNA that can easily amplified with universal ITS primer and serves as a marker of choice to explore the fungal diversity in environmental samples [Schoch *et al.*, 2012; Kõljalg *et al.*, 2013]. The fungal ITS region covers 600 - 800 bp and is thus often variable among different and distinct fungal species allowing for differentiation and affiliation [Gardes & Bruns, 1993; Hibbett *et al.*, 2011]. The in this study applied ITS primer pair (ITSF1 and ITS4) strongly supports the amplification of *Ascomycetes* and *Basidiomycetes* and

biases against plants or other eukaryotic organism because of the more specific forward primer [Gardes & Bruns, 1993].

Amplicons that were used for pyrosequencing were amplified in a two-step PCR approach including a PCR with the conventional primer set (step-1-PCR) followed by a PCR with barcoded fusion primers (step-2-PCR) [Berry *et al.*, 2011]. Barcoded primers (i.e., conventional primers including an oligonucleotide at the 5'-end) were necessary to re-identify amplicons in a multiplex sequencing and create different pyrosequencing libraries. Barcodes for the different experiments are listed in the appendix (Table A 1 & Table A 2). Barcoded fusion primers also include adaptor sequences that are necessary for the binding to capture beads before the emulsion PCR step of pyrosequencing (see Table 10).

Table 10 Structure of the barcoded fusion primers used for amplicon pyrosequencing.

fusion primer structure (5' – 3')			
adaptor sequence^a	key	barcode^b	gene specific primer^c
forward fusion primer			
CCATCTCATCCCTGCGTGTCTCCGAC	TCAG	NNNNNNN (6 or 10 bp)	'conventional' primer
reverse fusion primer			
CCTATCCCCTGTGTGCCTTGGCAGTC	TCAG		'conventional' primer

^a Adaptor sequences are provided by Roche (Mannheim, Germany). Forward fusion primer contains adaptor sequence A, reverse fusion primer contains adaptor sequence B.

^b Barcode sequences are given in Table A 1 for bacterial genes and Table A 2 for fungal genes and were used to create amplicon libraries and assign sequences to different samples.

^c Primer sequences of gene specific primers are given in Table 11. Forward fusion primer were constructed with the 'conventional' forward primer (bacterial genes) and the 'conventional' reverse primer (fungal bacterial genes), respectively. Reverse fusion primer were constructed with the 'conventional' reverse primer (bacterial genes) and the 'conventional' forward primer (fungal bacterial genes), respectively.

This table has been published in Morawe *et al.* 2017.

Table 11 Primer sequences of ‘conventional’ primers used to amplify 16S rRNA, *mxoF/xoxF*, *cmuA*, *pmoA*, and ITS gene fragments.

gene	primer ^a	sequence (5' – 3') ^b	amplicon	reference
16S rRNA	341f	(17 bp) CCT ACG GGN GGC WGC AG	444 –	Muyzer <i>et al.</i> , 1993
	785/805 r	(21 bp) GAC TAC HVG GGT ATC TAA TCC	464 bp	Herlemann <i>et al.</i> , 2011
	27F ^c	(18 bp) AGA GTT TGA TCM TGG CTC	900 bp	Lane, 1991
	907rm	(20 bp) CCG TCA ATT CMT TTG AGT TT		Lane, 1991
<i>mxoF/xoxF I</i>	<u>‘mxoF1’</u>		552 bp	McDonald & Murrell 1997 Neufeld <i>et al.</i> , 2007
	1003f	(21 bp) GCG GCA CCA ACT GGG GCT CGT		
	1555r	(21 bp) CAT GAA BGG CTC CCA RTC CAT		
	<u>‘mxoF2’</u>		455 bp	Moosvi <i>et al.</i> , 2005 Moosvi <i>et al.</i> , 2005
mxoF_for	(19 bp) TGG AAC GAG ACC ATG CGT C			
maxF_rev	(20 bp) CAT GCA GAT GTG GTT GAT GC			
<i>mxoF/xoxF II</i>	<u>‘MDH1’</u>		450 bp	Chaignaud, 2016 Chaignaud, 2016
	MDH_for1	(18 bp) GCG GIW SQA ICT GGG GYT		
	MDH_rev	(21 bp) GAA SGG YTC SYA RTC CAT GCA		
	<u>‘MDH2’</u>		450 bp	Chaignaud, 2016 Chaignaud, 2016
MDH_for2	(18 bp) GCG GIW SGA ICT GGG GYT			
MDH_rev	(21 bp) GAA SGG YTC SYA RTC CAT GCA			
<i>cmuA I</i>	cmuA802f	(23 bp) TTC AAC GGC GAY ATG TAT CCY GG		Miller <i>et al.</i> , 2004
	cmuA1609r	(21 bp) TCT CGA TGA ACT GCT CRG GCT	800 bp	Miller <i>et al.</i> , 2004
	cmuA1802r	(17 bp) TTV GCR TCR AGV CCG TA	1000 bp	Nadalig <i>et al.</i> , 2011
<i>cmuA II</i>	<u>‘cmuA-NGS’</u>		422 bp	Chaignaud, 2016 Chaignaud, 2016
	cmuAf422	(20 bp) GAR GTB GGI TAY AAY GGH GG		
cmuAr422	(23 bp) TCR TTG CGC TCR TAC ATG TCI CC			
<i>pmoA</i>	A189f	(18 bp) GGN GAC TGG GAC TTC TGG		Holmes <i>et al.</i> , 1995
	A682r	(18 bp) GAA SGC NGA GAA GAA SGC	525 bp	Holmes <i>et al.</i> , 1995
	A650r	(17 bp) ACG TCC TTA CCG AAG GT	500 bp	Bourne <i>et al.</i> , 2001
	mb661rm	(19 bp) CCG GMG CAA CGT CYT TAC C	470 bp	Costello & Lidstrom, 1999
<i>pxmA</i>	novelmo634r ^d	(22 bp) CTA TGA TGC GCA GAT ATT CTG G	500 bp	Tavormina <i>et al.</i> , 2008
<i>mmoX</i>	mmoX206f	(20 bp) ATC GCB AAR GAA TAY GCS CG	719 bp	Hutchens <i>et al.</i> , 2004
	mmoX886r	(20 bp) ACC CAN GGC TCG ACY TTG AA		Hutchens <i>et al.</i> , 2004
ITS	ITS1F	(22 bp) CTT GGT CAT TTA GAG GAA GTA A	700 –	Gardes & Bruns, 1993
	ITS4	(20 bp) TCC TCC GCT TAT TGA TAT GC	900 bp	White <i>et al.</i> , 1990

^a Primer notation according to the reference with primer length in brackets. ‘f’ or ‘F’ indicate the forward primers that are listed at first.

^b Primer sequence with wobble bases in bold faces.

^c Primer was labelled with the infra-red dye IRD700 at the 5' end.

^d in combination with the forward primer ‘A189f’

2.5.7.2. PCR approaches to amplify *pmoA*

The methanotrophic marker gene *pmoA* was amplified using different primer sets (see Table 11). As observed by Bourne and colleagues, each primer set reveal biases when applying in soils. The primer set A189f/A682r [Holmes *et al.*, 1995] targets *pmoA* as well as *amoA* sequences of ammonia-oxidizing nitrifiers. The primer sets A189f/A650r and A189f/mb661r are not targeting *amoA* sequences. However, A189f/A650r [Bourne *et al.*, 2001] might detect high-affinity methanotrophs of the USC α group but also seems to favour *pmoA* of *Methylococcus capsulatus* (type I methanotroph). The primer set A189f/mb661r was originally developed for freshwater environments [Costello & Lidstrom, 1999], detects the *pmoA* of type I and type II methanotrophs, but seems to bias against *pmoA* of high-affinity methanotrophs.

Several PCR conditions were tested with genomic DNA of *Methylococcus capsulatus* BATH, *Methylomonas methanica*, and *Methylosinus trichosporium* OB3b (kindly provided by Dr. Andrew Crombie) as positive template controls.

Table 12 Composition of reagents for PCR reactions of the assays for *pmoA*.

reagent (conc.)	Primers					
	<u>A189f / A862r</u>		<u>A189f / A650r</u>		<u>A189f / mb661r</u>	
	Vol. [μ l]	final conc.	Vol. [μ l]	final conc.	Vol. [μ l]	final conc.
SensiFast SYBR ^b (2x)	30	1x	30	1x	10	1x
Primer forward (10 μ M)	3	500 nM	1.5	250 nM	1.3	650 nM
Primer reverse (10 μ M)	3	500 nM	1.5	250 nM	1.3	650 nM
BSA (3%) ^c	1.5	0.1%	1.5	0.1%	0.5	0.1%
MgCl ₂ (50 mM) ^{b,d}					0.8	2 mM
PCR - H ₂ O ^e	7.5		10.5		1.1	
DNA-template ^f	5		5		5	
	Σ	50		50		20

^a Primer pair used in qPCR reaction was "M13_rev / T7-Prom"

^b Reagents from SensiMix™ SYBR® & Fluorescein Kit (Bioline GmbH, Luckenwalde, Germany)

^c Stocksolution (3 mg ml⁻¹) from crystallised BSA (Bovine Serum Albumin) from Merck (Darmstadt, Germany).

^d Additional supplementation of Mg²⁺ resulted in a final concentration of 5 mM.

^e Distilled Water (DNase/RNase free) from gibco (Paisley, United Kingdom)

^f Diluted DNA templates (1:100 or 1:100)

Table 13 PCR programs to amplify *pmoA*.

step	primers			
	<u>A189f / A862r OR A189f / A650r</u>		<u>A189f / mb661r</u>	
	temp.	time	temp.	time
initial denaturation	95°C	6 min	95°C	5 min
amplification cycles ^a			94°C	1 min
			62°C	1 min
			(-1°C / cycle)	8 x
			72°C	1 min
amplification cycles ^b	94°C	45 sec	94°C	1 min
	55°C	30 sec	55°C	1 min
	72°C	60 sec	72°C	1 min
terminal elongation	72°C	10 min	72°C	10 min
storage	10°C	∞	10°C	∞

^a Amplification cycles include denaturation, annealing and elongation in repeated cycles. PCR is a touchdown PCR with decreasing annealing temperatures by 1°C per cycle.

^b Amplification cycles include denaturation, annealing and elongation in repeated cycles.

2.5.7.3. PCR approaches to amplify *mmoX*

The methanotrophic marker gene *mmoX* encoding for the active site of a subunit of the sMMO was amplified using a primer set introduced by Hutchens and colleagues (see Table 11). The primer was designed on the basis of all available *mmoX* gene sequences in 2003 [Hutchens *et al.*, 2004] assuming a better coverage compared to other primer sets such as the firstly reported *mmoX* targeting primer set that was designed on the basis of sMMO gene cluster sequences of *Methylococcus capsulatus* BATH and *Methylosinus trichosporium* OB3b [McDonald *et al.*, 1995].

In this work several PCR conditions were tested in order to amplify *mmoX* gene sequences from the acid soil but the amplification was insufficient. In all PCR approaches genomic DNA of *Methylcella silvestris* BL2 (kindly provided by Dr. Andrew Crombie) was used as positive template control to check the PCR conditions. All PCR conditions tested are listed in order to show the attempts. In total 3 different assays were tested. Each assay consisted of a different PCR reaction mixture (see Table 14) and PCR program (see Table 15).

Table 14 Composition of reagents for PCR reactions of the assays for *mmoX*.

Assay 1			Assay 2			Assay 3		
Reagent (conc.)	Vol. [μ l]	final conc.	Reagent (conc.)	Vol. [μ l]	final conc.	Reagent (conc.)	Vol. [μ l]	final conc.
Buffer ^a (10x)	2	1 x	5PRIME (2.5 x) ^{d,e}	8	1 x	SensiFast SYBR (2x) ^f	10	1 x
dNTPs ^b (2 mM)	2	0.2 mM	MgCl ₂ (25 mM) ^d	0 or 1.2	1.5 mM or 3 mM ^e	MgCl ₂ (25 mM) ^d	1.6	5 mM ^e
Taq Polym. ^a (5 U/ μ l)	0.25					BSA ^g (3%)	1.3	0.2%
Primer forward (10 μ M)	1	500 nM	Primer forward (10 μ M)	1	500 nM	Primer forward (10 μ M)	0.4	200 nM
Primer reverse (10 μ M)	1	500 nM	Primer reverse (10 μ M)	1	500 nM	Primer reverse (10 μ M)	0.4	200 nM
PCR-H ₂ O ^c	8.75		PCR-H ₂ O ^c	to 15		PCR-H ₂ O ^c	1.3	
DNA template	5		DNA template	5		DNA template	5	
Σ	20		Σ	20		Σ	20	

^a Reagents from BILATEC AG, Viernheim, Germany.

^b Equimolar mixture from 100 mM stock solutions from ROTH (Karlsruhe, Germany)

^c Distilled Water (DNase/RNase free) from gibco (Paisley, United Kingdom)

^d Reagents from 5PRIME (Hamburg, Germany)

^e Master mix (2.5 x) contains Taq DNA polymerase (62.5 U ml⁻¹), 125 mM KCl, 75 mM Tris-HCl (pH 8.3), 4 mM Mg²⁺, 0.5% Igepal®-CA630⁺, 500 μ M of each dNTP, stabilizers.

^f Reagent from SensiMix™ SYBR® & Fluorescein Kit (Bioline GmbH, Luckenwalde, Germany)

^g Stock solution (3 mg ml⁻¹) from crystallised BSA (Bovine Serum Albumin) from Merck (Darmstadt, Germany).

Table 15 Different PCR programs to amplify *mmoX*.

step	Assay 1 & 2 ^a	Assay 3 ^a	time
	initial denaturation	95°C	
amplification cycles ^b	95°C	95°C	45 sec
	48 - 62°C ^c	60°C ^d	45 sec
	72°C	72°C	60 sec
terminal elongation	72°C	72°C	10 min
storage	10°C	10°C	∞

^a Assay numeration corresponds to PCR reactions listed in Table 14.

^b Amplification cycles include denaturation, annealing and elongation in repeated cycles. Annealing temperatures varied as noted.

^c Annealing temperature gradient range: 48°C / 49.3°C / 50.5°C / 51.8°C / 53.1°C / 54.4°C / 55.6°C / 56.9°C / 58.2°C / 59.5°C / 60.7°C / 62°C

^d Annealing temperature was chosen according to the study where the primers were applied for the first time (Hutchens *et al.*, 2004).

2.5.7.4. PCR approaches to amplify *pxmA*

The gene *pxmA* is a homolog of *pmoA* and has been described in gammaproteobacterial methanotrophs such as *Methylomonas*, *Methylobacter* and *Methylomicrobium* [Tavormina *et al.*, 2011]. However, genome sequencing revealed a more widespread occurrence and a *pxmA* copy was also detected in an alphaproteobacterial methanotrophic strain of *Methylocystis rosea* [Knief, 2015]. Just before the gene description of the *pxmA* gene, sequences were also detected in several other studies as ‘*pmoA/amoA* like’ sequences [Nold *et al.*, 2000; Lau *et al.*, 2007; Dörr *et al.*, 2010]. But yet, the function of *pxmA* remains still unknown [Knief, 2015].

In this work several PCR conditions were tested in order to amplify *pxmA* gene sequences from the acid soil, but the amplification was insufficient resulting in smeared bands. However, all PCR conditions resulting in smeared bands are listed in order to show the attempts and give further approaches to amplify *pxmA*. In total 4 different assays were tested. Each assay consisted of a different PCR reaction mixture (see Table 17) and PCR program (see Table 16).

Table 16 Different PCR programs to amplify *pxmA*.

	<u>Assay 1^a</u>	<u>Assay 2^a</u>	<u>Assay 3^a</u>	<u>Assay 4^a</u>		
step	temperature				time	
initial denaturation	95°C	95°C	95°C	95°C	6 min	
amplification cycles ^b	94°C	94°C	94°C	94°C	45 sec	
	48 - 62°C ^c	56°C	55 - 60°C ^d	54.5 - 58°C ^e	30 sec	35 x
	72°C	72°C	72°C	72°C	60 sec	
terminal elongation	72°C	72°C	72°C	72°C	10 min	
storage	10°C	10°C	10°C	10°C	∞	

^a Assay numeration corresponds to PCR reactions listed in Table 17.

^b Amplification cycles include denaturation, annealing and elongation in repeated cycles. Annealing temperatures varied as noted.

^c Annealing temperature gradient range: 48°C / 49.3°C / 50.5°C / 51.8°C / 53.1°C / 54.4°C / 55.6°C / 56.9°C / 58.2°C / 59.5°C / 60.7°C / 62°C

^d Annealing temperature gradient range: 55.1°C / 55.6°C / 56.2°C / 56.7°C / 57.3°C / 57.8°C / 58.4°C / 58.9°C / 59.5°C / 60°C

^e Annealing temperature gradient: 54.5°C / 56°C / 57°C / 58°C

Table 17 Composition of reagents for PCR reactions of the assays for *pxmA*.

Reagent (conc.)	<u>Assay 1</u>		Reagent (conc.)	<u>Assay 2</u>		<u>Assay 3</u>		<u>Assay 4</u>	
	Vol. [μ l]	final con.		Vol. [μ l]	final con.	Vol. [μ l]	final conc.	Vol. [μ l]	final conc.
5PRIME (2.5 x) ^{a,b}	8	1 x	SensiFast SYBR (2x) ^c	8	1 x	8	1 x	8	1 x
MgCl ₂ (25 mM) ^a	0 / 1.2	1.5 mM ^d	MgCl ₂ (25 mM) ^a	1.6	2 mM ^e				
			BSA (3%) ^f	1.5	0.2%	1.5	0.2%	1.5	0.2%
			DSMO (100%) ^g					0.2 / 0.4 / 0.6 / 0.8 / 1	1% / 2% / 3% / 4% / 5%
Primer 'A189f' (10 μ M)	1	500 nM	Primer 'A189f' (10 μ M)	1	500 nM	1 / 1.5 / 2	500 / 750 / 1000 nM	2	1000 nM
Primer 'novelmo634r' (10 μ M)	1	500 nM	Primer 'novelmo634r' (10 μ M)	1	500 nM	1 / 1.5 / 2	500 / 750 / 1000 nM	2	1000 nM
PCR-H ₂ O ^h	ad to 15		PCR-H ₂ O ^h	1.9		ad to 15		4.5	
DNA template	5		DNA template	5		5		5	
Σ	20		Σ	20		20		20	

^a Reagents from 5PRIME (Hamburg, Germany)

^b Master mix (2.5 x) contains Taq DNA polymerase (62.5 U ml⁻¹), 125 mM KCl, 75 mM Tris-HCl (pH 8.3), 4 mM Mg²⁺, 0.5% Igepal®-CA630+, 500 μ M of each dNTP, stabilizers.

^c Reagent from SensiMix™ SYBR® & Fluorescein Kit (Bioline GmbH, Luckenwalde, Germany)

^d Additional supplementation of Mg²⁺ resulted in a final concentration of 3 mM.

^e Additional supplementation of Mg²⁺ resulted in a final concentration of 5 mM.

^f Stock solution (3 mg ml⁻¹) from crystallised BSA (Bovine Serum Albumin) from Merck (Darmstadt, Germany).

^g Reagent from New England Biolabs, USA

^h Distilled Water (DNase/RNase free) from gibco (Paisley, United Kingdom)

2.5.7.5. PCR approaches to amplify *cmuA*

The marker gene *cmuA* for chloromethane utilisation was targeted with different primer pairs. The primer pairs listed as *cmuA I* were designed based on 4 *cmuA* sequences (*Methylobacterium extorquens* CM4, *Hyphomicrobium chloromethanicum* CM1, *Aminobacter lissarensis* CC495, and *Aminobacter ciceronei* IMB-1; Miller *et al.*, 2004) or based on *cmuA* sequences derived from the phyllosphere [Nadalig *et al.*, 2011]. These primers were already used to target the diversity of *cmuA* in several environments [Miller *et al.*, 2004; Borodina *et al.*, 2005; Nadalig *et al.*, 2011], but the rise of more and new *cmuA* sequences allowed the design of new primers (*cmuA II*) [Chaignaud, 2016]. These primers were tested on samples derived from the methanol / chloromethane SIP experiment (see 2.3.10) and are assumed to be more specific.

PCRs with the primer pairs of *cmuA I* were performed at the University of Bayreuth using genomic DNA of *Methylobacterium extorquens* CM4 (provided by Pauline Chaignaud) as positive template controls. PCRs with the primer pairs of *cmuA II* were performed by our cooperation partner at the Institute de botanique, Laboratoire GMG, Equipe AIME, Strasbourg.

Table 18 PCR programs to amplify *cmuA*.

step	<i>cmuA</i> gene sequences					
	<i>cmuA I</i> ^a		<i>cmuA II</i> ^b			
	temp.	time		temp.	time	
initial denaturation	95°C	8 min		95°C	10 min	
amplification cycles ^c	95°C 60°C 72°C	60 sec 60 sec 90 sec	35 x	95°C 56°C	15 sec 30 sec ^d	30 x
terminal elongation	72°C	10 min		72°C	5 min	
storage	10°C	∞		10°C	∞	

^a PCR was conducted at the department EMIC, University of Bayreuth

^b PCR was conducted at the Institute de botanique, Laboratoire GMG, Equipe AIME, Strasbourg

^c Amplification cycles include denaturation, annealing and elongation in repeated cycles.

^d Annealing and elongation are combined in one step.

Table 19 Composition of reagents for PCR reactions of the assays for *cmuA*.

<i>cmuA I</i> ^a			<i>cmuA II</i> ^e		
<i>cmuA802f / cmuA1609r or cmuA1802r</i>			<i>cmuAf422 / cmuAr422</i>		
reagent (conc.)	Vol. [μ l]	final concentr.	reagent (conc.)	Vol. [μ l]	final concentr.
SensiFast SYBR (2x) ^b	8	1 x	Buffer (10x) ^f	5	0.86 x
BSA (3%) ^c	1.5	0.2%	dNTPs (20 mM) ^f	0.5	0.17 mM
			<i>Taq</i> Polymerase Mix ^g	10	
Primer reverse (10 μ M)	1	500 nM	Primer reverse (20 μ M)	0.75	258 nM
Primer forward (10 μ M)	1	500 nM	Primer forward (20 μ M)	3.25	1121 nM
PCR-H ₂ O ^d	4.5		PCR-H ₂ O ^f	33.5	
DNA template	3		DNA template	5	
Σ	20		Σ	58	

^a PCR was conducted at the department EMIC, University of Bayreuth

^b Reagents from SensiMix™ SYBR® & Fluorescein Kit (Bioline GmbH, Luckenwalde, Germany)

^c Stock solution (3 mg ml⁻¹) from crystallised BSA (Bovine Serum Albumin) from Merck (Darmstadt, Germany).

^d Distilled Water (DNase/RNase free) from gibco (Paisley, United Kingdom)

^e PCR was conducted at the Institute de botanique, Laboratoire GMG, Equipe AIME, Strasbourg

^f Reagents from MP Biomedicals (buffer: 1x: Tris- HCl 10 mM, KCl 50 mM, MgCl₂ 1.5 mM, Triton 0.1%, BSA 0.2 mg mL⁻¹, pH 9.0)

^g *Taq* Polymerase Mix consistent of 2 μ l *Taq* polymerase (5U/ μ L, MP biomedical), 1 μ l 10x buffer and 7 μ L PCR-H₂O.

2.5.7.6. 2-step approach PCRs for pyrosequencing

The 2-step-approach was conducted for all amplicons that were used for pyrosequencing (samples of the substrate SIP experiment, see 2.3.3, and pH shift SIP experiment, see 2.3.4) including 16S rRNA, *mxaxoxF* I, and ITS (see Table 11). PCRs were performed in duplicates or triplicates with SIP-derived DNA of pooled ‘heavy’, ‘middle’, and ‘light’ fractions.

Amplification of *mxaxF* fragments with ‘mxaxF1’ in the step-1-PCR for the substrate SIP experiment samples was insufficient, leading to a second amplification with ‘mxaxF2’ targeting a region within the previously amplified segment. Amplicons from the first PCR were purified with columns (see 2.5.9.2) and re-amplified in a nested PCR employing nearly the same conditions (i.e., decreased amplification cycles; Table 20, Table 22).

In all 'pH shift SIP experiment DNA extracts' huge amounts of humic acids were detected and PCR inhibitory effects were still present after isopycnic centrifugation (Figure 29). Thus, step-1-PCR was conducted for all targeted marker genes with different PCR reagents (KAPA2G Ready Mix, KAPABIOSYSTEM (Boston, MA, USA)) showing increased inhibitor tolerance than reagents for substrate SIP experiments (Table 20, Table 22).

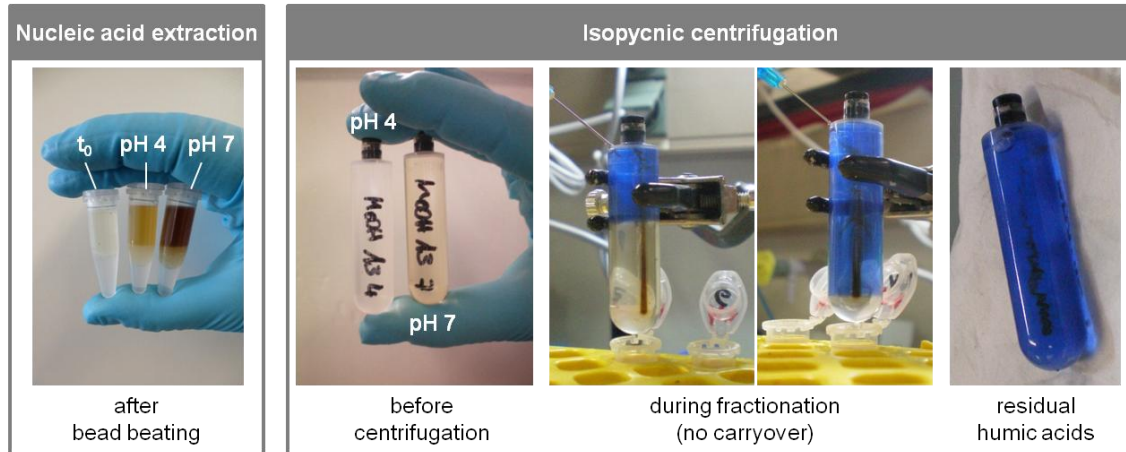


Figure 29 Humic acids contamination.

Strong contamination of humic acids during nucleic acid extractions, before and after isopycnic centrifugation complicated further molecular work. Residuals of humic acids were still recalcitrant after isopycnic centrifugation.

The amplification of ITS gene sequences of the substrate SIP experiment samples followed two different strategies. ITS gene fragments of pooled DNA of 'middle' and 'light' fractions were amplified in one PCR step (similar to step-1-PCR) with an ITS fusion primer pair. ITS gene fragments of pooled DNA of the 'heavy' fractions were amplified in the two-step PCR approach [Berry *et al.*, 2011] with the conventional primer pair in step-1-PCR and the fusion primer pair in step-2-PCR (Table 21, Table 22).

Table 20 Composition of reagents for PCR reactions in the 2-step approach PCR of barcoded amplification for bacterial gene fragments (16S rRNA, *mxoF/xoxF I*)

Step-1-PCR						Step-2-PCR		
(conventional primer pair)						(barcoded primer pair)		
Substrate SIP experiment			pH-SIP experiment					
reagent (conc.)	Vol. [μl]	final conc.	reagent (conc.)	Vol. [μl]	final conc.	reagent (conc.)	Vol. [μl]	final conc.
5PRIME ^{a,b} (2.5 x)	8	1 x	KAPA2G Ready Mix ^c (2 x)	12.5	1 x	Buffer ^{a,d} (10x)	5	1 x
						dNTPs ^e (2 mM)	5	0.2 mM
						Taq Poly. ^a (5U/μl)	0.25	0.025 U
TaqMaster PCR Enhancer ^a (5 x)	1	1 x				TaqMaster PCR Enhancer ^a (5 x)	10	1 x
BSA ^f (3%)	1.5	0.2%	BSA ^f (3%)	1.5	0.2%			
Primer reverse (10 μM)	1	500 nM	Primer reverse (10 μM)	1.25	500 nM	Primer reverse (10 μM)	2.5	500 nM
Primer forward (10 μM)	1	500 nM	Primer forward (10 μM)	1.25	500 nM	Primer forward (5 μM)	5	500 nM
PCR-H ₂ O ^g	4.5		PCR-H ₂ O ^g	3.5		PCR-H ₂ O ^g	17.25	
DNA template	3		DNA template	5		DNA template	5	
Σ	20		Σ	25		Σ	50	

^a Reagents from 5PRIME (Hamburg, Germany)

^b Master mix (2.5 x) contains Taq DNA polymerase (62.5 U ml⁻¹), 125 mM KCl, 75 mM Tris-HCl (pH 8.3), 4 mM Mg²⁺, 0.5% Igepal®-CA630+, 500 μM of each dNTP, stabilizers.

^c Reagents from KAPABIOSYSTEM (Boston, MA, USA).

^d Buffer (10 x) contains 500 mM KCl, 100 mM Tris-HCl pH 8.3 (at 25°C), 15 mM Mg²⁺

^e Equimolar mixture from 100 mM stock solutions from ROTH (Karlsruhe, Germany)

^f Stock solution (3 mg ml⁻¹) from crystallised BSA (Bovine Serum Albumin) from Merck (Darmstadt, Germany).

^g Distilled Water (DNase/RNase free) from gibco (Paisley, United Kingdom)

This table has been published in Morawe *et al.* 2017.

Table 21 Composition of reagents for PCR reactions in the two-step approach PCR of barcoded amplification for fungal gene fragments (ITS)

Step-1-PCR						Step-2-PCR		
(conventional primer pair or fusion primer pair)						(fusion primer pair)		
<u>Substrate SIP experiment</u>			<u>pH-SIP experiment</u>					
reagent (conc.)	Vol. [μ l]	final conc.	reagent (conc.)	Vol. [μ l]	final conc.	reagent (conc.)	Vol. [μ l]	final conc.
GoTaq Green			KAPA2G			GoTaq Green		
Mastermix (2 x) ^a	25	1 x	Ready Mix ^b (2 x)	12.5	1 x	Mastermix (2 x) ^a	25	1 x
			BSA ^c (3%)	1.5	0.2%			
Primer reverse (10 μ M) ^d	1	200 nM	Primer reverse (10 μ M)	1.25	500 nM	Primer reverse (10 μ M)	1	200 nM
Primer forward (10 μ M) ^d	1	200 nM	Primer forward (10 μ M)	1.25	500 nM	Primer forward (10 μ M)	1	200 nM
PCR-H ₂ O ^a	to 50		PCR-H ₂ O ^e	3.5		PCR-H ₂ O ^a	18	
DNA template ^f	1 to 10		DNA template	5		DNA template	5	
Σ	50		Σ	25		Σ	50	

^a Reagents from Promega (Madison, WI, USA)

^b Reagents from KAPABIOSYSTEM (Boston, MA, USA).

^c Stock solution (3 mg ml⁻¹) from crystallised BSA (Bovine Serum Albumin) from Merck (Darmstadt, Germany).

^d The conventional primer pair ITS1F and ITS4 or the fusion primer pair of these primers were used. Fusion primers possess at the 5'-end of the primer sequence an additional adaptor and barcode sequences (see Table 10)

^e Distilled Water (DNase/RNase free) from gibco (Paisley, United Kingdom)

^f DNA template was added in different volumes ranging from 1 to 10 μ l dependent of PCR result.

This table has been published in Morawe *et al.* 2017.

Table 22 PCR programs to amplify 16S rRNA, *mxoF/xoxFI* and ITS gene fragments in step-1-PCR and step-2-PCR of barcoded amplification.

Bacterial genes (16S rRNA and <i>mxoF</i> gene)						
step	Step-1-PCR (conventional primer pair)				Step-2-PCR (barcoded primer pair)	
	Substrate SIP exp.		pH-SIP experiment		temp.	time
	temp.	time	temp.	time		
initial denaturation	95°C	5 min	95°C	5 min	95°C	5 min
amplification cycles ^a	95°C	60 sec	25 x ^c	95°C	30 sec	15 x
	55°C	60 sec	30 x ^d	55°C	30 sec	
	72°C	60 sec	20 x ^e	72°C	60 sec	
terminal elongation	72°C	8 min	72°C	8 min	72°C	8 min
storage	10°C	∞	10°C	∞	10°C	∞
Fungal genes (ITS gene)						
step	Step-1-PCR (conventional primer pair or fusion primer pair)			Step-2-PCR (fusion primer pair)		
	both SIP experiments					
	temp.	time				
initial denaturation	95°C	6 min		95°C	6 min	
amplification cycles ^b	94°C	30 sec		10 x	94°C	45 sec
	60°C	30 sec			50°C	45 sec
	(-1°C / cycle)	72°C			72°C	60 sec
amplification cycles ^a	94°C	45 sec		20 x ^f 30 x ^g		
	50°C	45 sec				
	72°C	60 sec				
terminal elongation	72°C	10 min		72°C	10 min	
storage	10°C	∞		10°C	∞	

^a Amplification cycles include denaturation, annealing and elongation in repeated cycles.

^b Amplification cycles include denaturation, annealing and elongation in repeated cycles. PCR is a touchdown PCR with decreasing annealing temperatures by 1°C per cycle.

^c Number of repeated cycles for 16S rRNA gene fragment amplification.

^d Number of repeated cycles for *mxoF* gene fragment amplification with primer pair “*mxoF1*”.

^e Number of repeated cycles for *mxoF* gene fragment amplification with primer pair “*mxoF2*”.

^f Number of repeated cycles for step-1-PCR with the conventional primer pair (subsequently step-2-PCR conducted).

^g Number of repeated cycles for step-1-PCR with the fusion primer pair (no step-2-PCR conducted).

This table has been published in Morawe *et al.* 2017.

2.5.7.7. PCR approaches to amplify 16S rRNA and *mxoF/xoxF II* for 'ILLUMINA' sequencing

Previous to sequencing by synthesis ('ILLUMINA sequencing', see 2.5.12.3) amplicons of 16S rRNA and *mxoF/xoxF II* sequences were retrieved by PCR of SIP-derived DNA of pooled 'heavy', 'middle', and 'light' fractions. PCRs were performed in duplicates. The new designed primer pairs of *mxoF/xoxF II* were assumed to target also *xoxF*.

PCRs were performed using genomic DNA of *Escherichia coli* JM109 (for 16S rRNA, competent cells for cloning, see 2.5.10) and *Methylobacterium extorquens* CM4 (for *mxoF/xoxF II*, provided by Pauline Chaignaud) as positive template controls.

Table 23 Composition of reagents for PCR reactions of the assays for 16S rRNA and *mxoF/xoxF II* for 'ILLUMINA' sequencing.

16S rRNA			<i>mxoF/xoxF II</i>		
Reagent (conc.)	Vol. [μ l]	final conc.	Reagent (conc.)	Vol. [μ l]	final conc.
Buffer ^a (10x)	5	1x	5PRIME (2.5 x) ^{d,e}	8	1x
dNTPs ^b (2 mM)	5	0.2 mM	TaqMaster PCR Enhancer (5 x) ^d	3	1x
MgCl ₂ ^a (25 mM)	3	1.5 mM	BSA (3%) ^f	1.5	0.2%
Taq Polym. ^a (5 U/ μ l)	0.25				
Primer reverse (10 μ M)	2.5	500 nM	Primer reverse (10 μ M)	1	500 nM
Primer forward (10 μ M)	2.5	500 nM	Primer forward (10 μ M)	1	500 nM
PCR-H ₂ O ^c	26.75		PCR-H ₂ O ^c	0.5	
DNA template	5		DNA template	5	
Σ	50		Σ	20	

^a Reagents from BILATEC AG, Viernheim, Germany.

^b Equimolar mixture from 100 mM stock solutions from ROTH (Karlsruhe, Germany)

^c Distilled Water (DNase/RNase free) from gibco (Paisley, United Kingdom)

^d Reagents from 5PRIME (Hamburg, Germany)

^e Master mix (2.5 x) contains Taq DNA polymerase (62.5 U ml⁻¹), 125 mM KCl, 75 mM Tris-HCl (pH 8.3), 4 mM Mg²⁺, 0.5% Igepal®-CA630⁺, 500 μ M of each dNTP, stabilizers.

^f Stock solution (3 mg ml⁻¹) from crystallised BSA (Bovine Serum Albumin) from Merck (Darmstadt, Germany).

Table 24 PCR programs to amplify 16S rRNA and *mxoF/xoxF* II for 'ILUMINA' sequencing.

step	temperature	time	
initial denaturation	95°C	5 min	
amplification cycles ^a	95°C	1 min	30 x ^b 40 x ^c
	55°C	1 min	
	72°C	1 min	
terminal elongation	72°C	8 min	
storage	10°C	∞	

^a Amplification cycles include denaturation, annealing and elongation in repeated cycles.

^b Number of repeated cycles for 16S rRNA gene fragment amplification.

^c Number of repeated cycles for *mxoF/xoxF* gene fragment amplification with both primer pairs of *mxoF/xoxF* II.

2.5.7.8. PCR approaches to amplify 16S rRNA gene sequences for T-RFLP

16S rRNA amplicons used for the T-RFLP analysis (see 2.5.11) were terminal fluorescence labelled during PCR reactions by using a fluorescence dye-labelled primer.

Table 25 Composition of reagents for PCR reactions for amplifying 16S rRNA gene fragments with fluorescent dye labelled primer.

Reagent (conc.)	Vol. [μl]	final conc.
5PRIME (2.5 x) ^{a,b}	8	1x
TaqMaster PCR Enhancer (5 x) ^a	1	1x
MgCl ₂ (25 mM) ^{a,c}	1	1 mM
Primer reverse 907rm (10 μM)	1	500 nM
Primer forward 27F ^d (10 μM)	1	500 nM
PCR-H ₂ O ^e	10	
DNA template	3	
Σ	25	

^a Reagents from 5PRIME (Hamburg, Germany)

^b Master mix (2.5 x) contains Taq DNA polymerase (62.5 U ml⁻¹), 125 mM KCl, 75 mM Tris-HCl (pH 8.3), 4 mM Mg²⁺, 0.5% Igepal®-CA630⁺, 500 μM of each dNTP, stabilizers.

^c Additional supplementation of Mg²⁺ resulted in a final concentration of 2.5 mM.

^d Primer was labelled with the infra-red dye IRD700 at the 5' end.

^e Distilled water (DNase/RNase free) from gibco (Paisley, United Kingdom)

Table 26 PCR programs to amplify 16S rRNA and *mxoF/xoxF II* for 'ILUMINA' sequencing.

step	temperature	time	
initial denaturation	95°C	5 min	
amplification cycles ^a	95°C	60 sec	5 x
	40°C	60 sec	
	72°C	90 sec	
amplification cycles ^a	95°C	60 sec	33 x
	50°C	60 sec	
	72°C	90 sec	
terminal elongation	72°C	10 min	
storage	10°C	∞	

^a Amplification cycles include denaturation, annealing and elongation in repeated cycles.

2.5.8. Quantitative polymerase chain reaction (qPCR)

Quantities of gene numbers in different samples can be determined using quantitative PCR (qPCR) that is similar to PCRs with an additional quantification step [Raeymaekers, 2000; Čikoš & Koppel, 2009]. The qPCR is quite sensitive and detects even minimal changes in gene copy numbers or gene expression (in the case of mRNA analyses) [Heid *et al.*, 1996]. The operating principle of qPCR is based on fluorescent dyes such as SYBR Green I and their binding to dsDNA. The auto-fluorescence of unbound SYBR Green I is increased by the factor 10^4 when the fluorescent dye intercalates with dsDNA. Thus, increasing concentrations of dsDNA (= amplicons) correlates with an increasing fluorescence signal by SYBR Green I that is recorded in each qPCR cycle. At the beginning of the exponential phase of the qPCR the fluorescence exceeds a threshold value (C_T) that is linear proportional to the logarithm of the initial concentration of the targeted gene [Bustin *et al.*, 2009]. Basis for the quantification of the initial concentration in the analysed sample are quantitative standards with known gene concentrations (qPCR standards, see 2.5.8.2). The specific nature of the amplification is verified by the melting curve at the end of the qPCR. The continuous increase of temperature leads to the melting of dsDNA amplicons depending on their length and nucleotide composition and thus to the loss of fluorescence.

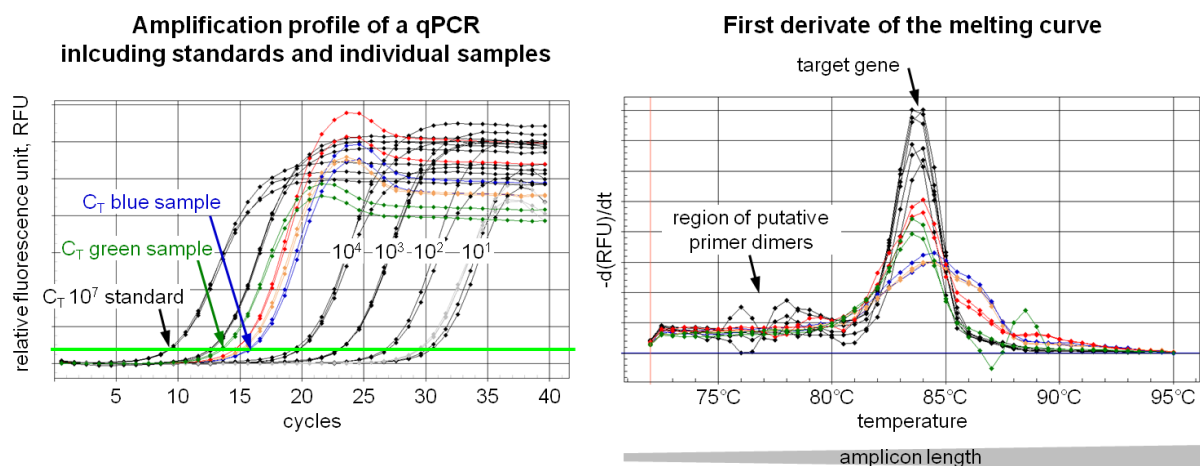


Figure 30 Schematic overview on the operating principle of qPCR analysis.

The figure shows amplification profiles recorded during a qPCR (target gene: 16S rRNA) and the first derivate of the melting curve. Gene numbers of individual samples (●, ●, ●, ●) are determined via their sample-specific threshold cycle (C_T) and qPCR standards with known concentrations (e.g. 10^7 - 10^1 target molecules, ●). The C_T is characterised as the cycle when the fluorescence signal exceeds the background fluorescence (green line). Negative controls (= PCR- H_2O , ●) serve as quality check. The levelling-out of the sigmoid curves is the result of primer and nucleotide consumption, i.e., no further amplicons are synthesized.

The melting curve shows the change of fluorescence over time depending on the temperature. The peaks resulting of the first derivate of the melting curves are depending on length and nucleotide composition of an amplicon as indicated. Short fragments (such as primer dimers) would exhibit a peak at lower temperatures.

2.5.8.1. qPCR primers

The primers used for qPCR analyses were shown to detect the target genes specifically and resulting amplicons were always short in order to enhance qPCR efficiency. These primers were also used to prepare the qPCR standards (see 2.5.8.2).

2.5.8.2. Preparation of qPCR standards

The qPCR standards of the target genes were amplified using the same primers as used for qPCR. Amplified PCR products were cloned (see 2.5.10) and finally specific amplicons (i.e., identical gene structure due to cloning) were enriched by PCR. The amplicons were purified by gel extraction (see 2.5.9.1) and quantified using a fluorescence dye based method (see 2.5.4.2).

PCRs for standard preparation were performed using genomic DNA of *Escherichia coli* JM109 (for 16S rRNA, competent cells for cloning, see 2.5.10), *Methylobacterium extorquens* CM4 (for *mxoF*, provided by Pauline Chaignaud), *Methylocella silvestris* BL2 (for *mmoX*, provided by Dr. Andrew Crombie), and forest soil (for *pmoA-USCa*) as templates. For the preparation of the artificial DNA the plasmid pCR 2.1-TOPO (Invitrogen, Karlsruhe, Germany) flanked by M13 priming sites without any insert served as template.

Table 27 Primer sequences of primers used for qPCR and to prepare qPCR standards.

gene	primer ^a	sequence (5' – 3') ^b	amplicon	reference
16S rRNA	341f (17 bp)	CCT ACG GGN GGC WGC AG	193 bp	Muyzer <i>et al.</i> , 1993
	534r (17 bp)	ATT ACC GCG GCT GCT GG		Muyzer <i>et al.</i> , 1993
<i>mxoF</i>	<i>mxoF</i> _for (19 bp)	TGG AAC GAG ACC ATG CGT C	455 bp	Moosvi <i>et al.</i> , 2005
	<i>mxoF</i> _rev (20 bp)	CAT GCA GAT GTG GTT GAT GC		Moosvi <i>et al.</i> , 2005
<i>mmoX</i>	<i>mmoX</i> Af (17 bp)	ACC AAG GAR CAR TTC AA	295 bp	Aumann <i>et al.</i> , 2000
	<i>MceI</i> 422r (18 bp)	GAA GCC GCA TTG ATG GGT		Kolb <i>et al.</i> , 2005
<i>pmoA</i> USCα	USCα346f (16 bp)	TGG GYG ATC CTN GCN C	185 bp	Degelmann <i>et al.</i> , 2010
	A682r (18 bp)	GAA SGC NGA GAA GAA SGC		Degelmann <i>et al.</i> , 2010
vector pCR 2.1	T7-Prom_f (20 bp)	TAA TAC GAC TCA CTA TAG GG	178 bp	ThermoScientific, 2011 ^e
	M13_rev (18 bp)	CAG GAA ACA GCT ATG ACC		ThermoScientific, 2011 ^e
vector pJET 1.2	M13_for (16 bp)	GTA AAA CGA CGG CCA G	199 bp ^c	ThermoScientific, 2011 ^e
	pJET_for (23 bp)	CGA CTC ACT ATA GGG AGA GCG GC	variable ^d	ThermoScientific, 2011 ^e
pJET_rev (24 bp)	AAG AAC ATC GAT TTT CCA TGG CAG	ThermoScientific, 2011 ^e		

^a Primer notation according to the reference with primer length in brackets. 'f' or 'for' indicate the forward primers that are listed at first.

^b Primer sequence with wobble bases in bold faces.

^c Amplicon length in combination with "M13_rev"

^d Amplicon length depends on ligated vector insert (i.e., ligated insert + 119 bp).

^e Primer sequences available in product information for "ThermoScientific CloneJET PCR Cloning Kit"

Table 28 Composition of reagents for PCR reactions of qPCR standard preparation (16S rRNA, *mxoF*, *mmoX*, M13) and cloning (pJET).

reagent (conc.)	16S rRNA / <i>mxoF</i>		<i>mmoX</i>		M13 ^a / pJET ^b	
	Vol. [μl]	final conc.	Vol. [μl]	final conc.	Vol. [μl]	final conc.
Buffer ^c (10x)	5	1 x	5	1 x	5	1 x
dNTPs ^d (2 mM)	5	200 μM	5	200 μM	5	200 μM
MgCl ₂ ^c (25 mM)	3	1.5 mM	6	3 mM	3	1.5 mM
Taq Polym. ^c (5 U/μl)	0.25	0.025 U	0.25	0.025 U	0.25	0.025 U
Primer forward (10 μM)	2.5	500 nM	2.5	500 nM	1	200 nM
Primer reverse (10 μM)	2.5	500 nM	2.5	500 nM	1	200 nM
PCR-H ₂ O ^e	26.75		23.75		29.75	
DNA-templat ^f	5		5		5	
Σ	50		50		50	

^a Reaction mixture for preparing artificial DNA using primer pair "M13_for/M13_rev"

^b Reaction mixture used to amplify clones with correct insert to prepare qPCR standards

^c Reagents from BILATEC AG, Viernheim, Germany.

^d Equimolar mixture from 100 mM stock solutions from ROTH (Karlsruhe, Germany)

^e Distilled Water (DNase/RNase free) from gibco (Paisley, United Kingdom)

^f DNA templates were genomic DNA (16S rRNA, *mxoF*, *mmoX*), circular plasmid pCR 2.1-TOPO from Invitrogen ("M13") or aqueous clone suspension ("pJET")

^g Primer pair used in qPCR reaction was "M13_rev / T7-Prom"

^h Reagents from SensiMix™ SYBR® & Fluorescein Kit (Bioline GmbH, Luckenwalde, Germany)

ⁱ Stock solution (3 mg ml⁻¹) from crystallised BSA (Bovine Serum Albumin) from Merck (Darmstadt, Germany).

^j Diluted DNA templates (1:100 or 1:100)

Table 29 Composition of reagents for PCR reactions of qPCR standard preparation of *pmoA-USCα*.

Reagent (conc.)	Vol. [μl]	final conc.
5PRIME (2.5 x) ^{a,b}	8	1x
MgCl ₂ (25 mM) ^{a,c}	1.2	1.5 mM
Primer reverse (10 μM)	1.5	750 nM
Primer forward (10 μM)	1.5	750 nM
PCR-H ₂ O ^d	2.8	
DNA template	5	
Σ	20	

^a Reagents from 5PRIME (Hamburg, Germany)

^b Master mix (2.5 x) contains Taq DNA polymerase (62.5 U ml⁻¹), 125 mM KCl, 75 mM Tris-HCl (pH 8.3), 4 mM Mg²⁺, 0.5% Igepal®-CA630⁺, 500 μM of each dNTP, stabilizers.

^c Additional supplementation of Mg²⁺ resulted in a final concentration of 3 mM.

^d Distilled Water (DNase/RNase free) from gibco (Paisley, United Kingdom)

Table 30 PCR programs to amplify gene fragments for qPCR standards.

step	gene fragments ^a					
	16S, <i>mmoX</i> , <i>mxoF</i> , M13			<i>pmoA-USCα</i>		
	temp	time		temp	time	
initial denaturation	95°C	5 ^b / 8 ^c min		95°C	5 min	
amplification cycles ^c	95°C	60 ^d / 30 ^e sec	30 x	95°C	30 sec	35 x
	55°C	60 ^d / 30 ^e sec		57.3°C	25 sec	
	72°C	60 sec		72°C	30 sec	
terminal elongation	72°C	8 min		72°C	8 min	
storage	10°C	∞		10°C	∞	

^a Genes were amplified from genomic DNA of *E.coli* JM109 (16S rRNA), *M. extorquens* CM4 (*mxoF*), and *M. silvestris* BL2 (*mmoX*) as well as from the plasmid pCR2.1 (M13 = Inhibit) and from fresh soil (*pmoA-USCα*)

^b Amplification conditions of gene fragments ligated into the vector pJET1.2/blunt with the primer pair 'pJET_for / pJET_rev'.

^c Amplification cycles include denaturation, annealing and elongation in repeated cycles.

^d Time applied in the PCR program for preparing gene fragments of 16S rRNA, *mxoF* and *mmoX* from pure cultures using specific primers.

^e Time applied in the PCR program for the amplification of artificial DNA using primer pair 'M13_for/M13_rev'.

----- Tables 27 to 31 (see p. 95) have been published in Morawe *et al.* 2017. -----

In order to obtain qPCR standards of known concentration of target molecules the gene copy number was calculated using Equation 11. Subsequently, the qPCR standard solutions were diluted to 10⁹ target molecules (5 μl)⁻¹ and stored as 5 μl aliquots at -20°C. The quantitative standards with known initial concentration (10¹ - 10⁷ target molecules (5 μl)⁻¹) were always prepared before each qPCR by dilution of a highly concentrated stock solution (10⁹ target

molecules ($5 \mu\text{l}^{-1}$). These standards were always the calculation reference in each qPCR approach.

Equation 11 **Number of molecules M_s in qPCR standard solutions [molecules μl^{-1}]**

$$M_s = \frac{C_s}{l_a \times m_{bp}} \times N_A$$

C_s , concentration of molecules in the standard solution [$\text{ng } \mu\text{l}^{-1}$]

l_a , exact length of amplicon (including target gene fragment, primer sequences and vector residuals)

m_{bp} , molecular weight of one base pair in dsDNA (= $649.5 \text{ ng nmol}^{-1}$)

N_A , Avogadro constant ($6.022 \times 10^{23} \text{ mol}^{-1} \triangleq 6.022 \times 10^{32} \text{ nmol}^{-1}$)

2.5.8.3. qPCR assay to evaluate gene copy numbers

All qPCR reactions were set-up as duplicates or triplicates and were conducted in specific qPCR plates (Thermosprint 96 PCR plates, Bilatec, Mannheim, Deutschland) sealed with a transparent adhesive foil (Thermosprint transparent sealing tapes, Bilatec, Mannheim, Deutschland) enabling the record of fluorescent signals. The mastermix contained the fluorescent dye SYBR Green I and Fluorescein (excitation at 490 nm; emission at 530 nm). Fluorescein was used to calibrate the qPCR at the beginning and does not intercalate with dsDNA amplicons. All DNA-templates were diluted (1:100 up to 1:1000) avoiding PCR inhibition.

Table 31 **Composition of reagents for PCR reactions of the qPCR assays.**

reagent (conc.)	16S rRNA		<i>mxoF</i> & <i>mnoX</i>		<i>pmoA-USCα</i> & Inhibit ^a	
	Vol. [μl]	final conc.	Vol. [μl]	final conc.	Vol. [μl]	final conc.
SensiFast SYBR ^b (2x)	10	1x	10	1x	10	1x
Primer forward (10 μM)	0.5	250 nM	1	500 nM	1	500 nM
Primer reverse (10 μM)	0.5	250 nM	1	500 nM	1	500 nM
BSA (3%) ^c			1	0.15%		
PCR - H ₂ O ^d	4		2		3	
DNA-template ^e	5		5		5	
Σ	20		20		20	

^a Primer pair used in qPCR reaction was "M13_rev / T7-Prom"

^b Reagents from SensiMix™ SYBR® & Fluorescein Kit (Bioline GmbH, Luckenwalde, Germany)

^c Stock solution (3 mg ml⁻¹) from crystallised BSA (Bovine Serum Albumin) from Merck (Darmstadt, Germany).

^d Distilled Water (DNase/RNase free) from gibco (Paisley, United Kingdom)

^e Diluted DNA templates (1:100 or 1:100)

The qPCRs were run in a qPCR cyler (iQ5 multicolor real-time PCR detection system, Bio-Rad Laboratories, Hercules, USA) using the corresponding assays (Table 32). The purity and amplification success was always checked by melting curves and agarose gel electrophoresis (see 2.5.5).

Table 32 Modified qPCR programs to amplify 16S rRNA, *pmoA-USCα*, *mxoF*, *mnoX* and artificial DNA (Inhibit).

step	<u>16S rRNA</u>		<u><i>pmoA-USCα</i></u>		<u><i>mxoF</i></u>		<u><i>mnoX</i></u>		<u>Inhibit</u>	
	temp.	time	temp.	time	temp.	time	temp.	time	temp.	time
initial denaturation	95°C	8 min	95°C	8 min	95°C	8 min	95°C	8 min	95°C	8 min
	3-step		4-step		4-step		4-step		3-step	
amplification	95°C	30 sec	95°C	30 sec	95°C	30 sec	95°C	30 sec	95°C	30 sec
cycles ^a	55.7°C	25 sec	57.3°C	15 sec	64°C	20 sec	61°C	30 sec	61.2°C	15 sec
40x	72°C	25 sec	72°C	10 sec	72°C	30 sec	72°C	30 sec	72°C	15 sec
			78°C	12 sec	78°C	12 sec	78°C	12 sec	72°C	15 sec
terminal elongation	72°C	10 min	72°C	10 min	72°C	10 min	72°C	10 min	72°C	10 min
	72°C		72°C		72°C		72°C		72°C	
	↓		↓		↓		↓		↓	
melting	(+0.5°C		(+0.5°C		(+0.5°C		(+0.5°C		(+0.5°C	
curve ^b	/cycle)	12 sec	/cycle)	12 sec	/cycle)	12 sec	/cycle)	12 sec	/cycle)	12 sec
47x	↓		↓		↓		↓		↓	
	95°C		95°C		95°C		95°C		95°C	
storage	10°C	∞	10°C	∞	10°C	∞	10°C	∞	10°C	∞
according to ^c	Zaprasis <i>et al.</i> , 2010		Degelmann <i>et al.</i> , 2010				“MCEL” Kolb <i>et al.</i> , 2005		“INHIB-CORR” Degelmann <i>et al.</i> , 2010	

^a Amplification cycles include denaturation, annealing and elongation in repeated cycles. Bold faces indicate the step when fluorescence signal was recorded, i.e., in a 3-step protocol the last 12 seconds of elongation step and in a 4-step protocol an extra step with higher temperatures than elongation to melt small unspecific PCR products and thus reduce bias of unspecific fluorescence signals.

^b Melting curve analysed was performed from 72°C to 95°C with increments of 0.5°C per cycle.

^c Established qPCR assays were slightly modified in this study, the original qPCR assay references are quoted.

This table has been published in Morawe *et al.* 2017

2.5.8.4. Evaluation of a putative qPCR inhibition

According to Degelmann *et al.* 2010 all qPCR measurements were inhibitor corrected since coextracted humic acids were obvious for example in the 'pH shift SIP experiment DNA extracts', and inhibition is well recorded [Tsai & Olson, 1992; Wilson, 1997; Wintzingerode *et al.*, 1997; Watson & Blackwell, 2000; Radstrom *et al.*, 2004; Zaprasis *et al.*, 2010]. In brief, all DNA templates were spiked with artificial DNA, so that 5×10^{-4} target molecules per qPCR reaction were expected. Inhibition qPCR assays 'Inhibit' were conducted as listed in Table 31 and Table 32.

2.5.8.5. Calculation of transcript numbers

The correct number of gene copies in each sample was calculated using Equation 12. Thus, putative inhibitory effects during each qPCR reaction and measurement were included.

Equation 12 **Calculation of corrected gene copy numbers $\lg(SQ_{cor})$ including putative qPCR inhibition**

$$\lg(SQ_{cor}) = \lg(SQ_m) \times \left(\frac{\lg(SQ_{Inhib-s})}{\lg(SQ_{Inhib-m})} \right) \times \left(\frac{E_{qPCR}}{E_{Inhibi}} \right)$$

SQ_m , measured gene copy numbers in the gene specific assay*

$SQ_{Inhib-s}$, spiked gene copy numbers in the Inhibition assay ($= 5 \times 10^4$)*

$SQ_{Inhib-m}$, measured gene copy numbers in the Inhibition assay*

E_{qPCR} , amplification efficiency of the gene specific assay

E_{Inhibi} , amplification efficiency of the Inhibition assay

*SQ, starting quantity

2.5.9. Purification of PCR products

2.5.9.1. Gel extraction

This type of purification was applied if more than the desired specific size amplicons or a smear (i.e., unspecific amplicons) were visible after agarose gel electrophoresis. For the gel extraction-based purification the montage Gel Extraction Kit (Millipore GmbH, Schwalbach, Germany) was used according to the manufactory's protocol. Agarose gel electrophoresis was done as described above (see 2.5.5). DNA-bands were excised from the gel with a sterile scalpel under UV light visualization. In order to keep the gel slice small all not stained gel parts (thus no DNA containing) were trimmed at all sites of the gel slice. In addition, gel parts that were not handled were stored out of the UV light range in order to keep UV-caused damages small. The trimmed gel slices were transferred to the montage gel extraction columns and centrifuged. The filtrate contained the purified DNA and was used for further molecular work.

2.5.9.2. Purification with columns

Amplicons after PCR reactions were purified using a column-based purification kit (OMEGA bio-tek (Norcross, GA, USA)) according to the manufactory's protocol. In short, samples were bind to a silica matrix of the column, washed twice with ethanol and finally eluted with a low salt elution buffer. In order to achieve higher yields of DNA the elution step was always conducted twice with 10 μl elution buffer for each step (final volume 20 μl).

2.5.10. Cloning

Cloning was performed in order to obtain standards for qPCR (see 2.5.8.2). For cloning of 16S rRNA gene fragments and marker genes the Thermo Scientific CloneJET PCR Cloning Kit (Thermo Fisher Scientific, Waltham, USA) was used. Amplicons of the correct size were purified by gel extraction (see 2.5.9.1) and spectrophotometrically quantified (see 2.5.4.1).

2.5.10.1. Ligation

The ligation of purified amplicons was mainly performed according to the manufactory's protocol. Depending on the fragment size the amplicon was diluted to the suitable concentration. At first 3'-overhangs formed during PCR with a *Taq* DNA polymerase were removed from the amplicons in a 'blunting reaction'. In total, 1 μl of amplicons, 10 μl of 2x reaction buffer, 1 μl of DNA blunting enzyme, and PCR- H_2O was mixed on ice to a final volume of 18 μl . The mixture was vortexed, incubated at 70°C for 5 min, and chilled on ice. Subsequently, the 'ligation reaction' was started by adding 1 μl plasmid (pJET1.2/blunt vector plasmid, 50 $\text{ng } \mu\text{l}^{-1}$) and 1 μl T4 DNA ligase (5 U μl^{-1}) to the 'blunting reaction' mixture. The ligation was performed at room temperature for at least 10 min and was ready to use for the transformation. A 'ligation control' was set-up in the same way according to manufactory's protocol.

2.5.10.2. Transformation

The ligation mix containing plasmids with amplicon DNA were transferred into competent cells of *Escherichia coli* JM109. Competent cells were thawed up on ice and mixed gently by flicking the tubes. Transformation was started by adding 2 μl 'ligation mixture' to 50 μl of competent cells. Tubes were gently mixed and placed on ice for 20 min allowing plasmids to attach to the outer cell membrane. The following heat-shock reaction permeabilized the cell membranes allowing the plasmids to enter cells. Heat-shock was conducted for 45 sec at exactly 42°C. Transformation mixtures were immediately placed on ice for 5 minutes. Subsequently 950 μl prewarmed SOC medium (37°C, see 2.2.7) was supplemented to heat shocked cells allowing the cells to regenerate. After 1.5 h of regeneration at 37°C cells were harvested by centrifugation (5'000 x g, 10 min, room temperature). 750 μl of supernatant were discarded, pelletized cells were gently resuspended in the residual 250 μl and approx.

50 - 100 µl were transferred to LB agar plates (see 2.2.7). A transformation control was set-up in the same manner using an uncut control plasmid 'pUC19'. This plasmid is a derivative of the 'pBR322' plasmids, has a size of 2868 bp and contains an ampicillin resistance gene [Vieira & Messing, 1982].

2.5.10.3. Screening for successful cloning

Transformed cells were plated onto LB agar plates with ampicillin and allowed to grow at 37°C over night. The used plasmid contains an ampicillin resistance gene (*bla*(ApR)) and thus only plasmid harbouring *E.coli* cells were able to grow. In addition, the used plasmid contains the lethal gene *eco47IR*. Thus, only cells that incorporated the plasmid containing ligated DNA revealed a disrupted lethal gene, were able to survive on the agar plates. For that reason all colonies growing over night on the agar plates should harbour the plasmid including the amplicon sequence. In total, 12 to 24 cells were picked and checked for the correct inserts by PCR reactions using plasmid applied primers (for primer pair see "vector pJET 1.2", Table 27; for PCR assay see 2.5.8.2, Table 28 and Table 30). Clones containing the correct inserts were chosen, sequenced by Macrogen (Sanger method, Amsterdam, Netherlands, see 2.5.12.1), and used for preparing qPCR standards (see 2.5.8.2).

2.5.11. Terminal restriction fragment length polymorphism (T-RFLP) analysis

The terminal restriction fragment length polymorphism (T-RFLP) analysis is an established fingerprinting technique enabling the estimation of the diversity and detection of abundant taxa in a microbial community itself, or the comparison of different microbial communities among each other [Liu *et al.*, 1997; Thies, 2007]. The operating principle of the T-RFLP is based on the dissimilarities of marker genes such as 16S rRNA. The marker genes are amplified with fluorescence labelled primers resulting in terminal labelled amplicons. Subsequently, these amplicons are digested with restriction enzymes (endonucleases) resulting in terminal labelled restriction fragments that can be separated on a polyacrylamide gel (PAGE) resulting in different T-RF patterns of different samples. Thereby, these T-RFs represent different phylogenetic taxa within the microbial community [Marsh, 2005].

In this work T-RFLP was used to compare the T-RF patterns of unlabelled (¹²C treatments) and partly labelled (¹²C treatments) DNA of a the methanol treatments of the substrate SIP experiment (see 2.3.3) in order to assign fractions 1 - 10 as 'heavy', 'middle', and 'light' fractions and thus to determine the threshold of the buoyant densities (see 2.5.6)

2.5.11.1. Amplification with fluorescence-dye tagged primers

Fractionated DNA derived from all fractions (#1 - #10) of the [^{12}C]- and [$^{13}\text{C}_1$]-methanol treatments of the substrate SIP experiment (see 2.3.3, 2.5.6.2) was used to amplify 16S rRNA gene sequences. Thereby the forward primer was labelled with a fluorescent dye. After PCR (see 2.5.7.8), amplicons of the correct size were purified by gel extraction (see 2.5.9.1) and used for further analysis.

2.5.11.2. Mung bean endonuclease digestion

During the PCR a premature termination of the elongation step can lead to single stranded terminal overhangs of the amplicons. These regions can lead to the formation of pseudo T-RFs during restriction digestion by the false cleavage of enzymes at non-terminal restriction sites [Egert & Friedrich, 2003]. Single stranded overhangs were removed by the digestion with mung bean endonuclease (New England Biolabs, Ipswich, USA). For this digestion 50 μl of purified PCR product (fluorescent labelled, see 2.5.7.8, 2.5.11.1) were mixed with 5.5 μl 10x mung bean reaction buffer and 2 μl mung bean endonuclease (0.5 U μl^{-1}) and incubated for 1 h at 30°C. Subsequently, the digestion was stopped by the precipitation with isopropyl alcohol (see 2.5.3.2).

2.5.11.3. Restriction enzyme digestion

After the mung bean digestion the terminal fluorescent labelled amplicons (see 2.5.11.2) were used for restriction enzyme digestion. Restriction enzymes are endonucleases recognizing specific restriction sites and thus cleaving dsDNA. Two different restriction enzymes with different restriction sites were used (*MspI*, *RsaI*, Figure 31).



Figure 31 Restriction sites of the applied restriction enzymes *MspI* and *RsaI*.

The restriction sites of *MspI* and *RsaI* (New England Biolabs, USA) are specific and different. Enzymes were derived from *E.coli* strain carrying *MspI* gene from *Moraxella* sp. ATCC 49670 and *RsaI* gene from *Rhodopseudomonas sphaeroides*, respectively. Information and images are taken from www.neb.com.

Each restriction digestion (15 μl final volume) was set-up with 10.5 μl of amplicon and 1.5 μl restriction enzyme (2 U μl^{-1}), 1.5 μl 10x reaction buffer 'NEB4' and 1.5 μl 10x BSA (all chemicals from New England Biolabs, USA). The digestion was performed at 37°C for 4 h and reaction was stopped by heat inactivation at 95°C for 5 min. Digested samples were quantified with Quant-iT-PicoGreen dsDNA reagent Kit (Invitrogen, Carlsbad, CA, USA) (see 2.5.4.2) and diluted with PCR- H_2O to obtain a final concentration of 0.5 ng μl^{-1} for further PAGE analysis (see 2.5.11.4).

2.5.11.4. Denaturing Polyacrylamide Gel Electrophoresis (PAGE)

In order to analyse the terminal labelled restriction enzymes a denaturing polyacrylamide gel electrophoresis (PAGE) was performed. Due to the small size of pores in the gel a better resolution and separation of DNA fragments than with agarose gels is possible.

The gel was poured between two glass plates (Boroflat glass plates, 25 cm x 25 cm x 0.5 cm) that were previously cleaned with ddH₂O, ethanol (70 %) and isopropyl alcohol (80 %) in order to remove disruptive particles. At the uppermost area of the plates a bind silane solution (1:1 bind silane plusOne, GE Healthcare, Piscataway, MD, USA; 10 % acetate) was applied as a thin film onto the plates to further stabilise the gel pockets. Spacers (0.2 mm) were placed on the glass plates to separate the two plates.

The gel was prepared by mixing 15 g urea (Roche Pharma, Reinach, Switzerland), 3.75 ml of a 40 % acrylamide-bis-solution (37.5:1, 2.6 % C; BioRad, Hercules, CA, USA), 5 ml 5x TBE buffer (450 mM Tris, 450 mM H₃Bo₃, 10 mM EDTA (pH 8), and 9.25 ml ddH₂O at a heating block set to 50°C to prepare the basic solution for the polyacrylamide gel. The solution was sterile-filtered (pore size 0.2 µm) to remove larger disruptive particles such as salts. The polymerisation of the solution was started by the supplementation of 175 µl ammonium persulfate (440 mM) and 17 µl ultra-pure N,N,N,N-tetramethylethylenediamine (Invitrogen, Karlsruhe, Germany). Immediately, the still fluid solution was poured between the two glass plates (disruptive bubbles were removed with a thin wire), a comb (48 lanes) was inserted at the uppermost part of the gel (area with binding solution) and the gel was allowed to polymerise for at least 30 minutes at room temperature.

Subsequently, the glass plates including the hardened gel were placed into a NEN 4300 DNA Analyser (Licor, Lincoln NE, USA). The upper and lower buffer tanks were filled with 1x TBE buffer, the comb was removed and the slots were flushed with buffer to remove residual urea. After a pre-run (1'200 V, 25 min, 45°C) the prepared samples were added.

Samples (2 µl) and size standard (µ-STEP-24a, 50 - 700 bp; Microzone, Haywards Heath, UK) were prepared by equally mixing with Stop-Solution (Licor, Lincoln, NE, USA), denaturated for 3 minutes at 94 °C on thermo cycler, and chilled on ice. A total of 0.5 µl per sample was added to flushed and urea-free slots. The gel electrophoresis was performed for 4 hours at 1'200 V and 45 °C.

2.5.11.5. Analysis of T-RF profiles

After the run the gel was scanned and images were analysed with GelQuest (Version 2.6.3.; Sequentix, Klein Raden, Germany). The program generates T-RFLP profiles, in which every peak represents a single T-RF and the height of the peak is linked to the relative fluorescence intensity. T-RFLP profiles of all fractions of [¹²C]- and [¹³C₁]-methanol treatments were compared and shifts of T-RFs towards heavier fractions were evaluated (Figure 58, 3.6.2). In addition, a virtual digestion by *MspI* and *RsaI* with the online available

tool 'NEBcutter V2.0' (New England Biolabs; <http://tools.neb.com/NEBcutter2/>) of a small selection of sequences from methylotrophic bacteria belonging to the alphaproteobacterial *Rhizobiales* and *Methylobacteriaceae* as well as members of the betaproteobacterial *Methylophilaceae* was conducted in order to roughly estimate phylogenetic affiliation of detected T-RFs (Table 35, 3.6.2).

2.5.12. Sequencing

2.5.12.1. Sequencing by chain-termination ('Sanger sequencing')

Sequencing by chain-termination ('Sanger sequencing', Sanger *et al.*, 1977) was performed to determine the exact lengths and verify the sequences of the qPCR standards (see 2.5.8.2). Amplicons (derived after cloning and amplification) were purified by gel extraction (see 2.5.9.1) and sequencing was done by Macrogen (Amsterdam, the Netherlands). The sequencing primers were always the plasmid applied primers (pJET1.2 sequencing primer, see 2.5.8.2, Table 27).

2.5.12.2. Pyrosequencing with barcoded amplicons

Sequencing by pyrosequencing [Margulies *et al.*, 2005] was performed for 16S rRNA gene sequences, *mxoF* sequences and ITS sequences from DNA of the substrate SIP and pH shift SIP experiment (see 2.3.3). In order to assign sequences derived from different samples all amplicons were tagged with an individual barcode by a PCR approach with barcoded fusion primers (see 2.5.7.6).

For bacterial genes (i.e., 16S rRNA amplicons and *mxoF* amplicons) a two-step PCR approach [Berry *et al.*, 2011] was always performed to decrease bias (see 2.5.7.6). Barcoded amplicons were gel-purified (see 2.5.9.1) and pooled equimolar resulting in different amplicon pools. All amplicon pools were treated with PreCR Repair MIX (NEB, Frankfurt am Main, Germany) according to manufacturer's protocol to reduce or eliminate possible DNA-damages that might have occurred during gel purification or amplicon storage (Table 33). The reaction was incubated for 20 min at 37°C.

Table 33 Composition of the reactions with PreCR Repair Mix

Reagent [concentration]	volume
PreCR Repair Mix [1x] ^a	1 µl
ThermoPol Reaction Buffer [10x] ^a	5 µl
BSA [10x] ^a	5 µl
dNTP mix [10 mM] ^b	0.5 µl
NAD ⁺ [25 mM] ^a	0.5 µl
Barcoded amplicon pool	38 µl
	Σ 50 µl

^a All reagents from the PreCR Repair MIX Kit (New England Biolabs)

^b Equimolar mixture from 100 mM stock solutions from ROTH (Karlsruhe, Germany)

Repaired amplicon pools were subsequently purified by isopropyl precipitation (see 2.5.3.2), concentrated by vaporizing (still solved in 10 mM TRIS, pH 8) and then pyrosequenced at the Göttingen Genomics Laboratory using Roche GS-FLX 454 Sequencer and GSL FLX Titanium series reagents according to manufacturer's protocol (Roche Diagnostics GmbH, Mannheim, Germany) as described elsewhere [Stacheter *et al.*, 2013].

For fungal genes (i.e., ITS amplicons) the amplification followed different strategies (see 2.5.7.6) all resulting in barcoded amplicons that were subsequently sequenced. Barcoded amplicon pools were further processed at the Department of Soil Ecology (UFZ, Halle, Germany). Before pyrosequencing all ITS amplicon-replicates were pooled and fragments between 400 bp and 1200 bp were gel-purified with QIAquick Gel Extraction Kit (Qiagen, Hilden, Germany) on a Dark Reader Transilluminator (Clare Chemical Research Inc, Dolores, CO, USA) using blue light instead of UV light. Thus, no damaging of amplicons was assumed reduntantising DNA repair kit. Amplicons were pooled equimolar and sequenced as described elsewhere [Wubet *et al.*, 2012].

2.5.12.3. Sequencing by synthesis ('ILLUMINA sequencing')

Sequences by synthesis ('ILLUMINA sequencing', Bentley *et al.*, 2008) was performed for 16S rRNA gene sequences, *mxoF/xoxF* and *cmuA* sequences from DNA of the methanol/chloromethane SIP experiment (see 2.3.10). The sequencing and creation of the individual amplicon libraries was done by LGC. For 16S rRNA the different PCR samples (i.e., 'heavy', 'middle' or 'light' fraction, ¹²C- or ¹³C-treatment, supplemented substrate; in total 24 different samples) were pooled equimolar, and one NuGen Library was prepared. For marker genes (*mxoF/xoxF*, *cmuA*) the PCR products were pooled equimolar at the University of Bayreuth and for each sample one NuGen Library was prepared by LGC. All libraries were sequenced using Illumina MiSeq V3 (300 bp paired-end read) with a sequencing amount of 2.5 mio read pairs.

2.5.13. Sequence analyses (filtering and clustering of raw reads)

2.5.13.1. Analyses of sequences derived from pyrosequencing

The sequence analyses of bacterial genes (i.e., 16S rRNA and *mxoF/xoxF* gene sequences) was conducted at the department EMIC of the University of Bayreuth and the sequence analyses of fungal genes (i.e., ITS gene sequences) was conducted at Department of Soil Ecology, UFZ - Helmholtz Centre for Environmental Research, Halle by Dr. Guillaume Lentendu. Thus, the filtering of sequences and the clustering of amplicon pyrosequencing reads were different. Finally, clustered reads (according to similarity) were used for further analyses (see 2.5.14, 2.5.15, 2.5.17).

Recovered reads of bacterial genes were trimmed to 446 nt (for 16S rRNA amplicons) and 461 nt (for *mxoF* amplicons), so that the reverse primer sequence was mostly removed.

Amplicon pyrosequencing errors were corrected using ACACIA, i.e., homopolymer error-correction and low quality reads were discarded [Bragg *et al.*, 2012]. Potential 16S rRNA chimeric sequences were filtered out using UCHIME algorithm implemented in USEARCH and the latest RDP Gold database for high quality 16S rRNA gene reference sequences [Edgar *et al.*, 2011]. Before sequence clustering initial barcode sequences were modified to re-assign amplicons (see Table A 1). Using JAguc v2.1 [Nebel *et al.*, 2011] sequences were clustered into operational taxonomic units (OTUs) using a pairwise sequence alignment before creating a distance matrix and clustering with the average similarity method. Only sequences with the correct forward primer sequence were further analysed. OTUs of 16S rRNA were clustered on family level with 90.1 % as pairwise similarity cut-off value [Yarza *et al.*, 2010] and *mxoF* OTUs were clustered with a cut-off value of 90 %. The *mxoF* cut-off was higher than previously reported [Stacheter *et al.*, 2013] to obtain a higher diversity with regard to exhibit still a relative constant number of retrieved OTUs (Figure 32). An overview of the total number of sequences derived from pyrosequencing and after clustering is given in Table A 4. Phylogenetic affiliation of ribosomal sequences was done by a local nucleotide BLAST using the latest NCBI GenBank release. Affiliation was verified by manual BLAST of the OTU's representative sequences and phylogenetic tree using MEGA Version 6.06 [Tamura *et al.*, 2013]. Affiliation of *mxoF* OTUs was performed by manual BLAST and phylogenetic trees.

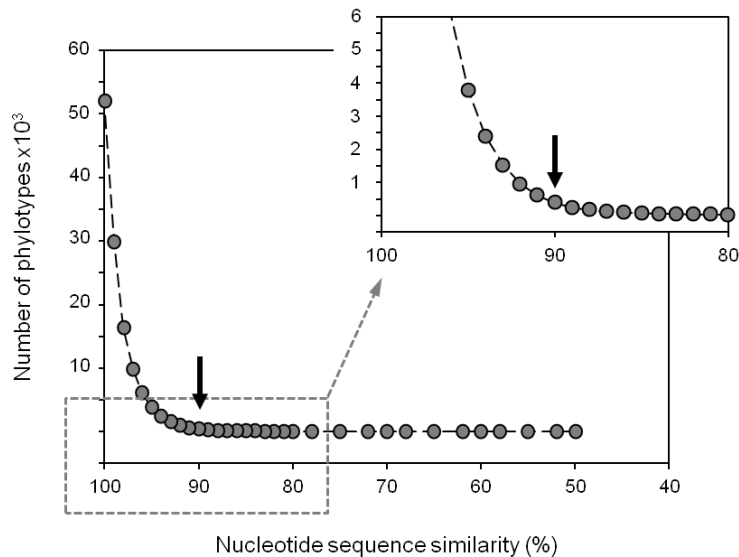


Figure 32 Correlation between the number of detected phylotypes and the nucleotide sequence similarities of *mxoF* gene sequences.

The shown correlation between all detected phylotypes and the nucleotide sequence similarity based on all detected *mxoF* gene sequences of both SIP experiments (i.e., 113 689 sequences) was used to determine the similarity threshold value of 90 % chosen for clustering and further analyses. Inset focuses on a sequence similarity range between 80 % and 100 %. This figure has been published in Morawe *et al.* 2017.

Recovered reads for fungal genes were demultiplexed and quality trimmed using MOTHUR [Schloss *et al.*, 2009]. Reads that met the following criteria were further analysed: holding one of the expected barcodes (1 mismatch allowed, for barcode sequences see Table A 2) and the forward fusion primer sequence (includes ITS4, 4 mismatches allowed), with a minimum length of 355 nt, a minimum average quality of 29 Phred score over the 355 first nucleotides, maximum homopolymer length of 8 nt, and without ambiguous nucleotides. The reads were cut to their 355 first nucleotides to avoid low quality ends and length sorting in the following clustering step. Normalised reads (1503 counts per sample) were checked for chimeric sequences using UCHIME [Edgar *et al.*, 2011] as implemented in MOTHUR. Unique sequences were sorted by decreasing abundances and were clustered into OTUs using CD-HIT-EST [Fu *et al.*, 2012] at a 97 % pairwise similarity cut-off value. Low abundant OTUs with 3 or less reads were removed as they potentially originated from artificial sequences [Kunin *et al.*, 2010]. Representative OTU sequences were classified against the dynamic UNITE database (v7 release 01.08.2015 [Kõljalg *et al.*, 2013]) using the MOTHUR implementation of Wang *et al.* (2007) classifier. Sequences that could not assigned further than to the kingdom Fungi were classified for a second time against a previous database including non-fungal ITS sequences retrieved from GenBank (release 207, accessed on 06.05.2015 [Benson *et al.*, 2008]) in order to detect and remove non-fungal sequences. Subsequently, remaining sequences assigned to the Fungi kingdom only were classified against the full UNITE database to improve the taxonomic affiliation. In addition, reference sequences of selected OTUs (representative sequence) were manually identified by 'massBLASTer analyses' of UNITE database to confirm affiliation. An overview of the total number of sequences derived from pyrosequencing and after clustering is given in Table A 4.

For general community analyses and the identification of labelled phylotypes of bacterial and fungal genes (see 2.5.14, 2.5.17.4, 2.5.17.5) sequences occurring only once within the complete data set of all received amplicon libraries were considered as artificial errors and thus were removed, whereas singletons in each individual amplicon library were preserved.

2.5.13.2. Analyses of sequences derived from synthesis-sequencing

The sequence analysis of raw reads obtained by 'ILLUMINA sequencing' was conducted by our cooperation partner at the Institute de botanique, Laboratoire GMG, Equipe AIME, Strasbourg (analyses done by Dr. Ludovic Besaury).

For the analyses of 16S rRNA reads, the Illumina reads were analysed using mothur software package v.1.33.2 [Kozich *et al.*, 2013] with the default parameters of the MiSeq standard operating protocol (http://www.mothur.org/wiki/MiSeq_SOP). Read pairs were assembled into contigs and contigs shorter than 420 bp or longer than 460 bp were discarded. Sequences were pre-clustered in groups of sequences with up to 2 nucleotide differences. Putative chimeric sequences were predicted by UCHIME [Edgar *et al.*, 2011] and subsequently removed. The remaining sequences were assigned using naïve Bayesian

taxonomic classification on the bacterial reference database SILVA (SSU_Ref database v.119), at a bootstrap cut-off set at 80 %. Only sequences affiliated to Bacteria and Archaea domains were selected and other non-bacterial or archeal sequences were discarded. The clustering into OTUs was done at a similarity threshold of 98 % sequence identity using the automated protocol within Mothur. This also yielded a representative consensus sequence for each OTU that was chosen as the most abundant sequence in a given OTU, and subsequently used for sequence alignments and further analyses.

For the analyses of functional genes (i.e., *mxoF/xoxF* and *cmuA*) the raw reads were processed using mothur software package v.1.33.2 [Kozich *et al.*, 2013] including length filtering and quality trimming, and allowing sequence lengths within 20 nucleotides of the expected length of the amplicon. The USEARCH software [Edgar, 2010] was used for clustering the obtained filtered reads. Sequences occurring only once within the complete dataset of gene amplicon libraries were considered as artificial and were removed, whereas singletons in individual amplicon libraries were retained. Reads were clustered iteratively at progressively lower cut-off values, and the maximum cut-off value at which the number of retrieved OTUs stabilized was selected according to Stacheter and colleagues (77 % for *mxoF/xoxF*-type MDH) and the similarity cut-off value for the other SIP experiments (90 % for *cmuA*) (see 2.5.13.1, Figure 32). In the case of all MDH related gene sequences only forward reads (R1) were analysed in this manner because of the amplicon length (569 bp) and poor assembly results when forward and reverse reads were assembled. Consensus sequences for each OTU were provided by mothur. These sequences were compared against a gene-specific database generated from GenBank using BLAST (<http://blast.ncbi.nlm.nih.gov>) for taxonomic identification. Thus, a cluster table for each gene and each sample was obtained and used for further analyses.

2.5.14. Identification of ‘¹³C-labelled’ phylotypes

The ‘labelling’ of taxa by the ¹³C-isotopologues was determined by analysing relative abundances of phylotypes in the amplicon libraries of ‘heavy’, ‘middle’ and ‘light’ fractions of [¹²C]- and [¹³C]-incubations of all SIP experiments (see 2.3.3, 2.3.4, 2.3.10).

The comparison of relative abundances in ‘heavy’ fractions of ¹³C-isotopologue incubations with ‘heavy’ fractions of ¹²C-isotopologue incubations as well as a comparison of the ‘heavy’ and ‘light’ fractions of the ¹³C-isotopologue were conducted. This procedure minimises the false evaluation of a false-positive signal due to migration of ‘light’ DNA into the ‘heavy’ fractions [Lueders *et al.*, 2004; Liu *et al.*, 2011; Dallinger *et al.*, 2014].

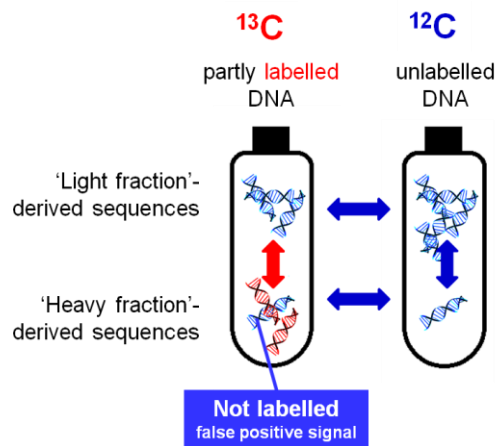


Figure 33 Identification of labelled phylotypes.

The identification of labelled phylotypes was based on the comparison of amplicon libraries derived from different fractions of the SIP treatments. The comparison of all corresponding fractions with each other enables the detection of false-positive phylotypes, i.e., they are detectable in the heavy fraction of ^{13}C -derived amplicon libraries but they are not labelled by ^{13}C -isotopologues.

Following 4 criteria had to be met determining taxa as putatively 'labelled':

- (1) the abundance in the appropriate fraction (i.e., 'heavy' and 'middle' fraction, respectively) of the ^{13}C -isotopologue incubation was higher than in the corresponding fraction of the ^{12}C - isotopologue incubation
- (2) the abundance in the 'light' fraction was lower than in the 'heavy' or 'middle' fraction of the ^{13}C - isotopologue incubation
- (3) the abundance in the 'heavy' or 'middle' fraction of the ^{13}C - isotopologue incubation was $\geq 0.5\%$
- (4) the difference between the abundance in the compared fractions of the ^{13}C - isotopologue incubation was higher than the individual threshold value compared to the ^{12}C - isotopologue incubation

In terms of the substrate SIP and pH shift SIP experiments (see 2.3.3, 2.3.4) this threshold value was equal for all treatments and was determined as $\geq 0.1\%$. The reason for this lowered value is justified in the dominating abundance of several phylotypes in the heavy fractions of all treatments distorting the abundances of other phylotypes (see 3.6.3). In terms of the methanol/chloromethane SIP experiment (see 2.3.10) the individual threshold was adapted to the different incubation approaches (i.e., solely methanol, solely chloromethane, and both substrates simultaneously supplemented). The individual T_x of each incubation approach was calculated using Equation 13.

Equation 13 Individual threshold T_x calculated for the methanol/chloromethane SIP experiment

$$T_x = \frac{1}{n} \sum_{i=1}^n RE_i$$

n , number of all detected taxa in an incubation approach (involves ^{12}C - and ^{13}C - isotopologue treatments)

$\frac{1}{n} \sum_{i=1}^n RE_i$, average of the relative errors* of detected taxa in an incubation approach (involves ^{12}C and ^{13}C - isotopologue treatments)

*calculated using Equation 14

Equation 14 Relative error RE_x

$$RE_x = \frac{100}{\sum_{i=1}^n RA_i} \times SD_x$$

$\sum_{i=1}^n RA_i$, is the average of all relative abundances of the detected taxa in the corresponding fraction of the ^{13}C - isotopologue treatment

SD_x , is the standard deviation of the detected taxa

Taxa that met all these criteria were considered 'potentially labelled' and were the basis for the calculation of the 'labelling proportion' (LP) as a measure of the relative importance (Equation 15).

Equation 15 Labelling proportion LP_x

$$LP_x = \frac{100}{\sum_{i=1}^n RA_i^{13\text{C}}} \times RA_x^{13\text{C}}$$

n , number of all 'potentially labelled' taxa

$\sum_{i=1}^n RA_i^{13\text{C}}$, sum of all relative abundances of 'potentially labelled' taxa in the corresponding fraction of the ^{13}C -isotopologue treatment

$RA_x^{13\text{C}}$, relative abundance of a certain taxon x in the corresponding fraction of the ^{13}C -isotopologue treatment

A threshold value of 5 % was used to distinguish between the labelled taxa of greater (i.e., $LP_x \geq 5\%$) or minor (i.e., $LP_x < 5\%$) importance [Liu *et al.*, 2011; Dallinger *et al.*, 2014]. The phylotypes that were identified as labelled in the M fraction were considered as weakly labelled, assuming that they possessed not fully labelled DNA and thus were not well separated from non-labelled DNA.

2.5.15. Calculation of phylogenetic trees

All phylogenetic trees are based on nucleotide sequences of the genes and were created using mainly the same approach. 16S rRNA and *mxoF/xoxF* tree databases include the first 1 to 3 BLAST hits of cultured and uncultured next hits (sorted by ID, nucleotide BLAST,

<https://blast.ncbi.nlm.nih.gov/BLAST.cgi>, using the nucleotide (nr/nt) database and the megablast algorithm (standards settings). Several type species of identified families or genera as well as known methylotrophic organisms were added to both of the sequence databases. The basis for the *mxoF/xoxF* database was kindly provided by Dr. Martin Taubert and was previously applied for *xoxF* analyses [Taubert *et al.*, 2015]. Before each alignment all sequences of the nucleotide databases were trimmed, i.e., the forward primer sequences were removed and the 3'-end were shortened to obtain consistent lengths of all sequences. Alignments for 16S rRNA were done using the SINA Alignment Service (<https://www.arb-silva.de/aligner/>) and the alignment for *mxoF/xoxF* sequences were done using the MUSCLE algorithm implemented in MEGA5 [Tamura *et al.*, 2011]. All phylogenetic trees were calculated using MEGA5 and maintaining the same conditions for each tree [Tamura *et al.*, 2011]. In total tree different trees were created.

'Neighbour joining trees' were constructed using the Neighbour-Joining method [Saitou & Nei, 1987]. Evolutionary distances were computed using the p-distance method [Nei & Kumar, 2000]. Codon positions included were 1st+2nd+3rd and all ambiguous positions were removed for each sequence pair. In total 100 to 1000 bootstrap replications were conducted [Felsenstein, 1985].

'Maximum likelihood trees' were calculated using the Maximum Likelihood method based on the Jukes-Cantor model [Jukes & Cantor, 1969]. In total 50 bootstrap replications were conducted and initial trees were obtained automatically by applying Neighbor-Join and BioNJ algorithms to a matrix of pairwise distances estimated using the Maximum Composite Likelihood (MCL) approach. Finally, the tree with the highest likelihood was shown. Codon positions included were 1st+2nd+3rd.

'Maximum parsimony trees' were calculated the Maximum Parsimony method. In total 50 bootstrap replications were conducted using the Subtree-Pruning-Regrafting (SPR) algorithm [Nei & Kumar, 2000] and the most parsimonious tree was finally shown. Codon positions included were 1st+2nd+3rd.

Neighbour joining trees are always shown in the figures and are the basis for congruency evaluation with the maximum likelihood and the maximum parsimony trees. Congruencies were indicated by circles at the nodes (i.e., congruency in all three trees is indicated by black filled circles; congruency with the neighbour joining tree and the maximum likelihood or the maximum parsimony tree is indicated by grey filled circles).

The phylogenetic tree of the *cmuA* phylotypes (Figure A 15) was created by our cooperation partner at the Institute de botanique, Laboratoire GMG, Equipe AIME, Strasbourg (created by Pauline Chaignaud) and is based on nucleotide sequences.

2.5.16. Nucleotide sequence accession numbers

Published sequences obtained in this work are available from the EMBL nucleotide sequence database (European Molecular Biology Laboratory; <http://www.embl.de>)

Representative sequences of labelled phylotypes derived from barcoded amplicon pyrosequencing (i.e., substrate SIP and pH shift SIP experiments) were deposited in EMBL under accession numbers LT607885 to LT607955 (for 16S rRNA gene), LT607956 to LT608017 (for *mxoF*), and LT608018 to LT608119 (for ITS). All raw pyrosequencing datasets were deposited in the ENA Short Read Archive under the study accession number ERP016444, including the 16S rRNA gene, *mxoF* and ITS datasets.

Representative sequences of labelled phylotypes based on 16S rRNA gene sequences as well as all detected phylotypes of *mxoF/xoxF*-type MDH and *cmuA* gene sequences derived from 'ILLUMINA sequencing' (i.e., methanol/chloromethane SIP experiments) were deposited in EMBL under accession numbers LT674486 to LT674490 (for 16S rRNA gene), LT674515 to LT674539 (for *mxoF/xoxF*-type MDH), and LT674491 to LT674498 (for *cmuA*). All raw datasets of the 'ILLUMINA sequencing' were deposited in the ENA Short Read Archive under the study accession number ERP016444, including the 16S rRNA gene (sample group accession number ERG010959), *mxoF* and *cmuA* datasets (sample group accession number ERG010984).

2.5.17. Statistical analyses and calculations

2.5.17.1. Arithmetic mean, standard deviation, standard error, error propagation

Since incubation experiments or measurements were conducted in replicates (duplicate / triplicates), the arithmetic mean values (Equation 16), standard deviations (Equation 17), standard errors (Equation 18), and error propagation (Equation 19) were calculated.

Equation 16 **Arithmetic mean \bar{x}**

$$\bar{x} = \frac{1}{n} \sum_{i=1}^n x_i$$

n , number of replicates
 $\sum_{i=1}^n x_i$, sum of all individual values x_i
 x_i , individual value for one replicate

Equation 17 **Standard deviation SD_i**

$$SD_i = \sqrt{\frac{1}{n-1} \sum_{i=1}^n (x_i - \bar{x})^2}$$

Equation 18 **Standard error SE_i .**

$$SE_i = \frac{SD}{\sqrt{n}}$$

Equation 19 **Error propagation EP .**

$$EP = \sqrt{\sum_{i=1}^n (SE_i)^2}$$

2.5.17.2. Calculation of the methane degradation rate ' $R\Delta CH_4$ '

The methane degradation rate ' $R\Delta CH_4$ ' was calculated (Equation 20) based on CH_4 concentration changes within one week in treatments with and without additional substrate supplementation of the long-term incubation under mixed substrate conditions (see 2.3.1). A stimulation of the supplemented alternative substrate was assumed if the calculated ratio was greater than 1, and an inhibition of the supplemented substrate was assumed if the calculated ratio was below 1.

Equation 20 **Methane degradation rate $R\Delta CH_4$**

$$R\Delta CH_4 = \frac{\Delta CH_4 \text{ substrate supplemented}}{\Delta CH_4 \text{ unsupplemented}}$$

ΔCH_4 *substrate supplemented*, changes of the CH_4 concentration in a given time period (for example one week) in treatments with additional alternative substrates supplemented [$\mu\text{mol ml}^{-1}$]

ΔCH_4 *unsupplemented*, changes of the CH_4 concentration in a given time period (for example one week) in treatments solely supplemented with methane [$\mu\text{mol ml}^{-1}$]

2.5.17.3. Coverage

The coverage was calculated for all data sets derived from sequencing and is an estimator of sufficient sampling. The coverage is an estimator concerning the amount of detected phylotypes in comparison to the absolute number of all detected phylotypes in a sequence database [Singleton *et al.*, 2001].

Equation 21 **Coverage C [%] of a sequence database.**

$$C = \frac{n_a - n_s}{n_a} \times 100$$

n_a , total number of sequences
 n_s , number of singletons (occurring only once in a sample database)

2.5.17.4. Community analyses (diversity indices, ANOSIM, NPMANOVA, SIMPER)

All filtered and clustered sequencing datasets (i.e., libraries of 'light', 'middle' and 'heavy' fractions) of ^{12}C - and ^{13}C -isotopologue treatments were combined to an entire data set for each treatment. Community analyses were always based on family level for 16S rRNA and

ITS phylotypes and 90 % similarity cut-off for *mxnF* phylotypes. All statistical analyses were performed using the software *PAleontological STatistics* (PAST, version 1.85 and version 3.08) [Hammer *et al.*, 2001].

Diversity and richness estimators (i.e., dominance D, Shannon index H, equitability J, and Chao1 index) were calculated with the in PAST V1.85 implemented diversity indices calculation (bootstrap replications: 9999; bootstrap type: percentile).

ANOSIM (ANalysis Of SIMilarities) is a non-parametric test of significant difference between two or more groups, based on any distance measure [Clarke, 1993]. It is based on comparing distances between groups with distances within groups. The calculated R value (up to 1) indicates dissimilarities. NPMANOVA (Non-Parametric Multivariate ANalysis Of Variance, also PERMANOVA) is a non-parametric test of significant difference between two or more groups, based on any distance measure [Anderson, 2001]. The calculated F value indicates dissimilarities. The significance of each analysis was computed by 10'000 replicates. Each analysis was based on the similarity index of Bray-Curtis [Bray & Curtis, 1957] considering also the abundances of detected phylotypes.

SIMPER (SIMilarity PERcentage) is a method for assessing which taxa are primarily responsible for an observed difference between groups of samples [Clarke, 1993]. SIMPER was conducted as pairwise analyses of two different conditions (t_0 vs. t_{END} or methanol incubation vs. substrate incubation). The overall average dissimilarity is computed using all the taxa, while the taxon-specific dissimilarities are computed for each taxon individually. SIMPER was always based on the similarity index of Bray-Curtis [Bray & Curtis, 1957].

2.5.17.5. Visualisation by NMDS plots and heatmaps

Multidimensional scaling (MDS) is an ordination technique based on a (dis)similarity matrix using a chosen distance metric. In nonmetric multidimensional scaling (NMDS), ranks of these distances among all objects are calculated and the algorithm then finds a configuration of objects in the chosen N-dimensional ordination space that matches differences in ranks best [Kruskal, 1964; Paliy & Shankar, 2016]. NMDS is a numerical and not an analytical method, thus it does not produce a unique solution. The calculated 'stress' value is computed in order to measure the lack of fit between object distances in the NMDS ordination space and the calculated dissimilarities among objects. The NMDS algorithm then iteratively repositions the objects in the ordination space to minimize the stress function [Dugard *et al.* 2014]. The stress value tends to zero when the rank orders reach perfect agreement and stress values ≤ 0.15 are considered generally acceptable [Clarke, 1993]. The NMDS plots in this work were created using PAST V1.85 and employing the Bray-Curtis similarity index.

All heatmaps in order to visualize congruency between analysed samples were individually created using the software 'R' (version 3.2.2; R development core team, Vienna, Austria) and the packages 'gplot' (version 2.17.0) and 'RColorBrewer' (version 1.1-2).

3. RESULTS

The following section is subdivided based on the respective C1 compounds (i.e., methane, methanol and chloromethane) and the microbial guilds of methylophiles utilising these compounds.

In addition, some presented data in this section were obtained by coworkers as part of their Bachelor thesis, Master thesis or Doctoral thesis [Gass, 2013; Ruffer, 2014; Steinen, 2014; Chaignaud, 2016]. Michael Gass (MG) collected qPCR data that are present in section 3.1. Vanessa Steinen (VG) established a qPCR-assay for the marker gene *mxnA* that was the basis for *mxnA* qPCR analyses of this current work. Michael Ruffer (MR) collected data on the CH₃Cl degradation potential of different forest compartments. These data are presented in the section 4.4.1. Pauline Chaignaud (PC) contributed to the methanol/chloromethane SIP experiment presented in section 3.10 & 3.11.

3.1. Methane degradation and abundance of ‘high-affinity’ USC α methanotrophs in an acidic forest soil

Methanotrophic microorganisms are the major sink for atmospheric methane [Kolb *et al.*, 2005, Kolb, 2009b]. Since atmospheric concentrations of methane are low, the question arises how these methanotrophs can grow or even persist under such growth-limiting conditions. One feasible survival mechanism might be the utilisation of other carbon substrates besides methane [Dunfield, 2007]. Indeed, some cultured facultative methanotrophs affiliated to *Beijerinckiaceae* and *Methylocystaceae* were described over the last years but are still an exception [Dedysh *et al.*, 2005; Dunfield *et al.*, 2010; Belova *et al.*, 2011; Im & Semrau, 2011]. Predominant methanotrophs at the sampling site were ‘high-affinity’ USC α [Degelmann *et al.*, 2010], which exhibit a close phylogenetic relation to known facultative methanotrophs, suspecting the ability of a hitherto underestimated substrate range of these high-affinity methanotrophs including common compounds within soil environments like acetate, sugars, aromatic compounds, and hydrocarbons. Thus, low concentrations of methane (20 ppm) and putatively alternative substrates (100 μ M) were supplemented in weekly pulses over a long incubation period to analyse the long-term effect of substrates and incubation on the methane degradation (see 2.3.1).

Soil slurry treatments without supplemented substrates revealed a constant methane degradation potential per week over the first 10 weeks of incubation (i.e., 50 μ M CH₄ in total). After 10 weeks the methane degradation per week decreased slightly and after 15 weeks of incubation (i.e., 75 μ M CH₄ in total) the methane degradation per week was the lowest (Figure 34). The analysis of 16S rRNA gene copy numbers revealed an initial slight increase of gene copy numbers from 5.9 x 10⁴ gene copies ng⁻¹ DNA at t₀ to 7.8 x 10⁴ gene copies ng⁻¹ DNA after 6 weeks, but finally bacterial abundance dropped to 3.6 x 10⁴ gene copies ng⁻¹

DNA after 14 weeks (Figure 34). Contrary to 16S rRNA genes USCα-specific *pmoA* gene numbers initially dropped from 3.8×10^3 gene copies ng^{-1} DNA at t_0 to 9.85×10^2 gene copies ng^{-1} DNA after 6 weeks of incubation, but increased again over time indicating a growth supporting effect of supplemented methane (Figure 34). However, the abundance of methanotrophic USCα-affiliated microorganisms never reached the initial abundance again.

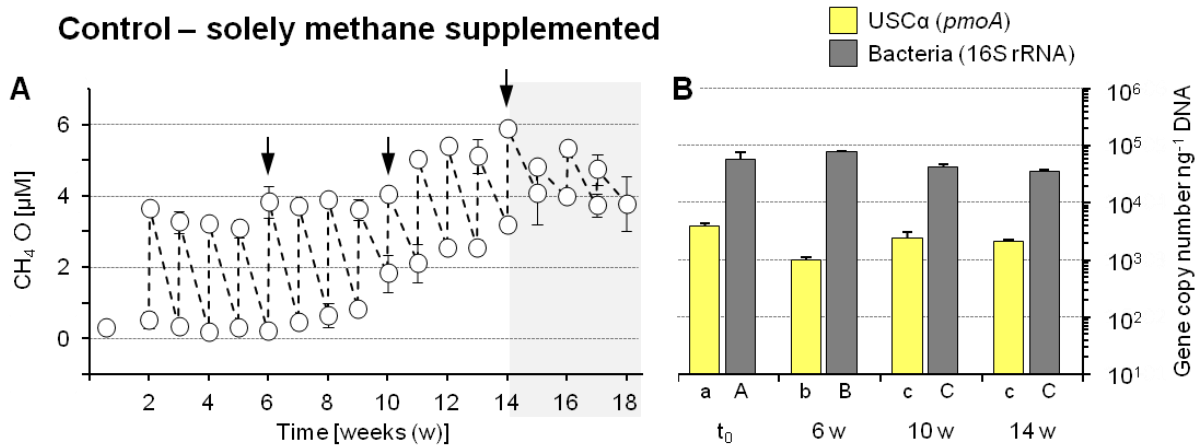


Figure 34 Methane degradation (A) and corresponding gene copy numbers of 16S rRNA and *pmoA* (USCα) (B) in soil slurry treatments during the long-term incubation.

Panel A, CH₄ concentrations (mean values) in methane-supplemented treatments before and after each weekly methane pulse. The grey background indicates the timeframe corresponding to increased pulses of alternative substrates in substrate pulsed treatments (not shown here). Error bars represent standard deviations. The arrows indicate the time points of qPCR analysis during the incubation.

Panel B, gene copy numbers of 16S rRNA and *pmoA* genes ng^{-1} DNA. Gene copy numbers for t_0 were determined by triplicated qPCR measurements. Gene copy numbers for treatments are mean values of replicates. Gene copy numbers for each replicate were determined by triplicated qPCR measurements. Error bars indicate standard deviation for mean values. Raw qPCR data were generated by MG [Gass, 2013]. Different letters indicate significant differences between *pmoA*-samples (small letters) and 16S rRNA-samples (capital letters) based on One-Way ANOVA (normal distribution was assumed based on Shapiro-Wilk-test, $n = 3$).

The observed changes in the decreasing methane degradation per week were not explainable by changes in the abundance of bacterial or methanotrophic cell numbers. In addition, the pH of the methane supplemented slurry incubations did not changed and remained constant at 3.92 ± 0.1 (data not shown), so that the influence of varying pH values within the incubation are deniable. As it was observed by Pratscher and colleagues [Pratscher *et al.*, 2011], methane oxidation can be obviously inhibited by the manner of incubation as shaken slurries. For that reason the incubation style might be the main reason for the observed decreasing methane degradation per week over time.

Assuming two 2 *pmoA* copies per USCα genome, as it is reported for cultured methanotrophs [Stolyar *et al.*, 1999], and 4.13 16S rRNA gene copies per bacterial genome [Klappenbach *et al.*, 2001], the relative amount of USCα with regard to the total bacterial community at the initial t_0 was 13.6 % (Table 34). Previous calculation of the relative amount of USCα in Steigerwald soil revealed a contribution of these methanotrophs to the total

bacterial community up to 2 % [Degelmann *et al.*, 2010], which is nearly 7 times lower than reported here. In addition, the relative amount of methanotrophs in another soil system was below 4 % [Lau *et al.*, 2007], emphasising the high proportion of methanotrophs calculated here. Interestingly, such high amounts of USC α were not reported for the different incubations with supplemented alternative substrates (exceptions are the incubation with methanol and guaiacol at 6 weeks) (Table 34). As mentioned before the incubation was suggested to have an initially negative effect on USC α methanotrophs, since their contribution to the total community dropped to 2.6 % after 6 weeks of incubation (Table 34) , whereas the total community was not negatively affected as indicated by slightly higher 16S rRNA gene numbers (7.8×10^4 gene copies ng⁻¹ DNA) (Figure 34). Methane supplementation was assumed to enrich USC α methanotrophs over the longer incubation to a relative amount more than 10 % of the total community (Table 34).

Table 34 Percentage of USC α methanotrophs on total bacterial cell numbers in different treatments with alternative substrates over time.

Values are calculated on the basis of determined gene copy numbers and average gene copy numbers per genome for *pmoA* and 16S rRNA.

Treatment	Incubation time			
	t_0^a	6 weeks	10 weeks	14 weeks
control ^b		2.6 %	11.4 %	12.0 %
acetate		1.2 %	2.7 %	4.6 %
n-alkanes		2.9 %	3.1 %	3.8 %
cellobiose		2.9 %	5.4 %	1.5 %
xylose	13.6 %	4.7 %	7.1 %	2.8 %
methylamine		0.7 %	4.3 %	0.6 %
methanol		18.0 %	8.3 %	1.7 %
vanillic acid		4.5 %	5.6 %	3.5 %
guaiacol		17.1 %	5.6 %	5.6 %

^a No incubation or no supplementation of substrates or additional CH₄. Initial analyses of t_0 serve as comparison for all treatments.

^b Unsupplemented control without additional substrates; only CH₄ was supplemented according to the other treatments.

3.2. Effects on the methane degradation by the simultaneous supplementation of methane and alternative substrates

3.2.1. Effects of acetate and n-alkanes

Supplementation of acetate changed the methane degradation per week dramatically. Even within the first weeks of incubation methane degradation was strongly inhibited and came to a standstill with longer incubation time (Figure 35). Higher weekly substrate pulses (500 μ M) showed apparently no stronger inhibition (Figure 35, grey box). Methane degradation ratios

' $R\Delta CH_4$ ' were always below the critical threshold, emphasising the inhibitory effect of acetate right from the start of the incubation (Figure 35).

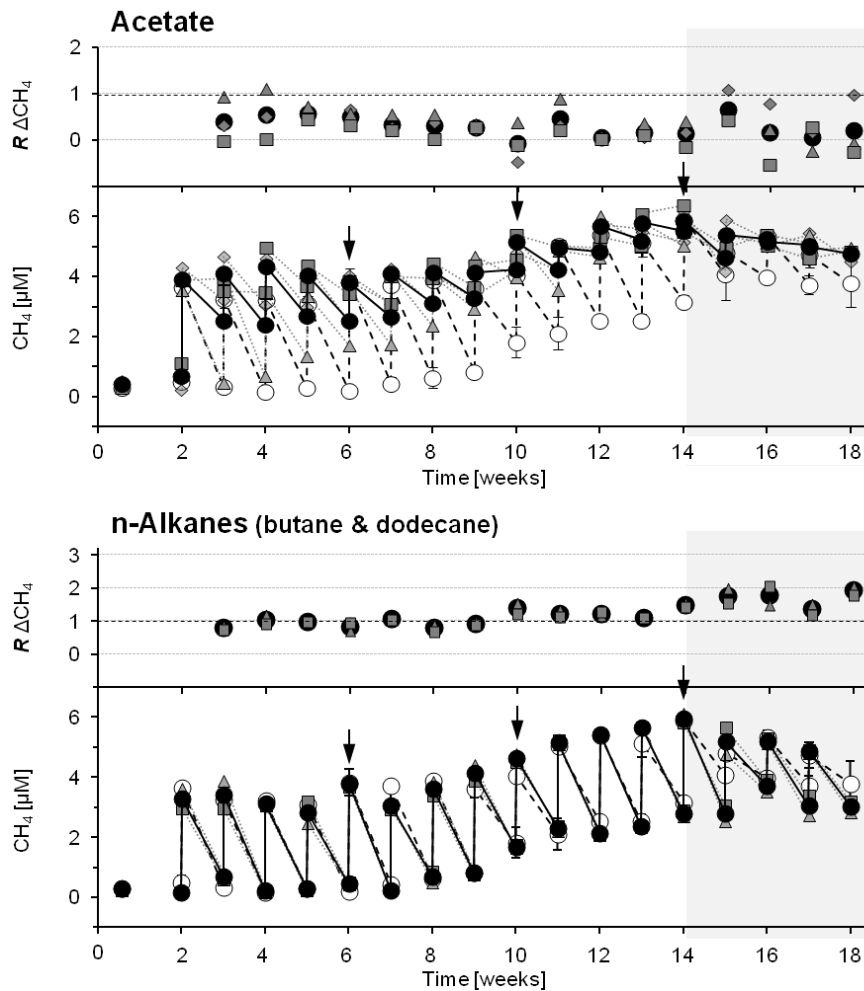


Figure 35 Effect of acetate and n-alkanes (butane & dodecane) on CH_4 degradation in soil slurry treatments.

Effects were evaluated by changes of the CH_4 concentrations in treatments before and after each substrate pulse (i.e., acetate or n-alkanes and CH_4 , weekly) and the corresponding CH_4 degradation ratio ' $R\Delta CH_4$ ' (ratio > 1 indicates stimulation of CH_4 degradation; ratio < 1 indicates inhibition of CH_4 degradation). Pulses of acetate or n-alkanes were 100 μM (no background, to 14 weeks of incubation) and 500 μM (grey background, from 14 weeks of incubation). Symbols: ●, mean value of all acetate or n-alkanes supplemented replicates (◆, replicate 1; ▲, replicate 2; ■, replicate 3); ○, mean value of unsupplemented controls. All treatments were supplemented with CH_4 in accordance with substrate pulses. Error bars represent standard deviations. Arrows indicate the time points of qPCR analysis during the incubation.

The gene abundance of 16S rRNA revealed constant values (1.4×10^5 to 1×10^5 gene copies ng^{-1} DNA) over the incubation time of 14 weeks, meaning an additional total amount of 1.5 mM acetate supplemented (Figure 36). Bacterial abundance was slightly higher than in controls indicating bacterial growth as a response on low acetate supplementation. USC α -specific *pmoA* gene numbers increased from 8×10^2 to 2.3×10^3 gene copies ng^{-1} DNA over the incubation time and were comparable to control incubations (Figure 36). Thus, the ratio of USC α gene copies per 16S rRNA gene copies increased slightly (Figure 36) and the

RESULTS

relative amount of USC α was increased up to 4.6 % after 14 weeks of incubation. Growth of methanotrophic USC α -affiliated organisms can be assumed, but no enhanced activity of their methane degradation suggesting preferred acetate utilisation and a slowdown in methane-utilisation. In addition, pH of the soil slurry increased from initial 3.94 to 4.49 ± 0.04 after 14 weeks (1.5 mM acetate in total) and to a final value of 4.78 ± 0.06 after 18 weeks of incubation (4 mM acetate in total) (data not shown).

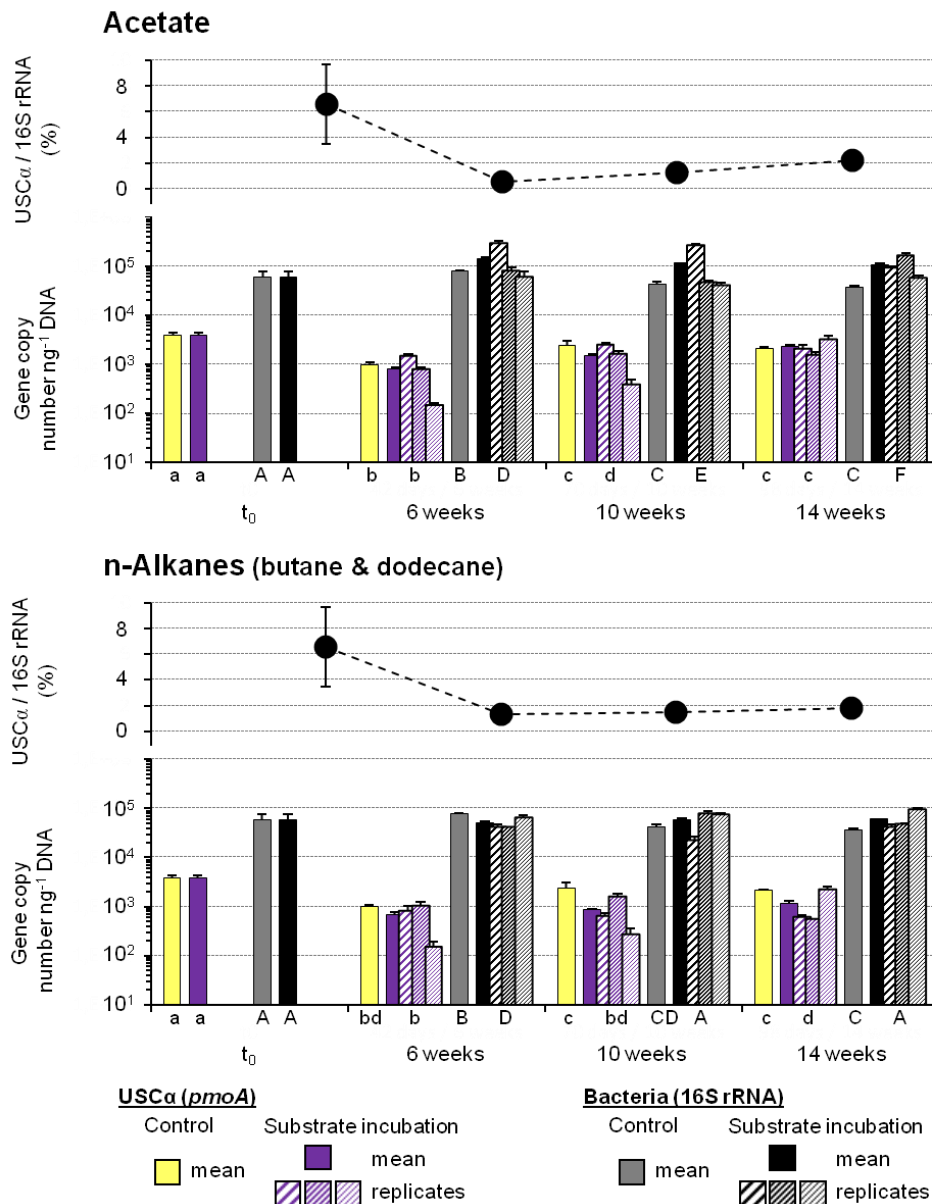


Figure 36 Influence of acetate and n-alkanes on gene copy numbers of 16S rRNA and *pmoA* (USC α) in soil slurry treatments.

The influence of substrates was evaluated by gene copy numbers ng⁻¹ DNA and the corresponding ratio of USC α -*pmoA* per 16S rRNA (%). Gene copy numbers for t₀ were determined by triplicated qPCR measurements. Gene copy numbers for different treatments are mean values of replicates (filled columns). Gene copy numbers for each replicate were determined by triplicated qPCR measurements (shaded columns); error bars indicate standard deviation for replicates and standard error for mean values. Raw qPCR data were generated by MG [Gass, 2013]. Different letters indicate significant differences between *pmoA*-samples (small letters) and 16S rRNA-samples (capital letters) based on One-Way ANOVA (normal distribution was assumed based on Shapiro-Wilk-test, n = 3).

The supplementation of n-alkanes was shown to have no effect on the methane degradation (Figure 35). Methane degradation ratios ' $R\Delta CH_4$ ' were always near the threshold value within the incubation period of 14 weeks (Figure 35). Higher amounts of supplemented n-alkanes revealed a putatively stimulating effect on methane degradation, as calculated ' $R\Delta CH_4$ ' were progressively above the threshold (Figure 35, grey box). In addition, pH of the soil slurry increased from initial 3.94 to 4.02 ± 0.07 after 14 weeks and to a final value of 4.25 ± 0.02 after 18 weeks of incubation (data not shown).

The gene abundance of 16S rRNA remained constant ranging from 5×10^5 to 6.3×10^5 gene copies ng^{-1} DNA over the incubation time of 14 weeks with increasingly higher bacterial abundance than in controls (Figure 36) indicating only minimal bacterial growth as response on the supplementation of n-alkanes. USC α -specific *pmoA* gene copy numbers increased slightly from 6.9×10^2 to 1.2×10^3 gene copies ng^{-1} DNA over the incubation, but values were always lowered compared to the control indicating no preferred growth on n-alkanes of USC α (Figure 36). Thus, the ratio of USC α gene copies per 16S rRNA gene copies remained almost constant (Figure 36) as well as the relative amount of USC α which ranged from 2.9 % to 3.8 % of the total community (Table 34).

3.2.2. Effects of sugars: cellobiose and xylose

Supplementation of sugars affected the methane degradation negatively (Figure 37). Methane degradation in treatments with cellobiose seemed to be inhibited from the beginning indicated by ' $R\Delta CH_4$ ' lower than the threshold, and came to a standstill with longer incubation time (i.e., after 10 weeks) (Figure 37). In comparison, xylose-treated slurries showed at first no effect of substrate supplementation indicated by ' $R\Delta CH_4$ ' values around the threshold value. Decreased methane degradation was observed after longer incubation time (i.e., 10 weeks) (Figure 37), and with increased substrate amounts per pulse (500 μM per pulse) methane degradation was stronger inhibited (Figure 37, grey box).

The pH in both sugar-treated approaches increased slightly from 3.94 at the beginning to values around 4.23 ± 0.05 after 18 weeks of incubation with 4 mM sugars supplemented in total (data not shown).

The supplementation of cellobiose resulted in slight bacterial growth indicated by slight increased 16S rRNA gene abundances. Values ranged from 9.2×10^4 after 6 weeks of incubation up to 2.2×10^5 gene copies ng^{-1} DNA after 14 weeks and were higher than in controls (Figure 38). The supplementation of xylose, however, did not affect 16S rRNA gene abundances and values remained constant over the incubation time (Figure 38). USC α -specific *pmoA* gene copy numbers also remained constant in both sugar-treated approaches, ranging from 1.3×10^3 to 2×10^3 gene copies ng^{-1} DNA (Figure 38). The lowest USC α -specific *pmoA* gene copy number was detected for xylose-treated samples after 14 weeks of

RESULTS

incubation indicating a degraded abundance of USC α methanotrophs, which is in accordance with the observed decreased methane degradation.

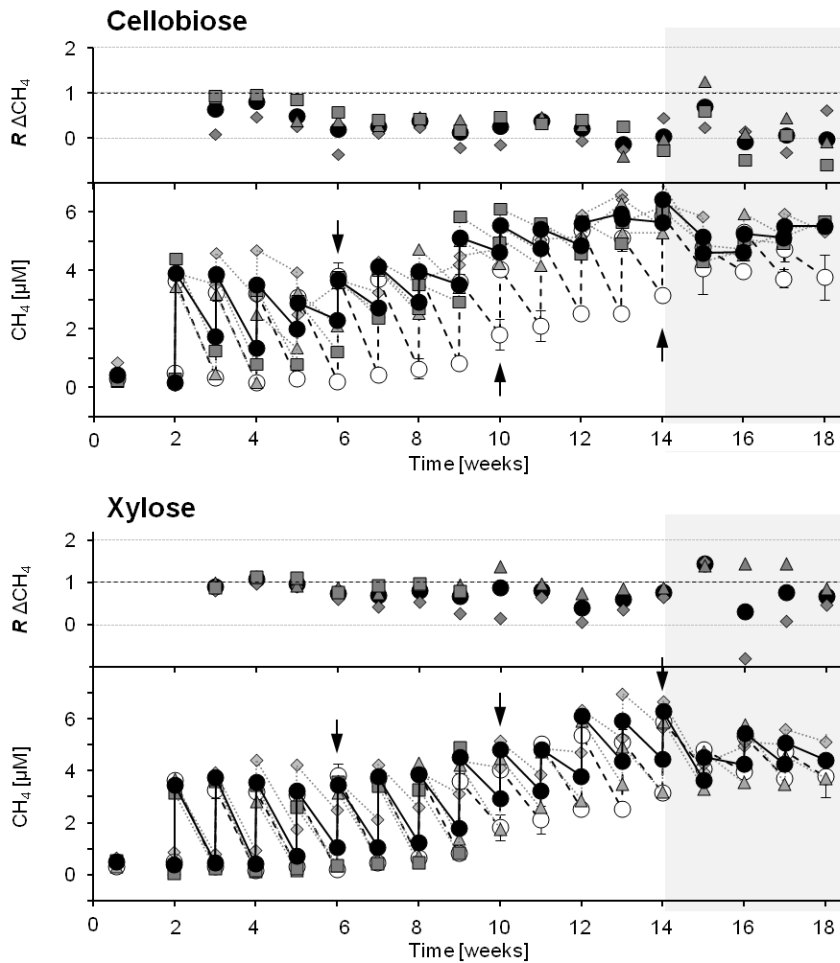


Figure 37 Effect of sugars (glucose & xylose) on CH_4 degradation in soil slurry treatments.

Effects were evaluated by changes of the CH_4 concentrations in treatments before and after each substrate pulse (i.e., glucose or xylose and CH_4 , weekly) and the corresponding CH_4 degradation ratio ' $R\Delta\text{CH}_4$ ' (ratio > 1 indicates stimulation of CH_4 degradation; ratio < 1 indicates inhibition of CH_4 degradation). Pulses of sugars were 100 μM (no background, to 14 weeks of incubation) and 500 μM (grey background, from 14 weeks of incubation). Symbols: ●, mean value of all glucose or xylose supplemented replicates (◆, replicate 1; ▲, replicate 2; ■, replicate 3); ○, mean value of unsupplemented controls. All treatments were supplemented with CH_4 in accordance with glucose and xylose pulses. Error bars represent standard deviations. Arrows indicate the time points of qPCR analysis during the incubation.

The ratios of USC α gene copies per 16S rRNA gene copies were fluctuating for both sugar treatments (Figure 38) as well as the relative amount of USC α of the total bacterial community ranging from 1.5 % to 7 % (Table 34) and growth enhancing effects of sugars for these methanotrophs were not assumed.

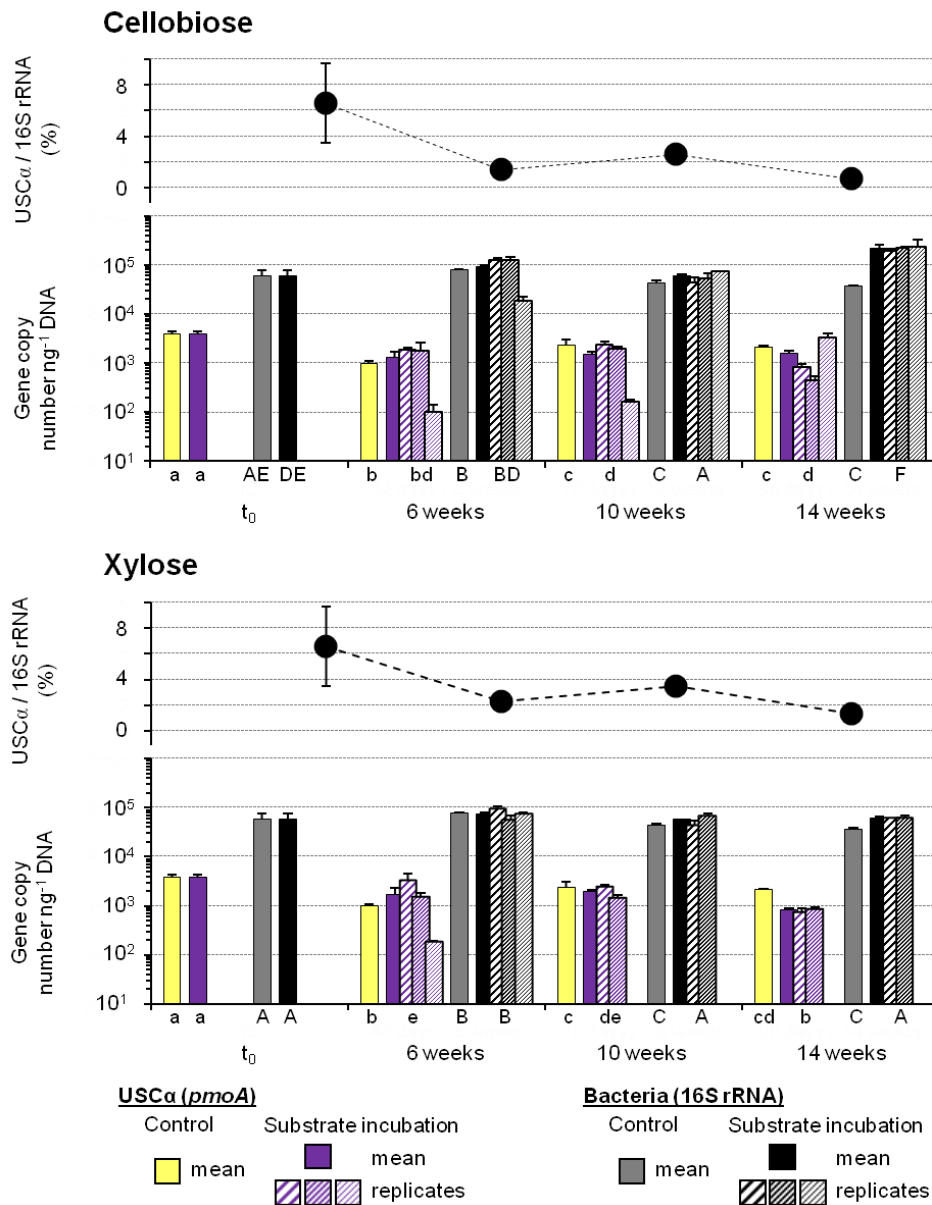


Figure 38 Influence of sugars (glucose and xylose) on gene copy numbers of 16S rRNA and *pmoA* (USC α) in soil slurry treatments.

The influence of substrates was evaluated by gene copy numbers ng⁻¹ DNA and the corresponding ratio of USC α -*pmoA* per 16S rRNA (%). Gene copy numbers for t₀ were determined by triplicated qPCR measurements. Gene copy numbers for different treatments are mean values of replicates (filled columns). Gene copy numbers for each replicate were determined by triplicated qPCR measurements (shaded columns); error bars indicate standard deviation for replicates and standard error for mean values. Raw qPCR data were generated by MG [Gass, 2013]. Different letters indicate significant differences between *pmoA*-samples (small letters) and 16S rRNA-samples (capital letters) based on One-Way ANOVA (normal distribution was assumed based on Shapiro-Wilk-test, n = 3).

3.2.3. Effects of other C1 compounds: methylamine and methanol

Methylamine and methanol did not affect the methane degradation per week significantly (Figure 39). Especially methylamine revealed no influence over the whole incubation time

RESULTS

and even an increased amount of methylamine per week (500 μM) did not alter methane degradation compared to controls (Figure 39).

For methanol a minor inhibiting effect on methane degradation can be assumed after longer incubation and mainly after increased methanol pulses (500 μM) as indicated by ' $R\Delta\text{CH}_4$ ' values below the threshold (Figure 39).

In addition, the pH in those incubations increased from 3.94 to 4.39 ± 0.01 in methylamine- and 4.28 ± 0.08 in methanol-treated incubations after 18 weeks of incubation (supplementation of 4 mM substrates in total) (data not shown).

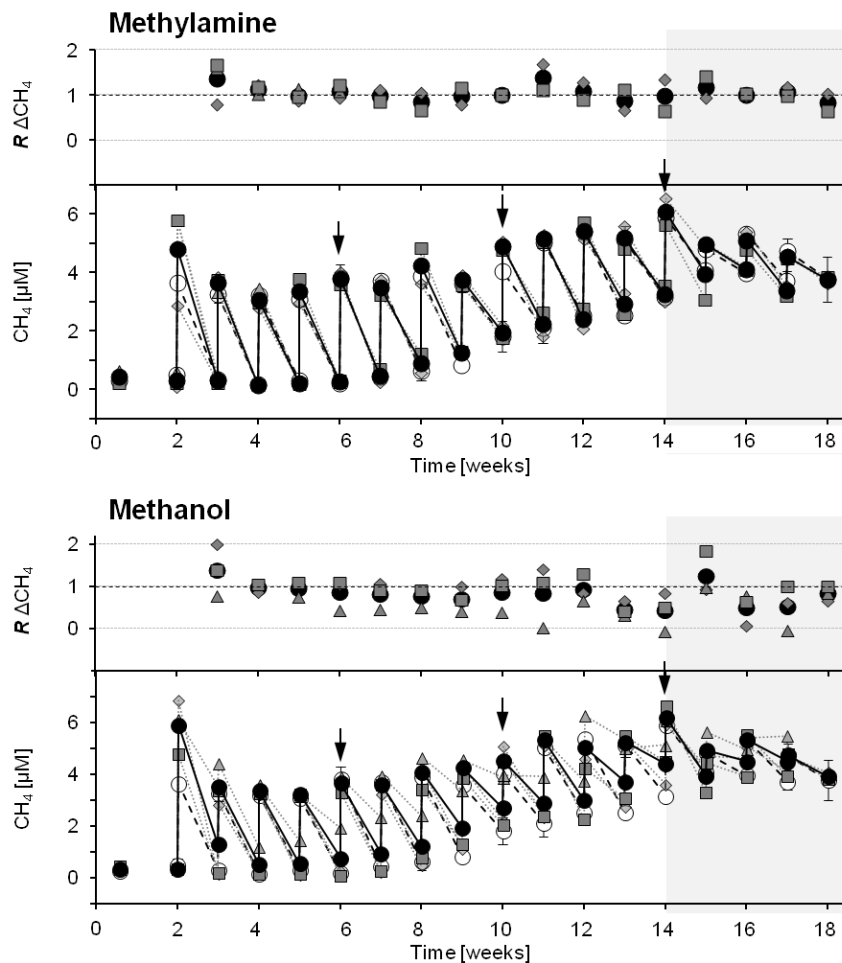


Figure 39 Effect of C1 compounds (methylamine & methanol) on CH_4 degradation in soil slurry treatments.

Effects were evaluated by changes of the CH_4 concentrations in treatments before and after each substrate pulse (i.e., methylamine or methanol and CH_4 , weekly) and the corresponding CH_4 degradation ratio ' $R\Delta\text{CH}_4$ ' (ratio > 1 indicates stimulation of CH_4 degradation; ratio < 1 indicates inhibition of CH_4 degradation). Pulses of C1 compounds were 100 μM (no background, to 14 weeks of incubation) and 500 μM (grey background, from 14 weeks of incubation). Symbols: ●, mean value of all methylamine or methanol supplemented replicates (◆, replicate 1; ▲, replicate 2; ■, replicate 3); ○, mean value of unsupplemented controls. All treatments were supplemented with CH_4 in accordance with methylamine and methanol pulses. Error bars represent standard deviations. Arrows indicate the time points of qPCR analysis during the incubation.

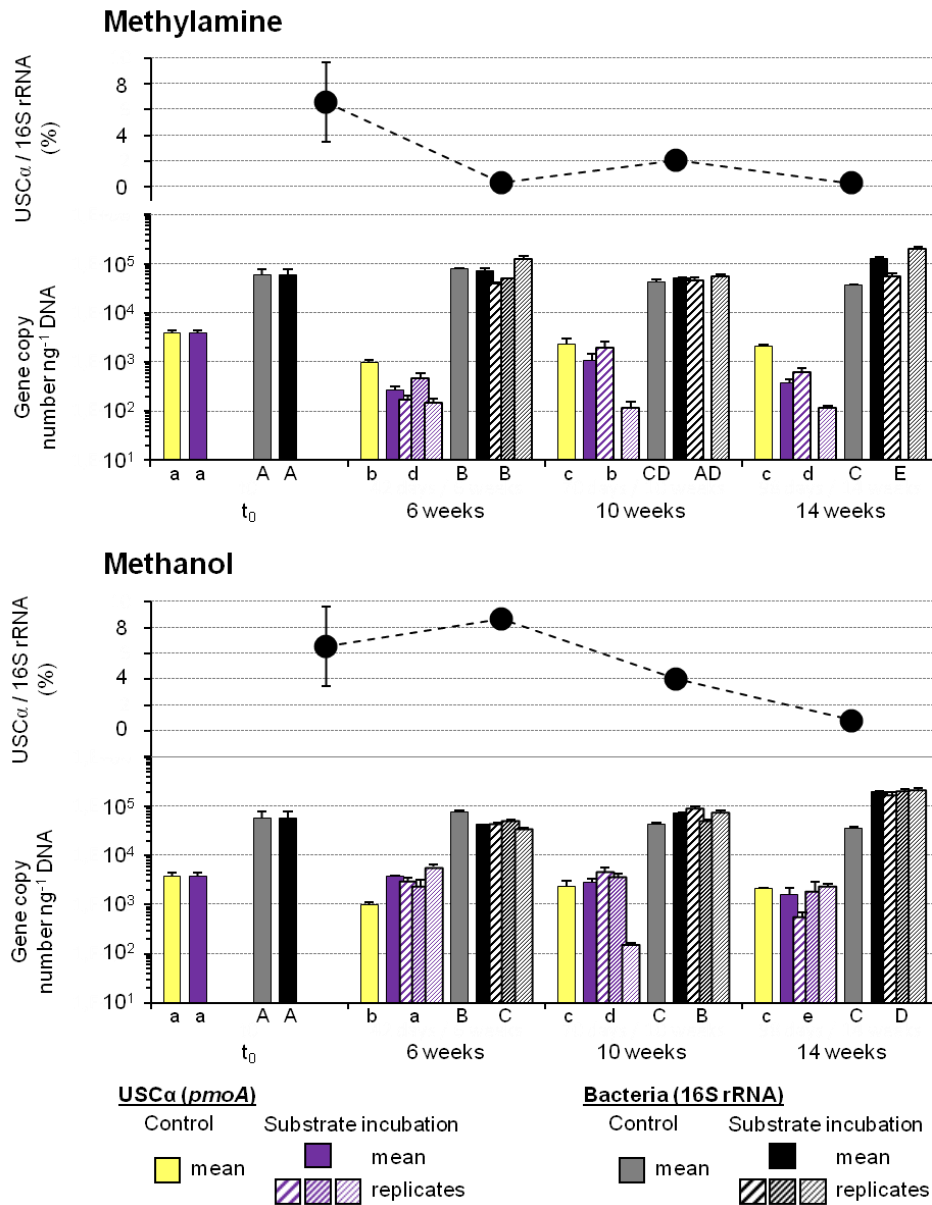


Figure 40 Influence of C1 compounds (methylamine and methanol) on gene copy numbers of 16S rRNA and *pmoA* (USCα) in soil slurry treatments.

The influence of substrates was evaluated by gene copy numbers per ng DNA and the corresponding ratio of USCα-*pmoA* per 16S rRNA (%). Gene copy numbers for t_0 were determined by triplicated qPCR measurements. Gene copy numbers for different treatments are mean values of replicates (filled columns). Gene copy numbers for each replicate were determined by triplicated qPCR measurements (shaded columns); error bars indicate standard deviation for replicates and standard error for mean values. Raw qPCR data were generated by MG [Gass, 2013]. Different letters indicate significant differences between *pmoA*-samples (small letters) and 16S rRNA-samples (capital letters) based on One-Way ANOVA (normal distribution was assumed based on Shapiro-Wilk-test, $n = 3$).

Both C1 compounds induced bacterial growth, as indicated by higher gene abundances of 16S rRNA over incubation time. On the contrary, the abundance of USCα-specific *pmoA* gene numbers was different for both substrates. Methylamine-treated samples revealed always lower values for USCα-specific *pmoA* genes than controls and gene numbers were fluctuating (2.7×10^2 to 1×10^3 gene copies ng⁻¹ DNA) (Figure 40) resulting in fluctuating

relative amounts of USC α methanotrophs contributing to the total community (Table 34). The number of USC α -specific *pmoA* genes in methanol-treated samples was higher after 6 weeks of incubation compared to controls, but showed a decreasing trend over time, ranging from 3.8×10^3 to 1.6×10^3 gene copies ng^{-1} DNA and finally, after 14 weeks the gene abundance of USC α -specific *pmoA* was comparable to controls (Figure 40).

Thus, the relative amount of USC α methanotrophs of the total bacterial community dropped from 18 % to only 1.7 % (Table 34) and indicated no growth stimulating effect of methanol on USC α methanotrophs. Growth inhibition was also not observed, since the USC α -specific *pmoA* gene numbers did not drop.

3.2.4. Effects of aromatic compounds: vanillic acid and guaiacol

Supplementation of aromatic compounds affected methane degradation obviously (Figure 41). An enhancing effect on methane degradation was observed for vanillic acid, whereas guaiacol affected methane degradation negatively (Figure 41). The stimulating effect of vanillic acid was remarkable after around 10 weeks of incubation as indicated by ' $R\Delta\text{CH}_4$ ' that showed higher values than the threshold (Figure 41). The inhibitory effect of guaiacol was detectable from the beginning of the incubation and increased over time corresponding with the decreasing ' $R\Delta\text{CH}_4$ ' values (Figure 41). The pH of both incubation approaches with aromatic compounds increased from 3.94 to 4.81 ± 0.01 for vanillic acid- and 4.27 ± 0.05 for guaiacol-treated incubations after 18 weeks of incubation (i.e., supplementation of 4mM substrates in total) (data not shown).

The 16S rRNA gene numbers increased over time in guaiacol-treated incubations from 4.7×10^4 to 1.3×10^5 gene copies ng^{-1} DNA assuming slight bacterial growth, whereas no growth could be observed for vanillic acid incubations indicated by slight decreasing 16S rRNA gene numbers (Figure 42). In general, after 6 weeks USC α -specific *pmoA* gene numbers were in aromatic compound-supplemented treatments higher than in controls, suggesting growth stimulating effects on USC α -methanotrophs by these compounds. For guaiacol-treated samples USC α -specific *pmoA* gene abundances remained constant over time (Figure 42). For vanillic acid treatments the USC α -specific *pmoA* gene abundances decreased between 10 and 14 weeks although enhanced methane degradation was observed assuming no further growth of USC α methanotrophs with vanillic acid but a stimulation of their activity (Figure 41 & Figure 42).

Thus, the resulting relative amount of USC α methanotrophs was around 5 % over the whole incubation (Table 34). On the other hand USC α -specific *pmoA* gene numbers were constant in guaiacol-treated incubations ranging from 2.4×10^3 to 3.9×10^3 gene copies ng^{-1} DNA. This indicates no growth influencing effects of guaiacol, although an inhibition of the methane degradation was observed (Figure 41 & Figure 42). The resulting relative amount of USC α

methanotrophs was around 5 % (with the exception of 18 % at the time point of 6 weeks of incubation) (Table 34).

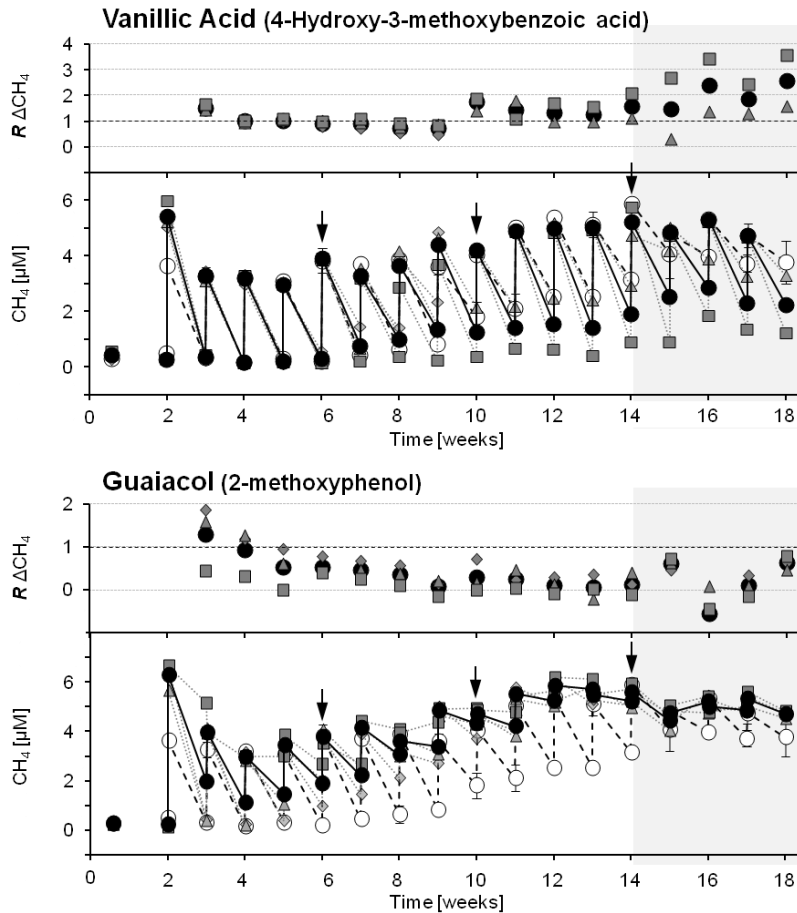


Figure 41 Effect of aromatic compounds (vanillic acid & guaiacol) on CH_4 degradation in soil slurry treatments.

Effects were evaluated by changes of the CH_4 concentrations in treatments before and after each substrate pulse (i.e., vanillic acid or guaiacol and CH_4 , weekly) and the corresponding CH_4 degradation ratio ' $R \Delta\text{CH}_4$ ' (ratio > 1 indicates stimulation of CH_4 degradation; ratio < 1 indicates inhibition of CH_4 degradation). Pulses of aromatic compounds were 100 μM (no background, to 14 weeks of incubation) and 500 μM (grey background, from 14 weeks of incubation). Symbols: ●, mean value of all vanillic acid or guaiacol supplemented replicates (◆, replicate 1; ▲, replicate 2; ■, replicate 3); ○, mean value of unsupplemented controls. All treatments were supplemented with CH_4 in accordance with vanillic acid and guaiacol pulses. Error bars represent standard deviations. Arrows indicate the time points of qPCR analysis during the incubation.

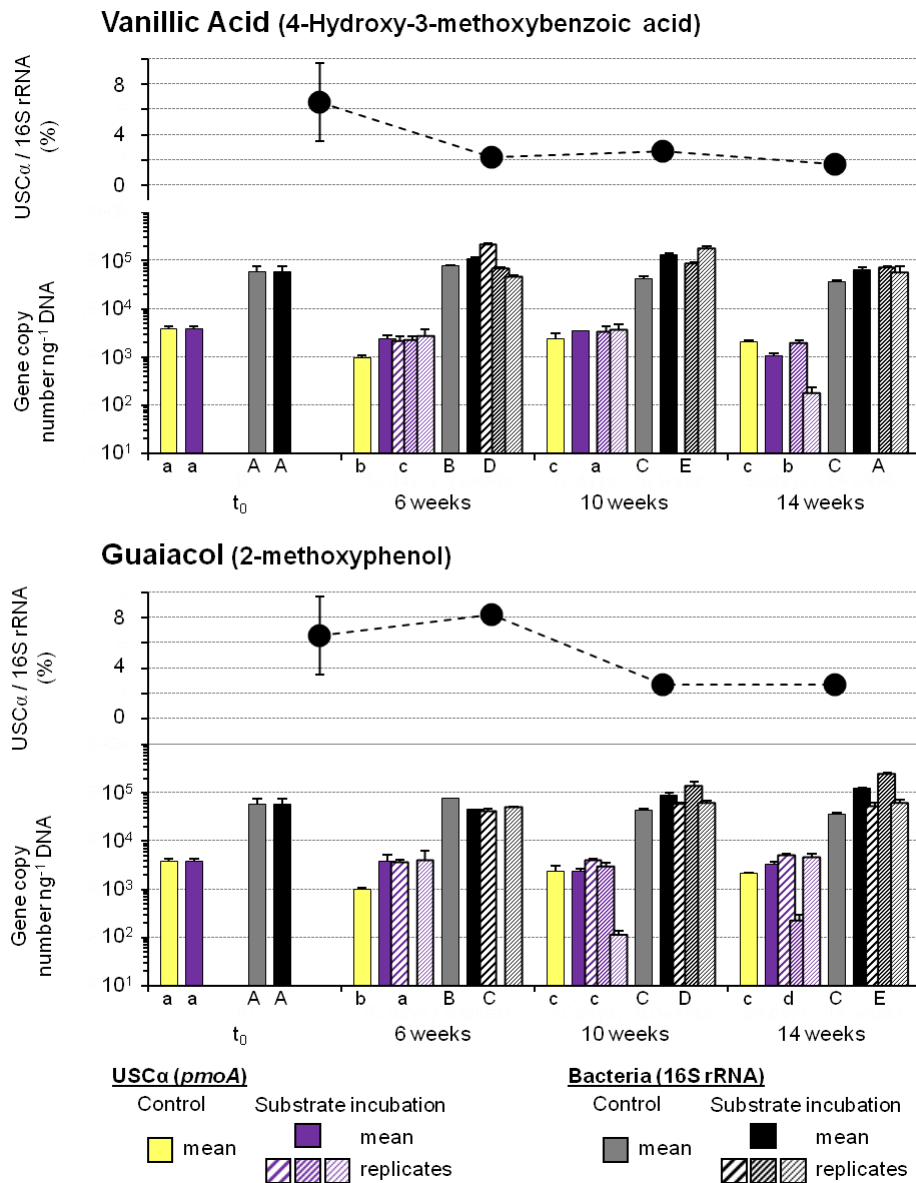


Figure 42 Influence of aromatic compounds (vanillic acid and guaiacol) on gene copy numbers of 16S rRNA and *pmoA* (USCα) in soil slurry treatments.

The influence of substrates was evaluated by gene copy numbers per ng DNA and the corresponding ratio of USCα-*pmoA* per 16S rRNA (%). Gene copy numbers for t_0 were determined by triplicated qPCR measurements. Gene copy numbers for different treatments are mean values of replicates (filled columns). Gene copy numbers for each replicate were determined by triplicated qPCR measurements (shaded columns); error bars indicate standard deviation for replicates and standard error for mean values. Raw qPCR data were generated by MG [Gass, 2013]. Different letters indicate significant differences between *pmoA*-samples (small letters) and 16S rRNA-samples (capital letters) based on One-Way ANOVA (normal distribution was assumed based on Shapiro-Wilk-test, $n = 3$).

3.2.5. Long-term effects on the methane degradation potential caused by alternative substrates under solely methanotrophic conditions

After 14 weeks of incubation (i.e., in total 1.5 mM substrates and 70 μM CH_4) the long-term effect of alternative substrates on the methane degradation in the microcosms was analysed.

RESULTS

Assuming that the apparently unaffected or partially observed lowered methane degradation rates per week were caused by preferential utilisation of alternative substrates over methane (since both substrates were supplemented) it is conceivable that methanotrophs were however stimulated, enriched and active. Thus, aliquots of soil slurries from one replicate per substrate incubation were tested separately on their methane degradation potential. Therefore, the conditions were methanotrophic.

The methane degradation potential of the control incubation (i.e., long-term incubation with solely $\text{CH}_4 = 70 \mu\text{M}$ in total) revealed only a minor methane degradation potential at the beginning ('initial period' over 7 hours) (Figure 43, open circles and dashed line). Even after 21 days, more than half amount of the initial supplemented methane was still detectable and the methane degradation potential of the control treatment was gradually lowered over incubation time. This observation, however, contradicts the analysed abundance of USC α methanotrophs that was indicated to be enriched over the incubation time (Table 34).

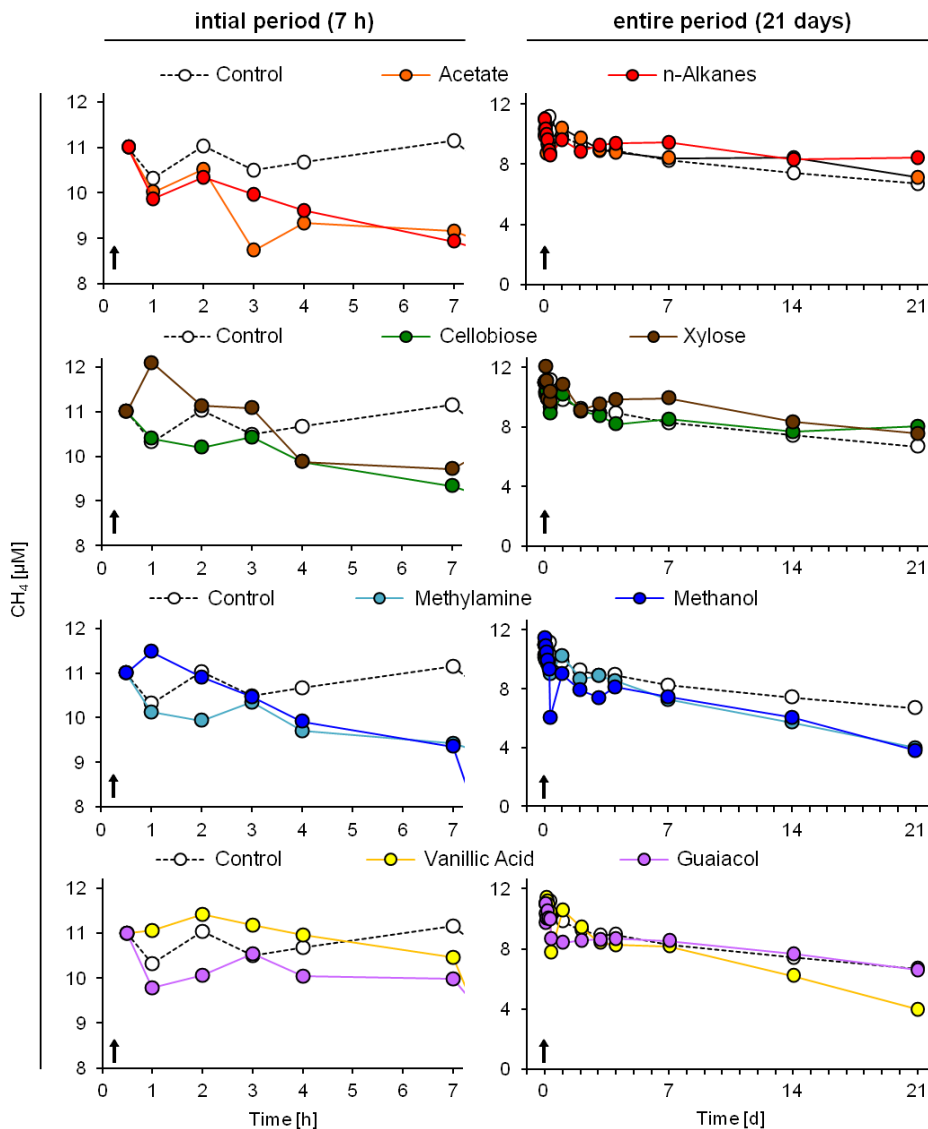


Figure 43 Long-term effect of alternative substrates on CH_4 degradation.

Explanation of Figure 43. Overview on the different CH₄ degradation potentials of slurry samples after 14 weeks of incubation with different alternative substrates (100 µM pulsed weekly; 1.5 mM in total) and CH₄ (200 ppm pulsed weekly; 70 µM total). Degradation potential was analysed with slurry aliquots after one initial CH₄ pulse (20 ppm; †) over a total period of 21 days. Slurry samples were taken from one replicate of each substrate treatment (conducted in triplicates) during the incubation and degradation was recorded from these slurry aliquots (n = 1 for each substrate).

The methane degradation potential in all aliquots derived from the methane- and alternative substrate-supplemented treatments revealed at the beginning ('initial period') no delay, but also no clear trend in methane degradation, preventing to determine methane degradation rates (Figure 43). However, the methane degradation potentials within the initial period over 7 hours were in almost all substrate-treated samples higher than in the control indicated by steeper curves (Figure 43, 'initial period'). Only for the vanillic acid-treated aliquot the initial methane degradation potential was not obviously higher than in the control.

Previously observed effects (inhibitory, neutral or stimulatory effects) in the long-term enrichments were only partially confirmed. The inhibitory effects on the methane degradation were again assumed for sugars, and a stimulatory effect was again observed for vanillic acid (Figure 43, 'entire period'). Interestingly, for some treatments the simultaneous availability of alternative substrates and methane revealed different effects on the methane degradation (observed in the long-term treatments) compared to the availability of solely methane. For example, both C1 compounds, i.e., methylamine and methanol, were previously assumed to have no or slight inhibitory effects on the methane degradation potential. When methane was the only available substrate, however, the methane degradation potential was apparently higher than in the control assuming indirect stimulatory effects of both C1 compounds (Figure 43, 'entire period'). Also, the previously observed inhibitory effects of acetate and guaiacol on the methane degradation were not confirmed when methane was the only substrate supplemented (Figure 43, 'entire period'). Methane degradation was similar to control in both, acetate and guaiacol treatment derived aliquots indicating a substrate preference towards these alternative substrates or an activity, altering effect on methanotrophs in the presence of acetate and guaiacol.

3.2.6. Long-term effects on the methane degradation potential caused by alternative substrates under methanotrophic and mixed substrate conditions

Estimating immediately and thus directly caused effects of alternative substrates, the methane degradation potentials before and after a substrate pulse were compared (Figure 44). Methane degradation potentials in long-term incubated samples (i.e., 18 weeks of incubation, 4 mM alternative substrates in total and 90 µM CH₄ in total) were recorded. Samples derived from the control treatments supplemented with methane solely revealed

again lowered methane degradation potentials (Figure 43) as it was observed in the previous experiment (see Figure 43, open circles and dashed line). Only samples derived from the acetate and guaiacol treatments revealed lower methane degradation potentials as the control (Figure 44), which is in comparison with the observed lowered methane degradation potential (Figure 35 & Figure 41). All other samples revealed almost higher potentials compared to the control assuming long-term stimulating effects after all. Interestingly, the methane degradation potential of the n-alkanes treatment derived samples was the highest (Figure 44), which was unexpected, since previous experiments did not demonstrate a stimulation of methanotrophs by n-alkanes (Figure 35 & Figure 43). However, substrate pulses did apparently not affect the methane degradation potentials in all samples with the exception of acetate and methanol treatment derived samples (Figure 44). As response to the acetate pulse, increasing, and as response on the methanol pulse, decreasing methane degradation potentials were assumed (Figure 44). Thus, acetate was suggested to stimulate the methane degradation capacity and methanol was suggested to be preferentially used over methane, resulting in an immediately down regulation of methane degradation pathway. The stimulatory effect of vanillic acid and the inhibitory effects of sugars as previously observed (see Figure 37, Figure 41 & Figure 43) were, however, not confirmed.

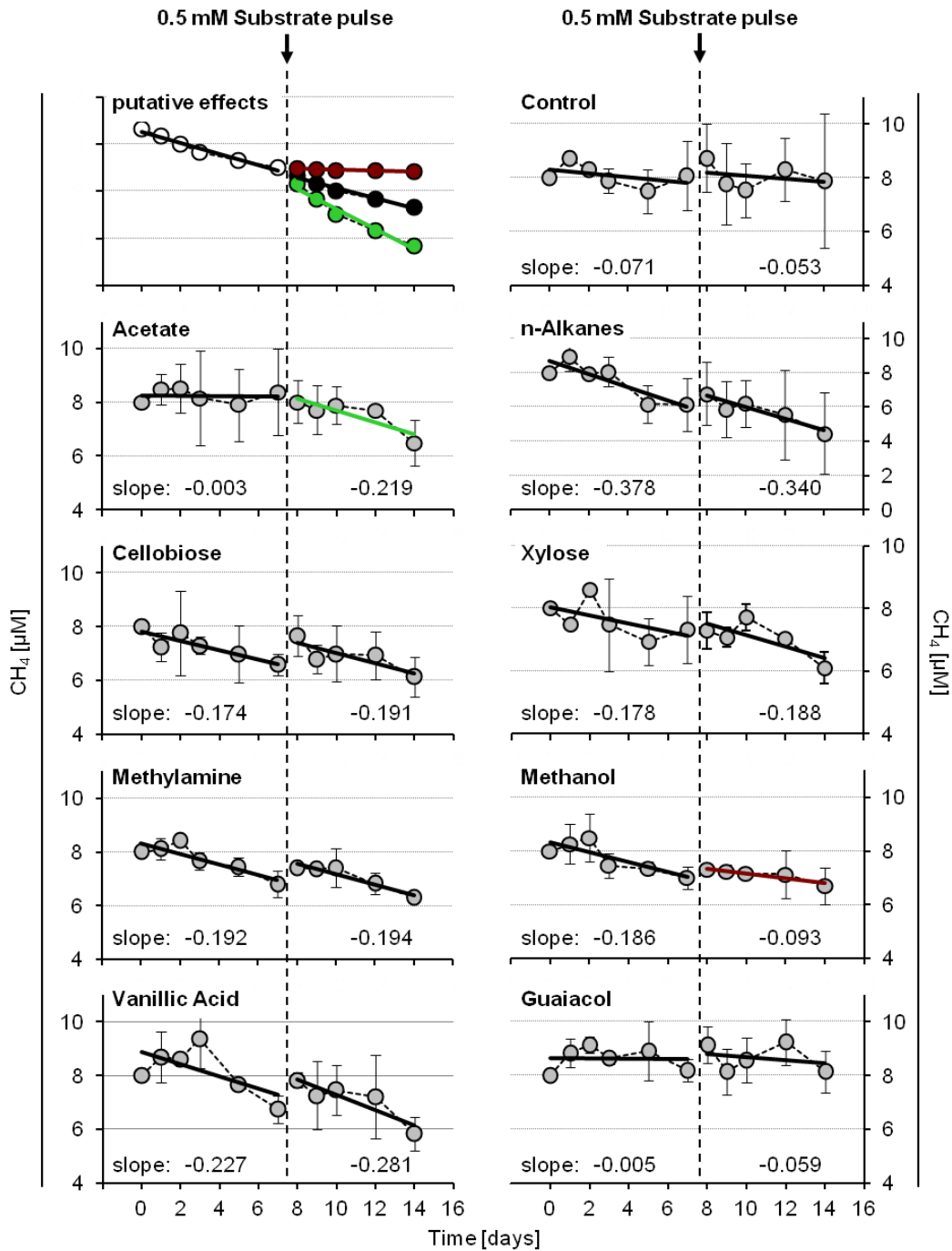


Figure 44 Long-term effect of alternative substrates on CH_4 degradation.

Overview on the CH_4 degradation potential of slurry samples after 18 weeks of incubation with CH_4 (90 μM total) and different alternative substrates (4 mM in total). Slurry samples were taken from each replicate of each substrate treatment. Samples were initially supplemented with CH_4 (20 ppm). An additional 0.5 mM substrate pulse (dashed lines) was conducted after 7 days. Substrate-induced changes in CH_4 degradation potential were indicated by regression curves. The panel 'putative effects' indicates the trend of methane degradation after substrate pulses (i.e. ●, slope decreased = inhibition; ●, slope constant = no effect; ●, slope increased = stimulation). Error bars represent standard deviations of mean values ($n = 2 - 3$).

3.2.7. Effects of alternative substrates on the methane degradation potential in fresh forest soil under changed substrate availabilities

The long-term incubation to analyse the effect of alternative substrates was conducted in soil slurries ensuring the homogeneous distribution of alternative substrates and to be able to compare samples (for example, providing similar slurry volumes and thus slurry-to-air ratios in the flasks, similar water content or preventing anoxic microzones by homogenous slurries). However, control slurry samples supplemented with methane as sole substrate revealed lowered methane degradation potentials over time indicating an inhibitory effect of the soil slurry itself. In addition, Pratscher and colleagues [Pratscher *et al.*, 2011] observed the same effect for soil slurries that were shaken. For that reason the effect of two selected alternative substrates on the methane degradation in fresh sieved soil without long-term incubation was analysed. The selected substrates were acetate and vanillic acid. Acetate was shown to have inhibitory effects on the methane oxidation in a fen soil [Wiezcorek *et al.*, 2011] and was also suggested to have inhibitory effects on the methane degradation potential in the long-term incubation (see 3.1 & 4.1.1). Vanillic acid was suggested to have stimulatory effects on the methane degradation potential in the long-term incubation (see section above). In addition, different concentrations were applied to detect alternative substrate concentration-dependent effects, and to verify the substrate induced effects. The stimulation of methane degradation should be indicated by an increased potential, whereas inhibition should be indicated by decreased potential in accordance with supplemented substrate concentrations - highest inhibition or stimulation is assumed with the highest substrate concentration tested (Figure 45, 'putative effects'). In addition, the potential for methanogenesis was also analysed in the presence of the different alternative substrates. No endogenously formed methane was detectable, assuming that no methanogenic processes happened.

For all samples, the initial methane degradation potential was comparable and served as 'control' to ensure that all replicates were comparable (Figure 45, 'initial'). The simultaneous substrate and methane pulse did not alter the methane degradation potential in both approaches and no influence based on different alternative substrate concentrations was observed (Figure 45, dark grey background 'Substrate pulse'). Thus, a direct effect of acetate or vanillic acid on the methane degradation was for that moment excluded. Since it is also conceivable that the supplemented alternative substrates could have an indirect impact on some methanotrophs in the soil (such as activating them, altering their general activity or supporting growth), a delayed effect of the alternative substrates was analysed, but no affected methane degradation potential was observable (Figure 45, light grey background '1d after Substrate').

RESULTS

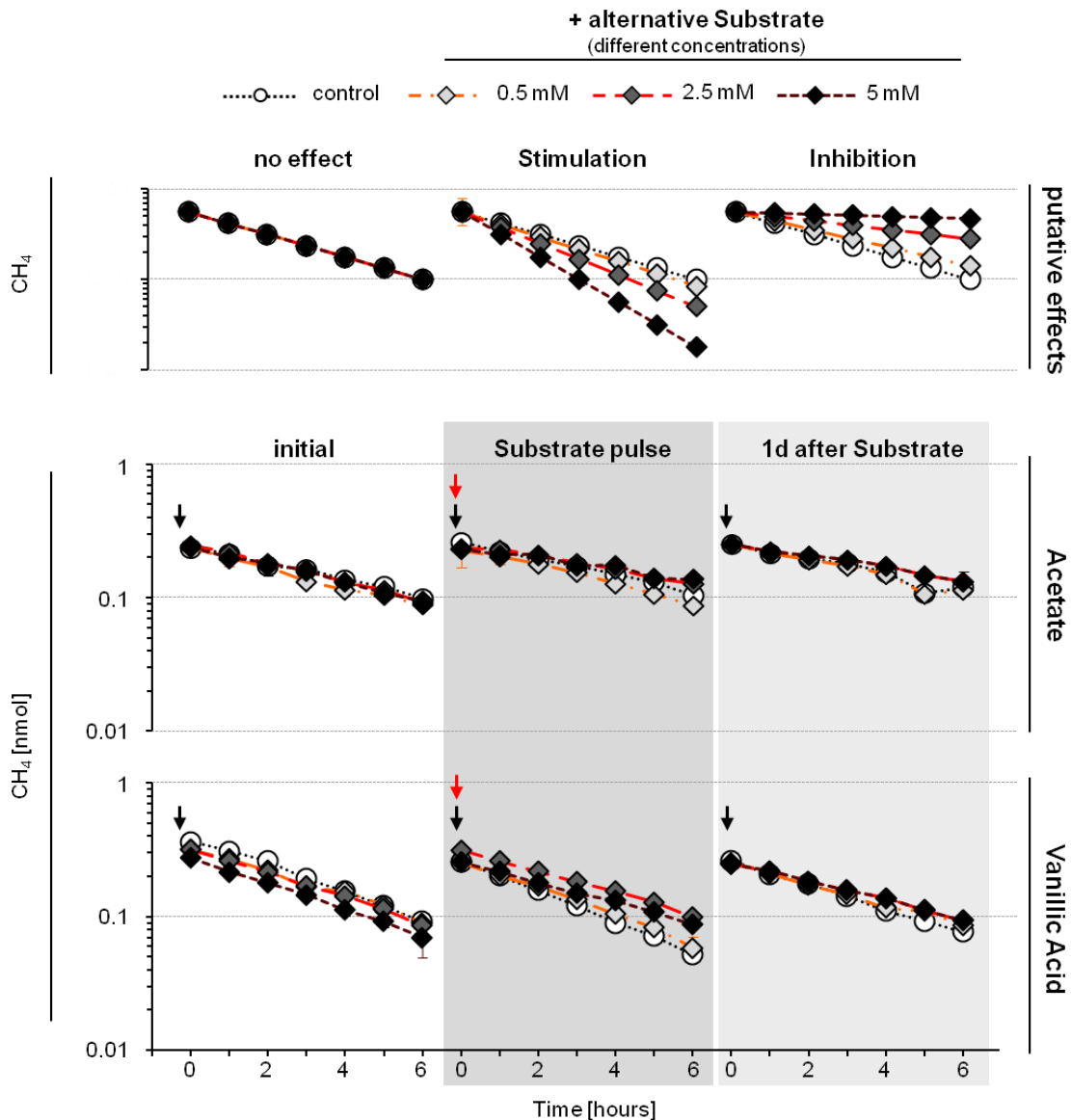


Figure 45 Effect of acetate and vanillic acid supplementation on CH₄ degradation in fresh soil samples.

The figure shows the CH₄ degradation (CH₄ pulse: ↓) in fresh soil samples (initial, no background), after one substrate pulse (↓, dark grey background), and one day after the alternative substrate pulse (light grey background). Values are a mean of triplicates (with triplicated measurements) and error bars indicate error of mean values. The panel 'putative effects' visualize the assumed methane degradation trends as response on supplemented alternative substrates (theoretical values).

3.3. Multi-carbon compound assimilation by methanol-utilising microorganisms in an acidic forest soil

3.3.1. Conversion of methanol and multi-carbon substrates and the formation of [¹³C]-CO₂ as evidence for substrate dissimilation

In order to investigate the multi-carbon substrate range of methylotrophic microorganisms homogenous soil slurry incubations of the acidic forest soil were conducted under methylotrophic and mixed substrate conditions (see 2.3.3). The initial pH of the soil slurry was low and stayed constant at 3.7 ± 0.1 during the incubation period. The only exception was the treatment supplemented with acetate that showed a slight increase of the pH up to 4.5 at the end resulting in a mean pH of 4.0 ± 0.2 .

The native microbial community in an acidic soil was tested for their capacity to utilise selected C1 and multi-carbon substrates. As typical C1 compounds methanol and methane were chosen. Methanol was supplemented daily as 1 mM pulse to mimic *in situ* conditions as well as avoiding accumulation and toxication. The utilisation of methanol was assumed by an increased formation of CO₂ evidently after five days of incubation (Figure 46A). Methane was supplemented consistently to methanol, in which the concentrations of methane were 100 times higher than atmospheric conditions, but still low compared to other studies to address methanotrophic microorganisms with high-affinity enzymes for methane utilisation in particular. However, no utilisation of methane was observed in any incubation of the substrate SIP experiment (Figure 46B).

Apart from the C1 compounds – methane and methanol – the capacity to utilise multi-carbon compounds by the methylotrophic microorganisms in soils was analysed. The multi-carbon compounds tested were acetate as a common intermediate in the soil matrix, a hexose sugar (glucose), a pentose sugar (xylose) and an aromatic compound (vanillic acid). All these compounds are assumed to be plant-derived *in situ*.

Preliminary conducted substrate consumption tests revealed that supplemented acetate and sugars were no longer detectable in soil slurry samples within a few hours resulting in degradation rates of 0.11 mM acetate h⁻¹, 0.2 mM glucose h⁻¹ and 0.125 mM xylose h⁻¹ in soil slurries (data not shown). Thus, in the substrate SIP experiment acetate and sugars were pulsed daily. The aromatic compound vanillic acid was hardly detectable in the soil slurry supernatant indicating a binding to soil particles. However, degradation of vanillic acid could be observed resulting in a degradation rate of 0.02 mM vanillic acid h⁻¹ in soil slurries (data not shown). Thus, vanillic acid was pulsed for a second time after 3 days. An adaption to the supplementation of vanillic acid could be observed resulting in an increased uptake rate with the outcome of an increased pulsing rate (up to daily pulses).

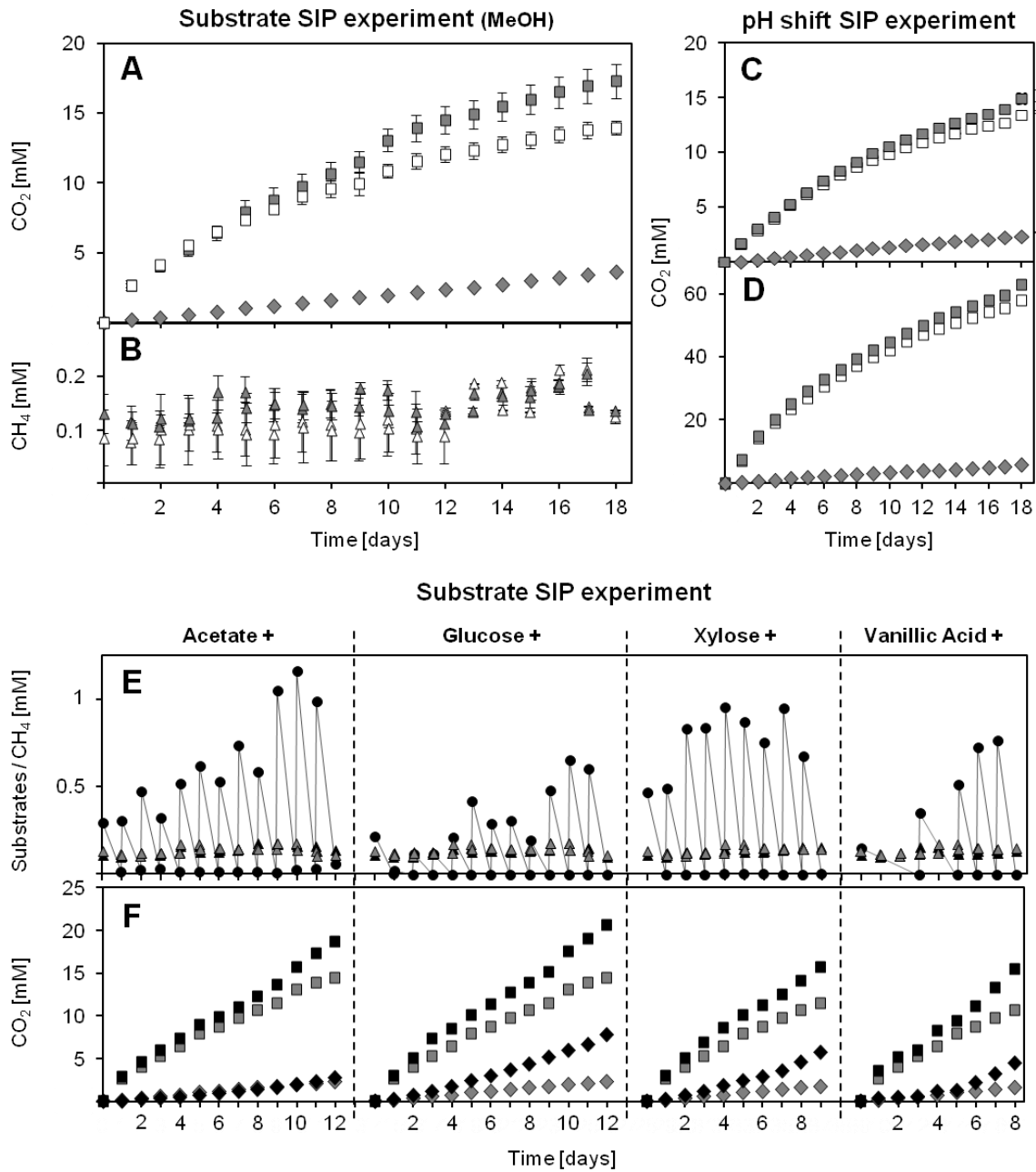


Figure 46 CO_2 formation and conversion of different multi-carbon substrates in soil slurry treatments.

$^{12}\text{CO}_2$ and $^{13}\text{CO}_2$ concentrations (cumulative) of substrate SIP experiment treatments pulsed with methanol (A) and other multi-carbon substrates (F) as well as methanol treatments of the pH shift SIP experiment with pH 4 (C) and pH 7 (D). A cross indicates additional methanol supplementation. Substrate utilisation is supposed by the conversion of supplemented substrates (E), methane utilisation in the substrate SIP experiment treatments is negligible (B, E). Methanol treatments serve as control treatments for supplemented multi-carbon substrate treatments. All values are mean values of replicates; error bars represent standard deviations. White symbols, unsupplemented control; grey symbols, methanol treatments; black symbols, multi-carbon substrate treatments; \diamond , ^{13}C - CO_2 ; \square , ^{12}C - CO_2 ; \circ , substrates; \triangle , methane. This figure has been published in Morawe *et al.* 2017.

The utilisation of multi-carbon substrates was indicated by the observed disappearance of supplemented substrates and a correlating increase of CO₂ formation (Figure 46E & F). Since methanol was also pulsed in the substrate treatments, the methanol incubation served as control for the different substrate treatments. Even after one day differences in CO₂ formation between substrate incubations and the methanol incubation were already detectable (Figure 46F). During the SIP incubation experiment methanol, acetate, glucose, xylose and vanillic acid were supplemented as ¹²C- or ¹³C-isotopologue. For vanillic acid only carbon atoms of the aromatic ring were ¹³C-isotopes, carbon atoms of the carboxyl and methyl group were ¹²C-isotopes. Thus, only the fate of aromatic ring-derived carbon atoms can be tracked as [¹³C]-CO₂ for vanillic acid. The amount of CO₂ detectable in ¹²C- and ¹³C-isotopologue substrate incubations was similarly, assuming no preference of [¹²C]-substrates utilisation (Figure 46F).

The utilisation of ¹³C-isotopologues was obviously proven by [¹³C]-CO₂ formation. On average the carbon recovery per 1 mM [¹³C₁]-methanol pulse as [¹³C]-CO₂ was approximately 20 % in the methanol supplemented incubations, and no increase of [¹³C]-CO₂ formation per 1 mM pulse was observed during the incubation period. In contrast, for all multi-carbon substrate treatments an increase in [¹³C]-CO₂ formation per 1 mM substrate pulse was observed. Acetate supplementation affected an approximately 5-fold increase per 1 mM of acetate assuming a carbon recovery of 4.30 % up to 22.26 % (on average 11.72 %). Glucose supplementation affected an approximately 4-fold increase per 1 mM of glucose assuming carbon recovery of 4.32 % up to 17.48 % (on average 10.82 %). Xylose supplementation affected an approximately 3.7-fold increase per 1 mM of xylose assuming a carbon recovery of 5.96 % up to 22.19 % (on average 12.80 %). Vanillic acid supplementation affected an approximately 2.5-fold increase per 1 mM of vanillic acid assuming a carbon recovery of 6.35 % up to 15.67 % (on average 11.37 %).

3.3.2. Influence of the soil pH on methanol utilisation and the [¹³C]-CO₂ formation

Soil samples for pH shift SIP experiment were taken at another time point than for the substrate SIP experiment (see 2.3.4). However, the initial pH of the soil slurry was still low (pH 3.6). In order to determine the effect of a higher pH on the methylotrophic microorganisms in an acidic soil the pH was adjusted to a more neutral value around 7. The incubation of *in situ* pH ('pH 4 incubation') and pH-adjusted ('pH 7 incubation') soil slurry treatments showed no dramatic changes in terms of pH over the incubation time. A slight increase in 'pH 4 incubation' up to a pH of 4.2 at the end was observed. Mean pH values of unsupplemented controls and methanol treatments were 4.0 ± 0.1 for 'pH 4 incubation' and 6.9 ± 0.1 for 'pH 7 incubation', respectively (data not shown).

In accordance to previously performed substrate SIP experiment (see 3.3.1), only methanol was supplemented. The utilisation of methanol was indicated by the increased formation of CO₂ even after one day of incubation compared to unsupplemented controls (Figure 46C & D). In general, the CO₂ formation was always higher in 'pH 7 incubations' (control and methanol treatments).

No preferred [¹²C]-methanol utilisation was indicated by similar amounts of CO₂ produced in [¹²C]- and [¹³C]-methanol incubations (Figure 46C & D). This is in accordance with the substrate SIP experiment as well as the constant formation of [¹³C]-CO₂ per 1 mM methanol pulse during both incubations. For 'pH 4 incubation' a mean carbon recovery of approximately 13.5 % was assumed, which is lowered compared to the methanol incubations of the preliminarily performed substrate SIP experiment, assuming a putatively less active methanol-utilising community. For 'pH 7 incubation' the [¹³C]-CO₂ formation was more than 2-fold higher compared to 'pH 4 incubation' revealing a mean carbon recovery of approximately 29.67 %.

3.4. Pyrosequencing read yield of 16S rRNA gene, ITS gene sequences and *mxoF* gene sequences

In order to obtain genetic information the nucleic acids were specifically amplified with different primer sets (see 2.5.7.1 & 2.5.7.6) and achieved amplicon libraries were further sequenced (see 2.5.12.2).

In total, 200'785 sequences of 16S rRNA gene sequences were obtained from pyrosequencing. A total of 105'689 16S rRNA gene sequences were obtained after further processing (i.e., quality filtering, checking for chimeric sequences and clustering based on primer and different barcodes at a family-level cut-off of 90.1 % similarity, see 2.5.13.1) resulting in only 1'492 sequences (i.e., t₀ of substrate SIP experiment) up to 13'979 sequences (i.e., [¹³C]-methanol treatment of the 'pH 4 incubation' of the pH shift SIP experiment) for samples.

139'329 sequences of *mxoF* were obtained in total from pyrosequencing. After processing (i.e., clustering based on primer and different barcodes at a threshold of 90% similarity, see 2.5.13.1) 113'689 sequences remained, resulting in only 955 sequences (i.e., [¹³C]-methanol incubation of the substrate SIP experiment) up to 14'934 sequences (i.e., [¹³C]-methanol treatment of the 'pH 7 incubation' of the pH shift SIP experiment) for each sample.

Due to the huge range of remaining sequence numbers of the different samples, a normalization step was not realized for 16S rRNA gene and *mxoF* sequence analysis to avoid a larger loss of information.

For ITS gene sequences a total of 237'495 sequences were obtained from pyrosequencing. The data sets were rarefied to 1'503 sequences per sample (i.e., 99'198 sequences in total)

and after processing (i.e., checking for chimeric sequences and confirming fungal origin of sequence, see 2.5.13.1) a total of 95'065 sequences remained, ranging from 4'246 sequences (i.e., [¹²C]-vanillic acid incubation of the substrate SIP experiment) up to 4'440 sequences (i.e., [¹³C]-xylose incubation of the substrate SIP experiment) for each sample.

3.5. The impact of methanol, multi-carbon substrates and pH on the microbial community in an acidic forest soil

The treatments with methanol and different multi-carbon substrates as well as shifted pH conditions were assumed to influence the native microbial community of an acidic forest soil. Not only specific microbial members or functional guilds were assumed to be influenced, but also microbial interactions such as interdependent food webs (for example the degradation of recalcitrant structures and thus the supply of oligo- and monomeric compounds) by the outcompeting of some taxa over others.

The methanol treatments of the substrate SIP and the pH shift SIP experiments were assumed to trigger especially methanol-utilising methylotrophs. The treatments with different multi-carbon substrates in the substrate SIP experiment were conducted under mixed substrate conditions, meaning that also methanol was supplemented. Thus, it was intended to trigger also methanol-utilising microorganisms and to assess their substrate spectrum in terms of multi-carbon compounds under competing conditions. Since the analysed forest soil was acidic the influence of an elevated pH on the native methylotrophic community was also tested and the elevated pH was assumed to change the microbial community.

3.5.1. The impact of substrates and pH on *Bacteria*

The mean coverage of all combined amplicon libraries of the different treatments (i.e., t_0 , substrate or pH incubations of both SIP experiments) of 16S rRNA gene sequences based on family-level cut-off was 98.8 ± 0.66 % (Figure 47A). The detected numbers of phylotypes (OTUs) were on average 109 ± 18 phylotypes for the substrate SIP experiment and 193 ± 74 phylotypes for pH shift SIP experiment. On average Chao 1 indices for all amplicon libraries hypothesised a species richness of 148 ± 35 phylotypes for the substrate SIP experiment and 262 ± 76 phylotypes for the pH shift SIP experiment (Figure 47B & F). Noticeable, the differences of phylotype numbers between the substrate SIP and pH shift SIP experiment can be explained by sampling time points of the fresh soil samples (see Table 2), PCR-based differences (i.e., chemicals and enzymes used, see 2.5.7.6) and the amount of sequences obtained in the independently conducted pyrosequencing for the different amplicon libraries (see 3.4 & Table A 4). However, values indicate a diverse active bacterial community at the beginning and after all incubations with different substrates, or under different pH conditions. For the substrate SIP experiment no domination of only a single or a

RESULTS

few phylotypes was observed. For the pH shift SIP experiment a domination of a few or a single phylotypes was obvious in methanol treatments at pH 4 (Figure 47C, D & E).

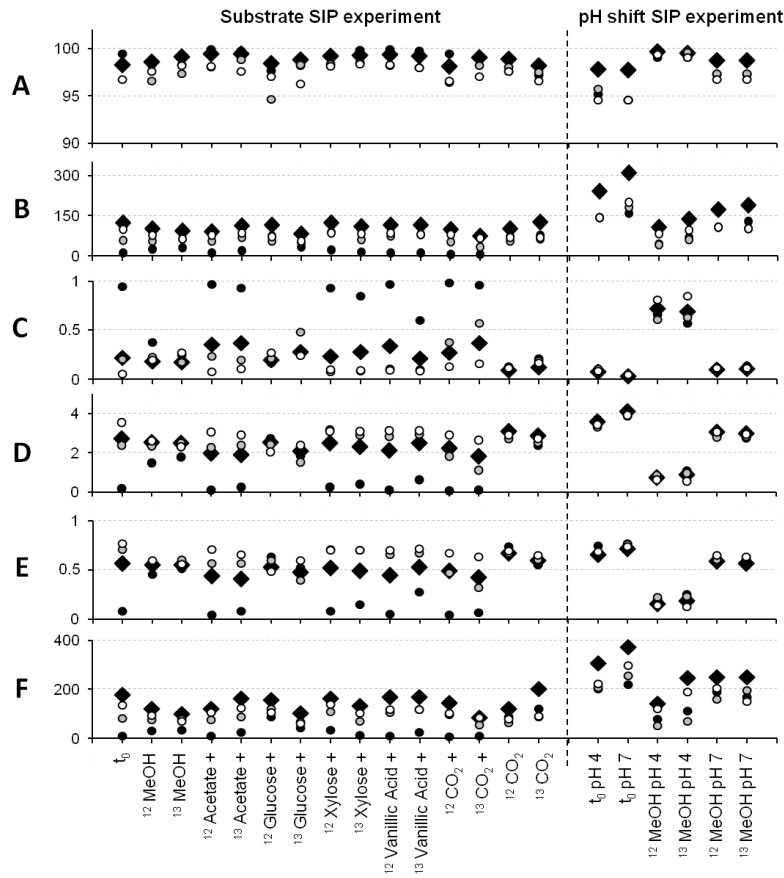


Figure 47 Diversity and richness estimators of 16S rRNA gene sequences from pyrosequencing amplicon pools at similarity level 90.1% (family level).

Figures indicating coverage (%) (A), numbers of OTUs (B), dominance D (C), Shannon index H (D), equitability J (E) and Chao1 index (F) of t_0 samples (no treatment, combined data sets of replicates for substrate SIP experiment t_0) and after treatment for both SIP experiments. A ¹² indicates [¹²C]-isotopologue, ¹³ indicates [¹³C]-isotopologues. A cross indicates additional supplementation of methanol in substrate treatments. Symbols: ◆, combined data sets of 'heavy', 'middle' and 'light' fractions; ●, 'heavy' fraction; ◐, 'middle' fraction; ○, 'light' fraction. This figure has been published in Morawe *et al.* 2017.

Differences between initial t_0 samples of the substrate SIP and pH shift SIP experiment were not significant, but a tendency for a separation of the initial community structures was indicated by ANOSIM (analysis of similarity; $R = 0.48$, $p = 0.06$) and with NPMANOVA (non-parametric multivariate analysis of variance; $F = 1.75$, $p = 0.07$) (Table A 7).

Substrate incubation as well as the incubation at different pH conditions affected bacterial community composition significantly as revealed by ANOSIM ($R = 0.75$, $p < 0.0001$) and NPMANOVA ($F = 8.23$, $p = 0.0001$). Lower R values for the substrate SIP experiment incubations ($R = 0.55$, $p = 0.001$) indicated lower dissimilarities than for the pH shift SIP experiment incubations ($R = 1$, $p = 0.02$). Following ANOSIM results, NPMANOVA revealed

RESULTS

that differences between the samples of the substrate SIP experiment ($F = 5.31$, $p = 0.0001$) were less distinct than the differences between the pH shift SIP experiment samples ($F = 19.71$, $p = 0.02$) suggesting a higher effect of pH conditions than available substrates on the bacterial community (Table A 7).

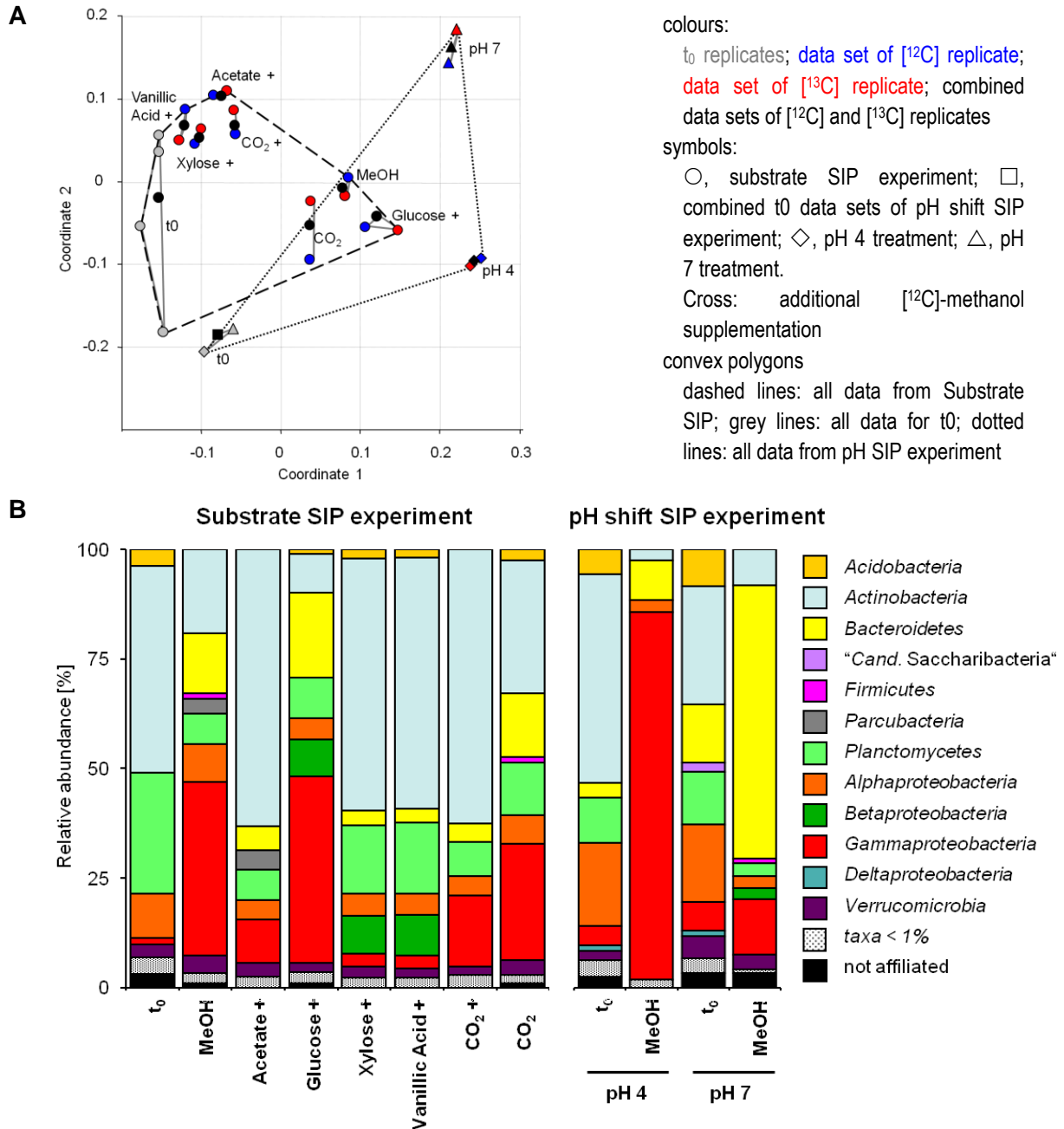


Figure 48 nMDS analyses (A) and the phylogenetic compositions (B) of the bacterial community after different substrate or pH treatments.

Panel A, nMDS analysis for the bacterial community based on 16S rRNA gene sequences (family-level, similarity cut-off 90.1 %). The analysis is based on the Bray-Curtis similarity index with a stress value of 0.1002.

Panel B, relative abundances of combined (^{12}C and ^{13}C) data sets of 16S rRNA gene sequences derived phylotypes from pyrosequencing pools of both SIP experiments at the beginning (t_0) and after treatment with substrates or different pH conditions. A cross indicates additional supplementation of methanol in substrate treatments. The phylogenetic affiliation was confirmed with a GenBank database for 16S rRNA gene sequences.

This figure has been published in Morawe *et al.* 2017.

The pairwise ANOSIM revealed that methanol and glucose ($R = 1$, both) were more responsible for dissimilarities between t_0 and t_{End} of the substrate incubation treatments, whereas the contribution of supplemented acetate ($R = 0.21$), vanillic acid ($R = 0.11$) and xylose ($R = 0.04$) was low. The dissimilarity between t_{End} samples of the substrate incubations and pH incubations with each other ($R = 0.5, 0.75$ or 1 , data not shown) is another explanation for the ANOSIM result. R values of 1 indicated that the replicates of treatments were more similar to each other than to any replicates from different treatments. Additionally, the pairwise NPMANOVA indicated considerably dissimilarities between incubations with methanol and incubations with acetate ($F = 23.69$), vanillic acid ($F = 21.60$) and xylose ($F = 24.74$), respectively. In contrast, incubations with glucose were not very distinct to methanol incubations ($F = 2.22$). Surprisingly, incubations with CO_2 and additional methanol ($F = 18.36$) were more distinct to the methanol incubation than incubations with only CO_2 supplemented ($F = 3.93$) (Table A 7).

In accordance to the ANOSIM and NPMANOVA results the t_0 replicates of the substrate SIP experiment scattered in a non-metric multidimensional scaling (nMDS) plot, indicating a small variance between replicates among each other due to methodical procedures (i.e., DNA extraction, PCR based amplification) (Figure 48A). However, the phylogenetic composition of the initial bacterial community in the acidic forest soil samples of the substrate SIP experiment showed on average a dominance of *Actinobacteria* and *Planctomycetes*, followed by *Alphaproteobacteria* and *Acidobacteria*. *Verrucomicrobia* as well as *Gammaproteobacteria* were detectable but their portion was only minor (Figure 48B).

3.5.1.1. Comparison of t_0 and t_{End} of the substrate-treated samples

The comparison of the bacterial community composition at t_0 and t_{End} of the substrate SIP experiment as well as the comparisons between the different treatments pointed out how the bacterial communities were influenced during the treatments with different substrates.

The analysis of the phylogenetic composition of t_0 and t_{End} revealed a dramatic increase in the abundance of *Gammaproteobacteria* and a high presence of *Bacteroidetes* in methanol and glucose treatments. Instead, the amounts of *Actinobacteria* and *Planctomycetes* were highly reduced (Figure 48B). In detail, SIMPER (similarity percentage) analysis uncovered *Xanthomonadaceae* (i.e., *Rhodanobacter*, OTU_{16S} 300), *Sphingobacteriaceae* (i.e., *Mucilaginibacter*, OTU_{16S} 1073) and *Corynebacteriaceae* (i.e., *Corynebacterium*, OTU_{16S} 748) being responsible for more than 50 % of dissimilarities between t_0 and t_{End} (Figure 49, Table A 9). The amount of *Alphaproteobacteria* in the methanol incubation remained constant and decreased in the glucose treatment. *Verrucomicrobia* were more abundant in the methanol treatment at t_{End} than t_0 , but in treatments with glucose no changes were observed. Also in methanol treatments small amounts of *Firmicutes* and *Parcubacteria* were detectable (Figure 48B).

Acetate, xylose and vanillic acid treatments revealed still a dominance of an increased amount of *Actinobacteria* (Figure 48B), and SIMPER analysis underlined that actinobacterial families contribute to this dissimilarities (Figure 49). Interestingly, the amount of *Corynebacteriaceae* (i.e., *Corynebacterium*, OTU_{16S} 748) was increased, whereat the amount of *Kineosporiaceae* (i.e., *Kineosporia*, OTU_{16S} 703) was decreased (Table A 9). Besides the actinobacterial dominance, the amount of *Planctomycetes* and *Alphaproteobacteria* was reduced (Figure 48B). *Gammaproteobacteria* were increased compared to t_0 samples but still low compared to methanol and glucose treatments. Also, *Bacteroidetes* were detectable but only to a minor part (Figure 48B). However, SIMPER analysis indicated *Xanthomonadaceae* (i.e., *Rhodanobacter*, OTU_{16S} 300) and *Sphingobacteriaceae* (i.e., *Mucilaginibacter*, OTU_{16S} 1073) being also responsible for dissimilarities between t_0 and t_{End} of acetate, xylose and vanillic acid treatments (Figure 49).

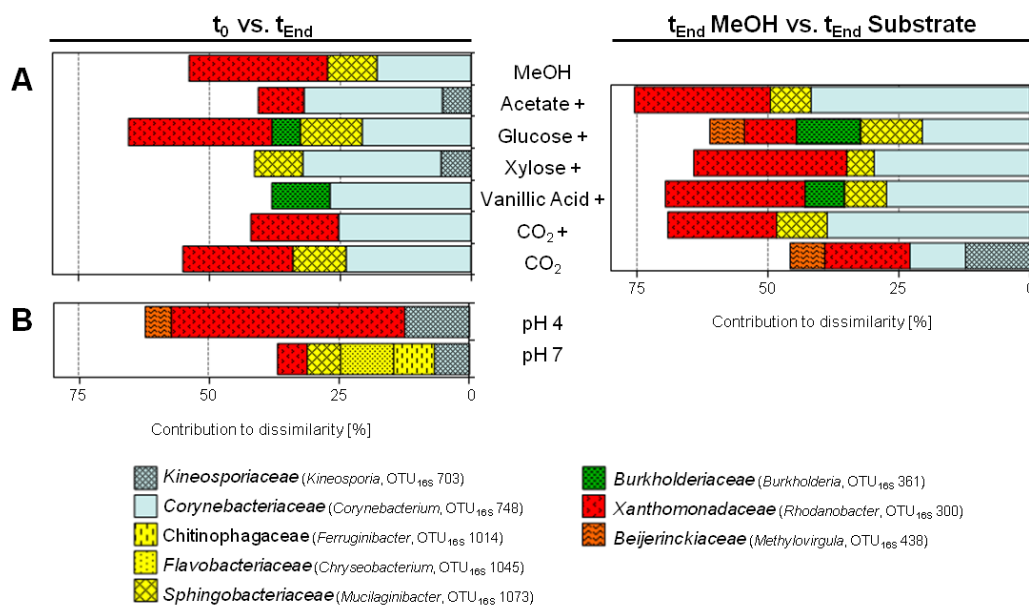


Figure 49 Bacterial taxa responsible for dissimilarity in substrate treatments.

Pairwise comparisons between t_0 (no treatment) and t_{END} of both SIP experiments (A, substrate SIP; B, pH shift SIP) as well as pairwise comparisons between t_{END} of methanol and substrate treatments of the Substrate SIP experiment determined by SIMPER (Similarity Percentage) analyses. SIMPER was performed with combined data sets (¹²C and ¹³C) of relative abundances based on family level (via 90.1 % clustering threshold). Shown are the main taxa contributing each to ≥ 5 % to the dissimilarity between samples. Phylogenetic affiliation (phylum level) is indicated by equal colours, different families are differentiated by shading. A cross indicates additional supplementation of methanol in substrate treatments.

Although samples of the glucose treatment were distinct from the xylose and vanillic acid treatments in the nMDS plot (Figure 48A), *Betaproteobacteria* were detectable in these treatments (Figure 48B, Table A 9). Only in glucose and vanillic acid treatments *Burkholderiaceae* (i.e., *Burkholderia*, OTU_{16S} 360) contributed with more than 5 % to the dissimilarity between t_0 and t_{END} in these incubations as revealed by SIMPER (Figure 49).

For CO₂ treatments the phylogenetic composition was similar, but with different percentages of phyla. *Actinobacteria* dominated in CO₂ treatment with additional methanol. *Bacteroidetes* and *Gammaproteobacteria* were more present in CO₂ treatments without additional methanol (Figure 48B). As before, *Corynebacteriaceae* (i.e., *Corynebacterium*, OTU_{16S} 748), *Xanthomonadaceae* (i.e., *Rhodanobacter*, OTU_{16S} 300) and *Sphingobacteriaceae* (i.e., *Mucilaginibacter*, OTU_{16S} 1073) were indicated to contribute to this composition (Figure 49, Table A 9). The amount of *Alphaproteobacteria* was similar in both CO₂ treatments. *Firmicutes* were minor detected in CO₂ treatment without additional methanol and the amount of *Verrucomicrobia* remained constant for t₀ and the different treatments (Figure 48B, Table A 9).

3.5.1.2. Comparison of the methanol-treated samples and multi-carbon-treated samples

Interestingly, the comparison of the bacterial community similarity between methanol and substrate treatments revealed that more than 50 % of the dissimilarity is contributed by only a few bacterial families including almost always *Corynebacteriaceae* (i.e., *Corynebacterium*, OTU_{16S} 748), *Xanthomonadaceae* (i.e., *Rhodanobacter*, OTU_{16S} 300) and *Sphingobacteriaceae* (i.e., *Mucilaginibacter*, OTU_{16S} 1073) (Figure 49).

In detail, *Corynebacteriaceae* (i.e., *Corynebacterium*, OTU_{16S} 748) were in treatments with acetate, xylose, vanillic acid and CO₂ with additional methanol highly abundant compared to methanol treatments, suggesting a higher competitiveness of these taxa at these conditions. On the other hand the amount of *Corynebacteriaceae* was lower in treatments with glucose and CO₂ without additional methanol compared to the methanol treatment (Table A 9). *Xanthomonadaceae* (i.e., *Rhodanobacter*, OTU_{16S} 300) and *Sphingobacteriaceae* (i.e., *Mucilaginibacter*, OTU_{16S} 1073) were highly abundant in methanol and glucose treatments, less abundant in CO₂ treatments and showed a low abundance in treatments with acetate, xylose and vanillic acid, indicating a lower competitiveness under these conditions (Table A 9).

3.5.1.3. Comparison of samples incubated under different pH conditions

The methanol treatments under different pH conditions were distinct from each other in an nMDS plot, indicating a huge community shaping effect of the pH (Figure 48A). The phylogenetic analysis of the community composition revealed also a domination of *Gammaproteobacteria* for *in situ* treatments with pH 4. The only other phyla detectable were *Bacteroidetes*, *Alphaproteobacteria* and *Actinobacteria* in minimal amounts (Figure 48B, Table A 9). SIMPER analysis indicated *Xanthomonadaceae* (i.e., *Rhodanobacter*, OTU_{16S} 300), *Kineosporiaceae* (i.e., *Kineosporia*, OTU_{16S} 703) and *Beijerinckiaceae* (i.e., *Methylovirgula*, OTU_{16S} 438) contributing to these differences in pH 4 treated samples

(Figure 49, Table A 9). An enormous increase of *Gammaproteobacteria* (i.e., *Rhodanobacter*, OTU_{16S} 300) was consistently observed in both methanol incubations of substrate SIP and pH shift SIP experiments (Figure 48B).

An increased number of *Bacteroidetes* dominated the methanol treatment at pH 7 followed by *Gammaproteobacteria* compared to its t_0 . A drastic decrease was obvious for *Alphaproteobacteria*, *Actinobacteria*, *Planctomycetes* and *Acidobacteria* (Figure 48B). In detail, SIMPER revealed *Flavobacteriaceae* (i.e., *Chryseobacterium*, OTU_{16S} 1045), *Sphingobacteriaceae* (i.e., *Mucilaginibacter*, OTU_{16S} 1073) and *Chitinophagaceae* (i.e., *Ferruginibacter*, OTU_{16S} 1014) as well as decreasing amounts of *Xanthomonadaceae* (i.e., *Rhodanobacter*, OTU_{16S} 300) and *Kineosporiaceae* (i.e., *Kineosporia*, OTU_{16S} 703) contributing to the dissimilarity of t_0 and t_{End} (Figure 49, Table A 9). In addition, *Betaproteobacteria* and a minor part of *Firmicutes* were also noticeable in the pH 7 treatments (Figure 48B, Table A 9).

3.5.2. The impact of substrates and pH on methylotrophs

The mean coverage of all combined amplicon libraries for *mxoF* gene sequences based on 90 % similarity cut-off was 99.08 ± 0.64 % (Figure 50A). Only methylotrophic microorganisms possessing *mxoF* genes encoding for the large subunit of the PQQ-methanol dehydrogenase were addressed. Thus, other methylotrophic microorganisms possessing further methylotrophic marker genes such as *xoxF* (also encoding a PQQ-methanol dehydrogenase) or other methanol-utilising enzymes were not included in this analysis.

The detected numbers of family-level based phylotypes were on average 65 ± 15 OTUs for the substrate SIP experiment incubations. For the pH shift SIP experiment a difference between pH 4 and pH 7 incubations was observed. The number of detected phylotypes was lower at pH 4 with an average of 54 ± 7 OTUs compared to a nearly 2-fold higher value for pH 7 incubation with an average of 96 ± 15 OTUs. (Figure 50B). The Chao 1 indices estimating *mxoF* gene richness followed the same pattern with average values of 94 ± 26 expected phylotypes for the substrate SIP experiment, 75 ± 29 expected phylotypes for pH 4 incubations and 115 ± 19 expected phylotypes for pH 7 incubations of the pH shift SIP experiment (Figure 50F). Thus, a higher influence of different pH conditions on the overall diversity of *mxoF* gene sequences in the initial acidic soil was assumed.

In addition, no domination of a few or only one phylotype was observed in all combined amplicon libraries of both SIP experiments (Figure 50C, D & E). Thus, a diverse *mxoF*-possessing methylotrophic community was assumed at the beginning as well as after the incubation with different substrates or at different pH conditions.

RESULTS

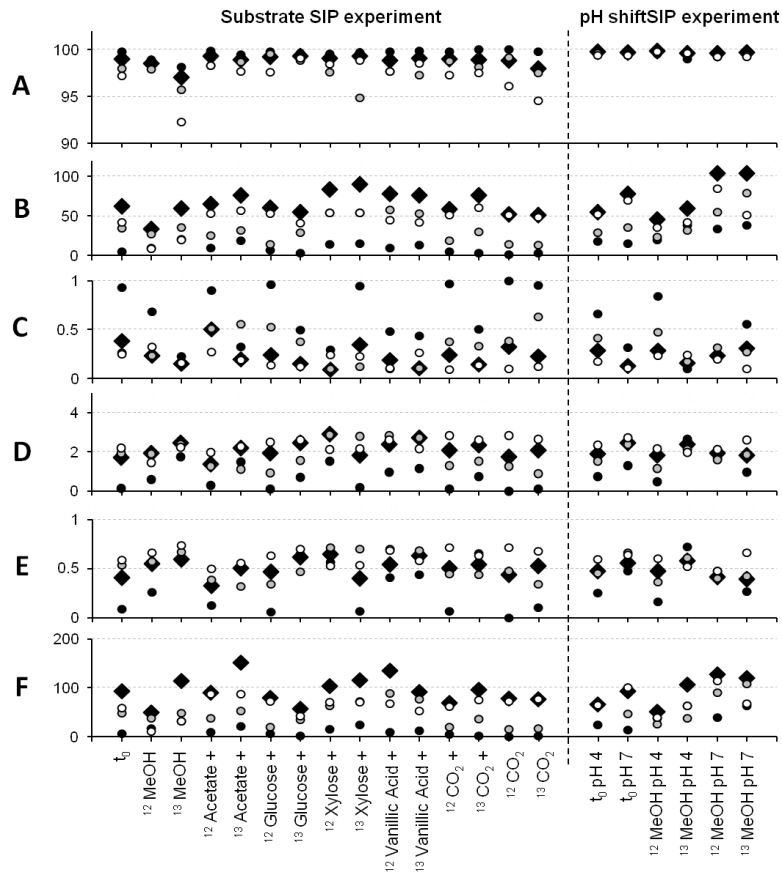


Figure 50 Diversity and richness estimators of *mxoF* gene sequences from pyrosequencing amplicon pools at similarity level 90%.

Figures indicating coverage (%) (A), numbers of OTUs (B), dominance D (C), Shannon index H (D), equitability J (E) and Chao1 index (F) of t_0 samples (no treatment, combined data sets of replicates for substrate SIP experiment t_0) and after treatment for both SIP experiments. A ¹² indicates [¹²C]-isotopologue, ¹³ indicates [¹³C]-isotopologue. A cross indicates additional supplementation of methanol in substrate treatments. Symbols: ◆, combined data sets of 'heavy', 'middle' and 'light' fractions; ●, 'heavy' fraction; ◐, 'middle' fraction; ◑, 'light' fraction. This figure has been published in Morawe *et al.* 2017.

In general, the methylotrophic community was significantly affected by different substrates as well as different pH incubations as shown with ANOSIM ($R = 0.33$, $p = 0.02$) and NPMANOVA ($F = 2.02$, $p = 0.0023$) analyses (Table A 7). As assumed by the numbers of detected and expected phylotypes (Chao 1 index) before, ANOSIM analysis revealed a high influence of pH ($R = 0.85$, $p = 0.02$) and only a minor effect of different substrates ($R = 0.18$, $p = 0.13$) on the methylotrophic community. This result was also confirmed by NPMANOVA analysis. The pairwise NPMANOVA indicated no obvious differences in the methylotrophic community between t_0 and t_{End} of different substrate incubations with the lowest influence of vanillic acid treatments ($F = 0.9$) and the highest influence for xylose treatments ($F = 2.01$) compared with t_0 (Table A 7). The same trend was shown for the comparison between methanol treatments and substrate treatments. The pairwise NPMANOVA of samples from the pH shift SIP experiment revealed a remarkable influence of a more neutral pH in

comparison with its t_0 ($F = 7.19$) as well as in comparison with the incubation at pH 4 ($F = 15.43$) (Table A 7).

Interestingly, all t_0 samples from the substrate SIP and pH shift SIP experiments were indicated to be not highly dissimilar as revealed by the pairwise ANOSIM and the pairwise NPMANOVA of these samples (Table A 7), suggesting a more similar initial community of methylotrophic microorganisms in the acidic soil samples of both SIP incubations. This is also in accordance with the analysis of the bacterial community (see 3.5.1).

Only small differences between [^{12}C]-, [^{13}C]- and combined dataset-derived communities were observed in an nMDS plot, which accords to the other nMDS plots for bacteria (based on 16S rRNA gene sequences, see 3.5.1 & Figure 48) and fungi (based on ITS gene sequences, see 3.5.3 & Figure 55). In addition, a clear clustering corresponding to the incubations with different substrates and under different pH conditions was obvious (Figure 51). Although ANOSIM and NPMANOVA analyses revealed no strong dissimilarities between the t_0 replicates a noticeable scattering effect in the nMDS plot was represented. This was also observed with the 16S rRNA gene sequence analyses (see 3.5.1 & Figure 48) and could be due to methodical reasons like PCR-based differences and the amount of sequences obtained in the independently conducted pyrosequencing for the different amplicon libraries. Another explainable reason for the scattering of t_0 replicates could be that the nMDS was conducted with the complete dataset and an nMDS plot attempts to illustrate as accurately as possible the pairwise dissimilarity between different samples based on a distance matrix in a two-dimensional plot. Nonetheless, a stress value below 0.2 indicates for an acceptable representation of the original structure of the data [Clarke, 1993].

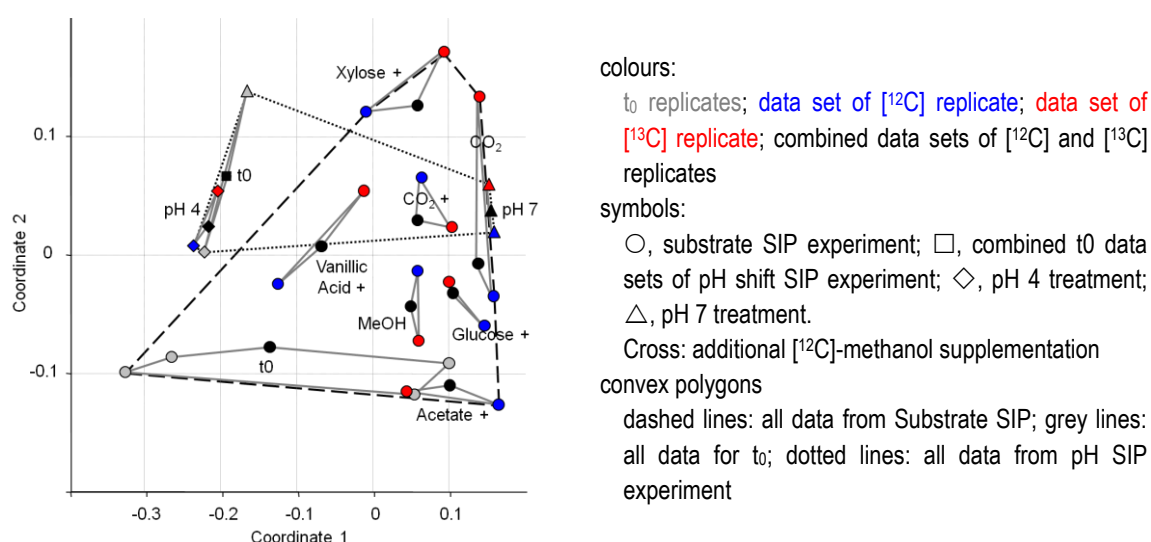


Figure 51 nMDS analyses of the *mxoF*-possessing bacterial community after different substrate or pH treatments.

The nMDS analysis for the bacterial methylotrophic community was based on *mxoF* gene sequences (similarity cut-off 90 %). The analysis is based on the Bray-Curtis similarity index with a stress value of 0.1868. This figure has been published in Morawe *et al.* 2017.

3.5.2.1. Comparison of the methanol treated samples and multi-carbon treated samples

Although the effect of different substrates on the responding methylotrophic community was assumed as low, the position of the substrate SIP experiment derived-samples in the nMDS plot hypothesised the grade of similarities between different substrate incubated-samples compared to each other and with its t_0 samples (Figure 51). Methanol- and glucose-treated samples revealed a closer positioning, assuming higher similarity between these incubations. Xylose- and acetate-treated samples showed the highest dissimilarity as indicated by their positioning of the samples (Figure 51).

Interestingly, the phylogenetic analysis revealed a decreasing amount of *Methylobacterium*-related phylotypes and an increase of *Hyphomicrobium*-related phylotypes in all incubations of the substrate SIP experiment (Figure 52 & Table A 10). In the methanol-treated samples only approximately 31 % of all OTUs were related to *Methylobacterium*. The at t_0 dominating OTU_{mx_aF 35} was no longer detectable, and instead OTU_{mx_aF 40} was the dominating sequence (i.e., approximately 20 % abundance) followed by OTU_{mx_aF 55} (i.e., approximately 10 % abundance). Acetate, glucose as well as treatments with CO₂ with and without additional methanol showed the same trend with a domination of increased OTU_{mx_aF 40} followed by OTU_{mx_aF 55}, and either no detection of OTU_{mx_aF 35} or a detection of OTU_{mx_aF 35} at a low level. Thus, a growth stimulating benefit for these phylotype possessing taxa might be suggested. Only xylose and vanillic acid treatments revealed another distribution of *Methylobacterium*-related phylotypes. OTU_{mx_aF 35} was still dominant in vanillic acid treatment, but decreased compared to t_0 and OTU_{mx_aF 55} was highly increased and thus dominant in xylose treatments.

The distribution of *Hyphomicrobium*-related sequences still showed the presence of OTU_{mx_aF 185} in all samples of the substrate SIP experiment with nearly equal amounts in methanol treatments (i.e., approximately 15 % abundance), a lower abundance in vanillic acid, glucose, xylose and both CO₂ treatments (i.e., approximately an abundance of 7.5 %, 7 %, 6 %, 6 % and 3 %, respectively) and an increase in acetate treatment (i.e., approximately 24 % abundance). Thus, acetate seemed to have a stimulating effect on OTU_{mx_aF 185}, whereat other multi-carbon substrates supported growth of other taxa. Further phylotypes that were present in all samples were OTU_{mx_aF 266} and OTU_{mx_aF 172}. The at t_0 more abundant phylotype OTU_{mx_aF 266} was highly increased in methanol treatments (i.e., approximately 25 % abundance) as well as in treatments with vanillic acid, glucose and CO₂ without methanol (i.e., approximately an abundance of 14 %, 9 % and 9 %, respectively) but decreased in treatments with acetate (i.e., abundance below 1 %) as well as xylose and CO₂ with additional methanol (i.e., approximately 2.5 % abundance). The low abundant phylotype OTU_{mx_aF 172} was increased but still low abundant in treatments with methanol, vanillic acid and CO₂ without additional methanol. Only in xylose treated samples OTU_{mx_aF 172} was detected as a high abundant *Hyphomicrobium*-related sequence.

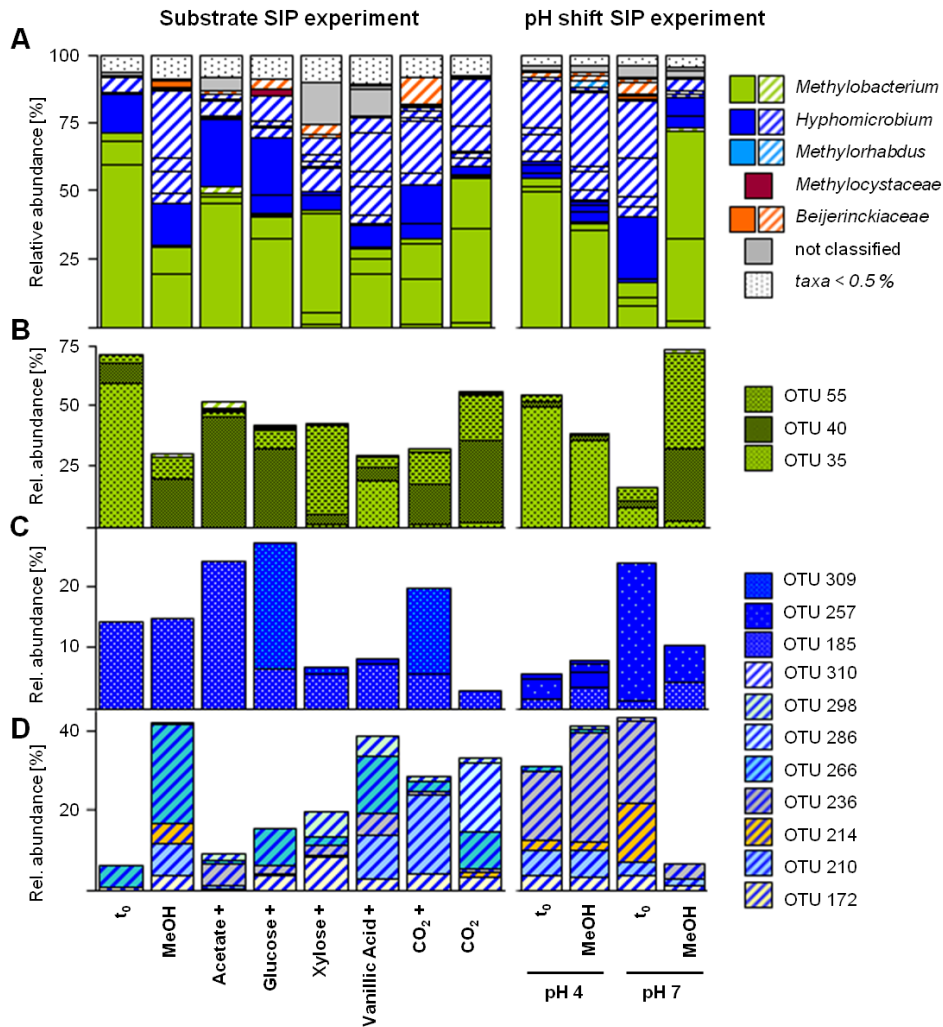


Figure 52 Composition of various *mxaF* genotypes after different substrate or pH treatments.**

Relative abundances of combined (¹²C and ¹³C) data sets of all *mx**aF*-affiliated genotypes (A) and in more detail *Methylobacterium*-affiliated (B) and *Hyphomicrobium*-affiliated genotypes (C, D). Phylogenetic affiliation is indicated by equal colours; ambiguous affiliation (i.e., sequence identity with BLASTn < 90 % as well as ambiguous position in phylogenetic tree) is indicated by shading. Additional [¹²C]-methanol supplementation in Substrate SIP experiment is indicated by a cross. Shown are genotypes with relative abundances ≥ 0.5 % in combined (¹²C and ¹³C) data sets. This figure has been published in Morawe *et al.* 2017.

In all substrate treatments the at *t*₀ marginal abundant phylotype OTU_{*mx**aF*} 210 increased, but only in treatments with methanol, vanillic acid and CO₂ with additional methanol the abundance was high (i.e., approximately 8 %, 11 % and 19 % abundance, respectively). A similar observation was made for the phylotype OTU_{*mx**aF*} 309, which was marginal abundant at *t*₀ (i.e., below 0.5 %), but highly increased in treatments with glucose and CO₂ with additional methanol (i.e., approximately 21 % and 14 % abundance, respectively).

3.5.2.2. Low abundant *mxoF* phylotypes in the substrate SIP experiment

Besides the domination of *Methylobacterium*- and *Hyphomicrobium*-related phylotypes smaller amounts (i.e., abundances mainly below 5 %) of phylotypes related to *Methylohabdus*, *Methylocystaceae* and *Beijerinckiaceae* were detected (Figure 52 & Table A 10). *Methylohabdus*-related phylotypes were present in all samples of the substrate SIP experiment but the abundance was almost always below 0.5 % (exception for the methanol treatment). Only in acetate and xylose treatments a slight higher abundance was detected (i.e., approximately 0.4 % abundance, data not shown) compared to other treatments, indicating a putative utilisation of these two multi-carbon substrates besides methanol. This is in accordance with the known substrate spectrum of this facultatively methylotrophic genera [Doronina *et al.*, 1996]. Although the generation time of *Methylohabdus* on glucose is higher than on methanol [Doronina *et al.*, 1996] the abundance of *Methylohabdus*-related phylotypes in glucose treated samples was only minimalistic, suggesting no utilisation of the hexose under the given conditions. Thus, it can be assumed that the competition for glucose in the forest soil is high and the low abundant *Methylohabdus* is not competitive enough.

Methylocystaceae-related phylotypes were only detectable at low abundances in the initial t_0 sample and after treatments with glucose and acetate. The abundance in the glucose treatment was high compared to the t_0 samples, indicating a growth supporting effect for this phylotype. For a long time methylotrophic members of the *Methylocystaceae* were known to be obligately methanotrophic organisms, and multi-carbon substrates such as glucose were not utilised as energy source. However, multi-carbon compounds can be used as supporting carbon source when organisms grow in the presence of methanol or methane [Hanson, 1992]. Another multi-carbon substrate known to be utilised by *Methylocystaceae*, especially *Methylocystis* species in acidic peat [Belova *et al.*, 2011] or bog [Im *et al.*, 2011a] environments, is acetate. Although the *Methylocystaceae*-related phylotype was detected in the acetate treatment a growth supporting effect of acetate on this phylotype was not observed, since the abundance was negligible.

Beijerinckiaceae-related phylotypes were detected in all samples from the substrate SIP experiment. This family is known to show a preference for acidic soils and includes facultatively methylotrophic genera such as *Methylocella*, *Methylosorus* and *Methylovirgula* [Dedysh *et al.*, 2005a; Vorob'ev *et al.*, 2009; Berestovskaya *et al.*, 2012; Marín & Arahal, 2013; Crombie & Murrell, 2014]. Interestingly, in the initial t_0 sample of the acidic soil the abundance of *Beijerinckiaceae*-related phylotypes is marginal. Incubations with different substrates revealed a stimulation of growth for *Beijerinckiaceae*-related taxa, but after the treatment with methanol only less than 3 % of all detected *mxoF*-correlated phylotypes are related to this family. The treatment with acetate revealed comparable amounts, whereas in samples treated with glucose and xylose the amount of *Beijerinckiaceae*-related phylotypes was higher, indicating a more stimulating effect for taxa comprising these phylotypes. Abundances for *Beijerinckiaceae*-related phylotypes in treatments with vanillic acid were less

than 2 % indicating a minor stimulating effect compared to methanol and other substrates tested. The highest and also the lowest abundance for *Beijerinckiaceae*-related phylotypes were detected in CO₂ incubations with (i.e., approximately 11 % abundance) and without additional methanol (i.e., approximately 0.9 % abundance), suggesting a clear growth supporting effect of CO₂ in combination with methanol for these phylotype included taxa.

Phylogenetic affiliation and reliable classification of *mxoF* sequences was not always possible. Contradictory, miscellaneous and ambiguous results from BLASTn analysis and phylogenetic trees made it impossible to affiliate the different phylotypes. The polyphyletic origin of methylotrophic organisms, gene transferring events such as horizontal gene transfer as well as the choice of a suitable primer pair set [Moosvi *et al.*, 2005; see 2.5.7.1] and the limited length of amplicons from pyrosequencing (i.e., approximately 460 bp) contributed to this problem. In all substrate treatments such unclassifiable phylotypes were detectable (Figure 52). Interestingly, their abundance was low at t₀ (i.e., abundances below 2 %) and in methanol-, glucose- and CO₂-treated samples (i.e., abundances below 1 %), whereas an increase in abundances was detected in treatments with acetate, vanillic acid and xylose (i.e., abundances of approximately 5 %, 12 % and 16 %, respectively), suggesting a growth stimulating effect on taxa including these unclassifiable phylotypes. Thus, putatively unknown methylotrophic species, which are capable of utilising acetate, aromatic compounds and pentoses and revealing supported growth through multi-carbon substrates, could be hypothesised. Since methanol did not led to higher abundances of this phylotypes it could be questioned how competitive these taxa are in nature and if methanol is not the preferred carbon source. However, missing phylogenetic affiliation prevented further conclusions and clearer assumptions.

3.5.2.3. Comparison of the *mxoF*-possessing methylotrophic community incubated under different pH conditions

As indicated by ANOSIM and NPMANOVA analyses, the effect of different pH conditions on the *mxoF*-possessing methylotrophic community was stronger than the treatment with different substrates (Table A 7). Interestingly, even in the different t₀ samples remarkable differences were obvious with a domination of *Methylobacterium*-related phylotypes at pH 4 and a domination of *Hyphomicrobium*-related phylotypes at pH 7 (Figure 52).

Similar to the methanol incubation of the substrate SIP experiment the amount of *Methylobacteriaceae*-related phylotypes was decreased, and *Hyphomicrobium*-related phylotypes were increased after the treatment with methanol at pH 4 (i.e., no adjustment of pH). The t₀ samples with the *in situ* pH 4 were dominated by the phylotypes OTU_{*mxoF*} 35, but only in the methanol treatments of the pH shift SIP experiment OTU_{*mxoF*} 35 was still most abundant (i.e., 36 % abundance), which revealed a different composition of *Methylobacterium*-related phylotypes of both methanol incubations (i.e., incubations of the substrate SIP and pH shift SIP experiment). The same was observed for *Hyphomicrobium*-

related phylotypes. The in the substrate SIP experiment detected OTU_{*mx*aF} 185 was in general less abundant in the pH shift SIP experiment, though an increase in the methanol treatment at pH 4 compared to t₀ was detected. Instead, the most abundant *Hyphomicrobium*-related phylotypes at t₀ as well as after the treatment with methanol at pH 4 was OTU_{*mx*aF} 236, which was only minor abundant in methanol incubations of the substrate SIP experiment. Besides the *Methylobacterium*- and *Hyphomicrobium*-related phylotypes, minor proportions of *Methylorhabdus*- and *Beijerinckiaceae*-related phylotypes (i.e., approximately 3 % and 3.5 % abundance, respectively) were detected. The *Methylorhabdus*-related phylotype OTU_{*mx*aF} 18 was indicated to be enriched, whereas the amount of *Beijerinckiaceae*-related phylotypes remained rather constant.

Under the elevated pH 7 conditions, samples of t₀ as well as methanol treatments revealed a contrary composition of the *mx*aF-possessing methylotrophic community compared to all incubations under *in situ* pH 4. The initial domination of the *Hyphomicrobium*-related phylotypes at pH 7 (i.e., approximately 69 % abundance) was highly decreased. The initial high abundant phylotypes OTU_{*mx*aF} 257 and OTU_{*mx*aF} 236 (i.e., approximately 23 % and 21 % abundance, respectively) remained still abundant, but at low amounts (i.e., approximately 6 % and 4 % abundance, respectively). Interestingly, the initial lower abundant phylotype OTU_{*mx*aF} 185 increased from approximately 1 % up to approximately 4 %. After the methanol treatment at pH 7 *Methylobacterium*-related phylotypes increased in abundance up to 74 %, especially OTU_{*mx*aF} 55 followed by OTU_{*mx*aF} 40 (i.e., up to approximately 40 % and 30 % abundance, respectively). The abundance of *Beijerinckiaceae*-related phylotypes however decreased from initial approximately 8 % to 1 %, indicating an inhibitory effect of this more neutral pH to this family with its preference for acidic soils [Marín & Arahal, 2013].

3.5.2.4. The effect of the pH on *mx*aF- and *m*moX-possessing methylotrophs

Despite the dissimilarities of the *mx*aF-possessing methylotrophic communities in the pH 4 and pH 7 treatments also the abundance of these bacteria was assumed to be influenced as well as the abundance of methanotrophs. Methanotrophs that were often detected in acidic soils are affiliated to *Beijerinckiaceae*. For example, the ‘restricted’ facultatively methanotrophic genus *Methylocella* seems to prefer acidic environments with a pH below 5 [Rahman *et al.*, 2011]. *Methylocella* possess solely the sMMO [Marín & Arahal, 2013], wherefore *Methylocella*-specific *m*moX genes were further targeted to briefly assess the effect of an elevated pH on methanotrophs in an inherently acidic forest soil.

The initial quantification of the bacterial abundance (based on 16S rRNA gene numbers) revealed an increase in both pH 7 treatments (i.e., the unsupplemented controls and methanol treatments), demonstrating the general growth restricting conditions at the *in situ* pH 4 for *Bacteria* (Figure 53). The same was observed for *mx*aF gene numbers.

Contrary to that, the gene numbers of *mmoX* were dramatically decreased in all pH 7 treatments emphasising that the acidic *in situ* pH conditions were advantageous especially for methanotrophic organisms such as *Methylocella* or further *Beijerinckiaceae*.

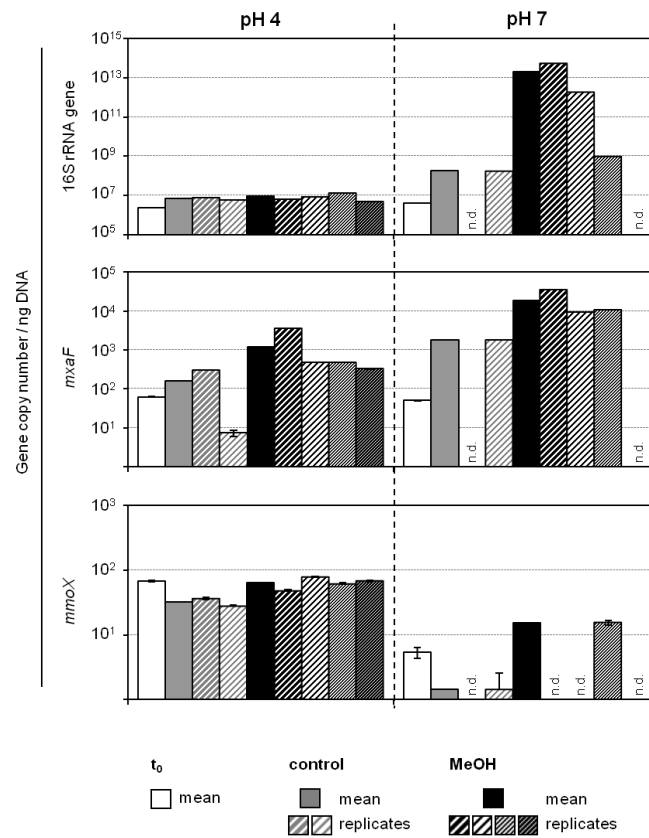


Figure 53 Influence of different pH conditions on 16S rRNA, *mxoF* and *mmoX* gene numbers in soil slurry treatments.

Comparison of the gene copy numbers ng^{-1} DNA at t_0 (no treatment; white) and after treatment (grey, unsupplemented control; black, methanol supplementation). Gene copy numbers for t_0 were determined by duplicated qPCR measurements. Gene copy numbers for different treatments are mean values of replicates (filled columns). Gene copy numbers for each replicate were determined by duplicated qPCR measurements (shaded columns); error bars indicate standard error; n.d., not detectable.

3.5.3. The impact of substrates and pH on Fungi in an acidic soil

The mean coverage of all combined amplicon libraries of the different treatments (i.e., t_0 , substrate or pH treatments of both SIP experiments) for ITS gene sequences based on a species-level cut-off was $98.44 \pm 0.29\%$ (Figure 54A). The detected numbers of phylotypes in the substrate SIP experiment were not similar for the different incubations, showing generally higher values of detected phylotypes for t_0 , methanol, vanillic acid and CO_2 incubations with an average of 241 ± 11 OTUs and lower values of detected phylotypes in acetate, glucose and xylose treatments with an average of 139 ± 26 OTUs. In terms of the pH shift SIP experiment no obvious differences were detectable for pH 4 and pH 7 incubations resulting in an average of 273 ± 25 detected phylotypes.

RESULTS

The Chao 1 indices calculated for the substrate SIP experiment amplicon libraries indicated on average a species richness of 317 ± 16 phylotypes for t_0 , methanol, vanillic acid and CO_2 treatments and 198 ± 40 phylotypes for acetate, glucose and xylose treatments, respectively. The estimated number of phylotypes for the pH shift SIP experiment was 334 ± 29 phylotypes (Figure 54B& F). In general, a diverse active fungal community was assumed at the beginning as well as after treatments with certain substrates (i.e., methanol, vanillic acid and CO_2) or under different pH conditions. Interestingly, the treatment with acetate and especially sugars led to the domination of a few fungal species (Figure 54C, D & E). No domination of one or a few fungal phylotypes was observed at different pH conditions. Although the sampling time points of fresh soil samples for the substrate SIP and pH shift SIP experiment were not identical, the number and diversity of phylotypes is comparable assuming a greater influence of given substrates on fungal diversity.

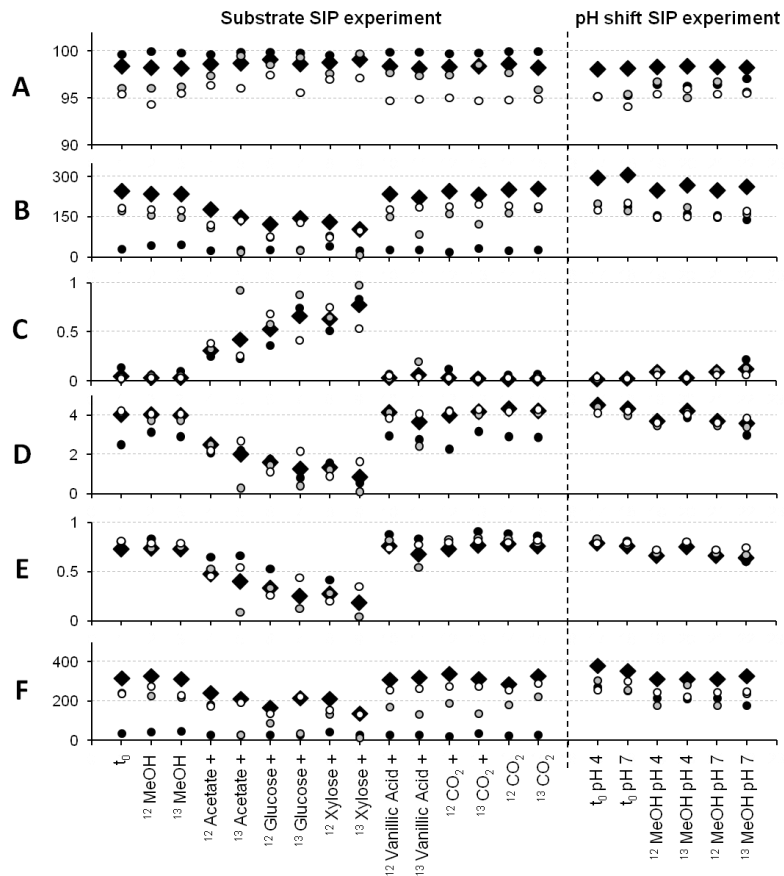


Figure 54 Diversity and richness estimators of ITS gene sequences from pyrosequencing amplicon pools at similarity level of 97% (species level).

Figures indicating coverage (%) (A), numbers of OTUs (B), dominance D (C), Shannon index H (D), equitability J (E) and Chao1 index (F) of t_0 samples (no treatment, combined data sets of replicates for substrate SIP experiment t_0) and after treatment for both SIP experiments. A ¹² indicates [¹²C]-isotopologue, ¹³ indicates [¹³C]-isotopologue. A cross indicates additional supplementation of methanol in substrate treatments. Symbols: ◆, combined data sets of 'heavy', 'middle' and 'light' fractions; ●, 'heavy' fraction; ●, 'middle' fraction; ○, 'light' fraction. This figure has been published in Morawe *et al.* 2017.

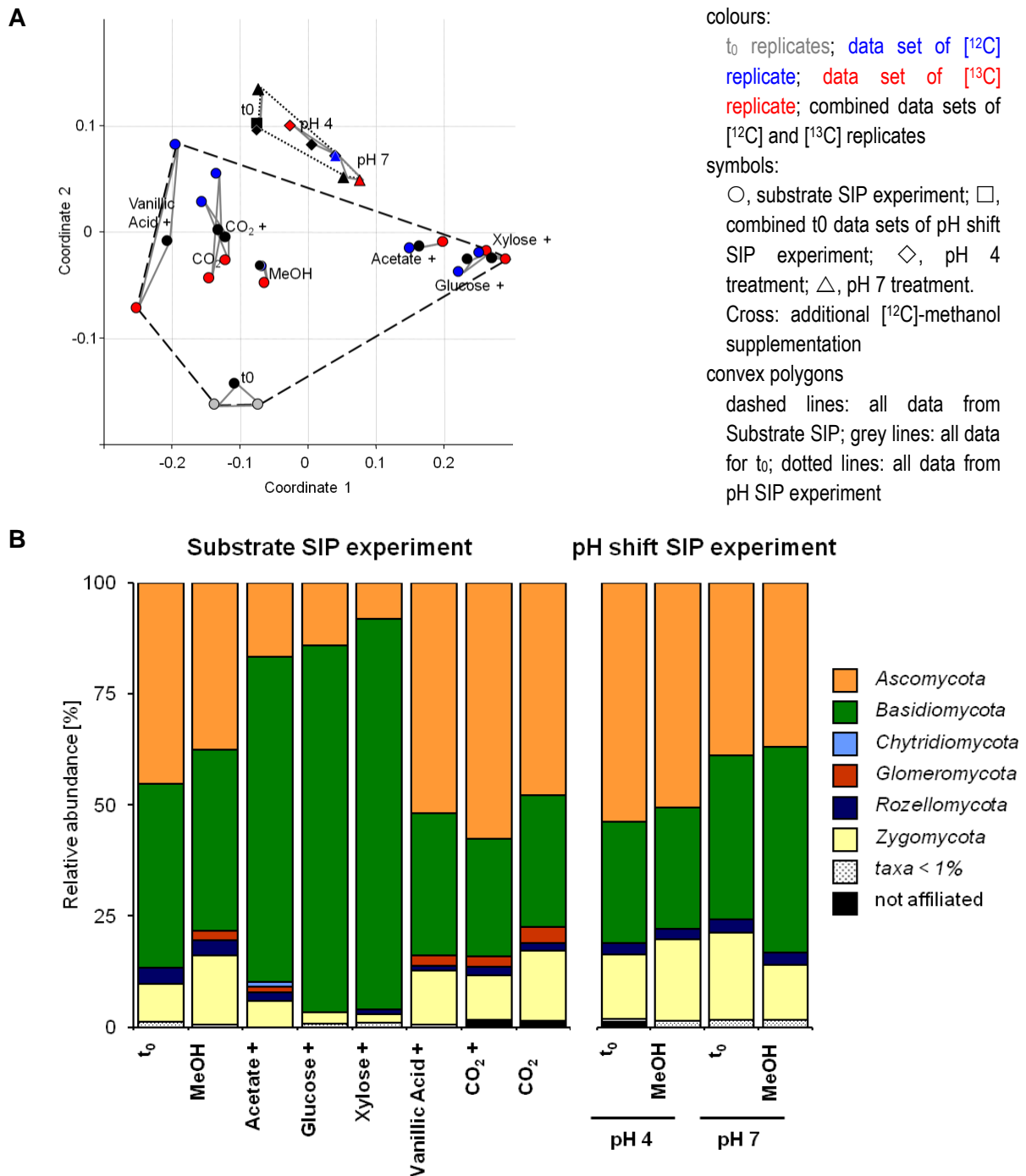


Figure 55 nMDS analyses (A) and the phylogenetic compositions (B) of the fungal community after different substrate or pH treatments.

Panel A, nMDS analysis of the fungal community based on ITS gene sequences (at species-level, similarity cut-off 98 %). The analysis is based on the Bray-Curtis similarity index with a stress value of 0.1245.

Panel B, relative abundances of combined (^{12}C and ^{13}C) data sets of ITS gene sequences derived OTUs from pyrosequencing pools of both SIP experiments at the beginning (t_0) and after treatment with substrates or different pH conditions. A cross indicates additional supplementation of methanol in substrate treatments. Phylogenetic affiliation was confirmed with UNITE database for ITS gene sequences.

This figure has been published in Morawe *et al.* 2017.

The similarity of the initial fungal community structure (based on family-level) between t_0 samples of the substrate SIP and pH shift SIP experiments was examined to address the question if the sampling time point affected both SIP experiments additionally. Interestingly, ANOSIM revealed no significant dissimilarity between t_0 samples ($R = 0.6$, $p = 0.33$), whereas NPMANOVA indicated a significant dissimilarity of samples ($F = 8.21$, $p = 0.0001$). Thus, both SIP experiments were presumably not set up under similar conditions in terms of the initial fungal community.

In accordance to ANOSIM and NPMANOVA, the nMDS plot revealed distinct positions of both t_0 samples for the substrate SIP and pH shift SIP experiment (Figure 55A). However, individual replicates of each t_0 time point showed no immense scattering effect, indicating that variances between replicates among each other due to methodical procedures (i.e., DNA extraction, PCR based amplification) are negligible.

Apart from the subordinated community shaping effect of different sampling time points, the fungal community composition in the different treatments was primarily significantly affected by supplemented substrates as well as different pH conditions, which was revealed by ANOSIM ($R = 0.82$, $p < 0.0001$) and NPMANOVA ($F = 8.11$, $p = 0.0001$). The effect of given substrates was higher (ANOSIM: $R = 0.78$, $p = 0.0001$; NPMANOVA: $F = 9.41$, $p = 0.0001$) than the effect of pH (ANOSIM: $R = 0.69$, $p = 0.07$; NPMANOVA: $F = 2.98$, $p = 0.09$) suggesting a smaller effect of pH than available substrates on the fungal community (Table A 7). The pairwise ANOSIM revealed an overall high effect of each substrate between fungal community compositions at t_0 and t_{End} ($R = 1$, each). Additionally, the pairwise NPMANOVA indicated a remarkable effect of xylose ($F = 30.91$) and glucose ($F = 24.93$) compared to acetate ($F = 13.17$) and methanol ($F = 7.23$). The lowest dissimilarity between t_0 and t_{End} was indicated for vanillic acid ($F = 3.58$) and CO_2 with methanol ($F = 3.64$) and without ($F = 2.69$).

The phylogenetic composition of t_0 samples from the substrate SIP experiment represented a nearly equal distribution of *Ascomycota* and *Basidiomycota* dominating the total fungal community as expected. Only a minor part of *Zygomycota* and *Rozellomycota* was detected. The initial t_0 samples from pH-SIP were also dominated by *Ascomycota* and *Basidiomycota*, whereat the t_0 of pH 4 (i.e., no adjustment of pH) showed a higher amount of *Ascomycota*, and the t_0 of pH 7 (i.e., adjustment of pH to 6.9) showed more equal distribution of the dominating phyla (Figure 55B). Interestingly, *Zygomycota* were approximately two times more abundant in pH-SIP t_0 samples compared to the substrate SIP experiment. Instead, the amount of *Rozellomycota* was comparable between the substrate SIP experiment and pH-SIP t_0 samples.

As previously observed for bacteria (see 3.5.1 & Figure 48) only marginal differences between [^{12}C]-, [^{13}C]- and combined dataset-derived communities were obvious in a nMDS plot (Figure 55A, species level). All fungal ITS gene sequences showed a clear clustering corresponding to their incubations with different substrates and pH, respectively.

3.5.3.1. Comparison of t_0 and t_{End} of the samples treated with different substrates

A community forming effect of methanol was indicated by distinct position of methanol-incubated samples to t_0 samples of the substrate SIP experiment. However, the distance between these samples and t_0 is the smallest compared with all other substrate-incubated samples (Figure 55A), indicating only a minor affected fungal community at species level. The analysis of the phylogenetic composition revealed still a nearly similar amount of *Basidiomycota* and *Ascomycota* dominating the fungal community as well as a stable amount of *Rozellomycota* compared to t_0 (Figure 55B). Although in general no changes for the amount of *Ascomycota* and *Basidiomycota* were observed fungal taxa like *Saccharomycetes* and *Russulaceae* (i.e., taxa decreased in abundance) as well as *Trichocomaceae*, *Ganodermataceae* and *Cryptococcus* (i.e., taxa increased in abundance), contributed to the dissimilarity between t_0 and methanol incubation as indicated by SIMPER (based on family level) (Figure 56, Table A 11). The treatment with methanol also resulted in an increase of *Zygomycota* (i.e., *Mortierella* indicated by SIMPER), the presence of *Glomeromycota* and similar amounts of *Rozellomycota* (Figure 55B).

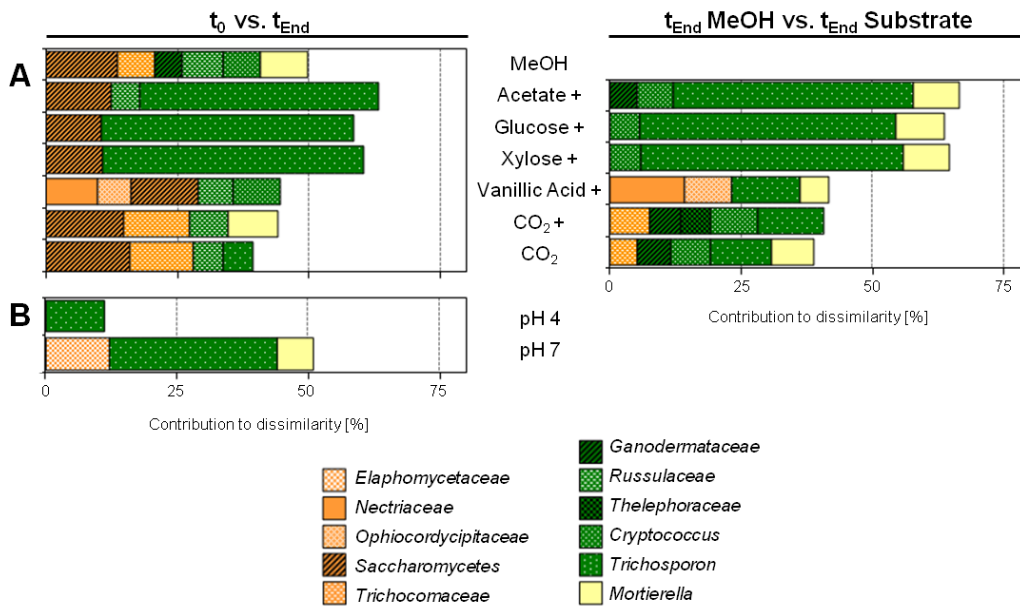


Figure 56 Fungal taxa responsible for dissimilarity in substrate treatments.

Pairwise comparisons between t_0 (no treatment) and t_{END} of both SIP experiments (A, substrate SIP; B, pH shift SIP) as well as pairwise comparisons between t_{END} of methanol and substrate treatments of the substrate SIP experiment determined by SIMPER (Similarity Percentage) analyses. SIMPER was performed with combined data sets (^{12}C and ^{13}C) of relative abundances based on family level (via phylogenetic affiliation of obtained OTUs). Shown are the main taxa contributing each to $\geq 5\%$ to the dissimilarity between samples. Phylogenetic affiliation (phylum level) is indicated by equal colours, different families are differentiated by shading. A cross indicates additional supplementation of methanol in substrate treatments.

Vanillic acid-treated samples were more distinct to t_0 than methanol samples (Figure 55A). The analysis of the phylogenetic composition revealed an increase in *Ascomycota* and a decrease of *Basidiomycota* due to the vanillic acid treatment (Figure 55B). In detail, taxa that contributed to more than 40 % of dissimilarity between t_0 and t_{End} were *Saccaromyces* and *Russulaceae* (i.e., taxa decreased in abundance) as well as *Nectriaceae*, *Ophiocordycipitaceae* and *Cryptococcus* (i.e., taxa increased in abundance) (Figure 56, Table A 11). The amount of *Zygomycota* (i.e., *Mortierella*) was increased. Only a minor part of *Rozellomycota* remained and *Glomeromycota* were present (Figure 55B).

Data from the samples of CO₂-supplemented treatments with and without methanol were positioned in between methanol and vanillic acid treatments, suggesting that the fungal community was somehow similar to communities from both treatments (Figure 55A). The phylogenetic analysis showed indeed a similar distribution of fungal phyla compared to methanol and vanillic acid treatments. In general, an increase of dominating *Ascomycota* and decrease of *Basidiomycota* was observed. The amount of *Zygomycota* detected was similar to methanol and vanillic acid treatments. In addition, the amount of *Rozellomycota* decreased compared to t_0 , and *Glomeromycota* were present (Figure 55B). SIMPER indicated that fungal taxa such as *Saccharomyces* and *Russulaceae* (i.e., taxa decreased in abundance) as well as *Trichocomaceae* (i.e., taxa increased in abundance) contributed mostly to the dissimilarity (Figure 56, Table A 11).

Interestingly, treatments with acetate, glucose and xylose were most distinct to t_0 and the other substrate incubations assuming a more different fungal community as shown with NPMANOVA before (Figure 55A). The phylogenetic analysis revealed an enormous increase and domination of *Basidiomycota* as well as a reduced amount of *Ascomycota* in these treatments (Figure 55B). *Trichosporon* (i.e., genus increased in abundance) and *Saccharomyces* (i.e., taxa decreased in abundance) were shown to contribute to more than 50 % of the dissimilarity between t_0 samples and t_{End} samples (Figure 56, Table A 11), and were assumed to be influenced by the supplementation of acetate and sugars. However, the position of acetate-treated samples to glucose- and xylose-treated samples in the nMDS plot indicated only slight dissimilarities of the fungal communities (Figure 55A). The amount of *Zygomycota* was mainly reduced in sugar treatments. In minor parts *Rozellomycota* were only detectable in acetate and xylose treatments and only in acetate treatments *Glomeromycota* and *Chytridiomycota* were present (Figure 55B). SIMPER analysis also indicated *Russulaceae* (i.e., taxa decreased in abundance) contributing to the dissimilarity between t_0 and acetate incubation (Figure 56, Table A 11).

3.5.3.2. Comparison of the methanol-treated samples and multi-carbon-treated samples

The comparison of the fungal communities of methanol and substrate treatments revealed that *Basidiomycota* (i.e., *Trichosporon*) as well as *Zygomycota* (i.e., *Mortierella*) were

responsible for more than 50 % of dissimilarities between methanol treatments and treatments with acetate and sugars. In addition, the abundance of *Mortierella* as well as *Cryptococcus* and *Ganodermataceae* was higher in methanol treatments compared to acetate and sugar treatments assuming that these taxa were not highly competitive for acetate and sugars. The SIMPER analysis indicated also *Trichosporon* and *Mortierella* (i.e., both taxa are more abundant in methanol treatment) as well as *Ascomycota* (i.e., *Netricaceae* and *Ophiocordycipitaceae*, both families are more abundant in vanillic acid treatments) as responsible for dissimilarities between the fungal community of methanol and vanillic acid treatments. Dissimilarities between methanol treatments and treatments with CO₂ with and without methanol were mainly caused by *Trichocomaceae* (i.e., family is more abundant in both CO₂ treatments), *Thelephoraceae*, (i.e., family is more abundant in CO₂ treatment without additional methanol), *Cryptococcus* and *Trichosporon* (i.e., genera are more abundant in methanol treatment) (Figure 56, Table A 11).

3.5.3.3. Comparison of samples incubated under different pH conditions

In general, all methanol treatments of the pH shift SIP experiment were closer located to each other than samples of the substrate SIP experiment as indicated by nMDS plot (Figure 55A), ANOSIM and NPMANOVA. Thus, fungal communities derived from samples of the pH shift SIP experiment were assumed to be more similar to each other. Phylogenetic analysis revealed a domination of *Ascomycota* followed by *Basidiomycota* for pH 4 treatments and similar amounts of *Ascomycota* and *Basidiomycota* detectable for pH 7 treatments (Figure 55B). Interestingly, *Trichosporon* were shown to contribute to the major dissimilarities between t₀ and t_{End} (i.e., more abundant at t₀), especially in pH 4 treatments *Trichosporon* was the only taxa with a higher influence (Figure 56). For pH 7 treatments also the ascomycotial family *Elaphomycetaceae* was indicated to contribute to dissimilarity as the family decreased in abundance at pH 7 treatments (Figure 56, Table A 11). As shown before, *Zygomycota* (i.e., *Mortierella*) were the third largest fungal phyla present in methanol treatments. In both pH treatments the amount of *Rozellomycota* was only low (Figure 55B).

3.6. Identification of methylotrophic microorganisms assimilating methanol or alternative substrates in an acidic forest soil by DNA-SIP

Stable isotope probing (SIP) was used to identify those microorganisms in an acidic forest soil that utilise a given [¹³C]-sources with an attention to methanol-utilising methylotrophs under *in situ* conditions (i.e., samples from the substrate SIP experiments, see 2.3.3) as well as under different pH conditions (i.e., samples from pH shift SIP experiment, see 2.3.4). SIP

was performed with DNA to identify not only metabolic active taxa, but also active growing taxa that assimilated the given carbon source.

The formation of [^{13}C]- CO_2 was observed (see 3.3.1 & 3.3.2), indicating the utilisation (i.e., at least the dissimilation) of the given [^{13}C]-source. Thus, also a cross feeding effect via CO_2 cannot be excluded, although [^{13}C]-isotopologues were always supplemented in minimal amounts. In addition, cross feeding could also occur by incorporation of ^{13}C that derived from [^{13}C]-breakdown products during the incubation or by ^{13}C derived from dead microbial material which assimilated ^{13}C before. In this way also the carbon flow and trophic interactions can be estimated via SIP.

3.6.1. Separation of DNA and distribution of nucleic acids along the gradient

Growing on [^{13}C]-isotopologues means assimilating the given ^{13}C , and thus incorporating these carbon into cell material such as DNA, whereof cell components of these microorganisms get higher buoyant densities. This 'heavier' DNA can be separated from non-labelled 'light' DNA in an isopycnic centrifugation caused by a density gradient. Extracted DNA from all samples of the substrate SIP experiment and the pH shift SIP experiment were subjected to such an isopycnic centrifugation step with 5 to 10 μg of DNA loaded on each gradient. The amount of samples as well as the different incubation time points led to the need of independent centrifugation runs. Nevertheless, comparability was still given by gradient solutions with the same density (i.e., $1.732 \pm 0.0006 \text{ g x ml}^{-1}$) as well as isopycnic centrifugation of corresponding DNA from [^{12}C]- and [^{13}C]-incubated samples of the corresponding treatments (e.g. DNA derived from [^{12}C]- and [^{13}C]-methanol incubations were subjected to the same centrifugation run).

In every run one DNA-free gradient was used to verify the developed gradient by determining the buoyant densities of all fractions. A linear decreasing gradient of buoyant densities was obvious in every centrifugation run suggesting that the required conditions for a successful separation of 'heavy' DNA were reached. For the substrate SIP experiment samples DNA was extracted for bacteria (i.e., 16S rRNA and *mxoF* gene sequence analyses) and for fungi (i.e., ITS gene sequence) independently resulting in two different gradients in which the average buoyant densities ranged from $1.750 \pm 0.003 \text{ g x ml}^{-1}$ to $1.697 \pm 0.007 \text{ g x ml}^{-1}$ and from $1.750 \pm 0.004 \text{ g x ml}^{-1}$ to $1.696 \pm 0.004 \text{ g x ml}^{-1}$, respectively. For the pH shift SIP experiment DNA was only extracted once and the average buoyant densities of the corresponding gradient ranged from $1.744 \pm 0.004 \text{ g x ml}^{-1}$ to $1.699 \pm 0.004 \text{ g x ml}^{-1}$.

After every centrifugation the distribution of DNA in the different fractions was determined and the majority of DNA was almost always re-detected in fractions 5 to 10 which are expected to be the 'middle' and 'light' fractions. In accordance to this observation the remaining fractions 1 to 4 contained minor amounts of DNA but were determined as 'heavy'

fractions and thus containing 'heavy' DNA of interest. Since all DNA was derived from environmental sample incubations, neither a shift of the $[^{13}\text{C}]$ -DNA distribution curves towards higher buoyant densities, nor any remarkable peak within 'heavier' fractions of $[^{13}\text{C}]$ -DNA was obvious. Interestingly, for methanol-treated samples of the substrate SIP experiment a small shoulder of the $[^{13}\text{C}]$ -DNA was detected in fraction 4 (i.e., buoyant density of $1.731 \text{ g x ml}^{-1}$) assuming successfully labelled $[^{13}\text{C}]$ -methanol-utilising microorganisms (Figure 57).

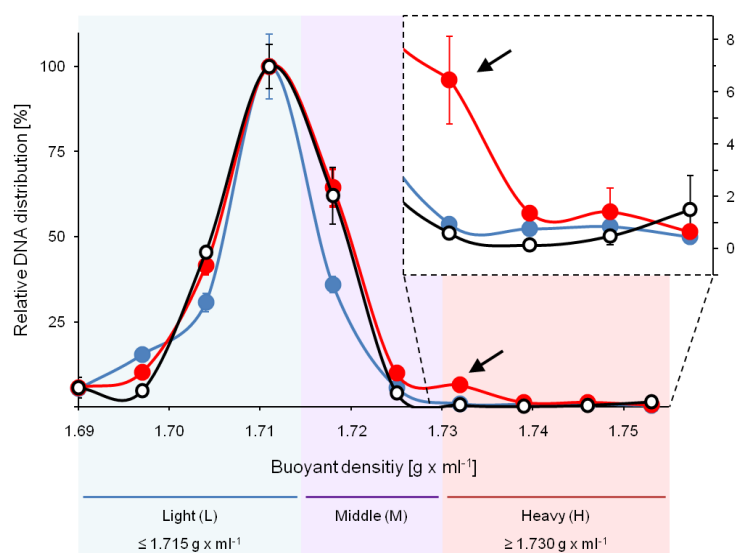


Figure 57 Distribution of DNA in the gradients of t_0 , $[^{12}\text{C}]$ - and $[^{13}\text{C}]$ -methanol treatments of Substrate SIP experiment and determination of 'heavy' (H), 'middle' (M) and 'light' (L) fractions.

Relative distribution of DNA derived from gradients of the initial t_0 ($-\circ-$) and both methanol treatments ($-\bullet-$, $[^{12}\text{C}]$ -methanol treatment; $-\bullet-$, $[^{13}\text{C}]$ -methanol treatment) and the determination of samples belonging to 'heavy' fractions (red background), 'middle' fractions (purple background), and 'light' fractions (blue background). The inset focuses on heavy fractions 1 to 4 with a clear shoulder (\leftarrow) in $[^{13}\text{C}]$ -methanol treatment indicating enrichment of 'heavy' DNA. Error bars indicate standard deviation of duplicated measurements. Threshold values for buoyant densities of different fractions are given.

3.6.2. Determination of heavy (H), middle (M) and light (L) fractions

Previous studies revealed that native DNA of organisms belonging to all three domains of life exhibit buoyant densities ranging from 1.69 g x ml^{-1} up to $1.725 \text{ g x ml}^{-1}$ [Carter *et al.*, 1983; Lueders *et al.*, 2004] and that the GC-content of an organism affects the native buoyant density within a range of 0.03 g x ml^{-1} in caesium chloride gradients [Lueders *et al.*, 2004]. Thus, the methanol-treated samples from the substrate SIP experiment were subjected to a more detailed fingerprinting-based approach in order to detect slight differences between $[^{12}\text{C}]$ - and $[^{13}\text{C}]$ -isotopologue incubations and to determine threshold buoyant densities for 'heavy', 'middle' and 'light' fractions. Consequently, a T-RFLP analysis

RESULTS

was performed with equal amounts of DNA from each fraction 1 to 10 of the [^{12}C]- and [$^{13}\text{C}_1$]-methanol incubations using restriction enzymes *MspI* and *RsaI*, which have specific recognition and restriction sites distinct from each other (see 2.5.11). Bacterial 16S rRNA gene sequences revealed different patterns of T-RFs in all fractions with a shift of some T-RFs towards heavier fractions. *RsaI* digestion revealed one T-RF with a length of 422 bp being enriched in the fractions 2 to 5 of the [^{13}C]-isotopologue treatment (Figure 58).

The *MspI* digestion revealed 3 different T-RFs, which were shifted to the heavier fractions in the [^{13}C]-DNA samples (i.e., T-RF with approximately 152 bp and 435 bp length) or were only detectable in fraction 2 to 4 of [^{13}C]-DNA samples (i.e., T-RF with a length of approximately 472 bp). Thus, an incorporation of [^{13}C]-carbon into DNA for a certain part of the microbial community as well as a successful separation of ‘heavy’ DNA from ‘light’ DNA was assumed. In addition, a virtual digestion with the online available tool ‘NEBcutter V2.0’ (New England Biolabs; <http://tools.neb.com/NEBcutter2/>) of a small selection of sequences from methylotrophic bacteria belonging to the alphaproteobacterial *Rhizobiales* and *Methylobacteriaceae* as well as members of the betaproteobacterial *Methylophilaceae* revealed that these noticeable T-RFs could be affiliated to alphaproteobacterial methylotrophs (Table 35).

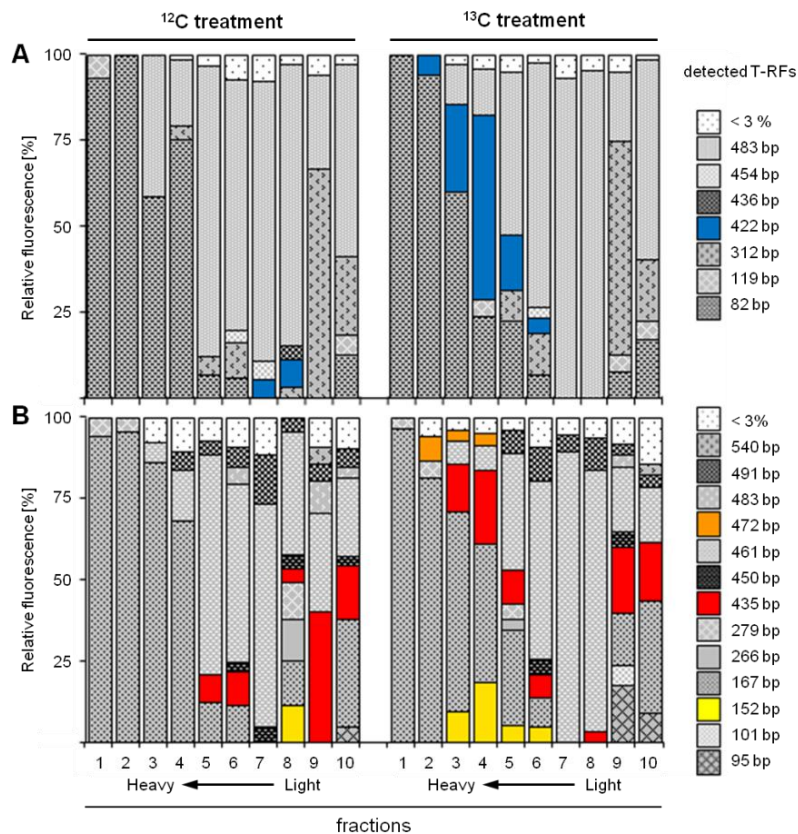


Figure 58 T-RF patterns of 16S rRNA gene sequences from methanol treatment of Substrate SIP experiments after digestion with *RsaI* (A) and *MspI* (B).

Overview on the relative fluorescence ($\geq 3\%$) of detected T-RFs in all fractions (1 – 10) of [^{12}C]- and [$^{13}\text{C}_1$]-methanol treatments to identify a potential incorporation of [^{13}C]-carbon resulting in a shift of T-RFs towards heavier fractions. Any Colouration indicates putatively affected T-RFs of interest; hatching indicates further T-RFs not of interest.

RESULTS

Based on the T-RFLP analysis threshold buoyant densities for 'heavy', 'middle' and 'light' fractions were determined. In accordance with buoyant densities for non-labelled native DNA (i.e., 1.69 g x ml⁻¹ up to 1.725 g x ml⁻¹ [Carter *et al.*, 1983; Lueders *et al.*, 2004]) as well as the shift and presence of specific T-RFs every fraction with a buoyant density \geq 1.730 g x ml⁻¹ were determined as 'heavy', fractions with buoyant densities \leq 1.715 g x ml⁻¹ were determined as 'light' fractions and remaining fractions with buoyant densities between 1.715 up to 1.730 g x ml⁻¹ were determined as 'middle' fractions.

Table 35 Potential T-RFs (based on 16S rRNA gene sequences) of known methylotrophic bacteria as a result of virtual digestion with MspI and RsaI.

Digestion was done with 'NEBcutter V2.0' (New England Biolabs; <http://tools.neb.com/NEBcutter2/>). Black bold, T-RFs were detected in T-RFLP analysis; grey bold, no suitable T-RF was detected in T-RFLP.

	taxa	Accession number	T-RFs (bp)				
			MspI ^a		RsaI ^a		
			1 st c	others ^d	1 st c	others ^d	
Alphaproteobacteria	Rhizobiales	Beijerinckiaceae					
		<i>Beijerinckia indica</i> subsp. <i>indica</i> ATCC 9039	NC_010581	150	439	422	
		<i>Methylocella silvestris</i> BL2	NC_011666	150	439	422	
		<i>Methylovirgula ligni</i> BW863	NR_044611	150	439	422	
		Bradyrhizobiaceae					
		<i>Bradyrhizobium japonicum</i> USDA110	NC_004463	152			424
		Hyphomicrobiaceae					
		<i>Hyphomicrobium nitratorans</i> NL23	NC_022997	439			422
		Methylobacteriaceae					
		<i>Methylobacterium extorquens</i> CM4	NC_011757	152	441		424
<i>Methylobacterium radiotolerans</i> JCM 2831	NC_010505	150	439	422			
Betaproteo		Methylophilaceae					
		<i>Methylobacillus flagellatus</i> KT	NC_007947	494		477	
		<i>Methylotenera versatilis</i> 301	NC_014207	490		473	

^a recognition and restriction site of *MspI*: C[▼]CG_▲G

^b recognition and restriction site of *RsaI*: GT[▼]_▲AC

^c length of T-RF if the first recognition site of the enzyme (located downstream) was cleaved

^d length of putative T-RFs detectable if other restrictions sites (located upstream) were not recognized and cleaved

3.6.3. Identification of labelled taxa

In order to identify only labelled taxa comparative analyses were conducted to minimize false positive signals caused by the a putative migration of 'light' DNA into the heavy fractions of a sample (see 2.5.14). Nevertheless, also inherently heavy DNA (i.e., high GC content) that was not labelled by ^{13}C might be detected in heavy fractions.

Analysing all fractions of the substrate SIP experiment a predominance of a *Corynebacterium*-related phylotype (OTU_{16S} 748; sequence identity 93 % (Table A 12)) in the acetate, xylose, vanillic acid and CO₂+methanol treatments was observed (Figure 59). *Corynebacteria* are a versatile clade of *Actinobacteria* and a remarkable variability in their GC-content of genomic DNA has been detected [Tauch & Sandbote, 2013]. For example, *C. kutscheri* has a GC-content of only 46 mol%, *C. glutamicum* (type species) reveals approximately 55 mol%, and *C. nuruki* possess inherently GC-rich DNA with a GC-content of 73.6 mol% [Tauch & Sandbote, 2013]. The detected phylotype exhibited a high sequence identity to the GC-rich species of *C. nuruki*, wherefore it might be possible that the detected phylotypes also possess inherently GC-rich and therefore heavy DNA. In addition, *Corynebacterium* species are not reported to grow on methanol as sole source of carbon or energy but *C. glutamicum* has the capability to use methanol fortuitously as source of energy by its alcohol dehydrogenase (i.e., the initial step: conversion of methanol to formaldehyde). Thus, *C. glutamicum* and likely other ethanol-utilising *Corynebacterium* species possess an endogenous pathway for the complete oxidation of methanol to CO₂ [Witthoff *et al.*, 2013].

Apart from the *Corynebacterium*-affiliated phylotype OTU_{16S} 748, samples of the pH shift SIP experiment revealed the domination of a *Rhodanobacter*-related phylotype (OTU_{16S} 300; sequence identity 99 % (Table A 12)) in the heavy fractions of the *in situ* pH 4 treatments (Figure 59). *Rhodanobacter* species are also not reported as methanol-utilising species, but some strains might be highly adapted to acidic soil environments where they dominate the microbial community and perform denitrification even at pH 4 conditions [van den Heuvel *et al.*, 2010]. Only one entry in the nucleotide database is available for an *mxoF*-like sequence of a *Rhodanobacter* species (accession number EU194907), but no further information on methanol utilisation by *Rhodanobacter* species could be gained.

In summary, both phylotypes (OTU_{16S} 748 and OTU_{16S} 300) were highly abundant in both [^{12}C] and [^{13}C] 'heavy' fractions in the different SIP experiments. Thus, a labelling of these phylotypes was not likely and both phylotypes were considered as artificial and were excluded from further analyses.

RESULTS

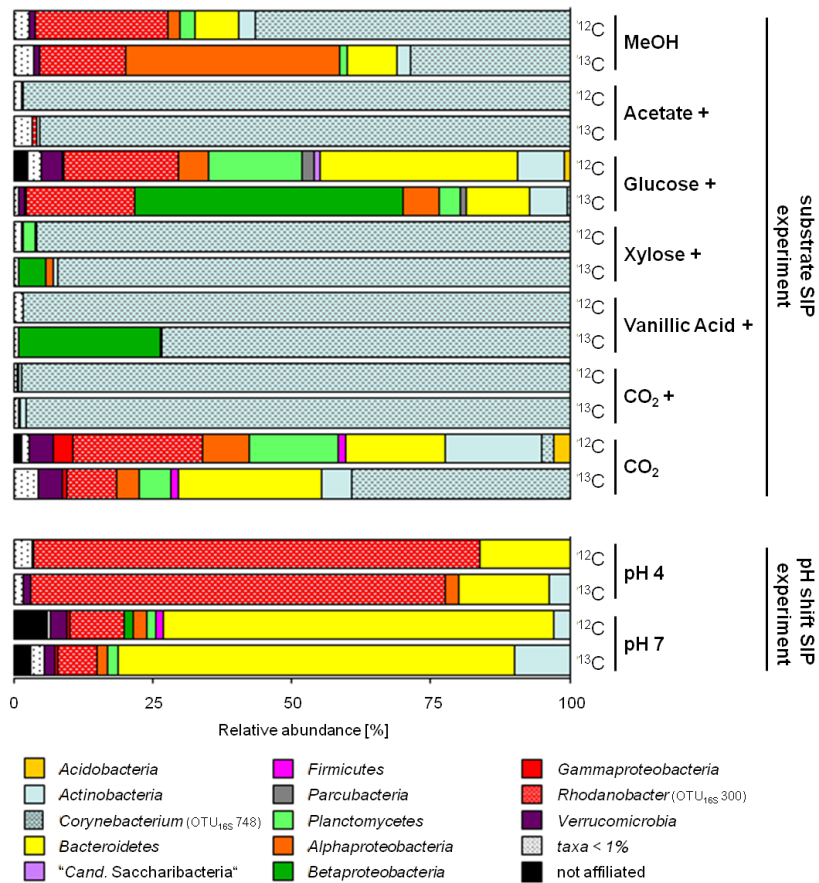


Figure 59 Bacterial phyla composition in 'heavy' fractions after different substrate or pH treatments based on all detected phylotypes.

Relative abundances ($\geq 1\%$) of bacterial phyla based on 16S rRNA gene sequences in 'heavy' fractions of [^{12}C]- and [^{13}C]-isotopologue treatments of both SIP experiments. Hatching indicates dominant families in 'heavy' fractions that were removed for the determination of labelled phylotypes. A cross indicates additional supplementation of methanol in substrate treatments. Phylotypes were clustered with 90.1% threshold for 16S rRNA genes (family-level) and phylogenetic affiliation was confirmed with a GenBank database. This figure has been published in Morawe *et al.* 2017.

3.7. Methanol-utilising microorganisms and their multi-carbon substrate range

The substrate SIP experiment under mixed substrate conditions (i.e., supplementation of [^{12}C]-methanol and [^{13}C]-isotopologues of a multi-carbon substrates) enabled the detection of methanol-utilisers (identified in the [$^{13}\text{C}_1$]-methanol treatment) in the alternative substrate treatments and might provided insights into the consumption habits of these microorganisms when multi-carbon substrates and methanol are simultaneously available.

3.7.1. Bacterial methylotrophs

In order to draw a more complete picture of all putative methanol-utilising bacteria, their abundance was analysed based on the bacterial marker gene 16S rRNA and the methylotrophic marker gene *mxoF*. However, a high competition for methanol, low abundance as well as no growth of some taxa, and an incomplete incorporation of ^{13}C into DNA might still mask methanol-utilisers in the soil. In addition, cross feeding effects (i.e., the assimilation of ^{13}C derived from formed $^{13}\text{CO}_2$, ^{13}C -enriched microbial debris or cell material) and thinning out effects (i.e., the simultaneously utilisation of labelled [^{13}C]-methanol and unlabelled endogenous substrates resulting in an incomplete labelling) should also be taken into account.

A successful 'labelling' of bacteria was assumed by the formation [^{13}C]- CO_2 (see 3.3). In addition, samples from 'heavy' fractions as well as from 'middle' fractions of [^{12}C]- and [^{13}C]-isotopologue treatments of each treatment were distinct to each other as revealed in the nMDS plot (Figure 60), indicating dissimilarities between the 'heavy' DNA samples of the different treatments.

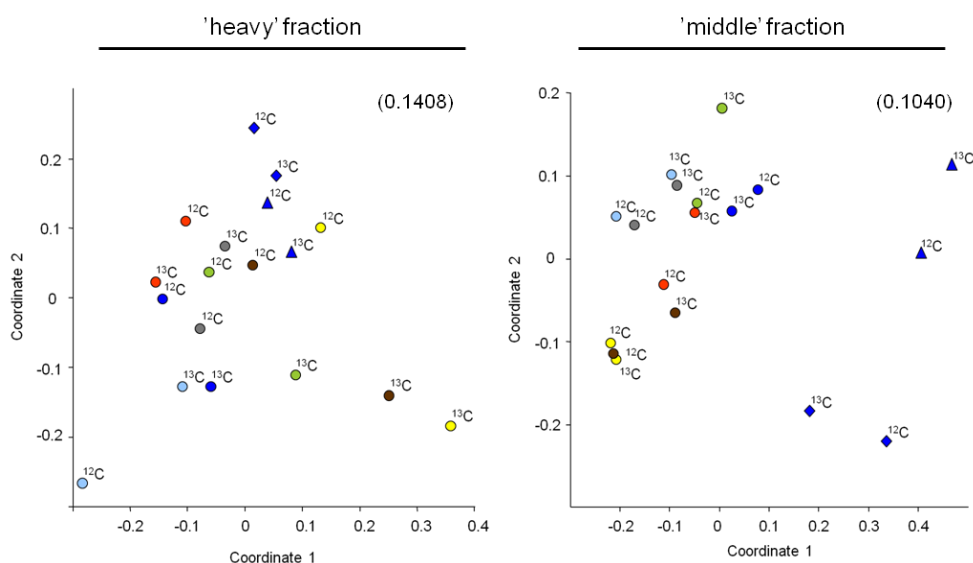


Figure 60 nMDS analyses of bacterial communities in 'heavy' and 'middle' fractions of both SIP experiments.

Analyses of relative abundances of all sequences in 'heavy' and 'middle' fractions of [^{12}C]- and [^{13}C]-treatments with cut-off values of 90.1% for bacteria (16S rRNA gene sequences, family-level; reduced data set, for detailed information see Materials and Methods). Stress values are given in brackets. All analyses are based on Bray-Curtis similarity index. Symbols according to SIP-experiment: ○, Substrate-SIP; ◇, pH 4; △, pH 7. ^{12}C indicates [^{12}C]-substrates and ^{13}C indicates [^{13}C]-isotopologue. Symbols according to supplemented [^{13}C]-isotopologue: ●, methanol; ●, acetate +; ●, glucose +; ●, xylose +; ●, vanillic acid +; ●, CO_2 +; ●, CO_2 (cross indicates additional supplementation of [^{12}C]-methanol in Substrate SIP experiment). This figure has been published in Morawe *et al.* 2017.

The number of phylotypes that were determined as labelled varies between the 'heavy' and 'middle' fractions of the different samples. Thus, a discriminative response and varying competitiveness for the given substrates was hypothesised and different taxa were expected

to be labelled by ^{13}C . In addition, the amount of labelled phylotypes showing labelling proportions $\geq 5\%$ was not identical to the total amount of detected labelled phylotypes, assuming a low assimilation of given substrates or a low abundance in general. Thus these weakly labelled phylotypes were defined to have only minor importance in the metabolic carbon flow of a certain substrate.

3.7.1.1. Methanol assimilating *Bacteria*

The analysis of [^{13}C]-methanol treatments revealed approximately 58 % of all detected phylotypes as labelled for the 'heavy' fraction and 17 % of all detected phylotypes as labelled for the 'middle' fraction. Interestingly, only OTU_{16S} 438 dominated the 'heavy' fraction and was affiliated to the family of *Beijerinckiaceae* (Figure 61A; Table A 14, Figure A 1; 98 % sequence identity to *Methylovirgula ligni*, (Table A 12)). This alphaproteobacterial family is well known for their methylotrophic members such as *Methylocella* and *Methylocapsa*, and seems to be ubiquitous in forest soil environments with a preference for acidic soils [Dedysh *et al.*, 2002; Dedysh *et al.*, 2005a; Marín & Arahal, 2013]. In addition, this *Beijerinckiaceae*-related phylotype was also highly labelled in the 'middle' fraction (i.e., an LP of 22 %) assuming also not fully labelled species as well as slower growing taxa that are not competitive for a faster uptake of [^{13}C]-methanol compared with other species of this family (Figure 61A; Table A 14).

Although the analysis of the phylogenetic composition of the responding community on methanol revealed *Gammaproteobacteria*, *Bacteroidetes* and *Actinobacteria* as dominant (see 3.5.1), no phylotype belonging to *Gammaproteobacteria* and *Bacteroidetes* was identified as labelled and only two phylotypes (i.e., OTU_{16S} 652 and OTU_{16S} 703) affiliated to *Actinobacteria* were labelled in 'middle' fractions (Figure 61A; Table A 14;

Figure A 5). Other phylotypes, which were labelled in the middle fractions and showing LPs $\geq 5\%$ were affiliated to *Verrucomicrobiales* (i.e., OTU_{16S} 18 with an LP of 20.5 %) and *Armatimonadetes* (i.e., *Fimbriimonadaceae*, OTU_{16S} 592 with an LP of 7.4 %) (Figure 61A; Table A 14; Figure A 8; Figure A 11). Sequence identities of these weakly labelled phylotypes to their next cultured hits ranged from 92 % to 94 % with an exception of the verrucomicrobial phylotype showing only 84 % sequence identity (Table A 12), suggesting hitherto unknown putatively methylotrophic bacteria in acidic forest soils.

Other phylotypes determined as putatively or weakly labelled (i.e., LP < 5 %) were affiliated to *Acetobacteraceae* (OTU_{16S} 467), *Methylophilaceae* (OTU_{16S} 360) and *Planctomycetes* (OTU_{16S} 836 and OTU_{16S} 968) (Figure 61A; Table A 14). For these taxa methylotrophic species are known or the potential for a C1-metabolism was proven [Urakiami *et al.*, 1989; Chistoserdova *et al.*, 2004; Greenberg *et al.*, 2006; Doronina *et al.*, 2013]. Sequence identities of these weakly labelled phylotypes to cultured organisms ranged from 94 % to

RESULTS

88 % (Table A 12, Figure A 1, Figure A 3, Figure A 10), suggesting also hitherto unknown methylotrophic organisms in this acidic forest soil sample.

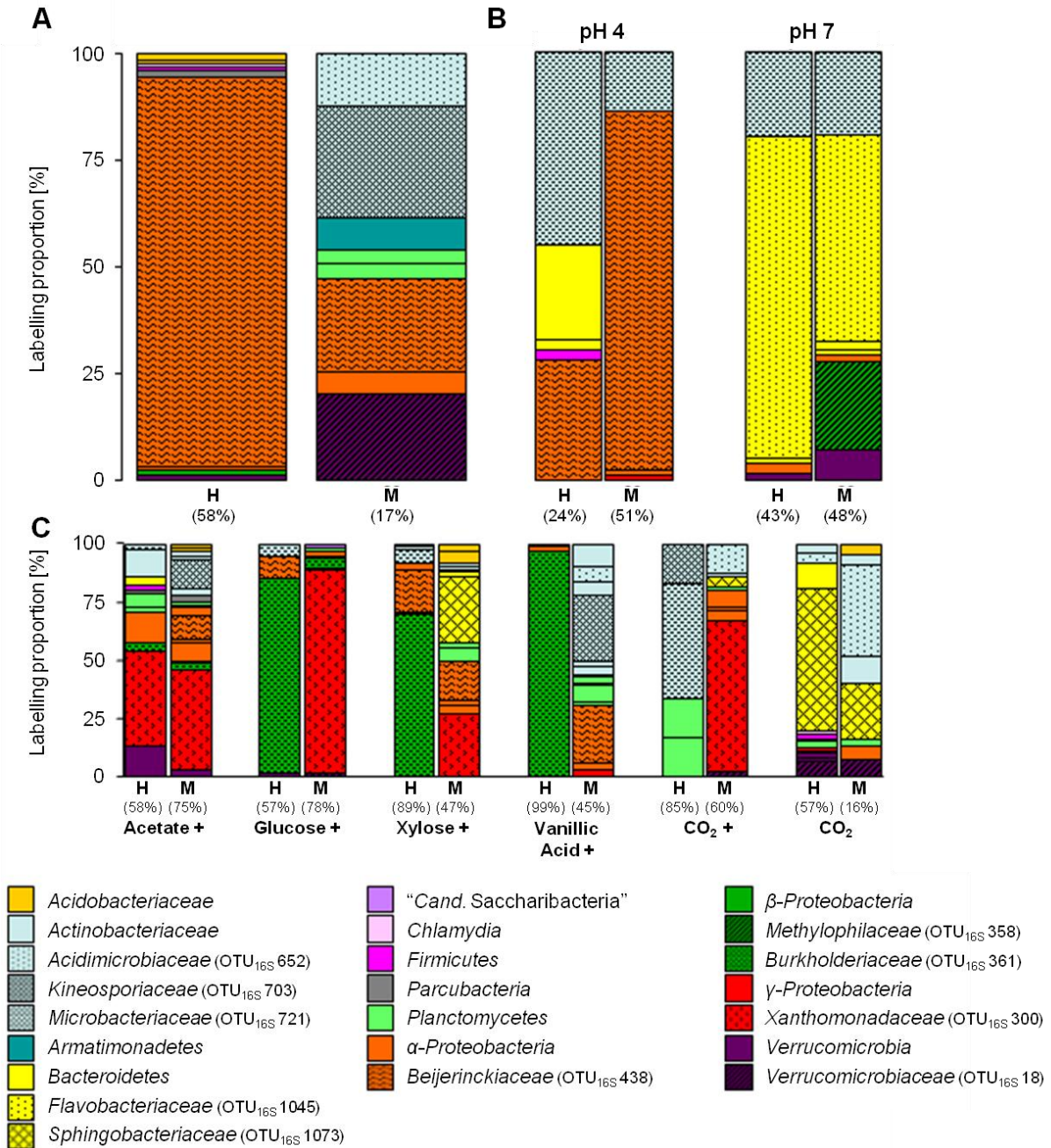


Figure 61 Labelled 16S rRNA phylotypes in 'heavy' and 'middle' fractions of different ¹³C-isotopologues treatments.

'Labelling proportions' ('LP') as indicator of relative importance of different bacterial taxa assimilating supplemented ¹³C-methanol (A) or ¹³C-isotopologues (C) in substrate SIP experiment as well as ¹³C-methanol at different pH conditions in pH SIP experiment (B). Additional ¹²C-methanol supplementation in substrate treatments is indicated by a cross. Phylogenetic affiliation is indicated by equal colours. 'H' and 'M' indicate 'heavy' and 'middle' fractions, respectively. Values in brackets indicate contribution of labelled OTUs to the total fraction. This figure has been published in Morawe *et al.* 2017.

3.7.1.2. Multi-carbon substrate assimilating *Bacteria*

The analysis of samples from the [$^{13}\text{C}_u$]-substrate treatments revealed a successful labelling of different taxa belonging to a wide range of heterotrophic bacterial phyla.

The highest number of labelled taxa was detected in [$^{13}\text{C}_2$]-acetate treatments. 58 % of all detected phylotypes in the 'heavy' fraction and 75 % of all detected phylotypes in the 'middle' fraction were determined as labelled. Within the 'heavy' fraction the highest LP was observed for a *Rhodanobacter*-affiliated phylotype (OTU_{16S} 300) with approximately 40 % LP, followed by a *Sphingomonas*-affiliated phylotype (OTU_{16S} 449), a *Spartobacteria*-affiliated phylotype (OTU_{16S} 6) and a *Corynebacterium*-affiliated phylotype (OTU_{16S} 752) with LPs around 11.5 % to 13.5 %. Within the 'middle' fraction a *Rhodanobacter*-affiliated phylotype (OTU_{16S} 300) still dominated the labelled community, followed by a *Kineosporiaceae*-affiliated phylotype (OTU_{16S} 703), a *Methylovirgula*-affiliated phylotype (OTU_{16S} 438) and an *Acetobacteraceae*-affiliated (OTU_{16S} 467). (Figure 61C; Table A 15)

Treatments with [$^{13}\text{C}_6$]-glucose resulted in a labelling of 57 % of all detected phylotypes in the 'heavy' fraction and 78 % of all detected phylotypes in the 'middle' fraction, whereas the incubation with [$^{13}\text{C}_5$]-xylose resulted in a labelling of 89 % of all detected phylotypes in the 'heavy' fraction and 47 % of all detected phylotypes in the 'middle' fraction. For both treatments with these sugars one phylotype (OTU_{16S} 361) affiliated to *Burkholderia* was dominant in the 'heavy' fractions, followed by the *Methylovirgula*-affiliated phylotype (OTU_{16S} 438). Additionally, a phylotype (OTU_{16S} 721) affiliated to the actinobacterial genus *Leifsonia* was determined as labelled in [$^{13}\text{C}_5$]-xylose treatments. The 'middle' fractions revealed the *Rhodanobacter*-affiliated phylotype (OTU_{16S} 300) as putatively labelled with xylose and glucose. For the xylose treatment also a *Mucilaginibacter*-affiliated phylotype (OTU_{16S} 1073), the *Methylovirgula*-affiliated phylotype (OTU_{16S} 438), an *Acidobacterium*-affiliated phylotype (OTU_{16S} 545) and a *Planctomycetales*-affiliated phylotype (OTU_{16S} 857) were indicated to be labelled. (Figure 61C; Table A 16, Table A 17)

The lowest number of labelled taxa was detected in [^{13}C]-vanillic acid treatments. Nearly all phylotypes (i.e., 99 %) in the 'heavy' fraction were identified as labelled and 45 % of all phylotypes in the 'middle' fraction were determined as labelled. In accordance with the sugar treatments the *Burkholderia*-affiliated phylotype (OTU_{16S} 361) was only highly labelled within the 'heavy' fraction (Figure 61C; Table A 18). Interestingly, in the 'middle' fraction 14 phylotypes were detected to be labelled in which 6 of them revealed LPs in the range of approximately 29 % to 5 %. The majority of these phylotypes were affiliated to *Actinobacteria* (i.e., OTU_{16S} 132, OTU_{16S} 652, OTU_{16S} 654 and OTU_{16S} 703), but also with *Methylovirgula* (OTU_{16S} 438) and *Planctomycetales* (OTU_{16S} 927) (Figure 61C; Table A 18).

Comparing the amount and phylogenetic affiliation of all labelled phylotypes of both [^{13}C]-CO₂ treatments, a higher number of labelled phylotypes in treatments without additional [^{12}C]-methanol is obvious. Treatments with [^{13}C]-CO₂ with additional [^{12}C]-methanol resulted in a labelling of 85 % of all detected phylotypes in 'heavy' fraction and 60 % of all detected

phylotypes in the 'middle' fraction, whereas the incubation with [¹³C]-CO₂ without additional [¹²C]-methanol resulted in labelling of 57 % of all detected phylotypes in 'heavy' fraction and only 16 % of all detected phylotypes in the 'middle' fraction (Figure 61C; Table A 19, Table A 20). In addition, the composition of labelled taxa is clearly different. In [¹³C]-CO₂ with additional [¹²C]-methanol *Actinobacteria*-affiliated phylotypes (OTU_{16S} 721 and OTU_{16S} 703) as well as *Planctomycetaceae*-affiliated phylotypes (OTU_{16S} 885 and OTU_{16S} 951) were highly labelled in 'heavy' fractions. 'Middle' fractions revealed a labelling of the *Rhodanobacter*-affiliated phylotype (OTU_{16S} 300), a *Caulobacter*-affiliated phylotype (OTU_{16S} 431) and the *Acidimicrobiaceae*-affiliated phylotype (OTU_{16S} 652) (Figure 61C; Table A 19). For [¹³C]-CO₂ treatments without additional [¹²C]-methanol a clear labelling of *Bacteroidetes*, in detail the *Mucilaginibacter*-affiliated phylotype (OTU_{16S} 1073) and a *Ferruginibacter*-affiliated phylotype (OTU_{16S} 1014) was obvious in 'heavy' fractions. Also OTU_{16S} 18 affiliated to *Verrucomicrobiales* was identified as labelled with an LP ≥ 5 % in 'heavy' fractions. The analysis of the 'middle' fraction revealed an additional labelling of phylotypes affiliated to *Actinobacteria* (OTU_{16S} 652 and OTU_{16S} 656) (Figure 61C; Table A 20).

3.7.1.3. Methanol-assimilating *Bacteria* under shifted pH conditions

As indicated by bacterial community analyses different pH conditions affected the microbial community (see 3.5.1) and thus, the indigenous methylophilic community determined as labelled was also expected to differ between incubations at *in situ* pH (i.e., pH 4) and incubations with a more neutral pH (i.e., pH 7).

The analysis of the [¹³C]-methanol treatments at pH 4 revealed weaker label efficiency compared to methanol samples from the substrate SIP experiment. 'Heavy' fractions revealed approximately 24 % of all detected phylotypes as labelled and in the 'middle' fraction approximately 51 % of all detected phylotypes were labelled. Interestingly, the *Methylovirgula*-affiliated phylotype (OTU_{16S} 438) that was highly labelled in the methanol treatment of the substrate SIP experiment was not the dominantly labelled phylotype in the 'heavy' fraction of the methanol treatment of the pH shift SIP experiment (Figure 61B; Table A 21). The most dominantly labelled phylotype was the actinobacterial *Leifsonia*-affiliated phylotype (OTU_{16S} 721) that was not detectable in methanol treatments of the substrate SIP experiment. Another phylotype also undetectable in methanol treatments of the substrate SIP experiment, but identified as labelled in pH shift SIP experiment at pH 4 was a *Chitinophaga*-affiliated phylotype (OTU_{16S} 1020). The analysis of the 'middle' fraction of the pH 4 methanol treatment revealed the *Methylovirgula*-affiliated phylotype (OTU_{16S} 438) as the most dominant phylotype, indicating a slower labelling of these taxa compared to methanol treatments of the substrate SIP experiment. (Figure 61B; Table A 21)

The analysis of the [¹³C]-methanol treatments at pH 7 revealed approximately 43 % of all detected phylotypes as labelled in the 'heavy' fraction, and approximately 48 % of all detected phylotypes in the 'middle' fraction were determined as labelled (Figure 61B; Table A

22). In accordance with the increasing amount of *Bacteroidetes* in pH 7 treatments (see 3.5.1, Figure 48) labelled phylotypes of both fractions were dominated by the *Chryseobacterium*-affiliated phylotype (OTU_{16S} 1045) that showed LPs of 75 % and 48 % for 'heavy' and 'middle' fractions, respectively (Figure 61B; Table A 22). The *Leifsonia*-affiliated phylotype (OTU_{16S} 721) was also identified as labelled at pH 7 in both fractions with lower LPs in the 'heavy' fraction compared to the 'heavy' fraction of the pH 4 treatment, indicating an advantageous effect of a more acidic pH for this taxon. Analysis of the 'middle' fraction of the pH 7 treatment revealed also a *Methylophilus*-affiliated phylotype (OTU_{16S} 358) and with lower LPs the verrucomicrobial *Terrimicrobium*-affiliated phylotype (OTU_{16S} 54) as labelled.

3.7.1.4. Comparative analysis and identification of putative facultatively methylotrophic bacteria

Several methylotrophic organisms are not only restricted to C1 compounds like methanol. These microorganisms are facultatively methylotrophic and are known to utilise different multi-carbon compounds [Anthony, 1982; Chistoserdova *et al.*, 2009; Semrau *et al.*, 2011; Kolb & Stacheter, 2013]. The availability of complete genomes as well as diverse metagenomic studies in various environments revealed a hitherto unknown methylotrophic potential of different organisms [Kaneko *et al.*, 2002; Greenberg *et al.*, 2006; Giovannoni *et al.*, 2008; Chistoserdova *et al.*, 2009; Halsey *et al.*, 2012]. Previous studies addressing methylotrophic organisms used typical C1 compounds such as methane or methanol as substrates and thus were not able to draw any conclusion about a broader substrate range of the detected methylotrophs. In addition, descriptions of new methylotrophic species include growth studies with a certain range of possible substrates utilised, but nonetheless these studies provide only hints for *in situ* relevant situations. The objective of the comparative SIP was to detect methylotrophs by identifying labelled phylotypes in a methanol-treated sample and estimate the potential substrate range of these identified methylotrophs by re-detecting the same phylotypes as labelled in multi-carbon substrate treatments.

In general, mainly the *Beijerinckiaceae*-affiliated phylotype (OTU_{16S} 438) was identified as the dominant methylotrophic taxon in the acidic forest soil sample (see 3.7.1.3) when samples were incubated with methanol. Several facultatively methylotrophic species are known for this family in which most cultivated species show only a narrow substrate range. Acetate is utilised by the majority of all cultured facultatively methylotrophic *Beijerinckiaceae* [Dunfield *et al.*, 2010; Dunfield *et al.*, 2003] and only *Methylorosula polaris* and *Beijerinckia mobilis* possess the ability to utilise sugars and polysaccharides [Berestovskaya *et al.*, 2012; Dedysh *et al.*, 2005b]. Interestingly, in all treatments of the substrate SIP experiment with multi-carbon compounds the *Beijerinckiaceae*-related phylotype was also identified as labelled in 'heavy' or 'middle' fractions indicating that the taxa comprised by OTU_{16S} 438 possess the ability to assimilate acetate, sugars and aromatic compounds in the presence of methanol since [¹²C]-methanol was always supplemented (Figure 62). The labelling was not as efficient

as it was observed for methanol indicated by lower LPs and a detected labelling in ‘middle’ fractions (Table A 15 – Table A 18). Thus, a higher competition or slower growth rates on multi-carbon substrates were suggested. Incorporation of [¹³C]-carbon via [¹³C]-CO₂ and thus a cross feeding effect was negligible, since the phylotype OTU_{16S} 438 was not identified as labelled in both CO₂ treatments (Figure 61C & Figure 62, Table A 19, Table A 20).

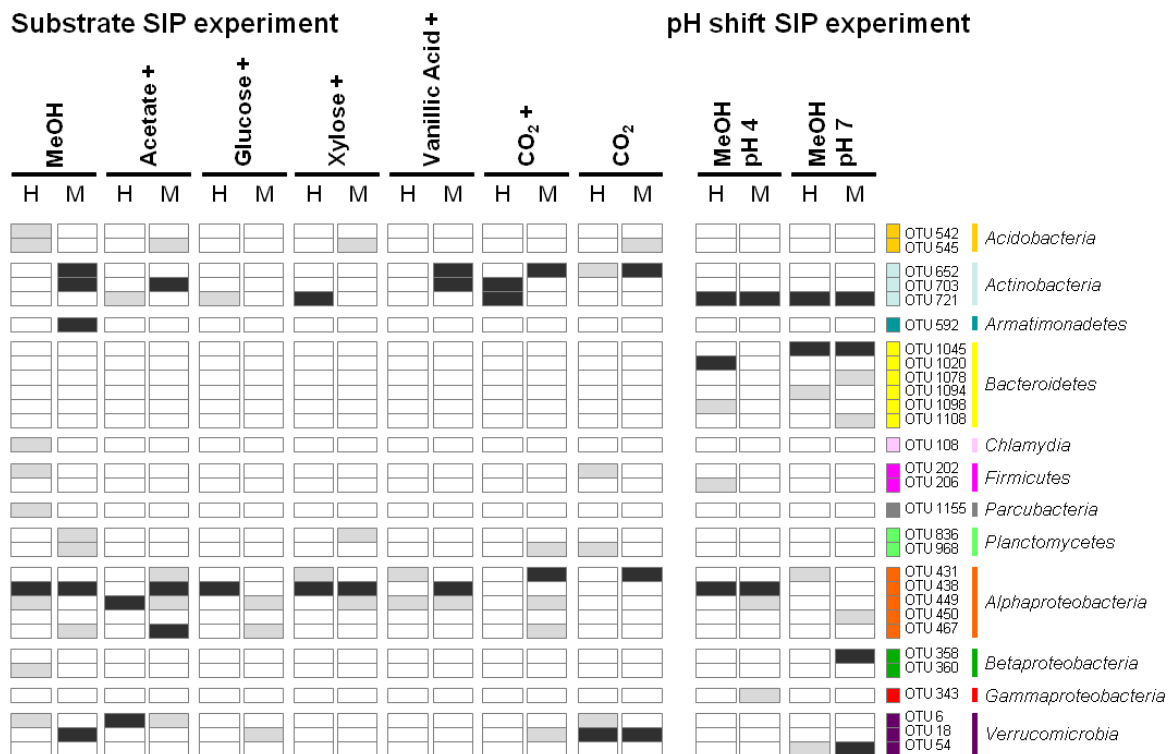


Figure 62 Congruently labelled bacterial phylotypes in treatments of both SIP experiments.

Labelled phylotypes (OTUs) in methanol treatments as well as the consistent presence of these phylotypes in the substrate SIP and pH shift SIP experiments (‘LP’ > 5 %, black; ‘LP’ < 5 %, grey). Phylotypes that are only labelled in treatments with multi-carbon substrates are not considered. Additional [¹²C]-methanol supplementation in the substrate SIP experiment is indicated by a cross. Phylogenetic affiliation is indicated by equal colours. ‘H’ and ‘M’ indicate ‘heavy’ and ‘middle’ fraction, respectively. This figure has been published in Morawe *et al.* 2017.

In order to resolve the putative trophic types that are comprised by the detected *Beijerinckiaceae*-affiliated phylotype the taxon OTU_{16S} 438 was further analysed on a species level cut-off value. Nine different phylotypes (A to I) were identified, that revealed three different trophic types including obligately methylotrophic (phylotype A, B and D), restricted facultatively methylotrophic (phylotype C) and chemoorganotrophic taxa (phylotype E, F, G, H) (see Table 36). All methylotrophic phylotypes (A - D) are affiliated to methylotrophic *Beijerinckiaceae* and the restricted facultatively methylotrophic phylotype C clustered next to *Methylocella* (see Figure A 2), emphasising that acetate was assimilated by a *Beijerinckiaceae*-phylotype affiliated to facultatively methylotrophic representatives. Although

for the family-level phylotype OTU_{16S} 438 CO₂ assimilation was not assumed, phylotype I was only detected in the treatments with CO₂ and methanol indicating that CO₂ was assimilated by this taxon, which seems affiliated to *Bradyrhizobiaceae* (see Figure A 2). The chemoorganotrophic taxa are affiliated to *Bradyrhizobiaceae* (phylotype E), *Hyphomicrobiaceae* (phylotype F & H), and *Roseiarcus fermentans* (phylotype G) (see Figure A 2) and are further distinguishable in taxa with a wide substrate range (phylotype E, F, G) including sugars, acetate and vanillic acid and a narrow substrate range (phylotype H) restricted to glucose. It is worth to mention that for the chemoorganotrophic phylotypes the utilisation of methanol is not verified, but is also not excluded, since SIP analysis are unable to resolve the dissimilatory utilisation of methanol that might have occurred. Nevertheless, the detected *Beijerinckiaceae*-affiliated taxon seems to be clearly distinguishable in taxa that are preferring methanol assimilation or multi-carbon compound assimilation, wherefore the substrate range – C1 and multi-carbon compounds – is one defining factors for their different ecological niches.

Table 36 Putative trophic types comprised by the *Beijerinckiaceae*-phylotype.

The resolution was done at species level. The 'X' means that the taxon was detected in the corresponding fraction ('H', 'heavy' fraction or 'M', 'middle' fraction)

phylotype	substrate SIP experiment												pH shift ^a				
	MeOH		Ace +		Glu +		Xyl +		Van +		CO ₂ +		CO ₂		pH4 ^b		
	H	M	H	M	H	M	H	M	H	M	H	M	H	M	H	M	
obligately methylophilic																	
A	X																X
D	X																
B	X	X															X X
restricted facultatively methylophilic																	
C	X			X													
chemoorganotrophic																	
E				X				X		X							
F				X		X				X							
G				X		X	X			X							
H				X		X	X			X							
'autotrophic'																	
I										X							

^a Abbreviation for the pH shift SIP experiment.

^b Cross indicates [¹²C]-methanol supplementation. 'H' and 'M' indicate 'heavy' and 'middle' fraction, respectively.

^c [¹³C₁]-methanol was supplemented

Another alphaproteobacterial phylotype that was putatively labelled in the methanol incubation as well as in the substrate incubations was the *Sphingomonas*-affiliated phylotype OTU_{16S} 449 with a broader substrate range including acetate, sugars and vanillic acid. The *Acetobacteraceae*-affiliated phylotype OTU_{16S} 467 that was also labelled in methanol treatments revealed a narrow substrate range including acetate and glucose (Figure 62). The actinobacterial phylotypes OTU_{16S} 652 (*Acidimicrobiaceae*-affiliated) and OTU_{16S} 703 (*Kineosporiaceae*-affiliated) were detected as labelled in the 'middle' fraction of the methanol

treatment indicating a delayed labelling. Both phylotypes were also detected in 'middle' fractions of vanillic acid treatments. The phylotype OTU_{16S} 703 was also labelled in 'middle' fraction of the acetate treatment. These delayed labelling could be explained by slow growth, utilisation of endogenous C-sources or cross feeding effects which could not be excluded, since both phylotypes were also identified as labelled in both CO₂ incubations (Figure 62). The verrucomicrobial phylotypes OTU_{16S} 6 and OTU_{16S} 18 labelled in methanol treatments were also labelled in treatments with acetate (i.e., for OTU_{16S} 6) and glucose (i.e., OTU_{16S} 18) and thus showed the ability to utilise multi-carbon substrates (Figure 62). In addition, both phylotypes were also detected as labelled in both CO₂ incubations not excluding cross feeding effects.

Interestingly, phylotypes that were only labelled in the pH 7 treatments were not detected as labelled in any treatment with the *in situ* pH 4. These phylotypes were affiliated to *Bacteroidetes* (i.e., OTU_{16S} 1045, OTU_{16S} 1078, OTU_{16S} 1094, and OTU_{16S} 1108), and the genera *Paracoccus* (OTU_{16S} 450), *Methylophilus* (OTU_{16S} 358) and *Terrimicrobium* (OTU_{16S} 54) assuming an inhibitory effect of a more acidic pH and thus no utilisation of any multi-carbon substrate at lowered pH. Only the *Leifsonia*-affiliated phylotype OTU_{16S} 721 that was labelled in both pH shift SIP experiment samples was also labelled in the acetate, glucose and xylose treatments as well as in the CO₂ with methanol treatment of substrate SIP experiment, suggesting a broader substrate range including acetate, sugars and CO₂ (Figure 62).

3.7.2. *mxoF*-possessing methylotrophs

Since a labelling of different taxa was detected for the 16S rRNA gene sequence based analyses (see 3.7.1), also a labelling for *mxoF*-derived sequences was assumed. Indeed the number of phylotypes that were determined as labelled varied between the 'heavy' and 'middle' fractions of the different samples indicating again discriminative response and varying competitiveness for the given substrates.

3.7.2.1. Methanol-assimilating methylotrophs

The analysis of the [¹³C]-methanol treatment of the substrate SIP experiment revealed that almost all phylotypes (i.e., approximately 97 %) of the 'heavy' fraction and approximately 43 % of all phylotypes from the 'middle' fraction were determined as labelled (Figure 63A; Table A 23). The 'heavy' fraction was dominated by three phylotypes that showed LPs ≥ 20 % and were affiliated to *Methylobacterium* (OTU_{*mxoF*} 40) and *Hyphomicrobium* (OTU_{*mxoF*} 185 and OTU_{*mxoF*} 210). Although the analysis of 16S rRNA gene sequences revealed *Beijerinckiaceae* as the dominantly labelled bacterial taxon only the *Beijerinckiaceae*-affiliated phylotype OTU_{*mxoF*} 144 was noticeable with an LP of approximately 9.7 % (Figure 63A; Table A 23). Though the number of potentially labelled

taxa in the 'middle' fraction was higher than in the 'heavy' fraction the majority of these phylotypes showed LPs < 5 % and thus their labelling is of minor interest.

3.7.2.2. Multi-carbon substrate-assimilating methylophs

The treatments of the substrate SIP experiment revealed that almost all detected phylotypes (i.e., 97 % to 100 %) in all individual 'heavy' fractions were identified as labelled. In contrast, the 'middle' fractions were not as clear as the 'heavy' fractions, showing only 14 % (for acetate treated samples) up to 73 % (for vanillic acid treated samples) of all detected phylotypes as labelled (Figure 63A; Table A 24 – Table A 27). Interestingly, all substrate treatments revealed only a rare labelling of *Methylobacterium*-affiliated phylotypes in their 'heavy' fractions with one exception (i.e., glucose-treated samples) (Figure 63A).

The analysis of the 'heavy' fraction of the [¹³C₂]-acetate treatment showed OTU_{mx_aF} 185 as highly labelled with an LP of approximately 51 % followed by OTU_{mx_aF} 236 that was also *Hyphomicrobium*-affiliated. In addition, the *Methylobacterium*-affiliated phylotype OTU_{mx_aF} 9 and *Beijerinckiaceae*-affiliated phylotype OTU_{mx_aF} 340 showed LPs of approximately 12 % and approximately 7 %, respectively (Table A 24).

The 'heavy' fraction of [¹³C₆]-glucose treatment revealed a singularity (Figure 63A; Table A 25). The only labelled phylotypes were affiliated to *Methylocystaceae* (OTU_{mx_aF} 137) and *Beijerinckiaceae* (OTU_{mx_aF} 340) and were highly labelled indicated by their LPs of approximately 50 % for each (Table A 25). Though the analysis of 16S rRNA gene sequences revealed *Beijerinckiaceae* as labelled in the 'heavy' fraction of the glucose treatment (see 3.7.1.2 & 3.7.1.4) no *Methylocystaceae*-affiliated phylotypes were detected neither in [¹²C]- nor in [¹³C]-glucose treatments (Table A 25). The analysis of the 'middle' fraction revealed again phylotypes affiliated to *Methylobacterium* and *Hyphomicrobium* as delayed labelled.

In the 'heavy' fraction of the [¹³C₅]-xylose treatment the *Methylobacterium*-affiliated phylotype OTU_{mx_aF} 55 was the only labelled taxon with an LP of 98.5 % (Table A 26). The analysis of the 'middle' fraction of the [¹³C₅]-xylose treatment revealed other phylotypes affiliated to *Hyphomicrobium* as labelled whereas only OTU_{mx_aF} 185 revealed a high LP of 50 % (Table A 26).

For the [¹³C₁₋₆]-vanillic acid treatment the only labelled phylotypes in the 'heavy' fraction were affiliated to *Hyphomicrobium* with a domination of OTU_{mx_aF} 210 (i.e., LP of approximately 61.5 %), followed by OTU_{mx_aF} 298 and OTU_{mx_aF} 185. The 'middle' fraction revealed a delayed labelling of *Methylobacterium*-affiliated phylotypes (Table A 27).

The majority of all detected phylotypes in 'heavy' fractions of both CO₂ incubations were determined as labelled. The CO₂ incubation with additional [¹²C]-methanol revealed approximately 58 %, and solely CO₂ incubation revealed approximately 85 % of all detected phylotypes as labelled in 'middle' fractions (Figure 63A, Table A 28, Table A 29). Both CO₂

treatments presented *Hyphomicrobium*-affiliated phylotypes as labelled but they were not identical in each 'heavy' fraction.

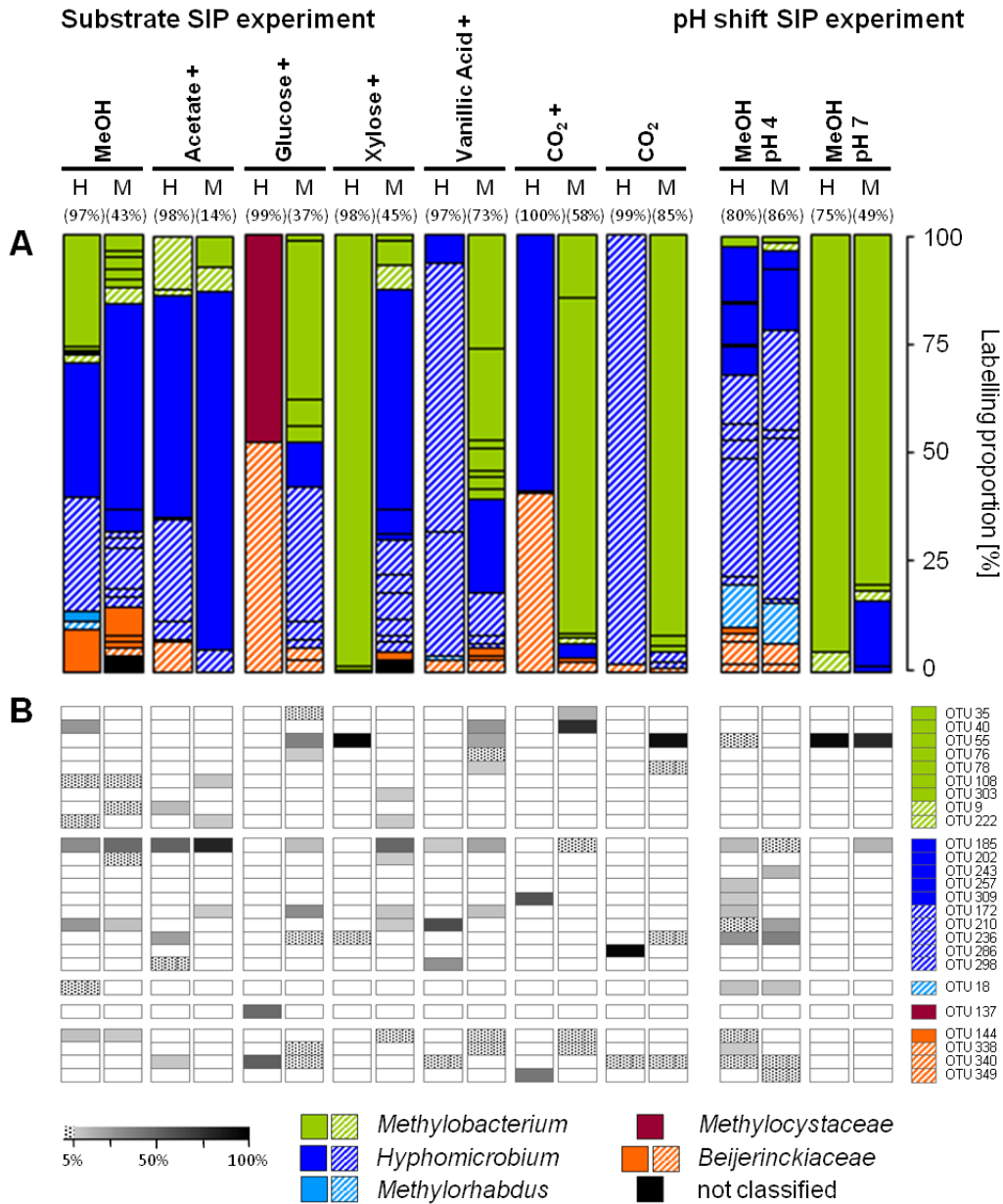


Figure 63 Labelled *mxoF* phylotypes in 'heavy' and 'middle' fractions of different [¹³C]-isotopologues treatments.

Overview on the composition of all labelled *mxoF* phylotypes depending on substrates or pH (A) as well as the consistent presence of phylotypes ('LP' > 5 %, greyish; 'LP' < 5 %, dotted) (B) in heavy ('H') and middle ('M') fractions. 'LPs' serve as indicator of the influence of supplemented [¹³C]-isotopologues on *mxoF* possessing methylotrophs after different treatments in both SIP experiments. Additional [¹²C]-methanol supplementation in the substrate SIP experiment is indicated by a cross. Phylogenetic affiliation is indicated by equal colours; ambiguous affiliation (i.e., sequence identity with BLASTn < 90 % as well as ambiguous position in phylogenetic tree) is indicated by shading. Values in brackets indicate contribution of labelled OTUs to the total fraction. This figure has been published in Morawe *et al.* 2017.

For CO₂ with additional [¹²C]-methanol also a *Beijerinckiaceae*-affiliated phylotype was identified as labelled in the 'heavy' fraction (Figure 63A, Table A 28, Table A 29). Some

Beijerinckiaceae such as *Methyloferula stellata* [Vorobev *et al.*, 2011], *Methylorosula polaris* [Berestovskaya *et al.*, 2012] and *Methylovirgula ligni* [Vorob'ev *et al.*, 2009] are known to harbour enzymes for the ribulose biphosphate pathway and thus are able to assimilate CO₂ as well. The 'middle' fractions of both CO₂ treatment approaches revealed *Methylobacterium*-affiliated phylotypes that were not identical in the different treatments as labelled with LPs between approximately 14 % and 92 % (Figure 63A, Table A 28, Table A 29).

3.7.2.3. Methanol-assimilating methylotrophs under shifted pH conditions

Since the community analysis of *mxoF*-possessing bacteria (see 3.5.2.3) as well as the identification of various labelled bacterial taxa (see 3.7.1.3) in the pH shift SIP experiment treatments revealed differences in responding taxa on changed pH conditions, a varying labelling pattern for *mxoF* was deductively expected. The numbers of potentially labelled taxa were not comparable between pH 4 and pH 7 treatments with lower counts for pH 7. In accordance to this observation only the *Methylobacterium*-affiliated phylotype OTU_{*mxoF*} 55 was labelled in the 'heavy' fractions of the pH 7 treatment, and the analysis of the 'middle' fraction revealed only one additional phylotype (*Hyphomicrobium*-affiliated OTU_{*mxoF*} 185) as delayed labelled with an LP of 14.7 % (Figure 63A, Table A 31). In contrast to the pH 7 treatment the 'heavy' fractions of the pH 4 treatment showed five *Hyphomicrobium*-affiliated phylotypes as labelled with LPs ranging from 27 % to 6.5 % (Figure 63A, Table A 30). In addition, a *Beijerinckiaceae*-affiliated phylotype (OTU_{*mxoF*} 338) and *Methylorhabdus*-affiliated phylotype (OTU_{*mxoF*} 18) were labelled in the 'heavy' fraction. The analysis of the 'middle' fraction revealed again a labelling for *Hyphomicrobium*-affiliated and *Beijerinckiaceae*-affiliated phylotypes (Figure 63A, Table A 30).

In comparison with the methanol treatment of the substrate SIP experiment the number of *Hyphomicrobium*-affiliated phylotypes was higher in the pH shift SIP experiment and the identified phylotypes were not identical. Also the *Beijerinckiaceae*-affiliated phylotypes were not identical. In addition, the *Methylorhabdus*-affiliated phylotypes revealed only in the pH shift SIP experiment an LP ≥ 5 %. The major difference between both methanol treatments at the *in situ* pH 4 was due to the detection of one *Methylobacterium*-affiliated phylotype identified as labelled in the methanol incubation of substrate SIP experiment (Figure 63A, Table A 23, Table A 30).

3.7.2.4. Comparative analysis and identification of facultative methylotrophs

The labelling pattern of all *mxoF*-derived phylotypes in all incubations of both SIP experiments revealed besides dissimilarities also congruence (Figure 63B). None of the four labelled phylotypes with an LP ≥ 5 % in the methanol treatment of the substrate SIP experiment occurred exclusively in this treatment. The *Methylobacterium*-affiliated phylotype (OTU_{*mxoF*} 40) was also labelled with LPs ≥ 5 % in the 'middle' fraction of the treatment with CO₂ with

additional methanol, indicating a preference for methanol but also a possibility of carbon assimilation via CO₂ for the species comprising this phylotype (Figure 63B, Table A 23, Table A 28). Both *Hyphomicrobium*-affiliated phylotypes (OTU_{mx_aF} 185 and OTU_{mx_aF} 210) were also labelled in [¹³C₀]-substrate treatments. In detail, OTU_{mx_aF} 185 was in both fractions (i.e., 'heavy' and 'middle') of methanol and acetate treatments the dominantly labelled phylotype, indicating an intense assimilation of these substrates (Figure 63B, Table A 23, Table A 24). The same phylotype was also identified as labelled in both fractions of the vanillic acid treatment with lower LPs, suggesting a delayed assimilation of this aromatic compound in the presence of methanol (Figure 63B, Table A 27). In the sugar treatments OTU_{mx_aF} 185 was identified as labelled in the 'middle' fractions only (Figure 63B, Table A 25, Table A 26), which indicated a delayed labelling of this taxon, and thus a preference for methanol assimilation was suspected. The LP of OTU_{mx_aF} 185 was higher in the [¹³C₅]-xylose treatment compared to the [¹³C₆]-glucose treatment, suggesting a preference for xylose or a higher competition for glucose (Figure 63B, Table A 25, Table A 26). OTU_{mx_aF} 185 was also detected in both incubations of the pH shift SIP experiment with lower LPs compared to the methanol treatment of the substrate SIP experiment (Figure 63B, Table A 30, Table A 31, Table A 23). In addition, OTU_{mx_aF} 185 was labelled in the 'middle' fraction of the pH 7 treatment. Thus, a preference for acidic conditions was assumable. The other *Hyphomicrobium*-affiliated phylotype (OTU_{mx_aF} 210) labelled in the methanol treatment was also determined as labelled in [¹³C₅]-xylose and [¹³C₁₋₆]-vanillic acid treatments (Figure 63B, Table A 26, Table A 27). Interestingly, the LP in the vanillic acid treatment was enormous compared to the methanol treatment, suggesting a preferred assimilation of aromatic compound-derived carbon or a higher competition for methanol in the methanol treatment (Figure 63B, Table A 23, Table A 27). The phylotype OTU_{mx_aF} 210 was not detectable in the methanol treatment at pH 7 but at both treatments with *in situ* pH, emphasising a preference for acidic conditions (Figure 63B, Table A 23, Table A 30, Table A 31). The last phylotype with an LP ≥ 5 % in the methanol treatment of the substrate SIP experiment was the *Beijerinckiaceae*-affiliated phylotype OTU_{mx_aF} 144. In treatments with xylose, vanillic acid and CO₂ with additional methanol this phylotype (OTU_{mx_aF} 144) was also detected as labelled but with LPs < 5 % (Figure 63B, Table A 26, Table A 27, Table A 28). In addition, the labelling was detected in the 'middle' fractions only, indicating a preference or a need for methanol. Slower growth on multi-carbon substrates could be assumed and putative cross feeding effects were not excluded.

The other methanol treatment at pH 4 (from the pH SIP experiment) revealed three other *Hyphomicrobium*-affiliated phylotypes (OTU_{mx_aF} 309, OTU_{mx_aF} 172, and OTU_{mx_aF} 236) additionally as labelled with [¹³C]-methanol (Figure 63B, Table A 30). OTU_{mx_aF} 309 was also identified as labelled in treatments with CO₂ with additional methanol, indicating a potential of assimilating CO₂ in the presence of methanol (Figure 63B, Table A 28, Table A 29). OTU_{mx_aF} 172 was also identified as labelled in all 'middle' fractions of treatments with acetate, sugars and vanillic acid (Figure 63B, Table A 24 - Table A 27), indicating a delayed labelling

and thus assuming a preference for methanol. OTU_{*mx*aF} 236 was also identified as labelled in the 'heavy' fraction of the acetate treatment and in different fractions of the sugar treatments (Figure 63B). The LP in the acetate treatment was almost equal compared to the methanol treatment (Table A 24, Table A 30) and below 5 % in the sugar treatments, assuming a preference for acetate than sugars or a higher competitiveness in terms of acetate (Table A 25, Table A 26).

The methanol treatment at pH 7 revealed the phylotype OTU_{*mx*aF} 55 affiliated to *Methylobacterium* as highly labelled (Figure 63, Table A 31). OTU_{*mx*aF} 55 was also detectable as labelled in the 'heavy' fraction of xylose treatment and in 'middle' fractions of treatments with glucose, vanillic acid and CO₂ (Figure 63B, Table A 25 - Table A 27). Minor amounts of OTU_{*mx*aF} 55 were also detected as labelled at pH 4 but the LP was < 5 % (Figure 63B, Table A 30). Thus, a preference for more neutral pH conditions of taxa composing this phylotype is assumed as well as facultative methylotrophy.

Apart from *mx*aF-phylotypes that were identified as labelled in methanol treatments, some phylotypes were only determined as labelled in substrate treatments (Figure 63B). These phylotypes were mainly affiliated to *Methylobacterium* (i.e., OTU_{*mx*aF} 35, OTU_{*mx*aF} 76, OTU_{*mx*aF} 78, and OTU_{*mx*aF} 303) and *Hyphomicrobium* (i.e., OTU_{*mx*aF} 286 and OTU_{*mx*aF} 298). Although *mx*aF is a well studied marker gene for the methanol dehydrogenase and methylotrophic microorganisms [McDonald & Murrell, 1997] the ability to assimilate methanol is not clearly proven by possessing this gene. Taxa composing these phylotypes could be assumed to grow only poor or very slow on methanol as it was demonstrated for some *Methylobacterium* species [Kelly *et al.*, 2013]. In addition, within the *Methylobacteriaceae* a huge variability of sequence similarity was shown. Similarity analysis of *mx*aF-sequences of certain *Methylobacteriaceae* revealed higher similarities to taxa such as *Mucilaginibacter* and *Flavisolibacter* (both *Bacteroidetes*), *Pseudomonas* (*Gammaproetobacteria*) or *Methylophilus* (*Betaproteobacteria*) than to other *Methylobacteriaceae* species [Kelly *et al.*, 2013]. Thus, the assumption of transferring *mx*aF-genes via the exchange of genetic material like horizontal gene transfer is emphasised. This increases the likelihood to receive *mx*aF accidentally without further metabolic advantage for the recipient, and thus a preferred utilisation of multi-carbon source by these recipients is conceivable.

3.7.3. Fungal methylotrophs

The role of fungal species in the methylotrophic community within a forest soil is not well resolved and most fungal organisms known to be methylotrophic belong to the diverse group of yeasts [Kolb & Stacheter, 2013]. Thus, also the diversity of fungal taxa and especially the assimilation of [¹³C]-carbon was targeted.

As it was observed for bacteria (see 3.7.1 & 3.7.2) a successful 'labelling' of fungi is assumed as samples from 'heavy' fractions as well as from 'middle' fractions of [¹²C]- and

[$^{13}\text{C}_u$]-substrate treatments of each treatment were distinct to each other as revealed in the nMDS plot (Figure 64) indicating dissimilarities between the ‘heavy’ DNA samples.

The number of labelled phylotypes varied between the ‘heavy’ and ‘middle’ fractions of the different samples. Thus, also varying response on the different [^{13}C]-isotopologues was suggested. As it was reported for bacteria (see 3.7.1) the amount of labelled phylotypes showing LPs $\geq 5\%$ was not identical with the total amount of detected labelled phylotypes. Thus, a low assimilation of given substrates or a low abundance of these taxa in general was assumed resulting in a weak labelling of these taxa. These weak labelled phylotypes were defined to have only minor importance to the metabolic carbon flow.

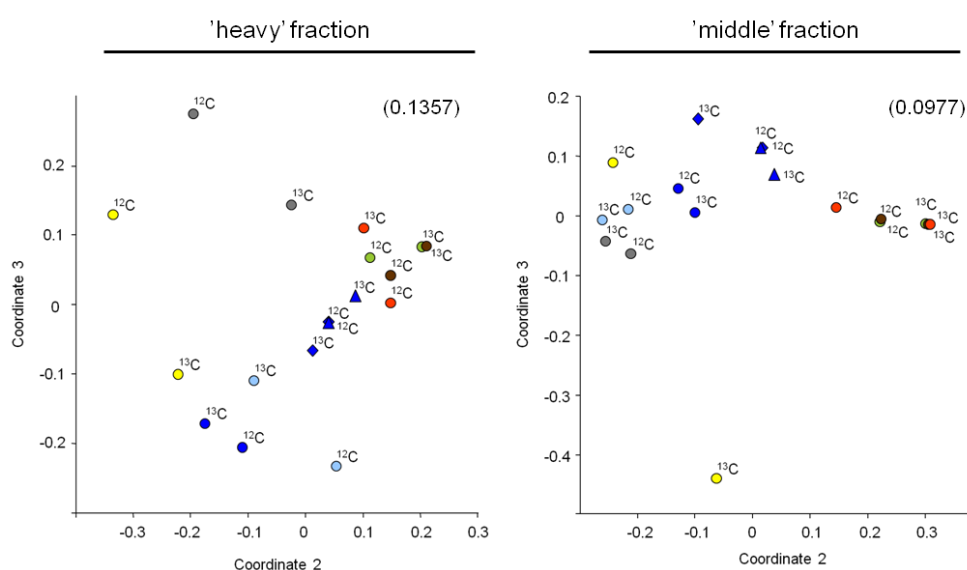


Figure 64 nMDS analyses of fungal communities in ‘heavy’ and ‘middle’ fractions of both SIP experiments.

Analyses of the relative abundances of all sequences in ‘heavy’ and ‘middle’ fractions of [^{12}C]- and [^{13}C]-isotopologue treatments with cut-off values of 97% for fungi (ITS gene sequences species-level). Stress values are given in brackets. All analyses are based on Bray-Curtis similarity index. Symbols according to SIP-experiment: ○, Substrate-SIP; ◇, pH 4; △, pH 7. ^{12}C indicates [^{12}C]-isotopologue and ^{13}C indicates [^{13}C]-isotopologue. Symbols according to supplemented [^{13}C]-isotopologue: ●, methanol; ●, acetate +; ●, glucose +; ●, xylose +; ●, vanillic acid +; ●, CO_2 +; ●, CO_2 (cross, additional supplementation of [^{12}C]-methanol in substrate SIP experiment). This figure has been published in Morawe *et al.* 2017.

3.7.3.1. Methanol-assimilating fungi

The analysis of the ‘heavy’ fraction of the [$^{13}\text{C}_1$]-methanol treatment of substrate SIP experiment revealed approximately 77 % of all detected phylotypes as labelled in the ‘heavy’ fraction and approximately 16 % of all detected phylotypes as labelled in the ‘middle’ fraction (Figure 65A, Table A 32). Five phylotypes showed LPs $\geq 5\%$, and thus are assumed to play a major role in methanol-derived carbon assimilation. The dominant phylotype (i.e., OTU_{ITS} 46 with an LP of approximately 31 %) was affiliated to the basidiomycetous yeast genus *Cryptococcus*. The second most abundant phylotype (OTU_{ITS} 10) was affiliated to the

ascomycetous mould fungi genus *Penicillium* and revealed LPs of approximately 19 %. In addition, two more phylotypes belonging to the *Ascomycota* were labelled. These phylotypes were affiliated to the mould fungi *Oidiodendron* (OTU_{ITS} 32) and *Saccharomyces* (OTU_{ITS} 2) that comprises budding yeasts such as *Pichia* and *Hansenula* with some known methylotrophic species (Figure 65A, Table A 32).

Another phylotype that was determined as labelled in the 'heavy' fraction of the methanol treatment was a *Mortierella*-affiliated phylotype (OTU_{ITS} 5) with an LP of approximately 7 % (Figure 65, Table A 32). The same phylotype was also identified as labelled in the 'middle' fraction with an LP of approximately 36 %, and in addition a second *Mortierella*-affiliated phylotype (OTU_{ITS} 112) was further labelled. Other phylotypes that were labelled in the 'middle' fraction were affiliated to the *Basidiomycota*, in detail to *Syzygospora* (OTU_{ITS} 22) and the ectomycorrhizal genus *Laccaria* (OTU_{ITS} 27) as well as to the *Ascomycota*, in detail to the saprobic *Hyaloscyphaceae* (OTU_{ITS} 135) (Figure 65, Table A 32).

3.7.3.2. Multi-carbon substrate-assimilating fungi

The treatments of the substrate SIP experiment revealed that for treatments with sugars and vanillic acid almost all detected phylotypes (i.e., 93 % to 95 %) in the individual 'heavy' fractions were identified as labelled. In contrast, the 'heavy' fraction of the [¹³C₂]-acetate treatment indicated only 47 % of all detected phylotypes as labelled. For all substrate treatments between 88 % and 98 % of all detected phylotypes were determined as labelled in the 'middle' fractions (Figure 65C; Table A 33 - Table A 36).

In both sugar treatments one phylotype (OTU_{ITS} 1) was highly abundant with LPs > 90 % (Figure 65C; Table A 34, Table A 35). This phylotype was affiliated to the basidiomycetous yeast *Trichosporon* and was also dominating the 'middle' fractions (Figure 65C; Table A 34, Table A 35). OTU_{ITS} 1 was also dominating the 'middle' fraction of the [¹³C₂]-acetate treatment, but was not detected in the 'heavy' fraction. Instead another *Trichosporon*-affiliated phylotype was labelled (OTU_{ITS} 73) with an LP of 9.6 % (Figure 65C, Table A 33). Other phylotypes in the 'heavy' fraction determined as labelled and affiliated to *Basidiomycota* were an *Inocybe*-affiliated phylotype (OTU_{ITS} 31) and a *Tomentella*-affiliated phylotype (OTU_{ITS} 49) (both genera are known to be ectomycorrhizal) as well as OTU_{ITS} 30 affiliated to the widespread genus *Trechispora* (Figure 65C, Table A 33). In addition, further phylotypes affiliated to *Ascomycota* were labelled. They were affiliated to the mould fungi *Oidiodendron* (OTU_{ITS} 9) and *Elaphocordyceps* (OTU_{ITS} 16) known to parasitise other fungi (Figure 65C, Table A 33). Moreover, phylotypes affiliated to the phyla *Chytridiomycota* (OTU_{ITS} 114) and *Rozellomycota* (OTU_{ITS} 141) were also labelled. One *Mortierella*-affiliated phylotype was labelled but with a low LP of only 5.6 % (Figure 65C, Table A 33). The numerous number of labelled phylotypes in the [¹³C₂]-acetate treatment hypothesised acetate as a well established direct or indirect substrate for fungi in the acidic forest soil. The same was observed for the aromatic compound. Half of the labelled phylotypes revealed LPs ≥ 5 %

in the 'heavy' fraction of the [$^{13}\text{C}_{1-6}$]-vanillic acid treatment (Figure 65C, Table A 36). The phylotypes OTU_{ITS} 2 and OTU_{ITS} 18 revealed the highest LPs and were both affiliated to *Ascomycota*. In detail, OTU_{ITS} 2 was affiliated to the yeasts comprising *Saccharomyces* and OTU_{ITS} 18 was affiliated to the genus *Nectria* (Table A 36). Further *Ascomycota*-affiliated and labelled phylotypes were OTU_{ITS} 32 affiliated to the mould fungi *Oidiodendron* and OTU_{ITS} 39 affiliated to *Leptodontidium*. In addition, phylotypes affiliated to *Basidiomycota* were also determined as labelled. In detail, they were affiliated to the yeast *Trichosporon* (OTU_{ITS} 1), the bracket fungi genus *Ganoderma* (OTU_{ITS} 7) and the ectomycorrhizal genus *Tomentella* (OTU_{ITS} 11) (Figure 65C, Table A 36). Moreover one *Mortierella*-affiliated phylotype (OTU_{ITS} 5) was also labelled with an LP of 9.4 % (Figure 65C, Table A 36). The analysis of the 'middle' fraction of the treatment with [$^{13}\text{C}_{1-6}$]-vanillic acid revealed a *Cryptococcus*-affiliated phylotype (OTU_{ITS} 6) as delayed labelled.

Interestingly, both treatments with [^{13}C]-CO₂ showed high amounts of potentially labelled phylotypes, in which the majority was related to *Ascomycota* (Figure 65C, Table A 37, Table A 38). LPs of these phylotypes in the 'heavy' fractions were almost always < 15 % and most of the potentially labelled phylotypes in the 'middle' fractions showed only LPs < 10 % (Table A 37, Table A 38), indicating a weak and possibly doubtful label, since fungi are known to be heterotrophic organisms gaining their nutrition mainly by absorption [Cannon & Kirk, 2007]. Thus, the labelling result for both CO₂ treatments should be examined with reservations.

In the treatment with CO₂ and additional methanol the labelled phylotypes were affiliated to *Ascomycota*, which were in detail the mainly saprotrophic living order *Helotiales* (OTU_{ITS} 62) and the included family *Dermataceae* (OTU_{ITS} 21), the widespread genus *Trichoderma* (OTU_{ITS} 8), the yeast comprising *Saccharomyces* (OTU_{ITS} 2). In addition, labelled phylotypes of *Basidiomycota* were affiliated to the major class of *Agaricomycetes* (OTU_{ITS} 12), the therein included bark fungi genus *Ganoderma* (OTU_{ITS} 7) and the ectomycorrhizal genus of *Inocybe* (OTU_{ITS} 31). Interestingly, the phylotype OTU_{ITS} 108 was also determined as labelled but could not be affiliated to any taxon indicating the potential of putatively hitherto unknown CO₂ assimilating fungi (Figure 65C, Table A 37).

In the treatment with solely CO₂ as additionally supplemented carbon source the majority of labelled phylotypes were affiliated to *Ascomycota* like the saprotrophic genus *Bulgaria* (OTU_{ITS} 41), the plant pathogenic genus *Volutella* (OTU_{ITS} 35), the mould fungi *Oidiodendron* (OTU_{ITS} 17), the widespread genus of *Trichoderma* (OTU_{ITS} 8) and the yeast comprising *Saccharomyces* (OTU_{ITS} 2). Labelled phylotypes that were affiliated to *Basidiomycota* were affiliated to the major class of *Agaricomycetes* (OTU_{ITS} 56, OTU_{ITS} 12) and the yeast *Cryptococcus* (OTU_{ITS} 28). Apart from one *Mortierella*-affiliated phylotype (OTU_{ITS} 5) another phylotype that could not be affiliated to any taxon (OTU_{ITS} 98) was also identified as labelled and indicates again the potential of putatively hitherto unknown CO₂ assimilating fungi (Figure 65C, Table A 38).

3.7.3.3. Methanol-assimilating methylotrophic fungi under shifted pH conditions

The analyses of the fungal communities in both pH treatments revealed no strong influence of different pH conditions on the fungal community composition in general (see 3.5.3). However, the number of labelled phylotypes was always higher in the pH 4 treatments compared to the pH 7 treatments indicating an effect of pH on the methanol-utilising methylotrophic fungal species. In addition, the numbers of phylotypes determined as labelled in both treatments with *in situ* pH (i.e., methanol treatment of the substrate SIP and the pH 4 treatment of the pH shift SIP experiment) were comparable, but the composition of labelled phylotypes revealed an inconsistent pattern (Figure 65A & B, Table A 32, Table A 39). The amount of labelled phylotypes in the pH 4 treatment revealed approximately 48 % of the phylotypes as labelled in the 'heavy' fraction, which is lower than in the methanol treatment of the substrate SIP experiment (Figure 65A & B, Table A 32, Table A 39) indicating a fungal community in the pH shift SIP experiment that is either less active in terms of methanol assimilation or the competition for methanol was higher. The amount of labelled phylotypes in the 'middle' fractions of both methanol treatments at the *in situ* pH is comparable instead (Figure 65A & B, Table A 32, Table A 39). Huge differences were observed for the phylogenetic affiliation of the labelled phylotypes. All labelled phylotypes of the 'heavy' fraction were affiliated to *Basidiomycota* or *Zygomycota* (Figure 65B, Table A 39). In accordance to the methanol treatment of the substrate SIP experiment all zygomycetous phylotypes (OTU_{ITS} 4, OTU_{ITS} 5, OTU_{ITS} 19, OTU_{ITS} 23, OTU_{ITS} 33, OTU_{ITS} 50) were affiliated to the genus *Mortierella* with LPs up to nearly 31 % (Figure 65B, Table A 39). The *Basidiomycota*-affiliated phylotypes showed only LPs around 8 % and below, and were affiliated to the widespread genera of *Trechispora* (OTU_{ITS} 30) and *Leucosporidiales* (OTU_{ITS} 15), the major class of *Agaricomycetes* (OTU_{ITS} 12) and the therein included bark fungi genus *Ganoderma* (OTU_{ITS} 7) (Figure 65B, Table A 39). In addition, the analysis of the 'middle' fraction revealed also the basidiomycetous yeast *Cryptococcus* (OTU_{ITS} 13) as labelled as well as one phylotype related to the ascomycetous saprotrophic family *Chaetomiaceae* (OTU_{ITS} 60) (Figure 65B, Table A 39).

The analysis of the 'heavy' fraction of the pH 7 treatment revealed approximately 64 % of all detected phylotypes as labelled, and approximately 49 % of all detected phylotypes in the 'middle' fraction were labelled (Figure 65B, Table A 40). The dominant labelled phylotype in both fractions was OTU_{ITS} 1 affiliated to the basidiomycetous yeast *Trichosporon* with LPs of > 70 % (Figure 65B; Table A 40). In the 'middle' fraction also the genus *Ganoderma* (OTU_{ITS} 7) and the ascomycetous mould fungi genus *Paecilomyces* (OTU_{ITS} 14) were identified as labelled (Figure 65B; Table A 40). Due to the labelling of only three fungal taxa, a reducing effect of a more neutral pH on the diversity of methanol-utilising fungi in an inherent acidic soil could be assumed. Another probable reason could be a high

RESULTS

competitiveness for methanol of *Trichosporon* at pH 7 resulting in a weak or even no label of other methylotrophic fungal taxa in this soil.

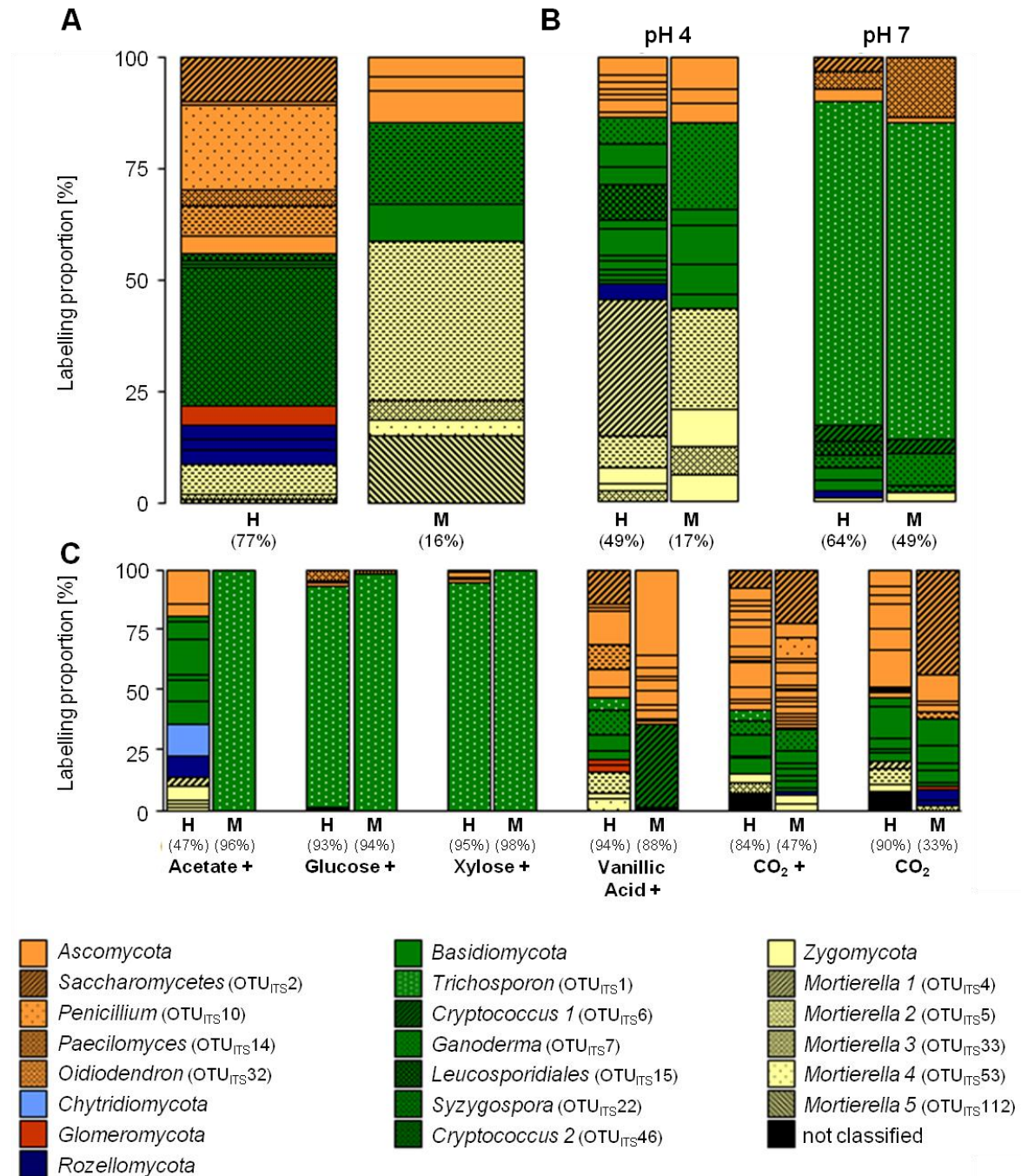


Figure 65 Labelled ITS phylotypes in ‘heavy’ and ‘middle’ fractions of different [¹³C]-isotopologue treatments.

‘LPs’ are indicators of relative importance of different fungal taxa assimilating supplemented [¹³C]-methanol (A) or [¹³C]-isotopologue (C) in the substrate SIP experiment as well as [¹³C]-methanol at different pH conditions in pH shift SIP experiment (B). Additional [¹²C]-methanol supplementation in substrate treatments is indicated by a cross. Phylogenetic affiliation is indicated by equal colours. ‘H’ and ‘M’ indicate ‘heavy’ and ‘middle’ fractions, respectively. Values in brackets indicate contribution of labelled OTUs to the total fraction. This figure has been published in Morawe *et al.* 2017.

3.7.3.4. Comparative analysis and assessment of the substrate range of methylotrophic fungi

In contrast to *Bacteria* no obligately methylotrophic fungi are known for which reason all fungi utilising methanol were assumed to be also facultatively methylotrophic. Thus, the attention of the comparative SIP was turned to the substrate range of the methylotrophic fungi in an acidic forest soil.

In the methanol treatment of the substrate SIP experiment the phylotype OTU_{ITS} 46 affiliated to the basidiomycetous yeast *Cryptococcus* showed the highest labelling proportion (Table A 32), and consequently was assumed to assimilate methanol. Interestingly, this phylotype was not detected in any other substrate treatment (Figure 66) although an increase in the relative abundance of *Cryptococcus*-related sequences was observed for vanillic acid treatments (Table A 11). No clear conclusion on the substrate range of *Cryptococcus* species was possible with the comment that these yeasts were assumed to possess the ability to utilise carbon derived from aromatic compounds (directly or from breakdown products). Another phylotype affiliated to the yeast comprising *Saccharomyces* was OTU_{ITS} 2, which was detected in methanol and vanillic acid treatments as well as in the CO₂ treatments, indicating the ability of this phylotype to utilise carbon derived from methanol and vanillic acid (Figure 66).

Two mould fungi were labelled in the [¹³C]-methanol treatment of the substrate SIP experiment. The *Penicillium*-affiliated phylotype OTU_{ITS} 10 was only re-detected as labelled in the treatment with CO₂ and additionally methanol (Figure 66), indicating the coincidental assimilation of CO₂ in the presence of methanol. Instead, the *Oidiodendron*-affiliated phylotype OTU_{ITS} 32 was re-detected as labelled in vanillic acid treatments indicating the possibility to utilise carbon from vanillic acid (Figure 66).

The same was observed for the *Mortierella*-affiliated phylotype OTU_{ITS} 5 that was additionally abundant in the methanol treatment at pH 4 of the pH shift SIP experiment, emphasising the methanol assimilation. Other *Mortierella*-affiliated phylotypes were also detectable with low labelling proportions in both methanol treatments at *in situ* conditions and the vanillic acid treatment indicating a general capacity to utilise these compounds.

Only OTU_{ITS} 1 affiliated to the yeast *Trichosporon* was detectable in all substrate treatments and even in the methanol treatment at pH 7 indicating a domination of this yeast, which is in accordance with relative abundances of these taxa within the fungal community (Figure 66, Table A 11). Interestingly, the labelling proportion of OTU_{ITS} 1 in the vanillic acid treatment assumed a lower assimilation of carbon derived from this aromatic compound indicating a preference for non complex substrates. The labelling of OTU_{ITS} 1 in the methanol treatment at pH 7 hypothesised the potentially assimilation of methanol under more neutral conditions as well as a growth optima for *Trichosporon* at neutral conditions.

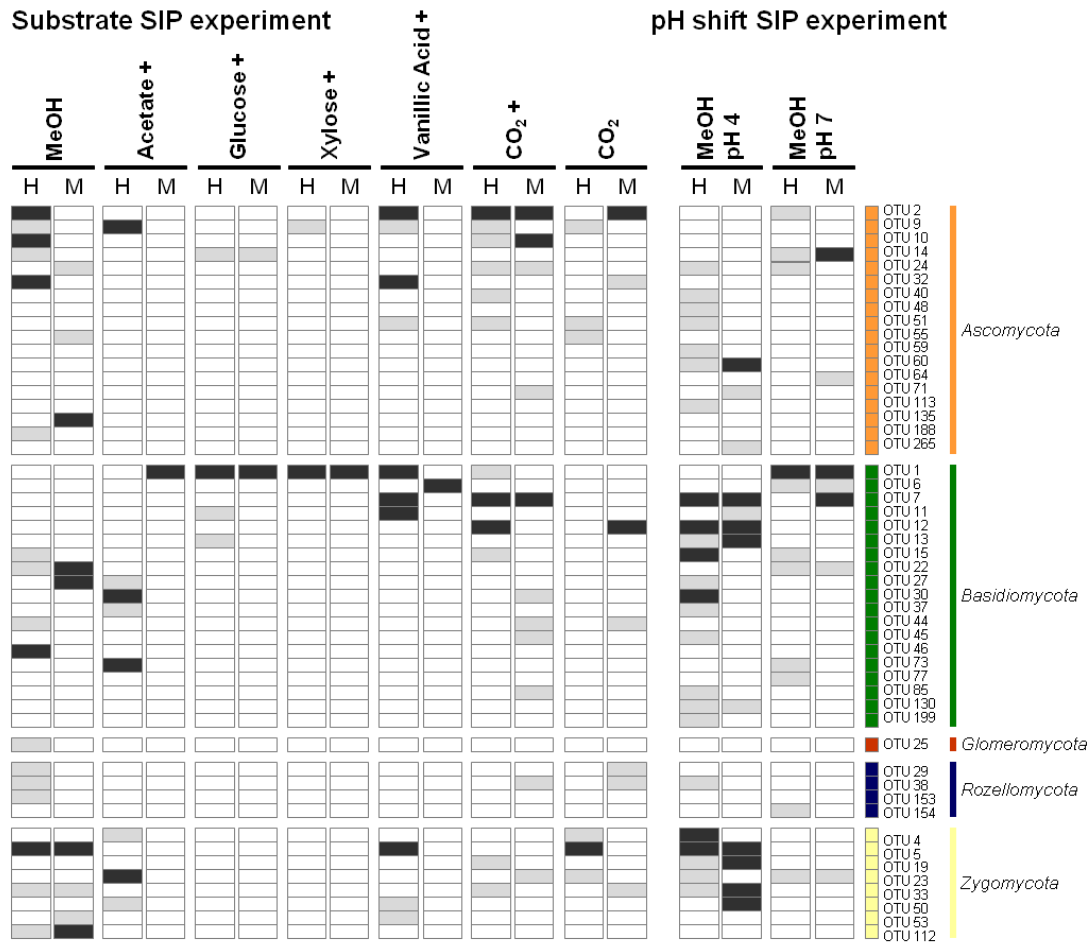


Figure 66 Congruently labelled fungal phylotypes in treatments of both SIP experiments.

Labelled phylotypes (OTUs) in methanol treatments as well as the consistent presence of these phylotypes in the substrate SIP and pH shift SIP experiments ('LP' > 5 %, black; 'LP' < 5 %, grey). Phylotypes that were only determined as labelled in treatments with multi-carbon substrates are not considered. Additional [¹²C]-methanol supplementation in the substrate SIP experiment is indicated by a cross. Phylogenetic affiliation is indicated by equal colours. 'H' and 'M' indicate 'heavy' and 'middle' fraction, respectively. This figure has been published in Morawe *et al.* 2017.

3.8. Methanol-utilisers in further soil environments

The main focus of this work was an acidic forest soil, but methanol utilisation is of course not restricted to such environments only. Methylophs are widespread in nature and the diversity of methylophic organisms is still growing (see 1.3, 1.2 & 1.3) [Kolb, 2009a; Chistoserdova, 2015]. In addition, the structure of a methylophic community is assumed to be correlated by the vegetation type of the environment [Degelmann *et al.*, 2009; Stacheter *et al.*, 2013], and tight interactions between methylophs and plants are reported [Zabetakis *et al.*, 1996; Pirttillä *et al.*, 2000; Ivanova *et al.*, 2001; Omer *et al.*, 2004; Madhaiyan *et al.*, 2006; Renier *et al.*, 2011; Irvine *et al.*, 2012]. Thus, it is conceivable that a vegetation-influenced environment such as herbage-dominated meadows or deciduous and coniferous forests might reveal different methylophic communities with different representatives present.

In order to estimate the abundance of methylotrophs and thus the importance of other soil environments in terms of methanol utilisation a selection of ten different soils (see 2.1.2 & Table 2) was analysed for their abundance of the methylotrophic marker gene *mxoF*. The sampling sites were chosen in order to cover several different soil environments with different but also common characteristics including forest-related soils (i.e., 'mixed forest'; 'beech'; 'birch' or 'pine'), herbaceous characterised soils (i.e., 'herbs' 'syringa', or 'blueberry'), meadow soils (i.e., 'meadow 1' and 'meadow 2') or an agricultural soil (i.e., 'canola') from geographically distinct areas.

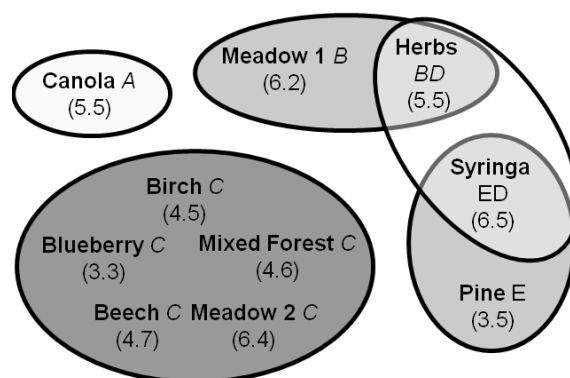


Figure 67 Comparison of different soil environments with a focus on methylotrophs.

(Dis)similarities of different soil environments by matched grouping based on significant differences of calculated *mxoF*/16S rRNA ratios (i.e., The gene copy number of *mxoF* per ng DNA against the gene copy number of 16S rRNA per ng DNA; see Table A 41 for values). The comparison refers to t_0 -ratios of all soil environments without any incubation. The significant differences of the ratios were calculated based on One-Way ANOVA with the assumption of a normal distribution (based on Shapiro-Wilk-test). An overview and a description of the environments are given (see 2.1.2 & Table 2) and the pH values for each soil (i.e., soil slurry) are given in brackets.

The initial comparisons of freshly taken and not methanol-treated soil samples were done based on the bacterial abundance (i.e., 16S rRNA gene sequence copy numbers) and the abundance of *mxoF* gene sequences. Contrary to the expectations no clear grouping of the different soil samples in terms of vegetation, geographical area or pH was obvious (Figure 67). For example, the samples 'beech', 'mixed forest' and 'herbs' were retrieved from the same sampling area with comparable impacts (i.e., soil type, bed rock, precipitation, climate, general vegetation, see 2.1.2 & Table 2), but did not group together. The same is also true for the samples 'blueberry' and 'pine' that were from the same sampling area. The distance of the sampling points was approximately 3 m, and both soils were covered by pine needles and revealed the lowest pH values. Thus, although a clear correlation between methylotrophs and the vegetation is already known [for example Degelmann *et al.*, 2009; Stacheter *et al.*, 2013], no clear statements could be constituted in terms of *mxoF*-possessing methylotrophic communities in this case.

RESULTS

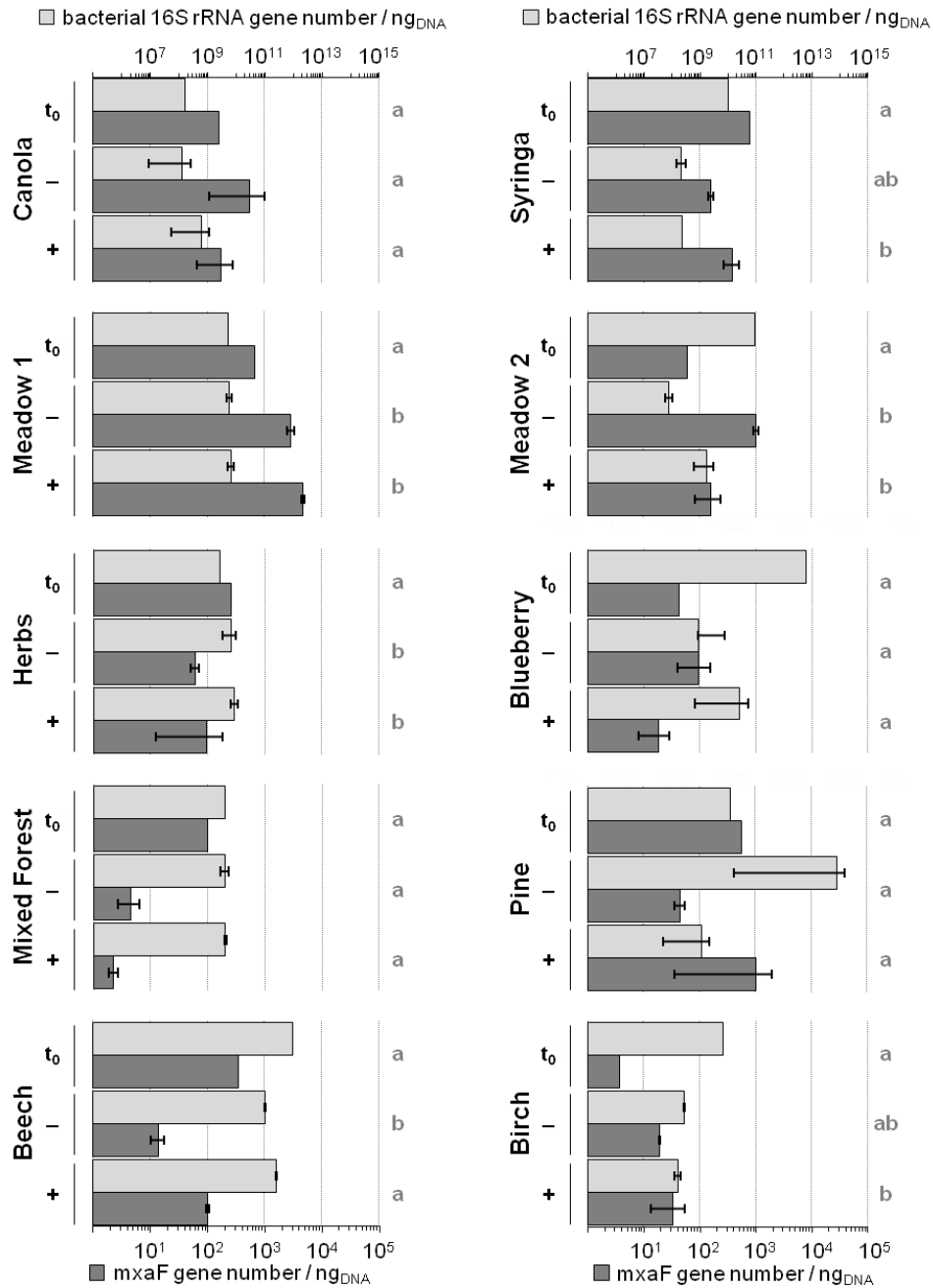


Figure 68 Influence of methanol on the *in situ* *mxoF*-possessing methylotrophs in different soil environments.

Gene numbers ng^{-1} DNA (mean values of duplicated qPCR measurements; error bars indicate highest and lowest values) of bacterial 16S rRNA gene sequences (light grey) and the methylotrophic specific marker gene *mxoF* (dark grey) at the beginning ($t_0 = \textit{in situ}$) and after a 20 days incubation period (i.e., '-', unsupplemented; '+', supplementation of methanol). Soil slurries were pulsed 4 times with 5 mM methanol (20 mM in total). Significant differences of calculated *mxoF*/16S rRNA ratios (see Table A 41 for values) within each soil environment approach are indicated by letters (One-Way ANOVA; normal distribution assumed based on Shapiro-Wilk-test).

Apart from the initial potential of methylotrophy also the response of *mxoF*-possessing methylotrophs on the supplementation of methanol was analysed (Figure 68). It was assumed that the supplementation of methanol could lead to an increase in *mxoF* gene copy

numbers, indicating growth of methylotrophic organisms in the soil samples. However, the comparison of methanol-supplemented and unsupplemented treatments revealed also no clear results. Only the samples 'syringa', 'birch' and 'beech' revealed significant differences between methanol-supplemented and unsupplemented treatments (based on ANOVA analyses of the resulting *mxoF*/16S RNA ratios and indicated by small letters in Figure 67). Interestingly, in some samples such as 'mixed forest', 'beech', and 'blueberry' the initial *mxoF* gene number was higher than in methanol-treated samples. An explanation might be that other methylotrophs besides the *mxoF*-possessing members might become more activated and are thus more important in these soils. For that reason also other methylotrophic marker genes such as *xoxF* genes should be additionally analysed in such environmental studies.

It is also worth to mention that the comparison of initial t_0 -samples and treated samples might be false leading, since the incubation itself might affect the microbial community to a greater importance than the supplemented methanol, i.e., the application of soil slurries changed the soil structure dramatically by disrupting established soil structures. For example the bacterial abundance in the samples 'syringa', 'meadow 2', 'blueberry', and 'birch' dropped dramatically assuming a negative effect of the incubation itself. Other samples such as 'meadow 1', 'herbs', and 'mixed forest', however, did not reveal such losses in bacterial abundance.

In summary, other soil environments also harbours *mxoF*-possessing methylotrophs but no clear trend on the abundances or importance of these methylotrophic representatives could be made. The requirement for suitable primers of other methylotrophic marker genes was also emphasised, which would lead to a more *in situ* close reflection of the diversity of methylotrophs in soils and other environments.

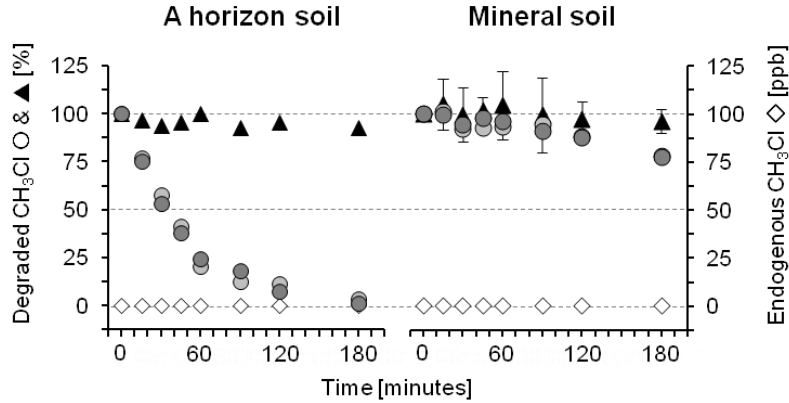
3.9. Forest soil – a microbial sink of chloromethane

Since natural sources of CH_3Cl are forest-associated (terrestrial plants, dead wood or wood-rotting fungi) and several isolates of CH_3Cl -utilising bacteria are soil-derived [Coulter *et al.*, 1999; McAnulla *et al.*, 2001; Borodina *et al.*, 2005], the potential of the forest soil inhabiting microbial community as a sink for CH_3Cl was tested.

Preliminary CH_3Cl oxidation analyses of different forest compartments (i.e., phyllosphere, senescent leaves / litter, rotting wood, soil) revealed the biodegradation of CH_3Cl in nearly all compartments tested with the exception of the mineral soil layer (Figure 69; all raw data are a result of the Master thesis of Michael Ruffer, 2014). The CH_3Cl degradation potential was highest in the approach with the A horizon of a forest soil (i.e., the upper layer, 0 to 5 cm depth) indicating the most abundant and active CH_3Cl utilisers therein. In addition, the approaches with almost fresh leaves and litter showed further apparently effective CH_3Cl degrading potentials, and thus represent both further important compartments. None of the tested compartments was shown to generate CH_3Cl endogenously, and all approaches with

KCN revealed lower to none CH_3Cl degradation, indicating the biotic origin of the observed CH_3Cl degradation (Figure 69).

Soil-derived material



Plant-derived material

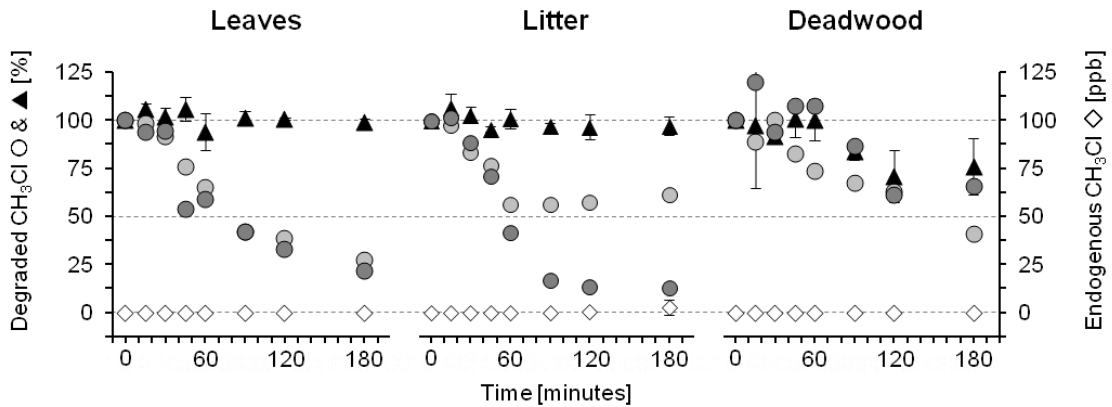


Figure 69 Degradation of low amounts of chloromethane in different forest-derived compartments.

Relative concentrations of CH_3Cl over time as indicator for its degradation and the amount of endogenous formed CH_3Cl (in ppb). The initial concentration of applied CH_3Cl was 100 ppb (\cong 100 % of relative amount). Symbols: \circ , relative CH_3Cl concentration in forest-derived samples (\bullet & \bullet , replicate 1 & 2); \blacktriangle , relative CH_3Cl concentration in the presence 20 mM KCN; \diamond , concentration of endogenously formed CH_3Cl (in ppb; no additional CH_3Cl applied). The KCN control was used to prove the biotic origin of the recorded CH_3Cl degradation. Shown are average values; error bars represent standard deviation ($n=2$). All data presented in this figure are a result of the Master thesis of Michael Ruffer, 2014.

In further approaches the CH_3Cl degradation potential of the upper layer (A horizon) was tested. Both, low and high concentrations of CH_3Cl were degraded within several hours and days, respectively (Figure 70 & Figure 71). If low amounts of CH_3Cl were applied (i.e., 100 ppb) approximately 50 % of the applied CH_3Cl was degraded within 1 hour and nearly all CH_3Cl was degraded after 3 hours (Figure 70), which is also consistent with previous observations holding comparable conditions (Figure 69; Ruffer, 2014). CH_3Cl is a water soluble gas, but although no soil slurries were used approximately 30 % of the applied CH_3Cl

were absorbed by the soil from the beginning of the experiment (Figure 70). The fate of this bound CH_3Cl could not elucidate but it is possible that the absorbed CH_3Cl was also degraded.

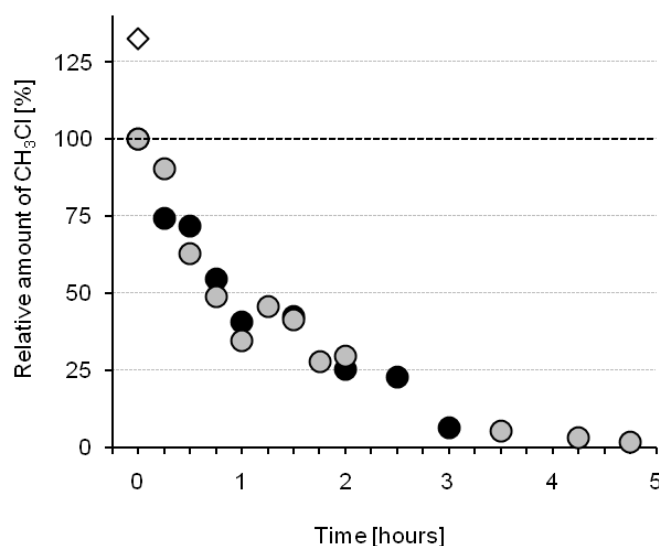


Figure 70 Degradation of low amounts (i.e., 100 ppb) of chloromethane of a forest soil.

Relative degradation potential of forest soil samples (coarse-grained, storage time below 24 hours) with low amounts of CH_3Cl as initial concentration (i.e., 100 ppb) applied. Symbols: ● & ●, replicates; ◇, 'no soil control'. 'No soil control' was conducted to estimate the absorption of CH_3Cl to soil particles or flask surfaces.

Although the atmospheric concentration of CH_3Cl is only about 600 ppt, CH_3Cl -utilising bacteria in terrestrial environments were isolated with higher amounts of CH_3Cl (at least 1 % v/v) [Hartmans *et al.*, 1986; Doronina *et al.*, 1996; Nadalig *et al.*, 2011; Coulter *et al.*, 1999], assuming that the in soil indigenous microorganisms are capable of CH_3Cl -degradation of non-atmospheric concentrations. The forest soil sample tested was capable of degrading an initial supplementation of 1 % CH_3Cl within 16 days (Figure 71, 1st cycle). The concentration of CH_3Cl in flasks without soil was stable over a longer period (i.e., 90 % of the initially supplemented CH_3Cl concentration) (Figure 71, 1st cycle). Thus, the reasons for the disappearance of CH_3Cl in the incubation flasks are neither any depletion by abiotic reactions in the gas phase nor any absorption to the surfaces are. In addition, an adaption to the high amounts of CH_3Cl and consequently an activation of CH_3Cl -utilising microorganisms could be assumed, since several subsequently pulsed CH_3Cl supplementations resulted in an increasing degradation potential (Figure 71). The second pulse of CH_3Cl revealed an enhanced degradation and resulted in a two times faster degradation potential (Figure 71, 2nd cycle). After the 4th cycle the biodegradation of 1 % CH_3Cl was approximately eight times faster than the initial biodegradation, assuming high adapted CH_3Cl -utilisers being indigenous in the forest soil (Figure 71, 4th cycle).

All these results emphasise the CH_3Cl degradation potential of pristine forest soil environments and thus their role as microbial sink for monohalocarbons. The observed

adaption also emphasise the quick response on elevated concentrations of CH_3Cl that are conceivable, since local concentrations of CH_3Cl (i.e., the local concentration next to plant leaves, litter, wood, fungi) are not evaluated.

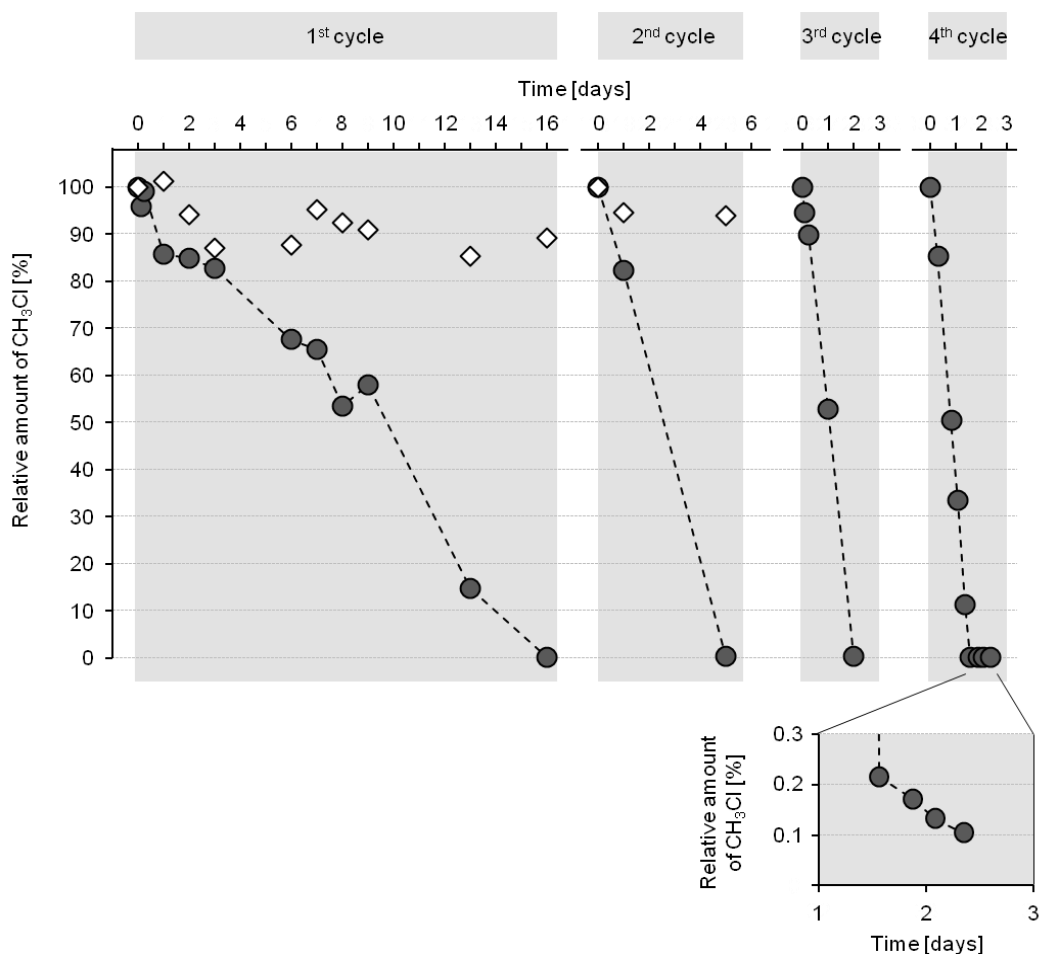


Figure 71 Degradation of high amounts (i.e., 1 %) of chloromethane of a forest soil.

The forest soil (coarse-grained) shows a subsequent adaption to repeated CH_3Cl supplementation with high amounts of CH_3Cl (i.e., 1 %) applied. Grey background indicates separate cycles of CH_3Cl degradation records (4 in total). Inset focuses on the relative CH_3Cl concentrations in the 4th cycle after 1 day. Symbols: ●, relative concentration of CH_3Cl in the approach with soil; ◇, relative concentration of CH_3Cl in the approach without soil to estimate non-biotic degradation effects (approach was conducted in the 1st and 2nd cycle).

3.10. Utilisation of methanol or chloromethane by methylotrophic organisms in an acidic soil

The highly specialised CH_3Cl -utilising microorganisms were isolated and detected in different ecosystem types [Schäfer *et al.*, 2007], but are not highly abundant within the pristine microbial communities. For example, only one cell out of thousand bacterial cells on the leaf surfaces of *Arabidopsis thaliana* is expected to be able to utilise CH_3Cl [Nadalig *et al.*, 2011]. For that reason the forest soil samples of this incubation experiment were pre-incubated with 1 % CH_3Cl (see 2.3.10) to activate chloromethane-utilisers. Previous CH_3Cl degradation studies revealed a quick adaption to elevated CH_3Cl concentrations (see 3.9).

3.10.1. Conversion of methanol and chloromethane and the formation of [¹³C]-CO₂ as evidence for substrate dissimilation

Over the whole incubation time five individual substrate pulses were conducted. While focussing on CH₃Cl-utilisers all methanol supplementations were conducted in accordance to the CH₃Cl substrate pulses (i.e., at the same time point and with a similar concentration) in the incubations where only one substrate was supplemented (i.e., solely methanol or solely CH₃Cl). Each CH₃Cl pulse was given when CH₃Cl was no longer detectable in the gas phase in at least one replicate. The incubation of samples, GC-measurements, and samplings were conducted by Pauline Chaignaud (PC).

Both incubation variants (i.e., solely CH₃Cl and the combined supplementation of methanol and CH₃Cl (MeOH&CH₃Cl)) revealed similar trends in CH₃Cl degradation. The additional methanol in the combined approaches (i.e., MeOH & CH₃Cl) had no stimulating effect on the CH₃Cl degradation (Figure 72A). In both incubation variants activated soil was used to achieve a quick response to CH₃Cl supplementation. As it was observed in previous studies (see 3.9) the CH₃Cl degradation potential was expected to be enhanced. This expectation was only met within the first two substrate pulses. After the third substrate pulse the degradation potentials were reduced in all treatments with CH₃Cl (Figure 72A). One explanation could be that with the sampling of soil before each substrate pulse the total potential for the CH₃Cl degradation was actually lowered causing this unexpected negative effect. However, this explanation is only speculative. As a compromise only samples taken after the 3rd pulse were further molecular analysed.

The utilisation of supplemented substrates was assumed by an increased formation of CO₂ compared to unsupplemented controls (Figure 72B). The amount of CO₂ detectable in [¹²C]- and [¹³C]-isotopologue treatments was similar assuming no preference of [¹²C]-substrates (Figure 72B). In addition, the formation of [¹³C]-CO₂ was analysed to proof the utilisation of the [¹³C]-isotopologues.

All incubations solely supplemented with methanol revealed the highest amounts of formed CO₂ compared to the incubations with simultaneously supplemented methanol and CH₃Cl (Figure 72B). Incubations solely supplemented with CH₃Cl revealed no obvious differences in the CO₂ formation than the unsupplemented controls, but the utilisation of supplemented CH₃Cl was proven via the detection of [¹³C]-CO₂ (Figure 72B). Although the formation of CO₂ showed different trends for all three approaches (i.e., solely methanol, solely CH₃Cl, methanol and CH₃Cl combined), the resulting [¹³C]-CO₂ revealed similar concentrations. On average in all [¹³C]-methanol treatments approximately 70 % of the supplemented ¹³C was recovered in [¹³C]-CO₂ and in all [¹³C]-CH₃Cl treatments approximately 60 % of the supplemented ¹³C was recovered as [¹³C]-CO₂ per [¹³C]-isotopologue indicating a higher dissimilation turnover for methanol than for CH₃Cl (Table 37).

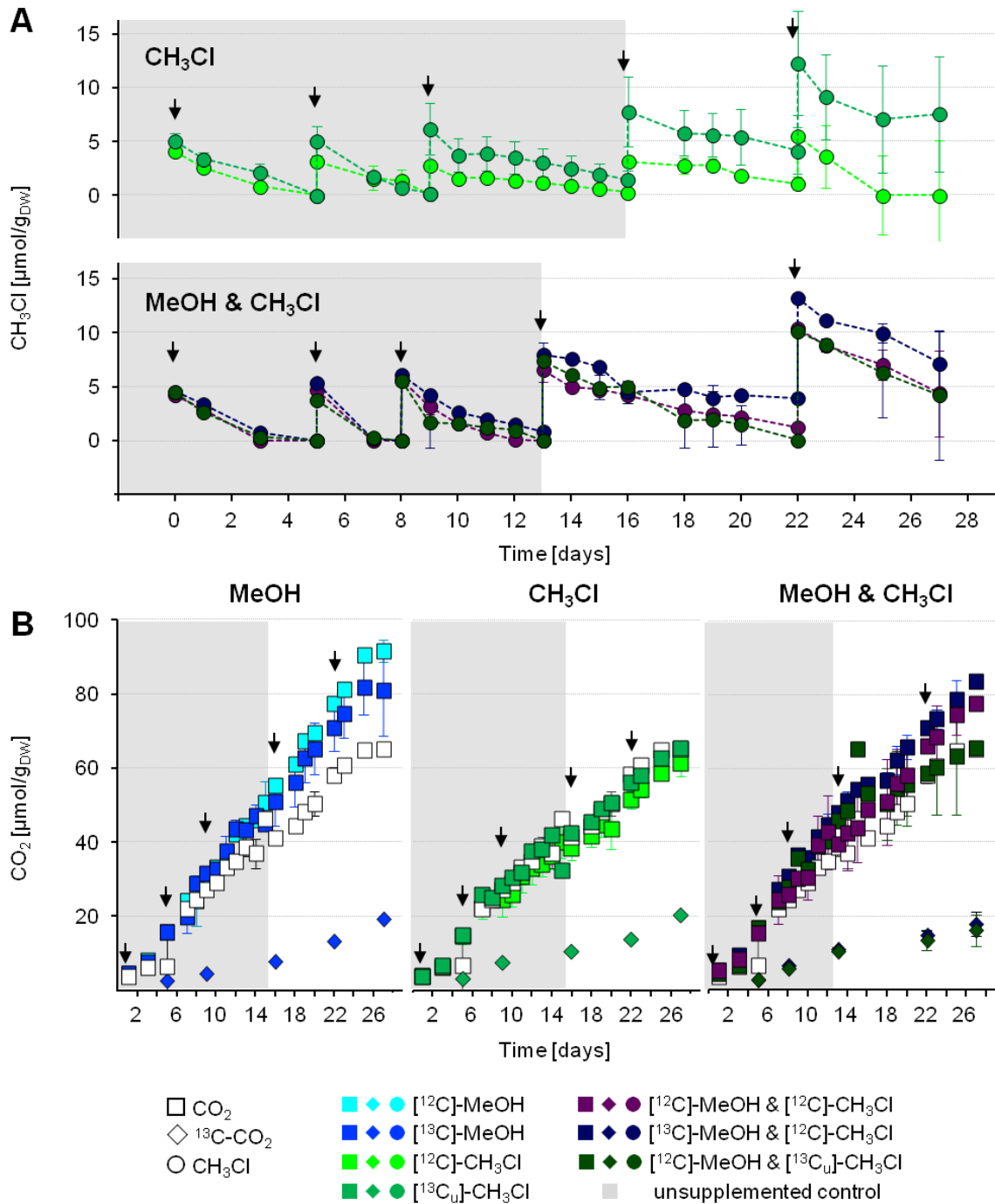


Figure 72 Degradation of CH₃Cl (A) and formation of CO₂ (B) in the methanol/chloromethane SIP experiment.

Trend of the CH₃Cl degradation in CH₃Cl supplemented approaches (i.e., CH₃Cl and MeOH & CH₃Cl approach; panel A) as well as the cumulative ¹²CO₂ and ¹³CO₂ concentrations of all three different approaches supplemented with methanol solely (MeOH approach), chloromethane solely (CH₃Cl approach) and a combination of methanol and chloromethane (MeOH & CH₃Cl approach) (panel B). Arrows (▼) indicate C1 compound substrate pulses (5 in total) in each approach. Grey background indicate the time of the first 3 substrate pulses; samples for molecular analyses were taken just before the 4th substrate pulse was supplemented. Shown are average values; error bars represent standard deviation (n=2). Raw data of CH₃Cl and CO₂ concentrations were collected by Pauline Chaignaud [Chaignaud, 2016].

Table 37 Amounts of supplemented [$^{13}\text{C}_n$]-isotopologues, $^{13}\text{CO}_2$ and the resulting C-recoveries of carbon per substrate pulse.

Values are average values and comprise all five substrate pulses. [^{13}C]-isotopologues are highlighted in bold.

Solely supplemented substrate approaches

Total amounts of	$^{13}\text{MeOH}$				$^{13}\text{CH}_3\text{Cl}$			
Supplemented ^{13}C -substrate ^a	216	±	0	μmol	273	±	5	μmol
Resulting $^{13}\text{CO}_2$ ^b	160	±	33	μmol	159	±	40	μmol
C-Recovery	74	±	15	%	59	±	15	%

Simultaneously supplemented substrate approaches

Total amounts of	$^{13}\text{MeOH}$ & $^{12}\text{CH}_3\text{Cl}$				$^{12}\text{MeOH}$ & $^{13}\text{CH}_3\text{Cl}$			
Supplemented ^{13}C -substrate ^a	216	±	0	μmol	235	±	13	μmol
Resulting $^{13}\text{CO}_2$ ^b	147	±	21	μmol	134	±	29	μmol
C-Recovery	68	±	10	%	59	±	13	%

^a The amount of supplemented [^{13}C]-methanol refers to theoretically calculated values; the amount of supplemented [$^{13}\text{C}_1$]- CH_3Cl refers to actually measured values.

^b The amount of $^{13}\text{CO}_2$ refers to the determined relative amount of $^{13}\text{CO}_2$ in gas samples relating to the total amount of CO_2 at the same time point.

3.10.2. The influence of methanol and chloromethane on *Bacteria* in an acidic soil

The mean coverage of all combined amplicon libraries of the different treatments (i.e., t_0 , solely methanol supplementation, solely chloromethane supplementation or simultaneously supplementation of methanol and chloromethane) of 16S rRNA gene sequences at a family-level was 99.98 ± 0.01 %, indicating a sufficient amount of amplicons sequenced (Figure 73A). The detected numbers of genotypes were on average 86 ± 2 OTUs and the Chao 1 indices hypothesised a species richness of 97 ± 7 genotypes (Figure 73 B & F). Diversity estimators indicate that the bacterial community was similar diverse at the beginning and in all different treatments of the incubation. No domination of only a single or a few genotypes was observed (Figure 73C, D & E).

Between [^{12}C]-, [^{13}C]- and combined dataset-derived sequences of the different treatments slight differences were noticeable in an nMDS plot (Figure 74A). All incubated samples were distinct from t_0 indicating a community forming effect of the supplemented substrates as it was expected. Treatments with solely methanol-supplemented were distinct from all other samples suggesting differences of the microbial community of these treatments (Figure 74A).

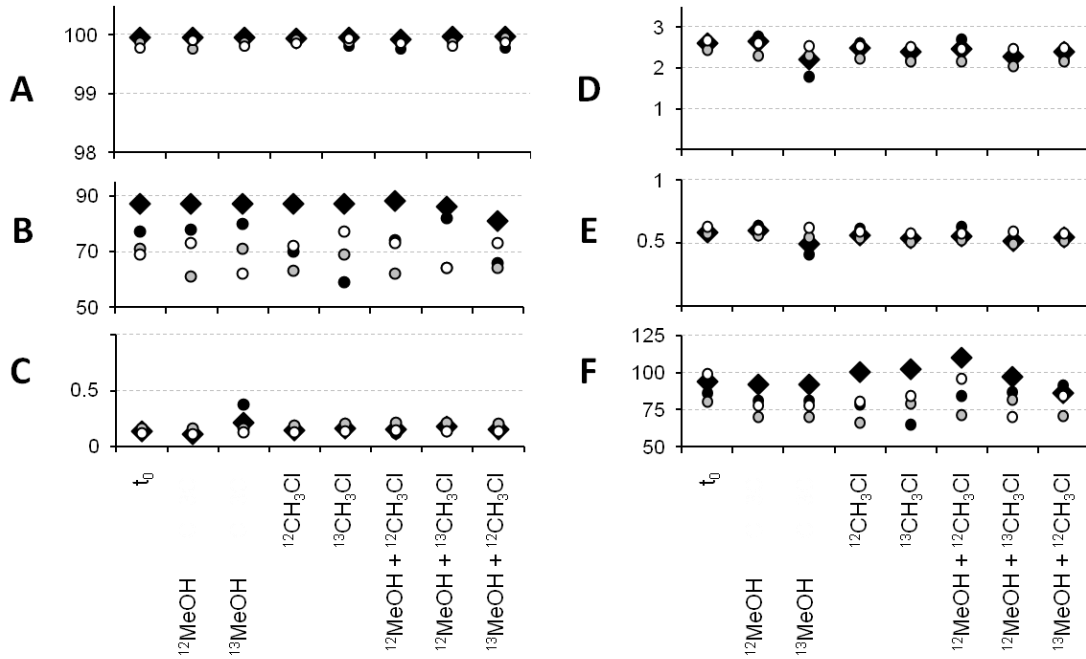


Figure 73 Diversity and richness estimators of 16S rRNA gene sequences of the methanol/chloromethane SIP experiment.

Figures indicating coverage (%) (A), numbers of OTUs (B), dominance D (C), Shannon index H (D), equitability J (E) and Chao1 index (F). Shown are values of t_0 (no treatment) and after the treatment with solely methanol supplemented (MeOH), solely chloromethane supplemented (CH_3Cl) or both compounds combined supplemented (MeOH + CH_3Cl). A 12 indicates [^{12}C]-substrate, 13 indicates [$^{13}\text{C}_\text{U}$]-substrate. Symbols: \blacklozenge , combined datasets of 'heavy', 'middle' and 'light' fractions; \bullet , 'heavy' fraction; \circ , 'middle' fraction; \circ , 'light' fraction.

However, all samples from the methanol/chloromethane SIP experiment (i.e., t_0 and all treatments) revealed no significant differences in their bacterial community structures as indicated by ANOSIM (analysis of similarity; $R = 0.30$, $p = 0.131$) as well as with NPMANOVA (non-parametric multivariate analysis of variance; $F = 1.92$, $p = 0.097$) (Table A 8). Nevertheless, the analyses indicated tendencies of how the supplemented substrates affected the bacterial communities. Treatments solely supplemented with methanol revealed apparently no differences compared to t_0 . The in the nMDS plot observed separation of t_0 and the methanol-supplemented samples could be due to the enrichment of methanol-utilisers in the samples. This would indicate that the microbial community was already well adapted to methanol as substrate. The supplementation of CH_3Cl affected the initial bacterial community and led to a higher separation between t_0 and CH_3Cl -supplemented treatments, which is indicated by the values of the pairwise analyses. The dissimilarities between t_0 and the solely CH_3Cl -supplemented treatments were highest, suggesting CH_3Cl as the strongest community affecting factor and thus an advantage of CH_3Cl -utilisers over the residual microbes in these treatments. In addition, higher differences of the microbial communities of the solely methanol-supplemented samples and the simultaneously supplemented (methanol and CH_3Cl) samples were obvious (i.e., pairwise analyses of t_{End} vs t_{End}). This emphasises again

RESULTS

CH₃Cl as a stronger community-affecting factor and suggests the presence of a few specialists in terms of CH₃Cl utilisation.

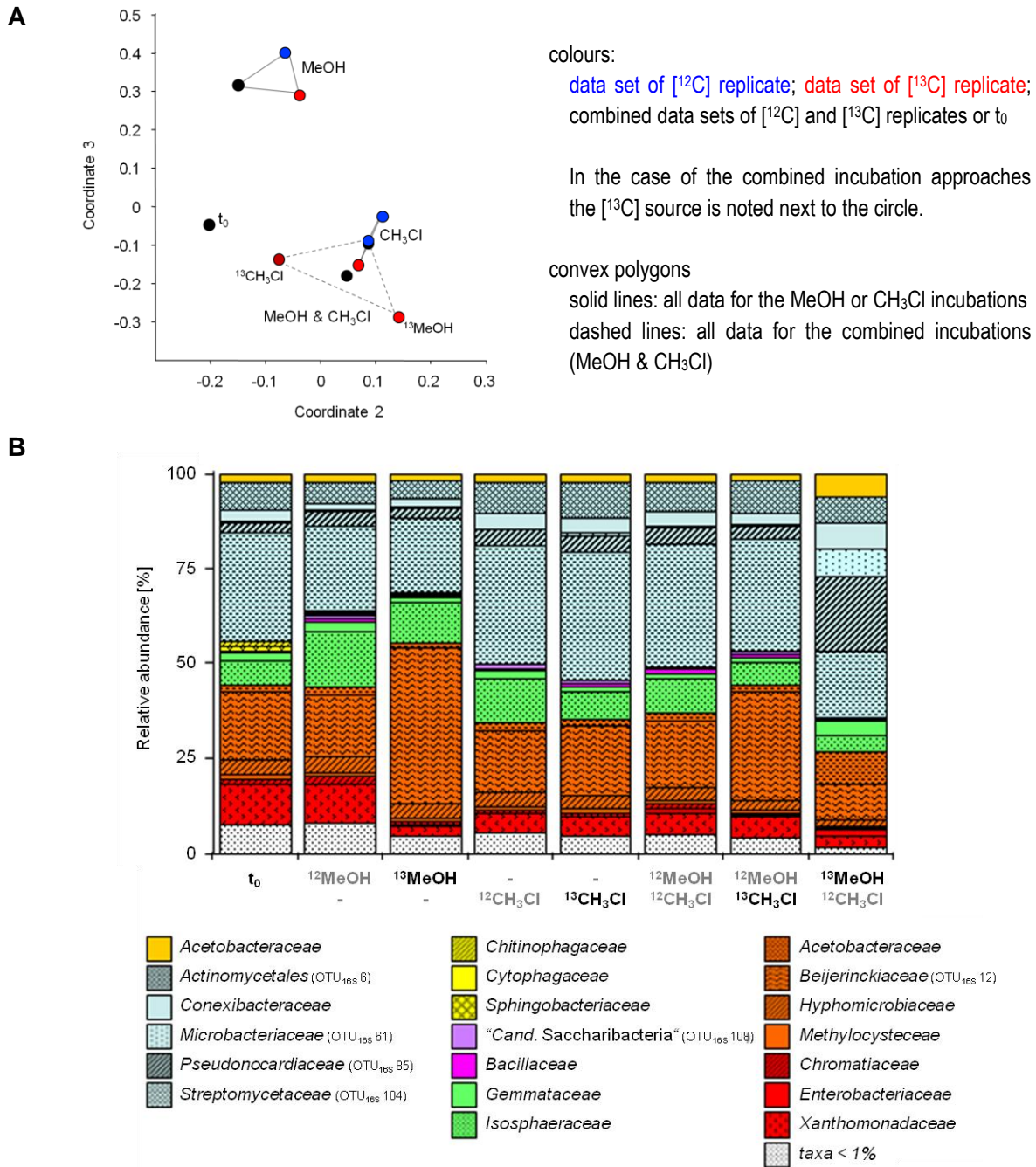


Figure 74 nMDS analyses (A) and the phylogenetic compositions (B) of the bacterial community after treatments with methanol or/and chloromethane.

Panel A, nMDS analysis of relative abundances of sequences for 16S rRNA gene sequences (based on family-level). The analysis is based on the Bray-Curtis similarity index with a stress value of 0.03.

Panel B, relative abundances of selected bacterial phylotypes of the methanol/chloromethane SIP experiment at the beginning (t₀) and after an incubation with solely methanol (MeOH), solely chloromethane (CH₃Cl) or a combination of both (MeOH & CH₃Cl). ¹³ indicates ¹³C isotopologue and ¹² indicates ¹²C isotopologue. The relative abundance is only shown for bacterial phylotypes with a relative abundance ≥ 1 %. Phylogenetic affiliation is indicated by equal colours (■, *Acidobacteria*; ■, *Actinobacteria*; ■, *Bacteroidetes*; ■, "*Candidatus Saccharibacteria*"; ■, *Firmicutes*; ■, *Planctomycetes*; ■, *Alphaproteobacteria*; ■, *Gammaproteobacteria*). The analysis of sequences (filtering, clustering, and affiliation) was done by Ludovic Besaury (LB).

The analysis of the phylogenetic composition of t_0 and all t_{End} samples revealed members of the *Actinobacteria* (especially the family *Streptomycetaceae*, OTU_{16S} 104) and *Alphaproteobacteria* (especially the family *Beijerinckiaceae*, OTU_{16S} 12) as dominant in all samples (Figure 74B). Further abundant phylotypes were affiliated to the *Planctomycetes* (especially the family *Isophaeraceae*) and *Gammaproteobacteria* (especially the family *Xanthomonadaceae*). Comparing the phylogenetic composition of the t_0 samples from the substrate SIP experiment and the pH shift SIP experiment (see 3.5.1, Figure 48) with the t_0 sample of the methanol/chloromethane SIP experiment the same phyla were detected as abundant (i.e., *Actinobacteria*, *Alphaproteobacteria*, *Planctomycetes* and *Acidobacteria*) (Figure 48B & Figure 74B). This finding indicates that the pristine microbial community is to some degree stable over time and thus assuming at least the same taxa as methanol-utilisers in the treatments solely supplemented with methanol.

3.10.3. The influence of methanol and chloromethane on *mxoF/xoxF*-type MDH and *cmuA* phylotypes in an acidic soil

The mean coverage of all combined amplicon libraries of the different treatments (i.e., t_0 , solely methanol supplementation, solely chloromethane supplementation or simultaneously supplementation of methanol and chloromethane) of the *mxoF/xoxF*-type MDH gene sequences was 100 % and for *cmuA* gene sequences 99.99 ± 0.02 % (Figure 75A). The numbers of detected (number of OTUs) and expected genotypes (hypothesised by the Chao 1) were identical for *mxoF/xoxF*-type MDH gene sequences and for *cmuA* gene sequences, respectively. In total 24 ± 1 *mxoF/xoxF*-type MDH phylotypes and 7 ± 1 *cmuA* phylotypes were detected and estimated (Figure 75B & F). Similar to the bacterial community all diversity estimators indicate that the *mxoF/xoxF*-type MDH phylotype resulting communities were similar diverse at the beginning and in all different treatments of the incubation. No domination of only a single or a few phylotypes was observed (Figure 75 C, D & E). The community based on all detected *cmuA* phylotypes revealed a tendency towards a less diverse community compared to the *mxoF/xoxF*-type MDH community even from the beginning of the whole incubation, indicating that *cmuA*-possessing microorganisms are more restricted in their diversity (Figure 75C, D & E).

In accordance to the microbial communities (based on 16S rRNA gene sequences, see 3.10.2) differences between all *mxoF/xoxF*-type MDH and *cmuA* phylotype communities of the different treatments were noticeable in the nMDS plots (Figure 76A). In general, all incubated samples were distinct from the t_0 sample and clustered together according to their supplemented substrate(s) (i.e., solely methanol, solely CH₃Cl or both combined) (Figure 76A).

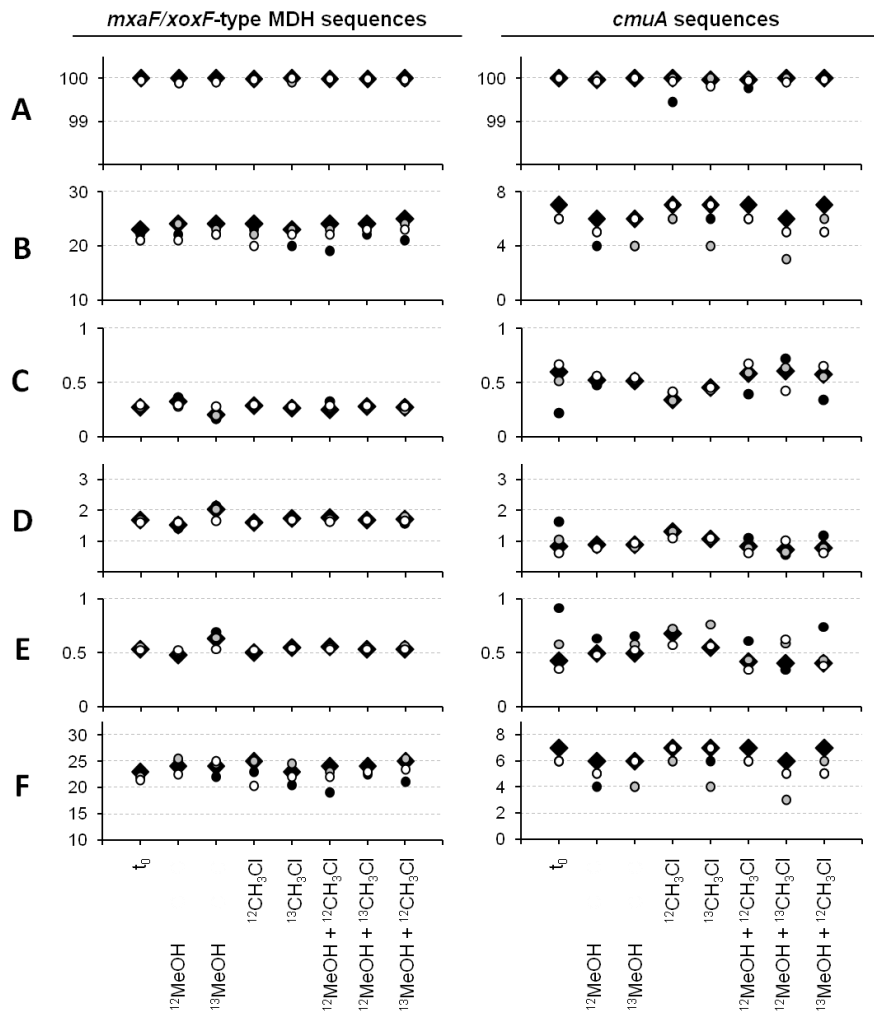


Figure 75 Diversity and richness estimators of *mxoF/oxoF*-type MDH and *cmuA* gene sequences of the methanol/chloromethane SIP experiment.

Figures indicating coverage (%) (A), numbers of OTUs (B), dominance D (C), Shannon index H (D), equitability J (E) and Chao1 index (F). Shown are values of t_0 (no treatment) and after the treatment with solely methanol supplemented (MeOH), solely chloromethane supplemented (CH_3Cl) or both compounds combined supplemented (MeOH + CH_3Cl). A 12 indicates [^{12}C]-substrate, 13 indicates [^{13}C]-substrate. Symbols: \blacklozenge , combined datasets of 'heavy', 'middle' and 'light' fractions; \bullet , 'heavy' fraction; \circ , 'light' fraction.

Within the detected *cmuA* phylotype communities all samples solely supplemented with CH_3Cl were most distinct from t_0 , indicating the highest influence of CH_3Cl compared to treatments with methanol or both substrates (Figure 76A). Significant differences of the *cmuA* phylotype communities were obvious and revealed well separated communities (ANOSIM: $R = 0.67$, $p = 0.011$; NPMANOVA: $F = 7.19$, $p = 0.018$). The pairwise analyses revealed that the supplementation of solely methanol or CH_3Cl affected the *cmuA* phylotype communities most (Table A 8). These results are somehow in accordance with the relative abundances of all eight detected *cmuA* phlotypes in all treatments (Figure 76B). In general most of the detected phlotypes were affiliated to *Methylobacteriaceae*, and OTU_{*cmuA*} 2 and OTU_{*cmuA*} 3 were consistently dominant (Figure 76B). Differences of the *cmuA* phylotype composition in the treatments were only remarkable for lower abundant phlotypes. One

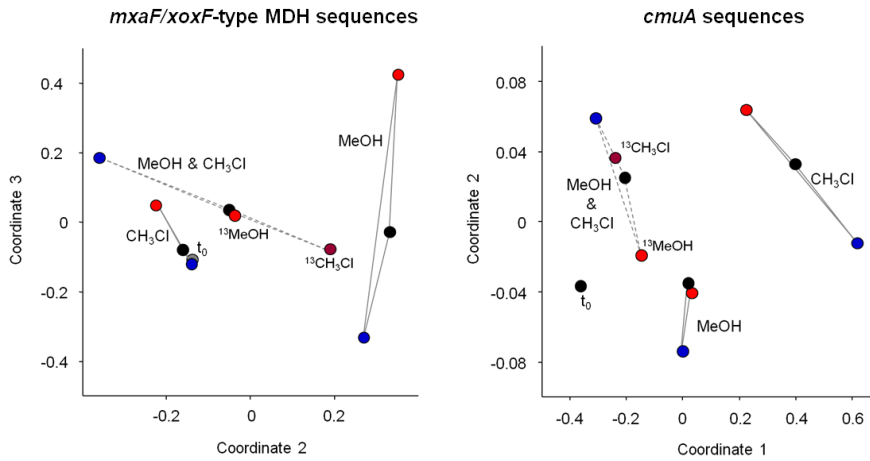
phylotype was only detectable in the treatments solely CH₃Cl-supplemented (OTU_{cmuA} 1, affiliated with *Alphaproteobacteria*), indicating that CH₃Cl triggered the growth of this phylotype and the supplementation of methanol was disadvantageous and led to the outcompeting of this phylotype by *Methylobacteriaceae*-related phylotypes in all other treatments (Figure 76B).

In the case of the *mxoF/xoxF*-type MDH phylotype communities all samples solely supplemented with methanol were most distinct from t₀, indicating the highest influence of solely methanol (Figure 76A). All samples solely supplemented with CH₃Cl were most similar to t₀ indicating only a minor influence of solely CH₃Cl on the *mxoF/xoxF*-type MDH phylotypes (Figure 76A). Somehow contrary to the picture the nMDS plot draws, the relative abundance of all detected *mxoF/xoxF*-type MDH phylotypes revealed a similar distribution pattern regardless of the treatment (i.e., t₀ or t_{End}) and also regardless of the supplemented substrate(s) (Figure 76B). Only the treatment with [¹³C]-methanol revealed a difference in the presence of detectable phylotypes (Figure 76B). The most abundant phylotypes were OTU_{MDH} 24 and OTU_{MDH} 25, which are both affiliated to *xoxF* gene sequences of *Bradyrhizobiaceae*, and OTU_{MDH} 17 affiliated to *xoxF* gene sequences of *Rhizobiaceae* (*Sinorhizobium*). In total, the majority of MDH phylotypes was affiliated to *xoxF* gene sequences and only 4 phylotypes were affiliated to *mxoF* gene sequences of *Beijerinckiaceae* (*Methylovirgula* or *Methyloferula*; OTU_{MDH} 4, OTU_{MDH} 8, and OTU_{MDH} 15) and *Hyphomicrobiaceae* (OTU_{MDH} 20). However, these *mxoF* phylotypes were only low abundant.

In addition, the ANOSIM and NPMANOVA analyses revealed both no significant differences of the different *mxoF/xoxF*-type MDH phylotypes communities (Table A 8). The pairwise ANOSIM analysis indicated that solely methanol affected the *mxoF/xoxF*-type MDH phylotypes communities most, whereas the pairwise NPMANOVA analysis revealed a higher influence of solely supplemented CH₃Cl (Table A 8). These different results are acceptable, since both analyses evaluate different properties of the data, i.e., ANOSIM is a distribution free analysis of the similarity between samples and NPMANOVA is a distribution free analysis of the variance between samples. Thus, the *mxoF/xoxF*-type MDH phylotypes communities are suggested to be in principle similar, but vary in their abundance of the detected phylotypes.

RESULTS

A



B

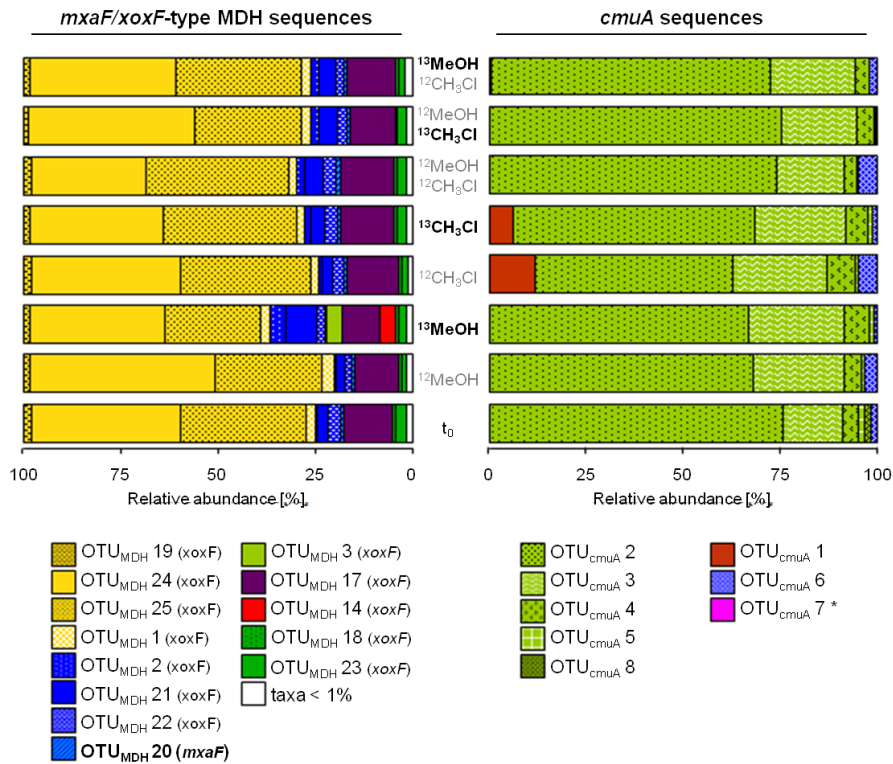


Figure 76 nMDS analyses of the *mdh*/*xoxF*-type MDH and *cmuA* sequences (A) and the corresponding phylogenetic compositions (B) after treatments with methanol or/and chloromethane.

Panel A, nMDS analysis of relative abundances of sequences for *mdh*/*xoxF*-type MDH and *cmuA* gene sequences (based on a similarity cut-off value of 77 % and 90 %, respectively). The analysis is based on the Bray-Curtis similarity index with a stress value of 0.04 for *mdh*/*xoxF*-type MDH and 0.0 for *cmuA* based analyses. Colours: data set of ¹²C replicates; data set of ¹³C replicates; combined data sets of ¹²C and ¹³C replicates or t₀. In the case of the combined incubation approaches the ¹³C source is noted next to the circle. Convex polygons: solid lines, all data for the MeOH or CH₃Cl incubations; dashed lines, all data for the combined incubations (MeOH & CH₃Cl).

Panel B, relative abundances of all *mdh*/*xoxF*-type MDH and *cmuA* phylotypes of the methanol/chloromethane SIP experiment at the beginning (t₀) and after an incubation with solely methanol (MeOH), solely chloromethane (CH₃Cl) or a combination of both (MeOH & CH₃Cl). ¹³ indicates ¹³C isotopologue and ¹² indicates ¹²C isotopologue. Phylogenetic affiliation is indicated by equal colours (■, *Bradyrhizobiaceae*; ■, *Hyphomicrobiaceae*; ■, *Methylobacteriaceae*; ■, *Rhizobiaceae*; ■, *Acetobacteraceae*; ■, *Burkholderiaceae*; ■, unclassified *Alphaproteobacteriaceae*; ■, *Firmicutes*). Hatching indicates different phylotypes. The "*" indicates that the relative abundance of was always < 0.5 %, thus OTU_{cmuA} 7 is not apparent in this figure.

3.11. Microorganisms assimilating methanol and chloromethane

In this experiment again stable isotope probing (SIP) was used to identify microorganisms that utilise a given [^{13}C]-isotopologue. Since the methanol-utilising bacteria were already addressed in another SIP experiment (see 3.7.1.1), the focus of this SIP experiment was to identify those methylotrophic organisms that assimilate CH_3Cl and to evaluate if these microbes are also important central methanol-utilisers in the acidic forest soil. Again SIP was only performed with DNA to identify the active growing taxa assimilating the supplemented carbon sources. This SIP study was a cooperation project (*university of strasbourg*), therefore Pauline Chaignaud (PC) and Ludovic Besaury (LB) contributed to this analysis by conducting the incubation (PC) and processing NGS-data (LB) as mentioned in the appropriate sections of 'Material and Methods' and at the beginning of the 'Results' part.

The formation of $^{13}\text{CO}_2$ was observed (see 3.10.1) indicating the utilisation (i.e., at least the dissimilation) of the supplemented [^{13}C]-isotopologues. The carbon recoveries of the ^{13}C as $^{13}\text{CO}_2$ revealed that in all cases most of the supplemented [^{13}C]-isotopologue was most likely used for dissimilation (see 3.10.1 & Table 37). Thus, also a cross feeding effect via CO_2 cannot be excluded and could occur by the incorporation of ^{13}C that derived from $^{13}\text{CO}_2$ or by ^{13}C derived from microbes, which assimilated ^{13}C before. In this way also the carbon flow and trophic interactions can be estimated.

In order to ensure comparability concerning all SIP experiments (i.e., substrate SIP experiment, pH shift SIP experiment, and methanol/chloromethane SIP experiment), the used gradient solution was adjusted to a density of $1.730 \pm 0.004 \text{ g x ml}^{-1}$ and isopycnic centrifugation was conducted under the same conditions. A linear decreasing gradient of buoyant densities was obvious, suggesting that the required conditions for a successful separation of 'heavy' DNA were reached. The average buoyant densities of the gradient ranged from $1.747 \pm 0.003 \text{ g x ml}^{-1}$ to $1.700 \pm 0.002 \text{ g x ml}^{-1}$. In accordance to the previous SIP experiments (see 3.7) the same threshold buoyant densities for 'heavy', 'middle' and 'light' fractions were applied (i.e., buoyant density of heavy fractions was $\geq 1.730 \text{ g x ml}^{-1}$, buoyant density of middle fractions was in between 1.715 and $1.730 \text{ g x ml}^{-1}$, buoyant density of light fractions was $\leq 1.715 \text{ g x ml}^{-1}$).

3.11.1. Identification of *Bacteria* assimilating methanol and chloromethane

A 'labelling' of bacterial taxa was assumed, since all samples from 'heavy' and 'middle' fractions of [^{12}C]- and [^{13}C]-isotopologue treatments of each treatment were distinct to each other as revealed in a nMDS plot, indicating dissimilarities between the 'heavy' and 'middle' fraction DNA samples (Figure 77). Compared to the previously conducted SIP experiments

(see 3.7.1) the number of labelled phylotypes was low, i.e., one to two labelled phylotypes were identified (Figure 78A, Table A 46). Moreover no phylotype was additionally identified as weakly labelled via the middle fractions (Figure 78A, Table A 46).

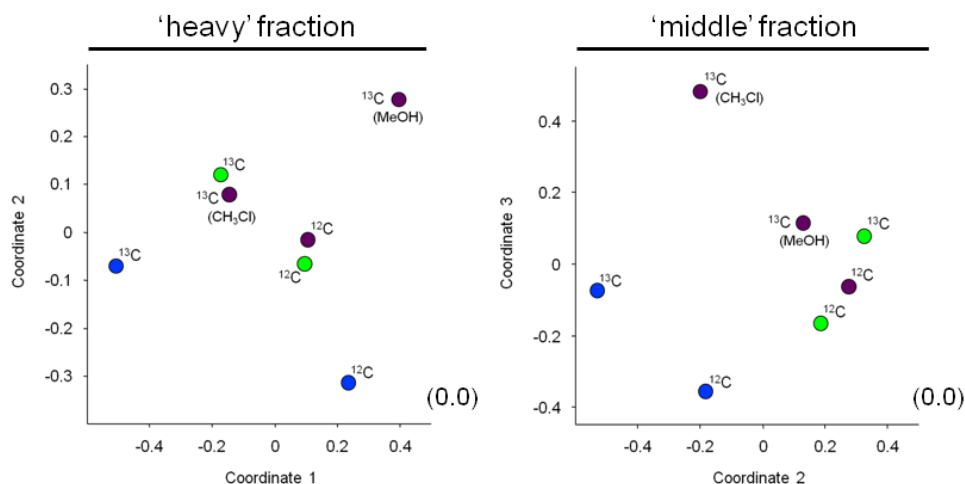


Figure 77 nMDS analyses of 16S rRNA gene sequences from the ‘heavy’ and ‘middle’ fractions of the methanol/chloromethane SIP experiment.

Analyses of relative abundances of all sequences in ‘heavy’ and ‘middle’ fractions of $[^{12}\text{C}]$ - and $[^{13}\text{C}]$ -isotopologue treatments for 16S rRNA gene sequences (based on family-level). Stress values are given in brackets. All analyses are based on Bray-Curtis similarity index. Symbols according to the incubation: ●, solely MeOH; ●, solely CH_3Cl ; ●, MeOH & CH_3Cl . In the case of the combined incubation approaches the $[^{13}\text{C}]$ source is noted next to the circle.

In the treatment solely supplemented with $[^{13}\text{C}_1]$ -methanol only one phylotype (OTU_{16S} 12) was clearly labelled (LP = 100 %) and constitutes about 59 % of the heavy fraction 16S rRNA phylotypes (Figure 78A, Table A 46). This phylotype was affiliated to *Beijerinckiaceae* and revealed a sequence identity of 99 % to *Methylovirgula ligni* (Table A 45, Figure A 13). The identification of this phylotype as exclusively labelled in the treatment solely supplemented with methanol is in an accurate accordance with the findings of the previously conducted SIP experiments (see 3.7.1.1). It also emphasises the suggested central role of the *Beijerinckiaceae*-phylotype dominating the methanol turnover in the forest soil. Interestingly, this phylotype was also identified as labelled in both treatments supplemented with $[^{13}\text{C}_1]$ - CH_3Cl and was detectable as an abundant phylotype in all treatments including the ^{12}C -control (Figure 78B).

In the treatment solely supplemented with $[^{13}\text{C}_1]$ - CH_3Cl the percentage of labelled phylotypes were 41 % of the heavy fraction 16S rRNA phylotypes (Figure 78, Table A 46). Besides the *Beijerinckiaceae*-phylotype a second phylotype (OTU_{16S} 6) was labelled affiliated to *Actinomycetales* (95 % sequence identity to *Kineosporia* sp., Table A 44) (Figure 78A, Table A 46). This phylotype was also detectable in all treatments where it was not identified as labelled, assuming a general role in the microbial food web (Figure 78A).

RESULTS

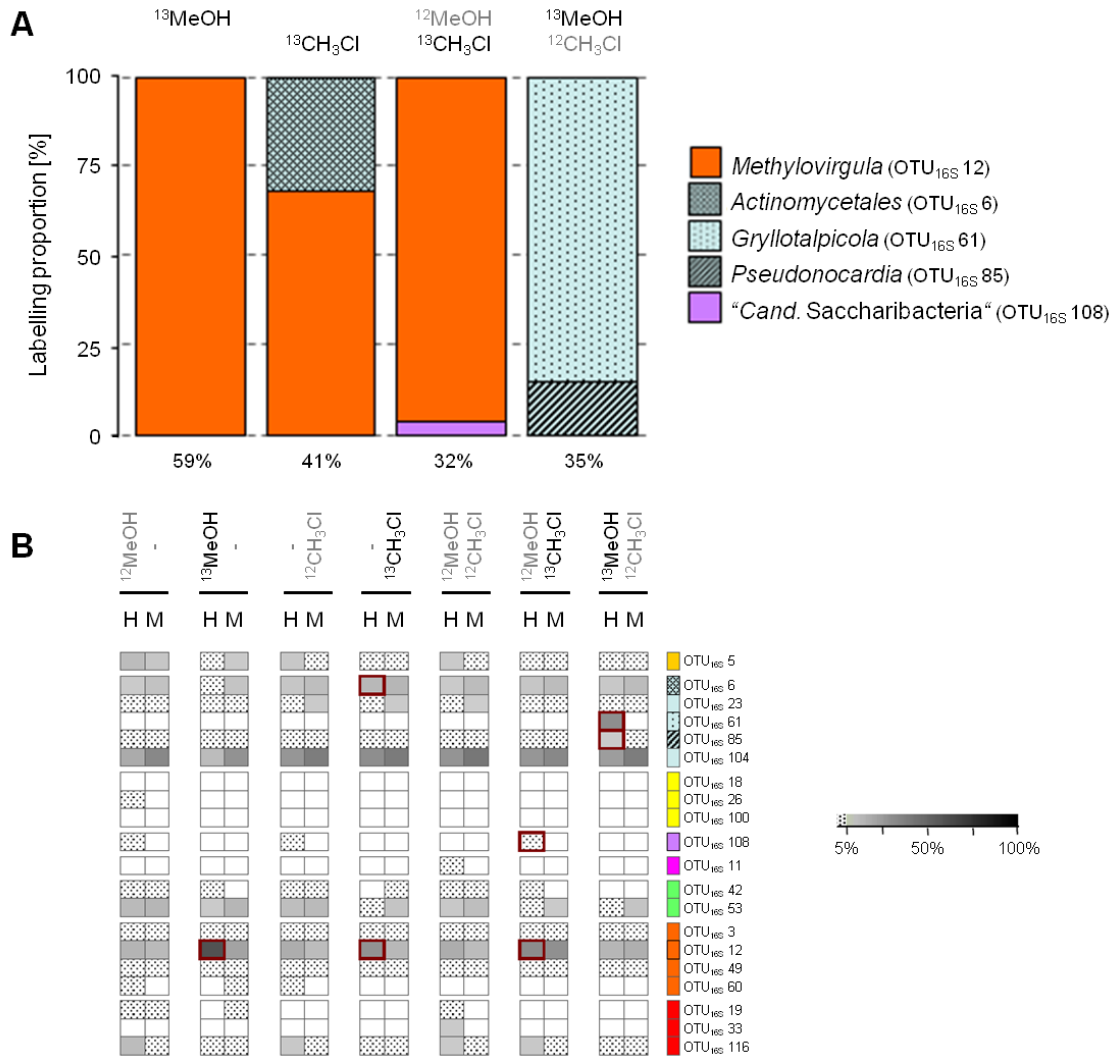


Figure 78 Phylotypes of 16S rRNA gene sequences in the 'heavy' and 'middle' fractions of the methanol/chloromethane SIP.

'LPs' of labelled phylotypes in the heavy fractions (A) and the relative abundances of selected labelled and unlabelled phylotypes (B). The 'LP' is an indicator of the relative importance of different bacterial taxa assimilating supplemented [¹³C]-methanol or [¹³C]-chloromethane under different conditions, i.e., different approaches where solely methanol (MeOH), solely chloromethane (CH₃Cl) or a combination of both (MeOH & CH₃Cl) was supplemented. Values in brackets indicate contribution of the labelled phylotype to the total fraction. The relative abundance for selected phylotypes is only shown for phylotypes with a relative abundance ≥ 1 % (relative abundance ≥ 5 %, greyish; relative abundance < 5 %, dotted). The dark red frame in panel B highlights the labelled phylotypes. '¹³' indicates ¹³C isotopologue and '¹²' indicates ¹²C isotopologue. 'H' and 'M' indicate 'heavy' and 'middle' fractions, respectively. Phylogenetic affiliation is indicated by equal colours (■, *Acidobacteria*; ■, *Actinobacteria*; ■, *Bacteroidetes*; ■, "*Candidatus Saccharibacteria*"; ■, *Firmicutes*; ■, *Planctomycetes*; ■, *Alphaproteobacteria*; ■, *Gammaproteobacteria*). NGS-data analysis (filtering, clustering) was done by Ludovic Besaury (LB).

The treatments simultaneously supplemented with methanol and CH₃Cl revealed again *Beijerinckiaceae* and *Actinobacteria* as labelled. In both treatment approaches (i.e., one approach with [¹³C₁]-methanol and one approach with [¹³C₁]-CH₃Cl) more than 30 % of the 'heavy' fraction 16S rRNA phylotypes were labelled (Figure 78A, Table A 46). The supplementation of [¹³C₁]-CH₃Cl in the combined approaches led to a labelling of the

Beijerinckiaceae-phylogroup (OTU_{16S} 12) with LPs > 5 % (Figure 78A, Table A 46). One phylotype (OTU_{16S} 108) affiliated to “*Candidatus* Saccharibacteria” was only minor labelled (LP < 5 %) but the relative abundance of this phylotype was in general low, and thus no important role concerning CH₃Cl-utilisation was assumed (Figure 78A, Table A 45, Table A 46). The supplementation of [¹³C₁]-methanol in the combined approaches led to an exclusive labelling of only *Actinobacteria*-affiliated phylotypes (Figure 78A, Table A 45, Table A 46). One phylotype (OTU_{16S} 61) was affiliated to *Microbacteriaceae* (99 % sequence identity to *Gryllotalpicola daejeonensis*) and the other phylotype (OTU_{16S} 85) was affiliated to *Pseudonocardiaceae* (98 % sequence identity to *Pseudonocardia hispaniensis*) (Figure 78A, Table A 45, Table A 46). Interestingly, the *Microbacteriaceae*-related phylotype was in almost all treatments only low abundant (relative abundance < 1 %, Table A 42) with the exception of the [¹³C₁]-methanol and CH₃Cl treatment, assuming a minor importance in the microbial food web. A similar observation was done for the *Pseudonocardiaceae*-phylogroup, which was in almost all treatments minor abundant (relative abundance < 5 %, Table A 42; Figure 78B) with the exception of the treatment supplemented with [¹³C₁]-methanol and CH₃Cl. Therefore both phylotypes (OTU_{16S} 61 and OTU_{16S} 85) might assimilate methanol at least in the presence of CH₃Cl, but the general competition for methanol in the treatments with supplemented methanol and CH₃Cl was higher resulting in other labelled methanol-utilising phylotypes. However, although expected, the *Beijerinckiaceae*-phylogroup (OTU_{16S} 12) was not identified as labelled in the [¹³C₁]-methanol approach of the combined approaches but the phylotype was detectable within the total community (Table A 46, grey background; Figure 78B). Therefore the assimilation of methanol by the *Beijerinckiaceae*-phylogroup was still suggested but ¹³C was not incorporated in a label-sufficient manner and other phylotypes might achieve their labelling more sufficiently.

3.11.2. Identification of *mxoF/xoxF*-type MDH-possessing methylotrophs assimilating methanol and chloromethane

In accordance with the 16S rRNA phylotype communities (see 3.11.1) a labelling of several taxa was assumed for the *mxoF/xoxF*-type MDH phylotype communities, since all samples from ‘heavy’ and ‘middle’ fractions of [¹²C]- and [¹³C]-isotopologue treatments of each treatment were again distinct to each other as revealed in a nMDS plot (Figure 79).

In the treatment solely supplemented with [¹³C₁]-methanol the highest number of *mxoF/xoxF*-type MDH phylotypes were identified as labelled (i.e., 41 % of the ‘heavy’ and 25 % of the ‘middle’ fraction) (Figure 80A). Two phylotypes affiliated to *xoxF* gene sequences (i.e., OTU_{MDH} 3, *Methylobacteriaceae*; OTU_{MDH} 14, *Acetobacteraceae*) were only labelled in the ‘heavy’ and ‘middle’ fraction of this treatment, indicating methanol utilisation but no CH₃Cl utilisation (Figure 80). Two *xoxF* gene phylotypes affiliated to *Hyphomicrobiaceae* (OTU_{MDH} 2 and OTU_{MDH} 21) were also labelled in treatments with CH₃Cl indicating that CH₃Cl might be somehow utilised by these taxa (Figure 80). Interestingly, both *Beijerinckiaceae*-affiliated

phylotypes (OTU_{MDH} 11 and OTU_{MDH} 15) were only minor labelled with LPs < 5 %, although based on 16S rRNA gene sequences a *Beijerinckiaceae*-affiliated phylotype was identified as important labelled taxa under several conditions and in previous conducted SIP experiments (see 3.7.1). However, based on previous *mxoF* gene sequence analyses no *Beijerinckiaceae*-affiliated phylotype was identified as labelled. *Methylovirgula ligni* was reported to possess a highly divergent *mxoF* gene sequence [Voro'bev *et al.*, 2009]. Thus, it might be possible that the important *Beijerinckiaceae*-affiliated phylotype in the acidic forest soil harbours an MDH gene sequence that is even more distinct from previously known sequences, in which the used molecular tools might bias against this sequence. Comparing the relative abundance of all detected *mxoF/xoxF*-type MDH phylotypes with the labelled ones it is obvious that the three dominating taxa (OTU_{MDH} 24, OTU_{MDH} 25, and OTU_{MDH} 17) might be not important in terms of methanol consumption, emphasising the specialisation of other methanol-utilising microorganisms (Figure 80B).

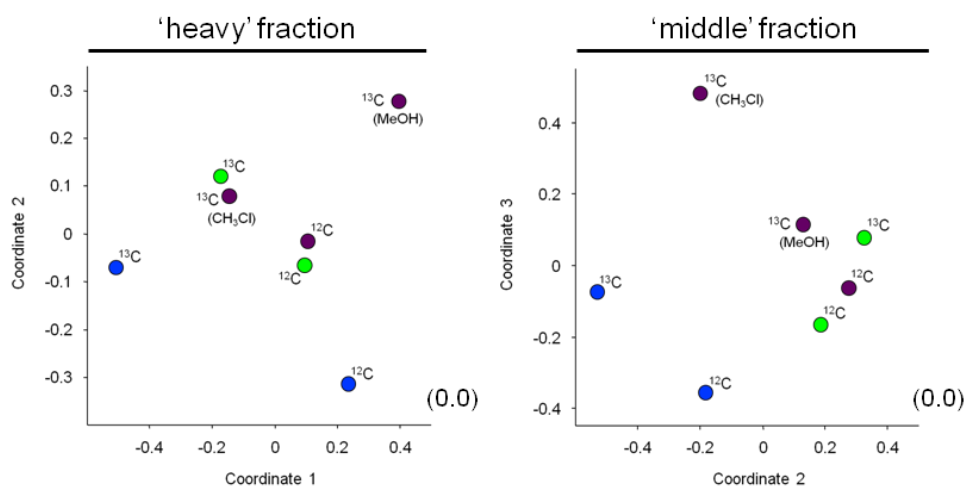


Figure 79 nMDS analyses of *mxoF/xoxF*-type MDH sequences from the 'heavy' and 'middle' fractions of the methanol/chloromethane SIP experiment.

Analyses of relative abundances of all sequences in 'heavy' and 'middle' fractions of [¹²C]- and [¹³C]-isotopologue treatments for *mxoF/xoxF*-type MDH sequences (based on a similarity cut-off value of 77 %). Stress values are given in brackets. All analyses are based on Bray-Curtis similarity index. Symbols according to the incubation: ●, solely MeOH; ●, solely CH₃Cl; ●, MeOH & CH₃Cl. In the case of the combined incubation approaches the [¹³C] source is noted next to the circle.

In the treatment solely supplemented with [¹³C₁]-CH₃Cl 79 % of the 'heavy' fraction *mxoF/xoxF*-type MDH phylotypes were labelled, in which a *Bradyrhizobiaceae*-affiliated phylotype (OTU_{MDH} 25) dominated (Figure 80A). This phylotype was also highly labelled in the combined treatment with [¹³C₁]-methanol and CH₃Cl, indicating that CH₃Cl and methanol are utilised by this phylotype with a putative preference for methanol if both substrates are simultaneously present (Figure 80). The same might be true for a *Rhizobiaceae*-affiliated (OTU_{MDH} 17, *Sinorhizobium*) and a *Hyphomicrobiaceae*-affiliated phylotype (OTU_{MDH} 22) (Figure 80).

RESULTS

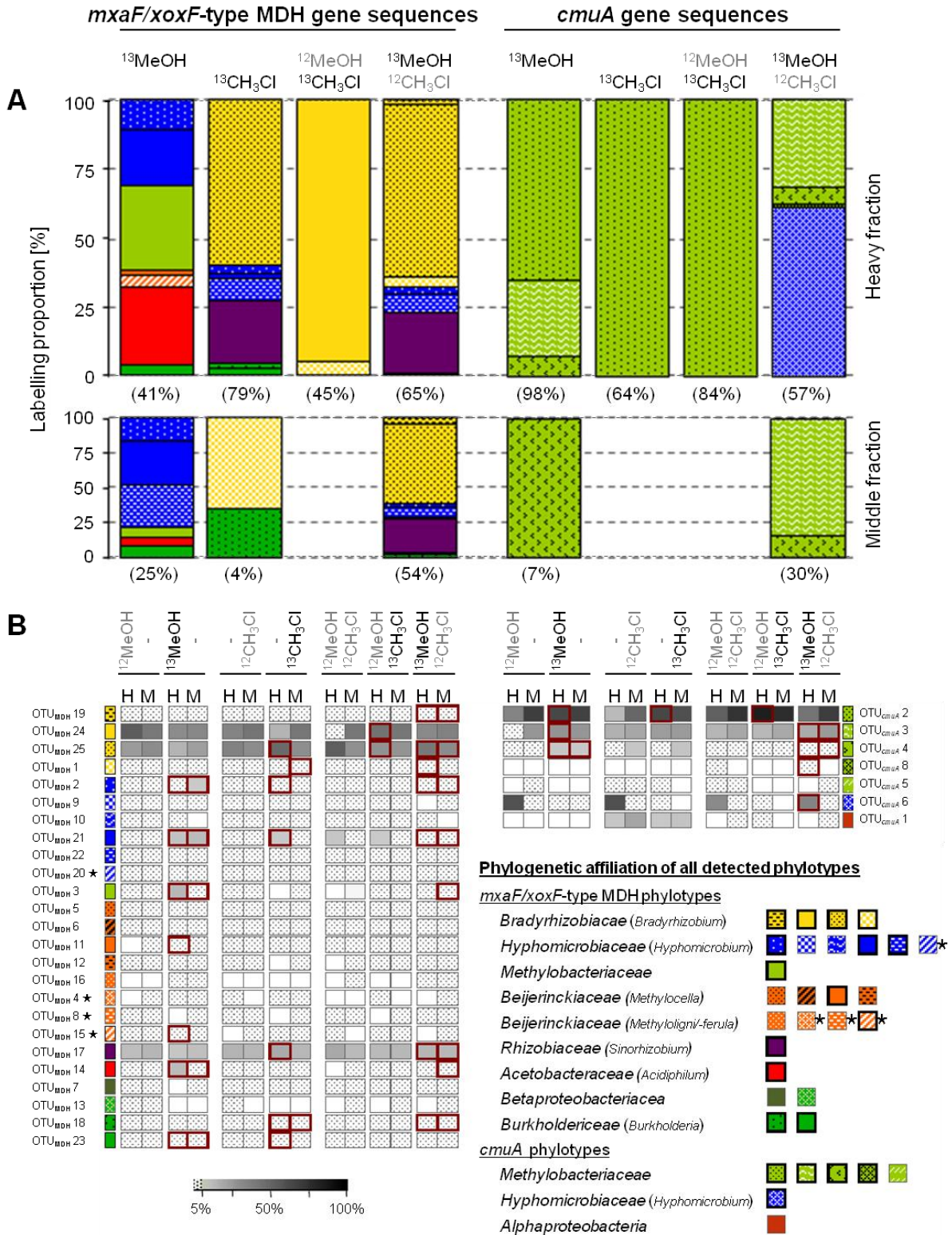


Figure 80 Phylotypes of *mxoF/xoxF*-type MDH and *cmuA* gene sequences in the 'heavy' and 'middle' fractions of the methanol/chloromethane SIP.

Explanation of Figure 80. 'Labelling proportions' ('LPs') of labelled phylotypes (A) and the relative abundances of all detected phylotypes (relative abundance $\geq 5\%$, greyish; relative abundance $< 5\%$, dotted) (B). The 'LPs' are an indicator of the relative importance of different bacterial taxa assimilating supplemented [^{13}C]-methanol or [^{13}C]-chloromethane under different conditions, i.e., different approaches where solely methanol (MeOH), solely chloromethane (CH_3Cl) or a combination of both (MeOH & CH_3Cl) was supplemented. Values in brackets in panel A indicate the contribution of the labelled phylotypes to the total fraction. The relative abundance for selected phylotypes is shown for all phylotypes. The dark red frame in panel B highlights the labelled phylotypes and an asterisk indicates all *mxoF* gene sequence phylotypes. ' 13 ' indicates ^{13}C isotopologue and ' 12 ' indicates ^{12}C isotopologue. 'H' and 'M' indicate 'heavy' and 'middle' fractions, respectively. Phylogenetic affiliation is indicated by equal colours (■, unclassified *Alphaproteobacteriaceae*; ■, *Bradyrhizobiaceae*; ■, *Hyphomicrobiaceae*; ■, *Methylobacteriaceae*; ■, *Beijerinckiaceae*; ■, *Rhizobiaceae*; ■, *Acetobateraceae*; ■, unclassified *Betaproteobacteria*; ■, *Burkholderiaceae*). Hatching indicates different phylotypes. Thick black frames in the legend indicate labelled phylotypes.

Two phylotypes affiliated to *Bradyrhizobiaceae* (OTU_{MDH} 1) and *Burkholderiaceae* (OTU_{MDH} 18) were only weakly labelled in the treatment solely supplemented with CH_3Cl . It might be possible that these phylotypes might be slower in CH_3Cl turnover rates or the competition for CH_3Cl was high resulting in a disadvantage for these taxa. Since the *Bradyrhizobiaceae*-affiliated phylotype was also labelled in both treatments simultaneously supplemented with CH_3Cl and methanol, it is also possible that methanol provides a growth benefit for these taxa, wherefore they are only weakly labelled if solely CH_3Cl is present (Figure 80).

In the combined treatment supplemented with [$^{13}\text{C}_1$]- CH_3Cl and methanol only two phylotypes were labelled that constitutes 45 % of the 'heavy' fraction *mxoF/xoxF*-type MDH (Figure 80A). Both phylotypes were affiliated to *Bradyrhizobiaceae*, in which the dominating phylotype (OTU_{MDH} 24) was only labelled under these conditions, indicating that both substrates might be necessary for growth with a preference for CH_3Cl or the utilisation of CH_3Cl as carbon source and methanol for energy supply.

In order to summarise the results obtained within the *mxoF/xoxF*-type MDH phylotype community, different phylotypes were labelled under conditions where solely methanol was present and conditions where CH_3Cl was present. In the treatment solely supplemented with methanol the labelled phylotypes were most different to all CH_3Cl -supplemented treatments (solely or in the combined treatments), indicating that CH_3Cl -utilisers in the forest soil might be not highly diverse. Nearly all labelled phylotypes were affiliated to *xoxF* gene sequences than *mxoF* gene sequences, indicating the dominance of these MDH type in the forest soil. The minor labelling of *Beijerinckiaceae*-affiliated phylotypes raises the question of further important methylotrophic microorganisms in the acidic forest soil or the detection limit of MDH based molecular analyses. The strong labelling of several *Bradyrhizobiaceae*-affiliated and *Sinorhizobium*-affiliated phylotypes in all CH_3Cl -supplemented treatments indicates a high adaption of these microorganisms to CH_3Cl and suggests a dominant role in carbon turnover of members of the *Rhizobiales* here.

3.11.3. Identification of *cmuA*-possessing methylotrophs assimilating methanol and chloromethane

Concerning the *cmuA* gene sequence samples of the methanol/chloromethane SIP experiment all samples from the 'heavy' and 'middle' fractions of [^{12}C]- and [^{13}C]-isotopologue treatments of each treatment were distinct to each other as revealed in a nMDS plot (Figure 81) and as it was observed for 16S rRNA and *mxoF/xoxF* gene sequence samples.

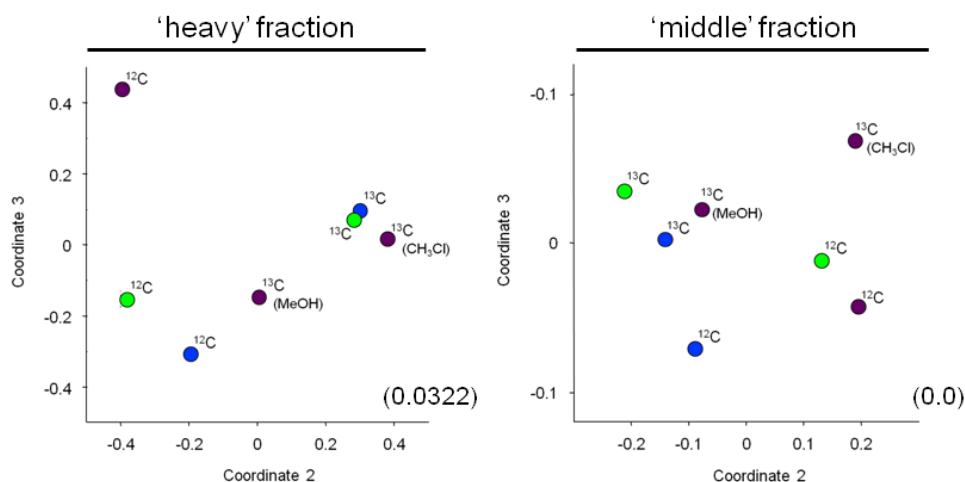


Figure 81 nMDS analyses of *cmuA* sequences from the 'heavy' and 'middle' fractions of the methanol/chloromethane SIP experiment.

Figures show analyses of relative abundances of all sequences in 'heavy' and 'middle' fractions of [^{12}C]- and [^{13}C]-treatments for *cmuA* sequences (based on a similarity cut-off value of 90 %). Stress values are given in brackets. All analyses are based on Bray-Curtis similarity index. Symbols according to the incubation: ●, solely MeOH; ●, solely CH_3Cl ; ●, MeOH & CH_3Cl . In the case of the combined incubation approaches the [^{13}C] source is noted next to the circle.

The amount of labelled taxa ranged from one phylotype in all treatments with [^{13}C]- CH_3Cl up to four different phlotypes in the combined treatment with [$^{13}\text{C}_1$]-methanol (Figure 80). One generally dominant phylotype in all treatments (i.e., OTU_{*cmuA*} 2; see Figure 80 & Figure 76B, Table A 44) was labelled in both approaches with [^{13}C]- CH_3Cl and comprises 64 % of the 'heavy' fraction *cmuA* phlotypes in the approach solely supplemented with [^{13}C]- CH_3Cl and 84 % of the 'heavy' fraction *cmuA* phlotypes in the approach with simultaneously supplemented [^{13}C]- CH_3Cl and methanol (Figure 80A). Phylogenetic analyses indicated that this phylotype might be affiliated to *Methylobacteriaceae* of which family members are known to utilise CH_3Cl even as sole source of carbon and energy [Doronina *et al.*, 1996] (Figure A 15). No further phylotype was labelled with [^{13}C]- CH_3Cl , indicating that species comprising this phylotype are specialised CH_3Cl -assimilating microorganisms and might play a crucial role in the CH_3Cl turnover in the forest soil. Apart from that suggestion OTU_{*cmuA*} 2 was also identified as labelled in the approach solely supplemented with methanol, suggesting that

methanol serves also as a carbon source (Figure 80). In addition, two further phylotypes were labelled in the approach solely supplemented with methanol resulting in 98 % of the 'heavy' and 7 % of the 'middle' fraction *cmuA* phylotypes as labelled (Figure 80A). Again, all these phylotypes were affiliated to the well known methylotrophic family *Methylobacteriaceae* (Figure A 15). One phylotype (OTU_{*cmuA*} 4) was also minor labelled, indicating a slower growth of this taxa or a high competition for methanol resulting in this observed delayed labelling (Figure 80A). In addition, OTU_{*cmuA*} 4 was detected as not highly abundant in the general *cmuA* phylotype community, emphasising the label and the role in methanol-derived carbon assimilation (Figure 76B). The other labelled phylotype in the approach solely supplemented with methanol was OTU_{*cmuA*} 3 that belongs to one of the two dominant phylotypes within the general *cmuA* phylotype community of the SIP experiment (Figure 80 & Figure 76B). The same phylotype was also labelled in the approach simultaneously supplemented with [¹³C₁]-methanol and CH₃Cl, indicating a preferred methanol assimilation (Figure 80). In the combined treatment with [¹³C₁]-methanol 57 % of the 'heavy' and 30 % of the 'middle' fraction *cmuA* phylotypes were labelled, and apart from the *Methylobacteriaceae*-affiliated phylotypes another phylotype (i.e., OTU_{*cmuA*} 6) was labelled (Figure 80A). This in the combined [¹³C₁]-methanol-supplemented treatment exclusively labelled phylotype is indicated to be affiliated to *Hyphomicrobiaceae* (Figure A 15). In general, OTU_{*cmuA*} 6 was only low abundant, but detectable in all treatments within the *cmuA* phylotype community (Figure 80B & Figure 76), and its labelling suggests that the putative *Hyphomicrobiaceae*-phylotype assimilates methanol but not CH₃Cl, although several members of this family are known to utilise CH₃Cl as sole source of carbon and energy [Doronina *et al.*, 1996; Nadalig *et al.*, 2011].

In order to summarise the results obtained within the *cmuA* phylotype community most phylotypes were affiliated to *Methylobacteriaceae* and only one phylotype was indicated to utilise CH₃Cl as carbon source, emphasising the specialisation of CH₃Cl-utilisers. This phylotype was also able to utilise methanol as carbon source. Moreover, the amount of labelled *cmuA* phylotypes regarding methanol was higher assuming a broader spectrum of methanol-assimilating microorganisms. Only one *Hyphomicrobiaceae*-affiliated phylotype was labelled but not in the treatment solely supplemented with [¹³C]-CH₃Cl, indicating that CH₃Cl-assimilating *Hyphomicrobiaceae* might play no important role in the CH₃Cl turnover in a forest soil and are more adapted to methanol.

3.12. Chloromethane degradation in different ecosystem types – a comparison of terrestrial and aquatic environments

Bacteria capable of utilising CH₃Cl were detected in several environments including pristine and contaminated soils [Doronina *et al.*, 1996; McAnulla *et al.*, 2001a; Borodina *et al.*, 2005], phyllosphere [Nadalig *et al.*, 2011], freshwater lake [McAnulla *et al.*, 2001a], and marine environments [Schäfer *et al.*, 2005]. Thus both, the ubiquity and the overall potential of CH₃Cl utilisation are obvious.

The CH₃Cl degradation of different ecosystem types was tested to estimate the role of forest soils as a terrestrial CH₃Cl sink. All environmental samples were not pre-incubated with CH₃Cl and surface water samples were not filtered or concentrated to achieve a more *in situ* relevant reflection.

Apart from the CH₃Cl degradation potential of different ecosystem types, also the possible endogenous formation of CH₃Cl was analysed. In all environmental samples CH₃Cl was endogenously formed (Figure 82). The formation of CH₃Cl was not continuous with the highest amounts detected at the beginning. Comparing the different ecosystem types marine environmental samples and the lakeshore samples revealed the highest amounts of endogenously formed CH₃Cl. However, endogenously formed CH₃Cl reached only marginal concentrations ranging up to approximately 2 µmol in total (Figure 82). Thus, the small amounts of endogenously formed CH₃Cl did not affect the recorded CH₃Cl degradation of the different ecosystem types (Figure 83).

In general, all environmental samples tested showed CH₃Cl degradation and an initial loss of CH₃Cl of approximately 20 % on average was detectable after 1 day assuming absorption of CH₃Cl onto surfaces and equilibration of the microcosms within the first hours (Figure 83). Both soil type approaches (i.e., forest soil and compost soil samples) revealed a higher degradation potential compared to all aquatic environments with the highest potential in the forest soil samples, since after 15 hours of incubation nearly all of the supplemented CH₃Cl was degraded (Figure 83).

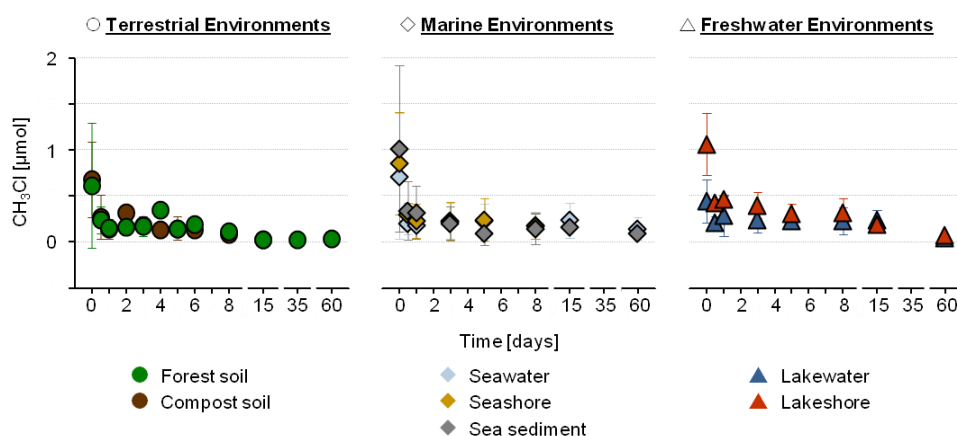


Figure 82 Comparison of endogenously formed chloromethane in different terrestrial and aquatic ecosystem type samples.

Overview on endogenously formed CH₃Cl in samples of different ecosystem types. Samples were sealed in gas tight bottles, gas samples were taken, but atmosphere was not flushed. Shown are average values; error bars represent standard deviation (n = 2).

RESULTS

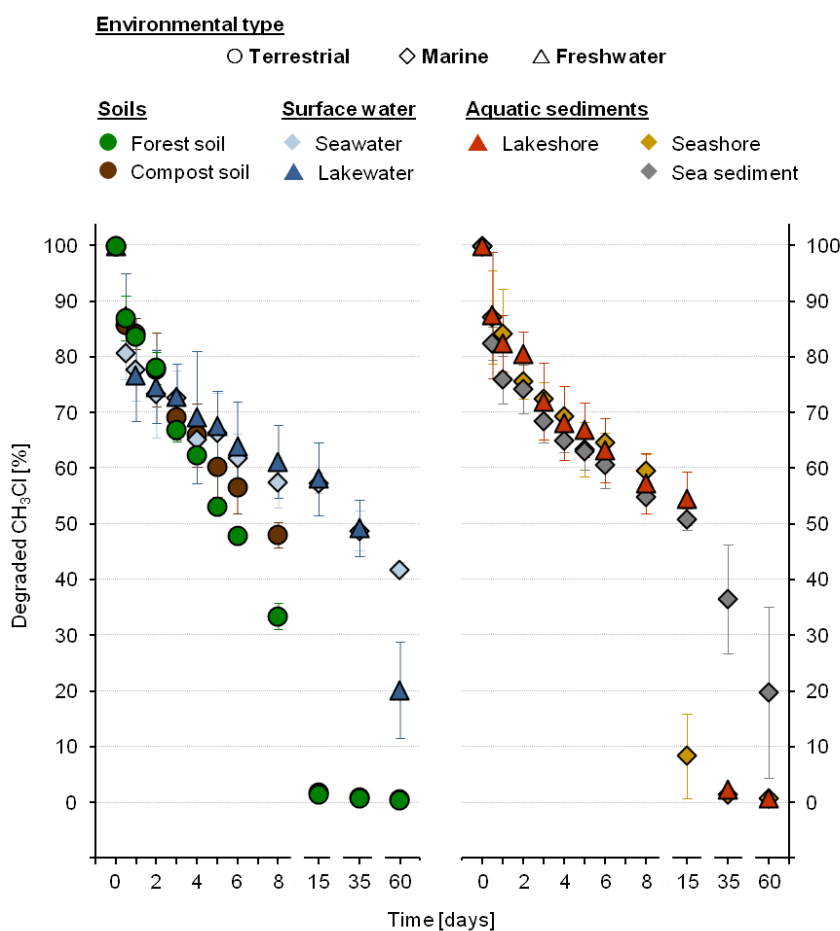


Figure 83 Initial chloromethane degradation potential of different terrestrial and aquatic ecosystem type samples.

Relative concentrations of CH_3Cl (mean values) over time as indicator for its degradation in different terrestrial and aquatic environmental samples (sample weight ~ 15 g). Initial concentration of applied CH_3Cl was 0.5 % (± 100 % of relative amount). Error bars represent standard deviation ($n = 2$).

In both shore sample types (i.e., lakeshore and seashore) the concentration of CH_3Cl was below 5 % (referred to the initial puls) after a longer incubation of 35 days. The seashore sample revealed even after 15 days significantly lower CH_3Cl concentrations indicating a slightly higher CH_3Cl degradation potential than the lakeshore sample (Figure 83). After 35 days of incubation both surface water samples (i.e., seawater and lakewater) revealed similar CH_3Cl degradation potentials (Figure 83). After a longer incubation (60 days) lakewater revealed a higher CH_3Cl degradation potential than the seawater (Figure 83). In addition, all shore and surface water samples showed an increasing turbidity during the whole incubation time indicating bacterial growth putatively caused by CH_3Cl . Degradation of CH_3Cl was also recorded for sea sediment samples. The CH_3Cl degradation was constant without any radical drop of CH_3Cl concentrations like it was observed for the seashore (i.e., time between 8 and 15 days revealed a loss of CH_3Cl of more than 50 %) (Figure 83). Thus, the sea sediment revealed a lowered degradation potential than the seashore, which act as another marine sediment related environment.

Recapitulating, soil samples were assumed to possess the highest CH₃Cl degradation potential followed by shore samples and even non-concentrated surface water of freshwater and marine environments revealed CH₃Cl biodegradation.

3.13. Halocarbons and aromatic compounds – the impact of toluene on chloromethane degradation

The two well studied CH₃Cl-utilising bacteria *Hyphomicrobium chloromethanicum* CM2 and *Methylobacterium extorquens* CM4 (synonym: *M. chloromethanicum* CM4) were isolated from soil at a petrochemical factory side [Doronina *et al.*, 1996]. Hydrocarbons such as aromatic compounds are compounds that are related to petroleum or natural gas. Thus, it is conceivable that aromatic compounds could have an impact on monohalomethane-utilisers.

An inhibitory effect of the aromatic compound toluene on the degradation of CH₃Cl and CH₃Br in natural seawater samples was shown [Goodwin *et al.*, 2005]. In addition, the authors described the marine isolate Oxy6 capable of CH₃Br biodegradation and growth on toluene. In general, for the biodegradation of CH₃Cl and CH₃Br the same pathway (cmu-pathway) is assumed. This cmu-pathway is initiated by a methyltransferase enabling the initial dehalogenation step of CH₃X compounds [Vannelli *et al.*, 1998; 1999]. Cultures of *Methylobacterium extorquens* CM4 grown on CH₃Cl are still capable to utilise CH₃Br, indicating that this pathway is common for the degradation of monohalomethanes. Genes for this cmu-pathway were also identified in *Hyphomicrobium chloromethanicum* CM2 emphasising this hypothesis [McAnulla *et al.*, 2001b].

A further correlation between halocarbons and aromatic compounds was demonstrated by Nelson and colleagues [Nelson *et al.*, 1987]. *Burkholderia (Pseudomonas) cepacia* strain G4 was capable of aerobic degradation of the halocarbon trichloroethylene (C₂HCl₃; abbreviation TCE) only in the presence of aromatic compounds such as phenol or toluene [Nelson *et al.*, 1987; Folsom *et al.*, 1990]. It was suggested that the aromatic compounds induce one or more enzymes that are required for the TCE degradation in strain G4 [Nelson *et al.*, 1987].

Since the focus of the present study was on a terrestrial environment, the impact of toluene on the degradation potential of forest soil was addressed. Low and high concentrations of CH₃Cl were tested as well as different concentrations of toluene. The biodegradation of CH₃Cl was already shown (see 3.9). An initial supplementation of 0.2 µM and 1 µM toluene resulted in a slight inhibition of the CH₃Cl biodegradation potential and a concentration dependent inhibitory effect could be also assumed (Figure 84). Contrary to this observation the biodegradation of higher amounts CH₃Cl (i.e., 1 % v/v; supplemented to the headspace) was not inhibited by toluene but seemed enhanced. This observed stimulation seemed to be concentration-dependent, in which the lowest concentration of toluene tested revealed the highest stimulatory effect (Figure 84).

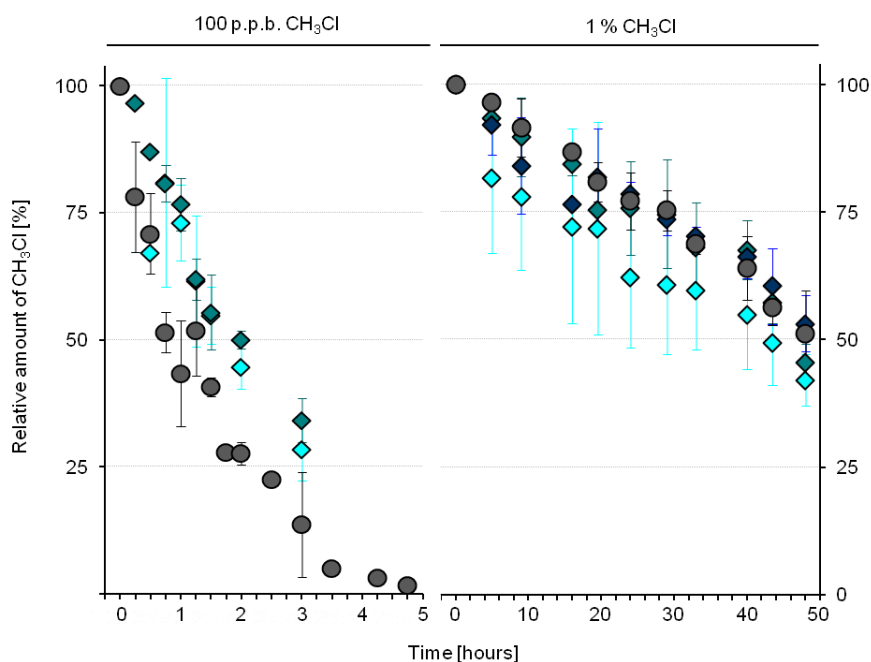


Figure 84 Chloromethane degradation potential of forest soil in the presence of toluene.

CH₃Cl concentrations over time as indicator for degradation of low (i.e., 100 ppb) and high (i.e., 1 %) amounts of halogenated gas in the presence of toluene. Toluene was present in different concentrations to evaluate the impact of this aromatic compound on the CH₃Cl degradation potential. Symbols: ●, relative CH₃Cl concentrations; ◇, relative CH₃Cl concentrations in the presence of toluene (◆, 0.2 μM toluene; ◆, 1 μM toluene; ◆, 50 μM toluene). Shown are average values; error bars represent standard deviation (n=2).

These observations should be interpreted with caution, since the results were not clear (meaning standard deviations were high), but with this approaches first insights as well as an indicative trend was demonstrated. Thus, aromatic compounds could provide an impact on the biodegradation of monohalomethanes.

The impulse to analyse the impact of toluene on the CH₃Cl degradation was promoted by the paper of Goodwin and colleagues, where the toluene inhibition in different marine environments (i.e., North Atlantic, North Pacific and Southern Ocean) was tested [Goodwin *et al.*, 2005]. In the present study no clear inhibition of the CH₃Cl degradation by toluene was obvious for the forest soil samples. For that reason the impact of toluene on the CH₃Cl degradation in other environmental samples covering terrestrial and aquatic environments was analysed. The degradation potential of all these environmental samples was already presented (see 3.12). According to Goodwin *et al.* 2005, only one concentration of toluene was chosen (i.e., 500 nM) for the inhibition assays. In general, neither an inhibition nor another effect on the CH₃Cl degradation caused by toluene was clearly detectable in any environmental sample (Figure 85). Contrary to Goodwin *et al.* 2005, also no inhibition of toluene on CH₃Cl degradation was indicative in the marine surface water samples. Interestingly, at an incubation time point of 15 days a clear difference between toluene-supplemented and unsupplemented replicates was obvious in the seashore sample

approach. However, this clear difference was not constant, since after 35 days of incubation again no differences were detectable (Figure 85).

Thus, the true effect of toluene on the CH_3Cl degradation in samples of different ecosystem types remains still unsolved. Detailed approaches including molecular techniques such as qPCR and rRNA based studies could be conducted to detect also a putative (co)utilisation and growth on toluene by the CH_3Cl -utilising bacteria.

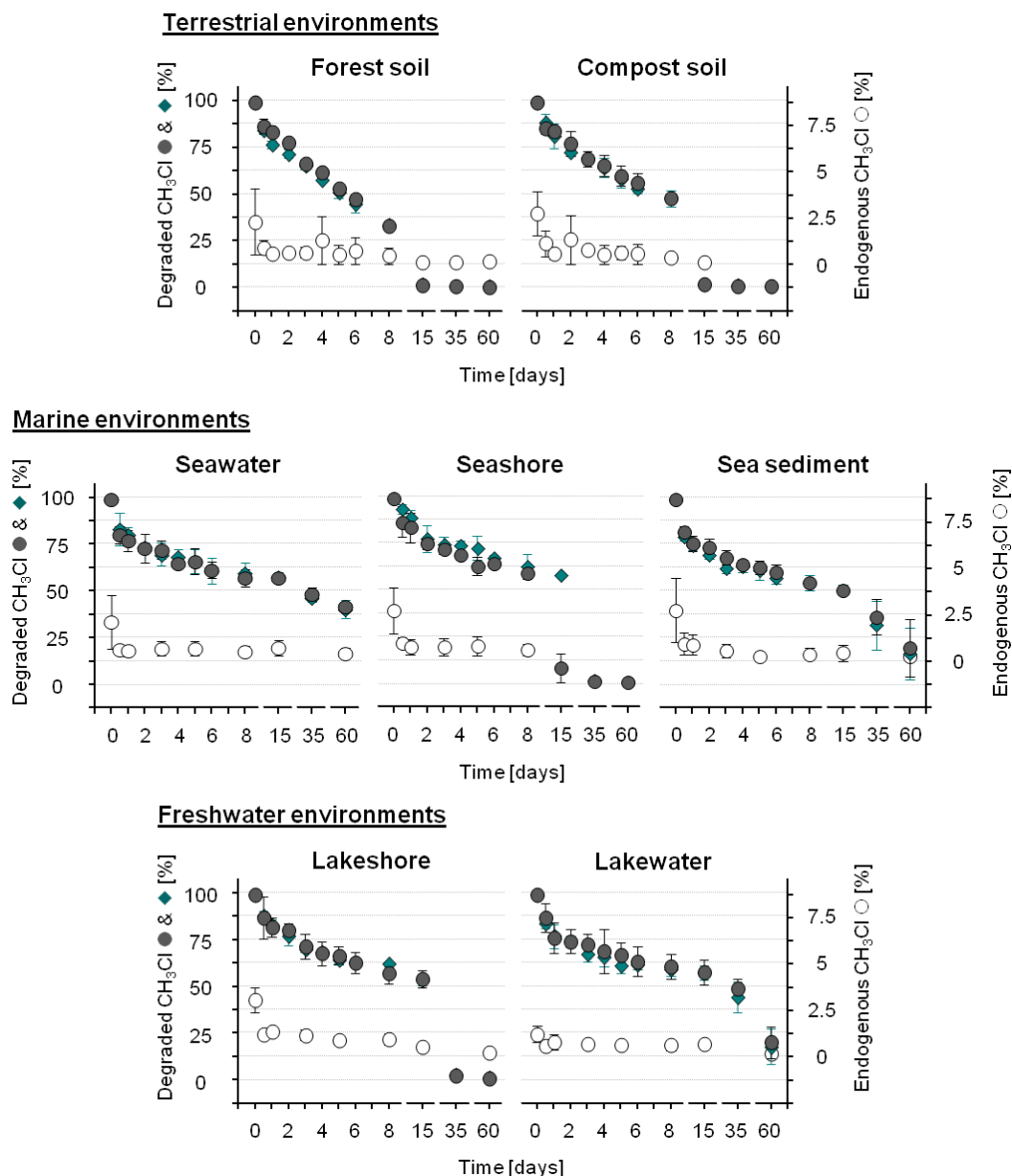


Figure 85 Degradation of chloromethane in different terrestrial and aquatic ecosystem type samples.

CH_3Cl concentrations over time as indicator for its degradation, the influence of toluene on these native degradation potentials and the amount of endogenously formed CH_3Cl referred to the amount of CH_3Cl applied in samples of different ecosystem types. Initial concentration of applied CH_3Cl was 0.5 % (\pm 100 % of relative amount). Symbols: ●, relative CH_3Cl concentration in environmental samples (corresponding with the initial degradation); ◆, relative CH_3Cl concentration in the presence of 500 nM toluene; ○, concentration of endogenously formed CH_3Cl (no additional CH_3Cl applied). Shown are average values; error bars represent standard deviation ($n = 2$).

4. DISCUSSION

According to the former sections also the discussion section is subdivided based on the respective C1 compounds (i.e., methane, methanol and chloromethane) and the microbial guild of methylotrophs utilising these compounds.

4.1. The methanotrophic community and their alternative substrate range in an acidic forest soil

Soils are the major sink for atmospheric methane due to the activity of methanotrophic microorganisms [Kolb *et al.*, 2005; Kolb, 2009b]. The predominant methanotrophs at the analysed sampling site are ‘high-affinity’ methanotrophs of the USC α group, which are to date not cultivated [Degelmann *et al.*, 2010]. USC methanotrophs are enigmatic, since estimated methane oxidation rates indicated lower values than effectively required for the maintenance of cell metabolism, arising the question how these methanotrophs can grow or even maintain under such substrate-limiting conditions [Degelmann *et al.*, 2010]. It might be possible that these ‘high-affinity’ methanotrophs can utilise other carbon substrates besides methane like it is known for some restricted facultative ‘low-affinity’ methanotroph such as *Methylocella* or *Methylocystis* [Dedysh *et al.*, 2005a; Dunfield, 2007 Dunfield *et al.*, 2010; Belova *et al.*, 2011; Im & Semrau, 2011]. Another possibility might be the utilisation of H₂ for energy conservation, enabling the preservation of the cell metabolism or even autotrophic growth under methane-limiting conditions as it was recently proven for methanotrophic *Verrucomicrobia* [Carere *et al.*, 2016; Mohammadi *et al.*, 2016].

4.1.1. The methane degradation potential by USC α and the presence of other methanotrophs

The *in situ* methane oxidation rates of the forest soil at the sampling site ‘Steigerwald’ were determined in a previous study conducted by Degelmann and colleagues [Degelmann *et al.*, 2009]. These *in situ* rates were comparable with methane oxidation rates measured by Smith and colleagues, who compared several North European soils [Smith *et al.*, 2000], emphasising that the forest soil of the ‘Steigerwald’ sampling area reflects an active and thus important methane sink. In addition, methanotrophs affiliated to USC α were predominant compared to other methanotrophs [Degelmann *et al.*, 2010]. Thus, a high and effective methane oxidation potential of soil slurries was expected in the long-term incubation experiment concentrating on ‘high-affinity’ USC α methanotrophs.

Within the first 10 weeks of incubation the methane degradation potential was mainly constant. However, after 10 weeks of incubation the degradation potential decreased and was lowest after 14 weeks (see 3.1). This decline of methane oxidation was not correlated

with the abundance of methanotrophs affiliated to USC α since gene copies of the USC α -specific *pmoA* gene revealed no dramatic collapse after longer incubation time (at least for 14 weeks of incubation). Contrary, the major decline of USC α -specific *pmoA* genes was obvious at the beginning between t_0 and the first sampling time point after 6 weeks of incubation. The supplementation of methane rather triggered USC α methanotrophs, since their relative abundance increased over time. Thus, the observed decrease of the methane degradation potential after 10 week of incubation must be explained by other reasons.

It might be possible that other methanotrophs besides the 'high-affinity' methanotrophs were also addressed during the incubation period. By supplementing methane to a final mixing ratio of 200 ppm it was expected to mainly address 'high-affinity' methanotrophs, although the amount of methane was 100-times higher than atmospheric methane concentrations. Known cultivated methanotrophs are 'low-affinity' methanotrophs that were only isolated using high methane concentrations [King, 1993; Roslev & King, 1994; Schnell & King, 1995; Knief & Dunfield, 2005]. The 'behaviour' (i.e., methane oxidation activity) of some of these known 'low-affinity' methanotrophs was evaluated under low methane mixing ratios. For example, when incubated at concentrations of 1000 ppm methane *Methylococcus capsulatus* BATH, *Methylocapsa acidiphila* B2, and several *Methylobacter* species stopped their methane degradation activity [Knief & Dunfield, 2005]. However, some 'low-affinity' methanotrophs might persevere lowered methane concentrations such as *Methylocystis* strain L6 or *Methylosinus trichosporium* OB3b, whose methane oxidation rates only declined gradually over time when incubated at 100 ppm methane concentrations [Knief & Dunfield, 2005]. There are also some 'low-affinity' methanotrophs that revealed even increased methane oxidation rates under these substrate-lowered conditions such as some *Methylocystis* strains or *Methylomicrobium album* NCIMB 11123 [Knief & Dunfield, 2005]. In addition, two *Methylocystis* strains (DWT and LR1) were also able to maintain under atmospheric methane concentrations for several weeks (i.e., 10 weeks in the conducted experiment) [Knief & Dunfield, 2005]. The metabolic reason for the utilisation of low methane concentrations by 'low-affinity' methanotrophs is explainable by the presence of two isoenzymes of the pMMO – pMMO1 (low substrate affinity, methane oxidation at mixing ratios > 600 ppm) and pMMO2 (high substrate affinity, methane oxidation down to atmospheric concentrations) [Baani & Liesack, 2008]. Interestingly, Baani and Liesack reported even growth of *Methylocystis* sp. SC2 under methane concentrations between 10 and 100 ppm, wherefore these initial 'low-affinity' methanotrophs soften the classification of 'low-affinity' and 'high-affinity' methanotrophs. Thus, it is very likely that not only 'high-affinity' methanotrophs of the USC α group were addressed during the long-term experiment, but also 'low-affinity' methanotrophs possessing the 'high-affinity' pMMO2 such as some *Methylocystis* and *Methylosinus* strains.

The observed decline of the methane degradation potential might be further in accordance with a decline of these incidentally addressed 'low-affinity' methanotrophs. Unfortunately, no molecular data on such other methanotrophic species besides USC α are available in this

work to test this suggestion. The gradually decrease of bacterial genes (based on 16S rRNA) is no unequivocal explanation, since the consumption of endogenous carbon sources might lead to the gradual decline of all heterotrophic microorganisms.

In addition, a gradual consumption of endogenous carbon sources or essential nutrients might also represent another explanation for the decline in the methane oxidation potential. Independently if facultatively methanotrophic USC α -organisms exist, no further nutrients or trace elements were provided over the entire incubation period. Thus, a putative depletion of endogenous nutrients might have led to the observed decline in methane degradation, since methanotrophs might stop their activity and cell growth. Thus, they might persist and maintain only marginal cell metabolism, wherefore they were still detectable via DNA targeting approaches such as qPCR. The formation of resting states by USC α methanotrophs might be also conceivable. Cultivated 'low-affinity' methanotrophs such as *Methylosinus trichosporium*, *Methylosinus sporium*, *Methylocystis parvus*, and *Methylobacter* species are known to survive unfavourable conditions by forming species-specific resting states such as spores and cysts, and their activity can be restored under more favourable conditions [Whittenbury *et al.*, 1970b].

Apart from the putative depletion of nutrients, an accumulation of inhibitory substances during the incubation could also be possible. The long-term incubation was conducted in screw-capped natural-rubber-stopped flask. Nieman and colleagues reported toxic effects of butyl-rubber stoppers on the aerobic methane oxidation in aqueous samples caused by organic (i.e., benzyltoluene, phenylalkane isomers and benzothiazole) and inorganic (i.e., heavy metals, zinc) contaminants leaching from the butyl elastomer into the medium [Nieman *et al.*, 2015]. The organic and inorganic contaminants might be on the one hand potentially toxic to microorganisms [Giller *et al.*, 1998; Heipieper & Martínez, 2010; Segura *et al.*, 2010; Ytreberg *et al.*, 2010; Nieman *et al.*, 2015]. On the other hand, however, it might be possible that methanotrophs fortuitously utilised the organic compounds, since the substrate spectrum of the MMOs is not restricted to methane only and aromatic compound utilisation (i.e., benzoic acid) by *Methylocystis* strain M was reported [Colby *et al.*, 1977; Uchiyama *et al.*, 1989; Smith & Dalton, 2004]. The fortuitous utilisation of other substrates than methane could cause also a depletion of reducing equivalents that are necessary for the initial hydroxylation step of methane. Further the natural-rubber stoppers used might also contain other additives such as metal oxides added during the vulcanisation process [Mark & Erman, 2005]. Regrettably, no further information on the natural rubber stopper was provided by the supplier upon request (Ochs Gerätebau, Bovenden, Germany), wherefore this 'leaching hypothesis' is highly speculative.

Another possible explanation for the decreased methane degradation potential over time might be the slurry itself. Soil slurries are by definition supersaturated with water. However, the solubility of methane in water is only low (approximately 22 mg L⁻¹ at 25°C; <https://www.ncbi.nlm.nih.gov/pccompound>), and the transport of methane in water is 10'000 times

slower than in air resulting in a limited methane diffusivity [Whalen & Reeburgh, 1992; Castro *et al.*, 1995]. Additionally, a negative correlation of the soil water content, the destructed soil structure and methane uptake rates was already documented for different soil environments [Striegl, 1993; MacDonald *et al.*, 1996; Mancinelli, 1995; Smith *et al.*, 2000; Price *et al.*, 2003; Price *et al.*, 2004; Shresta *et al.*, 2012]. An ongoing inhibition of methane oxidation in a forest soil caused by water saturation was also observed by Price and colleagues [Price *et al.*, 2004], and a negative effect of soil slurries on ‘high-affinity’ methanotrophs was also observed by Pratscher and colleagues, but the authors gave no further explanation [Pratscher *et al.*, 2011]. However, the incubation as soil slurries was done to ensure homogenous and thus comparable conditions in terms of multi-carbon substrate availability.

As a last explanation it might be possible that the methane degradation potential was not lowered over time, but methanogenesis might occur elevating the measurable methane concentration and thus lead to falsified conclusions. Several studies concerning methanotrophs in soil ecosystems assume that it might be possible that methanotrophs grow on methane produced by methanogenic *Archaea* occurring in anoxic microzones in the soil or in the humus layer or during periodically anoxic conditions such as after rain fall events or flooding [e.g. Megraw & Knowles, 1987; Dunfield *et al.*, 1995; Yavitt *et al.*, 1995; Andersen *et al.*, 1998; Horz *et al.*, 2002]. Although it might be conceivable that during the long-term incubation small anoxic microzones occurred that were favourable for methanogens, it is, however, highly unlikely that methanogenesis occurred, since the applied conditions were not favourable for methanogens.

Taken together, no clear explanations for the decline in the methane degradation potential over time are obvious, but the presence of ‘low-affinity’ methanotrophs, which survived for a longer time at the provided methane concentrations but died off with longer incubation time, might be the most likely explanation.

Nevertheless, it is obvious that the amount of USC α methanotrophs was not lowered over the incubation time, suggesting no extinction of these ‘high-affinity’ methanotrophs in the soil slurries. The slight increase of USC α -specific *pmoA* gene numbers even suggests the incorporation of methane and thus cell growth of USC α methanotrophs under the conditions during the long-term incubation. However, in a comparable study (200 ppm methane supplied, 10 weeks of incubation) no incorporation of methane-derived ¹³C was detected into the nucleic acids of methanotrophic microorganisms assuming no cell growth [Pratscher *et al.*, 2011]. The enrichment of USC α methanotrophs is therefore not verified (as well as not excluded). However, it might be possible that methanotrophs – ‘low-affinity’ and ‘high-affinity’ – survived in the long-term incubation by the utilisation of H₂. Methanotrophic bacteria such as *Methylococcus capsulatus* BATH (γ) and *Methylosinus trichosporium* (α) can gain reducing equivalents from H₂ [Hanczár *et al.*, 2002]. In addition, even autotrophic growth of *M. capsulatus* BATH was reported, but autotrophy could not be confirmed [Baxter *et al.*, 2002]. H₂ is mainly produced during anaerobic processes [Conrad, 1999; Schwartz *et al.*,

2013] but the fixation of nitrogen might also provide internal H₂ that can support N₂-fixing methanotrophs such as *Beijerinckiaceae* or *Methylocystaceae* [Bothe *et al.*, 2010; Marín & Arahal, 2013; Webb *et al.*, 2013]. Since USCα are affiliated to such N₂-fixing taxa, it might be possible that N₂-fixation might support these 'high-affinity' methanotrophs and enables the maintenance under methane-limited conditions. However, since no enrichments or cultured isolates of 'high-affinity' methanotrophs are available, all these assumptions remain speculative rendering USCα methanotrophs still enigmatic.

Although the 'high-affinity' methanotrophs belonging to the USCα group were addressed during the long-term incubation experiment, further other molecular marker genes were targeted to evaluate the diversity of methanotrophs in the soil. The marker genes tested were *pmoA* and *mmoX*, which encode for the two types of MMOs (see 1.6.1, 2.5.7.1). Several attempts to amplify *pmoA* and *mmoX* in the native acidic forest soil were made, but all attempts were not satisfying. The amplification of *mmoX* based on a 'general primer pair' of Hutchens and colleagues failed, indicating that the amount of *mmoX* in the soil might be under the detection limit. However, conducting qPCRs with a *Methylocella* specific *mmoX* primer pair [Kolb *et al.*, 2005] genes were detected (see 3.5.2.4). Thus, besides the 'high-affinity' USCα methanotrophs also methanotrophs affiliated to *Methylocella* species (*Beijerinckiaceae*, type II methanotrophs) seems to be present in the acidic soil. This observation was also emphasised by further molecular studies based on 16S rRNA gene sequences where a phylotype affiliated to *Beijerinckiaceae* was revealed as a central methylotrophic organism in the acidic soil (see 3.7.1.1 & 3.11.1; for further discussion on the phylotype please refer to 4.2.1). In the case of *pmoA* three different primer pairs were used with different features in terms of *pmoA* amplification biases (see 2.5.7.1). Almost always small bands or smears were visible after PCR, indicating that the amount of *pmoA* was not under the detection limit. However, further molecular steps such as the purification of amplicons leads to losses of amplicons rendering further analyses impossible.

Apart from both MMO marker genes *pmoA* and *mmoX* another gene *pxmA* encoding for a still enigmatic pXMO was analysed. This gene is a homolog of *pmoA* and *amoA* (encoding for a subunit of the ammonium monooxygenase [Hanson & Hanson, 1996]) with a still unknown function [Tavormina *et al.*, 2011; Knief, 2015]. It might be possible that the pXMO plays a role in detoxification processes or that the primary substrate might be similar to methane or ammonium [Tavormina *et al.*, 2011]. Genes of *pxmA* were mainly found in gammaproteobacterial type I methanotrophs affiliated to *Methylomonas*, *Methylomicrobium*, and *Methylobacter* [Tavormina *et al.*, 2011], but genomic studies revealed the presence of *pxmA* also in a strain of the alphaproteobacterial type II methanotroph *Methylocystis rosea* [Knief, 2015]. However, attempts to amplify *pxmA* in the acidic forest soil were not satisfying and further molecular analyses of all obtained amplicons (smearish or thin bands) were impossible. Thus, the presence of pXMOs in the acidic forest soil is not rejected, but rather not assumed, since no evidence for gammaproteobacterial methanotrophs were obtained

based on methanotrophic marker genes or 16S rRNA gene sequences (refer to 2.5.7.2, 3.7.1.1 & 3.11.1).

Taken together, in the acidic forest soil microorganisms affiliated to the USC α might be the predominating group in the methanotrophic community as it was also observed by Degelmann and colleagues [Degelmann *et al.*, 2010]. The presence of the 'high-affinity' pMMO2 of some type II methanotrophs such as *Methylocystis* and *Methylosinus* was not analysed, wherefore these methanotrophs might also contribute to the methane sink in the soil. Other methanotrophs that possess different types of MMO (sMMO, pXMO) and different affinities ('low-affinity') to methane might be present, but seem to play only a minor role under *in situ* conditions.

4.1.2. Alternative substrates of USC α methanotrophs

To date all known facultatively methanotrophic organisms belong to the *Alphaproteobacteria*, more detailed to the families *Beijerinckiaceae* and *Methylocystaceae*. They are type II methanotrophs assimilating carbon via the serine cycle and possess the complete TCA cycle [Marín & Arahal, 2013; Webb *et al.*, 2013]. The alternative multi-carbon substrates known are mainly limited to acetate and other short fatty acids (up to C4 compounds, see Table 38).

Table 38 Substrate spectrum of known facultatively methanotrophic representatives.
substrates^a

organism	C1	C1	C2	C3	C4	C4	C2	reference	Isolation source	reference
	methane	methanol	acetate	pyruvate	succinate	malate	ethanol			
<i>Methylocella</i>										
<i>palustris</i>	+	+	+	+	+	+	+	Dedysh <i>et al.</i> , 2005a	Acidic peat bog	Dedysh <i>et al.</i> , 1998; 2000
<i>silvestris</i>	+	+	+	+	+	+	+	Dedysh <i>et al.</i> , 2005a	Forest soil	Dunfield <i>et al.</i> , 2003
<i>tundrae</i>	+	+	+	+	+	+	+	Dedysh <i>et al.</i> , 2005a	Peat / tundra soil	Dedysh <i>et al.</i> , 2004
<i>Methylocapsa</i>										
<i>aurea</i>	+	+	+	-	-	-	-	Dunfield <i>et al.</i> , 2010	Forest soil	Dunfield <i>et al.</i> , 2010
<i>Methylocystis</i>										
<i>bryophila</i>	+	+	+	w	-	-	w	Belova <i>et al.</i> , 2011	peat-bog lake	Belova <i>et al.</i> , 2013
<i>heyeri</i>	+	+	w	-	-	-	-	Belova <i>et al.</i> , 2011	peat-bog lake	Dedysh <i>et al.</i> , 2007
<i>echinoides</i>	+	+	w	-	-	-	-	Belova <i>et al.</i> , 2011	n.a. ^b	Bowman <i>et al.</i> , 1993
<i>hirsuta</i>	+	+	w	-	-	-	-	Belova <i>et al.</i> , 2011	aquifer	Lindner <i>et al.</i> , 2007
strain SB2	+	+	+	-	-	-	+	Im <i>et al.</i> , 2011	Spring bog	Im <i>et al.</i> , 2011

^a +, growth; -, no growth; w, weak growth; grey coloured background indicate preferred substrate (dark grey, reported; light grey, assumed based on the behaviour of *M. silvestris*)

^b n.a., not available

Metabolic pathways for the assimilation of the multi-carbon compounds have not been examined in detail [Vorobev *et al.*, 2014], but it is assumed that the multi-carbon substrates are converted into intermediates of the serine pathway and other following interlinked

pathways that funnel for example acetyl-CoA into the metabolism [Starai & Escalante-Semerena, 2004]. In addition, several other alternative substrates such as malate or pyruvate are also intermediates of metabolic pathways, restricting the utilisation of these substrates only to the question of entering the cell. Smaller substrates such as acetate can enter the cell via a specific permease or passive by diffusion [Gimenez *et al.*, 2003]. Thus, the ability of being facultatively methano- or methylotrophic depends more probably on the existence of specific permeases or transporter proteins for the different substrates than on the presence of metabolic pathways.

4.1.2.1. Acetate

The most promising alternative substrate for the 'high-affinity' methanotrophs of the USC α group might be acetate that is a major intermediate of anaerobic metabolisms in soil environments, and can exceed the concentration of atmospheric methane by far. The concentration of acetate in the soil or litter layer can reach up to millimolar ranges [Küsel & Drake, 1999; Duddleston *et al.*, 2002]. The utilisation of acetate requires its activation before carbon can be assimilated into biomass, and such metabolic steps are already present in methanotrophs [Starai & Escalante-Semerena, 2004; Semrau *et al.*, 2011]. All known facultative methanotrophs have at least two similarities: (i) they can utilise acetate, and (ii) they were mainly isolated from acidic environments (see Table 38). The more acidic an environment is, the more acetate is available in its protonated form (pKa of acetate 4.76; http://www.chem.wisc.edu/areas/reich/pkatable/pKa_compilation-1-Williams.pdf) and thus its diffusion across the cell membrane is more facilitated [Axe & Bailey, 1995]. The pH of the soil slurries of the long-term incubation were between 3.9 and 4.8, wherefore acetate might be easily penetrated cell membranes making it available as alternative substrate for methanotrophs. It should be also mentioned that under acetate-rich and acidic conditions (i.e., pH > pKa_{acetate}) protonated acetate (and other organic acids) might cause negative effects by the streamlined diffusion into the cell. The cytosolic pH of neutrophilic and acidotolerant *Bacteria* is more neutral around pH values of 7.5 to 7.7 [Krulwich *et al.*, 2011]. Protonated acetate will subsequently dissociate into its anion (CH₃COO⁻) and H⁺ under the cytosolic pH conditions, and the increasing enrichment of protons can cause the decay of the proton gradient that is necessary for ATP synthesis [Krulwich *et al.*, 2011]. Therefore high amounts of protonated acetate can clearly inhibit the bacterial metabolism. Since the amounts of supplemented acetate were only low (100 μ M), such inhibiting effects are rejected.

The supplementation of acetate inhibited methane oxidation potentials apparently and an increase in acetate concentrations lead to a standstill, indicating that the methanotrophic organisms in the soil slurries might prefer acetate over methane (see 3.2.1). This observation is contrary to a study of an alpine tundra soil where the presence of acetate stimulated methane oxidation [West & Schmidt, 1999]. Since at that time the presence of facultatively methanotrophs was not proven, the authors suggested rather that acetate might trigger methanogenesis, and thus the elevated methane concentrations were stimulative for

methanotrophs. Regrettably, molecular data revealing the diversity of methanotrophs or the abundance of methanogens in this soil are lacking, wherefore no further assumptions or speculations on the operating principle of acetate on the enhanced methane degradation can be made. In another study concentrating on methanotrophs in a forest soil the utilisation of acetate by the 'high-affinity' USC α methanotrophs was demonstrated [Pratscher *et al.*, 2011]. However, acetate had no effect on the methane degradation, which indicates that the USC α methanotrophs might utilise methane and acetate simultaneously without any preference. An inhibitory effect of acetate on the methane degradation was observed in a mire soil [Wieczorek *et al.*, 2011]. The dominant methanotrophs detected in this study were affiliated to *Methylocystis* species (*M. bryophila* and *M. heyeri*) capable of utilising acetate, and thus a preferential use of acetate over methane might be possible. However, in summary the impact of acetate on the methane degradation potential of a methanotrophic community is not unequivocally evident.

Additionally, different behaviours concerning the acetate utilisation exist also along the facultative methanotrophs. For example, species of *Methylocystis* prefer methane over acetate if only one substrate is available, but if both substrates were simultaneously present acetate was consumed faster and the methane degradation was slowed down [Belova *et al.*, 2011]. This preference of acetate might be due to the requirement of reducing power for the methane oxidation, which strongly limits growth on methane if the concentration of methane is low [Anthony, 1982]. Thus, acetate might represent a more efficiently substrate at least on the level of reducing power supply. In the case of *Methylocystis* species the authors suggest that the utilisation of acetate might be a survival strategy if the concentrations of methane are not favourable, allowing these methanotrophs to maintain the methane oxidation machinery and enabling them to respond quickly on elevated methane concentrations [Belova *et al.*, 2011]. Another example for the acetate utilisation by facultative methanotrophs represents *Methylocella silvestris* BL2 that prefers acetate over methane [Dedysh *et al.*, 2005a]. The presence of acetate even inhibits the methane degradation rates dramatically [Dedysh *et al.*, 2005a]. If acetate is no longer available, the methane oxidation rates recover quickly, reaching even higher rates than before acetate supplementation. The expression of sMMO gene transcripts was shown being dependent on the presence or absence of methane rather than acetate [Theisen *et al.*, 2005]. This indicates that *Methylocella* species might possess a regulation mechanism that prefers acetate but is not working on gene expression levels. It was also observed, that the inhibitory effect of acetate on the methane degradation turns into a stimulation of methane degradation after a longer time caused by promoted cell growth rather than enhanced activities emphasising the preference of acetate over methane again.

In the current study of the long-term incubation the USC α -specific *pmoA* gene numbers increased slightly over time (see 3.2.1). Since USC α -specific *pmoA* gene numbers also increased under strict methanotrophic conditions, cell growth based on acetate is rejected. This is also in accordance with Pratscher and colleagues, who could also not verify cell growth of USC α methanotrophs caused by acetate [Pratscher *et al.*, 2011]. The inhibitory

effect of acetate on the methane degradation was obvious in the long-term incubation during mixed substrate conditions (methane and acetate were simultaneously present) conditions suggesting that acetate might be used preferentially as it was also observed for all known facultatively methanotrophs [Dedysh *et al.*, 2005a; Belova *et al.*, 2011]. Under strict methanotrophic conditions the acetate treated slurry revealed at first enhanced methane degradation potential compared to the control (see 3.2.5). It might be possible that during the previous mixotrophic conditions acetate was incorporated into the storage compound PHB as it was demonstrated for the *Methylocystis parvus* strain MTS [Vecherskaya *et al.*, 2001; 2009], and the subsequently utilisation of PHB under strict, but limiting methanotrophic conditions provided additional energy. The gradually slowdown of methane degradation under methanotrophic conditions might be due to the depletion of intracellular PHB in the active methanotrophs resulting in reduced energy supply. Another stimulating effect of acetate on the methane degradation was also observed after 18 weeks under mixed substrate incubation with changed conditions (methanotrophic turns to mixed substrate conditions) (see 3.2.6). The supplementation of acetate immediately enhanced the methane oxidation potential of the soil slurry treatments. It might be conceivable that the availability and utilisation of acetate increased the amount of reducing equivalents intracellular, and thus methane oxidation was no longer energy limited.

Taken together, acetate might be preferred by USC α methanotrophs under mixed substrate conditions as it was described for facultative methanotrophs [Dedysh *et al.*, 2005a; Belova *et al.*, 2011]. It might be possible that acetate is used to gain enough energy for methane oxidation, and that acetate is also incorporated into storage compounds that provide energy under unfavourable conditions [Vecherskaya *et al.*, 2001]. However, since no organism of the 'high-affinity' USC α methanotrophs is cultured yet, all these considerations remain still speculative and are only based on the knowledge gained from phylogenetic closely related methanotrophic isolates. Additionally, no statements on the methanotrophic diversity during the long-term incubation can be made, since only 'high-affinity' USC α methanotrophs were targeted by molecular analyses.

An effective strategy to enrich and even isolate the enigmatic 'high-affinity' USC α methanotrophs might be a combination of a selective long-term incubation of soil under low methane-mixing ratios for more than 10 weeks, since also 'low-affinity' methanotrophs can preserve under harsh conditions for several weeks [Knief & Dunfield, 2005], with sporadically acetate supplementations. During this 'selective' time other heterotrophic microorganisms that might compete for acetate should be reduced in their abundance resulting in a competitive advantage for 'high-affinity' USC α methanotrophs. Finally, growth of these methanotrophs could be triggered by subsequent mixed substrate conditions since, methane might be essential, but methanotrophic conditions only could be energy limited [Anthony, 1982] resulting in growth restriction.

4.1.2.2. n-Alkanes

Methane is the simplest alkane and its oxidation is facilitated by a methane monooxygenase (pMMO and/or sMMO). It has been reported that the substrate spectrum of MMOs is not restricted to methane only, wherefore a fortuitous oxidation of alkanes might occur if both compounds are present [Colby *et al.*, 1977; Stirling & Dalton, 1979; Smith & Dalton, 2004]. The MMO of *Methylococcus capuslatus* BATH was shown to hydroxylate n-alkanes (C1 - C8) to their corresponding 1- and 2-alcohols [Colby *et al.*, 1977]. However, all enzymatic tests revealed that the specific activity of the MMO of *Methylococcus capuslatus* BATH, *Methylosinus trichosporium* OB3b and *Methylomonas methanica* was always lowered if an n-alkane was the substrate compared to assays where methane was the substrate [Colby *et al.*, 1977; Stirling & Dalton, 1979]. Additionally, all these enzymatic tests were performed with purified proteins and not with methanotrophic cell cultures. Thus, in intact methanotrophic cells the first crucial step for the utilisation of n-alkanes is entering the cell, since MMOs are not extracellular. Also the enzyme assays were conducted under 'one-substrate' conditions that are also altering the enzyme activity compared to conditions in which more than one suitable substrates are present. However, the majority of all known facultative methanotrophs are not reported to utilise n-alkanes (see references in Table 38). The pMMO is evolutionary related to the ammonia monooxygenase of nitrifying microbes [Holmes *et al.*, 1995], but other monooxygenases (HMO, hydrocarbon monooxygenase) of the same superfamily that oxidise short chain hydrocarbons form only distantly related clusters in phylogenetic trees [Knief, 2015]. For example, a butane monooxygenase has less than 50 % amino acid similarity to the MMO and AMO [Sayavedra-Soto *et al.*, 2011], and a monooxygenase of a *Gammaproteobacteria* was not able to oxidise methane [Suzuki *et al.*, 2012]. In the current study n-alkanes also did not alter the methane degradation potential under all conditions tested (long-term incubation under mixotrophic, strictly methanotrophic conditions, and changed substrate availability conditions). Marginally increased numbers of USC α -specific *pmoA* gene numbers indicated no cell growth caused by n-alkanes. Thus, n-alkanes are obviously no alternative substrate for 'high-affinity' methanotrophs.

4.1.2.3. Sugars (D-cellobiose and D-xylose)

Plant cell walls consist of cellulose and hemicelluloses, making these polysaccharides the most abundant components of biomass on earth, and several microorganisms are capable of the degradation of these molecules [Lynd *et al.*, 2002; Scheller & Ulvskov, 2010]. The plant dry weight typically composes 35 - 50 % cellulose and 5 - 30 % structural biopolymers such as hemicelluloses or lignin [Lynd *et al.*, 2002]. Cellulose is a chemically homogeneous linear biopolymer of up to 10'000 β -1,4-linked-D-glucose units, but the structural subunit of cellulose is the disaccharide cellobiose [Schwarz, 2001]. Conversely, hemicellulose has a heterogeneous structure with β -1,4-linked backbones of different subunits such as xylans that are polysaccharides of D-xylose units [Scheller & Ulvskov, 2010]. For that reason

cellobiose and xylose are abundant in soil environments and thus might be putative alternative substrates for methanotrophic organisms. In the long-term incubation no effects up to a gradually inhibition of the methane degradation potential was observed for both sugars tested (see 3.2.2). At least cellobiose might act as growth substrate for several heterotrophic microorganisms, since cell numbers based on 16S rRNA increased. However, growth of USC α methanotrophs was not observed. Thus, both sugars tested are assumed to be no alternative substrates (neither for dissimilation nor for assimilation) of the 'high-affinity' methanotrophs. This finding is not unexpected, since all known facultative methanotrophs could not utilise sugars (refer to the references in Table 38). The utilisation of sugars might be restricted by the uptake of these compounds into the cell. Membrane transporters might be essential in this case, but methanotrophs are often lacking such key enzymes for substrate uptake [Shishkina & Trotsenko, 1982; Wood *et al.*, 2004; Dedysh *et al.*, 2005a; Semrau *et al.*, 2011]. There is only one vague report of the utilisation of glucose by putative facultative methanotrophs isolated from soils affiliated with *Gamma*- and *Alpha*-*proetobacteria*, but apparently none of these exceptional strains still exists, rendering verification impossible [Semrau *et al.*, 2011]. Additionally, there is one example of a 'low-affinity' methanotrophic bacterium, in detail the filamentous bacterium *Crenothrix polyspora* related to the gammaproteobacterial methanotrophic type I organisms, utilising methane and putatively also glucose [Stoecker *et al.*, 2006]. However, the intensity of glucose utilisation was not further proven and *Crenothrix polyspora* seems to be restricted to freshwater environments wherefore this organism is only a sparse example for facultative methanotrophy in terms of forest soils. In general, the utilisation of sugars is not excluded by other facultatively methylotrophic taxa such as *Methylohabdus multivorans* [Doronina *et al.*, 1995], *Methylosula polaris* [Berestovskaya *et al.*, 2012], and several *Methylobacterium* species [Kelly *et al.*, 2013], but based on the long-term incubation experiment in the current study the hypothesis that sugars are alternative substrates for methanotrophs is rejected.

4.1.2.4. Other C1 compounds (methanol and methylamine)

Methane is hydroxylated to methanol during the initial step of methanotrophy. Thus, the utilisation of methanol by methanotrophs is not unexpected, since enzymes necessary for the utilisation (i.e., assimilation and dissimilation) of methanol are already present in methanotrophic cells. Methanol oxidation provides also energy for the energy limited step of the methane oxidation [Anthony, 1982], and most methanotrophs utilise methanol if it is available [Bowman *et al.*, 1993]. However, too high concentrations of methanol are inhibitory and some methanotrophs are not able to grow on methanol as sole source of carbon and energy due to the toxicity of methanol itself or the accumulation of the toxic intermediate formaldehyde [Whittenbury *et al.*, 1970a; Wilkinson *et al.*, 1974; Linton & Vokes, 1978; Best & Higgins, 1981; Cornish *et al.*, 1984; Im *et al.*, 2011a]. Growth inhibition and toxication of methanotrophs caused by supplemented methanol is rejected in the current long-term incubation, since methanol concentrations were always low (100 – 500 μ M per pulse). Thus,

it is conceivable that the presence of methanol might affect the methane degradation of methanotrophs in either a stimulatory way, i.e., methanol oxidation provides more energy, or in an inhibitory way, i.e., methanol is the preferred substrate over methane. No effects on the methane degradation potential were obvious in the methanol-treated incubations during mixed substrate conditions (i.e., methane and methanol are present) indicating that (i) methanol might be not utilised at the expense of methane (i.e., ceasing of methane-utilisation) and (ii) the enhanced availability of energy did not increase methane oxidation potential. This observation is in accordance with a study conducted by Jensen and colleagues 1998 and a study conducted by West and Schmidt 1999, who could not observe an increase of methane oxidation rates in soil samples when methanol was present [Jensen *et al.*, 1998; West & Schmidt, 1999]. Under strict methanotrophic conditions, the methanol-treated slurry revealed a higher methane degradation potential compared to the control (see 3.2.5), assuming that methanol indeed support 'high-affinity' USC α methanotrophs as it was also reported for a soil that was incubated under methane-free atmosphere [Jensen *et al.*, 1998]. In addition, methanol helped also to maintain atmospheric methane oxidation rates in a soil [West & Schmidt, 1999]. Under changed substrate conditions (methanotrophic turns to mixed substrate conditions) the supplementation of methanol slowed the methane degradation down (see 3.2.6). It might be possible that the availability of methanol resulted in a short-term but preferred utilisation of methanol over methane. An inhibition of the methane oxidation by methanol was also obvious in soil samples, but was totally recovered after 98 % of the methanol was consumed [West & Schmidt, 1999]. Thus, the supplementation of methanol might lead to a short-term inhibition of methane oxidation, but did not alter methane oxidation rates over time, indicating that methanol might not cause extensive growth of 'high-affinity' methanotrophs. In the current study, the supplementation of methanol resulted only in a gradually and slight decrease of USC α -specific *pmoA* gene numbers over time (see 3.2.3). The increase of 16S rRNA gene numbers indicated that methanol caused also growth of other methanol-utilising methylotrophic organisms in the soil that might compete with methanotrophs. Thus, it might be possible that the high competition for methanol in a soil environment might hamper methanotrophs *in situ*. In addition, low methanol concentrations are also reported to support 'low-affinity' methanotrophs such as *Methylocystis* strain H2s (now *M. bryophila* [Belova *et al.*, 2013]) and help to maintain methane oxidation under atmospheric conditions [Belova *et al.*, 2011].

Apart from methanol also methylamine might be a putative C1 compound that could affect methane degradation, since some methanotrophs are capable of using this substrate [Bowman *et al.*, 1993]. The interface of methane-derived carbon and methylamine-derived carbon is on the level of formaldehyde, and the enzyme necessary for the initial step of methylamine utilisation is different than the initial enzymes for methane or methanol utilisation. In addition, methylamine can also serve as nitrogen source for methylotrophs providing an additional benefit [Bowman *et al.*, 1993]. In the current long-term incubation the supplementation of methylamine did not affect the methane oxidation potentials under mixed

substrate conditions over time, but USC α -specific *pmoA* gene numbers were lowered compared to the methanotrophic controls. An effect causing population decrease but activity increase is hardly conceivable, but could explain this observation. It might also be possible that other methanotrophs that were not targeted by the qPCR assay of USC α were triggered by methylamine. However, along the methanotrophs only a handful of species are capable in methylamine utilisation (see Table 39 and references therein). Along the methylotrophic *Betaproteobacteria* several species are capable of utilising methylamine, but they cannot use methane [Doronina *et al.*, 2013].

Table 39 Methylamine utilisation by methano- and methylotrophs.

The table shows only a selection and focuses on alphaproteobacterial methanotrophs.

<i>methanotrophic Alphaproteobacteria</i>			<i>methanotrophic Gammaproteobacteria</i>		
<i>Beijerinckiaceae</i>			<i>Methylococcaceae</i>		
	Methylamine utilisation	reference		Methylamine utilisation	reference
<i>Methylocella</i>			<i>Methylobacter</i>		
<i>palustris</i>	No	Dedysh <i>et al.</i> , 2000	<i>agilis</i>	Yes	Bowman <i>et al.</i> , 1993
<i>silvestris</i>	Slow growth	Dunfield <i>et al.</i> , 2003	<i>Methylomonas</i>		
<i>tundrae</i>	Slow growth	Dedysh <i>et al.</i> , 2004	<i>aurantica</i>	Yes	Bowman <i>et al.</i> , 1993
<i>Methylocapsa</i>			<i>Methylococcus</i>		
<i>acidiphila</i>	No	Dedysh <i>et al.</i> , 2002	<i>capsulatus</i>	Some strains	Bowman <i>et al.</i> , 1993
<i>aurea</i>	No	Dunfield <i>et al.</i> , 2010	<i>Methyloferula</i>		
<i>palsarum</i>	No	Dedysh <i>et al.</i> , 2015	<i>stellata</i>	No	Vorobev <i>et al.</i> , 2011
<i>Methylocystaceae</i>			<i>methylotrophic Betaproteobacteria</i>		
	Methylamine utilisation	reference	<i>Methylophilaceae</i>		
				Methylamine utilisation	reference
<i>Methylocystis</i>			<i>Methylophilus</i>		
<i>bryophila</i>	n.d.	Belova <i>et al.</i> , 2013	<i>methylotenera</i>	Yes	Kalyuzhnaya <i>et al.</i> , 2006
<i>heyeri</i>	n.d.	Dedysh <i>et al.</i> , 2007	<i>mobilis</i>		
<i>echinoides</i>	No	Bowman <i>et al.</i> , 1993	<i>Methylbacillus</i>		
<i>hirsuta</i>	No	Lindner <i>et al.</i> , 2007	<i>flagellatus</i>	Yes	Doronina <i>et al.</i> , 2013
strain SB2	No	Im <i>et al.</i> , 2011	<i>Methylphilus</i>		
<i>parvus</i>	No	Bowman <i>et al.</i> , 1993	<i>methylotrophus</i>	Yes	Jenkins <i>et al.</i> , 1987
<i>rosea</i>	n.d.	Wartiainen <i>et al.</i> , 2006	<i>Methylosinus</i>		
<i>Methylosinus</i>			<i>trichosporium</i>	No	Bowman <i>et al.</i> , 1993
<i>trichosporium</i>	No	Bowman <i>et al.</i> , 1993	<i>sporium</i>	N source	Bowman <i>et al.</i> , 1993
<i>sporium</i>	N source	Bowman <i>et al.</i> , 1993			

grey background indicates facultatively methanotrophs (see also Table 38)

grey scripture indicates facultatively methylotrophs but incapable in methane-utilisation

Thus, the utilisation of methylamine among the methanotrophs remains an exception, and the assumption of other methanotrophs being responsible for the methane degradation potential in the slurries is rejected. Under strict methanotrophic conditions the methane

degradation was enhanced (see 3.2.5). It might be possible that methylamine somehow stimulated methanotrophs in terms of the formation of storage compounds based on methylamine. But as already described methylamine utilisation along methanotrophs is the exception. Under changed substrate conditions (methanotrophic turns to mixed substrate conditions) no effect was obvious after the supplementation of methylamine (see 3.2.6). Thus, the effect of methylamine remains inconclusive. Finally, methylated amines are mainly generated in aquatic environments and most methylamine utilisers were also isolated from such environments [Chistoserdova, 2015; Doronina *et al.*, 2013], marginalise methylamine as an alternative substrate for methanotrophs in forest soils.

4.1.2.5. Aromatic compounds (vanillic acid and guaiacol)

Lignin is the most abundant polymer on earth after cellulose and wood or other vascular plant tissue contain 20 - 30 % lignin. It has a heterogeneous structure and arises biosynthetically from three different precursor alcohols, i.e., coumaryl alcohol (*p*-hydroxycinnamyl), coniferyl alcohol (4-hydroxy-3-methoxycinnamyl), and sinapyl alcohol (3,5-dimethoxy-4-hydroxycinnamyl) [Kirk & Farrell, 1987]. During the microbial degradation of the complex lignin structure aromatic compounds that are derivatives of these lignin units might become available for other microorganisms incapable in lignin degradation. Thus, vanillic acid (4-hydroxy-3-methoxybenzoic acid) and guaiacol (2-methoxyphenol) might become available as derivative compounds of coniferyl alcohols. These compounds also represent natural monomeric constituents of degraded wood and humus [Kirk & Farrell, 1987; Dorrestijn & Mulder, 1999; Keppler, 2000]. In the current study under mixed substrate conditions both aromatic compounds had effects on the methane oxidation potential, in detail vanillic acid stimulated and guaiacol inhibited (see 3.2.4). Under strict methanotrophic conditions only the vanillic acid-treated slurry revealed a higher methane degradation potential than the control, whereas the guaiacol treated slurry revealed no difference (see 3.2.5). The observed stimulation of the methane oxidation by vanillic acid is in accordance with a previous observation for another forest soil by Dr. Gunnar Börjesson (pers. communication, data not published). However, the stimulatory mechanism remains unclear. The MMO of methanotrophs is able to utilise some aromatic compounds caused by its wider substrate affinity. As an example the MMO of *Methylosinus trichosporium* OB3b can oxidise vanillyl alcohol to vanillin and further to vanillic acid, but the substrate specificity is two times lowered compared to methane [Mountfort *et al.*, 1990]. It might be possible that the availability of formaldehyde as by-product of the aromatic compound degradation effected the methane oxidation potential. The degradation of several aromatic compounds is often facilitated by the formation of protocatechuate (protocatechuic acid, 3,4-dihydroxybenzoic acid) or catechol (1,2-dihydroxybenzene) before the aromatic ring structure is cleaved [Fuchs *et al.*, 2011]. During the conversion of vanillic acid to protocatechuate and guaiacol to catechol, respectively, formaldehyde is build which might be utilised by present methano- or

methylotrophic organisms. The inhibitory effect of guaiacol under mixotrophic conditions (see 3.2.4) might be caused by a preferred utilisation of this alternative substrate. However, this assumption is very vague, since the supplementation of guaiacol did not alter the methane oxidation potential under changed substrate conditions (methanotrophic turns to mixed substrate conditions) (see 3.2.6). Additionally, to date only one betaproteobacterial methylotroph, *Methylotenera mobilis*, was reported to grow slowly on guaiacol as substrate in its natural environment (lake sediment) but not in the laboratory [Kalyuzhnaya *et al.*, 2010]. *M. mobilis* is also not able to utilise methane as carbon or energy source as well as other aromatic compounds such as vanillic acid or benzoic acid [Kalyuzhnaya *et al.*, 2006; 2010]. Apart from *M. mobilis* another methylotroph, *Methylibium petroleiphilum*, is also reported to utilise aromatic compounds (i.e., MTBE compounds and its derivatives) and represents a facultative methylotroph [Nakatsu *et al.*, 2006]. However, the different observed effects on the methane oxidation potential (stimulation vs. inhibition) remain still enigmatic. Growth enhancing effects caused by vanillic acid as well as lethal effects caused by guaiacol cannot be verified, since USC α -specific *pmoA* gene numbers were constant over the incubation time indicating no growth-influencing impacts on the 'high-affinity' methanotrophs due to the aromatic compounds (see 3.2.4). Thus, either the activity of USC α methanotrophs or other methanotrophic organisms that were not targeted by the molecular methods were influenced.

Apart from fungi also some bacterial species related to *Streptomyces* can degrade wood, facilitating a mechanism that might be similar to the one of white-rot fungi [Antai & Crawford, 1981; Kirk & Farrell, 1987]. Further, other bacterial species related to *Pseudomonas*, *Nocardia* and *Corynebacterium* have also the ability to grow on lignin-related aromatic compounds [Janshekar & Fiechter, 1982]. Within the current study, the analysis of the microbial community revealed also phylotypes affiliated to these species being present in the acidic forest soil (see 3.5.1, Figure 48B & 3.10.2, Figure 74B), assuming that a microbial network might be present in terms of lignin degradation. Thus, methano- and methylotrophs might scavenge on by-products of the aromatic compound degradation.

4.1.3. Concluding remarks on the substrate range of 'high-affinity' methanotrophs (USC α)

In the current study the effects of several multi-carbon substrates on the methane degradation and on the presumable abundant 'high-affinity' methanotrophs affiliated to USC α -group were examined. The obtained results were not as clear as expected remaining 'high-affinity' methanotrophs still enigmatic. Especially, acetate and methanol might be suitable alternative substrates besides methane, but a prevalent high competition for these substrates is assumed putatively outcompeting 'high-affinity' methanotrophs. Other substrates might affect also 'high-affinity' methanotrophs indirectly, since by-products in their degradation could be utilised (e.g. aromatic compounds). Moreover, the existence of other

endogenous carbon source in the soil not yet identified could be assumed as well as the formation of resting stages by 'high-affinity' methanotrophs to endure harsh conditions.

Based on the obtained results the following model (Figure 86) was constructed to summarise the findings and putative substrate range of 'high-affinity' methanotrophs in an acidic soil of a temperate deciduous forest.

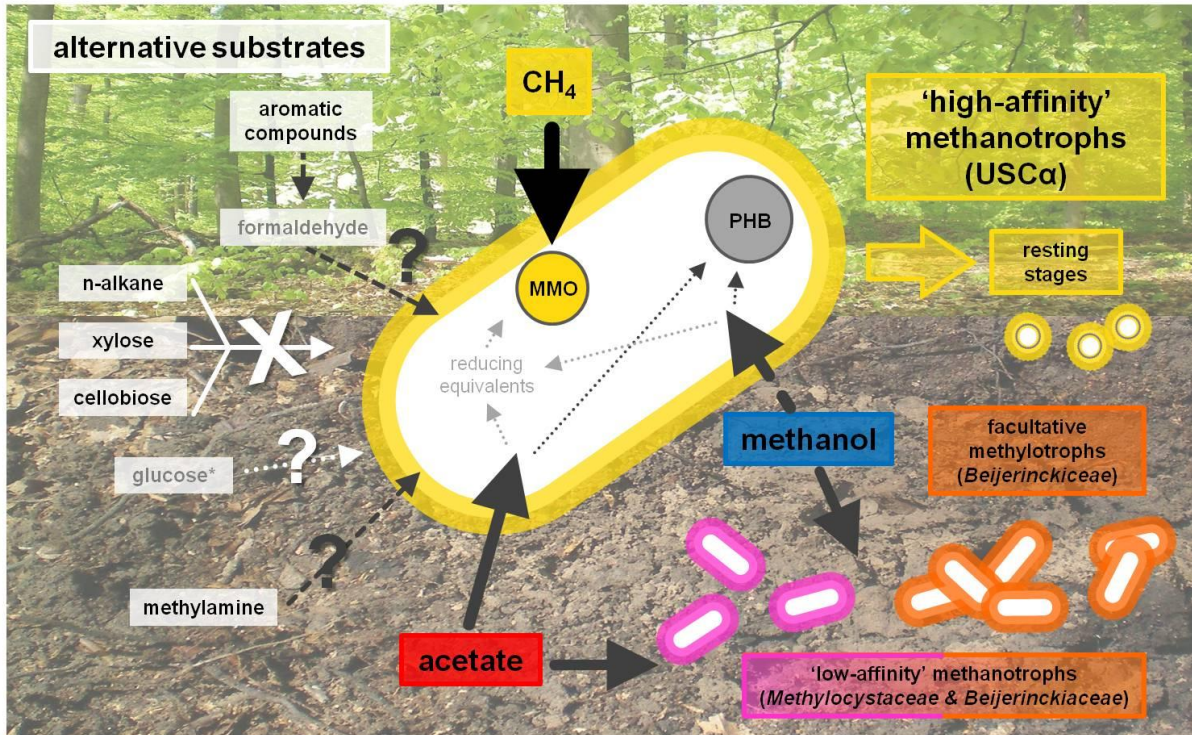


Figure 86 Substrate range of 'high-affinity' methanotrophs in an acidic soil of a temperate deciduous forest.

This figure summarises the obtained results of the conducted studies in terms of methanotrophs. For more information refer to the following sections: 1.6.2, 1.9, 3.1, 3.2, 4.1.

* Glucose was not tested in the experiments addressing methanotrophs, but in the conducted substrate SIP experiment (see 3.7.2.2) emerging evidence was given, that *Methylocystaceae*-affiliated phylotypes might utilise glucose. Based on the result glucose utilisation might be possible, since USCα are affiliated to *Methylocystaceae*.

4.2. The substrate range of methanol-utilising methylotrophs and methanol-derived carbon-utilising microorganisms in the acidic soil

Methylotrophic microorganisms have been studied over the last 100 years, have been shown to be ubiquitous and playing a crucial role in the global C1 metabolism of volatile organic compounds such as methane and methanol [Anthony, 1982; King, 1992; Kolb, 2009a; Chistoserdova & Lidstrom, 2013]. However, the crucial role of other not-methane-utilising methylotrophs seemed just overlooked, although terrestrial ecosystems are an important sink for atmospheric methanol having a direct impact on the atmospheric chemistry [Galbally & Kirstine, 2002; Kolb, 2009a; Stacheter *et al.*, 2013]. In addition, the role of eukaryotic methanol-utilisers in soils such as methylotrophic yeasts and fungi is hardly been researched [Lueders *et al.*, 2004; Kolb, 2009a]. Therefore factors defining the *in situ* abundance and activity of soil-derived methanol-utilisers are barely addressed. Since the majority of soil-derived methanol-utilisers are facultatively methylotrophic, the substrate range of these organisms might be one factor defining their ecological niche [Kolb, 2009a].

The conducted SIP experiment enabled the detection of methanol-utilisers and methanol-derived carbon-utilising microorganisms in the forest soil. Further, the comparative analysis of the different treatment approaches, i.e., strictly methylotrophic versus mixed substrate conditions, might provide insights into the consumption habits of these methanol-utilisers when multi-carbon substrates and methanol are simultaneously available as well as the evaluation of alternative multi-carbon substrates.

As expected, several primarily non-methylotrophic microbes such as phylotypes affiliated to *Rhodanobacter* (OTU_{16S} 300), *Burkholderia* (OTU_{16S} 361), *Mucilaginibacter* (OTU_{16S} 1073) were highly labelled in the multi-carbon substrate treatments (Figure 61). It might be possible that these organisms are utilising methanol as energy source, but SIP experiments cannot target the dissimilatory methanol-utilisation. Thus, methanol utilisation was not verified and these microorganisms were not further focused. The 'true' methanol-utilisers (i.e., the assimilation of methanol) were identified in the [¹³C₁]-methanol treatment and the congruent detection of the same phylotype in an alternative substrate treatment allowed for the assessment of a substrate spectrum. Thus, drawing conclusions on the trophic niches of the different methanol-utilisers occurring in the same soil and the assessment of a methanol-based food web was possible.

4.2.1. Methanol-utilising *Bacteria* and their multi-carbon substrate range

It is interesting, that a sufficient ^{13}C -assimilation and thus a labelling was achieved in a shortened incubation time (20 days) and with few amounts of methanol (20 mM) that were more than 100 times lower than in a comparable study by Radajewski and colleagues (i.e., oak forest soil [Radajewski *et al.*, 2000; 2002]) highlighting the adaption of the detected methylophilic *Beijerinckiaceae*-affiliated phylotype to lower methanol concentrations. This indicates also the existence of 'high-affinity' MDHs that were previously documented in grassland soils [Stacheter *et al.*, 2013].

The main methanol-utilising methylophilic in the analysed acidic forest soil was affiliated to *Beijerinckiaceae*, which is consistent with studies of other acidic systems such as an oak forest soil [Radajewski *et al.*, 2000; 2002] and environments dominated by peat / Sphagnum moss [Dedysh *et al.*, 2001; Morris *et al.*, 2002; Dedysh *et al.*, 2006; Gupta *et al.*, 2012] as well as with species descriptions of acidophilic methylophilic *Beijerinckiaceae* such as *Methylocella* spp. [Dedysh *et al.* 2000; Dunfield *et al.* 2003; Dedysh *et al.* 2004], *Methylocapsa* spp. [Dedysh *et al.*, 2002; Dunfield *et al.*, 2010; Dedysh *et al.*, 2015] and the latest described one-species-genera *Methylovirgula* [Vorob'ev *et al.*, 2009], *Methyloferula* [Vorob'ev *et al.*, 2011] and *Methylosorus* [Berestovskaya *et al.*, 2012].

The detected phylotype was indicated to be highly similar to *Methylovirgula ligni* (98 % sequence identity). However, due to the more general family-based analyses and the phylogenetic resolution limit of the analysed 16S rRNA gene fragment (444 bp), a detailed discussion on species-level is not possible, which prevents the unambiguous assessment of the substrate range. Therefore all findings were discussed on the basis of the knowledge on the family *Beijerinckiaceae* so far. However, the genera *Chelatococcus* and *Camelimonas* were excluded from all considerations on *Beijerinckiaceae*, since they are not capable of C1 compound utilisation and are nowadays assumed to be erroneously affiliated to this family [Dedysh *et al.*, 2016]. Further it is worth to mention that the family *Beijerinckiaceae* comprises isolates with remarkably different metabolic capacities – including chemoheterotrophy (*Beijerinckia*), facultative methylophilic (*Beijerinckia*, *Methylosorus*), 'restricted' facultative methanotrophy (*Methylocella*, *Methylocapsa*, *Methylovirgula*), and obligate methanotrophy (*Methylocapsa*, *Methyloferula*) – although they might have developed from a common ancestor [Marín & Arahal, 2013 and references therein; Tamas *et al.*, 2014; Dedysh *et al.*, 2016] (see 1.6.4). Nevertheless, the family *Beijerinckiaceae* was highly involved in methanol utilisation rendering this taxon the main methanol sink in the analysed forest soil.

The *Beijerinckiaceae*-phylotype was also indicated to utilise carbon derived from multi-carbon substrates. A closer look revealed that the family-based phylotype comprises several phylotypes at species-level that exhibit three different trophic types: obligately

methylotrophic, 'restricted' facultatively methylotrophic, chemoorganotroph (see 3.7.1.4). Among the facultatively methylotrophic *Beijerinckiaceae* the documented multi-carbon substrates are for example acetate (*Methylocella*, *Methylocapsa* [Marín & Arahal, 2013]), succinate, malate, pyruvate, and ethanol (*Methylocella*, *Methylovirgula* [Dedysh et al., 2005a; Vorob'ev et al., 2009; Marín & Arahal, 2013]) and thus the range is generally limited. However, two exceptions exist – (i) *Beijerinckia mobilis*, that is to date the only known methanol-utiliser of the metabolically versatile genus *Beijerinckia*, and (ii) *Methylosula polaris*, which exhibits a broad substrate range including sugars and polysaccharides [Dedysh et al., 2005b; Berestovskaya et al., 2012; Marín & Arahal, 2013]. Thus, acetate might be utilised by species such as *Methylocella* spp. and *Methylocapsa aurea*. The utilisation of both glucose and xylose might have been facilitated by *Beijerinckia* spp. (also non-methylotrophic ones) and *Methylosula* spp. preferring sugars.

It is well known that the sMMO of alphaproteobacterial methanotrophs can oxidise aromatic alcohols to their corresponding aldehydes and acids [Mountfort, 1990; Smith & Dalton, 2004], but ring cleavage and growth was not reported. Thus, the ability to assimilate carbon directly derived from the aromatic ring structures of vanillic acid as it was indicated for the detected phylotype might be facilitated by species like *Beijerinckia mobilis*, which possess the ability to grow on aromatic compounds [Chen et al., 1993]. However, the assimilation of aromatic compound derived carbon is further only documented for betaproteobacterial methylotrophs that reveal – albeit slow – growth on aromatic compounds such as lignin derivatives (i.e., 2-methoxyphenol) and petroleum derivatives (toluene, benzene, phenol, benzoates) [Nakatsu et al., 2006; Kalyuzhnaya et al., 2010]. It also remains speculative whether the detected *Beijerinckiaceae* can indeed cleave aromatic ring structures or assimilates [¹³C]-breakdown products resulted by fungal decomposition. Reported bacterial scavenging on easily available products released by the activity of white-rot fungi during lignin decomposition [Messner et al., 2003] emphasises the latter mentioned assumption. Also *Methylovirgula ligni* was isolated from a decaying beech wood inoculated by a white-rot fungus [Vorob'ev et al., 2009]. An advantageous relation between methylotrophic *Beijerinckiaceae* and saprotrophic *Basidiomycetes* was already reported [Folmann et al., 2008], and demonstrate a putatively mutualistic relationship in which the fungus release *inter alia* methanol during lignin degradation and thus increased the local availability and concentration. The methylotroph for its part provides nitrogen [Folmann et al., 2008], since all methylotrophic *Beijerinckiaceae* are capable of nitrogen fixation, with the exception of *Methylosula* [Marín & Arahal, 2013].

Apart from a direct substrate utilisation several methylotrophic *Beijerinckiaceae* assimilate carbon (also C₁-derived carbon) at the level of CO₂ via the ribulose-bisphosphate pathway such as *Methyloferula*, *Methylosula* and *Methylovirgula* [Marín & Arahal, 2013 and references therein; Vorobev et al., 2011]. Thus, the oxidation of [¹³C_u]-substrates to ¹³CO₂ by chemoheterotrophic microorganisms might enable the indirect assimilation of substrate-derived carbon by methylotrophic *Beijerinckiaceae* emphasising the tight trophic link in a microbial food web.

In addition, methane seemed to have growth stimulating effects on the *Beijerinckiaceae*-affiliated phylotype, since the labelling efficiency was higher in methane supplemented treatments. Only *mmoX* was detectable with molecular techniques (any effort to target *pmoA* failed, data not shown) indicating an sMMO and no pMMO catalyses the first step of methane oxidation. In addition, the inhibiting effect of a more neutral pH on these acidotolerant methanotrophs included within the phylotype is undisputed.

Besides *Beijerinckiaceae* the analyses of MDH marker genes revealed phlotypes mainly affiliated to *Methylobacteriaceae* and *Hyphomicrobiaceae* as further methanol and multi-carbon substrate-utilising taxa in the soil. For these taxa facultative methylotrophy is well known [Kelly et al., 2013; Oren & Wu, 2013]. However, *Methylobacteriaceae* and *Hyphomicrobiaceae* were not abundant in the microbial community and even not identified as labelled based on the bacterial 16S rRNA gene sequence analyses. In turn, *mxoF* sequences affiliated to the *Beijerinckiaceae* were only low abundant and minor labelled. Therefore, there is a discrepancy between the 16S rRNA gene sequence and the *mxoF*-based analyses, questioning the clear phylogenetic affiliation of *mxoF*-possessing taxa in the study. Although *mxoF* is a well recognized molecular tool for phylogenetic analyses and is encoded in all gram-negative *Proteobacteria* [McDonald & Murrell, 1997], it is highly conserved among distantly related methylotrophs and thus shows weak phylogenetic resolution power and an incongruent evolutionary topology of 16S rRNA and *mxoF* genes [Heyer et al., 2002; Lau et al., 2013; Kist & Tate, 2013; Marín & Arahal, 2013]. Several horizontal gene transfer (HGT) events are assumed, even for the genera *Methylobacterium* [Kist & Tate, 2013]. In addition, a putative localisation of *mxoF* genes on plasmids is partially assumed easily facilitating the exchange of genetic material [Kist & Tate, 2013]. Evolutionary theories within the putatively monophyletic group of *Beijerinckiaceae* and *Methylocystaceae* and genomic studies indicate a high genomic plasticity in which HGT plays crucial roles in developing 'specialists' (like methanotrophs) and 'generalists' (like *Beijerinckia* spp.) [Heyer et al., 2002; Tamas et al., 2014]. Thus, also multiple HGT events are suggested for *Beijerinckiaceae* and the *mxoF* genes [Lau et al., 2013]. Radajewski and colleagues detected in an acidic soil treated with methanol *mxoF* sequences that were distantly related to previously known *mxoF* sequences, but revealed still a high similarity to *Methylobacterium extorquens* (based on amino acid identity) [Radajewski et al., 2002]. The partial *mxoF* nucleotide sequences from the study of this work showed no high similarity to the distantly related *mxoF* sequences from the study of Radajewski and the highly divergent *mxoF* genes from *Methylovirgula ligni* [Vorob'ev et al., 2009] (analysed by BLASTn, data not shown, and phylogenetic trees, Figure A 12), which indicates the existence of an putative unknown methylotrophic *Beijerinckiaceae*-taxa possessing *mxoF* genes that are more similar to *mxoF* sequences of *Methylobacterium* or *Hyphomicrobium* leading to a false affiliation.

Interestingly, based on the MDH analyses one phylotype affiliated to *Methylocystaceae* (i.e., *Methylosinus* and *Methylocystis*; OTU_{*mxoF*} 137) was labelled under mixed substrate conditions with glucose, although *Methylocystaceae* were not abundant in the bacterial

community based on both gene markers (16S rRNA and *mxoF*). The detection of labelled *Methylocystaceae*-phylogenotypes based on 16S rRNA likely failed due to their low abundances, i.e., supplemented [¹³C₆]-glucose was predominantly assimilated by non-methylotrophs, which were enriched, and thus the *Methylocystaceae*-phylogenotype was only detectable through the more specific functional gene marker *mxoF*. *Methylocystaceae* comprise strongly 'restricted' facultatively methanotrophs which means that strains of the *Methylocystis* are capable of slow or weak growth on acetate or ethanol (Table 38) [Belova *et al.*, 2011]. However, the utilisation of glucose was never reported to date. Thus, it might be possible that the detected phylogenotype OTU_{*mxoF*} 137 is a hitherto unknown member of the *Methylocystaceae* utilising glucose and thus, broaden the multi-carbon substrate spectrum of this methylotrophic family.

Unexpectedly, no *xoxF* gene sequence were detected, although no preference of *mxoF* was assumed by the applied primers (see 2.5.7.1). Both marker genes are assumed to possess different functions and phylogenetic distributions (see 1.6.3). At the time of conducting the experiments an unequivocal grouping between *mxoF* genes and five distinct clades of *xoxF* genes (*xoxF1* to *xoxF5*) was already known [Chistoserdova, 2011; Keltjens *et al.*, 2014]. Only recently *xoxF* gene sequences were analysed in detail, which enabled the development of divergent *xoxF* primers for the different clades [Taubert *et al.*, 2015]. Thus, targeting both *mxoF* and *xoxF* genes with only one primer pair might result in biased amplification results towards *mxoF*. Therefore, the methylotrophic community in the soil was likely underestimated.

4.2.2. Putative fungal methanol-utilisers in the forest soil

The current knowledge on methylotrophic fungi is still strongly restricted, and only a limited number of methylotrophic fungi are reported. Methylotrophic taxa such as the well studied yeast genera *Candida*, *Hansenula* and *Pichia* (all belonging to the *Saccharomycetozoa*) [Gellissen, 2000] belong to yeasts or mould fungi (mainly *Ascomycota*) [Kolb, 2009a; Kolb & Stacheter, 2013]. For these fungi the methanol utilisation pathway (MUT pathway, see 1.7) is studied in detail, since they are of biotechnological importance [Wegner, 1990; Gellissen & Hollenberg, 1997; Gellissen, 2000; Hartner & Glieder, 2006]. Along the methylotrophic yeasts the MUT pathways and their regulation are fairly similar but also revealing significant differences in terms of involved genes and gene regulation [Hartner & Glieder, 2006]. Alcohol oxidases (AOx) catabolising the first crucial step in methanol oxidation within the peroxisoms of the methylotrophic fungal cells and different groups among the methylotrophic yeast are present in terms of their AOx [Ito *et al.*, 2007]. However, no marker genes are available to target these enzymes in a sufficient way to analyse and estimate the diversity of methylotrophic fungi. Thus, only more general ITS analyses were feasible.

Interestingly, no yeast or mould fungi affiliated to known methylotrophic fungi (especially *Ascomycota*) were abundantly labelled, and thus they were assumed as not important methanol-utilising fungal taxa in the acidic forest soil. Instead, fungal phylotypes that assimilated methanol-derived carbon were basidiomycetous yeasts belonging to the *Tremellomycetes* – namely *Cryptococcus* (at pH 4) and *Trichosporon* (at pH 7) – as well as the zygomycetous mould genus *Mortierella*. All these three genera are frequent in soils and possess different effects on soil and the soil ecosystem [El-Tarabily & Sivasithamparam, 2006; Voriskova & Baldrian, 2013].

Soil yeasts like *Cryptococcus* and *Trichosporon* are on the one hand saprotrophic and utilise degradation products of cellulose, hemicelluloses and lignin derivatives that originate from litter, wood or plant debris; on the other hand, they can even enhance plant-growth [Botha, 2011]. Thus, a methanol utilisation potential should not be rejected, since methanol can be released from both, decaying and growing plant material [Warneke *et al.*, 1999, Galbally & Kristine 2002, Millet *et al.*, 2008, Wohlfahrt *et al.*, 2015], and also methylotrophic bacteria (i.e., *Methylobacterium* spp.) are known to produce plant growth supporting compounds [Lidstrom & Chistoserdova, 2002]. *Cryptococcus* spp. are polyphyletic and belong to different clades within the *Tremellomycetes* [Liu *et al.*, 2015] making general statements on *Cryptococcus* difficult. They are ubiquitous and were even found at deep sea methane seeps where they are involved in the methane cycling in some way [Takishita *et al.*, 2006], as well as in highly acidic environments showing the existence of acidotolerant or acidophilic strains [Gadanhó & Sampaio, 2009; Delavat *et al.*, 2013]. Interestingly, Delavat and colleagues isolated *Cryptococcus* spp. as well as the facultative methylotroph *Methylorosula* sp. from the same acid mine drainage; but since the study was not focussing on methylotrophy these finding was not further commented (with no details on methanol concentrations or utilisation by the microorganisms) [Delavat *et al.*, 2013]. A physiological overview of known *Cryptococcus* sp. revealed that no species seems to utilise methanol; only ethanol can be utilised as carbon source by some strains [Barnett *et al.*, 2000]. However, it should be mentioned that this overview comprises only 35 type strains and the alcohol oxidases might fortuitously utilised methanol. To date no *Cryptococcus* sp. is reported being methylotroph, wherefore it might be possible that the *Cryptococcus* sp. was labelled due to cross feeding effects. However, the possibility of methylotrophy among these yeasts is not excluded because of their ubiquity, their polyphyletic nature and their versatility.

The enzyme facilitating the initial step of the MUT pathway (the AOX) was at first detected in a *Basidiomycota* but is also reported to be found in some mould fungi [Janssen *et al.*, 1965; Ito *et al.*, 2007]. Mould fungi are detectable among *Ascomycota* and *Zygomycota* [Hibbett *et al.*, 2007]. Indeed, several phylotypes of the zygomycetous *Mortierella* were labelled and are therefore putatively methanol-utilising. Never to date these fungi were reported to be methylotrophic, but mould fungi can indeed be found within the *Mortierella* [Kück *et al.*, 2009]. *Mortierella* belongs to the *Mortierellales*, a widespread and thus generalistic order comprising the most functionally diverse group of saprotrophic soil fungi with the capability to

degrade plant-polymeric structures such as hemicelluloses [Dix & Webster, 1995; Kjøller & Struwe, 2002; Cannon & Kirk, 2007, Hanson *et al.*, 2008; Buée *et al.*, 2009]. Therefore, the possibility for hitherto unknown methylotrophic strains among *Mortierella* is conceivable.

Regrettably, no clear evidence for methanol-utilising fungi was detected, since all under methylotrophic conditions labelled fungal taxa are not known to utilise methanol. They all possess a more saprotrophic lifestyle and are able to utilise a broad range of substrates and can even degrade complex and recalcitrant polymers. Thus, a labelling due to cross feeding processes on labelled bacteria might be possible. However, several studies on wild type strains of methylotrophic yeasts revealed diauxic growth when growing on glucose and methanol at the same time in batch cultures [Parpinello *et al.*, 1998; Sakai *et al.*, 1987; Stasyk *et al.*, 1997; Stasyk *et al.*, 2004; Hartner & Glieder, 2006], indicating a preference for one substrate over the other. Thus, the presence of a more preferable carbon sources in the forest soil during the incubation with [¹³C]-methanol can lead to a lowered utilisation and assimilation of ¹³C and thus resulted in a weaker labelling, wherefore the existence of methylotrophic fungi might be accidentally overlooked.

In addition, a putatively inhibitory effect on the methanol utilisation by repressors that are endogenously present in the soil is also considerable. For example, glucose showed an inhibiting effect on the key step of the MUT pathway and the following assimilatory pathways in biotechnologically relevant yeasts. The dissimilatory route however was not repressed – but dissimilation of methanol is not detectable via SIP studies. Unfortunately, no complete picture on this glucose-repressing mechanism has been generated so far [Hartner & Glieder, 2006]. Other sugars such as xylose revealed a de-repressing effect of the inhibiting effect of glucose, like it was reported for *Hansenula polymorpha* [Eggeling & Sahm, 1978; Hartner & Glieder, 2006], implying a complex interaction of different substrates on methanol utilisation in an even more complex environment.

4.2.3. Methanol-derived carbon assimilating *Bacteria*

Several other minor or weakly labelled phylotypes in the [¹³C₁]-methanol treatment were affiliated to different taxonomically unrelated phyla such as *Acidobacteria*, *Planctomycetes*, *Verrucomicrobia* and *Actinobacteria* (see 3.7.1). These phylotypes revealed, *inter alia*, low sequence similarities to cultured species and could be represent hitherto unknown bacteria involved in C1 assimilation processes. Due to their low labelling efficiencies (i.e., minor or weak labelling) these phylotypes might also be involved in a complex food web that is based on methanol and methanol-utilising *Beijerinckiaceae*, emphasising the role of this methylotrophic bacterial family in the acidic forest soil. In the following section the chance for methanol utilisation and the role of the detected taxa in a methanol-driven microbial food web are discussed.

4.2.3.1. *Acidobacteria*

Both phylotypes related to *Acidobacteria* were closely related to uncultured taxa among this phylum and showed highest similarity to *Acidobacter capsulatum* (98 % sequence identity for OTU_{16S} 545) and *Acidipila* sp. (93 % sequence identity for OTU_{16S} 542). *Acidobacteria* are predicted as abundant in soil environments and may reveal a significant high diversity and versatility [Ludwig *et al.*, 2010; Thrash & Coates, 2010]. The type genera of the two classes among the *Acidobacteria* (i.e., *Acidobacter* for *Acidobacteriia* and *Holophaga* for *Holophagae*) are not reported as being methylotrophic [Campell, 2013; Fukunaga & Ichikawa, 2013], but to date only a few representatives of this phylum are cultured and several new uncharacterized isolates still provide the possibility of hitherto unknown methylotrophs among this widespread phylum [Thrash & Coates, 2010]. In another study by Radajewski and colleagues in which *Beijerinckiaceae* (most likely *Methylovirgula* sp.) were identified as main methylotrophic taxa in an acidic forest soil, also *Acidobacteria* were shown to be involved in the methanol assimilation [Radajewski *et al.*, 2002]. Studies on decaying wood colonized by white-rot fungi revealed that besides *Beijerinckiaceae* (most likely *Methylovirgula* sp., since it was isolated from wood [Vorob'ev *et al.*, 2009]) also *Acidobacteria* were the only other bacteria colonizing the rotten wood [Folmann *et al.*, 2008], suggesting a relation or interaction between saprotrophic fungi, *Beijerinckiaceae* and *Acidobacteria*. Also, in different peatlands in which *Methylocystis* and *Methylocella* are important methylotrophs [Dedysh *et al.*, 2006] the supplementation of methanol significantly increased the abundance of *Acidobacteria* similar to a comparable glucose supplementation [Pankratov *et al.*, 2008], emphasising the involvement of *Acidobacteria* in a methanol based food web. However, the authors could not isolate methylotrophic *Acidobacteria* and assume a cross feeding effect in which *Acidobacteria* consume extracellular polysaccharides (EPS) produced by methylotrophs in the peat [Pankratov *et al.*, 2008]. Another example for such a cross feeding effect by EPS was shown with the isolation of *Edaphobacter aggregans* growing in co-culture with *Methylocella silvestris* as supplier of EPS as carbon source [Koch *et al.*, 2008]. In summary, an interaction between *Acidobacteria* and acidophilic / acidotolerant methylotrophs is obvious and although up to date no methylotrophic members of this phyla are reported, the chance for methylotrophs among the *Acidobacteria* should not be excluded.

4.2.3.2. *Planctomycetes*

Planctomycetes were first described in freshwater environments but increasing environmental studies and isolation techniques revealed an ubiquity of this deep branching phylum [Kulichevskaya *et al.*, 2007]. They are also common in diverse soil environments and are reported as an abundant bacterial group in acidic peat soils [Dedysh *et al.*, 2006; Kulichevskaya *et al.*, 2006; 2008; 2009; 2012]. Several acidophilic members of the *Planctomycetes* such as *Schlesneria paludicola* and *Singulisphaera acidiphila* were isolated

from the same peat environment like *Methylocapsa acidiphila* arising the question of a relation between acidophilic *Planctomycetes* and methylotrophs [Kulichevskaya *et al.*, 2007; 2008; Dedysh *et al.*, 2002]. *Singulisphaera acidiphila* was shown to be able to degrade different polysaccharides [Kulichevskaya *et al.*, 2008]. In general, *Planctomycetes* are known as heterotrophic organisms being able to degrade heteropolysaccharides such as EPS like it is produced by almost all members of the *Beijerinckiaceae* [Marin & Arahall, 2013]. Subsequently, the utilisation of EPS was proven by Wang and colleagues who could demonstrate the assimilation of [¹³C]-EPS (derived from *Beijerinckia indica*) by *Planctomycetes* affiliated to the genus *Singulisphaera* [Wang *et al.*, 2015]. In the conducted study with acidic forest soil the phylotypes related to *Planctomycetes* showed only a lower similarity to *Zavarzinella formosa* (90 % sequence identity for OTU_{16S} 938) and *Pirellula* sp. (88 % sequence identity for OTU_{16S} 836). Both genera are able to utilise sugars, sugar derivatives and heteropolysaccharides [Youssef & Elshahed, 2013; Wang *et al.*, 2015], and at least *Zavarzinella formosa* was isolated from acidic peat soils [Kulichevskaya *et al.*, 2009]. Thus, as it was also demonstrated for *Acidobacteria* (see 4.2.3.1), *Planctomycetes* could scavenge on EPS produced by methylotrophs, but to date it is not known whether the scavengers could provide something in return. If a beneficial relation for both partners is imagined *Planctomycetes* could provide methanol. Members of the *Phycisphaerae* were shown to be involved in wood degradation [Bienhold *et al.*, 2013], and thus it is also conceivable that the planctomyceteous activity increase the local concentration of methanol being advantageous for methylotrophs. Since wood and lignin are recalcitrant to degradation, EPS could serve as a more easily utilisable carbon source for *Planctomycetes*. However, only one described species of this class is reported (*Phycisphaera mikurensis*), providing a 'black box' and enough room for speculation on the realistic *in situ* relation between *Planctomycetes* and methylotrophs [Fukunaga *et al.*, 2009; Youssef & Elshahed, 2013]. In addition, methylotrophy among the phylum is still not excluded, since at least one species – *Planctomyces limnophilus* – was described to utilise methanol as carbon source [Hirsch & Müller, 1985; Youssef & Elshahed, 2013]. However, other species affiliated to the same genus were unable to utilise methanol and no further member of the *Planctomycetes* was reported assimilating methanol (albeit methanol utilisation was not always evaluated) [Youssef & Elshahed, 2013]. Several genomic studies revealed that *Planctomycetes* possess genes related to the C1 metabolism of methylotrophic and methanogenic organisms [Chistoserdova *et al.*, 2004; Kalyuzhnaya *et al.*, 2004; Fuerst & Sagulenko, 2011]. These genes are affiliated to C1 transfer reactions and are assumed to be important within the detoxification pathway of formaldehyde [Marx *et al.*, 2003]. However, *Planctomycetes* are lacking genes for the primary oxidation of C1 compounds such as *mxoF* and its homologue *xoxF*, and no growth or a stimulating effect of methanol was observed for isolated *Planctomycetes* gradually exclude this phylum from methylotrophic activity [Chistoserdova *et al.*, 2004; Chistoserdova, 2011].

4.2.3.3. *Verrucomicrobia*

Although increasing environmental studies revealed the phylum *Verrucomicrobia* as a widespread bacterial group detectable in soils, freshwater, marine or extreme environments such as hot springs, *Verrucomicrobia* are still underestimated and also poorly described [Hou *et al.*, 2008; Bergmann *et al.*, 2011]. To date *Verrucomicrobia* are divided into six subdivisions with only a few cultured species comprising three described classes and a wide range of environmental sequences complicating phylogenetic affiliations and precise physiological conclusions [Sangwan *et al.*, 2004; 2005; Ludwig *et al.*, 2010]. The verrucomicrobial phylotypes detected as labelled and thus are assumed to be involved in the methanol-based food web were affiliated to *Chthoniobacter flavus* (90 % sequence identity for OTU_{16S} 6) and *Prostheco bacter debontii* (84 % sequence identity for OTU_{16S} 18). The genus *Chthoniobacter* belongs to the class *Spartobacteria* (subdivision 2), which seems to be ubiquitous and the most abundant verrucomicrobial group [Sangwan *et al.*, 2004; 2005; Bergmann *et al.*, 2011]. Methanol utilisation was never reported for *Chthoniobacter flavus*, whereas the species is able to grow on mono- and disaccharides (such as glucose, xylose, cellobiose) as well as polysaccharides such as xylan, cellulose or pectin components [Sangwan *et al.*, 2004]. The inability of methanol utilisation but utilisation of saccharides is also characteristic for *Prostheco bacter* spp. belonging to the class *Verrucomicrobiae* (subdivision 1) [Stayley *et al.*, 1976; Hedlund *et al.*, 1997]. *Prostheco bacter* spp. are heterotrophic, and at least one species (i.e., *Prostheco bacter algae*) was shown to degrade polysaccharides (i.e., xylan) [Lee *et al.*, 2014]. Thus, the detected verrucomicrobial phylotypes could be also involved in the degradation of EPS from methylotrophic *Beijerinckiacae* as it was already assumed for *Acidobacteria* and *Planctomycetes* (see 4.2.3.1 & 4.2.3.2). Wang and colleagues could also identify *Verrucomicrobia* as EPS-assimilating microorganisms [Wang *et al.*, 2015], highlighting this possible explanation for the labelling of *Verrucomicrobia* in the conducted SIP-experiment.

Nonetheless, methylotrophy among the *Verrucomicrobia* is not excluded, since also methanotrophic members (also utilising methanol) were described belonging to a monophyletic subdivision comprising the genera *Methylacidiphilum* and *Methylacidimicrobium* [Dunfield *et al.*, 2007; Op den Camp *et al.*, 2009; van Teeseling *et al.*, 2014]. Genomic studies on *Methylacidiphilum infernorum* V4 revealed genes for a particulate methane monooxygenase that is distinct but homologue to methanotrophic *Proteobacteria*. These finding expands the view on methanotrophs and indicates the ancient divergence of both verrucomicrobial and proteobacterial methanotrophs [Dunfield *et al.*, 2007]. The common proteobacterial *pmoA* targeting primer systems showed multiple mismatches with the verrucomicrobial *pmoA* sequence [Dunfield *et al.*, 2007]. In addition, methylotrophic *Verrucomicrobia* possess *xoxF*, a homologue of *mxoF*, encoding for the large subunit of their methanol dehydrogenase [Hou *et al.*, 2008]. The distinct *pmoA* genes and the lack of *mxoF* appear to be good reasons why *Verrucomicrobia* were not often targeted in environmental

studies concerning methylotrophs [Sharp *et al.*, 2014]. In addition, the 'universal' 16S rRNA gene targeting primer pairs also discriminate against *Verrucomicrobia* and thus underestimate the total abundance and diversity of this phylum [Bergmann *et al.*, 2011]. In terms of the in this study conducted experiment such a biasing effect could not be excluded, although the 16S rRNA primers used in this study were recommended as 'universal' with a high coverage among *Bacteria* and *Archeae* [Klindworth *et al.*, 2013]. Further, SIP experiments enabling to elucidate [^{13}C]-carbon assimilating microorganisms in an environmental sample seem only of limited use to detect putative methylotrophic verrucomicrobial participants. Both, *Methylacidiphilum* and *Methylacidimicrobium* assimilate their carbon via the RuBP, thus they incorporate ^{13}C not directly derived from C1 compounds but indirectly from CO_2 [Khadem *et al.*, 2004; Sharp *et al.*, 2012; Van Teeseling *et al.*, 2014]. Subsequently, a high endogenous background consisting of $^{12}\text{CO}_2$ (that is assumed for the conducted incubations) would dilute the amount of arising $^{13}\text{CO}_2$ derived from labelled C1 compounds. Therefore, the assimilating and incorporation of ^{13}C would be weakened resulting in a weak labelling rendering the detecting of a labelling difficult. This phenomenon was observed by Sharp and colleagues who could not detect heavy verrucomicrobial DNA when using solely $^{13}\text{CH}_4$ in a SIP experiment. Combinations of different isotopologues of CH_4 and CO_2 were necessary to detect methanotrophic *Verrucomicrobia*, highlighting the requirement of a sufficient label [Sharp *et al.*, 2012].

Another problem could be the DNA of *Methylacidiphilum* spp. itself that are reported possessing a low GC-content of 40.5 mol% to 45.5 mol% [Op den Camp *et al.*, 2009]. The resulting buoyant density of labelled heavier DNA would be hard to distinguish from native not-labelled but GC-rich DNA. As a clarifying example, the GC contents of *Methanosarcina barkeri* and *Escherichia coli* are 40 mol% and 50 mol% with corresponding buoyant densities of about $1.70 \text{ g} \times \text{ml}^{-1}$ (applicable for DNA in CsCl solution) [Lueders *et al.*, 2004]. Fully labelled DNA of these organisms would be $0.038 \text{ g} \times \text{ml}^{-1}$ heavier (maximum value, according to the documented shift in buoyant densities from unlabelled to fully labelled DNA in *Methylobacterium extorquens* [Lueders *et al.*, 2004]) resulting in buoyant densities of around $1.74 \text{ g} \times \text{ml}^{-1}$ (Table 40). However, the SIP study done by Sharp and colleagues revealed even lower densities of around 1.72 to $1.73 \text{ g} \times \text{ml}^{-1}$ for labelled DNA of *Methylacidiphilum infernorum* V4 [Sharp *et al.*, 2012]. Thus, fully labelled DNA in environmental samples with a high diversity and competition for the supplemented [^{13}C]-isotopologue is hardly to obtain, therefore the resulting buoyant densities of GC-low organisms is still lower and could get lost in the total environmental DNA mixture. Contrary to *Methyloacidiphilum* spp. the second methanotrophic verrucomicrobial genus *Methyloacidimicrobium* possess a higher GC-content of 60.9 mol% to 63.8 mol%, wherefore the above mentioned problematic could be ignored [van Teeseling *et al.*, 2014].

Table 40 Buoyant densities according to the GC-mol% content of microbial species

	GC mol%	BD _{unlabelled} [g x ml ⁻¹]	→	BD _{fully labelled} [g x ml ⁻¹] ^b
<i>Methanosarcina barkeri</i>	40	1.692	→	1.730
<i>Escherichia coli</i>	50	1.704	→	1.742
<i>Methylobacterium extorquens</i>	66	1.719	→	1.757 ^a
<i>Micrococcus luteus</i>	71	1.725	→	1.763 ^a
<i>Methyloacidiphilum</i> spp.	40.5 – 45.5	Average: 1.695 (1.692 – 1.697)	→	Average: 1.733 (1.730 – 1.735)
<i>Methyloacidimicrobium</i> spp.	61 – 64	Average: 1.715 (1.713 – 1.716)	→	Average: 1.753 (1.751 – 1.754)

^a values taken from Lueder et al., 2004

^b fully labelled BD calculated based on the assumed shift in BD of + 0.038 g x ml⁻¹

Another difference between both methanotrophic genera is the ability to grow under highly acidic (i.e., growth at pH 0.5 for *Methyloacidimicrobium tartarophylax*) or highly temperate conditions (i.e., growth at 65°C for *Methyloacidiphilum fumariolicum* SolV), but both genera seem to be restricted to geothermal environments [Op den Camp *et al.*, 2009; Sharp *et al.*, 2012; 2014; van Teeseling *et al.*, 2014]. A survey of the distribution of methanotrophic *Verrucomicrobia* revealed a restriction to geothermal environments - in acidic peat soils they were never detected [Sharp *et al.*, 2014]. It can be speculated whether the pH in peat soils is not optimal for these *Verrucomicrobia* (i.e., too low pH), whether they are adapted to higher endogenous methane concentrations or whether they require higher concentrations of rare earth metals (REM). REMs are widespread in the earth's crust but their concentration is low and only in a nanomolar range within the most ecosystems including peat bogs, and excluding geothermal environments in which they are abundant up to a micromolar range [Vodyanitskii *et al.*, 2012; Pol *et al.*, 2014]. REMs were reported to enhance growth of *Methyloacidiphilum fumariolicum* SolV and its XoxF depends on REMs [Pol *et al.*, 2014]. Stimulating effects of REMs were also reported for XoxF-MDHs of *Bradyrhizobium* sp. and *Methylobacterium radiotolerans*, highlighting the special characteristic of Xox-MDHs and their physiological underestimation so far [Fitriyanto *et al.*, 2011; Hibi *et al.*, 2011].

In summary, methylotrophic verrucomicrobial members are described, are phylogenetically restricted to one subdivision and seem restricted to geothermal environments excluding acidic soils [Sharp *et al.*, 2014]. The detected verrucomicrobial phylotypes were mainly affiliated to *Chthoniobacter flavus* and *Prostheco bacter debontii* that are not reported as methylotrophic, mainly utilising sugars and being able to degrade polysaccharides [Sangwan *et al.*, 2004; Hedlund *et al.*, 1997]. Therefore, a cross feeding effect in which ¹³C was derived from [¹³C]-enriched EPS of the methylotrophic *Beijerinckiaceae* is most likely. This assumption is also accentuated by a SIP study in which *Verrucomicrobia* were detected as methane-based food web members [Morris *et al.*, 2002]. However, the low similarity of the detected phylotypes to cultured *Verrucomicrobia* and a putatively discriminating effect of the 'universal' primer against *Verrucomicrobia* [Bergmann *et al.*, 2011] still offers the possibility of

hitherto unknown methylophilic members of this phylum that are not restricted to geothermal environments such as *Methyloacidiphilum* and *Methyloacidimicrobium* [Op den Camp *et al.*, 2009; van Teeseling *et al.*, 2014]. In addition, if the assimilation of C1 compound-derived carbon would be always via the RuBP-pathway in all methylophilic *Verrucomicrobia* (known and hitherto unknown), the chance to detect unknown verrucomicrobial methylophilic members is hardly limited employing DNA SIP.

4.2.3.4. *Actinobacteria*

Actinobacteria were highly abundant among the total bacterial community in the acidic forest soil (see 3.5.1 & Figure 48B), which is not unexpected, since this phylum constitutes one of the main bacterial phyla widely distributed and includes a wide range of morphological and physiological characteristics [Goodfellow *et al.*, 2012]. *Actinomycetes*, the main class of *Actinobacteria*, produce a diverse range of exoenzymes for the degradation of recalcitrant polymers such as cellulose, hemicelluloses or lignin, and are thus playing an important role in plant-derived polymer degradation [McCarthy *et al.*, 1978; Kirk & Farrell, 1987; Crawford, 1988; Malhotra *et al.*, 2007; Suneetha & Khan, 2011]. The actinobacterial phylotypes detected as weakly labelled and thus only be minor involved in the methanol-driven food web were affiliated to *Aciditerrimonas ferrireducens* (92 % sequence similarity for OTU_{16S} 652) and *Kineosporia* sp. (94 % sequence similarity for OTU_{16S} 703).

Aciditerrimonas ferrireducens belongs to the acidophilic *Acidimicrobiaceae* that comprise also the genera *Acidimicrobium*, *Ferrimicrobium* and *Ferrithrix*. This family belongs to the rather small order *Acidimicrobiales* with only a handful of members described [Stackebrandt, 2013]. Interestingly, the detected phylotype revealed a higher similarity to *Ferrimicrobium* spp. (91 % sequence similarity) within a phylogenetic tree (Figure A 14). However, both genera are not reported to utilise methanol and show only a limited substrate range of carbon sources utilised [Johnson *et al.*, 2009; Itoh *et al.*, 2011]. Under anaerobic conditions *Aciditerrimonas* and *Acidimicrobium* were demonstrated to grow autotrophically by assimilating CO₂ [Johnson *et al.*, 2009], and an *Acidimicrobiaceae*-related phylotype in treatments supplemented with CO₂ was also detectable. Thus, a cross feeding effect via CO₂ in anoxic microzones within the soil slurry could be suggested. In addition, the lower similarity to the described species and the higher similarity to several environmental sequences from soil environments (i.e., 98 - 99 %, Figure A 14) opens the question of the *in situ* role of this phylotypes in the methanol-driven food web, since based on the described genera the acidophilic *Acidimicrobiaceae* reveal growth optima at higher temperatures (above 35°C to 50°C) and a higher acidity (pH of 1.8 – 3.0) and are thus not well adapted to forest soil environments [Johnson *et al.*, 2009]. However, methanol utilisation should still not be excluded. Johnson and colleagues reported that the isolate ‘Y005’, which was posterior classified as *Ferrithrix thermotolerans*, could be sub-cultured in media containing ferrous iron and methanol, indicating a possible utilisation of methanol [Johnson *et al.*, 2003].

The other actinobacterial phylotype weakly labelled was affiliated to *Kineosporia* spp. which are spore-bearing *Actinobacteria* belonging to the *Kineosporiaceae* within the large order of *Actinomycetales* [Zhi *et al.*, 2009; Tamura & Suzuki, 2013; entry for *Actinobacteria* at <http://www.bacterio.net/-classifphyla.html>]. They can utilise a wide range of saccharides such as glucose, xylose and cellobiose, and can decompose polymeric compounds such as starch, casein and DNA [Pagani & Parenti, 1978; Kudo *et al.*, 1998; Li *et al.*, 2009; Sakiyama *et al.*, 2009]. *Kineosporiaceae* are ubiquitous and were inter alia detected in soils, leaves, litter, root, stems and even Sphagnum moss [Tamura & Suzuki, 2013]. They show also tight relations with plants, and *Kineosporia mesophila* as well as *Kineococcus endophytica* were reported as plant growth enhancing organism [Hamedi & Mohammadipanah, 2015] like it was reported for some *Methylobacterium* spp. for instance [Lidstrom & Chistoserdova, 2002]. However, all described species of the *Kineosporiaceae* were not reported to utilise methanol (actual methanol utilisation was never been tested) [Pagani & Parenti, 1978; Kudo *et al.*, 1998; Li *et al.*, 2009; Sakiyama *et al.*, 2009]. In addition, *Kineosporia* spp. reveal a high GC-content of their DNA ranging from 69 mol% to 71 mol% [Tamura & Suzuki, 2013], and thus possessing inherently heavy DNA with a buoyant density of around 1.725 g x ml⁻¹ according to reported values for *Micrococcus luteus* (i.e., buoyant density of 1.725 g x ml⁻¹ reported for unlabelled DNA with a GC-content of 71 mol% [Lueders *et al.*, 2004], Table 40). This inherently heavy DNA is again hard to distinguish from labelled DNA of other microorganisms and the *Kineosporia*-affiliated phylotype was only detectable in the 'middle' fraction covering buoyant densities of 1.715 to 1.730 g x ml⁻¹. Therefore it is likely that the detected phylotype affiliated to *Kineosporia* sp. was not labelled. However, since a labelling is not excluded, it is also assumable that the phylotype probably achieved ¹³C indirectly from the [¹³C]-methanol by decomposing ¹³C-labelled DNA derived from labelled but dead methylotrophic organisms or from ¹³C-enriched EPS and EPS-derived saccharide components produced by the methylotrophic *Beijerinckiaceae*. It is still interesting that the *Kineosporia* spp. was only detectable in the acidic soil and not in the pH shift experiment in treatments with a more neutral pH, since described species were reported to show a growth range between pH 4 and 8, and no growth below 4 [Pagani & Parenti, 1978; Kudo *et al.*, 1998; Li *et al.*, 2009; Sakiyama *et al.*, 2009]. The low similarity of the detected phylotype to *Kineosporia* sp. (94 % sequence similarity) provides the opportunity of a hitherto unknown at least acidotolerant member of the actinobacterial family *Kineosporiaceae*.

In summary, both weakly labelled phylotypes were not clearly affiliated to known methylotrophic *Actinobacteria*, and their labelling was more likely achieved by cross feeding effects on ¹³C-labelled EPS or saccharides and ¹³CO₂ produced by methylotrophic *Beijerinckiaceae*. Nevertheless, the knowledge on methanol-utilising *Actinobacteria* is still limited and among the *Actinomycetes* methanol-utilising members are known belonging to seven families affiliated to three different suborders [Kolb, 2009a; Hung *et al.*, 2011; Hung *et al.*, 2012; Kolb & Stacheter, 2013; Witthoff *et al.*, 2013; Lynch *et al.*, 2014]. Some of them possess a methanol:NDMA oxidoreductase (MDO) catalyzing the first crucial step of

methanol utilisation which is different to proteobacterial methylotrophs [Bystrykh *et al.*, 1993; Park *et al.*, 2010; Kolb & Stacheter, 2013]. However to date, no applicable primers are available for these MDO enzymes disabling a more direct targeted molecular investigation [Kolb & Stacheter, 2013]. Interestingly, Anesti and colleagues reported that *Brevibacterium casei* 3Tg possess an *mxoF* sequence, which is more similar to the proteobacterial *Methylobacterium* spp., suggesting HGT events occurred and *mxoF* harbouring *Actinobacteria* exist [Anesti *et al.*, 2005]. Based on the general 16S rRNA gene sequence analysis no *Methylobacterium* spp. were detectable, but several phylotypes of *mxoF* related to *Methylobacterium* were detected. Thus, it is conceivable that actinobacterial methylotrophic taxa were indeed present in the soil samples and thus hitherto unknown members of the *Actinobacteria* are utilising methanol in the acidic forest soil and possess *mxoF* genes. In addition, Witthoff and colleagues demonstrated that *Corynebacterium glutamicum* was able to utilise methanol employing an alcohol dehydrogenase [Witthoff *et al.*, 2013]. No growth on methanol as sole carbon source was obtained, assuming that methanol was used for energy conservation in the dissimilatory pathway of the *Corynebacterium*. Thus, methanol dissimilation was proven and is also conceivable for *Actinobacteria*. Since SIP experiments can only target the assimilation of methanol, the utilisation of methanol as energy source by some actinobacterial members of the bacterial community in the forest soil is not excluded.

4.2.4. Hypothetical methanol-driven food web and ecological niches of associated microorganisms in the acidic soil

In the current study methanol-utilising microorganisms in an acidic forest soil were analysed and their multi-carbon substrate spectrum as ecological niche-defining parameter. *Beijerinckiaceae* are undisputable the main methanol-utilising microorganisms in the acidic soil, and the ability to utilise C1 compounds efficiently represents their ecological niche. The detected family-level phylotype was also able to utilise multi-carbon substrates including sugars, acetate and aromatic compounds. Thus, *Beijerinckiaceae* might occupy a central role in a methanol-driven food web. Further *Bacteria* and fungi assimilating methanol-derived carbon were likely linked with the *Beijerinckiaceae* by (i) providing methanol and multi-carbon substrates by degrading recalcitrant polymers, (ii) providing CO₂ as carbon source, and (iii) scavenging on *Beijerinckiaceae*-derived compounds such as EPS-sugars or cell debris.

Based on the obtained results the following graphical model (Figure 87) was constructed to summarise the findings on methanol-utilising microorganisms and the methanol-driven microbial food web in an acidic soil of a temperate deciduous forest.

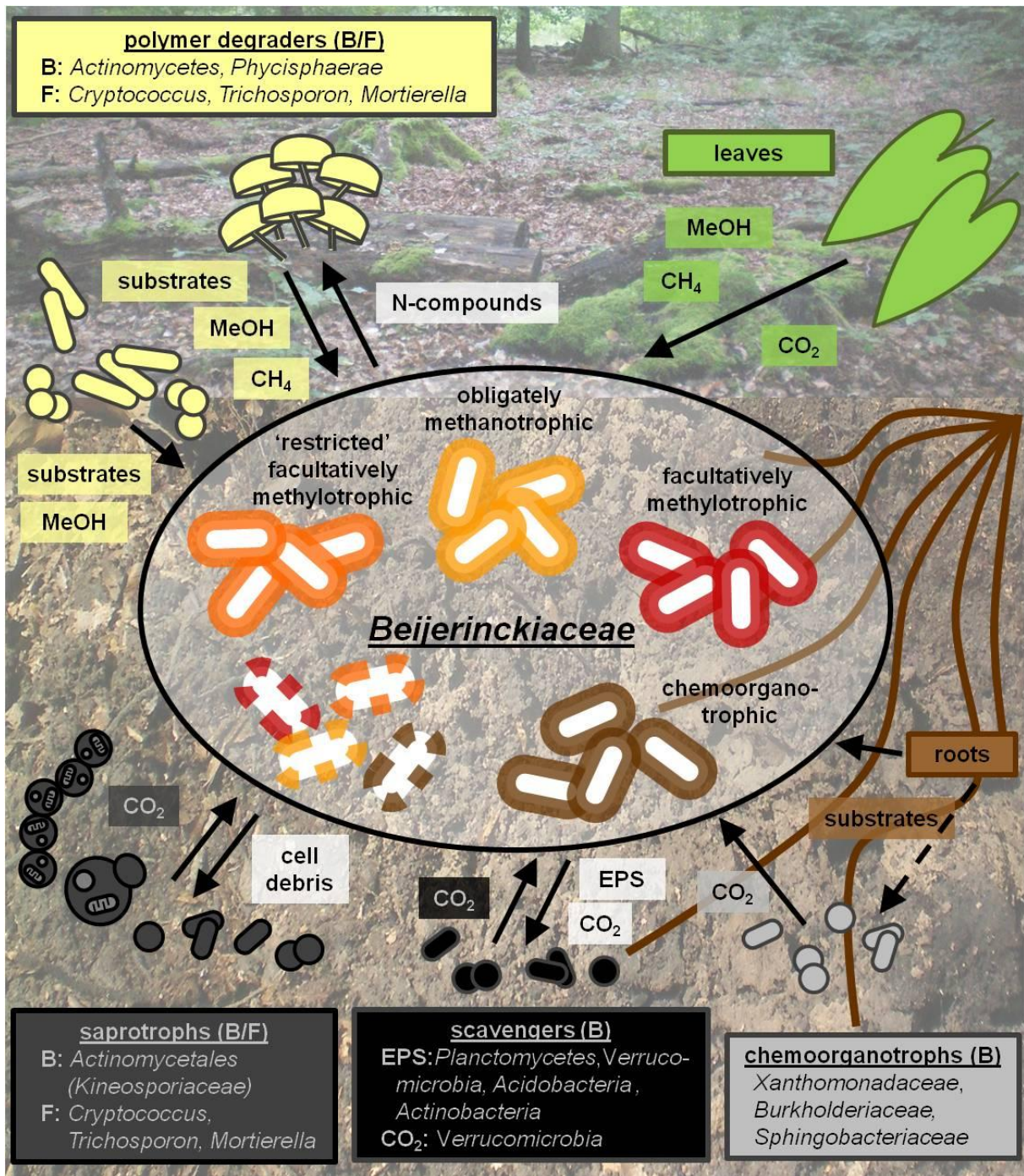


Figure 87 The central role of *Beijerinckiaceae* in a methanol-driven food web in a temperate deciduous forest with acidic soil.

This figure summarises the obtained results of the conducted studies in terms of direct and indirect methanol-utilising organisms and their interconnection in a methanol-driven food web (B = *Bacteria*; F = *Fungi*). For more information refer to the following sections: 1.6.4, 1.9, 3.7, 4.2, 4.2.3.

4.3. The influence of an elevated pH on the indigenous methanol-derived carbon-utilising microbiome

Soil is not homogeneous and microscale habitats exist. For example, within two millimetres of soil the pH can differ up to one pH unit [Or *et al.*, 2007]. Thus, the response of the indigenous methanol-utilisers on an elevated soil pH was addressed. The total bacterial community was significantly influenced by a changed pH and thus the detected methanol-utilising bacteria. Several phylotypes affiliated to *Chryseobacterium* sp. (*Bacteroidetes*), *Leifsonia* sp. (*Actinobacterium*) and *Methylophilum* sp. (*Betaproteobacteriaceae*) were detected as methanol-utilisers at a more neutral pH.

Among the *Bacteroidetes* a handful of methylotrophic taxa are reported such as species within the *Flavobacteriia* (*Flavobacterium* spp.) and *Sphingobacteriia* (*Mucilaginibacter* spp.) [Boden *et al.*, 2008; Madhaiyan *et al.*, 2010a; Madhaiyah *et al.*, 2010b; Kolb & Stacheter, 2013]. In addition, two different studies on methylotrophic communities suggest *Cytophaga* sp. (class *Cytophagia*) being also involved in methane oxidation as they were detected in methane-fed enrichments [Morris *et al.*, 2002; Radajewski *et al.*, 2002]. But to date *Chryseobacterium* spp. (affiliated to the same family like *Flavobacterium* spp.) were never reported as methylotrophic (and were not directly evaluated). However, the possibility of methylotrophs among the genus *Chryseobacterium* is conceivable, since members are widely distributed and several new species were assigned over the last years [Bernardet *et al.*, 2006; Venil *et al.*, 2014].

Among the *Actinobacteria* methylotrophs were already reported belonging to different taxa [Kolb & Stacheter, 2013]. For example, isolates affiliated to the genus *Leifsonia* are able to grow on methanol as sole carbon source [Hung *et al.*, 2011]. These isolates showed a high 16S rRNA gene sequence similarity to *Leifsonia xyli* (i.e., 98.7 - 99.8 %) as well as the in the pH shift SIP experiment detected phylotype (i.e., 99 %), emphasising a putative methylotrophic character. Although Hung and colleagues accentuate the ease of the isolation of methylotrophs in their study, best growth was obtained with higher methanol concentrations (50 mM) as they were used in the conducted SIP study and additional glass beads supporting a biofilm formation [Hung *et al.*, 2011]. Nevertheless this study demonstrated again that heterotrophic microorganisms are still underestimated in their metabolic flexibility. The utilisation of C1 compounds seems to be more common than previously assumed, since putative methylotrophic *Leifsonia* spp. were identified in two totally different environments (oral cavity [Hung *et al.*, 2011] and forest soil).

The detected *Methylophilus*-affiliated phylotype was only weakly labelled in slurries with the more neutral pH. *Methylophilaceae* are mainly isolated and detected in aqueous environments or plants and under more neutral or even alkaline conditions [Doronina *et al.*, 2012; Doronina *et al.*, 2013]. Thus, it is remarkable that a *Methylophilaceae*-related species seems to be indigenous in the acidic soil environment. This unfavourable condition could be

also the reason why the phylotype was only detected as weakly labelled but with a high LP indicating effective assimilation of the [¹³C]-methanol. It is conceivable that *in situ* the *Methylophilus* sp. has a lower competitiveness compared to the acidotolerant/-philic *Beijerinckiaceae* that dominate the methylophilic community. The resulting low abundance of this *Methylophilus* phylotype at *in situ* conditions might result in a delayed growth-based detection in the pH shift SIP experiment. Although *Methylophilaceae* are reported being versatile and possessing different metabolic pathways that can significantly differ within this methylophilic family [Doronina *et al.*, 2013], the *Methylophilus*-affiliated phylotype was not detectable in any multi-carbon substrate treatment, highlighting the unfavourable effect of the acidic pH.

Although the pH shift did not significantly affected the total fungal community (see 3.5.3.3) the amount of labelled methanol-utilising fungi was decreased, emphasising the reducing effect of more neutral pH on the diversity of putatively methanol-utilising fungi. The under acidic conditions labelled taxa *Cryptococcus* and *Mortierella* are assumed to grow also under more neutral conditions, however their pH optima seems more restricted to conditions below pH 7, explaining that they were not detected as methanol-utilisers at the more neutral pH condition [Gross & Robbins, 2000]. Instead, the basidiomycetous yeast genus *Trichosporon* was identified as methanol-utilising fungi at pH 7. Indeed, methylophilicity was reported for this versatile genus [Kaszycki *et al.*, 2006]. The *Trichosporon* species was isolated from an oil-polluted soil and revealed *inter alia* a tolerance for high methanol concentrations and degradation potential. Interestingly, the strain lacked the key enzyme of the MUT pathway (the AOx). Thus, *Trichosporon* seems to soften the dogma that an AOx is required for methanol utilisation. Since the above discussed *Cryptococcus* belongs to the same fungal class like *Trichosporon* and they are both belonging to different clades of the *Tremellomycetes*, it is also conceivable that taxa within the *Tremellomycetes* are indeed methylophilic possessing different enzymes and pathways than the hitherto known methylophilic yeasts of the *Ascomycota* and thus methylophilicity among the phyla could evolved in slight different ways.

4.4. The chloromethane-utilising guild of methylophilics

Several methylophilic microorganisms are able to utilise halogenated compounds such as chloromethane even as sole source of energy and carbon [Schäfer *et al.*, 2007; Kolb, 2009a; Nadalig *et al.*, 2011]. The source of chloromethane is mainly of natural origin (see 1.1.3) [Harper, 2000; Borodina *et al.*, 2005; Keppler *et al.*, 2005; Schäfer *et al.*, 2007; Nadalig *et al.*, 2011]. For that reason several CH₃Cl-utilising bacteria were isolated or enriched from these environments emphasising the ubiquity of these specialised methylophilics [Doronina *et al.*, 1996; Miller *et al.*, 1997; Coulter *et al.*, 1999; McAnulla *et al.*, 2001a; Borodina *et al.*, 2005; Schäfer *et al.*, 2005]. However, the true diversity and versatility of methyl halide-utilisers has hardly been investigated. In addition, although isolates are able to grow only on CH₃Cl, the

atmospheric concentration of CH₃Cl is marginal (i.e., 1 pM x g⁻¹ forest soil [Harper *et al.*, 2003]) and thus it is most likely conceivable that those *in situ* relevant CH₃Cl-utilisers are simultaneously utilising different substrates such as methanol.

4.4.1. Forest soils as chloromethane-sink

Several soil-derived and marine isolates possessing the ability to utilise CH₃Cl were already reported [Doronina *et al.*, 1996; McAnulla *et al.*, 2001a; Borodina *et al.*, 2005; Schäfer *et al.*, 2005]. Assessing the CH₃Cl degradation potential of soil environments in comparison to aquatic environments, different soil types (i.e., forest soil, compost soil), water and sediment types (i.e., marine or freshwater origin) were analysed (see 2.3.9 & 3.12). In order to achieve a more *in situ* relevant reflection samples were not pre-incubated or filtered. Both soil samples revealed the highest degradation potentials indicating a high active CH₃Cl-utilising microbial community. It is quite likely that the most pragmatically reason might be the number of microbial cells per gram or millilitre sample. Soil environments harbours on average 10⁶ up to 10⁹ bacterial cells x g⁻¹ soil [Reineke & Schlömann, 2015] (higher values were also reported ranging up to 10¹¹ cells x g⁻¹ soil [Peñuelas *et al.*, 2014]), whereas pristine aquatic environments (not sediments) are ranging up to values of 10⁶ bacterial cells x ml⁻¹. In addition, seasonal fluctuations are well known for aquatic environments mostly related with 'bloom and burst' cycles of the phytoplankton [Halsey *et al.*, 2012]. Surface water samples from the marine sampling site 'Boknis Eck' analysed in this study are known to range between 0.5 up to 8 x 10⁶ cells x ml⁻¹ in cell counts with lowered cell counts in the winter time (data obtained by flow cytometry; personal communication Dr. Sonja Endres). The sea sediment derived from the ocean floor at the sampling site 'Boknis Eck' was also capable to degrade CH₃Cl. Since it was assumed that the initial dehalogenation of CH₃Cl is not oxygen dependent, the following step depends on oxygen in the cmu pathway (i.e., at least CmuA is present) [Vannelli *et al.*, 1998]. The muddy sea sediments become sporadically anoxic due to seasonal stratification occurring from March to September [www.bokniseck.de]. Regrettably, nothing is known about the *in situ* oxygen concentration at the time of sampling but at least during sample transport (flask was sealed with a breathable cotton plug), preparation and incubation the sediments were exposed to oxygen. In addition, apart from the cmu pathway it is more likely that in marine environments different CH₃Cl-degrading pathways are established [Schäfer *et al.*, 2007]. Recapitulating, all environments tested were able to degrade CH₃Cl as it was previously reported by other authors [McAnulla *et al.*, 2001a; Borodina *et al.*, 2005; Schäfer *et al.*, 2005]. However, it is not possible to make a statement if the degradation was directly facilitated by CH₃Cl-utilisers or accidentally occurred due to reactions such as a co-oxidation by methanotrophs, which are not excluded from the tested environments. Nevertheless, it is worthy to mention that the aquatic samples (water and sediment) revealed lowered CH₃Cl degradation potentials, emphasising the importance of terrestrial environments such as forests as microbiological CH₃Cl sink.

In order to evaluate the compartment in a forest, which might be the most important CH₃Cl-sink, five different compartments (i.e., organic layer, mineral soil, 'fresh' leaves, litter, and deadwood) were evaluated in respect to their CH₃Cl degradation potential (see 2.3.6 & 3.9). Apart from soil and the phyllosphere as known active sinks (see 1.1.3) [Harper, 2000; Keppler *et al.*, 2005; Nadalig *et al.*, 2011], the CH₃Cl utilisation potential of other forest compartments such as the litter layer or dead and rotting wood is not known.

With the exception of the mineral soil, all compartments exhibited CH₃Cl degradation potential. This result is in accordance with a study by Redeker and Kalin that detected lowest fluxes in deeper soil horizons, indicating low CH₃Cl degradation potentials in the deep soil layers [Redeker & Kalin, 2012].

Both leaf-associated compartments (i.e., 'fresh' leaves and litter) revealed similar CH₃Cl degradation rates, and CH₃Cl degradation for these compartments was also proven in previous studies [Redeker & Kalin, 2012; Nadalig *et al.*, 2011]. Living leaves (= phyllosphere) produce CH₃Cl as a side reaction involved in plant defence mechanisms [Rhew *et al.*, 2003; Nagatoshi & Nakamura, 2007], and in decomposed plant material CH₃Cl is formed during demethylation processes of pectin [Hamilton *et al.*, 2003]. Therefore it is conceivable (and at least proven for the phyllosphere [Nadalig *et al.*, 2011]) that microorganism, which are associated with plant material, are capable of CH₃Cl degradation.

Another actively CH₃Cl degrading compartment was identified in the deadwood samples. During fungal wood degradation CH₃Cl is formed in methylation processes during the decomposition of aromatic structures derived from lignin [Keppler *et al.*, 2000]. These processes are also common in the fungal metabolism, especially during fungal growth, but here CH₃Cl acts as methyl group donor and is thus utilised by the fungi themselves [Harper, 2000; Moore *et al.*, 2005; Anke & Weber, 2006]. Thinking about fungi, it is worthy to mention that also the widespread and for plant growth essential mycorrhizal fungi produce methyl halides and are thus another fungal source of CH₃Cl [Redeker *et al.*, 2004]. Nevertheless, the release of CH₃Cl during decomposition of wood by white rot fungi could lead to the colonization of microorganism capable to utilise CH₃Cl. A reason for the lower activity in the deadwood samples, however, could be the decomposition state of the samples themselves. Since the rotten wood was spongy, soft and also of whitish colour, mainly white rot fungi were assumed as being active degrading lignin structures. Thus, it is also likely that the major part of lignin was already decomposed, resulting in lower CH₃Cl emission and thus in lowered abundances of CH₃Cl-utilisers at the wood surface.

The highest CH₃Cl degradation potential, by far, revealed the A horizon (see 3.9). This result matches up with several studies concerning CH₃Cl-utilisers in soils [McAnulla *et al.*, 2001a; Miller *et al.*, 2004; Borodina *et al.*, 2005]. Soils are rich in different substrates for various microorganisms resulting in diverse microbial communities [Torsvik & Øvreås, 2002; Peñuelas *et al.*, 2014]. In addition, abiotic reactions such as redox or substitution reactions that will form CH₃Cl were demonstrated in terrestrial environments [Harper, 2000; Keppler *et*

al., 2000; Hamilton *et al.*, 2003; Keppler *et al.*, 2005]. For example, Keppler and colleagues emphasised the enormous potential of organic-rich soils to release methyl halides by discovering that halide ions (i.e., Cl⁻, Br⁻, I⁻) can be alkylated during the oxidation of organic matter (i.e., humus) in the presence of a suitable electron acceptor such as Fe³⁺ [Keppler *et al.*, 2000]. Organic matter is thermodynamically labile, rich in methoxy group-possessing compounds, and a large amount of organic carbon (global 1500 ± 2200 Gt) is stored as humus [Post *et al.*, 1982]. Thus, organic rich soil layers might be an important source of CH₃Cl and simultaneously an important sink, since the availability of CH₃Cl leads to a successful establishment of CH₃Cl-utilising microorganisms and defines their ecological niche in this manner.

Interestingly, no endogenously formed CH₃Cl was detected in nearly all compartments. The only exception was litter in which CH₃Cl might be build by decomposing reactions of pectin [Hamilton *et al.*, 2003]. It might be also possible that endogenously formed CH₃Cl was immediately consumed by active microorganisms in the different compartments, assuming a closed CH₃Cl cycle in a forest.

4.4.2. (Co)utilisers of methanol and chloromethane in the acidic forest soil

Members affiliated to *Rhizobiales* (i.e., *Beijerinckiaceae*, *Bradyrhizobiaceae*, *Hyphomicrobiaceae*, *Methylobacteriaceae*, *Rhizobiaceae*), *Actinobacteria* and “*Candidatus Saccharibacteria*” were identified as CH₃Cl-utilisers based on the bacterial 16S rRNA gene sequences and marker genes for methanol- and CH₃Cl-initiated pathways (i.e., *mxoF*/*xoxF*-type MDH and *cmuA*) (see 3.11.1, 3.11.2 & 3.11.3). This large diversity was unexpected and new, since most isolates of CH₃Cl-assimilating microorganisms or enrichments with CH₃Cl revealed a few members along *Alphaproteobacteria* (such as species belonging to *Hyphomicrobium*, *Aminobacter*, *Leisingeria*, *Methylobacterium* or the *Roseobacter* group) as capable of growing on CH₃Cl [Miller *et al.*, 2004; Borodina *et al.*, 2005; Schäfer *et al.*, 2005; Nadalig *et al.*, 2011]. Currently only one species affiliated to *Actinobacteria* (i.e., *Nocardioides* sp. strain SAC-4) is described growing solely on CH₃Cl [McAnulla *et al.*, 2001a].

The *Beijerinckiaceae* phylotype was identified as main methanol-utilising methylotroph and revealed the highest similarity to *Methylovirgula ligni*. This finding is in accordance with the previous SIP experiments of the same sampling site, identifying *Beijerinckiaceae* as main methanol-utilisers occupying a central role in a methanol-based food web (see 3.7.1.1 & 4.2.1 & 4.2.4). All members of the acidophilic methylotrophic *Beijerinckiaceae* were never reported to use methyl halides (but were also never tested before) [Marín & Arahal, 2013]. An oxidation of CH₃Cl via an MMO is possible as it was already reported for the methanotrophs *Methylosinus trichosporium* OB3b (*Methylocystaceae*), *Methylococcus capsulatus* Bath, *Methylomonas methanica*, and *Methylomicrobium album* BG8 (all three

Methylococcaceae) [Stirling & Dalton, 1979; Han & Semrau, 2000]. Although CH₃Cl could not serve as a sole carbon source for them, *M. album* BG8 for example was able to assimilate carbon derived from CH₃Cl in the presence of methanol, presumably at the level of formaldehyde [Han & Semrau, 2000]. Thus, in the presence of a second substrate such as methanol, that allows generating enough reducing equivalents and is not competing for the same enzyme (i.e., the MMO here), CH₃Cl can act as an additional carbon source and support the methanotroph in its existence. This assumption is also emphasised by the fact that the *Beijerinckiaceae*-affiliated phylotype was labelled with high LPs in the approach with methanol and [¹³C₁]-CH₃Cl. On the other hand, not all members of the *Beijerinckiaceae* (i.e., *Methylovirgula* and *Methylorosula*) possess a MMO [Berestovskaya *et al.*, 2012; Vorob'ev *et al.*, 2009]. Another possible explanation for the labelling of the *Beijerinckiaceae* phylotype via [¹³C₁]-CH₃Cl-derived carbon could be a cross feeding effect via ¹³CO₂. Several genera (i.e., *Methyloferula*, *Methylovirgula* and *Methylorosula*) can assimilate their carbon via the ribulose biphosphate (RuBP) pathway [Vorob'ev *et al.*, 2009; Vorobev *et al.*, 2011; Berestovskaya *et al.*, 2012], and it is also likely that the supplemented CH₃Cl was primary dissimilated by other taxa in the forest soil, thus circumventing their identification using SIP. Since all analyses were done at the family-level, it is possible that different species or genera comprising the detected phylotype offer both possible pathways for assimilating ¹³C derived from CH₃Cl. In any case, the *Beijerinckiaceae*-affiliated phylotype provided a labelling signal that was highest in the treatment with solely supplemented [¹³C₁]-methanol, emphasising that methanol is preferred over CH₃Cl.

Another CH₃Cl-assimilating phylotype was affiliated to *Actinomycetales* (see 3.11.1). As mentioned before only one actinobacterial species (*Nocardioides* sp. strain SAC-4) affiliated to the *Nocardioidiaceae* (a family within the *Actinomycetales*) is described as growing on CH₃Cl so far [McAnulla *et al.*, 2001a]. The in the SIP experiment detected phylotype did not reveal a high sequence identity to members of the *Nocardioidiaceae* (maximal values of 92 % sequence identity; BLAST analyses done in October 2016, Figure A 13), instead the next hits of cultured species were found within *Kineosporiaceae* (i.e., *Kineosporia* and *Kineococcus*; maximal 95 % sequence identity), *Thermomonosporaceae* (i.e., *Actinomadura* and *Actinoallomurus*; maximal 94 % sequence identity), and *Acidothermaceae* (i.e., *Acidothermus cellolyticus*, maximal 93 % sequence identity), assuming a hitherto unknown *Actinomycetales*-affiliated organism capable of utilising CH₃Cl. In addition, the phylogenetic analyses indicated that the detected CH₃Cl-assimilating phylotype was mainly affiliated to a clade of several uncultured environmental actinobacterial sequences derived from various soil environments (Figure A 14). Moreover, the supplementation of CH₃Cl revealed increased relative abundances in the total bacterial community suggesting advantageous conditions for the phylotype. Such a benefit in utilising CH₃Cl was also assumed for isolates affiliated to the well known species *Methylobacterium extorquens* CM4, *Hyphomicrobium chloromethanicum* CM2 and the marine methylotrophic isolate HTCC2181 [Vannelli *et al.*, 1999; Coulter *et al.*, 1999; McAnulla *et al.*, 2001a; Halsey *et al.*, 2012].

Although generally low abundant, a phylotype affiliated to the Candidate phylum “*Candidatus Saccharibacteria*” (also known as “Candidate Division TM7”) was labelled to a minor extent in the approach with methanol and [$^{13}\text{C}_1$]- CH_3Cl assuming the assimilation of carbon derived from CH_3Cl (see 3.11.1). “*Candidatus Saccharibacteria*” were never reported as methylotrophic, but the present knowledge on this phylum is extremely limited. It is assumed to be ubiquitous in several environments, but members are recalcitrant to cultivation and most knowledge was gained from metagenome sequencing studies wherefore this phylum remains still one of the most enigmatic ones [Ferrari *et al.*, 2014; He *et al.*, 2015]. Actually, the highest abundances (data not shown; but relative abundances were $< 1\%$) were detected in all CH_3Cl -supplemented treatments indicating an enhancing effect of CH_3Cl . Beneficial effects were also reported for a marine betaproteobacterial isolate HTCC2181 that possess only a small genome like it is suggested for the “*Candidatus Saccharibacteria*” members [Albertsen *et al.*, 2013; He *et al.*, 2015], but the marine isolate is also capable of utilising C1 compounds and growth was enhanced with CH_3Cl in the presence of methanol [Halsey *et al.*, 2012]. Another example of an advantageously metabolic feature is the simultaneously utilisation of methanol and CH_3Cl by the methanotrophic species *Methylomicrobium album* BG8, that can assimilate CH_3Cl in the presence of an alternative substrate providing enough reducing equivalents [Han & Semrau, 2000]. However, the role of the detected “*Candidatus Saccharibacteria*” phylotype as a CH_3Cl -utiliser remains enigmatic and disputed.

Regarding the *mxoF*/*xoxF*-type MDH analyses, all labelled taxa were only low abundant in the total bacterial communities (i.e., *Hyphomicrobiaceae* $> 5\%$; *Bradyrhizobiaceae* and *Methylobacteriaceae* $> 1\%$) of the different treatments, suggesting well adapted and quick responding taxa in terms of methanol- and CH_3Cl utilisation that are highly specialised to this substrates and thus this substrate spectrum comprises their ecological niches.

In order to expand also the range of detectable putative methylotrophic taxa, another primer pair was used in the methanol/chloromethane SIP experiment than in the previous SIP experiments (see 2.5.7.1). For example, the reverse primer ‘1555r’ of the previously used primer pair ‘*mxoF1*’ is assumed to bias against *xoxF* sequences (pers. communication P. Chaignaud and F. Bringel), and thus a new primer pair was designed targeting also *xoxF* sequences. Interestingly by applying these primer pair mainly *xoxF* gene sequences were detected instead of *mxoF* gene sequences. At first this result is totally contrary to both previous conducted SIP experiments concerning the same sampling site in which only *mxoF* sequences affiliated to *Methylobacterium* and *Hyphomicrobium* were detected (see 3.7.2), but also indicates a bias of the first used primer pair and reveals the presence of *XoxF* methanol dehydrogenases in the forest soil. Phylogenetic analyses indicated that the majority of the MDH phlotypes detected in the methanol/chloromethane SIP experiment clustered within the *xoxF5* clade (Figure A 12). Only four phlotypes clustered within *mxoF* gene sequences (OTU_{MDH} 4, OTU_{MDH} 8, OTU_{MDH} 15, and OTU_{MDH} 20), three phlotypes were not further affiliated to any *xoxF* clade (OTU_{MDH} 17, OTU_{MDH} 18, and OTU_{MDH} 19) and one

phylotype (OTU_{MDH} 14) clustered with *xoxF* sequences of *Acidiphilium* (*Acetobacteraceae*) that are somehow distinct from the 5 *xoxF* clades.

However, despite the general diversity of MDH phylotypes only two phylotypes affiliated to *Bradyrhizobiaceae* (OTU_{MDH} 24 and OTU_{MDH} 25) dominated all *mxoF/xoxF*-type MDH communities in all treatments. Interestingly, some *Bradyrhizobiaceae*-affiliated phylotypes were detected as CH₃Cl-utilising organisms independent if methanol was present. *Bradyrhizobiaceae* are known to harbour *xoxF* genes and a methanol dehydrogenase activity is not excluded, but only weak growth was reported on methanol, assuming that this compound is not preferred [Sudtachat *et al.*, 2009]. However, growth on CH₃Cl was not reported to date [de Souza *et al.*, 2013]. A putative cross feeding effect cannot be excluded, since some species of the *Bradyrhizobiaceae* are known to assimilate carbon via the RuBP-cycle including *Bradyrhizobium japonicum* [Masuda *et al.*, 2010; de Souza *et al.*, 2013]. However, a true labelling of these *xoxF* phylotypes in the treatments with CH₃Cl is assumed, since cross feeding was avoided by ventilating the gas phase and thus removing accumulated ¹³CO₂ (see 2.3.10). Thus, with the present study a first hint for CH₃Cl-utilisation by *Bradyrhizobiaceae* might be evident.

A *Sinorhizobium*-affiliated phylotype (OTU_{MDH} 17) was dominant in the *mxoF/xoxF*-type MDH community and was assumed to utilise CH₃Cl. The genus *Sinorhizobium* belongs to the family *Rhizobiaceae*, which members are known to form tight association with leguminous plants and root nodules [Alves *et al.*, 2013]. During this tight association the bacterial partner provides nitrogen for its host and the plant provides carbon substrates for the bacterial partner such as carbohydrates and organic acids [Alves *et al.*, 2013]. Thus, it is also conceivable that during the tight association the plant provides also other plant-derived substrates such as methanol or CH₃Cl. To date species of *Sinorhizobium* are not known to utilise CH₃Cl, but some harbour *xoxF* gene sequences enabling methylotrophy. In addition, a putative cross feeding by CO₂ is not assumed since *Sinorhizobium* species are not capable of CO₂ fixation and the experimental design also avoids CO₂ cross feeding.

The putative CH₃Cl-utilising phylotypes affiliated with *Bradyrhizobiaceae* and *Sinorhizobium* were also capable in methanol utilisation (i.e., labelling in the treatment with [¹³C₁]-methanol and CH₃Cl), but might be outcompeted by other microorganisms if only methanol was the solely supplemented carbon source.

Some phylotypes affiliated to *Hyphomicrobiaceae* were labelled in treatments with methanol or CH₃Cl, and are thus assumed to be able to compete with other methanol-utilisers and also utilise CH₃Cl. Several strains of *Hyphomicrobium* were isolated with CH₃Cl as substrate and methanol utilisation is also well reported for several members of this family, wherefore the detection of *Hyphomicrobium*-affiliated phylotypes is in accordance with the current knowledge [Doronina *et al.*, 1996; McDonald *et al.*, 2001; Borodina *et al.*, 2005; Nadalig *et al.*, 2011; Oren & Wu, 2013].

In both treatments in which only one substrate (i.e., either [$^{13}\text{C}_1$]-methanol or [$^{13}\text{C}_1$]- CH_3Cl) was supplemented *Burkholderiaceae*-affiliated phylotypes were labelled to a minor extent indicating only minor importance in terms of the substrate utilisation or the ability by a labelling due to cross feeding on ^{13}C enriched substrates. For the non-methylotrophic *Burkholderia xenovorans* an expression of *xoxF* and other C1 pathway genes was only induced under starving conditions indicating that C1 compounds are not preferred substrates, but their utilisation in order to gain energy under harsh and competing conditions seems to be advantageous [Deneff *et al.*, 2005]. Interestingly, putative methyl halide utilisation was indicated in a SIP study conducted by Miller and colleagues in which *Burkholderia* was labelled in a soil microcosm supplemented with methyl bromide [Miller *et al.*, 2004]. For that reason the minor labelling of the *Burkholderiaceae*-affiliated phylotypes might be on the one hand indeed possible due to the methyl halide or methanol supplemented, or on the other hand (i.e., in the case of the [$^{13}\text{C}_1$]-methanol treatment) due to cross feeding on ^{13}C -enriched substrates like EPS or dead cell material.

Apart from the *Beijerinckiaceae* taxa (based on 16S rRNA gene sequences, see 3.11.1) two phylotypes were further detected as methanol-utilisers based on the *mxoF/xoxF*-type MDH gene sequence analyses. One phylotype is affiliated to the well known methylotrophic family *Methylobacteriaceae*. This family is large and members are widespread in nature and pursue a facultatively methylotrophic metabolism, but are not methanotrophic [Kelly *et al.*, 2013]. Several members are also able to utilise halomethanes such as *M. extorquens* CM4 [McDonald *et al.*, 2001; Studer *et al.*, 2002]. However, the detected phylotype OTU_{MDH} 3 was not labelled in any [$^{13}\text{C}_1$]- CH_3Cl treatment approach, assuming that the taxa is either not utilising CH_3Cl or is not detectable due to its general low abundance within the microbial community. Another methanol-utilising phylotype was affiliated to *xoxF* gene sequences of *Acetobacteraceae*, more precise to the genus *Acidiphilium*. Within the *Acetobacteraceae* methanol-utilising species are known such as *Granulibacter bethesdensis* or *Acidomonas methanolica* [Urakami *et al.*, 1989; Greenberg *et al.*, 2006]. In addition, *Acidiphilium multivorum* is also capable of methanol utilisation, whereas *Acidiphilium cryptum* is not, but both species possess *xoxF* gene sequences [Wakao *et al.*, 1994]. Thus, the detected phylotype might be another methanol-utilising member of the genus *Acidiphilium*.

By analysing the *cmuA* gene diversity, all detected phylotypes were assumed to utilise CH_3Cl . In total eight different *cmuA* phylotypes were detected, mainly affiliated to *Alphaproteobacteriaceae* (i.e., *Methylobacteriaceae*, *Hyphomicrobiaceae* and one unclassified phylotype) but also to *Firmicutes*. However, the question of a real functional enzyme in terms of CH_3Cl -utilisation remains, since the relative abundance of the *Firmicutes* phylotype (OTU_{cmuA} 7) was in all treatments below 0.5 %, and the phylotype clustered with *cmuA* sequences derived from genomes within the phylogenetic tree (see Figure A 15). Thus, only the residual six detected phylotypes are assumed to harbour functional enzymes.

Mainly *Methylobacteriaceae*-affiliated phylotypes were labelled in the treatments indicating methanol and CH₃Cl assimilation. This finding is partially not surprising, since the well characterised species *M. extorquens* CM4 is known as methanol- and CH₃Cl-utilising methylotroph [Studer *et al.*, 2002]. On the other hand the relative abundance of *Methylobacteriaceae* based on the 16S rRNA analyses was low (i.e., > 1 %) in all treatments. No member of this family was indicated as labelled based on 16S rRNA gene sequence or *mxoF/xoxF*-type MDH gene sequence analyses, raising the question of the 'true' or 'correct' affiliation of the detected *cmuA* phylotypes. Since the *cmu*-pathway is plasmid-borne in *M. extorquens* CM4, the chance for HGT events spreading *cmuA* genes in an environment is given and indeed evidences for this scenario are reported for the *cmu*-pathway [Roselli *et al.*, 2013; Nadalig *et al.*, 2014; Michener *et al.*, 2016]. Nevertheless, CH₃Cl as carbon source was only assumed for one phylotype (OTU_{*cmuA*} 2), whereas the supplementation of [¹³C₁]-methanol resulted in a higher diversity. If methanol was the solely substrate supplemented, only *Methylobacteriaceae*-affiliated phylotypes were labelled indicating that methanol is a preferred substrate for these taxa. If [¹³C₁]-methanol and CH₃Cl were simultaneously supplemented, another *Hyphomicrobium*-affiliated phylotype was additionally detected. Thus, a beneficial effect of CH₃Cl on the *Hyphomicrobium*-phylotype is assumed that might be the utilisation of CH₃Cl as energy source, since the taxon was not labelled in any [¹³C₁]-CH₃Cl treatment. Another explanation could be that the *Hyphomicrobium*-affiliated phylotype was slower in CH₃Cl utilisation than the *Methylobacterium*-affiliated taxa and thus less competitive. Incubation studies with pure cultures of *H. chloromethanicum* CM2 revealed that growth yields on methanol and CH₃Cl are nearly similar assuming no biasing effect of one substrate [McAnulla *et al.*, 2001b]. But enzymatic tests revealed that the dehalogenation rate of CH₃Cl was low compared to *Aminobacter lissarensis* CC495 suggesting a lowered specific activity for the CmuA enzyme of *H. chloromethanicum* CM2 [McAnulla *et al.*, 2001b]. Nevertheless, CH₃Cl served also as carbon source for this phylotype. Another *Methylobacteriaceae*-affiliated phylotype (i.e., OTU_{*cmuA*} 1) was not labelled, but this phylotype was only detected in treatments that were solely supplemented with CH₃Cl. Apparently, the taxon is able to utilise CH₃Cl as energy source; the utilisation as carbon source was not verifiable. The presence of methanol was also not growth enhancing, indicating that the phylotype is not utilising methanol like it is also reported for the CH₃Cl-utilising species *Aminobacter lissarensis* CC495 [McDonald *et al.*, 2005].

Apart from CH₃Cl being a carbon source the methyl halide could also serve as a source of energy like it was assumed for the marine isolate HTCC2181 [Halsey *et al.*, 2012]. CH₃Cl could not serve as solely carbon source, but when CH₃Cl was provided in the presence of low concentrations of methanol, growth rates, maximum cell density and cellular ATP content were significantly enhanced [Halsey *et al.*, 2012]. For that reason the authors suggested that under certain conditions (i.e., low amounts of the preferred assimilation substrate) C1 compounds are partitioned in compounds that are strictly assimilated (such as methanol) and

compounds that strictly serve as source of energy (such as CH₃Cl) [Halsey *et al.*, 2012]. These combined fluxes of substrates might be sufficient for obligate methylotrophs and it is also conceivable that such synergistic metabolic features are advantageous for other microorganisms in complex environments in which the competition for substrates is high by nature. In the treatment with [¹³C₁]-methanol and CH₃Cl such microorganisms might be detected that use CH₃Cl only as energy source, wherefore they were not detectable as CH₃Cl-assimilating taxa in both treatments with [¹³C₁]-CH₃Cl. Two phylotypes affiliated to *Actinobacteria* were identified as labelled in this way. Both are thus assumed to assimilate methanol and might use CH₃Cl as energy source. The dominant phylotype was affiliated to *Microbacteriaceae*, more detailed to the genus *Gryllotalpicola* (99 % sequence identity to *Gryllotalpicola daejeonensis*). *Microbacteriaceae*-affiliated methylotrophic isolates are reported belonging to the genus *Leifsonia* [Hung *et al.*, 2011], and in a previous SIP study of this doctoral thesis (pH shift experiment, see 3.7.1.3) focussing on the same sampling site a *Leifsonia*-affiliated phylotype (99 % sequence identity to *Leifsonia xyli*) was identified as methylotrophic taxon under pH neutral conditions. The identified *Gryllotalpicola* phylotype revealed only 94 % sequence identity to *Leifsonia* species offering the ability of a hitherto unknown methylotrophic member of this genus, since all members are currently not reported to be methylotrophic (they were also not tested) [Kim *et al.*, 2012; Moon *et al.*, 2014; Fang *et al.*, 2015]. In addition, the knowledge on this genus is still limited, since the hitherto described species (at the time of writing – October 2016 – there were six species validly listed at www.bacterio.net/gryllotalpicola.html) were isolated mainly from guts of wood- or root-feeding insect (termites and mole cricket) and only two species were soil-derived [Kim *et al.*, 2012; Moon *et al.*, 2014; Fang *et al.*, 2015].

The other phylotype putatively utilising CH₃Cl as energy source was affiliated to *Pseudonocardiaceae*. *Pseudonocardiaceae* comprises 26 different genera, in which the majority of all species was isolated from soils or other environmental sources [Franco & Labeda, 2013]. The detected phylotype revealed a sequence identity of 91 % to *Amycolatopsis methanolica*, which is a known methylotrophic species of the *Pseudonocardiaceae* [De Boer *et al.*, 1990]; instead a higher sequence identity to members of the genus *Pseudonocardia* (98 % sequence identity to *Pseudonocardia hispaniensis*) was obvious. *Pseudonocardia* species are metabolic versatile and some are even facultative autotrophs such as *P. carboxydivorans* that can grow with solely CO₂ as carbon source [Park *et al.*, 2008; Franco & Labeda, 2013]. Other species are also capable of utilising chlorobenzenes or chloroethene such as *P. benzenivorans* and *P. chloroethenivorans* [Kämpfer & Kroppenstedt, 2004; Lee *et al.*, 2004; Franco & Labeda, 2013]. Although their versatility and ability to utilise a broad range of different, even recalcitrant substrates, ‘true’ methylotrophy of cultured *Pseudonocardia* species was never reported (and also never tested) [Franco & Labeda, 2013]. However, one metagenomic studies in a harsh environment (i.e., the active Lullailaco Volcano in the Atacama Desert) revealed *Pseudonocardia* sp. as the dominant taxon there and several genes enabling a

methylotrophic lifestyle (complete pathways for methanol, formaldehyde and formate utilisation and for a putative sMMO) were detected [Lynch *et al.*, 2014]. Genome comparisons between several *Pseudonocardia* species revealed hints that MDH genes are spread over *Pseudonocardia* genomes, and thus the possibility of methanol-utilising *Pseudonocardia* species is clearly given [Lynch *et al.*, 2014]. In addition, CH₃Cl is mainly of naturally origin and is also emitted during volcanic activity and eruptions to concentrations that are 10⁶ times higher (i.e., up to 19 ppm) than the atmospheric concentration of CH₃Cl [Frische *et al.*, 2006]. For that reason, the utilisation of CH₃Cl – as energy source or even carbon source – might be beneficial for putative methylotrophic microorganism in such environments and thus speculations towards CH₃Cl utilisation by *Pseudonocardia* species are possible.

4.4.3. Striking differences between chloromethane-utilisers of different soil environments confirming their underestimation *in situ*

A large diversity of different taxa capable of CH₃Cl utilisation such as *Beijerinckiaceae* and actinobacterial taxa was detected in the methanol/chloromethane SIP experiment of this study confirming the current assumption that the *in situ* diversity of CH₃Cl-utilising microorganisms is much higher than currently known [Miller *et al.*, 2004; Borodina *et al.*, 2005; Schäfer *et al.*, 2005]. The additional application of marker genes revealed phylotypes as CH₃Cl-utilising taxa, although they were not abundant in the microbial community such as *Bradyrhizobiaceae* or *Sinorhizobium* based on *xoxF* gene sequences. Contrary, previous studies on terrestrial environments and the phyllosphere revealed mainly *Hyphomicrobium* species dominating enrichments and gene libraries [McAnulla *et al.*, 2001a; Borodina *et al.*, 2005; Nadalig *et al.*, 2011]. However, a study by Miller and colleagues revealed a more diverse community including further *Proteobacteria* and *Actinobacteria* (*Norcadioides*) as CH₃Cl-utilisers [Miller *et al.*, 2004]. It should be noted that the in this study conducted methanol/chloromethane SIP experiment focuses on a forest soil that differs especially in soil pH from all other soil environments investigated so far. Soil samples from the study of Borodina and colleagues as well as soil samples from the study of Miller and colleagues revealed nearly neutral pH [Miller *et al.*, 2004; Borodina *et al.*, 2005 – pers. communication C. Murrell], in which the soil of this study was acidic. Studies on phyllospheric and marine CH₃Cl-utilisers in a complex community were also conducted under pH neutral conditions [Schäfer *et al.*, 2005; Nadalig *et al.*, 2011]. Thus, there is a lack of knowledge on CH₃Cl-utilisers in acidic environments and it is undisputably conceivable that the pH of a system defines ecological niches more intensive than the available substrate spectrum. Further, the low abundance of *Methylobacteriaceae* and *Hyphomicrobiaceae* in the total community, but the exclusively labelling of *cmuA* gene sequences affiliated to these families opens the question of the achievable coverage of CH₃Cl-utilising microorganisms. Especially marine

isolates are not harbouring *cmuA* genes [Schäfer *et al.*, 2007; Halsey *et al.*, 2012], and putative HGT events are also contributing to misleading results [Michener *et al.*, 2016]. Since other pathways besides the well-analysed *cmu* pathway must also exist, the conceivable diversity of CH₃Cl-utilising microorganism increased [Schäfer *et al.*, 2007]. In addition, CH₃Cl is not always assimilated but can also serve as an energy source. The comparative character of the SIP experiment enabled (i) to further evaluate different metabolic profiles and (ii) also to detect such taxa like the two actinobacterial phylotypes (OTU_{16S} 61, *Gryllotalpicola*; OTU_{16S} 85, *Pseudonocardia*) that might use CH₃Cl as energy source. Recapitulated, all findings of the conducted methanol/chloromethane SIP experiment emphasise the assumption that the current known diversity of CH₃Cl-utilisers is indeed underestimated.

4.4.4. Variety of trophic types of methanol- and chloromethane-utilising methylotrophs

In the current study the co-utilisation of methanol and CH₃Cl in an acidic forest soil was evaluated. An unexpected diversity of CH₃Cl-utilisers was detected emphasising that the current knowledge on CH₃Cl-utilising microorganisms especially in acidic soils is weak. Phylotypes affiliated to alphaproteobacterial *Rhizobiales* (such as *Beijerinckiaceae*, *Bradyrhizobium*, *Methylobacterium*, and *Hyphomicrobium*) and some *Actinobacteria* were identified as CH₃Cl-utilisers. The conducted experiment enabled further the determination of four trophic types in terms of substrate utilisation that might be occurring simultaneously, only depending on the availability of the substrates ‘methanol’ and ‘CH₃Cl’. These trophic types are characterised by the simultaneously co-consumption, partitioning or the utilisation of only one C1 compound.

Trophic type 1 – Both substrates serve as carbon sources

Species such as the dominating phylotype affiliated to *Beijerinckiaceae* (OTU_{16S} 12), several MDH phylotypes (for example the *Hyphomicrobiaceae*-affiliated *xoxF* phylotypes OTU_{MDH} 2, OTU_{MDH} 21, OTU_{MDH} 22; *Bradyrhizobiaceae*-affiliated *xoxF* phylotypes OTU_{MDH} 25; *Sinorhizobium*-affiliated *xoxF* phylotype OTU_{MDH} 17) as well as the dominating *cmuA* phylotype (OTU_{cmuA} 2, *Methylobacteriaceae*) are suggested to utilise both given substrates as carbon sources, since they were consistently detected in approaches with solely one substrate supplemented (methanol or CH₃Cl) and/or they were detected in both combined approaches (methanol and CH₃Cl). Thus, they are also assumed to be able to respond on altering concentrations or availabilities of both C1 compounds. This metabolic profile seems to be common along alphaproteobacterial methylotrophs, since the simultaneously utilisation of methanol and CH₃Cl as source of carbon and energy was also described for known cultivated methylotrophs including well-characterized *Hyphomicrobium* and *Methylobacterium* strains [McDonald *et al.*, 2001]. In addition, the taxa are assumed to present no limited substrate range to C1 compounds only. The *Beijerinckiaceae*-affiliated phylotype was

assumed to utilise sugars, acetate and even aromatic compounds (see 4.2.1); the families *Hyphomicrobiaceae* and *Bradyrhizobiaceae* are metabolic versatile utilising several carbohydrates, organic acids or aromatic compounds [Oren & Wu, 2013; de Souza *et al.*, 2013], and *Methylobacterium* is a well-known genera including facultative methylotrophs [Kelly *et al.*, 2013]. Thus, this diverse substrate spectrum provides advantageous and might avoid starving states. In addition, the adaption to utilise methanol and CH₃Cl might improve the competitiveness of these taxa and defines their ecological niche in terms of substrate spectrum, substrate adaption, and substrate availability.

Trophic type 2 – Methanol serves as carbon and chloromethane serves as energy source

In the SIP experiment some taxa were only identified under certain conditions, assuming that methanol served as carbon source and that CH₃Cl had an enhancing effect, since it might be used as energy source. These taxa were mainly detected in the combined approach with [¹³C₁]-methanol and CH₃Cl (based on 16S rRNA) or in approaches with solely [¹³C₁]-methanol based on *cmuA* gene sequences analyses (presence of *cmuA* genes suggest the presence of the *cmu* pathway). Such taxa were affiliated to Actinobacteria (OTU_{16S} 61, *Gryllotalpicola*; OTU_{16S} 85, *Pseudonocardia*) and *Alphaproteobacteria* (OTU_{*cmuA*} 3 & 4, *Methylobacterium*; OTU_{*cmuA*} 6, *Hyphomicrobium*). Such trophic behaviours were conceivable during the co-oxidation of CH₃Cl enabled by an MMO as already observed for certain methanotrophs [Stirling & Dalton, 1979; Han & Semrau, 2000]. Interestingly, the specific activities of the MMO-containing extracts from *Methylosinus trichosporum* OB3b, *Methylococcus capsulatus* Bath and *Methylomonas methanica* to oxidise CH₃Cl were different compared to each other. Extracts of *M. capsulatus* BATH oxidises CH₃Cl as rapidly as methane; extracts of *M. trichosporum* OB3b revealed two times lowered activities, and extracts of *M. methanica* revealed nearly two times higher activities [Colby *et al.*, 1977; Stirling & Dalton, 1979]. Since genomic studies of *Pseudonocardia* species revealed the presence of a putative MMO, the ability to co-oxidise CH₃Cl enabled by this MMO might therefore be possible [Lynch *et al.*, 2014]. Apart from the actinobacterial phylotypes, also several phylotypes affiliated to the methylotrophic CH₃Cl-utilising genera *Methylobacterium* and *Hyphomicrobium* were suggested to belong to this described trophic type. In this way different preferences of *in situ* utilised carbon and energy source are assumable, indicating that the utilisation of both substrates as carbon source is not mandatory and a partition might be the preferred metabolic strategy for some taxa.

Trophic type 3 – Chloromethane serves as carbon and methanol serves as energy source

Another case of a partition of available substrates would be that CH₃Cl serves as carbon source and methanol serves an energy source. Taxa pursuing this trophic strategy are only detectable in the combined approach with [¹³C₁]-CH₃Cl and methanol (based on 16S rRNA) or in the approaches with supplemented [¹³C₁]-CH₃Cl based on the *mxoF/xoxF*-type MDH gene sequences analyses (presence of *mxoF* or *xoxF* genes suggest the presence of an

MDH and thus a methanol-based pathway). By this manner two different phylotypes were detected – one affiliated to the enigmatic phylum “*Candidatus* Saccharibacteria” (OTU_{16S} 108) and a *Bradyrhizobiaceae*-affiliated phylotype (OTU_{MDH} 24). Such a metabolic profile was already reported for the marine isolate HTCC2181 [Halsey *et al.*, 2012]. The authors assume that this metabolic profile is advantageous at conditions in which the availability of the primary substrate (methanol) is too low to maintain optimal growth rates and thus another low-molecular-weight substrate (CH₃Cl) serves as temporary energy source. As a well-fitting scenario the typically ‘boom and burst’ growth patterns of diatoms (they are provider of methanol or methylated compounds) are mentioned. For terrestrial environments modified scenarios are conceivable such as seasonal repeating events like plant growth (spring) or leaf fall (autumn) or unpredictable events such as increased deadwood amounts due to storm damage. Here the amount of methanol might be elevated due to plant release (growth) or wood-rotten fungi activity (dead wood), offering ideal conditions for some taxa. If these temporal and also spatial limited methanol-rich periods are gone, the taxa switch to the metabolic profile in which they strictly partitioned between carbon and energy sources that are available. In this manner cell maintaining is ensured and microorganisms can survive these starving conditions.

Trophic type 4 – Only one substrate serves as source of carbon and energy

Apart from taxa that might utilise both substrates, it is also possible that some taxa are only utilising one supplemented substrate and the presence of the second supplemented substrate is insignificant to them. Since only a handful isolates are known to utilise CH₃Cl, the amount of methanol- and not CH₃Cl-utilising microorganism must prevail. Based on *mxoF/oxoF*-type MDH gene analyses in total four different phylotypes affiliated to *Methylobacteriaceae* (OTU_{MDH} 3), *Acetobacteraceae* (OTU_{MDH} 14) and *Beijerinckiaceae* (OTU_{MDH} 11 and OTU_{MDH} 15) were detected as solely methanol-utilising taxa.

Based on 16S rRNA gene sequences only one phylotype was identified, which might be the only representative of the last mentioned metabolic profile in terms of CH₃Cl. This phylotype is affiliated to *Actinomycetales* (OTU_{16S} 6), and was only labelled in the treatment solely supplemented with [¹³C₁]-CH₃Cl. Currently, only one actinobacterial isolate was reported to grow on CH₃Cl, *Nocardioides* sp. SAC-4 [McAnulla *et al.*, 2001a]. Since this isolate was regrettably lost, no details of CH₃Cl utilisation or the *cmu* pathway of *Actinobacteria* can be obtained at the moment [Schäfer *et al.*, 2007]. However, *Aminobacter lissarensis* CC495 is an alphaproteobacterial species (*Phyllobacteriaceae*) that is reported to grow on CH₃Cl and other substrates such as glucose, pyruvate and methylamine, but it shows inability to grow on methanol, methane or formate [McDonald *et al.*, 2005]. Thus, taxa that are not depending on methanol might also have an advantage in the complex forest soil community, since they are not competing for methanol and so their ecological niche is defined in that way.

Based on the obtained results the following model (Figure 88) was constructed to summarize the findings on the occurring trophic types of methanol- and CH₃Cl-utilising microorganisms in an acidic soil of a temperate deciduous forest.

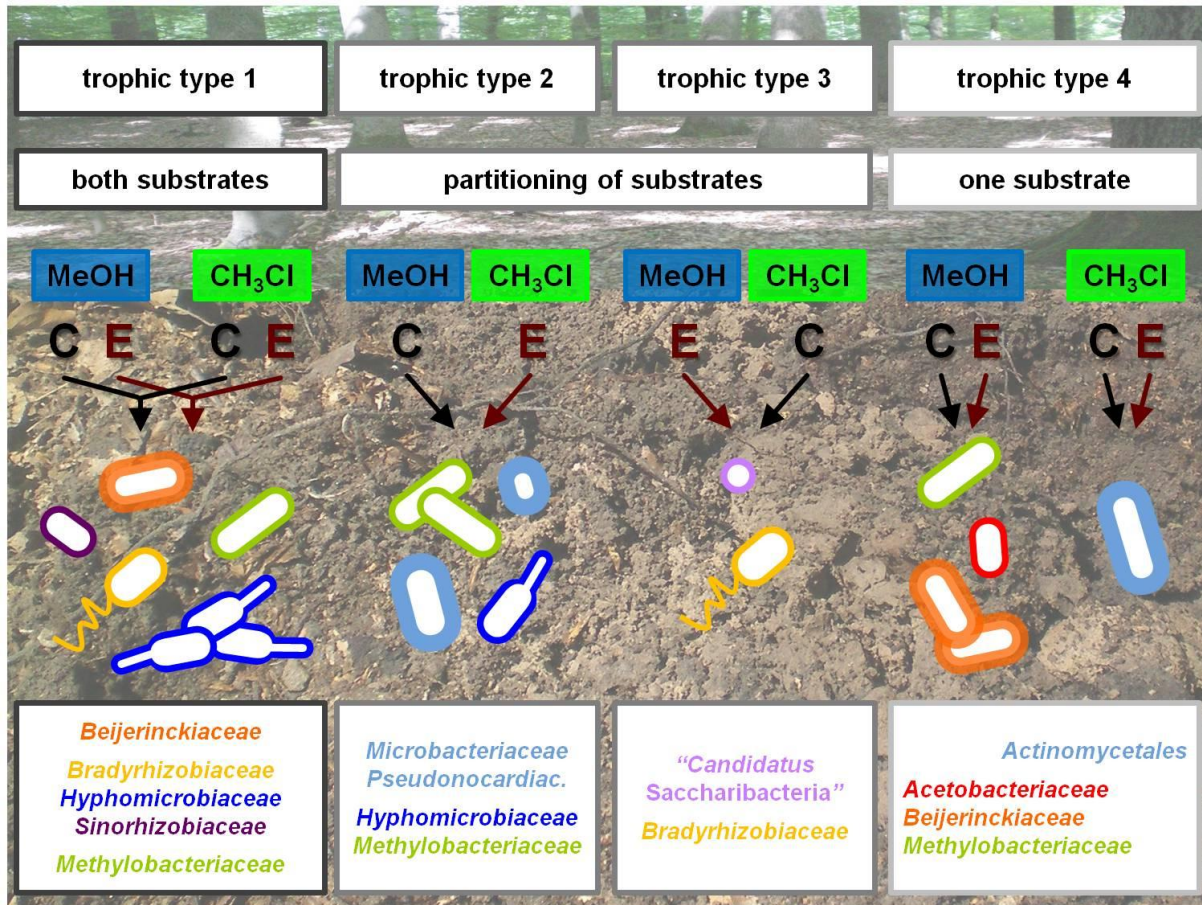


Figure 88 Variety of metabolic profiles of methanol- and chloromethane-utilising methylotrophs in a temperate deciduous forest with acidic soil.

This figure summarises the obtained results of the conducted study in terms of methanol and chloromethane (co)utilisation of methylotrophic organisms in the soil. For more information refer to the following sections: 1.6.5, 1.9, 2.3.10, 3.11, 4.2.4, 4.4.4.

4.4.5. Existing co-utilisation of aromatic compounds and chloromethane in soils?

Plant-derived aromatic compounds can serve as a biological soil-associated sources for CH₃Cl and are mainly originated from lignin (consisting of cross-linked phenolic polymeric compounds) [Keppler, 2000; Lebo *et al.*, 2015]. Another source of aromatic compounds, such as benzene, toluene, ethylbenzene and xylene (BTEX), is associated with natural gases, crude oil and petrolchemical industry [Deeb *et al.*, 2001]. A putative effect of aromatic compounds on CH₃Cl utilisation could be suggested and is also emphasised by the isolation of CH₃Cl-utilisers in pristine and contaminated environments [Hartmanns *et al.*, 1986;

Doronina *et al.*, 1996; McAnulla *et al.*, 2001a; Schäfer *et al.*, 2005; Nadalig *et al.*, 2011]. Indeed, a widespread inhibitory effect of toluene on the methyl halide degradation in marine water samples was reported [Goodwin *et al.*, 2005]. It was possible to gain a methyl halide-utilising isolate 'Oxy6', which was capable of growing on toluene and to oxidise several intermediates of the TOL pathway such as benzyl alcohol, benzoate or catechol [Goodwin *et al.*, 2005]. Regrettably, no further studies were conducted on toluene inhibition on the CH₃Cl degradation and also no further efforts were made to gain more physiological details on 'Oxy6' (person. communication Kelly Goodwin). Nevertheless, a co-utilisation of aromatic compounds and methyl halides might be possible in marine and terrestrial ecosystems. No inhibition of toluene on the CH₃Cl degradation was obvious in the soil samples tested (see 3.13) – contrary a putatively enhancing effect was observed at higher CH₃Cl concentrations. It might be possible that the co-oxidation of CH₃Cl might provide an advantageous effect in terms of energy production for aromatic compound utilising taxa.

Since the toluene inhibition was not unequivocal in the acidic forest soil samples and inhibitory effects were reported for seawater samples, it might be possible that the inhibition is only detectable in aquatic environments [Goodwin *et al.*, 2005]. Therefore the impact of toluene on the CH₃Cl degradation was additionally evaluated in several other environments (i.e., another soil type, 'compost soil'; freshwater environments, 'lakewater' and 'lakeshore'; marine environments, 'seawater', 'seashore', and 'seasediment') (see 3.13). The CH₃Cl degradation potential of these environments was already discussed (see 4.4.1). However, neither in any marine nor in any freshwater samples an obvious effect of toluene on the CH₃Cl degradation potential was detectable assuming that effects caused by toluene are negligible. In addition, further literature research (most recently performed in October 2016) and an overview on references citing the study by Goodwin and colleagues revealed no additional work on the inhibitory effect of toluene on methyl halide degradation. Thus, the observed toluene inhibition remains unique, the mechanisms behind remains unsolved and the putative metabolic interaction of aromatic compounds and methyl halides remains speculative and is rejected.

4.5. Addressing the hypotheses and future perspectives

This section summarises the main findings and how they address the main hypothesis (see 1.9). More detailed information on the results and conclusions were extensively discussed in the sections 3 and 4.1 - 4.4.

The main objective of the current study was to evaluate the substrate range of methylotrophic microorganisms in an acidic forest soil *in situ* as well as the influence of the soil's pH on the established methylotrophic community. The term 'substrate range' comprises thereby C1 compounds such as methane, methanol and chloromethane, but also multi-carbon substrates. In general, the three central C1 compounds were naturally occurring and mainly plant-derived. The tested multi-carbon compounds were assumed to be common in a

forest soil and thus served as example-substrates for different substrate classes such as organic acids, sugars or aromatic compounds. The conducted division of the study into three parts enabled a more concentrated addressing of the main hypothesis in terms of specific methylotrophic guilds.

The 'high-affinity' methanotrophs were mainly targeted by analysing USC α -methanotrophs (see 3.1, 4.1.1). The supplementation of alternative substrates did not provide clear results on the response of these 'high-affinity' methanotrophs on different alternative substrates, and rather confirmed the assumption that these microorganisms are obligate or restricted facultative methanotrophs (see 4.1.2, 4.1.3). The formulated sub-hypothesis could not be unequivocally confirmed, and thus the substrate range of USC α -methanotrophs seems restricted to methane, wherefore methane utilisation (especially the adaption to low concentrations) clearly defines their ecological niche.

Important methanol-utilising methylotrophs were identified as members of the *Rhizobiales* (i.e., *Beijerinckiaceae*, *Methylobacteriaceae*, *Hyphomicrobiaceae*, *Methylocystaceae*, *Rhizobiaceae*, *Bradyrhizobiaceae*) based on molecular studies applying general marker genes (16S rRNA gene) and methylotrophic specific marker genes (mx_AF/xoxF, cmuA, mmoX) (see 3.7, 4.2.1, 4.4.2). The utilisation of multi-carbon substrates was again not unequivocally verified. Especially the main methanol-utilising taxon *Beijerinckiaceae* seemed more restricted to C₁ compounds in their substrate range. Other taxa such as *Methylobacterium* or *Hyphomicrobium* are known as facultatively methylotrophic organisms, and they were indeed detectable possessing a broader substrate range including methanol, chloromethane, organic acids, sugars, and aromatic compounds (see 4.2.1 & 4.4.2). *Methylocystaceae*-affiliated taxa might be not the main methanol-utilising members of the methylotrophic community, but they seem to be capable in the utilisation of glucose, which was never reported before for this family (see 4.2.1). The (co)utilisation of methanol and chloromethane revealed different trophic types for methylotrophs (see 4.4.4). Therefore, the substrate utilisation regarding the trophic type (e.g. partitioning into energy and carbon source) further defines the ecological niche of methylotrophs.

In addition, fungi were addressed. Some methylotrophic yeasts are known, but the knowledge on methylotrophic fungi is restricted to biotechnological important strains. In the current work, yeast and mould fungi affiliated to *Basidiomycota* and *Zygomycota* were identified as methanol-derived carbon-utilisers (see 3.7.3). Thus, first slight hints on the presence and diversity of methylotrophic fungi in soil environments were gained

Apart from the different substrate ranges also the pH was clearly shown to be an important ecological niche-defining parameter, since the microbial community was dramatically changed under shifted pH conditions (see 4.3). The main methanol-utilising taxa were no longer detectable under elevated pH conditions, emphasising the growth-restricting conditions of an acidic soil pH and the adaption of acidotolerant taxa to this ecological niche-defining parameter.

Although the substrate spectrum of soil-derived methylotrophs was not satisfyingly evaluated, methanol-derived carbon-utilising taxa were recognized. Thus, a tight interaction between methylotrophs and other members of the microbial community could be assumed in which the methylotrophs occupy a central role in a methanol-based microbial food web (see 4.2.4).

In summary, all results gained confirm that the (co)utilisation of C1 compounds such as methane, methanol and chloromethane clearly defines the ecological niche of the soil-derived methylotrophs as well as the soil's pH. The presence of alternative substrates might be supporting, but inconclusive results could not verify the hypothesis in terms of the multi-carbon substrate range. It is very likely that the competition for multi-carbon substrates might be high in a soil under *in situ* conditions and that methylotrophs, which are not dominating the microbial community, are less competitive. This lowered competitiveness might be the crux, wherefore the detection of facultative methylotrophs based on multi-carbon compounds is extremely difficult.

Based on this knowledge so far and the experience gained in this work, targeting the multi-carbon substrate spectrum of soil-derived methylotrophs under *in situ* near conditions might be able by conducting 'selective long-term enrichments' as a starting point. A long-time incubation (several weeks) with low concentrations of methanol and methane supplemented might trigger methylotrophs, and might lead to an outcompeting of other heterotrophic microorganisms that would compete for multi-carbon compounds. Such 'in methylotrophs enriched' treatments could be further supplemented with mutlic-carbon substrates (as ^{13}C -isotopologues) and the response of the microbial community would lead to further conclusions. It might be advantageous to conduct such incubations not as soil slurries, since water saturation hampers methanotrophs (see 4.1.1). Also the supplementation of rare earth metals should be considered to not discriminate against XoxF-type MDH possessing methylotrophs (see 1.6.3). A more time-resolved analysis of the abundance (DNA-based) and activity (RNA-based) of microorganisms could further clarify the interaction of methylotrophs and further members of the microbial community. However, such incubations are also biased and depending on the methanol concentration used, some taxa could be still overlooked.

Another approach to evaluate the substrate utilisation potential of methylotrophs *in situ* could be addressed by an artificial community. Substrate ranges of facultative methylotrophs were assessed under laboratory conditions. Soil samples inoculated with such pure cultures and incubated under *in situ* close conditions could reveal whether under 'competitive conditions' the multi-carbon substrate is still utilisable by the methylotroph. In addition, carbon flux studies of known facultative methylotrophs besides *Methylobacterium* sp. might also reveal the 'metabolic behaviour' of these methylotrophs and could give further insights such as a possible substrate preference or partitioning. (Meta)genome studies combined with transcriptome or metabolome analyses could also answer questions on activity, diversity and

carbon fluxes under methylotrophic or mixed substrate conditions of a microorganism or a microbiome. Another approach to estimate the methylotrophic diversity of environmental samples might be a SIP incubation with labelled $^{13}\text{C}_1$ compounds (e.g. methanol or methane), and subsequently whole genome shotgun sequencing approaches. In this manner, C1 compound-utilising taxa could be identified without the implementation of known methylotrophic marker genes.

In addition, evidences for mixotrophic methanotrophs emerged by the proof of the mixotrophic growth (utilising H_2 as source of energy) of methanotrophic *Verrucomicrobia* (see 4.1.1 and Carerer *et al.*, 2016; Mohammadi *et al.*, 2016). Therefore, targeting the enigmatic USC α and other 'high-affinity' methanotrophs by treatments solely supplemented with H_2 and CH_4 as sole sources of energy and carbon might provide insights whether mixotrophic growth is a survival strategy of 'high-affinity' methanotrophs. Further, *Methylocystaceae* and the pMMO2 should be routinely taken into account when targeting 'high-affinity' methanotrophs, since these 'low-affinity' methanotrophs might substantially contribute to the atmospheric methane oxidation.

Apart from all these considerations, also the need for a broader spectrum of molecular tools is clearly given. Although the 16S rRNA gene might be a suitable phylogenetic marker for *Bacteria* in general, the application of gene markers based on the 'microbial guild' of methylotrophs might be more expedient. However, the tool box of methylotrophic marker genes regarding methanol is insufficient (see 1.6.3). Therefore, the development of primers targeting the broad range of marker genes encoding for known but not frequently addressed enzymes such as the PQQ-MDH2 of *Betaproteobacteria*, NAD-MDH of gram-positive *Bacilli* or the FAD-AOx of *Fungi* (see 1.6.3, 1.7), is absolutely essential. The development of qPCR assays based on different methylotrophic marker enzymes might be further beneficial to estimate the abundance of methylotrophic guilds in a microbial community.

Regarding the utilisation of CH_3Cl , the uncovering of pathways apart from the known cmu-pathway should be focussed to gain a more complex comprehension on the methyl halide utilisation and to identify further marker enzymes and genes which in turn can be applied in further environmental studies.

Last but not least, pure cultures of methylotrophs should be re-analysed in terms of the utilisation of alternative substrates as concentration depending studies, since substrate spectrum studies often concentrate solely on one concentration (often in mM range). Trials to isolate methylotrophic organisms from different environments with different isolation techniques should be further conducted, since pure culture and isolates can sometimes provide more hints than culture-independent studies.

5. REFERENCES

- Alber BE.** (2010). Biotechnological potential of the ethylmalonyl-CoA pathway. *Appl Microbiol Biotechnol* 89: 17–25.
- Albertsen M, Hugenholtz P, Skarshewski A, Nielsen KL, Tyson GW, Nielsen PH.** (2013). Genome sequences of rare, uncultured bacteria obtained by differential coverage binning of multiple metagenomes. *Nat Biotechnol* 31: 533–538.
- Allan W, Struthers H, Lowe DC.** (2007). Methane carbon isotope effects caused by atomic chlorine in the marine boundary layer: Global model results compared with Southern Hemisphere measurements. *J Geophys Res Atmos* 112: D04306.
- Allredge, A.L., and Cohen, Y.** (1987). Can microscale chemical patches persist in the sea? Microelectrode study of marine snow, fecal pellets. *Science* 235: 689–691.
- Alves LMC, de Souza JAM, de Mello Varani A, de Macedo Lemos EG.** (2013). The Family *Rhizobiaceae*. In: Rosenberg E, DeLong EF, Lory S, Stackebrandt E, Thompson F (eds). *The Prokaryotes – Alphaproteobacteria and Betaproteobacteria*. Springer: New York, pp 419–437.
- Anda M, Ikeda S, Eda S, Okubo T, Sato S, Tabata S, et al.** (2011). Isolation and genetic characterization of Aurantimonas and Methylobacterium strains from stems of hypermodulated soybeans. *Microbes Environ* 26: 172–180.
- Andersen BL, Bidoglio G, Leip A, Rembges D.** (1998). A new method to study simultaneous methane oxidation and methane production in soils. *Glob Biogeochem Cy* 12: 587–594.
- Anderson MJ.** (2001). A new method for non-parametric multivariate analysis of variance. *Austral Ecology* 26:32-46.
- Anesti V, McDonald IR, Ramaswamy M, Wade WG, Kelly DP, Wood AP.** (2005). Isolation and molecular detection of methylotrophic bacteria occurring in the human mouth. *Environ Microbiol* 7: 1227–1238.
- Anke H, Weber RWS.** (2006). White-rots, chlorine and the environment – a tale of many twists. *Mycologist* 20: 83–89.
- Antai SP, Crawford DL.** (1981). Degradation of softwood, hardwood, and grass lignocelluloses by two *Streptomyces* strains. *Appl Environ Microbiol* 42: 378–380.
- Anthony C, Williams P.** (2002). The structure and mechanism of methanol dehydrogenase. *Biochem Biophys Acta* 1647:18–23.
- Anthony C.** (1982). The biochemistry of methylotrophs. Academic Press: New York.
- Anthony, C.** (2011). How half a century of research was required to understand bacterial growth on C1 and C2 compounds; the story of the serine cycle and the ethylmalonyl-CoA pathway. *Science progress* 94: 109–137.
- Antony CP, Kumaresan D, Ferrando L, Boden R, Moussard H, Scavino AF, et al.** (2010). Active methylotrophs in the sediments of Lonar Lake, a saline and alkaline ecosystem formed by meteor impact. *ISME J* 4:1470–1480.
- Arfman N, Van Beeumen J, De Vries GE, Harder W, Dijkhuizen L.** (1991). Purification and characterization of an activator protein for methanol dehydrogenase from thermotolerant *Bacillus* spp. *J Biol Chem* 266: 3955–3960.
- Arfman N, Watling EM, Clement W, van Oosterwijk RJ, de Vries GE, Harder W, et al.** (1989). Methanol metabolism in thermotolerant methylotrophic *Bacillus* strains involving a novel catabolic NAD-dependent methanol dehydrogenase as a key enzyme. *Arch Microbiol* 152: 280–288.
- Auman AJ, Stolyar S, Costello AM, Lidstrom ME.** (2000). Molecular characterization of Methanotrophic Isolates from Freshwater Lake Sediment. *Appl Environ Microbiol* 66:5259–5266.
- Axe DE & Bailey JE.** (1995). Transport of lactate and acetate through the energized cytoplasmic membrane of *Escherichia coli*. *Biotechnol Bioeng* 47: 8–19.
- Baani M, Liesack W.** (2008). Two isozymes of particulate methane monooxygenase with different methane oxidation kinetics are found in *Methylocystis* sp. strain SC2. *Proc Natl Acad Sci USA* 105:10203–10208.
- Barnett JA, Payne RW, Yarrow D.** (2000) Yeasts: characteristics and identification. 3rd edition. Cambridge University Press: Cambridge, U.K.; New York, NY, USA
- Baxter NJ, Hirt RP, Bodrossy L, Kovacs KL, Embley TM, Prosser JI, et al.** (2002). The ribulose-1,5-bisphosphate carboxylase/oxygenase gene cluster of *Methylococcus capsulatus* (Bath). *Arch Microbiol* 177: 279–289.
- Beck DA, McTaggart TL, Setboonsarng U, Vorobev A, Goodwin L, Shapiro N, et al.** (2015). Multiphyletic origins of methylotrophy in Alphaproteobacteria, exemplified by comparative genomics of Lake Washington isolates. *Environ Microbiol* 17: 547–554.
- Belova SE, Baani M, Suzina NE, Bodelier PL, Liesack W, Dedysh SN.** (2011). Acetate utilization as a survival strategy of peat-inhabiting *Methylocystis* spp. *Environ Microbiol Rep* 3: 36–46.
- Belova SE, Kulichevskaya IS, Bodelier PL, Dedysh SN.** (2013). *Methylocystis bryophila* sp. nov., a facultatively methanotrophic bacterium from acidic *Sphagnum* peat, and emended description of the genus *Methylocystis* (ex Whittenbury et al. 1970) Bowman et al. 1993. *Int J Syst Evol Microbiol* 63:1096–1104.
- Bender M, Conrad R.** (1992). Kinetics of CH₄ oxidation in oxic soils exposed to ambient air or high CH₄ mixing ratios. *FEMS Microbiol Ecol* 101: 261-270.

- Benson DA, Karsch-Mizrachi I, Lipman DJ, Ostell J, Wheeler DL. (2008). GenBank. *Nucleic Acids Res* (36): D25–D30.
- Bentley DR, Balasubramanian S, Swerdlow HP, Smith GP, Milton M, Brown CG, et al. (2008). Accurate whole human genome sequencing using reversible terminator chemistry. *Nature* 456: 53–59.
- Berestovskaya JJ, Kotsyurbenko OR, Tourova TP, Kolganova TV, Doronina NV, Golyshev PN, et al. (2012). *Methylorosula polaris* gen. nov., sp. nov., an aerobic, facultatively methylotrophic psychrotolerant bacterium from tundra wetland soil. *Int J Syst Evol Microbiol* 62: 638–646.
- Bergmann GT, Bates ST, Eilers KG, Lauber CL, Caporaso JG, Walters WA, et al. (2011). The under-recognized dominance of *Verrucomicrobia* in soil bacterial communities. *Soil Biol Biochem* 43: 1450–1455.
- Bernardet JF, Bruun B, Hugo C. (2006). The genera *Chryseobacterium* and *Elizabethkingia*. In: Dworkin M, Falkow S, Rosenberg E, Schleifer K-H, Stackebrandt E. The *Prokaryotes*. Volume 7: *Proteobacteria*: Delta, Epsilon subclass. Springer: New York, pp. 638–676.
- Berry D, Mahfoudh KB, Wagner M, Loy A. (2011). Barcoded primers used in multiplex amplicon pyrosequencing bias amplification. *Appl Environ Microbiol* 77: 7846–7849.
- Best DJ, Higgins IJ. (1981) Methane oxidizing activity and membrane morphology in methanol grown obligate methanotroph, *Methylosinus trichosporium* OB3b. *J Gen Microbiol* 125: 73–84.
- Bienhold C, Pop Ristova P, Wenzhöfer F, Dittmar T, Boetius A. (2013). How deep-sea wood falls sustain chemosynthetic life. *PLoS One* 8:e53590.
- Blachnik R. (1998). D'Ans Lax Taschenbuch für Chemiker und Physiker. 4th edn. vol. 3. Springer: Berlin, Germany.
- Borodina E, Cox MJ, McDonald IR, Murrell JC. (2005). Use of DNA-stable isotope probing and functional gene probes to investigate the diversity of methyl chloride-utilizing bacteria in soil. *Environ Microbiol* 7:1318–1328.
- Bosch G, Wang T, Latypova E, Kalyuzhnaya MG, Hackett M, Chistoserdova L. (2009). Insights into the physiology of *Methylotenera mobilis* as revealed by metagenome-based shotgun proteomic analysis. *Microbiology* 155:1103–1110.
- Bosch G, Skovran E, Xia Q, Wang T, Taub F, Miller JA, et al. (2008). Comprehensive proteomics of *Methylobacterium extorquens* AM1 metabolism under single carbon and nonmethylotrophic conditions. *Proteomics* 8: 3494–3505.
- Botha A. (2011). The importance and ecology of yeasts in soil. *Soil Biol Biochem* 43: 1–8.
- Bothe H, Schmitz O, Yates MG, Newton WE. (2010). Nitrogen fixation and hydrogen metabolism in Cyanobacteria. *Microbiol Mol Biol Rev* 74: 529–555.
- Bourne DG, McDonald IR, Murrell JC. (2001). Comparison of *pmoA* PCR Primer Sets as Tools for Investigating Methanotroph Diversity in Three Danish Soils. *Appl Environ Microbiol* 67: 3802–3809.
- Bowman JP, Sly LI, Nichols PD, Hayward AC. (1993). Revised taxonomy of the methanotrophs: description of *Methylobacter* gen. nov., emendation of *Methylococcus*, validation of *Methylosinus* and *Methylocystis* species, and a proposal that the family *Methylococcaceae* includes only the group I methanotrophs. *Int J Syst Bacteriol* 43: 735–753.
- Bowman JP. (2013). The Family *Methylococcaceae*. In: Rosenberg E, DeLong EF, Lory S, Stackebrandt E, Thompson F (eds). *The Prokaryotes – Gammaproteobacteria*. Springer: New York, pp 411–441.
- Bragg L, Glenn Stone G, Imelfort M, Hugenholtz P, Tyson GW. (2012). Fast, accurate error-correction of amplicon pyrosequences using Acacia. *Nat Methods* 9:425–426.
- Brautaset T, Jakobsen ØM, Flickinger MC, Valla S, Ellingsen TE. (2004). Plasmid-dependent methylotrophy in thermotolerant *Bacillus methanolicus*. *J Bacteriol* 186: 1229–1238.
- Brautaset T, Jakobsen ØM, Josefsen KD, Flickinger MC, Ellingsen TE. (2007). *Bacillus methanolicus*: a candidate for industrial production of amino acids from methanol at 50°C. *Appl Microbiol Biotechnol* 74: 22–34.
- Bray JR, Curtis JT. (1957). An ordination of upland forest communities of southern Wisconsin. *Ecol Monogr* 27: 325–349.
- Brilli F, Ruuskanen TM, Schnitzhofer R, Müller M, Breitenlechner M, Bittner V, et al. (2011). Detection of plant volatiles after leaf wounding and darkening by proton transfer reaction “time-of-flight” mass spectrometry (PTRTOF). *PLoS One* 6(5): e20419.
- Bringel F, Couée I. (2015). Pivotal roles of phyllosphere microorganisms at the interface between plant functioning and atmospheric trace gas dynamics. *Front Microbiol* 22:486.
- Buchan A, Collier LS, Neidle EL, Moran MA. (2000). Key aromatic ring-cleaving enzyme, protocatechuate 3,4-dioxygenase, in the ecologically important marine *Roseobacter* lineage. *Appl Environ Microbiol* 66:4662–4672.
- Buée M, Reich M, Murat C, Morin E, Nilsson RH, Uroz S, et al. (2009). 454 Pyrosequencing analyses of forest soils reveal an unexpectedly high fungal diversity. *New Phytol* 184: 449–456.
- Bustin SA, Benes V, Garson JA, Hellemans J, Huggett J, Kubista M, et al. (2009). The MIQE Guidelines: minimum information for publication of quantitative real-time PCR experiments. *Clin Chem* 55: 611–622.

- Bystrkyh LD, Vonck J, van Bruggen EFJ, van Beeumen J, Samyn B, Govorukhina NI, et al.** (1993). Electron microscopic analysis and structural characterization of novel NADP(H)-containing methanol:N,N'-dimethyl-4-nitrosoaniline oxidoreductases from the gram-positive methylotrophic bacteria *Amycolatopsis methanolica* and *Mycobacterium gastri* MB19. *J Bacteriol* 175: 1814-1822.
- Bystrykh LV, Govorukhina NI, Dijkhuizen L, Duine JA.** (1997). Tetrazolium-dye-linked alcohol dehydrogenase of the methylotrophic actinomycete *Amycolatopsis methanolica* is a three-component complex. *Eur J Biochem* 247: 280-287.
- Campbell BJ.** (2013). The family *Acidobacteriaceae*. In: Rosenberg E, DeLong EF, Lory S, Stackebrandt E, Thompson F (eds). *The Prokaryotes – other major lineages of Bacteria and the Archaea*. Springer: New York, pp 405–415.
- Cannon PF and Kirk PM.** (2007). *Fungal families of the world*. 1st edition. CABI: Wallingford, Oxfordshire, UK.
- Carere CR, Hards K, Houghton KM, Power JF, McDonald B, Collet C, et al.** (2016). Mixotrophy drives niche expansion of verrucomicrobial methanotrophs. *ISMEJ: in press*
- Carter C, Britton VG, Haff L.** (1983). CsTFA: a centrifugation medium for nucleic acid isolation. *Biotechniques* 1: 142–147.
- Castelle CJ, Hug LA, Wrighton KC, Thomas BC, Williams KH, Wu D, et al.** (2013). Extraordinary phylogenetic diversity and metabolic versatility in aquifer sediment. *Nat Commun* 4: 2120.
- Castro MS, Steudler PA, Melillo JM, Aber JD, Bowden RD.** (1995). Factors controlling atmospheric methane consumption by temperate forest soils. *Global Biogeochem Cy* 9: 1–10.
- Chaignaud P.** (2016). *Le rôle des bactéries dans le filtrage du chlorométhane, un gaz destructeur de la couche d'ozone – des souches modèles aux communautés microbiennes de sols forestiers*. (in french and english). Doctoral thesis at the University of Strasbourg.
- Chain P, Lamerdin J, Larimer F, Regala W, Lao V, Land M, et al.** (2003). Complete genome sequence of the ammonia-oxidizing bacterium and obligate chemolithoautotroph *Nitrosomonas europaea*. *J Bacteriol* 185: 2759–2773.
- Chen Y, Crombie A, Rahman MT, Dedys SN, Liesack W, Stott MB, et al.** (2010) Complete genome sequence of the aerobic facultative methanotroph *Methylocella silvestris* BL2. *J Bacteriol* 192: 3840–3841.
- Chen YP, Lopez-de-Victoria G, Lovell CR.** (1993). Utilization of aromatic compounds as carbon and energy sources during growth and N₂-fixation by free-living nitrogen fixing bacteria. *Arch Microbiol* 159: 207–212.
- Cheng L, Qiu TL, Yin XB, Wu XL, Hu GQ, Deng Y, et al.** (2007). *Methermicoccus shengliensis* gen. nov., sp. nov., a thermophilic, methylotrophic methanogen isolated from oil-production water, and proposal of *Methermicoccaceae* fam. nov. *Int J Syst Evol Microbiol* 57: 2964–2969.
- Chien A, Edgar DB, Trela JM.** (1976). Deoxyribonucleic acid polymerase from the extreme thermophile *Thermus aquaticus*. *J Bacteriol* 127: 1550–1557.
- Chistoserdova L, Chen SW, Lapidus A, Lidstrom ME.** (2003). Methylotrophy in *Methylobacterium extorquens* AM1 from a genomic point of view. *J Bacteriol* 185: 2980–2987.
- Chistoserdova L, Jenkins C, Kalyuzhnaya MG, Marx CJ, Lapidus A, Vorholt JA, et al.** (2004). The enigmatic *Planctomycetes* may hold a key to the origins of methanogenesis and methylotrophy. *Mol Biol Evol* 21: 1234-1241.
- Chistoserdova L, Kalyuzhnaya MG, Lidstrom ME.** (2009). The expanding world of methylotrophic metabolism. *Annu Rev Microbiol* 63: 477–499.
- Chistoserdova L, Lidstrom ME.** (2013). Aerobic methylotrophic prokaryotes. In: Rosenberg E, DeLong EF, Lory S, Stackebrandt E, Thompson F (eds). *The Prokaryotes – Prokaryotic physiology and biochemistry*. Springer: New York, pp 267-285.
- Chistoserdova L, Vorholt JA, Lidstrom ME.** (2005). A genomic view of methane oxidation by aerobic bacteria and anaerobic archaea. *Genome Biol* 6: 208.
- Chistoserdova L.** (2011). Modularity of methylotrophy, revisited. *Environ Microbiol* 13: 2603–2622.
- Chistoserdova L.** (2015). Methylotrophs in natural habitats: current insights through metagenomics. *Appl Microbiol Biotechnol* 99: 5763–5779.
- Chistoserdova L.** (2016). Lanthanides: New life metals? *World J Microbiol Biotechnol* 32:138.
- Ciais P, Sabine C, Bala G, Bopp L, Brovkin V, Canadell J, et al.** (2013). Carbon and Other Biogeochemical Cycles. In: Stocker TF, Qin D, Plattner G-K, Tignor M, Allen SK, Boschung J, Nauels A, Xia Y, Bex V, Midgley PM (eds). *Climate Change 2013: The Physical Science Basis. Contribution of Working Group I to the Fifth Assessment Report of the Intergovernmental Panel on Climate Change*. Cambridge University Press, Cambridge, United Kingdom and New York, NY, USA, pp 465–470.
- Cicerone RJ, Oremland RS.** (1988). Biogeochemical aspects of atmospheric methane. *Glob Chang Biol* 2: 299–327.
- Čikoš Š, Koppel J.** (2009). Transformation of real-time PCR fluorescence data to target gene quantity. *Anal Biochem* 384: 1–10.

- Clarke KR. (1993). Non-parametric multivariate analysis of changes in community structure. *Australian Journal of Ecology* 18: 117–143.
- Colby J, Stirling DI, Dalton H. (1977). The soluble methane mono-oxygenase of *Methylococcus capsulatus* (Bath). Its ability to oxygenate n-alkanes, n-alkenes, ethers, and alicyclic, aromatic and heterocyclic compounds. *Biochem J* 165: 395–402.
- Conrad R. (1996). Soil microorganisms as controllers of atmospheric trace gases (H₂, CO, CH₄, OCS, N₂O, and NO). *Microbiol Rev* 60: 609–640.
- Conrad R. (1999). Contribution of hydrogen to methane production and control of hydrogen concentrations in methanogenic soils and sediments. *FEMS Microbiol Ecol* 28: 193–202.
- Conrad R. (2009). The global methane cycle: recent advances in understanding the microbial processes involved. *Environ Microbiol Rep* 1: 285–292.
- Cornish A, Nicholis KM, Scott D, Hunter BK, Aston WJ, Higgins IJ, et al. (1984). In vivo ¹³C NMR investigations of methanol oxidation by the obligate methanotroph *Methylosinus trichosporium* OB3b. *J Gen Microbiol* 130: 2564–2575.
- Costello AM, Lidstrom ME. (1999). Molecular characterization of functional and phylogenetic genes from natural populations of methanotrophs in lake sediments. *Appl Environ Microbiol* 65: 5066–5074.
- Coulter C, Hamilton JTG, McRoberts WC, Kulakov L, Larkin MJ, Harper DB. (1999). Halomethane:bisulfide/halide ion methyltransferase, an unusual corrinoid enzyme of environmental significance isolated from an aerobic methylotroph using chloromethane as the sole carbon source. *Appl Environ Microbiol* 65: 4301–4312.
- Cowan MI, Glen AT, Hutchinson SA, MacCartney ME, Mackintosh JM, Moss AM. (1973). Production of volatile metabolites by species of fomes. *Trans Br mycol Soc* 60: 347–360.
- Craveri R, Cavazoni V, Sarra PG, Succi G, Molteni L, Cardini G, et al. (1976). Taxonomical examination and characterization of a methanol-utilising yeast. *Antonie van Leeuwenhoek* 42: 533–540.
- Crawford DL. (1988). Biodegradation of agricultural and urban wastes. In: Goodfellow M, Williams ST, Mordarski M (eds). *Actinomycetes in biotechnology*. Academic Press Ltd: London, UK, pp 433–439.
- Crombie AT, Murrell JC. (2014). Trace-gas metabolic versatility of the facultative methanotroph *Methylocella silvestris*. *Nature* 510: 148–151.
- Crowther GJ, Kosaly G, Lidstrom ME. (2008). Formate as the Main Branchpoint for Methylotrophic Metabolism in *Methylobacterium extorquens* AM1. *J Bacteriol* 14: 5057–5062.
- Culpepper MA, Rosenzweig AC. (2012). Architecture and active site of particulate methane monooxygenase. *Crit Rev Biochem Mol* 47: 483–492.
- Dallinger A, Horn MA. (2014). Agricultural soil and drilosphere as reservoirs of new and unusual assimilators of 2,4-dichlorophenol carbon. *Environ Microbiol* 16: 84–100.
- de Boer L, Dijkhuizen L, Grobben G, Goodfellow M, Stackebrandt E, Parlett JH, et al. (1990). *Amycolatopsis methanolica* sp. nov., a facultatively methylotrophic actinomycete. *Int J Syst Bacteriol* 40: 194–204.
- de Souza JAM, Alves LMC, Mello Varani A, de Macedo Lemos EG. (2013). The Family *Bradyrhizobiaceae*. In: Rosenberg E, DeLong EF, Lory S, Stackebrandt E, Thompson F (eds). *The Prokaryotes – Alphaproteobacteria and Betaproteobacteria*. Springer: New York, pp 135–154.
- de Vries GE, Arfman N, Terpstra P, Dijkhuizen L. (1992). Cloning, expression, and sequence analysis of the *Bacillus methanolicus* C1 methanol dehydrogenase gene. *J Bacteriol* 174: 5346–5353.
- Dedysh SN, Belova SE, Bodelier PLE, Smirnova KV, Khmelenina VN, Chidthaisong A, et al. (2007). *Methylocystis heyeri* sp. nov., a novel type II methanotrophic bacterium possessing ‘signature’ fatty acids of type I methanotrophs. *Int J Syst Evol Microbiol* 57: 472–479.
- Dedysh SN, Berestovskaya YY, Vasylieva LV, Belova SE, Khmelenina VN, Suzina NE, et al. (2004). *Methylocella tundrae* sp. nov., a novel methanotrophic bacterium from acidic tundra peatlands. *Int J Syst Evol Microbiol* 54: 151–56.
- Dedysh SN, Berestovskaya YY, Vasylieva LV, Belova SE, Khmelenina VN, Suzina NE, et al. (2004). *Methylocella tundrae* sp. nov., a novel methanotrophic bacterium from acidic peatlands of tundra. *Int J Syst Evol Microbiol* 54: 151–156.
- Dedysh SN, Derakshani M, Liesack W. (2001). Detection and enumeration of methanotrophs in acidic *Sphagnum* peat by 16S rRNA fluorescence *in situ* hybridization, including the use of newly developed oligonucleotide probes for *Methylocella palustris*. *Appl Environ Microbiol* 67: 4850–4857.
- Dedysh SN, Didriksen A, Danilova OV, Belova SE, Liebner S, Svenning MM. (2015). *Methylocapsa palsarum* sp. nov., a methanotroph isolated from a subarctic discontinuous permafrost ecosystem. *Int J Syst Evol Microbiol* 65: 3618–3624.

- Dedysh SN, Khmelenina VN, Suzina NE, Trotsenko YA, Semrau JD, Liesack W, et al. (2002). *Methylocapsa acidiphila* gen. nov., sp. nov., a novel methane-oxidizing and dinitrogen-fixing acidophilic bacterium from *Sphagnum* bog. *Int J Syst Evol Microbiol* 52: 251–261.
- Dedysh SN, Knief C, Dunfield PF. (2005a). *Methylocella* species are facultatively methanotrophic. *J Bacteriol* 187: 4665–4670.
- Dedysh SN, Liesack W, Khmelenina VN, Suzina NE, Trotsenko YA, Semrau JD, et al. (2000). *Methylocella palustris* gen. nov., sp. nov., a new methane-oxidizing acidophilic bacterium from peat bogs, representing a novel subtype of serine-pathway methanotrophs. *Int J Syst Evol Microbiol* 50: 955–969.
- Dedysh SN, Panikov NS, Liesack W, Grosskopf R, Zhou J, Tiedje JM. (1998). Isolation of acidophilic methane-oxidizing bacteria from northern peat wetlands. *Science* 282: 281–284.
- Dedysh SN, Pankratov TA, Belova SE, Kulichevskaya IS, Liesack W. (2006). Phylogenetic analysis and *in situ* identification of bacteria community composition in an acidic *Sphagnum* peat bog. *Appl Environ Microbiol* 72: 2110–2117.
- Dedysh SN, Smirnova KV, Khmelenina VN, Suzina NE, Liesack W, Trotsenko YA. (2005b). Methylophilic autotrophy in *Beijerinckia mobilis*. *J Bacteriol* 187: 3884–3888.
- Dedysh SN, Haupt ES, Dunfield PF. (2016). Emended description of the family *Beijerinckiaceae* and transfer of the genera *Chelatococcus* and *Camelimonas* to the family *Chelatococcaceae* fam. nov. *Int J Syst Evol Microbiol*. 66: 3177–3182.
- Deeb RA, Hu HY, Hanson JR, Scow KM, Alvarez-Cohen L. (2001). Substrate interactions in BTEX and MTBE mixtures by an MTBE-degrading isolate. *Environ Sci Technol* 35: 312–317.
- Degelmann DM, Borken W, Drake HL, Kolb S. (2010). Different atmospheric methane-oxidizing communities in European Beech and Norway Spruce Soils. *Appl Environ Microbiol* 76: 3228–3235.
- Degelmann DM, Borken W, Kolb S. (2009). Methane oxidation kinetics differ in European beech and Norway spruce soils. *Eur J Soil Sci* 60: 499–506.
- Degelmann DM. (2010). *Bedeutung der Baumart für die Aktivität, Diversität und Abundanz methanoxidierender Bakterien in temperaten Waldböden* (in German). Doctoral thesis at the University of Bayreuth.
- Delavat F, Lett MC, Lièvreumont D. (2013). Yeast and bacterial diversity along a transect in an acidic, As–Fe rich environment revealed by cultural approaches. *Sci Total Environ* 463–464: 823–828.
- Denef VJ, Patrauchan MA, Florizone C, Park J, Tsoi TV, Verstraete W, et al. (2005). Growth substrate- and phase-specific expression of biphenyl, benzoate, and C1 metabolic pathways in *Burkholderia xenovorans* LB400. *J Bacteriol* 187: 7996–8005.
- Dix NJ, Webster J. (1995). *Fungal Ecology*. Chapman and Hall: London.
- Dlugokencky EJ, Nisbet EG, Fisher R, Lowry D. (2011). Global atmospheric methane: budget, changes and dangers. *Philos Trans A Math Phys Eng Sci* 369: 2058–2072.
- Dorokhov YL, Shindyapina AV, Sheshukova EV, Komarova TV. (2015). Metabolic methanol: molecular pathways and physiological roles. *Physiol Rev* 95: 603–644.
- Doronina N, Kaparullina E, Trotsenko Y. (2013). The Family *Methylophilaceae*. In: Rosenberg E, DeLong EF, Lory S, Stackebrandt E, Thompson F (eds). *The Prokaryotes – Alphaproteobacteria and Betaproteobacteria*. Springer: New York, pp 869–880.
- Doronina NV, Braus-Strohmeyer SA, Leisinger T, Trotsenko YA. (1995). Isolation and characterization of a new facultatively methylotrophic bacterium: description of *Methylorhabdus multivorans* gen. nov., sp. nov. *Syst Appl Microbiol* 18: 92–98.
- Doronina NV, Gogleva AA, Trotsenko YA. (2012). *Methylophilus glucosoxydans* sp. nov., a restricted facultative methylotroph from rice rhizosphere. *Int J Syst Evol Microbiol* 62: 196–201.
- Doronina NV, Sokolov AP, Trotsenko YA. (1996). Isolation and initial characterization of aerobic chloromethane-utilizing bacteria. *FEMS Microbiol Lett* 142: 179–183.
- Dörr N, Glaser B, Kolb S. (2010). Methanotrophic communities in Brazilian ferralsols from naturally forested, afforested, and agricultural sites. *Appl Environ Microbiol* 76: 1307–1310.
- Dorrestijn E, Mulder P. (1999). The radical-induced decomposition of 2-methoxyphenol. *J Chem Soc Perkin Trans 2*: 777–780.
- Drake HL, Küsel K, Matthies C. (2013). Acetogenic prokaryotes. In: Rosenberg E, DeLong EF, Lory S, Stackebrandt E, Thompson F (eds). *The Prokaryotes – Prokaryotic physiology and biochemistry*. Springer: New York, pp 3–60.
- Duddlestone KN, Kinney MA, Kiene RP, Hines ME. (2002). Anaerobic microbial biogeochemistry in a northern bog: acetate as a dominant metabolic end product. *Global Biogeochem Cyc* 16: 11–1 – 11–9.
- Dugard P, Todman J, Staines H. (2014). *Approaching Multivariate Analysis. A Practical Introduction*. Routledge, New York.

- Dumont MG, Murrell JC. (2005). Community-level analysis: key genes of aerobic methane oxidation. *Methods Enzymol* 397: 413–427.
- Dunfield PF, Belova SE, Vorob'ev AV, Cornish SL, Dedysh SN. (2010). *Methylocapsa aurea* sp. nov., a facultative methanotroph possessing a particulate methane monooxygenase, and emended description of the genus *Methylocapsa*. *Int J Syst Evol Microbiol* 60: 2659–2664.
- Dunfield PF, Khmelenina VN, Suzina NE, Trotsenko YA, Dedysh SN. (2003). *Methylocella silvestris* sp. nov., a novel methanotroph isolated from an acidic forest cambisol. *Int J Syst Evol Microbiol* 53: 1231–1239.
- Dunfield PF, Khmelenina VN, Suzina NE, Trotsenko YA, Dedysh SN. (2003). *Methylocella silvestris* sp. nov., a novel methanotroph isolated from an acidic forest cambisol. *Int J Syst Evol Microbiol* 53: 1231–1239.
- Dunfield PF, Topp E, Archambault C, Knowles R. (1995). Effect of nitrogen fertilizers and moisture content on CH₄ and N₂ fluxes in a humisol: measurements in the field and intact soil cores. *Biogeochemistry* 29: 199–222.
- Dunfield PF, Yuryev A, Senin P, Smirnova AV, Stott MB, Hou S, et al. (2007). Methane oxidation by an extremely acidophilic bacterium of the phylum *Verrucomicrobia*. *Nature* 450: 879–882.
- Dunfield PF, Dedysh SN. (2014). *Methylocella*: a gourmand among methanotrophs. *Trends Microbiol* 22: 368–369.
- Dunfield PF, Liesack W, Henckel T, Knowles R, Conrad R. (1999). High-affinity methane oxidation by a soil enrichment culture containing a type II methanotroph. *Appl Environ Microbiol* 65:1009–1014.
- Dunfield, P.F. (2007) The soil methane sink. In: Reay, D.S., Hewitt, N., Smith, K.A., and Grace, J. (eds). *Greenhouse Gas Sinks*. Wallingford, UK: CABI Publishing, pp. 152–170.
- Eccleston M, Kelly DP. (1973). Assimilation and toxicity of some exogenous C1 compounds, alcohols, sugars and acetate in the methane oxidizing bacterium *Methylococcus capsulatus*. *J Gen Microbiol* 75: 211–221.
- Edgar RC, Haas BJ, Clemente JC, Quince C, Knight R. (2011). UCHIME improves sensitivity and speed of chimera detection. *Bioinformatics* 27: 2194–2200.
- Edgar RC. (2010). Search and clustering orders of magnitude faster than BLAST. *Bioinformatics* 26: 2460–2461.
- Egert M, Friedrich MW. (2003). Formation of pseudo-terminal restriction fragments, a PCR-related bias affecting terminal restriction fragment length polymorphism analysis of microbial community structure. *Appl Environ Microbiol* 69: 2555–2562.
- Eggeling L, Sahn H. (1978). Derepression and partial insensitivity to carbon catabolite repression of the methanol dissimilating enzymes in *Hansenula polymorpha*. *Eur J Appl Microbiol Biotechnol* 5: 197–202.
- Ellerbrock RH, Gerke HH, Bachmann J, Goebel MO. (2005). Composition of organic matter fractions for explaining wettability of three forest soils. *Soil Sci Soc Am J* 69: 57–66.
- Elliott SM, Rowland FS. (1995). Methyl halide hydrolysis rates in natural waters. *J Atmos Chem* 20: 229–236.
- El-Tarabily KA, Sivasithamparam K. (2006). Potential of yeasts as biocontrol agents of soilborne fungal plant pathogens and as plant growth promoters. *Mycoscience* 47: 25–35.
- Ettwig KF, Butler MK, Le Paslier D, Pelletier E, Mangenot S, Kuypers MM, et al. (2010). Nitrite-driven anaerobic methane oxidation by oxygenic bacteria. *Nature* 464:543–548.
- Ettwig KF, Shima S, van de Pas-Schoonen KT, Kahnt J, Medema MH, Op den Camp HJ, et al. (2008). Denitrifying bacteria anaerobically oxidize methane in the absence of Archaea. *Environ Microbiol*. 10: 3164–3173.
- Ettwig KF, Zhu B, Speth D, Keltjens JT, Jetten MS, Kartal B. (2016). Archaea catalyze iron-dependent anaerobic oxidation of methane. *Proc Natl Acad Sci USA* 113: 12792–12796.
- Fall R, Benson AA. (1996). Leaf methanol – the simplest natural product from plants. *Trends Plant Sci* 1: 296–301.
- Fang H, Lv W, Huang Z, Liu SJ, Yang H. (2015). *Gryllotalpicola reticulitermitis* sp. nov., isolated from a termite gut. *Int J Syst Evol Microbiol*. 65: 85–89.
- Felsenstein J. (1985). Confidence limits on phylogenies: An approach using the bootstrap. *Evolution* 39:783-791.
- Ferrari B, Winsley T, Ji M, Neilan B. (2014). Insights into the distribution and abundance of the ubiquitous candidatus Saccharibacteria phylum following tag pyrosequencing. *Sci Rep* 4: 3957.
- Fitriyanto NA, Fushimi M, Matsunaga M, Petriwinigrum A, Iwama T, Kawai,K. (2011). Molecular structure and gene analysis of Ce³⁺-induced methanol dehydrogenase of *Bradyrhizobium* sp. MAFF211645. *J Biosci Bioeng* 111: 613–617.
- Folman LB, Klein Gunnewiek PJA, Boddy L, de Boer W. (2008). Impact of white-rot fungi on numbers and community composition of bacteria colonizing beech wood from forest soil. *FEMS Microbiol Ecol* 63: 181–191.
- Folsom BR, Chapman PJ, Pritchard PH. (1990). Phenol and trichloroethylene degradation by *Pseudomonas cepacia* G4: kinetics and interactions between substrates. *Appl Environ Microbiol* 56: 1279–1285.
- Franco CMM, Labeda DP. (2013). The Order *Pseudonocardiales*. In: Rosenberg E, DeLong EF, Lory S, Stackebrandt E, Thompson F (eds). *The Prokaryotes – Actinobacteria*. Springer: New York, pp 743–860.

- Freedman DL, Swamy M, Bell NC, Verce MF.** (2004). Biodegradation of chloromethane by *Pseudomonas aeruginosa* strain NB1 under nitrate-reducing and aerobic conditions. *Appl Environ Microbiol* 70: 4629–4634.
- Friedrich MW.** (2006). Stable-isotope probing of DNA: insights into the function of uncultivated microorganisms from isotopically labeled metagenomes. *Curr Opin Biotechnol* 17: 59–66.
- Frische M, Garofalo K, Hansteen TH, Borchers R.** (2006). Fluxes and origin of halogenated organic trace gases from Momotombo volcano (Nicaragua). *Geochem Geophys Geosyst* 7: Q05020.
- Fu L, Niu B, Zhu Z, Wu S, Li W.** (2012). CD-HIT: accelerated for clustering the next generation sequencing data. *Bioinformatics* 28: 3150–3152.
- Fuchs G, Boll M, Heider J.** (2011). Microbial degradation of aromatic compounds - from one strategy to four. *Nat Rev Microbiol* 9: 803–816.
- Fuerst JA, Sagulenko E.** (2011). Beyond the bacterium: planctomycetes challenge our concepts of microbial structure and function. *Nat Rev Microbiol* 9: 403–413.
- Fukunaga Y, Ichikawa N.** (2013). The Class *Holophagaceae*. In: Rosenberg E, DeLong EF, Lory S, Stackebrandt E, Thompson F (eds). *The Prokaryotes – other major lineages of Bacteria and the Archaea*. Springer: New York, pp 683–687.
- Fukunaga Y, Kurahashi M, Sakiyama Y, Ohuchi M, Yokota A, Harayama S.** (2009). *Phycisphaera mikurensis* gen. nov., sp. nov., isolated from a marine alga, and proposal of *Phycisphaeraceae* fam. nov., *Phycisphaerales* ord. nov. and *Phycisphaerae* classis nov. in the phylum *Planctomycetes*. *J Gen Appl Microbiol* 55: 267–275.
- Gadanhó M, Sampaio JP.** (2009). *Cryptococcus ibericus* sp. nov., *Cryptococcus aciditolerans* sp. nov. and *Cryptococcus metallitolerans* sp. nov., a new ecoclade of anamorphic basidiomycetous yeast species from an extreme environment associated with acid rock drainage in São Domingos pyrite mine, Portugal. *Int J Syst Evol Microbiol* 59: 2375–2379.
- Galbally IE, Kirstine W.** (2002). The production of methanol by flowering plants and the global cycle of methanol. *J Atmos Chem* 43: 195–229.
- Gardes M, Bruns TD.** (1993). ITS primers with enhanced specificity for *Basidiomycetes* - application to the identification of mycorrhizae and rusts. *Mol Ecol* 2: 113–118.
- Gass MJ.** (2013). *Der Effekt von Acetat, n-Alkanen, Cellobiose, Xylose, Methylamin, Methanol, Vanillinsäure und Guajacol auf die Abundanz von Methanotrophen in Waldböden.* (in German). Bachelor thesis at the University of Bayreuth.
- Gellissen G, Hollenberg CP.** (1997). Application of yeasts in gene expression studies: a comparison of *Saccharomyces cerevisiae*, *Hansenula polymorpha* and *Kluyveromyces lactis* – a review. *Gene* 190: 87–97.
- Gellissen G, Hollenberg CP.** (1997). Application of yeasts in gene expression studies: a comparison of *Saccharomyces cerevisiae*, *Hansenula polymorpha* and *Kluyveromyces lactis* – a review. *Gene* 190: 87–97.
- Gellissen G.** (2000). Heterologous protein production in methylotrophic yeasts. *Appl Microbiol Biotechnol* 54: 741 – 750.
- Ghosh M, Anthony C, Harlos K, Goodwin MG, Blake CCF.** (1995). The refined structure of the quinoprotein methanol dehydrogenase from *Methylobacterium extorquens* at 1.94 Å. *Structure* 3: 177– 187.
- Giller KE, Witter E, Mcgrath SP.** (1998). Toxicity of heavy metals to microorganisms and microbial processes in agricultural soils: A review. *Soil Biol Biochem* 30: 1389–1414.
- Gimenez R, Nuñez MF, Badia J, Aguilar J, Baldoma L.** (2003). The gene *yjcG*, cotranscribed with the gene *acs*, encodes an acetate permease in *Escherichia coli*. *J Bacteriol* 185: 6448–6455.
- Giovannoni SJ, Hayakawa DH, Tripp HJ, Stingl U, Givan SA, Cho JC, et al.** (2008). The small genome of an abundant coastal ocean methylotroph. *Environ Microbiol* 10: 1771–1782.
- Goeppert A, Czaun M, Jones JP, Surya Prakash GK, Olah GA.** (2014). Recycling of carbon dioxide to methanol and derived products: closing the loop. *Chem Soc Rev* 43: 7995–8048.
- Gonzalez JM, Mayer F, Moran MA, Hodson RE, Whitman WB.** (1997). *Sagittula stellata* gen. nov., sp. nov., a lignin-transforming bacterium from a coastal environment. *Int J Syst Bacteriol* 47: 773–780.
- Goodfellow M.** (2012). Phylum XXVI. *Actinobacteria* phyl. nov. In: Goodfellow M, Kämpfer P, Busse H-J, Trujillo ME, Suzuki K-I, Ludwig W, Whitman WB (eds). *Bergey's Manual of Systematic Bacteriology*. 2nd edition, Vol 5: *The Actinobacteria, Part A and B*. New York: Springer, pp 33–34.
- Goodwin KD, Schaefer JK, Oremland RS.** (1998). Bacterial oxidation of dibromomethane and methyl bromide in natural waters and enrichment cultures. *Appl Environ Microbiol* 64: 4629–4636.
- Goodwin KD, Tokarczyk R, Stephens FC, Saltzman ES.** (2005). Description of toluene inhibition of methyl bromide biodegradation in seawater and isolation of a marine toluene oxidizer that degrades methyl bromide. *Appl Environ Microbiol* 71: 3495–3503.
- Goodwin KDR, Varner RK, Crill PM, Oremland RS.** (2001). Consumption of tropospheric levels of methyl bromide by C1 compound utilising bacteria and comparison to saturation kinetics. *Appl Environ Microbiol* 67: 5437–5443.

- Green Mr, Sambrook J.** (2012). *Molecular cloning. A laboratory manual*. 4th edn. Cold Spring Harbor Laboratory Press: New York.
- Greenberg DE, Porcella SF, Stock F, Wong A, Conville PS, Murray PR, et al.** (2005). *Granulibacter bethesdensis* gen. nov., sp. nov., a distinctive pathogenic acetic acid bacterium in the family *Acetobacteraceae*. *Int J Syst Evol Microbiol* 56: 2609–2616.
- Griffiths RI, Whiteley AS, O'Donnell AG, Bailey MJ.** (2000). Rapid method for coextraction of DNA and RNA from natural environments for analysis of ribosomal DNA and rRNA-based microbial community composition. *Appl Environ Microbiol* 66: 5488–5491.
- Gross S, Robbins EI.** (2000). Acidophilic and acid-tolerant fungi and yeasts. *Hydrobiologia* 433: 91–109.
- Gülensoy N, Alvarez PJJ.** (1999). Diversity and correlation of aromatic hydrocarbon biodegradation capabilities. *Biodegradation* 10: 331–340.
- Gupta V, Smemo KA, Yavitt JB, Basiliiko N.** (2012). Active methanotrophs in two contrasting North American peatland ecosystems revealed using DNA-SIP. *Microb Ecol* 63: 438–445.
- Gvozdev AR, Tukhvatullin IA, Gvozdev RI.** (2012). Quinone-dependent alcohol dehydrogenases and FAD-dependent alcohol oxidases. *Biochemistry (Moscow)* 77: 843–856.
- Hakemian AS, Rosenzweig AC.** (2007). The biochemistry of methane oxidation. *Annu Rev Biochem* 76: 223–241.
- Halsey KH, Carter AE, Giovannoni SJ.** (2012). Synergistic metabolism of a broad range of C1 compounds in the marine methylotrophic bacterium HTCC2181. *Environ Microbiol* 14: 630–640.
- Hamedí J, Mohammadipanah F.** (2015). Biotechnological application and taxonomical distribution of plant growth promoting actinobacteria. *J Ind Microbiol Biotechnol* 42:157–171.
- Hamilton JT, McRoberts WC, Keppler F, Kalin RM, Harper DB.** (2003). Chloride methylation by plant pectin: an efficient environmentally significant process. *Science* 301:206–209.
- Hammer Ø, Harper DAT, Ryan PD.** (2001). PAST: Palaeontological Statistics software package for education and data analysis. *Palaeontol Electron* 4: 1–9.
- Han JI, Semrau JD.** (2000). Chloromethane stimulates growth of *Methylococcum album* BG8 on methanol. *FEMS Microbiol Lett* 187: 77–81.
- Hanczár T, Csáki R, Bodrossy L, Murrell JC, Kovács KL.** (2002). Detection and localization of two hydrogenases in *Methylococcus capsulatus* (Bath) and their potential role in methane metabolism. *Arch Microbiol* 177: 167–172.
- Hanson CA, Allison SD, Bradford MA, Wallenstein MD, Treseder KK.** (2008). Fungal taxa target different carbon sources in forest soil. *Ecosystems* 11: 1157–1167.
- Hanson RS, Hanson TE.** (1996). Methanotrophic bacteria. *Microbiol Rev* 60: 439–471.
- Hanson RS.** (1992). Introduction. In: Murrell JC, H. Dalton H. (eds). *Methane and methanol utilizers*. Plenum Press, New York, pp. 1–22.
- Harms N, Ras J, Reijnders WNM, Van Spanning RJM, Stouthamer AH.** (1996). S-formylglutathione hydrolase of *Paracoccus denitrificans* is homologous to human esterase D: a universal pathway for formaldehyde detoxification? *Journal of Bacteriology* 178: 6296–6299.
- Harper DB, Hamilton JTG, Ducrocq V, Kennedy JT, Downey A, Kalin RM.** (2003). The distinctive isotopic signature of plant-derived chloromethane: possible application in constraining the atmospheric chloromethane budget. *Chemosphere* 52: 433–436.
- Harper DB.** (2000). The global chloromethane cycle: biosynthesis, biodegradation and metabolic role. *Nat Prod Rep* 17: 337–348.
- Hartmann DL, Klein Tank AMG, Rusticucci M, Alexander LV, Brönnimann S, Charabi Y, et al.** (2013). Observations: Atmosphere and Surface. In: Stocker TF, Qin D, Plattner G-K, Tignor M, Allen SK, Boschung J, Nauels A, Xia Y, Bex V, Midgley PM (eds). *Climate Change 2013: The Physical Science Basis. Contribution of Working Group I to the Fifth Assessment Report of the Intergovernmental Panel on Climate Change*. Cambridge University Press, Cambridge, United Kingdom and New York, NY, USA, pp 159–254.
- Hartmans S, Schmuckle A, Cook AM, Leisinger T.** (1986). Methyl Chloride: Naturally Occurring Toxicant and C-1 Growth Substrate. *Microbiology* 132: 1139-1142.
- Hartner FS, Glieder A.** (2006). Regulation of methanol utilisation pathway genes in yeasts. *Microb Cell Fact* 5: 1–29.
- He X, McLean JS, Edlund A, Yooseph S, Hall AP, Liu SY, et al.** (2015). Cultivation of a human-associated TM7 phylotype reveals a reduced genome and epibiotic parasitic lifestyle. *Proc Natl Acad Sci USA*. 112: 244–249.
- Hedlund BP, Gosink JJ, Staley JT.** (1997). *Verrucomicrobia* div. nov., a new division of the *Bacteria* containing three new species of *Prostheco bacter*. *Antonie van Leeuwenhoek* 72: 29–38.
- Heid CA, Stevens J, Livak KJ, Williams PM.** (1996). Real time quantitative PCR. *Genome Res* 6: 986–994.

- Heikes BG, Chang WN, Pilson MEQ, Swift E, Singh HB, Günther A, et al. (2002). Atmospheric methanol budget and ocean implication. *Glob Biogeochem Cy* 16: 1–30.
- Heipieper HJ, Martínez A. (2010). Toxicity of Hydrocarbons to Microorganisms. In: Timmis KN (eds). *Handbook of hydrocarbon and lipid microbiology*. Springer, pp. 1565–1573.
- Hektor HJ, Kloosterman H, Dijkhuizen L. (2002). Identification of a magnesium-dependent NAD(P)(H)-binding domain in the nicotinoprotein methanol dehydrogenase from *Bacillus methanolicus*. *J Biol Chem* 277: 46966–46973.
- Henckel T, Jäckel U, Schnell S, Conrad R. (2000). Molecular analyses of novel methanotrophic communities in forest soil that oxidize atmospheric methane. *Appl Environ Microbiol* 66: 1801–1808.
- Herlemann DPR, Labrenz M, Juergens K, Bertilsson S, Waniek JJ, Andersson AF. (2011). Transition in bacterial communities along the 2000 km salinity gradient of the Baltic Sea. *ISME J* 5: 1571–1579.
- Heyer J, Galchenko VF, Dunfield PF. (2002). Molecular phylogeny of type II methane oxidizing bacteria isolated from various environments. *Microbiology* 148: 2831–2846.
- Hibbett DS, Binder M, Bischoff JF, Blackwell M, Cannon PF, Eriksson OE, et al. (2007). A higher level phylogenetic classification of the Fungi. *Mycological Research* 111: 509–547.
- Hibbett DS, Ohman A, Glotzer D, Nuhn M, Kirk P, Nilsson RH. (2011). Progress in molecular and morphological taxon discovery in Fungi and options for formal classification of environmental sequences. *Fungal Biology Reviews* 25: 38–47.
- Hibi Y, Asai K, Arafuka H, Hamajima M, Iwama T, Kawai K. (2011). Molecular structure of La³⁺-induced methanol dehydrogenase-like protein in *Methylobacterium radiotolerans*. *J Biosci Bioeng* 111: 547–549.
- Hirsch P, Müller M. (1985). *Planctomyces limnophilus* sp. nov., a stalked and budding bacterium from freshwater. *Syst Appl Microbiol* 6: 276–280.
- Holmes AJ, Costello A, Lidstrom ME, Murrell JC. (1995). Evidence that particulate methane monooxygenase and ammoniamonooxygenase maybe evolutionarily related. *FEMS Microbiol Lett* 132: 203–208.
- Holmes AJ, Roslev P, McDonald IR, Iversen N, Henriksen K, Murrell JC. (1999). Characterization of methanotrophic bacterial populations in soils showing atmospheric methane uptake. *Appl Environ Microbiol* 65: 3312–3318.
- Horn MA, Schramm A, Drake HL. (2003). The earthworm gut: an ideal habitat for ingested N₂O-producing microorganisms. *Appl Environ Microbiol* 69: 1662–1669.
- Horz H-P, Raghubanshi AS, Heyer J, Kammann C, Conrad R, Dunfield PF. (2002). Activity and community structure of methane-oxidising bacteria in a wet meadow soil. *FEMS Microbiol Ecol* 41: 247–257.
- Horz HP, Yimga MT, Liesack W. (2001). Detection of methanotroph diversity on roots of submerged rice plants by molecular retrieval of *pmoA*, *mmoX*, *mxoF*, and 16S rRNA and ribosomal DNA, including *pmoA*-based terminal restriction fragment length polymorphism profiling. *Appl Environ Microbiol* 67: 4177–4185.
- Hou S, Makarova KS, Saw JHW, Senin P, Ly BV, Zhou Z, et al. (2008). Complete genome sequence of the extremely acidophilic methanotroph isolate V4, *Methylacidiphilum infernorum*, a representative of the bacterial phylum *Verrucomicrobia*. *Biology Direct* 3: 26.
- Howard P H. (1990). *Handbook of Environmental Fate and Exposure Data for Organic Chemicals, Volume II – Solvents*. CRC Press, New York.
- Howe AC, Jansson JK, Malfatti SA, Tringe SG, Tiedje JM, Brown CT. (2014). Tackling soil diversity with the assembly of large, complex metagenomes. *Proc Natl Acad Sci USA* 111: 4904–4909.
- Hung W-L, Wade WG, Chen Y, Kelly DP, Wood AP. (2012). Design and evaluation of novel primers for the detection of genes encoding diverse enzymes of methylotrophy and autotrophy. *Pol J Microbiol* 61: 11–22.
- Hung W-L, Wade WG, Boden R, Kelly DP, Wood AP. (2011). Facultative methylotrophs from the human oral cavity and methylotrophy in strains of *Gordonia*, *Leifsonia*, and *Microbacterium*. *Arch Microbiol* 193: 407.
- Hutchens E, Radajewski S, Dumont MG, McDonald IR, Murrell JC. (2004). Analysis of methanotrophic bacteria in Movile Cave by stable isotope probing. *Environ Microbiol* 6: 111–120.
- Hutchinson, GE. (1978). *An introduction to population ecology*. Yale University Press, New Haven.
- Hüve K, Christ MM, Kleist E, Uerlings R, Niinemets U, Walter A, et al. (2007). Simultaneous growth and emission measurements demonstrate an interactive control of methanol release by leaf expansion and stomata. *J Exp Bot* 58: 1783–1793.
- Im J, Lee SW, Yoon S, Dispirito AA, Semrau JD. (2011). Characterization of a novel facultative *Methylocystis* species capable of growth on methane, acetate and ethanol. *Environ Microbiol Rep* 3: 174–181.
- Im J, Semrau JD. (2011). Pollutant degradation by a *Methylocystis* strain SB2 grown on ethanol: bioremediation via facultative methanotrophy. *FEMS Microbiol Lett* 318: 137–142.
- Irvine IC, Brigham CA, Suding KN, Martiny JB. (2012). The abundance of pink-pigmented facultative methylotrophs in the root zone of plant species in invaded coastal sage scrub habitat. *PLoS One* 7: e31026.

- Islam T, Jensen S, Reigstad LJ, Larsen O, Birkeland NK. (2008). Methane oxidation at 55 degrees C and pH 2 by a thermoacidophilic bacterium belonging to the *Verrucomicrobia* phylum. *Proc Natl Acad Sci USA* 105: 300–304.
- Ito T, Fujimura S, Uchino M, Tanaka N, Matsufuji Y, Miyaji T, et al. (2007). Distribution, diversity and regulation of alcohol oxidase isozymes, and phylogenetic relationships of methylotrophic yeasts. *Yeast* 24: 523–532.
- Itoh T, Yamanoi K, Kudo T, Ohkuma M, Takashina T. (2011). *Aciditerrimonas ferrireducens* gen. nov., sp. nov., an iron-reducing thermoacidophilic *Actinobacterium* isolated from a solfataric field. *Int J Syst Evol Microbiol* 61: 1281–1285.
- Ivanova EG, Doronina NV, Trotsenko YA. (2001). Aerobic Methylobacteria Are Capable of Synthesizing Auxins. *Microbiology* 70: 392–397.
- Jaatinen K, Knief C, Dunfield PF, Yrjälä K, Fritze H. (2004). Methanotrophic bacteria in boreal forest soil after fire. *FEMS Microbiol Ecol* 50: 195–202.
- Jacob DJ, Field BD, Li QB, Blake DR, DeGouw J, Warneke C, et al. (2005). Global budget of methanol: constraints from atmospheric observations. *J Geophys Res Atmos* 110: D08303.
- Jacob DJ. (1999). *Introduction to Atmospheric Chemistry*. Princeton University Press.
- Janshekar H, Fiechter, A. (1982). On the bacterial degradation of lignin. *Appl Microbiol Biotechnol* 14: 47–50.
- Janssen FM, Kerwin RM, Ruelius HW. (1965). Alcohol oxidase, a novel enzyme from a basidiomycete. *Biochem Biophys Res Commun* 20: 630–636.
- Jenkins O, Byrom D, Jones D. (1987). *Methylophilus*: a new genus of methanol utilizing bacteria. *Int J Syst Bacteriol* 37: 446–448.
- Jensen S, Priemé A, Bakken L. (1998). Methanol improves methane uptake in starved methanotrophic microorganisms. *Appl Environ Microbiol* 64: 1143–1146.
- Johnson DB, Bacelar-Nicolau P, Okibe N, Thomas A, Kevin B. Hallberg KB. (2009). *Ferrimicrobium acidiphilum* gen. nov., sp. nov. and *Ferrithrix thermotolerans* gen. nov., sp. nov.: heterotrophic, iron-oxidizing, extremely acidophilic actinobacteria. *Int J Syst Evol Microbiol* 59: 1082–1089.
- Johnson DB, Naoko Okibe N, Roberto FF. (2003). Novel thermo-acidophilic bacteria isolated from geothermal sites in Yellowstone National Park: physiological and phylogenetic characteristics. *Arch Microbiol* 180: 60–68.
- Jukes TH, Cantor CR. (1969). Evolution of protein molecules. In: Munro HN (eds). *Mammalian Protein Metabolism*. Academic Press, New York, pp. 21–132.
- Kähkönen MA, Wittmann C, Ilvesniemi H, Westman CJ, Salkinoja-Salonen MS. (2002). Mineralization of detritus and oxidation of methane in acid boreal coniferous forest soils: seasonal and vertical distribution and effects of clear-cut. *Soil Biol Biochem* 34: 1191–1200.
- Kalyuzhnaya MG, Martens-Habbena W, Wang T, Hackett M, Stolyar SM, Stahl DA, et al. (2009). *Methylophilaceae* link methanol oxidation to denitrification in freshwater lake sediment as suggested by stable isotope probing and pure culture analysis. *Environ Microbiol Rep* 1: 385–392.
- Kalyuzhnaya MG, Beck DAC, Suciú D, Pozhitkov A, Lidstrom ME, Chistoserdova L. (2010). Functioning *in situ*: gene expression in *Methylotenera mobilis* in its native environment as assessed through transcriptomics. *ISME J* 4: 388–398.
- Kalyuzhnaya MG, Hristova KR, Lidstrom ME, Chistoserdova L. (2008a). Characterization of a novel methanol dehydrogenase in representatives of *Burkholderiales*: implications for environmental detection of methylotrophy and evidence for convergent evolution. *J Bacteriol* 190: 3817–3823.
- Kalyuzhnaya MG, Lapidus A, Ivanova N, Copeland AC, McHardy AC, Szeto E, et al. (2008b). High-resolution metagenomics targets specific functional types in complex microbial communities. *Nat Biotechnol* 26: 1029–1034.
- Kalyuzhnaya MG, Lidstrom ME, Chistoserdova L. (2004). Utility of environmental primers targeting ancient enzymes: methylotroph detection in Lake Washington. *Microb Ecol* 48: 463–472.
- Kalyuzhnaya MG, Zabinsky R, Bowerman S, Baker DR, Lidstrom ME, Chistoserdova L. (2006). Fluorescence *in situ* hybridization-flow cytometry-cell sorting-based method for separation and enrichment of type I and type II methanotroph populations. *Appl Environ Microbiol* 72: 4293–4301.
- Kämpfer P, Kroppenstedt RM. (2004). *Pseudonocardia benzenivorans* sp. nov. *Int J Syst Evol Microbiol* 54: 749–751.
- Kane SR, Chakicherla AY, Chain PS, Schmidt R, Shin MW, Legler TC, et al. (2007). Whole-genome analysis of the methyl tert-butyl ether-degrading beta-proteobacterium *Methylibium petroleiphilum* PM1. *J Bacteriol* 189: 1931–1945. Erratum (2007) *J Bacteriol* 189: 4973.
- Kaneko T, Nakamura Y, Sato S, Minamisawa K, Uchiumi T, Sasamoto S, et al. (2002). Complete genomic sequence of nitrogen-fixing symbiotic bacterium *Bradyrhizobium japonicum* USDA110. *DNA Res* 9:189–197.
- Karl T, Guenther A, Lindinger C, Jordan A, Fall R, Lindinger W. (2001). Eddy covariance measurements of oxygenated volatile organic compound fluxes from crop harvesting using a redesigned proton-transfer-reaction mass spectrometer. *J Geophys Res Atmospheres* 106: 24157–24167.

- Karl T, Harren F, Warneke C, de Gouw J, Grayless C, Fall R. (2005). Senescing grass crops as regional sources of reactive volatile organic compounds. *J Geophys Res* 110: D15302.
- Kaserer, H. (1905). Über die Oxidation des Wasserstoffes und des Methan durch Mikroorganismen. *Z landw Versuchsw in Osterreich* 8: 789–792.
- Kaszycki P, Czechowska K, Petryszak P, Międzobrodzki J, Pawlik B, Kołoczek H. (2006). Methylophilic extremophilic yeast *Trichosporon* sp.: a soil-derived isolate with potential applications in environmental biotechnology. *Acta Biochim Pol* 53: 463–473.
- Keene WC, Khalil MAK, Erickson DJ, McCulloch A, Graedel TE, Lobert JM, et al. (1999). Composite global emissions of reactive chlorine from anthropogenic and natural sources: reactive chlorine emissions inventory. *J Geophys Res* 104: 8429–8440.
- Kelly DP, Anthony C, Murrell JC. (2005). Insights into the obligate methanotroph *Methylococcus capsulatus*. *Trends Microbiol* 13: 195–198.
- Kelly DP, McDonald IR, Wood AP. (2013). The Family *Methylobacteriaceae*. In: Rosenberg E, DeLong EF, Lory S, Stackebrandt E, Thompson F (eds). *The Prokaryotes – Alphaproteobacteria and Betaproteobacteria*. Springer: New York, pp 313–340.
- Keltjens JT, Pol A, Reimann J, Op den Camp HJM. (2014). PQQ-dependent methanol dehydrogenases: rare-earth elements make a difference. *Appl Microbiol Biotechnol* 98: 6163–6183.
- Keppler F, Eiden R, Niedan V, Pracht J, Schöler HF. (2000). Halocarbons produced by natural oxidation processes during degradation of organic matter. *Nature* 403: 298–301.
- Keppler F, Harper DB, Röckmann T, Moore RM, Hamilton JTG. (2005). New insight into the atmospheric chloromethane budget gained using stable carbon isotope ratios. *Atmos Chem Phys* 5: 2403–2411.
- Keppler F, Hamilton JT, Brass M, Röckmann T. (2006). Methane emissions from terrestrial plants under aerobic conditions. *Nature* 439: 187–191.
- Khadem AF, Pol A, Wiczorek A, Mohammadi SS, Francoijs KJ, Stunnenberg HG, et al. (2004). Autotrophic methanotrophy in *Verrucomicrobia*: *Methylacidiphilum fumariolicum* SolV uses the Calvin-Benson-Bassham cycle for carbon dioxide fixation. *J Bacteriol* 193: 4438–4446.
- Khalil MAK, Rasmussen RA. (1999) Atmospheric methyl chloride. *Atmos Environ* 33: 1305–1321.
- Kim H, Park DS, Oh HW, Lee KH, Chung DH, Park HY, et al. (2012). *Gryllotalpicola* gen. nov., with descriptions of *Gryllotalpicola koreensis* sp. nov., *Gryllotalpicola daejeonensis* sp. nov. and *Gryllotalpicola kribbensis* sp. nov. from the gut of the African mole cricket, *Gryllotalpa africana*, and reclassification of *Curtobacterium ginsengisoli* as *Gryllotalpicola ginsengisoli* comb. nov. *Int J Syst Evol Microbiol* 62: 2363–2370.
- King GM. (1992). Ecological aspects of methane oxidation, a key determinant of global methane dynamics. *Adv Microb Ecol* 12: 431–474
- King GM. (1993) Ecophysiological characteristics of obligate methanotrophic bacteria and methane oxidation in situ. In: Murrell JC, Kelly DP. (eds). *Microbial Growth on C1-Compounds*. Andover, Andorra: Intercept, pp. 303–313.
- Kirk TK, Farrell RL. (1987). Enzymatic “combustion”: the microbial degradation of lignin. *Ann Rev Microbiol* 41:465–505.
- Kist J, Tate III RL. (2013). Phylogeny of bacterial methylophilic genes reveals robustness in *Methylobacterium mxaF* sequences and *mxo* operon construction. *Soil Biol Biochem* 59: 49–57.
- Kjøller AH, Struwe S. (2002). Fungal communities, succession, enzymes, and decomposition. In: Burns RG, Dick RP, (eds). *Enzymes in the environment: activity, ecology and applications*. Marcel Dekker, Inc.: New York, pp 267–284.
- Klappenbach JA, Saxman PR, Cole JR, Schmidt TM. (2001). rrndb: the ribosomal RNA operon copy number database. *Nucleic Acids Res.* 29: 181-184.
- Klindworth A, Pruesse E, Schweer T, Peplies J, Quast C, Horn M, et al. (2013). Evaluation of general 16S ribosomal RNA gene PCR primers for classical and next-generation sequencing-based diversity studies. *Nucleic Acids Res* 41: e1.
- Knief C, Lipski A, Dunfield PF. (2003). Diversity and activity of methanotrophic bacteria in different upland soils. *Appl Environ Microbiol* 69: 6703–6714.
- Knief C, Dunfield PF. (2005). Response and adaptation of different methanotrophic bacteria to low methane mixing ratios. *Environ Microbiol* 7: 1307–1317.
- Knief C. (2015). Diversity and Habitat Preferences of Cultivated and Uncultivated Aerobic Methanotrophic Bacteria Evaluated Based on *pmoA* as Molecular Marker. *Front Microbiol* 6: 1346.
- Knittel K, Boetius A. (2009). Anaerobic oxidation of methane: progress with an unknown process. *Annu Rev Microbiol* 63:311–334.
- Koch C, Neumann P, Valerius O, Feussner I, Ficner R. (2016). Crystal Structure of Alcohol Oxidase from *Pichia pastoris*. *PLoS One* 11: e0149846.

REFERENCES

- Koch IH, Gich F, Dunfield PF, Overmann J.** (2008). *Edaphobacter modestus* gen. nov., sp. nov., and *Edaphobacter aggregans* sp. nov., *Acidobacteria* isolated from alpine and forest soils. *Int J Syst Evol Microbiol* 58: 1114–1122.
- Kolb S, Knief C, Dunfield PF, Conrad R.** (2005). Abundance and activity of uncultured methanotrophic bacteria involved in the consumption of atmospheric methane in two forest soils. *Environ Microbiol* 7: 1150–1161.
- Kolb S, Stacheter A.** (2013). Prerequisites for amplicon pyrosequencing of microbial methanol utilizers in the environment. *Front Microbiol* 4: 1–12.
- Kolb S.** (2009a). Aerobic methanol-oxidizing *Bacteria* in soil. *FEMS Microbiol Lett.* 300: 1–10.
- Kolb S.** (2009b). The quest for atmospheric methane oxidizers in forest soils. *Environ Microbiol Rep* 1: 336–346.
- Kõljalg U, Nilsson RH, Abarenkov K, Tedersoo L, Taylor AFS, Bahram M, et al.** (2013). Towards a unified paradigm for sequence-based identification of fungi. *Mol Ecol* 22: 5271–5277.
- Kondo, T., Morikawa, Y. & Hayashi, N.** (2008). Purification and characterization of alcohol oxidase from *Paecilomyces variotii* isolated as a formaldehyde-resistant fungus. *Appl Microbiol Biotechnol* 77: 995–1002.
- Kozich JJ, Westcott SL, Baxter NT, Highlander SK, Schloss PD.** (2013). Development of a dual-Index sequencing strategy and curation pipeline for analyzing amplicon sequence data on the MiSeq Illumina sequencing platform. *Appl Environ Microbiol* 79: 5112–5120.
- Krog A, Heggeset TMB, Muller JEN, Kupper CE, Schneider O, Vorholt JA, et al.** (2013). Methylophilic *Bacillus methanolicus* encodes two chromosomal and one plasmid born NAD⁺ dependent methanol dehydrogenase paralogs with different catalytic and biochemical properties. *PLoS ONE* 8: e59188.
- Krulwich TA, Sachs G, Padan E.** (2011). Molecular aspects of bacterial pH sensing and homeostasis. *Nat Rev Microbiol* 9(5): 330–343.
- Kruskal JB.** (1964). Multidimensional scaling by optimizing goodness of fit to a nonmetric hypothesis. *Psychometrika* 29: 1–27.
- Kück U, Nowrousian M, Hoff B, Eng H.** (2009). *Schimmelpilze - Lebensweise, Nutzen, Schaden, Bekämpfung*. Springer Berlin Heidelberg, 3. Auflage.
- Kudo T, Matsushima K, Itoh T, Sasaki J, Suzuki K-I.** (1998). Description of four new species of the genus *Kineosporia*: *Kineosporia succinea* sp. nov., *Kineosporia rhizophila* sp. nov., *Kineosporia mikuniensis* sp. nov. and *Kineosporia rhamnosa* sp. nov., isolated from plant samples, and amended description of the genus *Kineosporia*. *Int J Syst Evol Microbiol* 48: 1245–1255.
- Kuivila KM, Murray JW, Devol AH, Lidstrom ME, Reimers CE.** (1988). Methane cycling in the sediments of Lake Washington. *Limnol Oceanogr* 33: 571–581.
- Kulichevskaya IS, Ivanova AO, Baulina OI, Bodelier PLE, Sinninghe Damsté JS, Dedysh SN.** (2008). *Singulisphaera acidiphila* gen. nov., sp. nov., a non-filamentous, *Isosphaera*-like planctomycete from acidic northern wetlands. *Int J Syst Evol Microbiol* 58: 1186–1193.
- Kulichevskaya IS, Ivanova AO, Belova SE, Baulina OI, Bodelier PLE, Rijpstra WIC, et al.** (2007). *Schlesneria paludicola* gen. nov., sp. nov., the first acidophilic member of the order *Planctomycetales*, from *Sphagnum*-dominated boreal wetlands. *Int J Syst Evol Microbiol* 57: 2680–2687.
- Kulichevskaya IS, Pankratov T A, Dedysh SN.** (2006). Detection of representatives of the *Planctomycetes* in *Sphagnum* peat bogs by molecular and cultivation approaches. *Microbiology (English translation of Mikrobiologiya)* 75: 329–335.
- Kulichevskaya IS, Serkebaeva YM, Kim Y, Rijpstra WIC, Sinninghe Damsté JS, Liesack W, et al.** (2012). *Telmatocola sphagniphila* gen. nov., sp. nov., a novel dendriform planctomycete from northern wetlands. *Front Microbiol* 3: 146.
- Kulichevskaya IS, Baulina OI, Bodelier PL, Rijpstra WI, Damsté JS, Dedysh SN.** (2009). *Zavarzinella formosa* gen. nov., sp. nov., a novel stalked, *Gemmata*-like planctomycete from a Siberian peat bog. *Int J Syst Evol Microbiol* 59: 357–364.
- Kunin V, Engelbrekton A, Ochman H, Hugenholtz P.** (2010). Wrinkles in the rare biosphere: pyrosequencing errors can lead to artificial inflation of diversity estimates. *Environ Microbiol* 12: 118–123.
- Küsel K, Drake HL.** (1995). Effects of environmental parameters on the formation and turnover of acetate by forest soils. *Appl Environ Microbiol* 61: 3667–3675.
- Kvenvolden KA, Rogers BW.** (2005) Gaia's breath – global methane exhalations. *Mar Petrol Geol* 22: 579–590.
- Lane D.** (1991). *16S/23S rRNA sequencing: Nucleic Acid Techniques in Bacterial Systematics*. Wiley, Chichester UK.
- Large PJ, Bamforth CW.** (1988). *Methylophilicity and Biotechnology*. Longman Scientific & Technical, Harlow, UK.
- Large PJ, Peel D, Quayle JR.** (1961). Microbial growth on C1 compounds. II. Synthesis of cell constituents by methanol- and formate-grown *Pseudomonas* AM 1, and methanol-grown *Hyphomicrobium vulgare*. *Biochem J* 81: 470–480.
- Lau E, Ahmad A, Steudler PA, Cavanaugh CM.** (2007). Molecular characterization of methanotrophic communities in forest soils that consume atmospheric methane. *FEMS Microbiol Ecol* 60: 490–500.

- Lau E, Fisher MC, Steudler PA, Cavanaugh CM. (2013). The methanol dehydrogenase gene, *mxhF*, as a functional and phylogenetic marker for proteobacterial methanotrophs in natural environments. *PLoS ONE* 8: e56993.
- Leahy JG, Batchelor PJ, Morcomb SM. (2003). Evolution of the soluble diiron monooxygenases. *FEMS Microbiol Rev* 27: 449–479.
- Lebo Jr SE, Gargulak JD, McNally TJ. (2001). *Lignin*. In: Kirk-Othmer Encyclopedia of Chemical Technology. LignoTech USA, Inc.
- Lee B, Yurimoto H, Sakai Y, Kato N. (2002). Physiological role of the glutathione-dependent formaldehyde dehydrogenase in the methylotrophic yeast *Candida boidinii*. *Microbiology* 148: 2697–2704.
- Lee J, Park B, Woo S-G, Lee J, Park J. (2014). *Prostheco bacter* *algae* sp. nov., isolated from activated sludge using algal metabolites. *Int J Syst Evol Microbiol* 64: 663–667.
- Lee SB, Strand SE, Stensel HD, Herwig RP. (2004). *Pseudonocardia chloroethenivorans* sp. nov., a chloroethene-degrading actinomycete. *Int J Syst Evol Microbiol* 54: 131–139.
- LeMer J, Roger P. (2011). Production, oxidation, emission and consumption of methane by soils: a review. *Eur J Soil Biol* 37: 25–50.
- Lenhart K, Bunge M, Ratering S, Neu TR, Schüttmann I, Greule M, et al. (2012). Evidence for methane production by saprotrophic fungi. *Nat Commun* 3:1046.
- Lewin B. (1998). *Molekularbiologie der Gene*. Spektrum Verlag Heidelberg, Deutschland
- Li J, Zhao G-Z, Huang H-Y, Qin S, Zhu W-Y, Xu L-H, et al. (2009). *Kineosporia mesophila* sp. nov., isolated from surface-sterilized stems of *Tripterygium wilfordii*. *Int J Syst Evol Microbiol* 59: 3150–3154.
- Lidstrom ME, Anthony C, Biville F, Gasser F, Goodwin P, Hanson RS, et al. (1994). New unified nomenclature for genes involved in the oxidation of methanol in gram-negative bacteria. *FEMS Microbiol Lett* 117: 103–106.
- Lidstrom ME, Chistoserdova L. (2002). Plants in the pink: cytokinin production by *Methylobacterium*. *J Bacteriol* 184: 1818.
- Lidstrom ME. (2006). Aerobic methylotrophic bacteria. In: Dworkin M, Falkow S, Rosenberg E, Schleifer K-H, Stackebrandt E (eds). *The Prokaryotes – Volume 2: Ecophysiology and Biochemistry*. Springer: New York, pp 618–634.
- Lieberman RL, Rosenzweig AC. (2005). The quest for the particulate methane monooxygenase active site. *Dalton Trans* 21: 3390-3396.
- Liebner S, Zeyer J, Wagner D, Schubert C, Pfeiffer E-M, Knoblauch C. (2011). Methane oxidation associated with submerged brown mosses reduces methane emissions from Siberian polygonal tundra. *J Ecol* 99: 914–922.
- Limtong S, Srisuk N, Yongmanitchai W, Yurimoto H, Nakase T. (2008). *Ogataea chonburiensis* sp. nov. and *Ogataea nakhonphanomensis* sp. nov., thermotolerant, methylotrophic yeast species isolated in Thailand, and transfer of *Pichia siamensis* and *Pichia thermomethanolica* to the genus *Ogataea*. *Int J Syst Evol Microbiol* 58: 302–307.
- Lindner AS, Pacheco A, Aldrich HC, Costello Staniec A, Uz I, Hodson DJ. (2007). *Methylocystis hirsuta* sp. nov., a novel methanotroph isolated from a groundwater aquifer. *Int J Syst Evol Microbiol* 57, 1891–1900.
- Linton, J.D., and Vokes, J. (1978) Growth of the methane utilizing bacterium *Methylococcus* NCIB 11083 in mineral salts medium with methanol as a sole source of carbon. *FEMS Microbiol Lett* 4: 125–128.
- Liu WT, Marsh TL, Cheng H, Forney LJ. (1997). Characterization of microbial diversity by determining terminal restriction fragment length polymorphisms of genes encoding 16S rRNA. *Appl Environ Microbiol*. 63: 4516–4522.
- Liu X-Z, Wang Q-M, Theelen B, Groenewald M, Bai F-Y, Boekhout T. (2015). Phylogeny of tremellomycetous yeasts and related dimorphic and filamentous *Basidiomycetes* reconstructed from multiple gene sequence analyses. *Stud Mycol* 81: 1-26.
- Liu YJ, Liu SJ, Drake HL, Horn MA. (2011). *Alphaproteobacteria* dominate active 2-methyl-4-chlorophenoxyacetic acid herbicide degraders in agricultural soil and drilosphere. *Environ Microbiol* 13: 991–1009.
- Loew O (1892) Ueber einen Bacillus, welcher Ameisensäure und Formaldehyd assimiliren kann. *Centralblatt Bakteriologie, Parasitenkunde, Infektionskrankheiten Hygiene, Abteilung II* 12: 462–465.
- Lovelock JE. (1975). Natural halocarbons in the air and the sea. *Nature* 256: 193–194.
- Ludwig ML, Matthews RG. (1997). Structure-based perspectives on B₁₂-dependent enzymes. *Annu Rev Biochem* 66: 269–313.
- Ludwig W, Euzéby J, Whitman WB. (2010). Road map of the phyla *Bacteroidetes*, *Spirochaetes*, *Tenericutes* (*Mollicutes*), *Acidobacteria*, *Fibrobacteres*, *Fusobacteria*, *Dictyoglomi*, *Gemmatimonadetes*, *Lentisphaerae*, *Verrucomicrobia*, *Chlamydiae*, and *Planctomycetes*. In: Krieg NR, Staley JT, Brown DR, Hedlund BP, Paster BJ, Ward NL, Ludwig W, Whitman WB (eds). *Bergey's Manual of Systematic Bacteriology*. 2nd edition, Vol 4: *The Bacteroidetes*, *Spirochaetes*, *Tenericutes* (*Mollicutes*), *Acidobacteria*, *Fibrobacteres*, *Fusobacteria*, *Dictyoglomi*, *Gemmatimonadetes*, *Lentisphaerae*, *Verrucomicrobia*, *Chlamydiae*, and *Planctomycetes*. New York: Springer, pp 1-19.

- Lueders T, Manefield M, Friedrich MW. (2004). Enhanced sensitivity of DNA- and rRNA-based stable isotope probing by fractionation and quantitative analysis of isopycnic centrifugation gradients. *Environ Microbiol* 1: 73–78.
- Lynch RC, Darcy JL, Kane NC, Nemergut DR, Schmidt SK. (2014). Metagenomic evidence for metabolism of trace atmospheric gases by high-elevation desert Actinobacteria. *Front Microbiol* 5: 698.
- Lynd RL, Weimer PJ, van Zyl WH, Pretorius IS. (2002). Microbial Cellulose Utilization: Fundamentals and Biotechnology. *Microbiol Mol Biol R* 66: 506–577.
- MacDonald JA, Skiba U, Sheppard LJ, Hargreaves KJ, Smith KA, Fowler D. (1996). Soil environment variables affecting the flux of methane from a range of forest, moorland and agricultural soils. *Biogeochemistry* 34: 113–132.
- Madhaiyan M, Poonguzhali S, Lee J-S, Lee KC, Sundaram S. (2010a). *Flavobacterium glycines* sp. nov., a facultative methylotroph isolated from the rhizosphere of soybean. *Int J Syst Evol Microbiol* 60: 2187–2192.
- Madhaiyan M, Poonguzhali S, Lee J-S, Senthilkumar M, Lee KC, Sundaram S. (2010b). *Mucilaginibacter gossypii* sp. nov. and *Mucilaginibacter gossypicola* sp. nov., plant-growth-promoting bacteria isolated from cotton rhizosphere soils. *J Syst Evol Microbiol* 60: 2451–2457.
- Madhaiyan M, Poonguzhali S, Senthilkumar M, Lee JS, Lee KC. (2012) *Methylobacterium gossypicola* sp. nov., a pink-pigmented, facultatively methylotrophic bacterium isolated from the cotton phyllosphere. *Int J Syst Evol Microbiol* 62: 162–167.
- Madhaiyan M, Suresh Reddy BV, Anandham R, Senthilkumar M, Poonguzhali S, Sundaram SP, Sa T. (2006). Plant growth-promoting *Methylobacterium* induces defense responses in groundnut (*Arachis hypogaea* L.) compared with rot pathogens. *Curr Microbiol* 53: 270–276.
- Maleknia SD, Vail TM, Cody RB, Sparkman DO, Bell TL, Adams MA. (2009). Temperature-dependent release of volatile organic compounds of eucalypts by direct analysis in real time (DART) mass spectrometry. *Rapid Commun Mass Spectrom* 23: 2241–2246.
- Malhotra S, Lal R. (2007). The genus *Amycolatopsis*: indigenous plasmids, cloning vectors and gene transfer systems. *Indian J Microbiol* 47: 3–14.
- Mancinelli RL. (1995). The regulation of methane oxidation in soil. *Annu Rev Microbiol* 49: 581–605.
- Manley SL, Dastoor MN. (1987). Methyl halide (CH₃X) production from the giant kelp, *Macrocystis*, and estimates of global CH₃X production by kelp. *Limnol Oceanogr* 32: 70–715.
- Margulies M, Egholm M, Altman W, Attiya S, Bader JS, Bemben L, et al. (2005) Genome sequencing in microfabricated high density picolitre reactors. *Nature* 437: 376–380
- Marin I, Arahal DR. (2013). The Family *Beijerinckiaceae*. In: Rosenberg E, DeLong EF, Lory S, Stackebrandt E, Thompson F (eds). *The Prokaryotes – Alphaproteobacteria and Betaproteobacteria*. Springer: New York, pp 115–133.
- Mark JE, Erman B. (2005). Science and technology of rubber. Academic Pr Inc, 3rd edition. ISBN 0-12-464786-3.
- Marsh TL. (2005). Culture-independent microbial community analysis with terminal restriction fragment length polymorphism. *Environmental Microbiology* 397: 308–329.
- Marx CJ, Chistoserdova L, Lidstrom ME. (2003). Formaldehyde detoxifying role of the tetrahydromethanopterin-linked pathway *Methylobacterium extorquens* AM1. *J Bacteriol* 185: 760–768.
- Masuda S, Eda S, Sugawara C, Mitsui H, Minamisawa K. (2010). The *cbbL* gene is required for thiosulfate-dependent autotrophic growth of *Bradyrhizobium japonicum*. *Microbes Environ* 25: 220–223.
- McAnulla C, Woodall CA, McDonald IR, Studer A, Vuilleumier S, Leisinger T, et al. (2001b). Chloromethane Utilization Gene Cluster from *Hyphomicrobium chloromethanicum* Strain CM2T and Development of Functional Gene Probes To Detect Halomethane-Degrading Bacteria. *Appl Environ Microbiol* 67: 307–316.
- McAnulla C, McDonald IR, Murrell JC. (2001a). Methyl chloride utilising bacteria are ubiquitous in the natural environment. *FEMS Microbiol Lett* 201: 151–155.
- McCarthy AJ. (1978). Lignocellulose-degrading actinomycetes. *FEMS Microbiol Rev* 46: 145–163.
- McDonald IR, Bodrossy L, Chen Y, Murrell JC. (2008). Molecular ecology techniques for the study of aerobic methanotrophs. *Appl Environ Microbiol* 74: 1305–1315.
- McDonald IR, Doronina NV, Trotsenko YA, McAnulla C, Murrell JC. (2001). *Hyphomicrobium chloromethanicum* sp. nov. and *Methylobacterium chloromethanicum* sp. nov., chloromethane-utilising bacteria isolated from a polluted environment. *Int J Syst Evol Microbiol* 51: 119–122.
- McDonald IR, Kenna EM, Murrell JC. (1995). Detection of Methanotrophic Bacteria in Environmental Samples with the PCR. *Appl Environ Microbiol* 61: 116–121
- McDonald IR, Murrell JC. (1997). The methanol dehydrogenase structural gene *mxoF* and its use as a functional gene probe for methanotrophs and methylotrophs. *Appl Environ Microbiol* 63: 3218–3224.

- McDonald IR, Radajewski S, Murrell JC. (2005). Stable isotope probing of nucleic acids in methanotrophs and methylotrophs: A review. *Organic Geochemistry* 36: 779–787.
- McDonald IR, Uchiyama H, Kambe S, Yagi O, Murrell JC. (1997). The soluble methane monooxygenase gene cluster of the trichloroethylene-degrading methanotroph *Methylocystis* sp. strain M. *Appl Environ Microbiol* 63: 1898–1904.
- McDonald IR, Warner KL, McAnulla C, Woodall CA, Oremland RS, et al. (2002). A review of bacterial methyl halide degradation: biochemistry, genetics and molecular ecology. *Environ Microbiol* 4: 193–203.
- McNerney T, O'connor ML. (1980). Regulation of enzymes associated with C-1 metabolism in three facultative methylotrophs. *Appl Environ Microbiol* 40: 370–375.
- Medeiros PM, Simoneit BRT. (2008). Source profiles of organic compounds emitted upon combustion of green vegetation from temperate climate forests. *Environ Sci Technol* 42: 8310–8316.
- Meena KK, Kumar M, Kalyuzhnaya MG, Yandigeri MS, Singh DP, Saxena AK, Arora DK. (2012). Epiphytic pink-pigmented methylotrophic bacteria enhance germination and seedling growth of wheat (*Triticum aestivum*) by producing phytohormone. *Antonie Van Leeuwenhoek* 101: 777–786.
- Megraw SR, Knowles R. (1987). Methane production and consumption in a cultivated humisol. *Biofertil Soils* 5: 56–60.
- Messner K, Fackler K, Pongsak L, Gindl W, Srebotnik E, Watanabe T. (2003). Overview of white-rot research: where we are today. In: Goodell B, Nicholas DD & Schultz TR (eds). *Wood Deterioration and Preservation: Advances in our Changing World (ACS symposium series 845)*. American Chemical Society: Washington, DC, pp 73–96.
- Meßmer M, Wohlfarth G, Diekert G. (1993). Methyl chloride metabolism of the strictly anaerobic, methyl chloride-utilizing homoacetogen strain MC. *Arch Microbiol* 160: 383–387.
- Meßmer M, Reinhardt S, Wohlfarth G, Diekert G. (1996). Studies on methyl chloride dehalogenase and O-demethylase in cell extracts of the homoacetogen strain MC based on a newly developed coupled enzyme assay. *Arch Microbiol* 165: 18–25.
- Michener JK, Vuilleumier S, Bringel F, Marx CJ. (2016). Transfer of a Catabolic Pathway for Chloromethane in *Methylobacterium* Strains Highlights Different Limitations for Growth with Chloromethane or with Dichloromethane. *Front Microbiol* 7: 1116.
- Miller LG, Warner KL, Baesman SM, Oremland RS, McDonald IR, Radajewski S, et al. (2004). Degradation of methyl bromide and methyl chloride in soil microcosms: use of stable C isotope fractionation and stable isotope probing to identify reactions and the responsible microorganisms. *Geochim Cosmochim Acta* 68: 3271–3283.
- Miller LG, Connell TL, Guidetti JR, Oremland RS. (1997). Bacterial oxidation of methyl bromide in fumigated agricultural soils. *Appl Environ Microbiol* 63: 4346–4354.
- Millet DB, Jacob DJ, Custer TG, de Gouw JA, Goldstein AH, Karl T, et al. (2008). New constraints on terrestrial and oceanic sources of atmospheric methanol. *Atmos Chem Phys* 8: 6887–6905.
- Mohammadi S, Pol A, van Alen TA, Jetten MS, Op den Camp HJ. (2016). Methylacidiphilum fumariolicum SolV, a thermoacidophilic 'Knallgas' methanotroph with both an oxygen-sensitive and -insensitive hydrogenase. *ISME J* 9: 1–14. doi: 10.1038/ismej.2016.171.
- Montzka SA, Reimann S, Engel A, Krüger K, O'Doherty S, Sturges WT, et al. (2011). Scientific assessment of ozone depletion: 2010. *Global ozone research and monitoring project, World Meteorological Organization*. Geneva Report no. 52: Chapter 1, pp 1-86.
- Moon J-Y, Kim S-J, Hamada M, Ahn J-H, Weon H-Y, Suzuki K-I, et al. (2014). *Gryllotalpicola soli* sp. nov., isolated from soil. *Int J Syst Evol Microbiol* 64: 4079–4083.
- Moore RM, Tokarczyk R, Tait VK, Paulin M, Geen C. (1995). Marine phytoplankton as a natural source of volatile organohalogens. In: Grimvall A, de Leer EWB (eds). *Naturally-Produced Organohalogens*. Kluwer Academic Publishers, Dordrecht, pp. 283–294.
- Moore RM, Gut A, Andreae MO. (2005). A pilot study of methyl chloride emissions from tropical wood rot fungi. *Chemosphere* 58: 221–225.
- Moosvi SA, McDonald IR, Pearce DA, Kelly DP, Wood AP. (2005). Molecular detection and isolation from Antarctica of methylotrophic bacteria able to grow with methylated sulfur compounds. *Syst Appl Microbiol* 28: 541–554.
- Morawe M, Hoeke H, Wissenbach DK, Lentendu G, Wubet T, Kröber E, and Kolb S. (2017). Acidotolerant Bacteria and Fungi as a Sink of Methanol-Derived Carbon in a Deciduous Forest Soil. *Front Microbiol*.8: 1361. doi: 10.3389/fmicb.2017.01361
- Morris SA, Radajewski S, Willison TW, Murrell JC. (2002). Identification of the functionally active methanotroph population in a peat soil microcosm by stable-isotope probing. *Appl Environ Microbiol* 68: 1446–1453.
- Mountfort DO. (1990). Oxidation of aromatic alcohols by purified methanol dehydrogenase from *Methylosinus trichosporium*. *J Bacteriol* 172: 3690–3694.

- Mukhin VA, Voronin PY.** (2009). Methanogenic Activity of Woody Debris. *Russian Journal of Ecology* 40: 149–153.
- Müller J, Bußler H, Kneib T.** (2008). Saprophytic beetle assemblages related to silvicultural management intensity and stand structures in a beech forest in Southern Germany. *J Insect Conserv* 12: 107–124.
- Murrell JC, McDonald IR, Gilbert B.** (2000). Regulation of expression of methane monoxygenases by copper ions. *Trends Microbiol* 8 : 221–225.
- Muyzer G, Brinkhoff T, Nuebel U, Santegoeds C, Schaefer H, Waver C.** (1998). Denaturing gradient gel electrophoresis (DGGE) in microbial ecology. In: Akkermans ADL, van Elsas JD, de Bruijn FJ. (eds). *Molecular Microbial Ecology Manual*. Kluwer Academic Publishers, Dordrecht, The Netherlands, pp. 1–27.
- Myhre G, Shindell D, Bréon F-M, Collins W, Fuglestedt J, Huang J, et al.** (2013). Anthropogenic and Natural Radiative Forcing. . In: Stocker TF, Qin D, Plattner G-K, Tignor M, Allen SK, Boschung J, Nauels A, Xia Y, Bex V, Midgley PM (eds). *Climate Change 2013: The Physical Science Basis. Contribution of Working Group I to the Fifth Assessment Report of the Intergovernmental Panel on Climate Change*. Cambridge University Press, Cambridge, United Kingdom and New York, NY, USA, pp 659–740.
- Myronova N, Kitmitto A, Collins RF, Miyaji A, Dalton H.** (2006) Three-dimensional structure determination of a protein supercomplex that oxidizes methane to formaldehyde in *Methylococcus capsulatus* (Bath). *Biochemistry* 45 : 11905–11914.
- Nadalig T, Greule M, Bringel F, Keppler F, Vuilleumier S.** (2014). Probing the diversity of chloromethane-degrading bacteria by comparative genomics and isotopic fractionation. *Front Microbiol* 5: 523.
- Nadalig T, Farhan UI Haque M, Roselli S, Schaller H, Bringel F, Vuilleumier S.** (2011). Detection and isolation of chloromethane-degrading bacteria from the *Arabidopsis thaliana* phyllosphere, and characterization of chloromethane utilization genes. *FEMS Microbiol Ecol* 77: 438–448.
- Nagatoshi Y, Nakamura T.** (2007). Characterization of three halide methyltransferases in *Arabidopsis thaliana*. *Plant Biotechnol* 24 : 503–506.
- Nakagawa T, Inagaki A, Ito T, Fujimura S, Miyaji T, Yurimoto H, et al.** (2006). Regulation of two distinct alcohol oxidase promoters in the methylotrophic yeast *Pichia methanolica*. *Yeast* 23: 15–22.
- Nakagawa T, Mitsui R, Tani A, Sasa K, Tashiro S, Iwama T, et al.** (2012). A catalytic role of XoxF1 as La³⁺-dependent methanol dehydrogenase in *Methylobacterium extorquens* strain AM1. *PLoS ONE* 7: e50480.
- Nakatsu CH, Hristova K, Hanada S, Meng X-Y, Hanson JR, Scow KM, Kamagata Y.** (2006). *Methylbium petroleiphilum* gen. nov., sp. nov., a novel methyl tert-butyl ether-degrading methylotroph of the *Betaproteobacteria*. *J Syst Evol Microbiol* 56: 983–989.
- Nayak DD, Marx CJ.** (2014). Genetic and phenotypic comparison of facultative methylotrophy between *Methylobacterium extorquens* strains PA1 and AM1. *PLoS One* 9:e107887.
- Nazaries L, Murrell JC, Millard P, Baggs L, Singh BK.** (2013). Methane, microbes and models: fundamental understanding of the soil methane cycle for future predictions. *Environ Microbiol* 15: 2395–2417.
- Nebel ME, Holzhauser M, Hüttenberger L, Reitzig R, Sperber M, Wild S, et al.** (2011). Jaguc – a software package for environmental diversity analyses. *J Bioinform Comput Biol* 9: 749–773.
- Neef L, van Weele M, van Velthoven P.** (2010). Optimal estimation of the present-day global methane budget. *Global Biogeochem Cy* 24: GB4024.
- Negruță O, Csutak O, Stoica I, Rusu E, Vassu T.** (2010). Methylotrophic yeasts: diversity and methanol metabolism. *Rom Biotech Lett* 15: 5369–5375.
- Nei M, Kumar S.** (2000). *Molecular Evolution and Phylogenetics*. Oxford University Press, New York.
- Nelson MJ, Montgomery SO, Mahaffey WR, Pritchard PH.** (1987). Biodegradation of trichloroethylene and involvement of an aromatic biodegradative pathway. *Appl Environ Microbiol* 53: 949–954.
- Nemecek-Marshall M, MacDonald RC, Franzen JJ, Wojciechowski CL, Fall R.** (1995). Methanol Emission from Leaves (Enzymatic Detection of Gas-Phase Methanol and Relation of Methanol Fluxes to Stomatal Conductance and Leaf Development). *Plant Physiol* 108: 1359–1368.
- Neufeld JD, Vohra J, Dumont MG, Lueders T, Manefield M, Friedrich MW, et al.** (2007) DNA stable-isotope probing. *Nat Protoc* 2: 860-866.
- Neufeld JD, Dumont MG, Vohra J, Murrell JC.** (2006). Methodological considerations for the use of stable isotope probing in microbial ecology. *Microb Ecol* 53: 435–442.
- Niemann H, Steinle L, Blees J, Bussmann I, Treude T, Krause S, et al.** (2015). Toxic effects of lab-grade butyl rubber stoppers on aerobic methane oxidation. *Limnol Oceanogr Methods* 13: 40–52.
- Nisbet EG, Dlugokencky EJ, Bousquet P.** (2014). Atmospheric science. Methane on the rise-again. *Science* 343:493–495.

- Nold SC, Zhou J, Devol AH, Tiedje JM.** (2000). Pacific Northwest marine sediments contain ammonia-oxidizing bacteria in the beta subdivision of the Proteobacteria. *Appl Environ Microbiol* 66: 4532–4525.
- Ochsner AM, Sonntag F, Buchhaupt M, Schrader J, Vorholt JA.** (2015). *Methylobacterium extorquens*: methylotrophy and biotechnological applications. *Appl Microbiol Biotechnol* 99: 517–534.
- Ogata K, Nishikawa H, Ohsugi M.** (1969). A yeast capable of utilizing methanol. *Agric Biol Chem* 33: 1519–1520.
- Okubo Y, Yang S, Chistoserdova L, Lidstrom ME.** (2010). Alternative route for glyoxylate consumption during growth on two-carbon compounds by *Methylobacterium extorquens* AM1. *J Bacteriol* 192: 1813–1823.
- Omer ZS, Tombolini R, Gerhardson B.** (2004). Plant colonization by pink-pigmented facultative methylotrophic bacteria (PPFMs). *FEMS Microbiol Ecol* 47: 319–326.
- Op den Camp HJM, Islam T, Stott MB, Harhangi HR, Hynes A, Schouten S, et al.** (2009). Environmental, genomic and taxonomic perspectives on methanotrophic *Verrucomicrobia*. *Environ Microbiol Rep* 1: 293–306.
- Or D, Smets BF, Wraith JM, Dechesne A, Friedman SP.** (2007). Physical constraints affecting bacterial habitats and activity in unsaturated porous media – a review. *Adv Water Resour* 30: 1505–1527.
- Oremland RS, Culbertson CW.** (1992). Importance of methane-oxidizing bacteria in the methane budget as revealed by the use of a specific inhibitor. *Nature* 356: 421–423.
- Oren A, Xu X-W.** (2013). The Family *Hyphomicrobiaceae*. In: Rosenberg E, DeLong EF, Lory S, Stackebrandt E, Thompson F (eds). *The Prokaryotes – Alphaproteobacteria and Betaproteobacteria*. Springer: New York, pp 248–281.
- Oren A.** (2013). The Family *Methanosarcinaceae*. In: Rosenberg E, DeLong EF, Lory S, Stackebrandt E, Thompson F (eds). *The Prokaryotes – Other Major Lineages of Bacteria and the Archaea*. Springer: New York, pp 259–281.
- Pagan H, Parent F.** (1978). *Kineosporia*, a new genus of the order *Actinomycetales*. *Int J Syst Bacteriol* 28: 401–406.
- Paliy O, Shankar V.** (2016). Application of multivariate statistical techniques in microbial ecology. *Mol Ecol* 25: 1032–1057.
- Pankratov TA, Serkebaeva YM, Kulichevskaya IS, Liesack W, Dedysn SN.** (2008). Substrate-induced growth and isolation of *Acidobacteria* from acidic *Sphagnum* peat. *ISME J* 2: 551–560.
- Park H, Lee H, Ro YT, Kim YM.** (2010). Identification and functional characterization of a gene for the methanol:N,N9-dimethyl-4-nitrosoaniline oxidoreductase from *Mycobacterium* sp. strain JC1 (DSM 3803). *Microbiology* 156: 463–471.
- Park SW, Park ST, Lee JE, Kim YM.** (2008). *Pseudonocardia carboxydivorans* sp. nov., a carbon monoxide-oxidizing actinomycete, and an emended description of the genus *Pseudonocardia*. *Int J Syst Evol Microbiol* 58: 2475–2478.
- Parpinello G, Berardi E, Strabbioli R.** (1998). A regulatory mutant of *Hansenula polymorpha* exhibiting methanol utilization metabolism and peroxisome proliferation in glucose. *J Bacteriol* 180: 2958–2967.
- Penger J, Conrad R, Blaser M.** (2012). Stable carbon isotope fractionation by methylotrophic methanogenic archaea. *Appl Environ Microbiol* 78: 7596–7602.
- Peñuelas J, Asensio D, Tholl D, Wenke K, Rosenkranz M, Piechulla B, et al.** (2014). Biogenic volatile emissions from the soil: Biogenic volatile emissions from the soil. *Plant Cell Environ* 37: 1866–1891.
- Peñuelas J, Filella I, Stefanescu C, Llusà J.** (2005). Caterpillars of *Euphydryas aurinia* (Lepidoptera: Nymphalidae) feeding on *Succisa pratensis* leaves induce large foliar emissions of methanol. *New Phytologist* 167: 851–857.
- Peyraud R, Kiefer P, Christen P, Massou S, Portais JC, Vorholt JA.** (2009). Demonstration of the ethylmalonyl-CoA pathway by using ¹³C metabolomics. *Proc Natl Acad Sci USA* 106: 4846–4851.
- Peyraud R, Kiefer P, Christen P, Portais J-C, Vorholt JA.** (2012). Co-Consumption of Methanol and Succinate by *Methylobacterium extorquens* AM1. *PLoS One* 7: e48271.
- Peyraud R, Schneider K, Kiefer P, Massou S, Vorholt JA, Portais JC.** (2011). Genome-scale reconstruction and system level investigation of the metabolic network of *Methylobacterium extorquens* AM1. *BMC Syst Biol* 5:189.
- Pirttilä AM, Laukkanen H, Pospiech H, Myllylä R, Hohtola A.** (2000). Detection of intracellular bacteria in the buds of Scotch pine (*Pinus sylvestris* L.) by *in situ* hybridization. *Appl Environ Microbiol*. 66: 3073–3077.
- Pol A, Heijmans K, Harhangi HR, Tedesco D, Jetten MS, Op den Camp HJ.** (2007). Methanotrophy below pH 1 by a new *Verrucomicrobia* species. *Nature* 450: 874–878.
- Pol A, Barends TR, Dietl A, Khadem AF, Eygensteyn J, Jetten MS, et al.** (2014). Rare earth metals are essential for methanotrophic life in volcanic mudpots. *Environ Microbiol* 16: 255–264.
- Post WM, Emanuel WR, Zinke PJ, Stangenberger AL.** (1982). Soil carbon pools and world life zones. *Nature* 298, 156–159.
- Pratscher J, Dumont MG, Conrad R.** (2011). Assimilation of acetate by the putative atmospheric methane oxidizers belonging to the USCa clade. *Environ Microbiol* 13: 2692–2701.
- Price SJ, Kelliher FM, Sherlock RR, Tate KR, Condon L.** (2004). Environmental and chemical factors regulating methane oxidation in a New Zealand forest soil. *Australian Journal of Soil Research* 42: 767–776.

- Price SJ, Sherlock RR, Kelliher FM, McSeveny TM, Tate KR, Condron LM. (2003). Pristine New Zealand forest soil is a strong methane sink. *Global Change Biology* 10: 16–26.
- Radajewski S, Ineson P, Parekh NR, Murrell JC. (2000). Stable-isotope probing as a tool in microbial ecology. *Nature* 403: 646–649.
- Radajewski S, Webster G, Reay DS, Morris SA, Ineson P, Nedwell DB, et al. (2002). Identification of active methyloph populations in an acidic forest soil by stable-isotope probing. *Microbiology* 148: 2331–2342.
- Radstrom P, Knutsson R, Wolffs P, Lovenklev M, Lofstrom C. (2004). Pre-PCR processing—strategies to generate PCR-compatible samples. *Mol Biotechnol* (26): 133–146.
- Raeymaekers L. (2000). Basic principles of quantitative PCR. *Mol Biotechnol* 15: 115–122.
- Rahman MT, Crombie A, Moussard H, Chen Y, Murrell JC. (2011). Acetate repression of methane oxidation by supplemental *Methylocella silvestris* in a peat soil microcosm. *Appl Environ Microbiol* 77: 4234–4236.
- Rasche ME, Hyman HR, Arp DJ. (1990). Biodegradation of halogenated hydrocarbon fumigants by nitrifying bacteria. *Appl Environ Microbiol* 56: 2568–2571.
- Reay DS, Nedwell DB, McNamara N, Ineson P. (2005). Effect of tree species on methane and ammonium oxidation capacity in forest soils. *Soil Biol Biochem* 37: 719–730.
- Redeker KR, Kalin RM. (2012). Methyl chloride isotopic signatures from Irish forest soils and a comparison between abiotic and biogenic methyl halide soil fluxes. *Global Change Biology* 18: 1453–1467.
- Redeker KR, Treseder KK, Allen MF. (2004). Ectomycorrhizal fungi: A new source of atmospheric methyl halides? *Global Change Biology* 10: 1009–1016.
- Reeburgh WS. (2003). Global methane biogeochemistry. In: Heinrich, D.H., and Karl, K.T. (eds). *Treatise on Geochemistry*. Oxford: Pergamon, pp 1–32.
- Reineke W, Schlömann M. (2015): Umweltmikrobiologie. 2. Auflage. Springer Verlag, München
- Renier A, De Faria SM, Jourand P, Giraud E, Dreyfus B, Rapior S, et al. (2011). Nodulation of *Crotalaria podocarpa* DC by *Methylobacterium nodulans* displays very unusual features. *J Exp Bot* 62: 3693–3697.
- Rhew RC, Miller BR, Weiss RF. (2000) Natural methyl bromide and methyl chloride emissions from coastal salt marshes. *Nature* 403: 292–295.
- Rhew RC, Østergaard L, Saltzman ES, Yanofsky MF. (2003). Genetic control of methyl halide production in *Arabidopsis*. *Curr Biol* 13: 1809–1813.
- Ricke P, Kube M, Nakagawa S, Erkel C, Reinhardt R, Liesack W. (2005). First genome data from uncultured upland soil cluster alpha methanotrophs provide further evidence for a close phylogenetic relationship to *Methylocapsa acidiphila* B2 and for high-affinity methanotrophy involving particulate methane monooxygenase. *Appl Environ Microbiol* 71: 7472–7482.
- Roselli S, Nadalig T, Vuilleumier S, Bringel F. (2013). The 380kbp CMU01 plasmid encodes chloromethane utilisation genes and redundant genes for vitamin B12- and tetra hydrofolate-dependent chloromethane metabolism in *Methylobacterium extorquens* CM4: a proteomic and bioinformatics study. *PLoS ONE* 8:e56598.
- Roslev P, Iversen N, Henriksen K. (1997). Oxidation and assimilation of atmospheric methane by soil methane oxidizers. *Appl Environ Microbiol* 63: 874–880.
- Roslev P, King GM. (1994). Survival and recovery of methanotrophic bacteria starved under oxic and anoxic conditions. *Appl Environ Microbiol* 60: 2602–2608.
- Rüffer MJ. (2014). *Die räumliche Verteilung der Chlormethan-Oxidation und die assoziierte cmuA-Genotyp-Diversität in einem Waldboden.* (in english). Matser thesis at the University of Bayreuth.
- Rusch DB, Halpern AL, Sutton G, Heidelberg KB, Williamson S, Yooseph S, et al. (2007). The Sorcerer II global ocean sampling expedition: Northwest Atlantic through Eastern tropical Pacific. *PLoS Biol* 5: e77.
- Rusch H, Rennenberg H. (1998). Black alder [*Alnus glutinosa* (L.) Gaertn.] trees mediate methane and nitrous oxide emission from the soil to the atmosphere. *Plant Soil* 201: 1–7.
- Saari A, Rinnan R, Martikainen PJ. (2004). Methane oxidation in boreal forest soils: Kinetics and sensitivity to pH and ammonium. *Soil Biol Biochem* 36: 1037–1046.
- Saiki RK, Gelfand DH, Stoffel S, Scharf SJ, Higuchi R, Horn GT, Mullis KB, Erlich HA. (1988). Primer-directed enzymatic amplification of DNA with a thermostable DNA-polymerase. *Science* 239: 487–491.
- Saitou N, Nei M. (1987). The neighbor-joining method: A new method for reconstructing phylogenetic trees. *Mol Biol Evol* 4: 406–425.
- Sakai Y, Murdanoto AP, Konishi T, Iwamatsu A, Kato N. (1997). Regulation of the formate dehydrogenase gene, FDH1, in the methylophic yeast *Candida boidinii* and growth characteristics of an FDH1-disrupted strain on methanol, methylamine, and choline. *J Bacteriol* 179: 4480–4485.

- Sakai Y, Sawai T, Tani Y.** (1987). Isolation and characterization of a catabolite repression-insensitive mutant of a methanol yeast, *Candida boidinii* A5, producing alcohol oxidase in glucose-containing medium. *Appl Environ Microbiol* 53: 1812–1818.
- Sakiyama Y, Thao NKN, Giang NM, Miyadoh S, Hop DV, Ando K.** (2009). *Kineosporia babensis* sp. nov., isolated from plant litter in Vietnam. *Int J Syst Bacteriol* 59: 550–554.
- Sambrook J, Russell D.** (2001). *Molecular cloning: A Laboratory Manual*. 3rd ed. Cold Spring Harbor, New York, USA
- Sanger F, Nicklen S, Coulson AR.** (1977). DNA sequencing with chain-terminating inhibitors. *Proc Natl Acad Sci USA* 74: 5463–5467.
- Sangwan P, Chen X, Hugenholtz P, Janssen PH.** (2004). *Chthoniobacter flavus* gen. nov., sp. nov., the first pure-culture representative of subdivision two, *Spartobacteria* classis nov., of the phylum *Verrucomicrobia*. *Appl Environ Microbiol* 70: 5875–5881.
- Sangwan P, Kovac S, Davis KER, Sait M, Janssen PH.** (2005). Detection and Cultivation of Soil *Verrucomicrobia*. *Appl Environ Microbiol*. 71: 8402–8410.
- Sayavedra-Soto LA, Hamamura N, Liu CW, Kimbrel JA, Chang JH, Arp DJ.** (2011). The membrane-associated monooxygenase in the butane-oxidizing Gram-positive bacterium *Nocardioides* sp. Strain CF8 is a novel member of the AMO/PMO family. *Environ Microbiol Rep* 3: 390–396.
- Scarratt MG, Moore RM.** (1996). Production of methyl chloride and methyl bromide in laboratory cultures of phytoplankton. *Mar Chem* 54: 263–272.
- Scarratt MG, Moore RM.** (1998) Production of methyl bromide and methyl chloride in laboratory cultures of marine phytoplankton II. *Marine Chemistry* 59: 311–320.
- Schade GW, Custer TG.** (2004). OVOC emissions from agricultural soil in northern Germany during the 2003 European heat wave. *Atmos Environ* 38: 6105–6114.
- Schaefer JK, Goodwin KD, McDonald IR, Murrell JC, Oremland RS.** (2002). *Leisingera methylohalidivorans* gen. nov., sp. nov., a marine methylotroph that grows on methyl bromide. *Int J Syst Evol Microbiol* 52: 851–859.
- Schäfer H, Miller LG, Oremland RS, Murrell JC.** (2007). Bacterial cycling of methyl halides. *Adv Appl Microbiol*. 61: 307–346.
- Schäfer H, McDonald IR, Nightingale PD, Murrell JC.** (2005). Evidence for the presence of a CmuA methyltransferase pathway in novel marine methyl halide-oxidizing bacteria. *Environ Microbiol* 7: 839–352.
- Scheller HV, Ulvskov P.** (2010). Hemicelluloses. *Annu Rev Plant Biol* 61: 263–289.
- Schink B, Zeikus JG.** (1980). Microbial Methanol Formation: A Major End Product of Pectin Metabolism. *Current Microbiol* 4: 387–389.
- Schloss PD, Westcott SL, Ryabin T, Hall JR, Hartmann M, Hollister EB, et al.** (2009). Introducing mothur: open-source, platform-independent, community-supported software for describing and comparing microbial communities. *Appl Environ Microbiol* 75: 7537–7541.
- Schmidt S, Christen P, Kiefer P, Vorholt JA.** (2010). Functional investigation of methanol dehydrogenase-like protein XoxF in *Methylobacterium extorquens* AM1. *Microbiology* 156: 2575–2586.
- Schmidt S, Christen P, Kiefer P, Vorholt JA.** (2010). Functional investigation of methanol dehydrogenase-like protein XoxF in *Methylobacterium extorquens* AM1. *Microbiology* 156: 2575–2586.
- Schneider K, Peyraud R, Kiefer P, Christen P, Delmotte N, Massou S, et al.** (2011). The ethylmalonyl-CoA pathway is used in place of the glyoxylate cycle by *Methylobacterium extorquens* AM1 during growth on acetate. *J Biol Chem* 287: 757–766.
- Schnell S, King GM.** (1995) Stability of methane oxidation capacity to variations in methane and nutrient concentrations. *FEMS Microbiol Ecol* 17: 285–294.
- Schoch CL, Seifert KA, Huhndorf S, Robert V, Spouge JL, Levesque CA, et al.** (2012). Nuclear ribosomal internal transcribed spacer (ITS) region as a universal DNA barcode marker for Fungi. *Proc Natl Acad Sci* 109: 6241–6246.
- Schwartz E, Fritsch J, Friedrich B.** (2013). H₂-metabolizing prokaryotes. In: Rosenberg E, DeLong E, Lory S, Stackebrandt E, Thompson F (eds). *The Prokaryotes: Prokaryotic physiology and biochemistry*. Vol 3, 4th ed. Springer: New York pp 120-199.
- Schwarz WH.** (2001). The cellulosome and cellulose degradation by anaerobic bacteria. *Appl Microbiol Biotechnol* 56: 634–649.
- Seco R, Peñuelas J, Filella I, Llusà J, Molowny-Horas R, Schallhart S, et al.** (2011). Contrasting winter and summer VOC mixing ratios at a forest site in the Western Mediterranean Basin: the effect of local biogenic emissions. *Atmos Chem Phys* 11: 13161–13179.

- Seco R, Peñuelas J, Filella I.** (2007). Short-chain oxygenated VOCs: Emission and uptake by plants and atmospheric sources, sinks, and concentrations. *Atmospheric Environment* 41: 2477–2499.
- Segura A, Bernal P, Pini C, Krell T, Daniels C, Ramos J.** (2010). Membrane composition and modifications in response to aromatic hydrocarbons in gram negative bacteria. In: Timmis KN (ed). *Handbook of hydrocarbon and lipid microbiology*. Springer Berlin Heidelberg, pp 1595–1603.
- Semrau JD, DiSpirito AA, Vuilleumier S.** (2011). Facultativemethanotrophy: false leads, true results, and suggestions for future research. *FEMS Microbiol Lett* 323: 1–12.
- Semrau JD, DiSpirito AA, Yoon S.** (2010). Methanotrophs and copper. *FEMS Microbiol Rev* 34: 496–531.
- Sharp CE, Smirnova AV, Graham JM, Stott MB, Khadka R, Moore TR, et al.** (2014). Distribution and diversity of *Verrucomicrobia* methanotrophs in geothermal and acidic environments. *Environ Microbiol* 16: 1867–1878.
- Sharp CE, Stott MB, Dunfield PF.** (2012). Detection of autotrophic verrucomicrobial methanotrophs in a geothermal environment using stable isotope probing. *Front Microbiol* 3: 303.
- Shishkina VN, Trotsenko YA.** (1982). Multiple enzymic lesions in obligate methanotrophic bacteria. *FEMS Microbiol Lett* 13: 237–242.
- Shrestha PM, Kammann C, Lenhart K, Dam B, Liesack W.** (2012). Linking activity, composition and seasonal dynamics of atmospheric methane oxidizers in a meadow soil. *ISME J* 6: 1115–1126.
- Singh H, Chen Y, Tabazadeh A, Fukui Y, Bey I, Yantosca R, et al.** (2000). Distribution and fate of selected oxygenated organic species in the troposphere and lower stratosphere over the Atlantic. *J Geophys Res* 105: 3795–3805.
- Singleton DR, Furlong MA, Rathbun SL, Whitman WB.** (2001). Quantitative comparisons of 16S rRNA gene sequence libraries from environmental samples. *Appl Environ Microbiol* 67: 4374–4376.
- Skovran E, Palmer AD, Rountree AM, Good NM, Lidstrom ME.** (2011). *XoxF* is required for expression of methanol dehydrogenase in *Methylobacterium extorquens* AM1. *J Bacteriol* 193: 6032–6038.
- Skovran E, Crowther GJ, Guo X, Yang S, Lidstrom ME.** (2010). A systems biology approach uncovers cellular strategies used by *Methylobacterium extorquens* AM1 during the switch from multi- to single-carbon growth. *PLoS One* 5: e14091.
- Smejkalová H, Erb TJ, Fuchs G.** (2010). Methanol assimilation in *Methylobacterium extorquens* AM1: demonstration of all enzymes and their regulation. *PLoS One* 5: e13001.
- Smith KA, Dobbie KE, Ball BC, Bakken LR, Sitaula BK, Hansen S, et al.** (2000). Oxidation of atmospheric methane in Northern European soils, comparison with other ecosystems, and uncertainties in the global terrestrial sink. *Glob Change Biol* 6: 791–803.
- Smith TJ, Dalton H.** (2004). Biocatalysis by methane monooxygenases and its implications for the petroleum industry. In: Vazquez- Duhalt R., Quintero-Ramirez R (eds). *Petroleum biotechnology, developments and perspectives*. Elsevier, Amsterdam, The Netherlands, p. 177–192.
- Söhngen NL.** (1906). Ueber Bakterien welche Methan als Kohlenstoffnahrung und Energiequelle gebrauchen (On bacteria which use methane as a carbon and energy source). *Z Bakteriol Parasitenk (Infektionster)* 15: 513–517.
- Sorokin DY, Trotsenko YA, Doronina NV, Tourova TP, Galinski EA, Kolganova TV, et al.** (2007). *Methylohalomonas lacus* gen. nov., sp. nov. and *Methylonatrum kenyense* gen. nov., sp. nov., methylotrophic gammaproteobacteria from hypersaline lakes. *Int J Syst Evol Microbiol* 57: 2762–2769.
- Sowell SM, Abraham PE, Shah M, Verberkmoes NC, Smith DP, Barofsky DF, et al.** (2011). Environmental proteomics of microbial plankton in a highly productive coastal upwelling system. *ISME J* 5: 856–865.
- Stacheter A, Noll M, Lee CK, Selzer M, Glowik B, Ebertsch L, et al.** (2013). Methanol oxidation by temperate soils and environmental determinants of associated methylotrophs. *ISME J* (7):1051-64
- Stackebrandt E.** (2013). The Family *Acidimicrobiaceae*. In: Rosenberg E, DeLong EF, Lory S, Stackebrandt E, Thompson F (eds). *The Prokaryotes – Actinobacteria*. Springer: New York, pp 5–12.
- Staley JT, DeBont JAM, DeJonge K.** (1976). *Prostheco bacter fusiformis* nov. gen. et sp., the fusiform caulobacter. *Antonie van Leeuwenhoek* 42: 333–342.
- Starai VJ, Escalante-Semerena JC.** (2004). Acetyl-coenzyme A synthetase (AMP forming). *Cell Mol Life Sci* 61: 2020–2030.
- Stasyk OV, Ksheminskaya GP, Kulachkovskii AR, Sibirnyi AA.** (1997). Mutants of the methylotrophic yeast *Hansenula polymorpha* with impaired catabolite repression. *Microbiology (Moscow)* 66: 631–636.
- Stasyk OV, Stasyk OG, Komduur J, Veenhuis M, Cregg JM, Sibirny AA.** (2004). A hexose transporter homologue controls glucose repression in the methylotrophic yeast *Hansenula polymorpha*. *J Biol Chem* 279: 8116–8125.
- Steinen V.** (2014). *Effekt von Mehrkohlenstoffsubstraten auf die Abundanzen Methanolnutzender methylotropher Bakterien in einem Waldboden.* (in german). Bachelor thesis at the University of Jena (FSU).

- Stirling DI, Colby J, Dalton H.** (1979). A comparison of the substrate and electron-donor specificities of the methane mono-oxygenases from three strains of methane-oxidizing bacteria. *Biochem J* 177: 361–364.
- Stoecker K, Bendinger B, Schöning B, Nielsen PH, Nielsen JL, Baranyi C, et al.** (2006). Cohn's *Crenothrix* is a filamentous methane oxidizer with an unusual methane monooxygenase. *Proc Natl Acad Sci* 103: 2363–2367.
- Stolaroff JK, Bhattacharyya S, Smith CA, Bourcier WL, Cameron-Smith PJ, Aines RD.** (2012). Review of methane mitigation technologies with application to rapid release of methane from the Arctic. *Environ Sci Technol* 46: 6455–6469.
- Stolyar S, Costello AM, Peeples TL, Lidstrom ME.** (1999). Role of multiple gene copies in particulate methane monooxygenase activity in the methane-oxidizing bacterium *Methylococcus capsulatus* Bath. *Microbiol* 145: 1235–1244.
- Striegl RG.** (1993). Diffusional limits to the consumption of atmospheric methane by soils. *Chemosphere* 26: 715–720.
- Studer A, McAnulla C, Buchele R, Leisinger T, Vuilleumier S.** (2002). Chloromethane-induced genes define a third C-1 utilisation pathway in *Methylobacterium chloromethanicum* CM4. *J Bacteriol* 184: 3476–3484.
- Studer A, Stupperich E, Vuilleumier S, Leisinger T.** (2001). Chloromethane: tetrahydrofolate methyl transfer by two proteins from *Methylobacterium chloromethanicum* strain CM4. *Eur. J. Biochem.* 268:2931–2938.
- Studer A, Vuilleumier S, Leisinger T.** (1999). Properties of the methylcobalamin: H₄folate methyltransferase involved in chloromethane utilization by *Methylobacterium* sp. strain CM4. *Eur J Biochem* 264: 242–249.
- Studer A.** (2001). *Aerobic Microbial Degradation of Chloromethane*. Doctoral thesis at the Swiss Federal Institute of Technology, Zürich.
- Sudtachat N, Ito N, Itakura M, Masuda S, Eda S, Mitsui H, et al.** (2009). Aerobic vanillate degradation and C1 compound metabolism in *Bradyrhizobium japonicum*. *Appl Environ Microbiol* 75: 5012–5017.
- Suneetha V, Khan ZA.** (2011). *Actinomycetes: Sources for Soil Enzymes*. In: Shukla G, Varma A (eds). *Soil Enzymology* 22. Springer: Berlin, Heidelberg, pp 259–269.
- Suzuki T, Nakamura T, Fuse H.** (2012). Isolation of two novel marine ethylene-assimilating bacteria, *Haliea* species ETY-MandETY-NAG, containing particulate methane monooxygenase-like genes. *Microbes Environ* 27: 54–60.
- Tait VK, Moore RM.** (1995). Methyl chloride (CH₃Cl) production in phytoplankton cultures. *Limnol Oceanogr* 40: 189–195.
- Takishita K, Tsuchiya M, Reimer JD, Maruyama T.** (2006). Molecular evidence demonstrating the basidiomycetous fungus *Cryptococcus curvatus* is the dominant microbial eukaryote in sediment at the Kuroshima Knoll methane seep. *Extremophiles* 10: 165–169
- Tamas I, Smirnova AV, He Z, Dunfield PF.** (2014). The (d)evolution of methanotrophy in the *Beijerinckiaceae* – a comparative genomics analysis. *ISME J* 8: 369–382.
- Tamura K, Peterson D, Peterson N, Stecher G, Nei M, Kumar S.** (2011). MEGA5: Molecular Evolutionary Genetics Analysis using Maximum Likelihood, Evolutionary Distance, and Maximum Parsimony Methods. *Mol Biol Evol* 28: 2731–2739.
- Tamura K, Stecher G, Peterson D, Filipowski A, Kumar S.** (2013). MEGA6: Molecular evolutionary genetics analysis version 6.0. *Mol Biol Evol* 30: 2725–2729.
- Tamura T, Suzuki K-I.** (2013). The suborder *Kineosporiineae*. In: Rosenberg E, DeLong EF, Lory S, Stackebrandt E, Thompson F (eds). *The Prokaryotes – Actinobacteria*. Springer: New York, pp 443–453.
- Tani Y.** (1984). Microbiology and biochemistry of methylotrophic Yeasts. In: C. T. Hou (ed). *Methylotrophs: Microbiology, Biochemistry, and Genetics*. CRC Press, Boca Raton, Fla, USA, pp 55–86.
- Taubert M, Grob C, Howat AM, Burns OJ, Dixon JL, Chen Y, et al.** (2015). *XoxF* encoding an alternative methanol dehydrogenase is widespread in coastal marine environments. *Environ Microbiol* 17: 3937–3948.
- Tauch A, Sandbote J.** (2013). The Family *Corynebacteriaceae*. In: Rosenberg E, DeLong EF, Lory S, Stackebrandt E, Thompson F (eds). *The Prokaryotes – Actinobacteria*. Springer: New York, pp 239–277.
- Tavormina PL, Orphan VJ, Kalyuzhnaya MG, Jetten MS, Klotz MG.** (2011). A novel family of functional operons encoding methane/ammonia monooxygenase-related proteins in gammaproteobacterial methanotrophs. *Environ Microbiol Rep* 3: 91–100.
- Tavormina PL, Ussler W III, Orphan VJ.** (2008). Planktonic and sediment-associated aerobic methanotrophs in two seep systems along the North American margin. *Appl Environ Microbiol* 74: 3985–3995.
- Terazawa K, Ishizuka S, Sakatac T, Yamada K, Takahashi M.** (2007). Methane emissions from stems of *Fraxinus mandshurica* var. *japonica* trees in a floodplain forest. *Soil Biol Biochem* 39: 2689–2692.
- Theisen AR, Ali MH, Radajewski S, Dumont MG, Dunfield PF, McDonald IR, et al.** (2005). Regulation of methane oxidation in the facultative methanotroph *Methylocella silvestris* BL2. *Mol Microbiol* 58: 682–692.
- Theisen AR, Murrell JC.** (2005). Facultative methanotrophs revisited. *J Bacteriol* 187: 4303–4305.
- Thies JE.** (2007). Soil microbial community analysis using terminal restriction fragment length polymorphisms. *Soil Sci Soc Amer J* 71: 579–591.

- Thrash JC, Coates JD.** (2010). Phylum XVII. *Acidobacteria* phyl. nov. In: Krieg NR, Staley JT, Brown DR, Hedlund BP, Paster BJ, Ward NL, Ludwig W, Whitman WB (eds). *Bergey's Manual of Systematic Bacteriology*. 2nd edition, Vol 4: The *Bacteroidetes*, *Spirochaetes*, *Tenericutes (Mollicutes)*, *Acidobacteria*, *Fibrobacteres*, *Fusobacteria*, *Dictyoglomi*, *Gemmatimonadetes*, *Lentisphaerae*, *Verrucomicrobia*, *Chlamydiae*, and *Planctomycetes*. New York: Springer, pp 725–735.
- Tie X, Guenther A, Holland E.** (2003). Biogenic methanol and its impacts on tropospheric oxidants. *Geophys. Res Lett* 30. doi:10.1029/2003GL017167.
- Torsvik V, Øvreås L, Thingstad TF.** (2002). Prokaryotic diversity—magnitude, dynamics, and controlling factors. *Science* 296: 1064–1066.
- Trauneecker J, Preuß A, Diekert G.** (1991). Isolation and characterization of a methyl chloride utilizing, strictly anaerobic bacterium. *Arch Microbiol* 156: 416–421.
- Trotsenko YA, Murrell JC.** (2008). Metabolic aspects of aerobic obligate methanotrophy. *Adv Appl Microbiol* 63: 183–229.
- Tsai YL, Olson BH.** (1992). Rapid method for separation of bacterial DNA from humic substances in sediments for polymerase chain reaction. *Appl Environ Microbiol* 58: 2292–2295.
- Tsutsuki K, Kuwatsuka S.** (1979). Chemical studies on soil humic acids. VI. pH dependent nature of the ultraviolet and visible absorption spectra of humic acids. *Soil Sci Plant Nutr.* 25: 373–384.
- Turner EM, Wright M, Ward T, Osborne DJ, Self R.** (1975). Production of ethylene and other volatiles and changes in cellulase and laccase activities during the life cycle of the cultivated mushroom, *Agaricus bisporus*. *J gen Microbiol* 91: 167–176.
- Uchiyama H, Nakajima T, Yagi O, Tabuchi T.** (1989). Aerobic Degradation of Trichloroethylene by a New Type II Methane-Utilizing Bacterium, Strain M. *Agric Biol Chem* 53: 2903–2907.
- Urakami T, Tamaoka J, Suzuki K-I, Komagata K.** (1989). *Acidomonas* gen. nov. Incorporating *Acetobacter methanolicus* as *Acidomonas methanolica* comb. nov. *Int J Syst Evol Microbiol* 39: 50–55.
- van den Heuvel RN, van der Biezen E, Jetten MS, Heffing MM, Kartal B.** (2010) Denitrification at pH 4 by a soil-derived *Rhodanobacter*-dominated community. *Environ Microbiol* 12: 3264–3271.
- van Ophem PW, Vanbeeumen J, Duine JA.** (1993). Nicotinoprotein [Nad(P)-Containing] Alcohol Aldehyde Oxidoreductases - Purification and Characterization of a Novel Type from *Amycolatopsis methanolica*. *Eur J Biochem* 212: 819–826.
- van Ophem P, Euverink GJ, Dijkhuizen L, Duine JA.** (1991). A novel dye-linked alcohol dehydrogenase activity present in some Gram-positive bacteria. *FEMS Microbiol Lett* 80: 57–64.
- van Teeseling MCF, Pol A, Harhangi HR, van der Zwart S, Jetten MSM, Op den Camp HJM, van Niftrik L.** (2014). Expanding the verrucomicrobial methanotrophic world: description of three novel species of *Methylococcoides* gen. nov. *Appl Environ Microbiol* 80: 6782–6791.
- Vannelli T, Studer A, Kertesz M, Leisinger T.** (1998). Chloromethane metabolism by *Methylobacterium* sp. strain CM4. *Appl Environ Microbiol* 64:1933–1936.
- Vannelli, T., Messmer, M., Studer, A., Vuilleumier, S. and Leisinger, T.** (1999) A corrinoid-dependent catabolic pathway for growth of a *Methylobacterium* strain with chloromethane. *Proc Natl Acad Sci* 96: 4615–4620.
- Vecherskaya M, Dijkema C, Saad HR, Stams AJ.** (2009). Microaerobic and anaerobic metabolism of a *Methylocystis parvus* strain isolated from a denitrifying bioreactor. *Environ Microbiol Rep* 1: 442–449.
- Vecherskaya M, Dijkema C, Stams AJ.** (2001). Intracellular PHB conversion in a Type II methanotroph studied by ¹³C NMR. *J Ind Microbiol Biotechnol* 26: 15–21.
- Veenhuis M, Dijken JPV, Harder W.** (1983). The significance of peroxisomes in the metabolism of one-carbon compounds in yeasts. *Adv Microb Physiol* 24: 1–82.
- Venil CK, Nordin N, Zakaria ZA, Ahmad WA.** (2014). *Chryseobacterium artocarpis* sp. nov., isolated from the rhizosphere soil of *Artocarpus integer*. *Int J Syst Evol Microbiol* 64: 3153–3159.
- Vieira J, Messing J.** (1982). The pUC plasmids, an M13mp7-derived system for insertion mutagenesis and sequencing with synthetic universal primers. *Gene* 19: 259–268.
- Vodyanitskii YN, Savichev AT, Trofimov SY, Shishkonakova EA.** (2012). Accumulation of heavy metals in oil-contaminated peat soils. *Eurasian Soil Sci* 45: 977–982.
- Von Dahl CC, Hävecker M, Schlögl R, Baldwin IT.** (2006). Caterpillar-elicited methanol emission: a new signal in plant–herbivore interactions? *Plant J* 46: 948–960.
- Vonck J, Arfman N, de Vries GE, Van Beeumen J, van Bruggen EFJ, Dijkhuizen L.** (1991). Electron microscopic analysis and biochemical characterization of a novel methanol dehydrogenase from the thermotolerant *Bacillus* sp. Cl. *J Biol Chem* 266: 3949–3954.

- Voragen AGJ, Coenen G-J, Verhoef RP, Schols HA.** (2009). Pectin, a versatile polysaccharide present in plant cell walls. *Struct Chem* 20: 263–275.
- Vorholt JA.** (2012). Microbial life in the phyllosphere. *Nat Rev Microbiol* 10: 828–840.
- Voříšková J, Baldrian P.** (2013). Fungal community on decomposing leaf litter undergoes rapid successional changes. *ISME J* 7: 477–486.
- Vorob'ev AV, de Boer W, Folman LB, Bodelier PLE, Doronina NV, Suzina NE, et al.** (2009). *Methylovirgula ligni* gen. nov., sp. nov., an obligately acidophilic, facultatively methylotrophic bacterium with a highly divergent *mxoF* gene. *J Syst Evol Microbiol* 59: 2538–2545.
- Vorobev A, Jagadevan S, Jain S, Anantharaman K, Dick GJ, Vuilleumier S, et al.** (2014). How Do Facultative Methanotrophs Utilize Multi-Carbon Compounds for Growth? Genomic and Transcriptomic Analysis of *Methylocystis* Strain SB2 Grown on Methane and on Ethanol. *Appl Environ Microbiol* doi:10.1128/AEM.00218-14
- Vorobev AV, Baani M, Doronina NV, Brady AL, Liesack W, Dunfield PF, et al.** (2011). *Methyloferula stellata* gen. nov., sp. nov., an acidophilic, obligately methanotrophic bacterium that possesses only a soluble methane monooxygenase. *J Syst Evol Microbiol* 61: 2456–2463.
- Wackett LP, Logan MSP, Blocki FA, Bao-li C.** (1992). A mechanistic perspective on bacterial metabolism of chlorinated methanes. *Biodegradation* 3: 19–36.
- Waitling R, Harper DB.** (1998) Chloromethane production by woodrotting fungi and an estimate of global flux to the atmosphere. *Mycol Res* 107:769–787.
- Wakao N, Nagasawa N, Matsuura T, Matsukura H, Matsumoto T, Hiraishi A, et al.** (1994). *Acidiphilium multivorum* sp. nov., an acidophilic chemoorganotrophic bacterium from pyritic acid mine drainage. *J Gen Appl Microbiol* 40: 143–159.
- Wang Q, Garrity GM, Tiedje JM, Cole JR.** (2007). Naive bayesian classifier for rapid assignment of rRNA sequences into the new bacterial taxonomy. *Appl Environ Microbiol* 73: 5261–5267.
- Wang X, Sharp CE, Jones GM, Grasby SE, Brady AL, Dunfield PF.** (2015). Stable-isotope probing identifies uncultured *Planctomycetes* as primary degraders of a complex heteropolysaccharide in soil. *Appl Environ Microbiol* 81: 4607–4615.
- Ward N, Larsen O, Sakwa J, Bruseth L, Khouri H, Durkin AS, et al.** (2004). Genomic insights into methanotrophy: the complete genome sequence of *Methylococcus capsulatus* (Bath). *PLoS Biol* 2: e303.
- Warneke C, Karl T, Judmaier H, Hansel A, Jordan A, Lindinger W.** (1999). Acetone, methanol, and other partially oxidized volatile organic emissions from dead plant matter by abiological processes: Significance for atmospheric HO_x chemistry. *Global Biogeochem Cy* 13: 9–17.
- Warneke C, Luxembourg SL, de Gouw JA, Rinne HJI, Guenther AB, Fall R.** (2002). Disjunct eddy covariance measurements of oxygenated volatile organic compounds fluxes from an alfalfa field before and after cutting. *J Geophys Res Atmospheres* 107: ACH 6-1 – ACH 6-10.
- Wartiainen I, Hestnes AG, McDonald IR, Svenning MM.** (2006). *Methylocystis rosea* sp. nov., a novel methanotrophic bacterium from Arctic wetland soil, Svalbard, Norway (78° N). *Int J Syst Evol Microbiol* 56: 541–547.
- Watson RJ, Blackwell B.** (2000). Purification and characterization of a common soil component which inhibits the polymerase chain reaction. *Can J Microbiol* (43): 633–642.
- Webb HK, Ng HJ, Ivanova EP.** (2013). The Family *Methylocystaceae*. In: Rosenberg E, DeLong EF, Lory S, Stackebrandt E, Thompson F (eds). *The Prokaryotes – Alphaproteobacteria and Betaproteobacteria*. Springer: New York, pp 341–347.
- Wegner GH.** (1990). Emerging applications of the methylotrophic yeasts. *FEMS Microbiol Rev* 7: 279–283.
- Wellner S, Lodders N, Kämpfer P.** (2011) Diversity and biogeography of selected phyllosphere bacteria with special emphasis on *Methylobacterium* spp. *Syst Appl Microbiol* 34: 621–630.
- West AE, Schmidt SK.** (1999). Acetate stimulates atmospheric CH₄ oxidation by an alpine tundra soil. *Soil Biol Biochem* 31: 1649–1655.
- Whalen SC, Reeburgh WS.** (1992) Interannual variations in tundra methane emission: a 4-year time series at fixed sites. *Global Biogeochem Cycles* 6: 139–159.
- White TJ, Bruns TD, Lee SB, Taylor JW.** (1990). Amplification and direct sequencing of fungal ribosomal RNA genes for phylogenetics. In: Innis MA, Gelfand DH, Sninsky JJ, White TJ (eds). *PCR Protocols – a Guide to Methods and Applications*. San Diego, CA: Academic Press. 315–322.
- Whittenbury R, Davies SL, Davey JF.** (1970b). Exospores and Cysts Formed by Methane-utilizing Bacteria. *Gen Microbiol* 61: 219–226.
- Whittenbury R, Phillips KC, Wilkinson JF.** (1970a). Enrichment, Isolation and Some Properties of Methane-utilizing Bacteria. *Gen Microbiol* 61: 205–218.
- Wieczorek AS, Drake HL, Kolb S.** (2011). Organic acids and ethanol inhibit the oxidation of methane by mire methanotrophs. *FEMS Microbiol Ecol* 77: 28–39.

- Wilkinson TG, Topiwara HH, Hamer G. (1974). Interactions in a mixed bacterial population growing on methane in continuous culture. *Biotechnol Bioeng* 16: 41–59.
- Willats WGT, McCartney, Mackie W, Knox JP. (2001). Pectin: cell biology and prospects for functional analysis. *Plant Mol Biol* 47: 9–27.
- Wilson IG. (1997). Inhibition and facilitation of nucleic acid amplification. *Appl Environ Microbiol* 63: 3741–3751.
- Wintzingerode FV, Goebel UB, Stackebrandt E. (1997). Determination of microbial diversity in environmental samples: pitfalls of PCR-based rRNA analysis. *FEMS Microbiol Rev* 21: 213–229.
- Witthoff S, Mühlroth A, Marienhagen J, Bott M. (2013). C₁ metabolism in *Corynebacterium glutamicum*: an endogenous pathway for oxidation of methanol to carbon dioxide. *Appl Environ Microbiol* 79: 6974–6983.
- Wohlfahrt G, Amelynck C, Ammann C, Arneth A, Bamberger I, Goldstein AH, et al. (2015). An ecosystem-scale perspective of the net land methanol flux: synthesis of micrometeorological flux measurements. *Atmos Chem Phys* 15: 7413–7427.
- Wohlfarth G, Diekert G. (1997) Anaerobic dehalogenases. *Curr Op Biotechnol* 8: 290–295.
- Wolf HJ, RS Hanson. (1980). Isolation and characterization of methane-oxidizing yeasts. *J Gen Microbiol* 114: 187–194.
- Wood AP, Aurikko JP, Kelly DP. (2004). A challenge for 21st century molecular biology and biochemistry: what are the causes of obligate autotrophy and methanotrophy? *FEMS Microbiol Rev* 28: 335–352.
- Woolf D, Lehmann J, Fisher EM, Angenent LT. (2014) Biofuels from pyrolysis in perspective: trade-offs between energy yields and soil-carbon additions. *Environ Sci Technol* 48: 6492–6499.
- Wubet T, Christ S, Schöning I, Boch S, Gawlich M, Schnabel B, et al. (2012). Differences in soil fungal communities between European Beech (*Fagus sylvatica* L.) dominated forests are related to soil and understory vegetation. *PLoS ONE* 7(10): e47500.
- Wuosmaa AM, Hager LP. (1990). Methyl chloride transferase: a carbocation route for biosynthesis of halometabolites. *Science* 249: 160–162.
- Yarza P, Ludwig W, Jean Euzéby J, Amann R, Schleifer K-H, Glöckner FO, et al. (2010). Update of the all-species living tree project based on 16S and 23S rRNA sequence analyses. *Syst Appl Microbiol* 33: 291–299.
- Yasueda H, Kawahara Y, Sugimoto S. (1999). *Bacillus subtilis* yckG and yckF encode two key enzymes of the ribulose monophosphate pathway used by methylotrophs, and yckH is required for their expression. *J Bacteriol* 181:7154–7160.
- Yavitt JB, Fahey TJ, Simmons JA. (1995). Methane and carbon dioxide dynamics in a northern hardwood ecosystem. *Soil Sci Soc Am J* 59: 796–804.
- Yoon MH, Ten LN, Im WT, Lee ST. (2007). *Methylibium fulvum* sp. nov., a member of the *Betaproteobacteria* isolated from ginseng field soil, and emended description of the genus *Methylibium*. *Int J Syst Evol Microbiol* 57: 2062–2066.
- Youssef NH, Elshahed MS. (2013). The phylum *Planctomycetes*. In: Rosenberg E, DeLong EF, Lory S, Stackebrandt E, Thompson F (eds). *The Prokaryotes – other major lineages of Bacteria and the Archaea*. Springer: New York, pp 759–810.
- Ytreberg E, Karlsson J, Eklund B. (2010). Comparison of toxicity and release rates of Cu and Zn from anti-fouling paints leached in natural and artificial brackish seawater. *Sci Total Environ*. 408: 2459–2466.
- Yurimoto H, Oku M, Sakai Y. (2011). Yeast methylotrophy: metabolism, gene regulation and peroxisome homeostasis. *Int J Microbiol* 2011:101298.
- Zabetakis I. (1996). Enhancement of flavour biosynthesis from strawberry (*Fragaria x ananassa*) callus cultures by *Methylobacterium* species. *Plant Cell Tiss Org* 50: 179–183.
- Zahn JA, DiSpirito AA. (1996) Membrane-associated methane monooxygenase from *Methylococcus capsulatus* (Bath). *J Bacteriol* 178: 1018–1029.
- Zapras A, Liu Y-J, Liu S-J, Drake HL, Horn MA. (2010). Abundance of novel and diverse tfdA-like genes, encoding putative phenoxyalkanoic acid herbicide-degrading dioxygenases, in soil. *Appl Environ Microbiol* 76: 119–128.
- Zeikus, JG, Ward JC. (1974) Methane formation in living trees: a microbial origin. *Science* 184: 1181–1183.
- Zhi XY, Li WJ, Stackebrandt E. (2009). An update of the structure and 16S rRNA gene sequence-based definition of higher ranks of the class *Actinobacteria*, with the proposal of two new suborders and four new families and emended descriptions of the existing higher taxa. *Int J Syst Evol Microbiol* 59: 589–608.
- Zhou J, He Z, Yang Y, Deng Y, Tringe SG, Alvarez-Cohen L. (2015). High-throughput metagenomic technologies for complex microbial community analysis: open and closed formats. *M Bio* 6.
- Zinder SH. (1993). Physiological ecology of methanogens. In: Ferry JG (ed). *Methanogenesis: ecology, physiology, biochemistry and genetics*. Chapman and Hall, New York: pp 128–206.

6. ACKNOWLEDGMENTS

I think this is highly informal, but since this work comprises already numerous amounts of pages and since I will NOT forget someone to mention, I decided not to list all the names of all the magnificent people contributing to this work in a scientific, amicable, spiritual, and further supporting manner. I rather feel confident that all these people already know HOW well they supported me in any respect, in every situation, and at any time.

So – this work is dedicated to all my magnificent *OMs*, friends & colleagues.

I guess YOU know, that I mean YOU.

In order to be also a bit more formal.

I would like to thank my supervisor *Dr. Steffen Kolb* providing this research topic to me, giving me the opportunity to immerse myself into methylotrophy and getting scientific experience, providing financial support, and having patience with me.

I also would like to thank *Prof. Harold L Drake* giving me the opportunity to do and finish my doctorate at the department of ecological microbiology.

I also have to thank the *Deutsche Forschungsgemeinschaft DFG* and the Stabsabteilung Chancengleichheit Frauenförderung at the University of Bayreuth for financial support since 'no mon, no fun'.

OM.

7. PUBLICATIONS

Selected results of this current work are envisaged to be published (*submitted / in preparation*) or were presented at national and international conferences.

Publications

Morawe M, Hoeke H, Wissenbach DK, Lentendu G, Wubet T, Kröber E, and Kolb S. (2017). Acidotolerant *Bacteria* and *Fungi* as a Sink of Methanol-Derived Carbon in a Deciduous Forest Soil. *Front Microbiol.*8: 1361. doi: 10.3389/fmicb.2017.01361

Chaignaud P, Morawe M, Besaury L, Kröber E, Rüffer M, Vuilleumier S, Bringel F, Kolb S. (2017). An unexpected large diversity of bacterial ecotypes is involved in chloromethane degradation of a European beech soil. *in preparation*

Presentations

Morawe M, Kolb S. (2014). Multi-Carbon Compounds As Substrates For Methanol Utilizing Methylophs in a Soil Community. Poster presentation at the 'Gordon Research Conference - Molecular Basis of Microbial One-Carbon Metabolism'.

Morawe M, Steinen V, Wubet T, Kolb S. (2014). Multi-Carbon Compounds As Substrates For Methanol Utilizing Methylophs in a Soil Community. Poster presentation at the 'Gemeinsame Jahrestagung der Deutschen Gesellschaft für Hygiene und Mikrobiologie (DGHM) e. V. zusammen mit der Vereinigung für Allgemeine und Angewandte Mikrobiologie (VAAM) e. V.', BIOSpectrum Tagungsband, Abstract DEP59.

Kolb S, Morawe M, Stacheter A. (2014). Unveiling the Microbial Sink of Methanol in Terrestrial Ecosystems. Lecture presentation at the 'Gemeinsame Jahrestagung der Deutschen Gesellschaft für Hygiene und Mikrobiologie (DGHM) e. V. zusammen mit der Vereinigung für Allgemeine und Angewandte Mikrobiologie (VAAM) e. V.', BIOSpectrum Tagungsband, Abstract DEV09.

Morawe M, Wubet T, Kolb S. (2015). Multicarbon Substrate Spectrum and pH - Drivers of Fungal and Bacterial Methyloph Diversity in a Forest Soil. Poster presentation at the 'Jahrestagung der Vereinigung für Allgemeine und Angewandte Mikrobiologie (VAAM) e. V.', BIOSpectrum Tagungsband, Abstract EMP43.

8. APPENDICES

Table A 1 Sequences of the barcodes for 16S rRNA and *mxoF* sequence classification of PYRO-sequencing derived sequences.

	treatm. ^a	lib ^b	Pool ^c	barcode (5'-3')		treatm. ^a	lib ^b	Pool ^c	barcode (5'-3')			
				Initial	modified ^d				Initial	modified ^d		
substrate SIP experiment	t0₁	H	1	TACTAG	ACTAG ^e	¹²C	H	2	TCTCAC	TCTCA ^f		
		M	1	TACGTG	ACGTG ^e		M	2	TCTAGC	TCTAG ^f		
		L	1	ATAGTG	TAGTG ^e		Xylose +	L	2	TATCGC	TATCG ^f	
	t0₂	H	2	TACTAG	TACTA ^f		¹³C	H	2	AGTCAC	AGTCA ^f	
		M	2	TACGTG	TACGT ^f			M	2	AGCTAC	AGCTA ^f	
		L	2	ATAGTG	ATAGT ^f			Xylose +	L	2	AGCGTC	AGCGT ^f
	t0₃	H	2	TATCAG	TATCA ^f	¹²C		H	2	TGTGAC	TGTGA ^f	
		M	2	TATATG	TATAT ^f			Vanillic	M	2	TGTCTC	TGTCT ^f
		L	2	TAGCTG	TAGCT ^f			Acid +	L	2	TGCATC	TGCAT ^f
	t0₄	H	2	AGTATG	AGTAT ^f		¹³C	H	2	ATCTGC	ATCTG ^f	
		M	2	AGCACG	ACACG ^h			Vanillic	M	2	ATCATC	ATCAT ^f
		L	2	ACACTG	ACACT ^f			Acid +	L	2	ATACTC	ATACT ^f
	¹²C	H	1	TATCAG	ATCAG ^e	¹²C		H	1	TCTCAC	CTCAC ^e	
		Methanol	M	1	TATATG			ATATG ^e	M	1	TCTAGC	CTAGC ^e
		L	1	TAGCTG	AGCTG ^e			CO₂ +	L	1	TATCGC	ATCGC ^e
	¹³C	H	1	AGTATG	GTATG ^e		¹³C	H	1	AGTCAC	GTCAC ^e	
		Methanol	M	1	AGCACG			GCACG ^e	M	1	AGCTAC	GCTAC ^e
		L	1	ACACTG	CACTG ^e			L	1	AGCGTC	GCGTC ^e	
	¹²C	H	2	TAGTGC	TGTGC ^h	¹²C		H	1	TGTGAC	GTGAC ^e	
		Acetate +	M	2	TAGCAC			TAGCA ^f	M	1	TGTCTC	GTCTC ^e
L		2	TACAGC	TACAG ^f	L			1	TGCATC	GCATC ^e		
¹³C	H	2	ACTCGC	ACTCG ^f	¹³C		H	1	ATCTGC	TCTGC ^e		
	Acetate +	M	2	ACTATC			ACTAT ^f	M	1	ATCATC	TCATC ^e	
	L	2	ACGAGC	ACGAG ^f			L	1	ATACTC	TACTC ^e		
¹²C	H	1	TAGTGC	AGTGC ^e		t0	H	3	ACTATC	ACATC ^g		
	Glucose +	M	1	TAGCAC			AGCAC ^h	M	3	TAGTGC	TATGC ^g	
	L	1	TACAGC	ACAGC ^e			L	3	TAGCAC	TACAC ^g		
¹³C	H	1	ACTCGC	CTCGC ^e	¹²C		H	3	ATATAC	ATTAC ^g		
	Glucose +	M	1	ACTATC			CTATC ^e	M	3	ATCATC	ATATC ^g	
	L	1	ACGAGC	CGAGC ^e			pH 4	L	3	ATACTC	ATCTC ^g	
¹²C	H	2	TCTCAC	TCTCA ^f		¹³C	H	3	AGCTAC	AGTAC ^g		
	Xylose +	M	2	TCTAGC			TCTAG ^f	M	3	AGCGTC	AGGTC ^g	
	L	2	TATCGC	TATCG ^f			pH 4	L	3	AGCACG	AGACG ^g	
¹³C	H	2	AGTCAC	AGTCA ^f	t0		H	3	ATAGTG	ATGTG ^g		
	Xylose +	M	2	AGCTAC			AGCTA ^f	M	3	TCTAGC	TCAGC ^g	
	L	2	AGCGTC	AGCGT ^f			pH 7	L	3	TATCGC	TACGC ^g	
pH shift SIP experiment	¹²C	H	3	TGTGAC		TGGAC ^g	Methanol	H	3	TGTGAC	TGGAC ^g	
		M	3	TGTCTC		TGCTC ^g		M	3	TGTCTC	TGCTC ^g	
		L	3	TGCATC		TGATC ^g		pH 7	L	3	TGCATC	TGATC ^g

¹³ C	H	3	TACAGC	TAAGC ^g
Methanol	M	3	TACTAG	TATAG ^g
pH 7	L	3	TACGTG	TCGTG ^h

^a Abbreviation for 'treatment'; indicates supplemented substrate. '¹²C' indicates [¹²C]- isotopologue; '¹³C' indicates [¹³C]-isotopologue. A cross indicates additionally supplemented [¹²C]-methanol in substrate SIP experiment treatments

^b Abbreviation for 'library'; indicates pyrosequencing amplicon library. 'H', library of heavy fraction; 'M', library of middle fraction; 'L', library of light fraction.

^c Amplicons were pooled for pyrosequencing to minimize number of barcodes required. Number 1 to 3 indicates different 'amplicon sequence pools'.

^d Barcode sequence after manually modification.

^e Modification: First base of initial barcode was removed to create a unique barcode.

^f Modification: Last base of initial barcode was removed to create a unique barcode.

^g Modification: Third base of initial barcode was removed to create a unique barcode.

^h Modification: Second base of initial barcode was removed to create a unique barcode.

This table has been published in Morawe *et al.* 2017.

Table A 2 Sequences of the barcodes for ITS sequence classification of PYRO-sequencing derived sequences.

	treatm. ^a	lib ^b	10 nt barcode ^c (5'-3')	treatm. ^a	lib ^b	10 nt barcode ^c (5'-3')
Substrate SIP experiment	t0₁	H	CTCGCGTGTC	¹² C	H	AGCACTGTAG
		M	CGTCTAGTAC	Xylose +	M	CATAGTAGTG
		L	TCGTCGCTCG		L	CGTAGACTAG
	t0₂	H	CACGCTACGT	¹³ C	H	AGACTATACT
		M	TCTAGCGACT	Xylose +	M	TACAGATCGT
		L	AGTATACATA		L	ACAGTATATA
	¹² C Methanol	H	ACGAGTGCGT	¹² C	H	AGACGCACTC
		M	TAGTATCAGC	Vanillic Acid +	M	TACTGAGCTA
		L	TCTACGTAGC		L	ACGACTACAG
	¹³ C Methanol	H	ACATACGCGT	¹³ C	H	ACTGTACAGT
		M	CAGTAGACGT	Vanillic Acid +	M	TACACGTGAT
		L	TCTATACTAT		L	TGTGAGTAGT
¹² C Acetate +	H	ACGCTCGACA	¹² C	H	CGTGTCTCTA	
	M	TGATACGTCT	CO₂ +	M	TCACGTA	
	L	TGTACTACTC		L	TAGAGACGAG	
¹³ C Acetate +	H	ACGCGAGTAT	¹³ C	H	ATAGAGTACT	
	M	TGAGTCAGTA	CO₂ +	M	TCGCACTAGT	
	L	TGACGTATGT		L	AGCTCACGTA	
¹² C Glucose +	H	ATCAGACACG	¹² C	H	ATATCGCGAG	
	M	CGAGAGATAC	CO₂ +	M	ATACGACGTA	
	L	TACGAGTATG		L	TACTCTCGTG	
¹³ C Glucose +	H	AGCGTCGTCT	¹³ C	H	AGTACGCTAT	
	M	TACGCTGTCT	CO₂ +	M	TCGATCACGT	
	L	ACGCGATCGA		L	ACTAGCAGTA	
pH shift SIP experiment	t0 pH 4	H	TCGATCACGT	t0	H	TCTATACTAT
		M	ACAGTATATA	pH 7	M	AGCTCACGTA
		L	CGATCGTATA		L	CGTACAGTCA
	¹² C Methanol pH 4	H	TCGCACTAGT	¹² C	H	TGACGTATGT
		M	ACGCGATCGA	Methanol pH 7	M	AGTATACATA
		L	CGCAGTACGA		L	CGTACTCAGA
	¹³ C Methanol pH 4	H	TCTAGCGACT	¹³ C	H	TGTGAGTAGT
		M	ACTAGCAGTA	Methanol pH 7	M	AGTCGAGAGA
		L	CGCGTATACA		L	CTATAGCGTA

^a Abbreviation for 'treatment'; indicates supplemented substrate. '¹²C' indicates [¹²C]-isotopologue; '¹³C' indicates [¹³C]-isotopologue. A cross indicates additionally supplemented [¹²C]-methanol in substrate-SIP treatments

^b Abbreviation for 'library'; indicates pyrosequencing amplicon library. 'H', library of heavy fraction; 'M', library of middle fraction; 'L', library of light fraction.

^c 10 nt barcodes are internal provided by Roche (Roche Applied Science).

This table has been published in Morawe *et al.* 2017.

Table A 3 Sequences of the barcodes used to identify individual samples in ILLUMINA amplicon libraries (methanol/chloromethane SIP experiment).

treatm.^a	lib^b	Inline barcode^c	treatm.^a	lib^b	Inline barcode^c
t₀	H	ACACGTA	¹²MeOH & ¹²CH₃Cl	H	NNN ACGAGTC
	M	N ACACTAG		M	ACGATAC
	L	NN ACACTGA		L	N ACGATCA
¹²MeOH	H	NNN ACAGATC	¹²MeOH & ¹²CH₃Cl	H	NN ACGCATA
	M	ACAGCTA		M	NNN ACGTACA
	L	N ACAGTAC		L	ACGTATC
¹³MeOH	H	NN ACAGTCA	¹²MeOH & ¹²CH₃Cl	H	N ACGTCAC
	M	NNN ACATACG		M	NN ACGTCTG
	L	ACATAGC		L	NNN ACGTGAG
¹²CH₃Cl	H	N ACATCAG			
	M	NN ACATCGA			
	L	NNN ACATGAC			
¹³CH₃Cl	H	ACATGCA			
	M	N ACATGTG			
	L	NN ACGACTA			

^a Abbreviation for 'treatment'; indicates supplemented substrate. 't₀' indicates activated soil served as initial soil sample for the SIP experiment; '¹²' indicates [¹²C]-isotopologue; '¹³' indicates [¹³C]-isotopologue.

^b Abbreviation for 'library'; indicates ILLUMINA amplicon library. 'H', library of heavy fraction; 'M', library of middle fraction; 'L', library of light fraction.

^c Inline barcode always precedes primer (applicable for both forward and reverse primer). Barcode and primer are linked with an additional T. 'N' indicates for A, C, T or G.

APPENDICES

Table A 4 Number of all sequences obtained from pyrosequencing amplicon libraries.

The dash indicates no sample / no data / no amplicon library. This table has been published in Morawe *et al.* 2017.

treatm. ^a	lib ^b	16S rRNA		mxαF		ITS		
		raw	filtered ^c	raw	filtered ^c	raw	filtered ^c	
total		200785	105689	139329	113689	237495	95065	
Substrate SIP experiment	t₀	ALL	2939	1492	3479	2521	11282	4303
		H	1225	760	1223	898	3315	1477
		M	22	10	1049	773	4093	1440
		L	1692	722	1207	850	3874	1386
	t₀	ALL	5014	2882	6423	5756	11298	4316
		H	495	292	2605	2302	3391	1489
		M	2152	1133	1890	1734	4097	1456
		L	2367	1457	1928	1720	3810	1371
	t₀	ALL	6763	4376	2277	2040	-	-
		H	2277	1506	1025	945	-	-
		M	2323	1496	710	621	-	-
		L	2163	1374	542	474	-	-
	t₀	ALL	5354	3283	3741	3285	-	-
		H	260	185	2197	1995	-	-
		M	2650	1615	752	600	-	-
		L	2444	1483	792	690	-	-
	¹²C Methanol	ALL	4270	2103	1513	1081	10970	4263
		H	1060	528	719	551	3694	1466
		M	1117	586	694	474	3632	1437
		L	2093	989	100	56	3644	1360
	¹³C Methanol	ALL	4770	2328	1495	955	11043	4272
		H	1134	571	694	497	3122	1460
		M	1810	868	566	328	3980	1435
		L	1826	889	235	130	3941	1377
	¹²C Acetate +	ALL	7034	4454	3666	3220	13117	4348
		H	3061	2128	1543	1384	3750	1474
		M	1685	960	865	717	4827	1449
		L	2288	1366	1258	1119	4540	1425
¹³C Acetate +	ALL	9039	5666	4291	3743	11431	4322	
	H	3854	2536	1743	1484	3552	1397	
	M	3028	1902	1173	1067	3955	1499	
	L	2157	1228	1375	1192	3924	1426	

APPENDICES

	treatm. ^a	lib ^b	16S rRNA		mxαF		ITS	
			raw	modified ^c	raw	modified ^c	raw	modified ^c
substrate SIP experiment		ALL	5281	2536	3513	2767	13211	4427
	¹² C	H	1820	903	1136	973	3776	1469
	Glucose +	M	1272	543	1261	994	5154	1497
		L	2189	1090	1116	800	4281	1461
		ALL	5306	2217	2525	1837	13270	4406
	¹³ C	H	1961	661	397	266	4616	1481
	Glucose +	M	2407	1097	1197	930	4105	1477
		L	938	459	931	641	4549	1448
		ALL	7588	4667	3300	2923	12712	4420
	¹² C	H	2823	1864	1045	945	3984	1457
	Xylose +	M	2203	1415	782	710	4902	1489
		L	2562	1388	1473	1268	3826	1474
		ALL	8039	4525	5194	4645	12067	4440
	¹³ C	H	3352	2004	2967	2676	3977	1491
	Xylose +	M	2206	1117	561	469	4201	1501
		L	2481	1404	1666	1500	3889	1448
		ALL	9161	5476	3248	2871	12947	4246
	¹² C	H	3677	2498	1296	1125	2706	1467
	Vanillic Acid +	M	2952	1414	1017	913	6294	1424
		L	2532	1564	935	833	3947	1355
		ALL	7890	4675	2910	2501	11384	4270
	¹³ C	H	2783	2035	1061	852	3499	1428
	Vanillic Acid +	M	2638	1327	893	805	3852	1444
		L	2469	1313	956	844	4033	1398
		ALL	4311	2094	2835	2103	11783	4340
	¹² C	H	827	522	1180	935	2696	1493
	CO ₂ +	M	1454	731	774	501	5393	1471
		L	2030	841	881	667	3694	1376
	ALL	4453	2120	3830	2759	12435	4307	
¹³ C	H	705	393	1558	1166	3329	1454	
CO ₂ +	M	1886	923	1033	707	4691	1452	
	L	1862	804	1239	886	4415	1401	
	ALL	5642	2338	2390	1780	12351	4258	
¹² C	H	1818	795	1008	759	3808	1413	
CO ₂	M	2008	754	662	483	4365	1436	
	L	1816	789	720	538	4178	1409	

APPENDICES

	treatm. ^a	lib ^b	16S rRNA		mxαF		ITS	
			raw	modified ^c	raw	modified ^c	raw	modified ^c
sub. SIP exp	¹³ C CO2	ALL	5941	2704	1661	1224	16841	4268
		H	2347	1122	703	526	3534	1488
		M	1877	884	342	239	8430	1390
		L	1717	698	616	459	4877	1390
pH shift SIP experiment	t0 pH 4	ALL	9096	3917	10014	8364	5940	4301
		H	2852	1243	2797	2443	1767	1440
		M	3217	1397	3435	2880	2030	1441
		L	3027	1277	3782	3041	2143	1420
	Methanol pH 4	ALL	19781	12097	10795	9110	6340	4326
		H	4334	2587	2314	1928	2329	1422
		M	4866	3107	3533	3003	1986	1455
		L	10581	6403	4948	4179	2025	1449
	Methanol pH 4	ALL	23530	13979	10348	7716	6383	4286
		H	6775	3737	1698	1306	2324	1429
		M	8454	4757	3588	2949	1654	1434
		L	8301	5485	5062	3461	2405	1423
	t0 pH 7	ALL	10662	4460	13726	11167	6430	4251
		H	3117	1310	5407	4360	2114	1408
		M	3281	1480	2860	2370	2269	1416
		L	4264	1670	5459	4437	2047	1427
	Methanol pH 7	ALL	13412	4968	17830	14387	6947	4348
		H	4556	1741	5734	4591	2525	1459
		M	5189	1701	4889	4008	2153	1451
		L	3667	1526	7207	5788	2269	1438
Methanol pH 7	ALL	15509	6332	18325	14934	7313	4347	
	H	6848	2980	8171	6776	2551	1462	
	M	4277	1744	7173	5811	2288	1438	
	L	4384	1608	2981	2347	2474	1447	

^a Abbreviation for 'treatment'; indicates supplemented substrates. '¹²C' indicates [¹²C]-isotopologue; '¹³C' indicates [¹³C]-isotopologue. A cross indicates additionally supplemented [¹²C]-methanol in substrate SIP experiment.

^b Abbreviation for 'library'; indicates pyrosequencing amplicon library. 'ALL', library of combined data set of 'H', 'M' and 'L'; 'H', library of heavy fraction; 'M', library of middle fraction; 'L', library of light fraction.

^c Number of all remained sequences after quality and chimera check, clustering with specific cut-off values and detection of the correct forward primer sequence.

Table A 5 Number of all 16S rRNA gene sequences obtained from ILLUMINA amplicon libraries.

Raw paired reads are noted in grey faces; processed data are noted in black faces.

treatm. ^a	lib ^b	Number of 16S rRNA gene sequences		
		raw ^c	filtered ^d	analysed ^e
	total	1120929	1494462	257054
	ALL	124191	120362	28936
to	H	51497	50016	12037
	M	41314	39947	9483
	L	31380	30399	7416
	ALL	125952	122201	30854
¹² MeOH	H	46810	45411	12328
	M	25801	24992	5988
	L	53341	51798	12538
	ALL	117048	113677	29404
¹³ MeOH	H	50300	49166	14235
	M	47215	45568	10400
	L	19533	18943	4769
	ALL	128486	124127	28958
¹² CH ₃ Cl	H	37354	36261	9400
	M	53871	51925	11257
	L	37261	35941	8301
	ALL	158522	153202	34490
¹³ CH ₃ Cl	H	23765	23055	5607
	M	55957	53973	11452
	L	78800	76174	17431
	ALL	113760	519996	25383
¹² MeOH & ¹² CH ₃ Cl	H	24540	23618	5963
	M	42282	40786	8888
	L	46938	455592	10532
	ALL	171620	165902	39626
¹² MeOH & ¹² CH ₃ Cl	H	91930	89021	21694
	M	53641	51680	12020
	L	26049	25201	5912
	ALL	181350	174995	39403
¹² MeOH & ¹² CH ₃ Cl	H	39755	38345	8408
	M	86572	83539	18825
	L	55023	53111	12170
	ALL	181350	174995	39403

^a Abbreviation for 'treatment'; indicates supplemented substrates. 'to' indicates activated soil served as initial soil sample for the SIP experiment; ¹² indicates [¹²C]-isotopologue; ¹³ indicates [¹³C]-isotopologue.

^b Abbreviation for 'library'; indicates ILLUMINA amplicon libraries. 'ALL', library of combined data set of 'H', 'M' and 'L'; 'H', library of heavy fraction; 'M', library of middle fraction; 'L', library of light fraction.

^c Number of all raw reads obtained with ILLUMINA sequencing.

^d Number of all filtered paired reads obtained from raw reads by following the standard operating procedure (SOP) in mother (www.mothur.org/wiki/MiSeq_SOP).

^e Number of all sequences that were analysed and used to identify labelled taxa and to run community analyses.

Table A 6 Number of all *mxoF/xoxF*-type MDH and *cmuA* gene sequences obtained from ILLUMINA sequencing amplicon libraries.

Raw paired reads are noted in grey faces; processed data are noted in black faces.

treatm. ^a	lib ^b	Number of gene sequences		
		raw ^c	<i>mxoF/xoxF</i> filtered ^d	<i>cmuA</i> filtered ^d
	total	785203	18477	28290
	ALL	90590	3077	2345
t ₀	H	25443	1355	92
	M	32258	886	438
	L	32889	836	1815
	ALL	78762	2717	2289
¹² MeOH	H	25143	1473	123
	M	31856	711	936
	L	21763	533	1230
	ALL	92576	1431	3072
¹³ MeOH	H	36178	294	943
	M	33428	543	1692
	L	22970	594	437
	ALL	102828	3346	2719
¹² CH ₃ Cl	H	28847	1308	185
	M	38886	1108	994
	L	35095	930	1540
	ALL	104577	1678	3719
¹³ CH ₃ Cl	H	48095	393	2141
	M	29278	559	1028
	L	27204	726	550
	ALL	95674	1922	3262
¹² MeOH & ¹² CH ₃ Cl	H	37537	431	461
	M	23061	650	1115
	L	35076	841	1686
	ALL	107909	2406	5160
¹² MeOH & ¹³ CH ₃ Cl	H	37135	767	1889
	M	41860	846	2192
	L	28914	793	1079
	ALL	112287	1900	5724
¹³ MeOH & ¹² CH ₃ Cl	H	38425	459	307
	M	37378	697	2792
	L	36484	744	2625
	ALL	112287	1900	5724

^a Abbreviation for 'treatment'; indicates supplemented substrates. 't₀' indicates activated soil served as initial soil sample for the SIP experiment; '¹²' indicates [¹²C]-isotopologue; '¹³' indicates [¹³C]-isotopologue.

^b Abbreviation for 'library'; indicates ILLUMINA amplicon libraries. 'ALL', library of combined data set of 'H', 'M' and 'L'; 'H', library of heavy fraction; 'M', library of middle fraction; 'L', library of light fraction.

^c Number of all raw reads obtained with ILLUMINA sequencing comprising sequences of *mxoF/xoxF*, *cmuA* and a third gene sequence (not further analysed, presented and discussed in this thesis).

^d Number of all filtered paired reads obtained from the raw reads meeting certain criteria

Table A 7 ANOSIM and NPMANOVA of microbial communities (substrate SIP and pH shift SIP experiments).

Values of total analyses in bold, pairwise analyses in cursive.

bacterial communities (family-level, 90.1% cut-off)

ANOSIM R 0.75 / p 0.0001

Substrate SIP experiment^a R 0.55 / p 0.001							pH SIP exp.^b R 1.00 / p 0.02		t₀ R 0.48 / p 0.06			
MeOH	Ace +	Glu +	Xyl +	Van +	CO ₂ +	CO ₂	pH4	pH7	Sub vs pH4 ^c	Sub vs pH7 ^c	pH4 vs pH7 ^c	
t ₀ vs t _{End}							t ₀ vs t ₀					
R	1.00	0.21	1.00	0.04	0.11	0.18	0.61	1.00	1.00	0.58	0.67	2.00
t _{End} MeOH VS t _{End} Substrate							t _{End} pH4 VS t _{End} pH7					
R	-	1.00	0.50	1.00	1.00	1.00	0.50	1.00				

NPMANOVA F 8.23 / p 0.0001

Substrate SIP experiment^a F 5.31 / p 0.0001							pH SIP exp.^b F 19.71 / p 0.02		t₀ F 1.75 / p 0.07			
MeOH	Ace +	Glu +	Xyl +	Van +	CO ₂ +	CO ₂	pH4	pH7	Sub vs pH4 ^c	Sub vs pH7 ^c	pH4 vs pH7 ^c	
t ₀ vs t _{End}							t ₀ vs t ₀					
F	6.31	3.63	6.85	1.66	1.90	2.80	3.57	262.50	8.94	2.02	1.98	28.69
t _{End} MeOH VS t _{End} Substrate							t _{End} pH4 VS t _{End} pH7					
F	-	23.69	2.22	24.74	21.60	18.36	3.93	23.99				

mxαF-possessing methylotrophic communities (90% similarity cut-off)

ANOSIM R 0.33 / p 0.02

Substrate SIP experiment^a R 0.18 / p 0.13							pH SIP exp.^b R 0.85 / p 0.02		t₀ R -0.04 / p 0.66			
MeOH	Ace +	Glu +	Xyl +	Van +	CO ₂ +	CO ₂	pH4	pH7	Sub vs pH4 ^c	Sub vs pH7 ^c	pH4 vs pH7 ^c	
t ₀ vs t _{End}							t ₀ vs t ₀					
R	0.14	0.14	0.11	0.14	-0.11	0.14	0.11	0.00	1.00	0.00	0.00	2.00
t _{End} MeOH VS t _{End} Substrate							t _{End} pH4 VS t _{End} pH7					
R	-	0.25	0.25	1.00	0.25	-0.5	0.00	1.00				

NPMANOVA F 2.02 / p 0.0023

Substrate SIP experiment^a F 1.49 / p 0.07							pH SIP exp.^b F 7.52 / p 0.04		t₀ F 1.59 / p 0.03			
MeOH	Ace +	Glu +	Xyl +	Van +	CO ₂ +	CO ₂	pH4	pH7	Sub vs pH4 ^c	Sub vs pH7 ^c	pH4 vs pH7 ^c	
t ₀ vs t _{End}							t ₀ vs t ₀					
F	1.30	1.47	1.63	2.01	0.90	1.56	1.53	0.99	7.19	0.77	1.50	1.97
t _{End} MeOH VS t _{End} Substrate							t _{End} pH4 VS t _{End} pH7					
F	-	1.46	1.13	2.20	1.23	0.81	1.13	15.43				

fungus communities (family-level, 98% cut-off)

ANOSIM R 0.82 / p 0.0001

Substrate SIP experiment^a R 0.78 / p 0.0001							pH SIP exp.^b R 0.69 / p 0.07		t₀ R 0.60 / p 0.33		
MeOH	Ace +	Glu +	Xyl +	Van +	CO ₂ +	CO ₂	pH4	pH7	Sub vs pH4 ^c	Sub vs pH7 ^c	pH4 vs pH7 ^c
t ₀ vs t _{End}							t ₀ vs t ₀				
R	1.00	1.00	1.00	1.00	1.00	1.00	1.00	1.00	1.00	1.00	2.00
t _{End} MeOH VS t _{End} Substrate							t _{End} pH4 VS t _{End} pH7				
R	-	1.00	1.00	1.00	0	0.75	1.00	0.00			

NPMANOVA F 8.11 / p 0.0001

APPENDICES

Substrate SIP experiment^a F 9.41 / p 0.0001							pH SIP exp.^b F 2.98 / p 0.09		t₀ F 8.21 / p 0.0001			
MeOH	Ace +	Glu +	Xyl +	Van +	CO ₂ +	CO ₂	pH4	pH7	Sub vs pH4 ^c	Sub vs pH7 ^c	pH4 vs pH7 ^c	
t ₀ VS t _{End}							t ₀ vs t ₀					
F	7.23	13.17	24.93	30.91	3.58	3.64	2.69	2.95	4.62	3.39	3.79	0.99
t _{End} MeOH VS t _{End} Substrate							t _{End} pH4 VS t _{End} pH7					
F	-	19.50	47.01	65.45	1.82	2.55	2.77	1.46				

^a Treatment with methanol (MeOH), acetate (Ace), glucose (Glu), xylose (Xyl), vanillic acid (Van) and carbon dioxide (CO₂); cross (+) indicates additional methanol supplementation

^b Treatment with methanol at different pH conditions (pH 4 and pH 7)

^c Comparison between t₀ of Substrate SIP experiment and pH-SIP experiment (Sub vs pH) and between both t₀ of pH-SIP (pH4 vs pH7)

Table A 8 ANOSIM and NPMANOVA of microbial communities (methanol/chloromethane SIP experiments).

Values of total analyses in bold, pairwise analyses in cursive.

bacterial communities (family-level of 16S rRNA gene sequence)

ANOSIM R 0.30 / p 0.131			NPMANOVA F 1.92 / p 0.097		
<i>t₀^a vs t_{End}^b</i>			<i>t₀^a vs t_{End}^b</i>		
MeOH	CH ₃ Cl	MeOH & CH ₃ Cl	MeOH	CH ₃ Cl	MeOH & CH ₃ Cl
<i>0.00</i>	<i>1.00</i>	<i>0.56</i>	<i>0.77</i>	<i>3.57</i>	<i>1.54</i>
<i>t_{End}^b vs t_{End}^b</i>			<i>t_{End}^b vs t_{End}^b</i>		
MeOH vs CH ₃ Cl	MeOH & CH ₃ Cl vs MeOH	MeOH & CH ₃ Cl vs CH ₃ Cl	MeOH vs CH ₃ Cl	MeOH & CH ₃ Cl vs MeOH	MeOH & CH ₃ Cl vs CH ₃ Cl
<i>0.25</i>	<i>0.75</i>	<i>-0.33</i>	<i>2.16</i>	<i>3.30</i>	<i>0.36</i>

mxoF/xoxF-type MDH-possessing bacterial communities^c

ANOSIM R 0.01 / p 0.489			NPMANOVA F 0.91 / p 0.565		
<i>t₀^a vs t_{End}^b</i>			<i>t₀^a vs t_{End}^b</i>		
MeOH	CH ₃ Cl	MeOH & CH ₃ Cl	MeOH	CH ₃ Cl	MeOH & CH ₃ Cl
<i>1.00</i>	<i>0.66</i>	<i>0.75</i>	<i>0.50</i>	<i>0.73</i>	<i>0.34</i>
<i>t_{End}^b vs t_{End}^b</i>			<i>t_{End}^b vs t_{End}^b</i>		
MeOH vs CH ₃ Cl	MeOH & CH ₃ Cl vs MeOH	MeOH & CH ₃ Cl vs CH ₃ Cl	MeOH vs CH ₃ Cl	MeOH & CH ₃ Cl vs MeOH	MeOH & CH ₃ Cl vs CH ₃ Cl
<i>0.66</i>	<i>0.40</i>	<i>0.71</i>	<i>1.55</i>	<i>1.24</i>	<i>0.48</i>

cmuA-possessing bacterial communities^d

ANOSIM R 0.67 / p 0.011			NPMANOVA F 7.19 / p 0.018		
<i>t₀^a vs t_{End}^b</i>			<i>t₀^a vs t_{End}^b</i>		
MeOH	CH ₃ Cl	MeOH & CH ₃ Cl	MeOH	CH ₃ Cl	MeOH & CH ₃ Cl
<i>1.00</i>	<i>1.00</i>	<i>0.33</i>	<i>11.99</i>	<i>4.38</i>	<i>1.61</i>
<i>t_{End}^b vs t_{End}^b</i>			<i>t_{End}^b vs t_{End}^b</i>		
MeOH vs CH ₃ Cl	MeOH & CH ₃ Cl vs MeOH	MeOH & CH ₃ Cl vs CH ₃ Cl	MeOH vs CH ₃ Cl	MeOH & CH ₃ Cl vs MeOH	MeOH & CH ₃ Cl vs CH ₃ Cl
<i>0.50</i>	<i>0.92</i>	<i>0.92</i>	<i>3.47</i>	<i>8.51</i>	<i>13.53</i>

^a t₀ means "activated" soil (i.e., pristine soil was supplemented with one pulse 1% CH₃Cl to trigger chloromethane-utilizers and used as starting material for the treatments with [¹²C]- and [¹³C]-isotopologues)^b t_{End} means time point after 3 substrate pulses (i.e., with solely supplemented methanol (MeOH), solely supplemented chloromethane (CH₃Cl) or both simultaneously supplemented (MeOH & CH₃Cl) used for molecular analyses.^c based on 77% similarity cut-off^d based on a 90% similarity cut-off

APPENDICES

Table A 9 Relative abundance of bacterial taxa (16S rRNA gene sequences) in the substrate and pH shift SIP experiment.

Data derived from combined pyrosequencing data sets of [¹²C]- and [¹³C]-isotopologue treatments of both SIP experiments. Only taxa with a relative abundance ≥0.5% are listed, abundance <0.5% is indicated by *, no presence is indicated by -. Percentages are always related to filtered datasets of 16S rRNA gene sequence of pyrosequencing amplicon libraries. This table has been published in Morawe *et al.* 2017.

	Substrate SIP experiment ^c								pH SIP experiment ^d			
	t ₀	MeOH	Ace +	Glu +	Xyl +	Van +	CO ₂ +	CO ₂	pH 4		pH 7	
									t ₀	MeOH	t ₀	MeOH
number of sequences combined data sets & singletons removed	11979	4405	10105	4744	8098	10145	4203	5023	3796	26042	4281	11188
Phylogenetic affiliation ^a	Relative abundance [%]											
<i>Acidobacteria</i>	3.89	0.98	0.89	1.05	2.09	1.86	0.88	2.43	5.64	*	8.36	*
<i>Actinobacteria</i>	47.14	19.25	63.29	8.79	57.56	57.38	62.62	30.38	47.63	2.49	26.98	8.13
<i>Actinomycetales</i>	7.89	1.98	2.11	4.22	2.84	3.44	5.19	11.09	25.66	0.89	14.48	1.47
<i>Kineosporiaceae</i> (<i>Kineosporia</i> . OTU 703) ^b	7.61	1.82	2.04	3.96	2.80	3.40	4.83	10.55	23.29	0.70	11.42	0.88
<i>Corynebacteriales</i>	33.32	15.12	59.72	0.51	52.14	51.10	54.15	10.23	1.24	*	*	*
<i>Corynebacteriaceae</i> (<i>Corynebacterium</i> . OTU 748) ^b	32.62	14.71	59.31	*	51.67	50.63	53.91	9.06	-	-	-	-
<i>Mycobacteriaceae</i> (<i>Mycobacterium</i> . OTU 750) ^b	0.63	*	*	*	*	*	*	1.17	1.24	*	*	*
<i>Micrococcales</i>												
<i>Microbacteriaceae</i> (<i>Leifsonia</i> . OTU 721) ^b	*	*	*	*	*	*	*	*	*	0.78	*	4.45
<i>Streptosporangiales</i>	0.99	*	*	0.53	*	*	*	1.19	2.29	*	1.40	*
<i>other Actinobacteria</i>	12.39	3.70	3.27	6.91	5.08	5.81	7.71	18.12	41.07	1.33	21.16	2.57

APPENDICES

	Substrate SIP experiment ^c								pH SIP experiment ^d			
	t ₀	MeOH	Ace +	Glu +	Xyl +	Van +	CO ₂ +	CO ₂	pH 4		pH 7	
									t ₀	MeOH	t ₀	MeOH
Bacteroidetes	*	13.62	5.31	19.50	3.42	3.13	4.21	14.57	3.29	9.15	13.38	62.34
<i>Flavobacteriales</i>	-	-	-	-	-	-	-	-	-	-	*	18.25
<i>Flavobacteriaceae</i>	-	-	-	-	-	-	-	-	-	-	*	17.31
(<i>Chryseobacterium</i> . OTU 1045) ^b	-	-	-	-	-	-	-	-	-	-	*	17.31
<i>Sphingobacteriales</i>	*	13.55	5.18	19.39	3.30	3.03	4.07	14.19	1.21	9.02	8.11	38.63
<i>Chitinophagaceae</i>	-	*	*	*	*	*	0.57	2.29	*	-	*	12.14
(<i>Ferruginibacter</i> . OTU 1014) ^b	-	*	*	*	*	*	0.57	2.29	*	-	*	12.14
<i>Sphingobacteriaceae</i>	-	13.14	4.86	18.82	3.03	2.79	3.50	11.83	0.76	7.96	6.73	15.99
(<i>Mucilagibacter</i> ; OTU 1073) ^b	-	13.14	4.86	18.82	3.03	2.79	3.50	11.83	0.76	7.96	6.73	15.99
other <i>Bacteroidetes</i>	*	*	*	*	*	*	*	*	2.08	*	5.21	5.13
“Cand. Saccharibacteria”	0.63	*	*	*	*	*	*	*	0.61	*	1.94	*
Chlamydiae	0.86	*	*	*	*	*	-	*	0.74	*	0.96	*
Firmicutes	0.51	1.20	*	0.53	0.68	0.78	*	1.17	0.53	*	0.93	1.04
<i>Bacilli</i>	*	*	*	*	*	*	*	*	*	*	*	0.76
Parcubacteria	*	3.50	4.46	0.84	*	*	*	*	*	*	*	-
Planctomycetes	27.53	6.97	6.95	9.19	15.46	16.25	7.73	12.06	10.48	*	12.01	3.12
<i>Planctomycetia</i>	16.13	4.31	4.74	5.35	10.40	11.21	4.71	7.76	7.03	*	6.82	2.61
Proteobacteria	12.62	48.42	14.66	56.11	16.84	17.13	20.99	33.76	25.37	86.68	26.26	18.10
Alphaproteobacteria	10.03	8.58	4.50	4.93	5.01	4.77	4.43	6.67	18.97	2.61	17.75	2.61
<i>Rhizobiales</i>	6.09	6.61	1.92	3.35	3.87	3.59	2.78	4.38	11.01	2.03	8.25	0.92
<i>Beijerinckiaceae</i>	6.04	6.61	1.92	2.91	3.87	3.58	2.78	4.38	10.96	2.03	8.11	0.86
(<i>Methylovirgula</i> . OTU 438) ^b	6.04	6.61	1.92	2.91	3.87	3.58	2.78	4.38	10.96	2.03	8.11	0.86
<i>Rhodospirillales</i>	2.59	0.54	1.16	*	*	*	0.64	1.39	4.37	*	4.51	*
<i>Acetobacteraceae</i>	0.98	*	1.03	*	*	*	*	0.86	2.00	*	2.27	*
<i>Sphingomonadales</i>	0.55	*	*	0.89	*	*	*	*	1.77	*	2.31	0.73
other <i>Alphaproteobacteria</i>	0.79	1.09	0.98	*	*	*	0.59	*	1.82	*	2.69	0.72

APPENDICES

	Substrate SIP experiment ^c								pH SIP experiment ^d			
	t ₀	MeOH	Ace +	Glu +	Xyl +	Van +	CO ₂ +	CO ₂	pH 4		pH 7	
									t ₀	MeOH	t ₀	MeOH
Betaproteobacteria	*	*	*	8.31	8.74	9.31	*	*	0.76	*	0.61	2.53
<i>Burkholderiales</i>	*	-	*	8.31	8.74	9.29	*	*	0.71	*	*	0.79
<i>Burkholderiaceae</i>												
(<i>Burkholderia</i> . OTU 361) ^b	*	-	*	8.26	8.74	9.29	*	*	0.55	*	*	*
<i>Methylophilales</i>												
(<i>Methylophilus</i> . OTU 358) ^b	-	-	-	-	-	-	-	*	*	-	-	1.73
Gammaproteobacteria	1.58	39.50	9.77	42.58	3.03	2.97	16.23	26.54	4.45	83.98	6.59	12.80
<i>Xanthomonadales</i>	0.60	37.25	9.61	42.22	2.69	2.63	15.92	25.24	3.53	83.70	4.18	12.27
<i>Xanthomonadaceae</i>												
(<i>Rhodanobacter</i> . OTU 300) ^b	0.58	37.09	9.45	42.12	2.62	2.57	15.92	25.20	3.45	83.65	4.09	12.16
other <i>Gammaproteobacteria</i>	0.98	2.25	*	*	*	*	*	0.72	0.87	*	2.29	*
Deltaproteobacteria	0.83	*	*	*	*	*	*	*	1.19	*	1.31	*
Verrucomicrobia	2.88	4.09	3.19	2.19	2.49	2.13	1.95	3.30	2.03	0.56	4.93	3.31
<i>Methylacidiphilales</i>	*	*	*	*	*	*	*	*	-	*	0.56	-
<i>Spartobacteria</i>	*	0.59	1.02	*	*	*	*	0.58	*	*	0.77	2.65
<i>Verrucomicrobiae</i>	1.56	2.07	1.46	1.05	1.52	1.29	1.24	2.07	1.21	*	3.01	0.50
other <i>Verrucomicrobia</i>	*	1.18	0.50	*	0.54	*	*	*	*	*	*	*
not affiliated bacteria	3.19	1.04	0.75	1.01	*	*	0.67	1.08	2.48	*	3.22	3.36

^a Phylogenetic affiliation was done with JAguc2 and is based on GenBank Release (Oct 2015)

^b Genera in brackets dominated bacterial taxa

^c Treatment with methanol (MeOH), acetate (Ace), glucose (Glu), xylose (Xyl), vanillic acid (Van) and carbon dioxide (CO₂); cross (+) indicates additional methanol supplementation

^d Treatment with methanol at different pH conditions (pH 4 and pH 7)

APPENDICES

Table A 10 Relative abundance of methylotrophic taxa (*mxoF* gene sequences) in the substrate and pH shift SIP experiment

Data derived from combined pyrosequencing data sets of [¹²C]- and [¹³C]-isotopologue treatments of both SIP experiments. Only taxa with a relative abundance ≥0.5% are listed, abundance <0.5% is indicated by *, no presence is indicated by -. Percentages are always related to filtered datasets of *mxoF* gene sequence of pyrosequencing amplicon libraries. This table has been published in Morawe *et al.* 2017.

	Substrate SIP experiment ^c								pH SIP experiment ^d			
	t ₀	MeOH	Ace +	Glu +	Xyl +	Van +	CO ₂ +	CO ₂	pH 4		pH 7	
									t ₀	MeOH	t ₀	MeOH
number of sequences combined data sets & singletons removed	13602	2036	6963	4604	7568	5372	4862	3004	8364	16826	11167	29321
Phylogenetic affiliation^a	Relative abundance [%]											
<i>Methylobacterium</i>	72.43	31.14	50.29	43.22	44.37	31.24	33.63	56.79	55.26	39.24	16.79	72.92
OTU 35	60.23	-	*	*	1.10	19.62	1.25	1.76	50.12	35.88	8.08	2.56
OTU 40	8.34	19.94	45.91	32.78	4.47	5.64	16.97	34.79	2.00	2.41	3.00	30.17
OTU 55	2.98	9.63	2.11	7.84	36.87	3.80	13.00	18.28	3.13	0.90	5.71	39.61
OTU 76	*	*	*	0.52	*	*	*	*	-	-	-	*
OTU 78	*	*	0.56	*	0.81	1.01	1.44	0.93	-	-	-	*
OTU 79	*	*	*	0.52	*	*	*	0.53	-	*	-	*
OTU 107	*	*	*	0.52	*	*	*	*	*	-	-	*
OTU 108	*	*	0.95	*	*	*	*	*	-	*	-	*
ambiguous ^b	*	1.33	2.77	*	*	*	*	*	*	*	*	1.44
OTU 9	-	*	2.56	-	*	-	-	-	*	*	*	-
OTU 141	-	-	-	-	-	-	-	-	-	-	-	1.39
OTU 222	*	1.03	*	*	*	*	*	*	*	-	-	*

APPENDICES

	Substrate SIP experiment ^c								pH SIP experiment ^d			
	t ₀	MeOH	Ace +	Glu +	Xyl +	Van +	CO ₂ +	CO ₂	pH 4		pH 7	
									t ₀	MeOH	t ₀	MeOH
<i>Hyphomicrobium</i>	14.80	15.86	24.67	27.65	7.60	8.41	20.16	3.36	6.22	8.31	24.89	10.85
OTU 185	14.36	15.13	24.44	6.75	5.92	7.48	5.90	3.10	1.52	3.55	1.29	4.27
OTU 202	*	*	*	*	*	0.76	*	*	-	*	*	*
OTU 243	*	*	*	*	*	-	*	-	*	2.49	*	*
OTU 257	*	*	-	-	*	*	*	-	3.32	1.36	22.78	6.36
OTU 308	*	-	-	-	*	-	-	-	0.98	*	*	*
OTU 309	*	*	-	20.79	1.15	*	14.01	*	*	0.56	*	*
ambiguous ^b	7.47	42.19	9.31	16.36	19.87	39.02	29.08	33.16	31.79	41.16	43.69	7.32
OTU 172	0.82	3.88	0.69	3.78	8.31	3.11	4.44	3.36	3.71	3.34	3.73	1.48
OTU 210	*	7.91	0.80	0.54	0.54	10.67	19.29	*	6.37	6.85	3.54	1.42
OTU 214	*	4.86	*	*	*	*	*	1.33	2.61	1.86	14.56	-
OTU 236	*	*	5.20	2.04	2.34	5.53	0.93	0.83	17.19	27.56	20.50	3.89
OTU 266	5.65	24.90	0.85	9.30	2.48	14.09	2.45	9.15	1.26	0.58	*	*
OTU 286	*	-	*	-	-	*	*	17.31	-	-	-	-
OTU 298	*	0.54	1.61	*	6.01	5.32	1.56	1.00	*	0.75	*	*
OTU 310	-	-	-	-	-	-	-	-	*	*	0.68	*
<i>Methylorhabdus</i>	*	0.54	*	*	*	*	*	*	-	*	-	*
OTU 190	*	0.54	*	*	*	*	*	*	-	*	-	*
ambiguous ^b	*	*	*	*	-	-	*	-	*	2.81	*	-
OTU 18	*	*	*	*	-	-	*	-	*	2.81	*	-
<i>Methylocystaceae</i>	0.57	-	*	2.74	-	-	-	-	-	-	-	-
OTU 137	0.57	-	*	2.74	-	-	-	-	-	-	-	-

APPENDICES

	Substrate SIP experiment ^c								pH SIP experiment ^d			
	t ₀	MeOH	Ace +	Glu +	Xyl +	Van +	CO ₂ +	CO ₂	pH 4		pH 7	
									t ₀	MeOH	t ₀	MeOH
<i>Beijerinckiaceae</i>	*	2.85	*	*	*	1.04	0.51	-	*	*	1.33	0.69
OTU 144	*	2.85	*	*	*	1.04	0.51	-	*	*	1.33	0.69
ambiguous ^b	*	*	1.82	4.17	4.78	0.86	10.51	0.87	2.76	3.55	6.12	0.34
OTU 338	*	*	*	*	1.03	*	0.58	*	*	*	0.55	*
OTU 340	*	-	1.77	3.50	3.74	*	*	0.60	1.69	1.60	4.32	*
OTU 349	-	-	-	*	*	-	9.79	-	0.62	1.47	1.25	*
<i>not affiliated</i>	1.53	0.54	4.87	0.76	15.86	11.93	0.76	0.80	2.28	2.29	5.01	3.91
OTU 21	0.76	-	4.64	-	15.31	9.94	*	-	2.18	2.20	1.01	*
OTU 90	*	-	*	*	*	0.74	*	*	-	-	-	-
OTU 200	*	0.54	*	*	*	*	*	*	-	-	-	*
OTU 234	*	-	-	*	-	0.54	*	*	-	*	-	*
OTU 268	*	-	*	*	*	0.58	*	*	-	-	-	-
OTU 282	*	-	-	-	-	-	-	-	*	*	*	2.58
OTU 325	-	-	-	-	*	-	-	-	*	*	3.81	1.27

^a Phylogenetic affiliation was done with BLASTn (Dezember 2015) and confirmed by positioning in phylogenetic tree (for further information see

Figure A 12)

^b Sequence identity with BLASTn <90% as well as ambiguous position in phylogenetic tree

^c Treatment with methanol (MeOH), acetate (Ace), glucose (Glu), xylose (Xyl), vanillic acid (Van) and carbon dioxide (CO₂); cross (+) indicates additional methanol supplementation

^d Treatment with methanol at different pH conditions (pH 4 and pH 7)

APPENDICES

Table A 11 Relative abundance of fungal taxa (ITS gene sequences) in the substrate and pH shift SIP experiment.

Data derived from combined pyrosequencing data sets of [¹²C]- and [¹³C]-isotopologue treatments of both SIP experiments. Only taxa with a relative abundance ≥ 0.5% are listed, abundance < 0.5% is indicated by *, no presence is indicated by -. Percentages are always related to filtered datasets of ITS gene sequence of pyrosequencing amplicon libraries. This table has been published in Morawe *et al.* 2017.

	Substrate SIP experiment ^c								pH SIP experiment ^d			
	t ₀	MeOH	Ace +	Glu +	Xyl +	Van +	CO ₂ + +	CO ₂	pH 4		pH 7	
									t ₀	MeOH	t ₀	MeOH
number of sequences combined data sets & singletons removed	8619	8535	8670	8833	8860	8516	8647	8526	4301	8612	4251	8673
Phylogenetic affiliation^a	Relative abundance [%]											
Ascomycota	45.16	37.56	16.68	14.00	8.18	51.89	47.84	57.71	53.80	38.76	50.60	36.87
<i>Dothideomycetes</i>	1.13	*	*	*	*	*	1.41	1.38	1.74	*	1.11	*
<i>Eurotiomycetes</i>	5.80	9.31	4.35	5.38	2.61	10.24	13.81	12.68	17.41	9.72	24.84	11.54
<i>Chaetothyriales</i>	*	0.71	0.60	1.23	*	4.20	*	*	*	0.82	*	0.65
<i>Eurotiales</i>	5.53	8.60	3.75	4.14	2.44	6.04	13.58	12.30	16.93	8.89	24.35	10.90
<i>Trichocomaceae</i>	3.03	8.54	3.70	4.11	2.42	5.86	12.83	11.93	14.76	8.69	13.67	10.80
<i>Elaphomycetaceae</i>	2.49	*	*	*	*	*	0.75	*	2.16	*	10.63	*
<i>Leotiomycetes</i>	10.85	10.03	4.86	2.94	2.00	11.16	12.41	18.21	10.72	8.19	8.52	7.11
<i>Helotiales</i>	2.84	5.21	1.30	1.31	0.63	5.28	7.49	7.95	2.53	2.04	2.35	2.08
<i>Leotiales</i>	*	*	1.23	*	*	*	*	2.50	*	*	-	*
<i>Incertae sedis</i>	7.08	4.18	2.16	1.06	1.08	4.94	3.99	6.69	8.07	5.84	5.01	4.77
<i>Saccharomycetes</i>	18.49	7.05	2.70	2.34	0.80	6.11	6.27	7.86	1.86	0.60	2.49	0.90
<i>Sordariomycetes</i>	6.89	9.82	4.12	2.62	2.51	22.91	12.17	15.66	19.81	18.32	11.46	15.81
<i>Chaetosphaeriales</i>	0.68	1.65	*	*	*	0.72	0.87	1.02	3.30	4.30	1.91	3.46
<i>Hypocreales</i>	5.70	7.44	3.44	1.64	2.12	21.54	10.48	13.65	15.02	11.83	7.60	10.73
<i>Nectriaceae</i>	0.70	1.07	*	*	0.51	9.63	2.73	2.78	1.05	1.45	0.73	1.25
<i>Ophiocordycipitaceae</i>	*	*	1.03	*	*	5.97	1.33	3.19	2.58	1.58	1.51	1.52

APPENDICES

	Substrate SIP experiment ^c								pH SIP experiment ^d			
	t ₀	MeOH	Ace +	Glu +	Xyl +	Van +	CO ₂ +	CO ₂	pH 4		pH 7	
									t ₀	MeOH	t ₀	MeOH
Basidiomycota	41.39	40.79	73.18	82.57	87.88	32.02	29.58	26.34	27.23	36.88	27.26	46.24
Agaricomycetes	27.18	13.90	6.74	2.22	1.52	13.45	18.53	16.16	14.83	10.62	14.04	8.14
<i>Agaricales</i>	7.05	2.25	1.90	0.96	0.55	4.00	3.03	4.45	2.60	2.46	3.74	1.84
<i>Boletales</i>	1.18	*	*	-	-	*	*	*	*	*	*	*
<i>Phallales</i>	1.50	*	*	*	-	*	*	*	*	*	*	*
<i>Polyporales (Ganodermataceae)^b</i>	2.42	6.55	0.81	*	*	3.60	3.43	2.31	1.98	2.96	1.79	2.57
<i>Russulales</i>	6.44	*	*	*	*	*	0.71	2.31	2.49	*	1.36	*
(<i>Russulaceae</i>) ^b												
<i>Thelephorales</i>	3.11	2.41	1.98	0.62	*	2.89	5.57	2.44	0.70	0.71	0.59	0.55
(<i>Thelephoraceae</i>) ^b												
<i>Trechisporales</i>	1.39	*	0.80	*	*	1.22	1.42	0.80	2.46	2.58	2.80	1.89
Microbotryomycetes	1.18	2.94	1.13	*	*	2.42	1.40	1.01	1.49	2.57	1.65	2.04
<i>Leucosporidiales</i>	1.06	2.36	1.08	*	*	0.97	0.95	0.76	1.42	2.33	1.46	1.68
<i>Sporidiobolales</i>	*	*	-	*	*	1.23	*	*	-	-	-	*
Tremellomycetes	12.62	22.12	65.16	79.90	85.98	15.78	9.21	8.64	9.88	22.71	9.81	34.94
<i>Cystofilobasidiales (Syzygospora)^b</i>	1.25	1.56	1.64	*	*	0.67	0.76	0.83	0.88	0.60	*	0.92
<i>Tremellales</i>	4.81	10.44	2.58	2.56	1.73	12.99	5.35	5.40	4.51	2.08	5.65	2.42
(<i>Cryptococcus</i>) ^b												
<i>Trichosporonaceae (Trichosporon)^b</i>	6.46	9.84	60.85	77.14	84.05	1.98	2.95	2.36	4.44	19.89	3.65	31.36
Chytridiomycota	*	*	1.06	*	-	-	*	*	-	*	*	*
Glomeromycota	0.52	2.03	1.18	*	0.55	2.21	3.70	2.40	0.65	0.52	*	0.62
Rozellomycota	3.78	3.55	1.89	*	1.07	1.10	1.73	1.94	2.70	3.04	2.42	2.97
Zygomycota	8.54	15.51	5.76	2.68	1.95	12.09	15.74	9.90	14.46	19.71	18.30	12.30
<i>Mortierellales (Mortierellaceae)^b</i>	8.24	15.22	5.61	2.66	1.94	11.91	15.64	9.75	14.35	19.66	18.14	12.11
not affiliated	0.60	0.54	*	*	*	0.68	1.33	1.58	1.16	0.92	0.87	0.84

^a Phylogenetic affiliation was done by BLASTn (see Table A 13)

^b Taxa in brackets dominated fungal order or family

^c Treatment with methanol (MeOH), acetate (Ace), glucose (Glu), xylose (Xyl), vanillic acid (Van) and carbon dioxide (CO₂); cross (+) indicates additional methanol supplementation

^d Treatment with methanol at different pH conditions (pH 4 and pH 7)

APPENDICES

Table A 12 Phylogenetic affiliation of bacterial taxa in the substrate and pH shift SIP experiment.

Sequences were derived at family-level cut-off (90.1%). Listed are closest related sequences including cultured and environmental hits (closest related sequences are mentioned if they differ from closest related sequence). BLASTn analyses based on OTU sequence lengths of 400 – 449 bp. This table has been published in Morawe *et al.* 2017.

OTU	closest cultured related sequence ^a				closest related sequence ^b (environmental samples included)					
	strain ^c	Query ^d	Id ^e	Accession ^f	strain ^c	Query ^d	Id ^e	Accession ^f		
6	<i>Chthoniobacter flavus</i>	Ellin428	100	90	NR_115225	uncult. <i>Verrucomicrobia</i>	100	97	JQ368535	
9	<i>Chthoniobacter flavus</i>	Ellin428	100	89	NR_115225	uncult. <i>Verrucomicrobia</i>	100	99	JQ369834	
17	<i>Chthoniobacter flavus</i>	Ellin428	100	83	NR_115225	uncult. <i>Verrucomicrobia</i>	100	93	JQ366335	
18	<i>Prostheco bacter debontii</i>	DSM 14044	100	84	AJ966882	uncult. <i>Verrucomicrobia</i>	100	99	AM945528	
54	<i>Terrimicrobium sacchariphilum</i>	NM-5	99	97	GU129926	uncult. <i>Verrucomicrobia</i>	99	98	JF168305	
93	<i>Parachlamydia acanthamoebae</i>	NS2	100	95	JN051144	uncult. <i>Chlamydiae</i>	96	99	AB504668	
108	<i>Parachlamydia acanthamoebae</i>	UV-7	100	91	NR_074972	" <i>Candidatus</i> <i>Metachlamydia lacustris</i> "	CHSL	99	93	GQ221847
132	<i>Conexibacter woesei</i>	DSM 14684	100	94	NR_074830	uncult. <i>Bacteria</i>	96	99	LC011356	
142	<i>Gaiella occulta</i>	F2-233	100	93	NR_118138	uncult. <i>Bacteria</i>	100	99	JX100028	
202	<i>Bacillus</i> sp.	DMV7	99	99	GU584205	<i>Bacillus</i> sp.	DMV7	99	99	GU584205
206	<i>Paenibacillus</i> sp.	YN14-20	100	98	AM162325	uncult. <i>Firmicutes</i>	100	99	EU810868	
278	<i>Povalibacter uvarum</i>	Zumi 37	100	92	NR_126172	uncult. <i>Gammaproteobacterium</i>	100	99	JF301246	
280	<i>Steroidobacter</i> sp.	JC2986	100	98	KP185148	uncult. <i>Gammaproteobacterium</i>	100	99	HF952308	
300	<i>Rhodanobacter</i> sp.	BJC16-A24	99	99	JX483760	uncult. <i>Gammaproteobacterium</i>	99	99	HF952332	
343	<i>Rhodanobacter</i> sp.	D46	72	98	AF250415	uncult. <i>Gammaproteobacterium</i> (<i>Xanthomonadales</i>)	72	98	LC016556	

APPENDICES

OTU	closest cultured related sequence ^a					closest related sequence ^b (environmental samples included)				
		strain ^c	Query ^d	Id ^e	Accession ^f		strain ^c	Query ^d	Id ^e	Accession ^f
358	<i>Methylophilus methylotrophus</i>	HME9441	99	96	KF911346	uncult. <i>Betaproteobacterium</i>		99	98	JQ371286
360	<i>Methylophilus</i> sp.	TWE2	100	91	CP012020	uncult. <i>Betaproteobacterium</i>		100	98	HG529147
361	<i>Burkholderia</i> sp.	EC-V30-gmG7	100	99	AB627009	uncult. <i>Bacterium</i>		100	99	KP726299
379	<i>Acinetobacter</i> sp.	IMCC12751	100	95	JF715439.	uncult. <i>Gammaproteobacterium</i>		100	99	HM113016
431	<i>Caulobacter mirabilis</i>	0112ALTE9*	98	95	LN867237	uncult. <i>Alphaproteobacterium</i>		94	99	JN032148
438	<i>Methylovirgula ligni</i>	BW872	99	98	FM252035	uncult. <i>Alphaproteobacterium</i>		99	99	AM992784
449	<i>Sphingomonas</i> sp.	A37C6	97	99	KJ654808	uncult. <i>Alphaproteobacterium</i> (<i>Sphingobium</i> sp.)		97	99	JN860403
450	<i>Paracoccus</i> sp.	gyp-1	100	99	LN879490	<i>Paracoccus</i> sp.	gyp-1	100	99	LN879490
460	<i>Skermanella</i> sp.	B-121-1-2	99	94	KF561388	uncult. <i>Alphaproteobacterium</i>		99	99	EU849340
467	<i>Acidisphaera</i> sp.	X5	100	94	KM369919	uncult. <i>Alphaproteobacterium</i>		100	98	JQ383603
479	<i>Phaeospirillum</i> sp.	JA812	97	94	HG417062	uncult. <i>Alphaproteobacterium</i>		97	97	JQ386981
528	<i>Solibacter usitatus</i>	Ellin6076	99	93	CP000473	uncult. <i>Acidobacterium</i>		99	99	JX981716
542	<i>Acidipila</i> sp.	DHOF10	100	93	KM083127	uncult. <i>Acidobacterium</i>		100	99	GU598605
545	<i>Acidobacterium capsulatum</i>	20 0D9*	98	98	AM086241	uncult. <i>Acidobacterium</i>		98	99	JF300928
592	<i>Fimbriimonas ginsengisoli</i>	Gsoil 348	100	93	CP007139	uncult. <i>Armatimonadetes</i>		100	98	JN851205
615	<i>Gelria glutamica</i>	TGO	99	85	NR_041819	uncult. <i>Bacterium</i>		95	99	HQ629022

APPENDICES

OTU	closest cultured related sequence ^a					closest related sequence ^b (environmental samples included)				
	strain ^c	Query ^d	Id ^e	Accession ^f	strain ^c	Query ^d	Id ^e	Accession ^f		
652	<i>Aciditerrimonas ferrireducens</i>	IC-180	98	92	NR_112972	uncult. <i>Actinobacterium</i>	98	97	HQ845571	
654	<i>Aciditerrimonas ferrireducens</i>	IC-180	99	92	NR_112972	uncult. <i>Actinobacterium</i>	99	98	JQ376471	
656	<i>Aciditerrimonas ferrireducens</i>	IC-180	100	93	NR_112972	uncult. <i>Actinobacterium</i>	100	99	JQ376189	
668	<i>Aciditerrimonas ferrireducens</i>	IC-180	100	89	NR_112972	uncult. <i>Actinobacterium</i>	92	99	JX204369	
703	<i>Kineosporia</i> sp.	OTSz_A_216	100	94	FM886845	uncult. <i>Actinobacterium</i>	100	99	FJ661525	
721	<i>Leifsonia xyli</i>	HC37	97	99	HG794292	<i>Leifsonia xyli</i>	HC37	97	99	HG794292
723	<i>Pseudonocardia spinosispora</i>	LM 141	98	98	NR_025367	uncult. <i>Actinobacterium</i>	98	98	JN615726	
748	<i>Corynebacterium nuruki</i>	S6-4	100	93	NR_117816	uncult. <i>Actinobacterium</i>	100	94	FN667204	
750	<i>Mycobacterium branderi</i>	AFP-000NM48	100	98	JX266696	uncult. <i>Actinobacterium</i>	100	98	KF530052	
752	<i>Corynebacterium nuruki</i>	S6-4	99	96	NR_117816	uncult. <i>Actinobacterium</i>	99	97	JF208992	
758	<i>Actinospica robiniae</i>	GE134769	99	99	NR_042364	uncult. <i>Actinobacterium</i>	99	99	AB180777	
796	<i>Tepidisphaera mucosa</i>	2813	99	92	KM052380	uncult. <i>Bacterium</i>	99	99	KJ407548	
800	<i>Tepidisphaera mucosa</i>	2813	100	89	KM052380	uncult. <i>Planctomycetes</i>	100	98	JQ663701	
816	<i>Actinoallomurus</i> sp.	145541	70	92	KR781096	uncult. <i>Bacterium</i>	71	95	FQ744029	
836	<i>Pirellula</i> sp.	Schlesner 678	99	88	X81947	" <i>Candidatus Anammoxi-microbium moscowii</i> "	99	90	KC467065	
840	<i>Thermogutta terrifontis</i>	R1	100	86	KC867694	uncult. <i>Planctomycetes</i>	100	93	LK025317	
844	<i>Thermogutta hypogea</i>	SBP2	99	88	KC867695	uncult. <i>Planctomycetes</i>	99	90	LK025387	

APPENDICES

OTU	closest cultured related sequence ^a					closest related sequence ^b (environmental samples included)				
		strain ^c	Query ^d	Id ^e	Accession ^f		strain ^c	Query ^d	Id ^e	Accession ^f
857	<i>Planctopirus limnophilus</i>	DSM 3776	100	88	NR_074670	<i>Gimesia maris</i>	A11-0AF47_11038	100	93	KF228168
885	<i>Nostocoida limicola</i> III	Ben225	100	94	AF244752	<i>Nostocoida limicola</i> III	Ben225	100	94	AF244752
904	<i>Singulisphaera</i> sp.	lo3-4	100	92	GQ889439	uncult. <i>Planctomycetes</i>		100	92	HM748671
923	<i>Gemmata</i> sp.	SD2-6	99	90	GQ889476	uncult. <i>Planctomycetes</i>		99	95	AB127858
927	<i>Gemmata</i> sp.	Br1-2	100	89	GQ889455	uncult. <i>Planctomycetes</i>		100	93	LK025439
939	<i>Gemmata</i> sp.	Br1-2	100	90	GQ889455	uncult. <i>Planctomycetes</i>		100	93	LK025552
945	<i>Isosphaera</i> sp.	Br2-1	100	89	GQ889426	uncult. <i>Planctomycetes</i>		100	89	FJ405890
951	<i>Gemmata</i> sp.	lo1-6	99	91	GQ889466	<i>Gemmata</i> sp.	lo1-6	99	91	GQ889466
968	<i>Zavarzinella formosa</i>	A10	99	90	NR_042465	uncult. <i>Planctomycetes</i>		99	98	LK024693
1014	<i>Ferruginibacter lapsinans</i>	HU1-HG42	100	97	NR_044589	<i>Ferruginibacter lapsinans</i>	HU1-HG42	100	97	NR_044589
1018	<i>Heliimonas saccharivorans</i>	L2-4	100	95	JX458466	<i>Heliimonas saccharivorans</i>	L2-4	100	95	JX458466
1020	<i>Chitinophaga</i> sp.	BS20	99	96	JF806524	<i>Chitinophaga</i> sp.	BS20	99	96	JF806524
1045	<i>Chryseobacterium</i> sp.	WR21	100	99	JF700394	<i>Chryseobacterium</i> sp.	WR21	100	99	JF700394
1073	<i>Mucilaginibacter mallensis</i>	MP1X4	100	98	NR_116978	<i>Mucilaginibacter mallensis</i>	MP1X4	100	98	NR_116978
1078	<i>Sphingobacterium</i> sp.	TB1	100	99	LN867309	<i>Sphingobacterium</i> sp.	TB1	100	99	LN867309
1094	<i>Pedobacter westerhofensis</i>	WB 3.3-22	97	91	NR_042602	<i>Pedobacter westerhofensis</i>	WB 3.3-22	97	91	NR_042602
1098	<i>Solitalea koreensis</i>	R2A36-4	100	86	NR_044568	uncult. <i>Bacteroidetes</i>		95	90	HQ663372
1108	<i>Cytophaga hutchinsonii</i>	ATCC 33406	100	99	NR_102866	<i>Cytophaga hutchinsonii</i>	ATCC 33406	100	99	NR_102866

APPENDICES

OTU	closest cultured related sequence ^a				closest related sequence ^b (environmental samples included)					
	strain ^c	Query ^d	Id ^e	Accession ^f	strain ^c	Query ^d	Id ^e	Accession ^f		
1116	" <i>Candidatus</i> <i>Saccharimonas aalborgensis</i> "	genome	99	86	CP005957	uncult. <i>Bacterium</i>	99	90	EF197025	
1136	" <i>Candidatus</i> <i>Sonnebornia yantaiensis</i> "	<i>YTParaBac3</i>	99	83	KC495062	uncult. <i>Parcubacterium</i>	99	87	HQ290495	
1140	" <i>Candidatus</i> <i>Sonnebornia yantaiensis</i> "	<i>YTParaBac3</i>	100	85	KC495062	" <i>Candidatus</i> <i>Sonnebornia yantaiensis</i> "	<i>YTParaBac3</i>	100	85	KC495062
1155	" <i>Candidatus</i> <i>Sonnebornia yantaiensis</i> "	<i>YTParaBac2</i>	100	83	KC495061	uncult. <i>Parcubacterium</i>	98	86	CP011215	
1158	<i>Parcubacterium</i>	genome	100	84	CP011215	uncult. <i>Parcubacterium</i>	100	95	JN128702	

^a Closest cultured sequences includes validly published names of bacterial species with known strains. No Candidates are listed here with the exception for the candidates' phyla *Saccharibacteria* (OTU 1116) and *Parcubacteria* (OTU 1136, OTU 1140, OTU 1155).

^b Closest related sequences includes uncultured hits and are affiliated at least to phylum level using NCBI and SILVA SSU databases.

^c For detailed specification strains of closest related sequences are mentioned; * indicates an isolate; clones are presented in italics, and "genome" indicates complete genome sequence (from metagenome study).

^d Query values in %.

^e Maximum sequence identity [%] in BLASTn.

^f Accession number of closest sequence hit.

Figure A 1

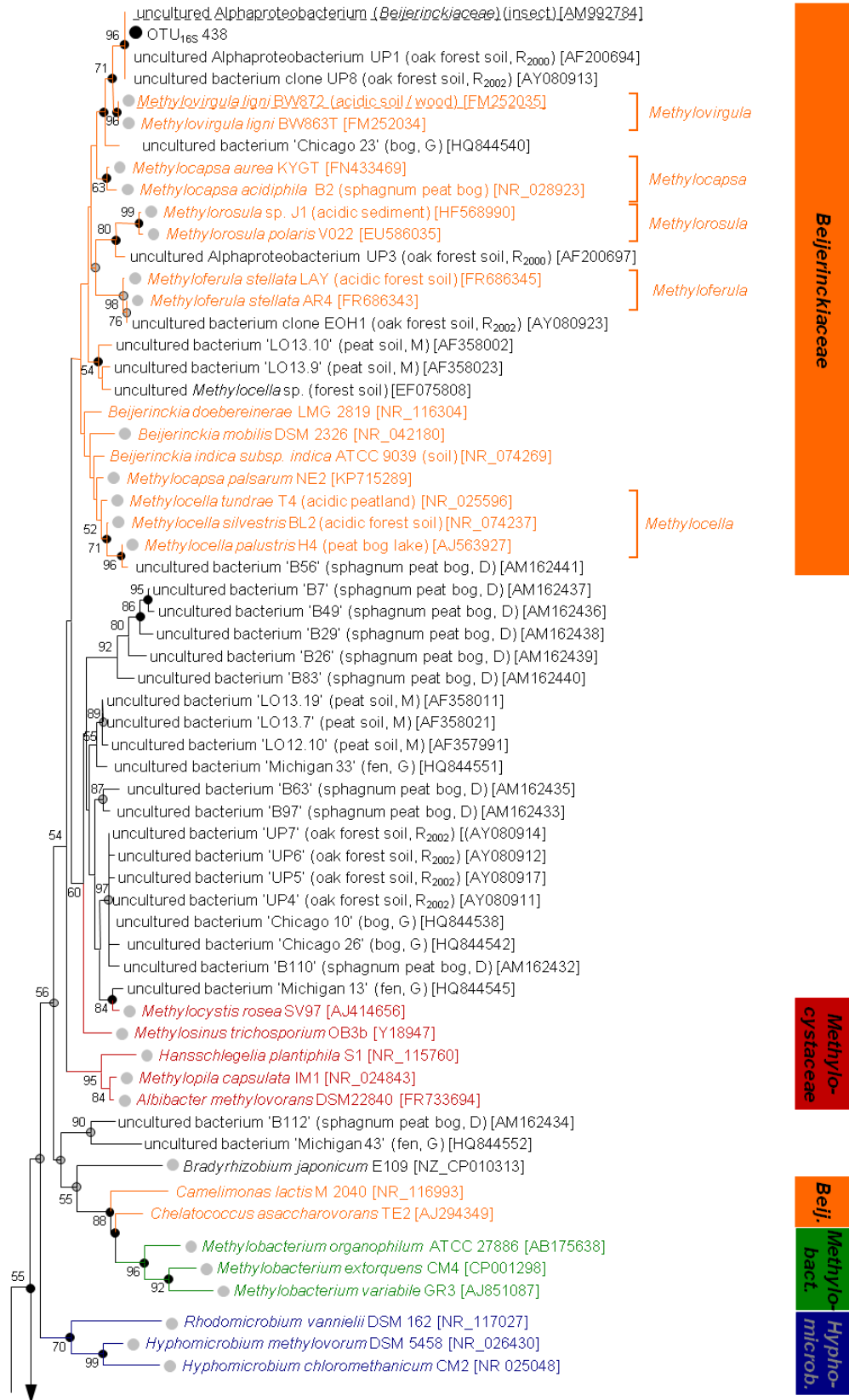
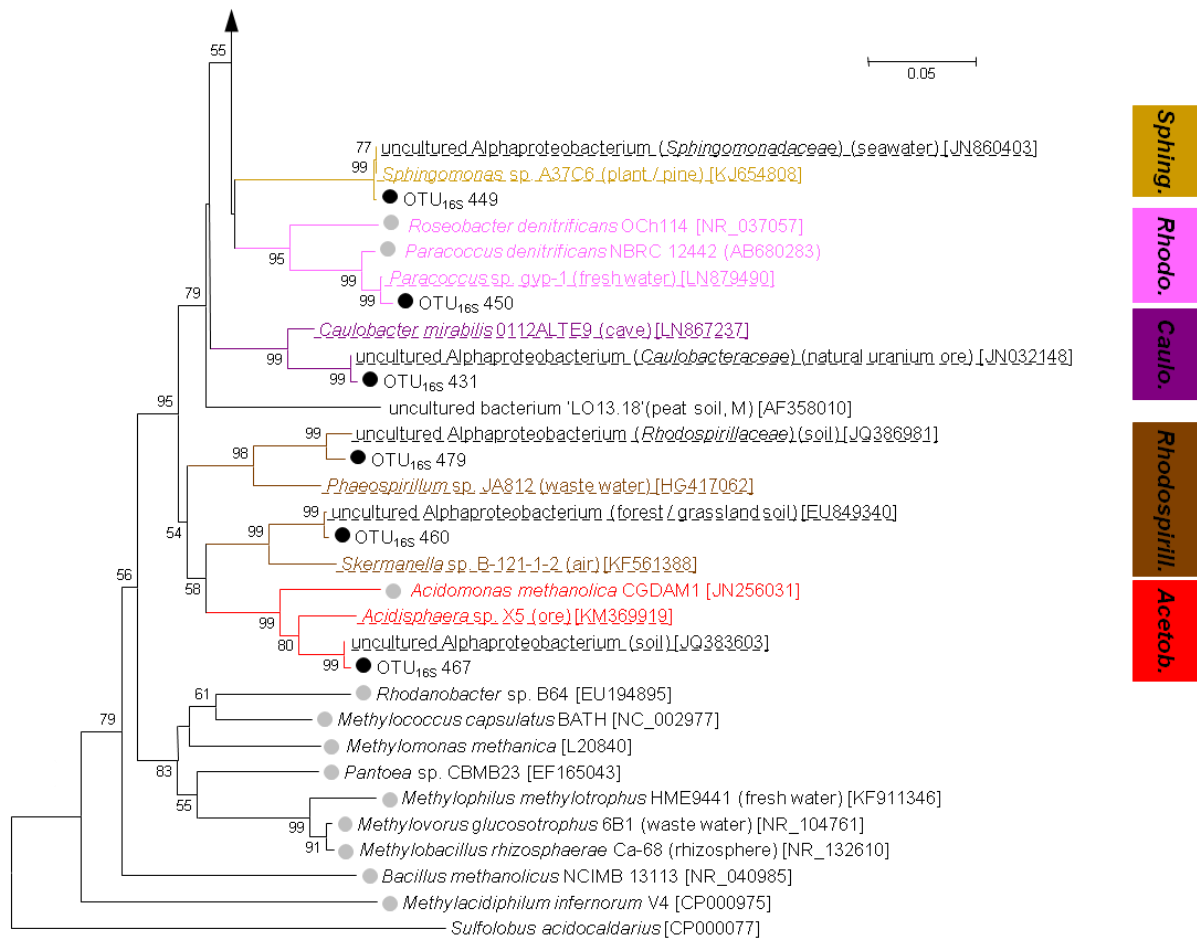


Figure A 1 continued on next page

Figure A 1 continued on previous page

**Figure A 1 Phylogenetic tree of Alphaproteobacteria-affiliated phylotypes.**

Phylotypes (●) are derived from the substrate and pH shift SIP experiments. The shown neighbour joining tree is based on 92 nucleotide sequences in total. The partial 16S rRNA sequence from the archaeal species *S. acidocaldarius* served as outgroup. Bootstrap values were calculated from 100 replicates and are shown for values ≥ 50 . Dots at the nodes indicate congruent nodes with trees based on the maximum likelihood and maximum parsimony method (●, true for both phylogenetic trees; ●, only true for one phylogenetic tree). The tree includes sequences from the next hits of the BLAST analysis (dashed underlined), sequences from uncultured microorganisms obtained in studies focussing on methane- and methanol-utilizing microorganisms in a forest soil and in acidic peat and bog soil environments (R₂₀₀₀, Radajewski *et al.*, 2000; R₂₀₀₂, Radajewski *et al.*, 2002; M, Morris *et al.*, 2002; D, Dedysh *et al.*, 2006; G, Gupta *et al.*, 2012) and sequences from known methanol-utilizing species (●). The phylogenetic affiliation on family level is indicated by the same font colour and coloured boxes (i.e., *Beijerinckiaceae*, *Methylocystaceae*, *Methylobacteriaceae*, *Hyphomicrobiaceae*, *Sphingomonadaceae*, *Rhodobacteraceae*, *Caulobacteraceae*, *Rhodospirillaceae*, *Acetobacteriaceae*). Sequences from methylotrophs affiliated with *Betaproteobacteria* (β) and *Gammaproteobacteria* (γ) are indicated with a grey box. If known the isolation origin of each sequence is given in brackets. Accession numbers are given in squared brackets. The bar indicates 0.05 change per nucleotide.

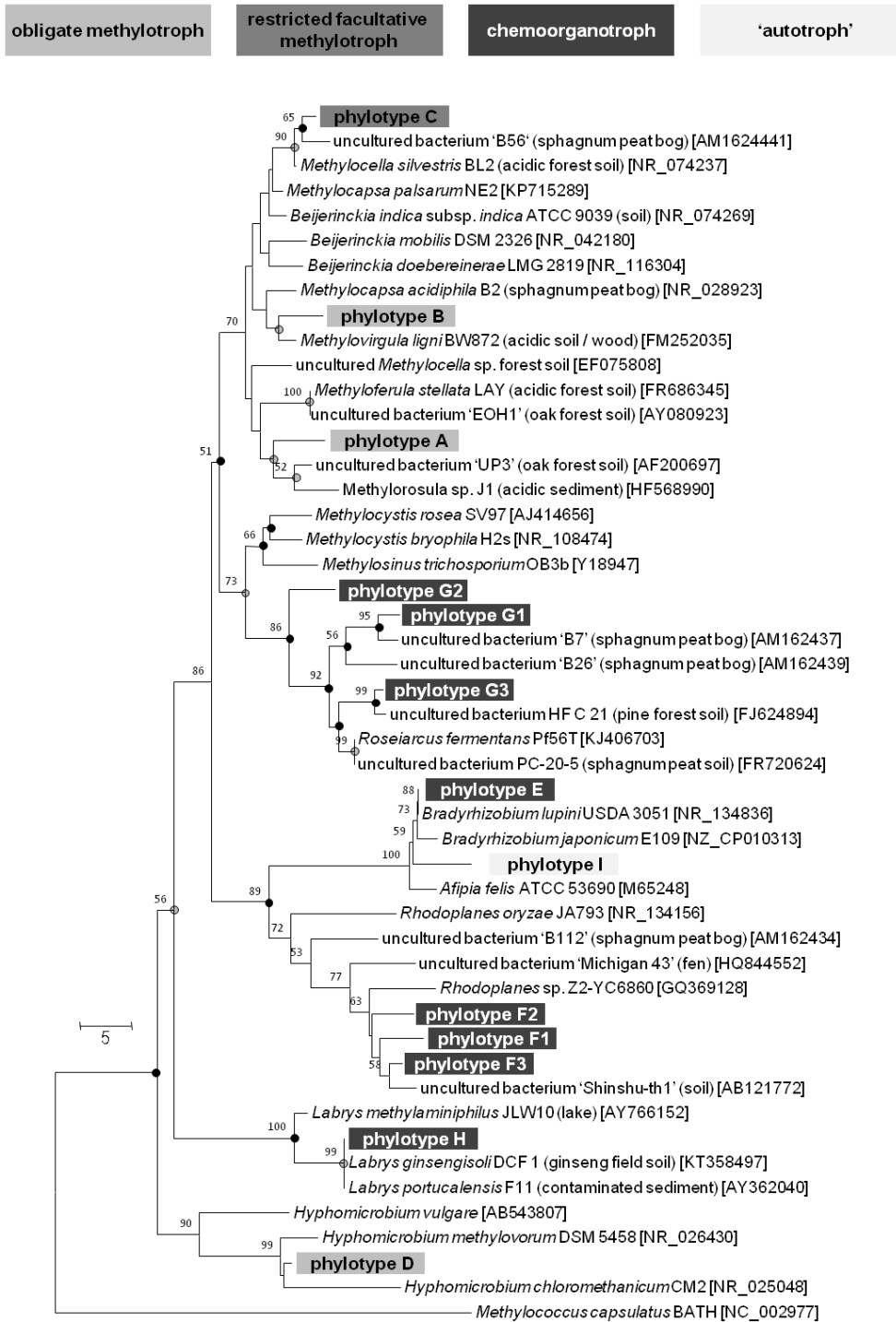


Figure A 2 Resolution of the *Beijerinckiaceae*-affiliated phylotype OTU_{16S}438

Taxa (phylotype A – I, based on species level similarity cut-off) comprised by the *Beijerinckiaceae*-affiliated phylotype OTU_{16S}438 and their trophic classification based on the conducted substrate SIP experiment (■ obligately methanolytrophic, only detected in methanol treatments; ■ restricted facultatively methylotrophic, detected in methanol and acetate treatments; ■ chemoorganotrophic, detected in multi-carbon substrate treatments; ■ autotrophic, detected in CO₂+methanol treatment). The shown neighbour joining tree is based on 49 nucleotide sequences in total. The partial 16S rRNA sequence of *Methylococcus capsulatus* BATH serves as outgroup. Bootstrap values were calculated from 1000 replicates and are shown for values ≥ 50. Dots at the nodes indicate congruent nodes with trees based on the maximum likelihood and maximum parsimony method (●, true for both phylogenetic trees; ○, only true for one phylogenetic tree). If known the isolation origin of each sequence is given in brackets. Accession numbers are given in squared brackets. The bar indicates 5 changes per nucleotide. This figure has been published in Morawe *et al.* 2017.

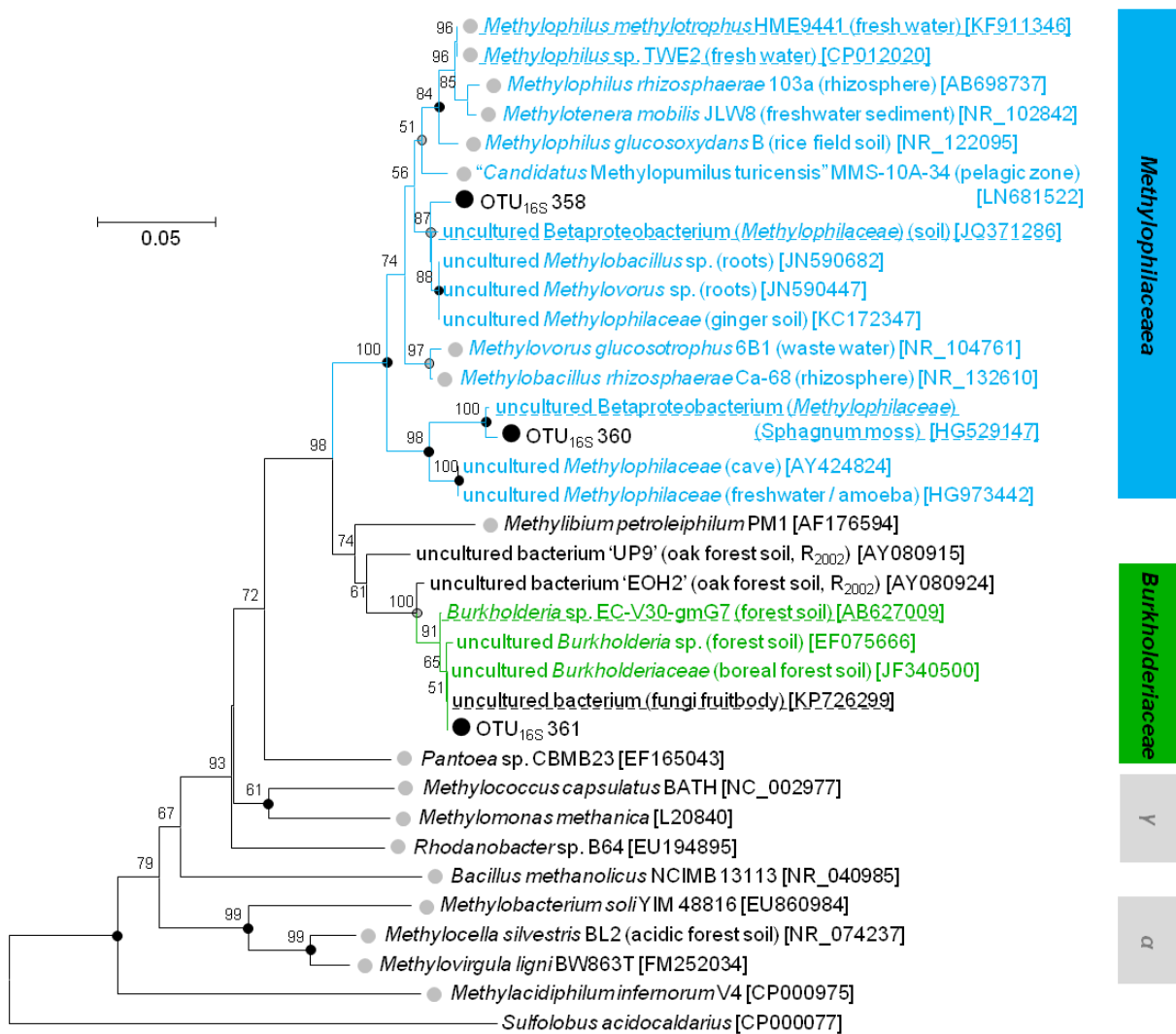


Figure A 3 Phylogenetic tree of *Betaproteobacteria*-affiliated phylotypes.

Phylotypes (●) are derived from the substrate and pH shift SIP experiments. The shown neighbour joining tree is based on 35 nucleotide sequences in total. The partial 16S rRNA sequence from the archaeal species *S. acidocaldarius* served as outgroup. Bootstrap values were calculated from 100 replicates and are shown for values ≥ 50 . Dots at the nodes indicate congruent nodes with trees based on the maximum likelihood and maximum parsimony method (●, true for both phylogenetic trees; ○, only true for one phylogenetic tree). The tree includes sequences from the next hits of the BLAST analysis (dashed underlined), sequences from uncultured microorganisms obtained in a study focussing on methanol-utilizing microorganisms in a forest soil [Radajewski *et al.*, 2002] (indicated with "R₂₀₀₂"), and sequences from known methanol-utilizing species (●). The phylogenetic affiliation on family level is indicated by coloured boxes (i.e., *Methylophilaceae*, *Burkholderiaceae*). Sequences from methylophilids affiliated with *Alphaproteobacteria* (α) and *Gammaproteobacteria* (γ) are indicated with a grey box. If known the isolation origin of each sequence is given in brackets. Accession numbers are given in squared brackets. The bar indicates 0.05 change per nucleotide.

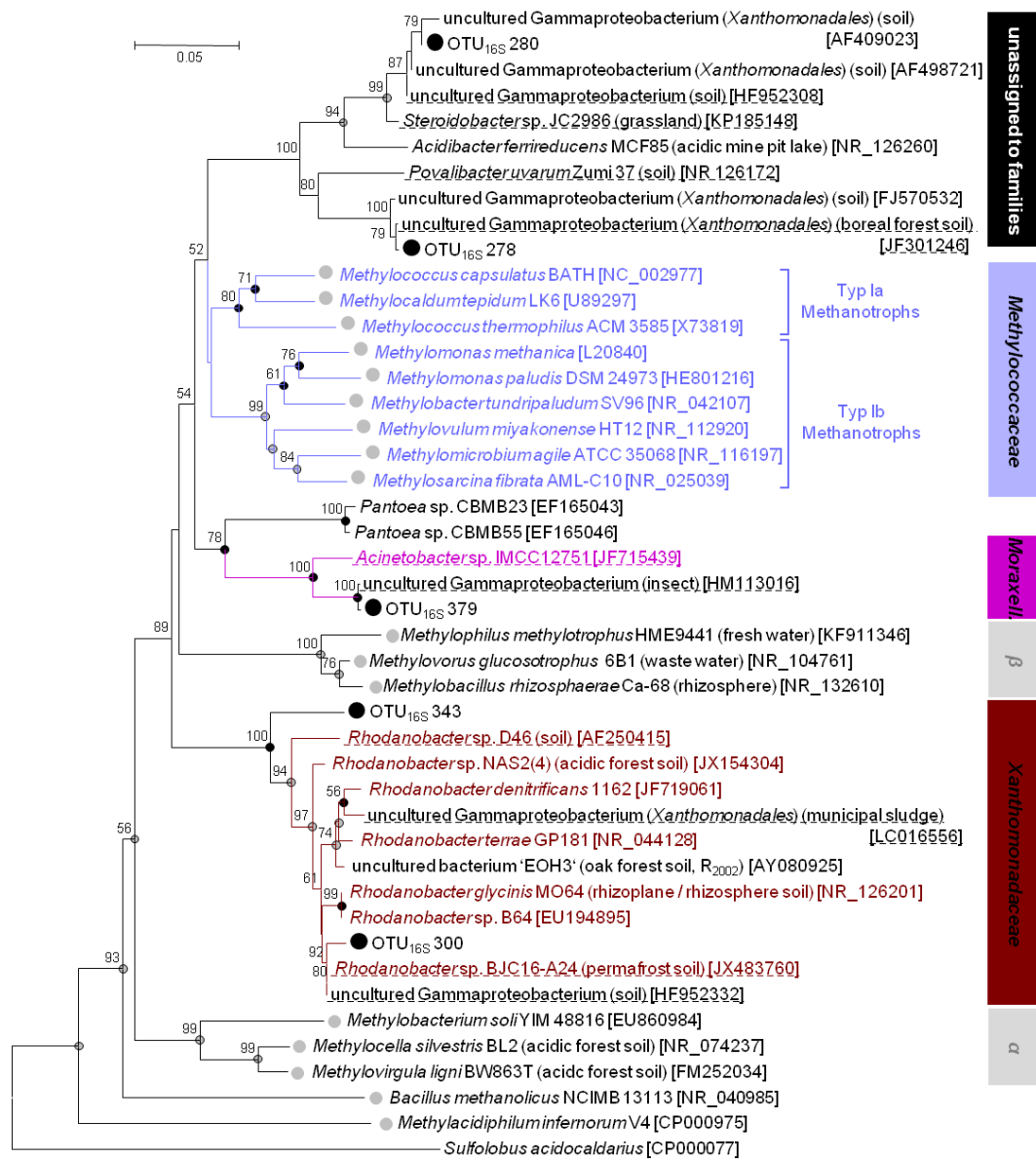


Figure A 4 Phylogenetic tree of Gammaproteobacteria -affiliated phylotypes.

Phylotypes (●) are derived from the substrate and pH shift SIP experiments. The shown neighbour joining tree is based on 45 nucleotide sequences in total. The partial 16S rRNA sequence from the archaeal species *S. acidocaldarius* served as outgroup. Bootstrap values were calculated from 1000 replicates and are shown for values ≥ 50 . Dots at the nodes indicate congruent nodes with trees based on the maximum likelihood and maximum parsimony method (●, true for both phylogenetic trees; ●, only true for one phylogenetic tree). The tree includes sequences from the next hits of the BLAST analysis (dashed underlined), sequences from uncultured microorganisms obtained in a study focussing on methanol-utilizing microorganisms in a forest soil [Radajewski *et al.*, 2002] (indicated with "R₂₀₀₂"), and sequences from known methanol-utilizing species (●). The phylogenetic affiliation to family level is indicated by the same font colour and coloured boxes (i.e., *Methylococcaceae*, *Moraxellaceae*, *Xanthomonadaceae*). Sequences from methylotrophs affiliated with *Alphaproteobacteria* ('α') and *Betaproteobacteria* ('β') are indicated with a grey box. If known the isolation origin of each sequence is given in brackets. Accession numbers are given in squared brackets. The bar indicates 0.05 change per nucleotide.

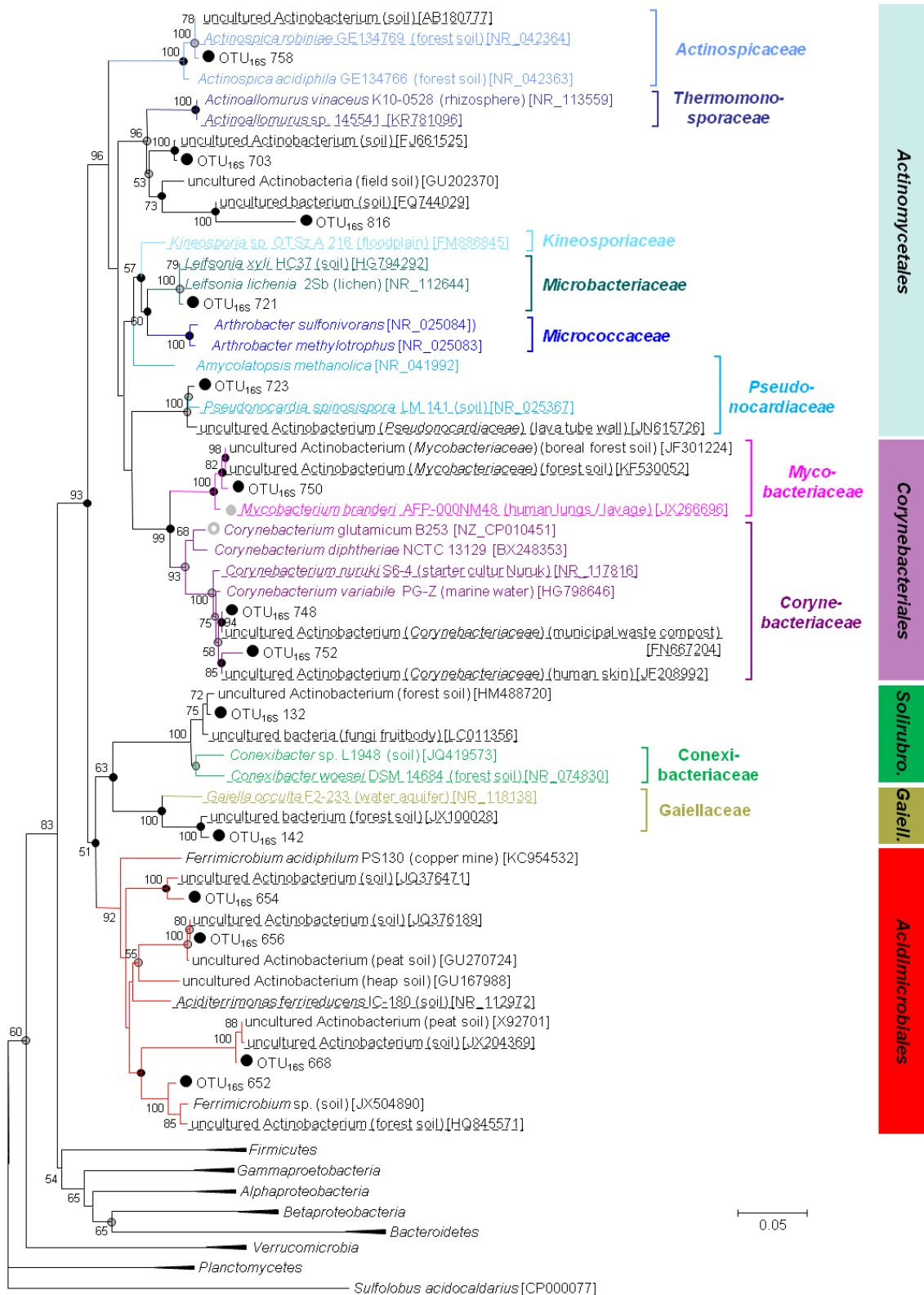


Figure A 5 Phylogenetic tree of Actinobacteria-affiliated phylotypes.

Phylotypes (●) are derived from the substrate and pH shift SIP experiments. The shown neighbour joining tree is based on 63 nucleotide sequences in total. The partial 16S rRNA sequence from the archaeal species *S. acidocaldarius* served as outgroup and phyla besides *Actinobacteria* are condensed. Bootstrap values were calculated from 100 replicates and are shown for values ≥ 50 . Dots at the nodes indicate congruent nodes with trees based on the maximum likelihood and maximum parsimony method (●, true for both phylogenetic trees; ●, only true for one phylogenetic tree). The tree includes i.a. sequences from the next hits of the BLAST analysis (dashed

underlined) and sequences from known methanol-utilizing species (indicated with ●, methanol used as carbon source; ○, methanol not used as carbon source). Phylogenetic affiliation on family level is indicated by the same font colour and the phylogenetic affiliation on order level is indicated by coloured boxes (i.e., *Actinomycetales*, *Corynebacteriales*, *Solirubrobacterales*, *Gaiellales*, *Acidimicrobiales*). If known the isolation origin of each sequence is given in brackets. Accession numbers are given in squared brackets. The bar indicates 0.05 change per nucleotide.

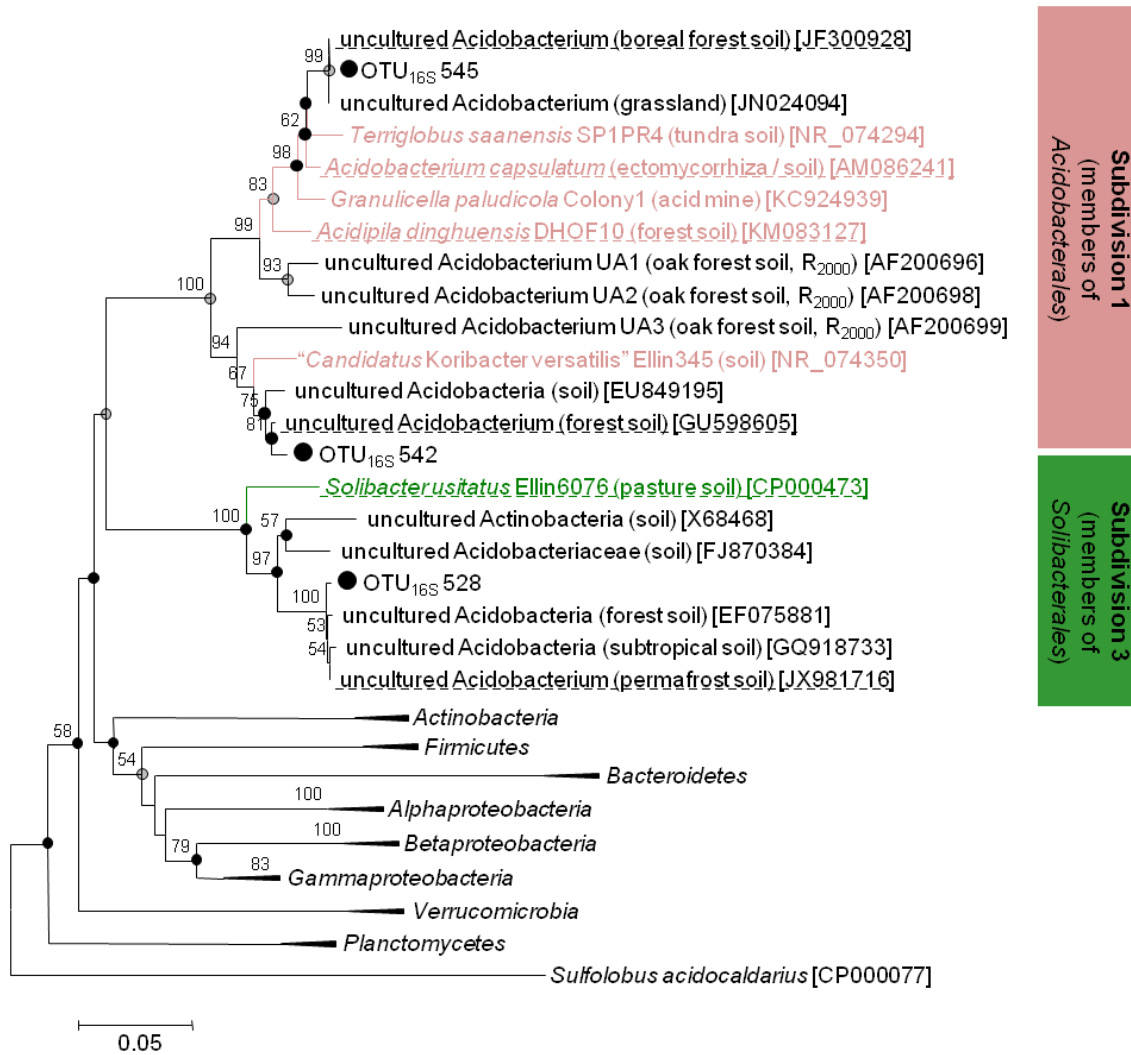


Figure A 6 Phylogenetic tree of *Acidobacteria*-affiliated phylotypes.

Phylotypes (●) are derived from the substrate and pH shift SIP experiments. The shown neighbour joining tree includes is based on 33 nucleotide sequences in total. The partial 16S rRNA sequence from the archaeal species *S. acidocaldarius* served as outgroup and phyla besides *Acidobacteria* are condensed. Bootstrap values were calculated from 100 replicates and are shown for values ≥ 50 . Dots at the nodes indicate congruent nodes with trees based on the maximum likelihood and maximum parsimony method (●, true for both phylogenetic trees; ○, only true for one phylogenetic tree). The tree includes sequences from the next hits of the BLAST analysis (dashed underlined) and sequences of putatively methanol-utilizing uncultured *Acidobacteria* obtained in a methanol based SIP experiment [Radajewski *et al.*, 2000] (indicated with 'R₂₀₀₀'). If known the isolation origin of each sequence is given in brackets. Accession numbers are given in squared brackets. The bar indicates 0.05 change per nucleotide.

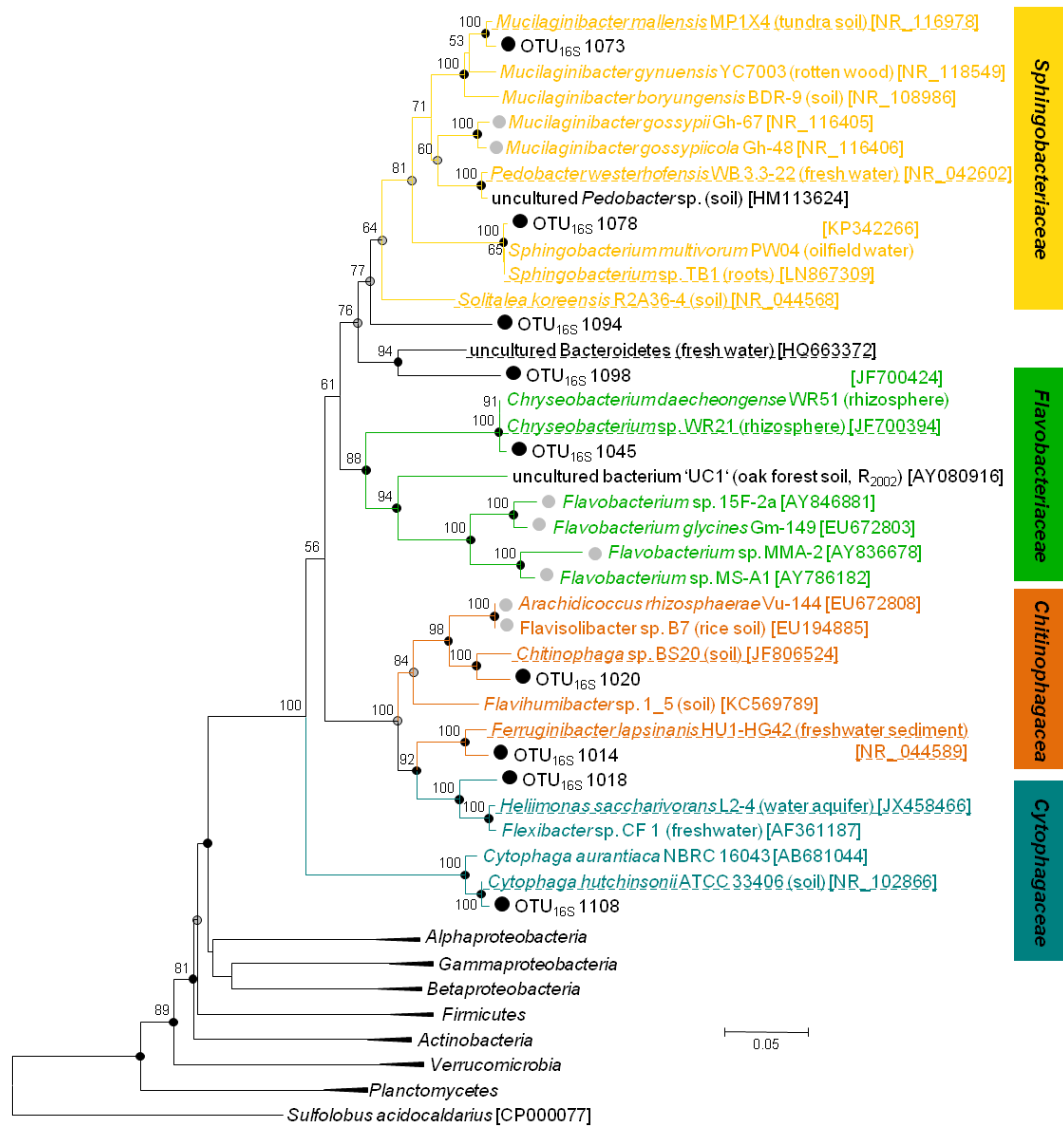


Figure A 7 Phylogenetic tree of *Bacteroidetes*-affiliated phylotypes.

Phylotypes (●) are derived from the substrate and pH shift SIP experiments. The shown neighbour joining tree is based on 45 nucleotide sequences in total. The partial 16S rRNA sequence from the archaeal species *S. acidocaldarius* served as outgroup and phyla besides *Bacteroidetes* are condensed. Bootstrap values were calculated from 1000 replicates and are shown for values ≥ 50 . Dots at the nodes indicate congruent nodes with trees based on the maximum likelihood and maximum parsimony method (●, true for both phylogenetic trees; ●, only true for one phylogenetic tree). The tree includes sequences from the next hits of the BLAST analysis (dashed underlined), sequences from uncultured microorganisms obtained in a study focussing on methanol-utilizing microorganisms in a forest soil [Radajewski *et al.*, 2002] (indicated with "R₂₀₀₂"), and sequences from known or putatively methanol-utilizing species (●). The phylogenetic affiliation on family level is indicate by the same font colour and coloured boxes (i.e., *Sphingobacteriaceae*, *Flavobacteriaceae*, *Chitinophagaceae*, *Cytophagaceae*). If known the isolation origin of each sequence is given in brackets. Accession numbers are given in squared brackets. The bar indicates 0.05 change per nucleotide.

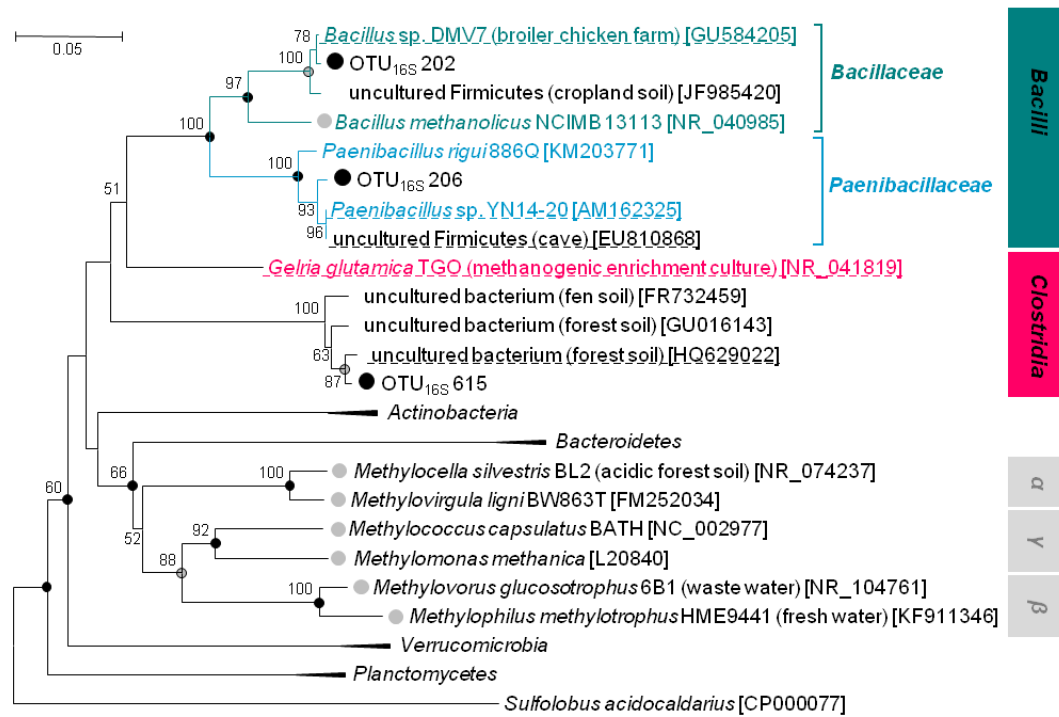


Figure A 8 Phylogenetic tree of *Firmicutes* -affiliated phylotypes.

Phylotypes (●) are derived from the substrate and pH shift SIP experiments. The shown neighbour joining tree is based on 24 nucleotide sequences in total. The partial 16S rRNA sequence from the archaeal species *S. acidocaldarius* served as outgroup and phyla besides *Firmicutes* are condensed. Bootstrap values were calculated from 1000 replicates and are shown for values ≥ 50 . Dots at the nodes indicate congruent nodes with trees based on the maximum likelihood and maximum parsimony method (●, true for both phylogenetic trees; ●, only true for one phylogenetic tree). The tree includes i.a. sequences from the next hits of the BLAST analysis (dashed underlined) and sequences from known methanol-utilizing species (●). The phylogenetic affiliation on family level is indicated by the same font colour and the phylogenetic affiliation on class level is indicated by coloured boxes (i.e., **Bacilli**, **Clostridia**). Sequences from methylophils affiliated with Alpha- (' α '), Beta- (' β '), and Gammaproteobacteria (' γ ') are indicated with a grey box. If known the isolation origin of each sequence is given in brackets. Accession numbers are given in squared brackets. The bar indicates 0.05 changes per nucleotide.

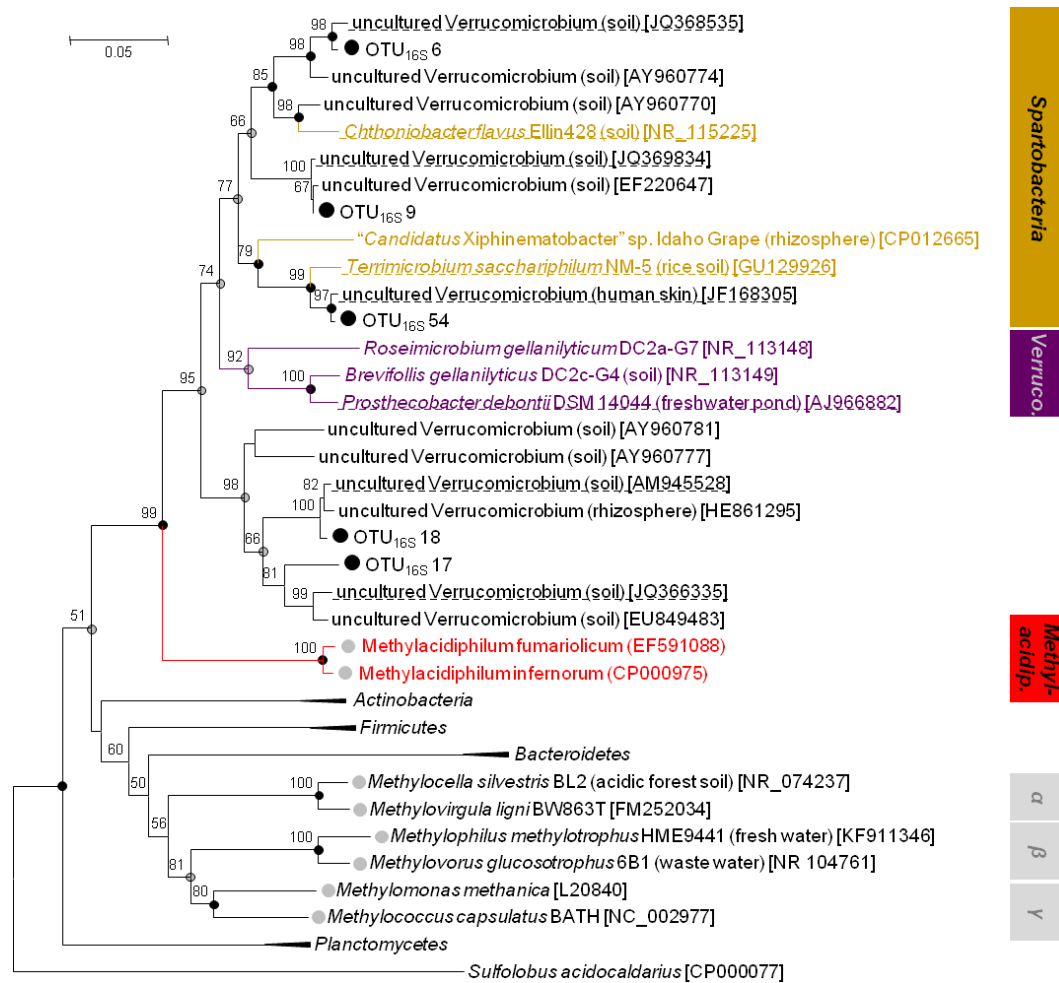


Figure A 9 Phylogenetic tree of *Verrucomicrobia*-affiliated phylotypes.

Phylotypes (●) are derived from the substrate and pH shift SIP experiments. The shown neighbour joining tree is based on 36 nucleotide sequences in total. The partial 16S rRNA sequence from the archaeal species *S. acidocaldarius* served as outgroup and phyla besides *Verrucomicrobia* are condensed. Bootstrap values were calculated from 1000 replicates and are shown for values ≥ 50 . Dots at the nodes indicate congruent nodes with trees based on the maximum likelihood and maximum parsimony method (●, true for both phylogenetic trees; •, only true for one phylogenetic tree). The tree includes i.a. sequences from the next hits of the BLAST analysis (dashed underlined) and sequences from known methanol-utilizing species (●). The phylogenetic affiliation on class or family level is indicated by the same font colour coloured boxes (i.e., *Spartobacteria*, *Verrucomicrobia*, *Methyloacidipilaceae*). Sequences from methylophilus affiliated with *Alpha-* (α), *Beta-* (β), and *Gammaproteobacteria* (γ) are indicated with a grey box. If known the isolation origin of each sequence is given in brackets. Accession numbers are given in squared brackets. The bar indicates 0.05 changes per nucleotide.

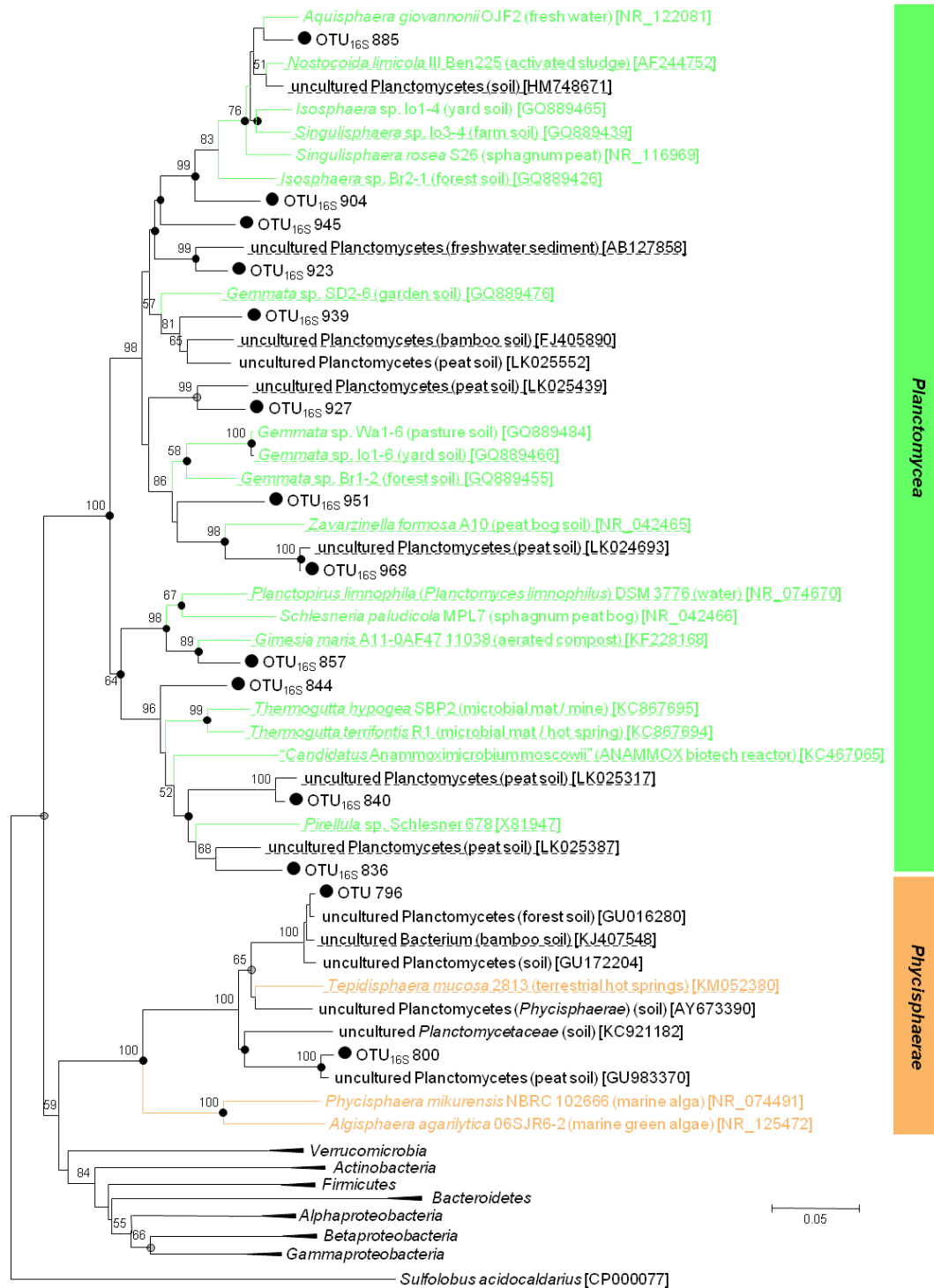


Figure A 10 Phylogenetic tree of *Planctomycetes*-affiliated phylotypes.

Phylotypes (●) are derived from the substrate and pH shift SIP experiments. The shown neighbour joining tree is based on 58 nucleotide sequences in total. The partial 16S rRNA sequence from the archaeal species *S. acidocaldarius* served as outgroup and phyla besides *Planctomycetes* are condensed. Bootstrap values were calculated from 1000 replicates and are shown for values ≥ 50 . Dots at the nodes indicate congruent nodes with trees based on the maximum likelihood and maximum parsimony method (●, true for both phylogenetic trees; •, only true for one phylogenetic tree). The tree includes sequences from the next hits of the BLAST analysis (dashed underlined,). The phylogenetic affiliation on class level is indicate by coloured boxes (i.e., *Planctomycea*, *Phycisphaerae*). If known the isolation origin of each sequence is given in brackets. Accession numbers are given in squared brackets. The bar indicates 0.05 change per nucleotide.

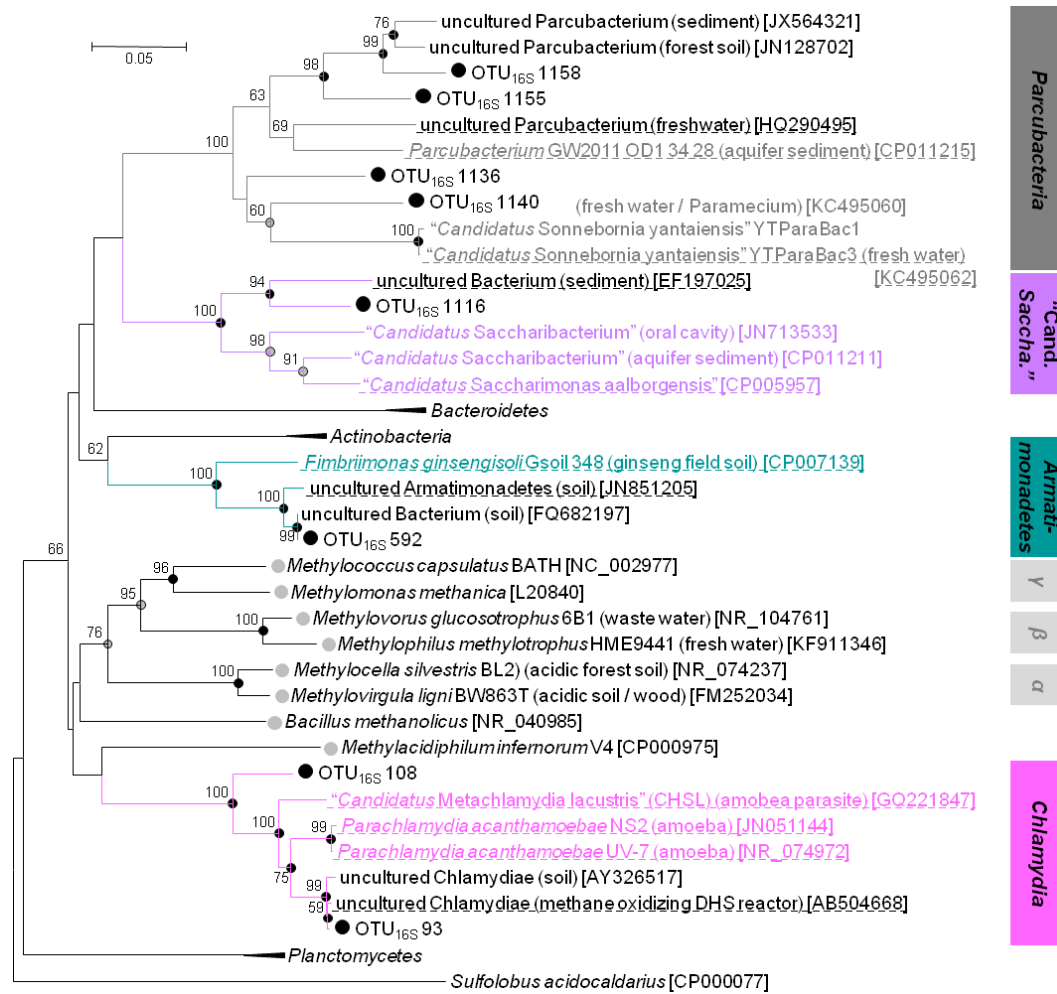


Figure A 11 Phylogenetic tree of phylotypes affiliated to *Parcubacteria*, *Armatimonadetes*, *Chlamydia*, and "Candidatus *Saccharibacteria*".

Phylotypes (●) are derived from the substrate and pH shift SIP experiments. The shown neighbour joining tree is based on 38 nucleotide sequences in total. The partial 16S rRNA sequence from the archaeal species *S. acidocaldarius* served as outgroup and phyla besides the four mentioned phyla are condensed. Bootstrap values were calculated from 1000 replicates and are shown for values ≥ 50 . Dots at the nodes indicate congruent nodes with trees based on the maximum likelihood and maximum parsimony method (●, true for both phylogenetic trees; ●, only true for one phylogenetic tree). The tree includes sequences from the next hits of the BLAST analysis (dashed underlined) and sequences from known methanol-utilizing species (●). The phylogenetic affiliation on phylum level is indicated by coloured boxes (i.e., *Parcubacteria*, *Armatimonadetes*, *Chlamydia*, and "Candidatus *Saccharibacteria*"). If known the isolation origin of each sequence is given in brackets. Accession numbers are given in squared brackets. The bar indicates 0.05 change per nucleotide.

Figure A 12

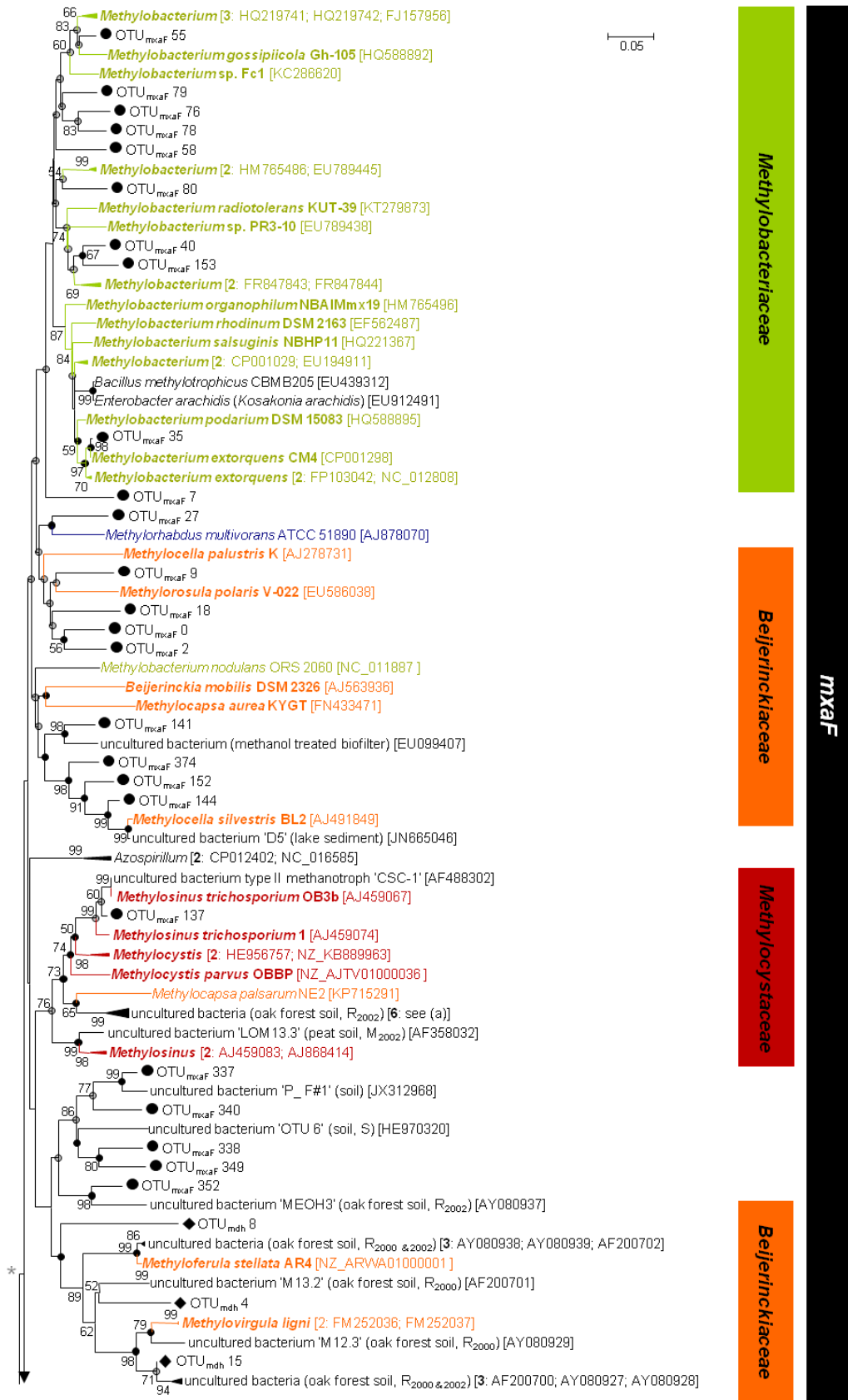


Figure A 12 Figure A 12 continued on next page

Figure A 12 continued on previous page

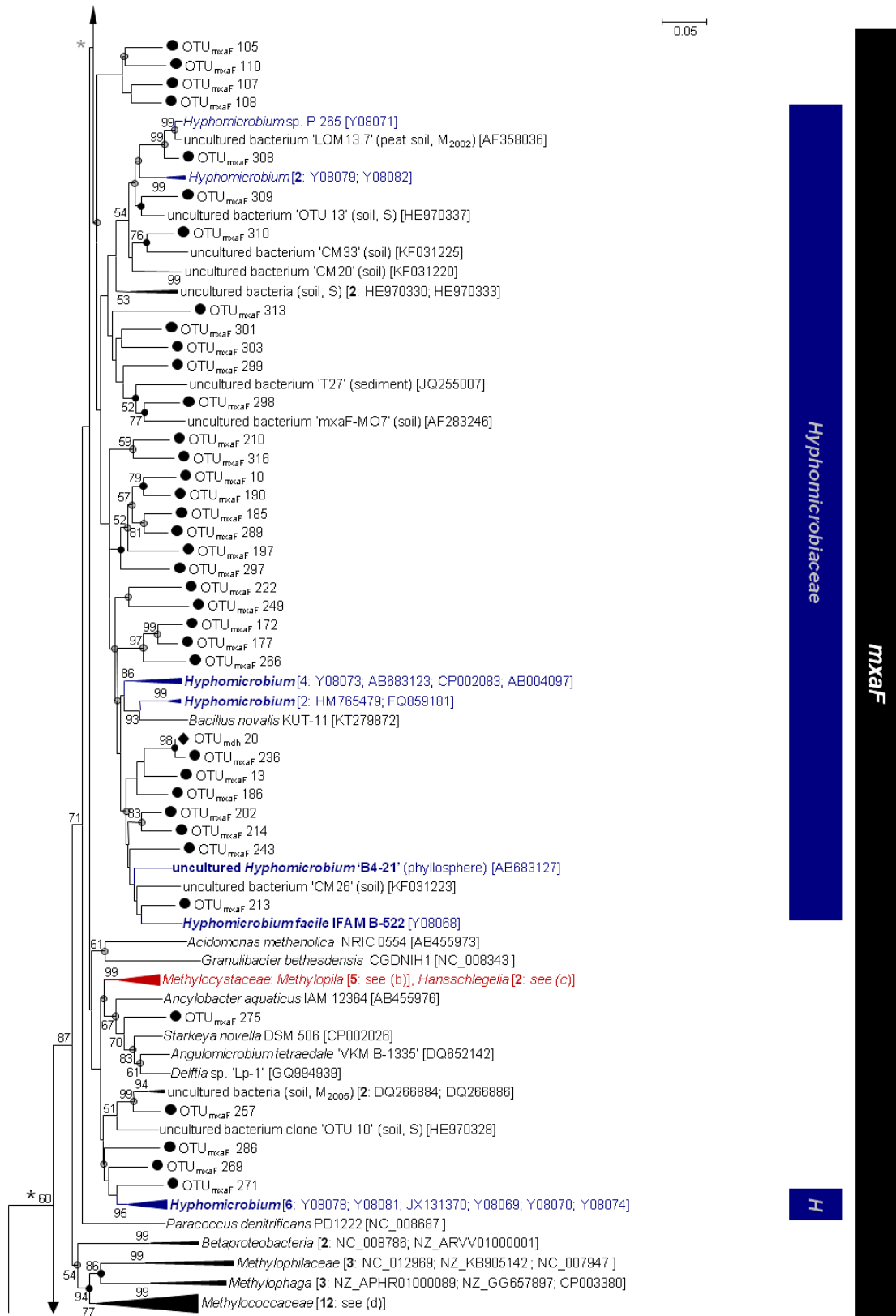


Figure A 12

Figure A 12 continued on next page

Figure A 12 continued on previous page

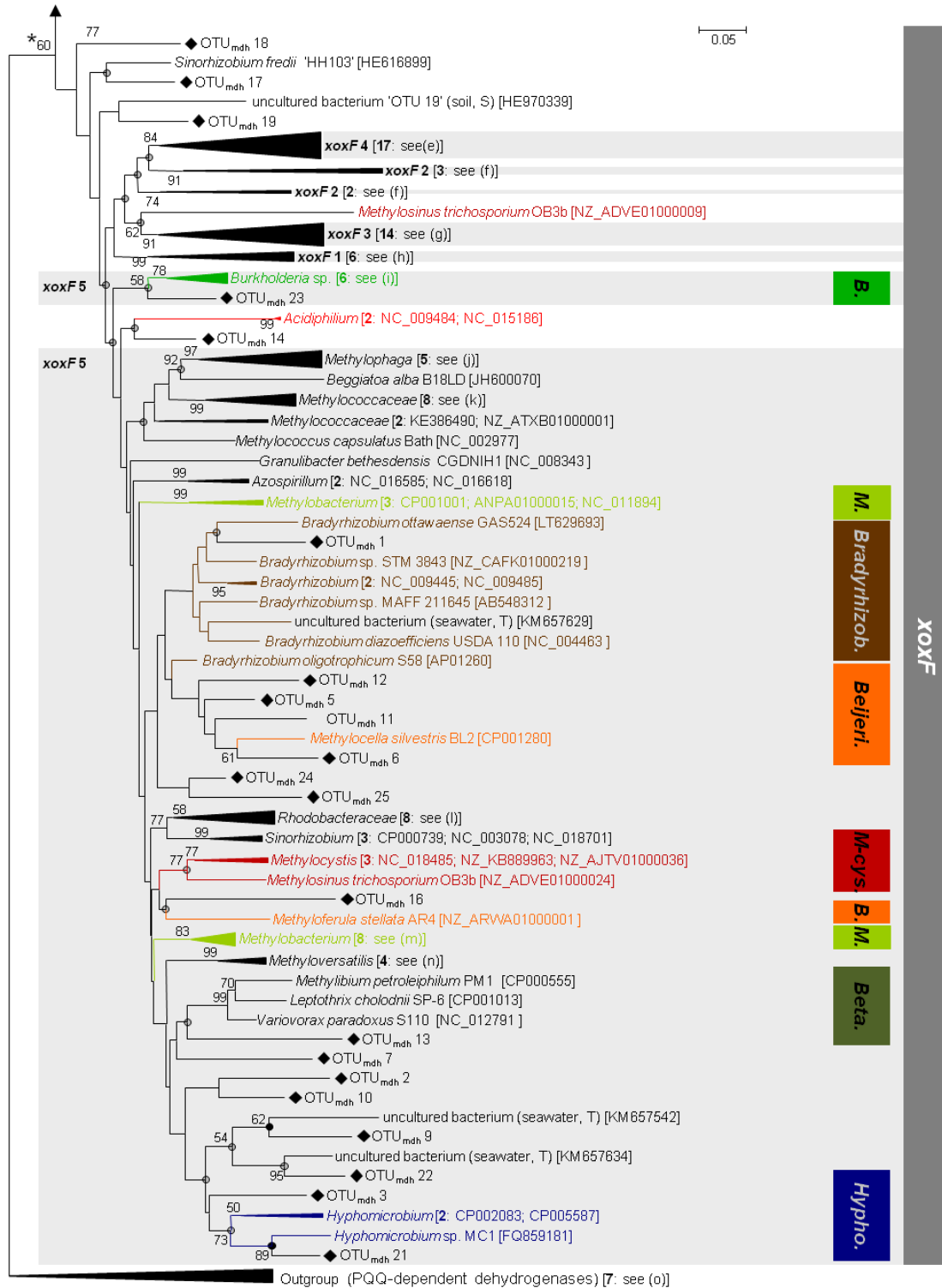


Figure A 12 Phylogenetic tree of all *mxoF* and *xoxF* phylotypes obtained in all SIP experiments.

Explanation of Figure A 12. Neighbour joining tree of all detected *mxoF* and *xoxF* phylotypes of the substrate SIP and pH shift SIP experiment (OTU_{*mxoF*} 0 to 374; indicated with ●) and the methanol/chloromethane SIP experiment (OTU_{MDH} 1 to 25; indicated with ◆). The tree is based on 352 nucleotide sequences. Sequences from other PQQ-dependent dehydrogenases served as outgroup. Bootstrap values were calculated from 100 replicates and are shown for values ≥ 50. Dots at the nodes indicate congruent nodes with trees based on the maximum likelihood and maximum parsimony method (●, congruent in all phylogenetic trees; •, only congruent with one phylogenetic tree). The bar indicates 0.05 change per nucleotide.

The tree includes known *mxoF* and *xoxF* sequences of several bacteria and from genomic annotations. Phylogenetic affiliation is indicated by the same font colour and coloured boxes (i.e., **Methylobacteriaceae**, **Beijerinckiaceae**, **Methylocystaceae**, **Hyphomicrobiaceae**, **Burkholderiaceae**, **Bradyrhizobiaceae**, and **unclassified Betaproteobacteria**). The tree includes also sequences of uncultured bacteria from different studies focussing on methylotrophs. The origin of the sequences as well as the study is given in brackets (i.e., M₂₀₀₂, Morris *et al.*, 2002; M₂₀₀₅, Moosvi *et al.*, 2005; R₂₀₀₀, Radajewski *et al.*, 2000; R₂₀₀₂, Radajewski *et al.*, 2002; S, Stacheter *et al.*, 2013; T, Taubert *et al.*, 2015).

Accession numbers of sequences are always given in squared brackets. In the case of condensed branches the number of sequences (in bold) and the accession numbers are given in squared brackets or listed below (condensed branch name is given):

mxoF

uncultured bacteria (oak forest soil, R₂₀₀₂) [**6**: AY080930; AY080932; AY080933; AY080934; AY080935; AY080936]

Methylocystaceae - *Methylopila* [**5**: AJ878071; JQ582798; KP407883; JX134090; JX134089]

Methylocystaceae - *Hansschlegelia* [**2**: DQ652143; DQ652144]

Methylococcaceae [**12**: *Methylohalobius* [NZ_ATXB01000001]; *Methylocaldum* [KE386490]; *Methylococcus* [NC_002977]; *Methylomicrobium* [**3**: NC_016112; NZ_KB455575; CM001475]; *Methylovulum* [NZ_KB913025]; *Methylobacter* [JX312967]; *Methylomonas* [NC_015572]; *Methylosarcina* [NZ_KB889965]; *Methylobacter* [**2**: NZ_JH109154; KB912877]]

xoxF 4 (*Methylophilaceae*)

CP001672; NC_014207; NZ_KB905141; NZ_KB905146; NZ_AAUX01000001; DS995299; NC_007947; NC_012969; CP001672; NC_014207; NC_012969; NZ_KB905145; NC_007947; NC_012969; NC_014207; NC_007947

xoxF 2 (*Verrucomicrobia*)

CP002221; NC_010794; NZ_CAHT01000021; NC_013260; DQ084247

xoxF 3 (*Rhizobiales*, some *Betaproteobacteria*, and *Gammaproteobacteria*)

NC_018485; NZ_KB889963; NZ_CAFK01000299; NC_008536; NZ_KB912877; KE386490; NC_007947; NC_011666; NZ_ARWA01000001; NC_012791; CP000741; NC_011894; CP002279; NC_016617

xoxF 1 (*Xanthomonas* and *Beijerinckiaceae*)

NC_003919; NZ_AEQX01000324; NC_010688; NC_013260; NC_011666; NZ_ARWA01000001

xoxF 5 (various *Alphaproteobacteria*, *Betaproteobacteria* and *Gammaproteobacteria*)

Burkholderia sp. [**6**: NC_015137; NC_007952; NC_016625; NC_010625; CP012748; CP002014]

Methylophaga [**5**: NZ_GG657899; NC_017857; CP003380; NZ_APHR01000021; NZ_APHR01000099]

Methylococcaceae [**8**: NC_016112; NZ_KB455575; CM001475; NZ_KB889965; NZ_KB912877; NC_015572; NZ_KB913025]

Rhodobacteraceae [**8**: CH902584; ABCL01000006; NZ_DS022277; NC_008686; NC_022041; NZ_AAYA01000026; NC_008209; NC_015730]

Methylobacterium [**8**: CP000943; AP014809; CP001298; NC_012808; NC_011894; CP017640; CP001001; ANPA01000003]

Methyloversatilis [**4**: NZ_AFHG01000059; NZ_ARVV01000001; NZ_KB900539; EU548065]

Outgroup (PQQ-dependent dehydrogenases)

NC_008825; AF355798; CP000555; AF326086; JN808865; EU548063; EU548066

APPENDICES

Table A 13 Phylogenetic affiliation of fungal taxa in the substrate and pH shift SIP experiment

Sequences were derived at species-level cut-off (98.1%). Listed are reference sequences of the UNITE database (<https://unite.ut.ee/analysis.php>) and their phylogenetic affiliation based on the dynamic UNITE database (v7 release 1.08.2015) using MOTHUR. This table has been published in Morawe *et al.* 2017.

OTU	Reference sequence ^a					Phylogeny ^b				
		Accession ^c	SH code ^d	Q ^e	Id ^f	Phyl ^g	Class	Order	Family	Genus
1	<i>Trichosporon porosum</i>	NR_073209	SH196641.07FU	100	100	Baso	Tremellomycetes	Trichosporonales	Trichosporonaceae	<i>Trichosporon</i>
2	<i>Saccharomycetales</i>	FN610974	SH180919.07FU	100	100	Asco	Saccharomycetes	NA	NA	NA
4	<i>Mortierella humilis</i>	KP772755		100	100	Zygo	<i>Incertae sedis</i>	Mortierellales	Mortierellaceae	<i>Mortierella</i>
5	<i>Mortierella</i>	JQ312759		99	98	Zygo	<i>Incertae sedis</i>	Mortierellales	Mortierellaceae	<i>Mortierella</i>
6	<i>Cryptococcus terricola</i>	NR_073221	SH190017.07FU	100	100	Baso	Tremellomycetes	Tremellales	<i>Incertae sedis</i>	<i>Cryptococcus</i>
7	<i>Ganoderma applanatum</i>	KJ857258	SH187220.07FU	100	100	Baso	Agaricomycetes	Polyporales	Ganodermataceae	<i>Ganoderma</i>
8	<i>Trichoderma viride</i>	X93980	SH187755.07FU	100	100	Asco	Sordariomycetes	Hypocreales	Hypocreaceae	<i>Trichoderma</i>
9	<i>Oidiodendron</i>	HM488481	SH216993.07FU	100	100	Asco	Leotiomycetes	<i>Incertae sedis</i>	Myxotrichaceae	<i>Oidiodendron</i>
10	<i>Penicillium</i>	FJ379809	SH182493.07FU	100	100	Asco	Eurotiomycetes	Eurotiales	Trichocomaceae	<i>Penicillium</i>
11	<i>Tomentella radiosa</i>	UDB017828	SH184517.07FU	100	100	Baso	Agaricomycetes	Thelephorales	Thelephoraceae	<i>Tomentella</i>
12	<i>Hyaloriaceae</i>	HQ021773	SH021770.07FU	97	96	Baso	Agaricomycetes	NA	NA	NA
13	<i>Cryptococcus podzolicus</i>	NR_073213	SH181879.07FU	100	100	Baso	Tremellomycetes	Tremellales	<i>Incertae sedis</i>	<i>Cryptococcus</i>
14	<i>Paecilomyces</i>	LN886697		98	97	Asco	Eurotiomycetes	Eurotiales	Trichocomaceae	<i>Paecilomyces</i>
15	<i>Leucosporidiales</i>	FN565254	SH193764.07FU	100	100	Baso	Microbotryomycetes	Leucosporidiales	NA	NA
16	<i>Tolypocladium cylindrosporum</i>	KJ028796	SH184933.07FU	100	99	Asco	Sordariomycetes	Hypocreales	Ophiocordycipitaceae	<i>Elaphocordyceps</i>
17	<i>Oidiodendron</i>	KF212286	SH217009.07FU	98	98	Asco	Leotiomycetes	<i>Incertae sedis</i>	Myxotrichaceae	<i>Oidiodendron</i>
18	<i>Nectria ramulariae</i>	FR717232	SH217194.07FU	100	100	Asco	Sordariomycetes	Hypocreales	Nectriaceae	<i>Nectria</i>
19	<i>Mortierellales</i>	GU366727	SH026735.07FU	100	100	Zygo	<i>Incertae sedis</i>	Mortierellales	Mortierellaceae	<i>Mortierella</i>
20	<i>Elaphomyces</i>	HQ021974	SH190236.07FU	100	100	Asco	Eurotiomycetes	Eurotiales	Elaphomycetaceae	<i>Elaphomyces</i>
21	<i>Dermateaceae</i>	HQ021920	SH196224.07FU	99	98	Asco	Leotiomycetes	Helotiales	Dermateaceae	NA

APPENDICES

OTU	Reference sequence ^a				Phylogeny ^b					
	Accession ^c	SH code ^d	Q ^e	Id ^f	Phyl ^g	Class	Order	Family	Genus	
22	<i>Syzygospora</i>	HQ211619	SH182180.07FU	100	100	Baso	Tremellomycetes	Cystofilobasidiales	Incertae sedis	<i>Syzygospora</i>
23	<i>Mortierella gamsii</i>	AJ878509	SH193938.07FU	100	100	Zygo	Incertae sedis	Mortierellales	Mortierellaceae	<i>Mortierella</i>
24	<i>Bionectria</i>	GQ219910	SH211202.07FU	100	100	Asco	Sordariomycetes	Hypocreales	Bionectriaceae	<i>Bionectria</i>
25	<i>Glomeromycetes</i>	JF300543	SH462390.07FU	98	96	Glom	Glomeromycetes	NA	NA	NA
26	<i>Glomeromycetes</i>	JF300543	SH462390.07FU	97	95	Glom	Glomeromycetes	NA	NA	NA
27	<i>Laccaria amethystina</i>	HM189774	SH220959.07FU	100	100	Baso	Agaricomycetes	Agaricales	Hydnangiaceae	<i>Laccaria</i>
28	<i>Cryptococcus podzolicus</i>	DQ069015	SH181879.07FU	97	96	Baso	Tremellomycetes	Tremellales	Incertae sedis	<i>Cryptococcus</i>
29	<i>Rozellomycota</i>	AF504877	SH211778.07FU	100	99	Roz	NA	NA	NA	NA
30	<i>Trechispora</i>	FJ820706	SH009022.07FU	99	99	Baso	Agaricomycetes	Trechisporales	Hydnodontaceae	<i>Trechispora</i>
31	<i>Inocybe napipes</i>	AM882927	SH196058.07FU	100	100	Baso	Agaricomycetes	Agaricales	Inocybaceae	<i>Inocybe</i>
32	<i>Oidiodendron</i>	FJ475564	SH216991.07FU	99	99	Asco	Leotiomycetes	Incertae sedis	Myxotrichaceae	<i>Oidiodendron</i>
33	Mortierellaceae	JQ666581	SH208762.07FU	100	100	Zygo	Incertae sedis	Mortierellales	Mortierellaceae	<i>Mortierella</i>
35	<i>Volutella</i>	HM136667	SH474556.07FU	100	100	Asco	Sordariomycetes	Hypocreales	Nectriaceae	<i>Volutella</i>
37	<i>Mycena cinerella</i>	UDB021984	SH220720.07FU	100	100	Baso	Agaricomycetes	Agaricales	Mycenaceae	<i>Mycena</i>
38	<i>Rozellomycota</i>	JQ666464	SH001662.07FU	99	99	Roz	NA	NA	NA	NA
39	<i>Leptodontidium trabinellum</i>	GU934588	SH019513.07FU	100	100	Asco	Leotiomycetes	Helotiales	Incertae sedis	<i>Leptodontidium</i>
40	<i>Chaunopycnis</i>	GQ302677	SH184950.07FU	99	98	Asco	Sordariomycetes	Hypocreales	Ophiocordycipitaceae	<i>Chaunopycnis</i>
41	<i>Bulgaria inquinans</i>	JN033386	SH194396.07FU	100	100	Asco	Leotiomycetes	Leotiales	Bulgariaceae	<i>Bulgaria</i>
42	<i>Mortierella simplex</i>	JX975982	SH189943.07FU	99	98	Zygo	Incertae sedis	Mortierellales	Mortierellaceae	<i>Mortierella</i>
44	<i>Cortinarius diasemospermus</i>	UDB000066	SH188559.07FU	100	100	Baso	Agaricomycetes	Agaricales	Cortinariaceae	<i>Cortinarius</i>
45	<i>Fungi</i>	KF297116	SH032387.07FU	98	95	Baso	NA	NA	NA	NA
46	<i>Cryptococcus oeirensis</i>	NR_077106	SH197623.07FU	100	100	Baso	Tremellomycetes	Tremellales	Incertae sedis	<i>Cryptococcus</i>
48	<i>Pochonia</i>	HM439557	SH012122.07FU	100	100	Asco	Sordariomycetes	Hypocreales	Clavicipitaceae	NA

APPENDICES

OTU	Reference sequence ^a				Phylogeny ^b					
	Accession ^c	SH code ^d	Q ^e	Id ^f	Phyl ^g	Class	Order	Family	Genus	
49	<i>Tomentella</i>	KM576633		100	100	Baso	Agaricomycetes	Thelephorales	Thelephoraceae	<i>Tomentella</i>
50	<i>Mortierella longigemmata</i>	JX976055	SH180129.07FU	99	99	Zygo	<i>Incertae sedis</i>	Mortierellales	Mortierellaceae	<i>Mortierella</i>
51	<i>Penicillium daleae</i>	GU981583	SH182497.07FU	100	100	Asco	Eurotiomycetes	Eurotiales	Trichocomaceae	<i>Penicillium</i>
53	<i>Mortierella macrocystis</i>	JQ272448	SH187863.07FU	100	100	Zygo	<i>Incertae sedis</i>	Mortierellales	Mortierellaceae	<i>Mortierella</i>
55	<i>Geomyces auratus</i>	KF039895	SH183331.07FU	100	100	Asco	Leotiomycetes	<i>Incertae sedis</i>	<i>Incertae sedis</i>	<i>Geomyces</i>
56	Hyaloriaceae	FJ475763	SH207620.07FU	100	100	Baso	Agaricomycetes	NA	NA	NA
57	<i>Lactarius camphoratus</i>	KF432971	SH220116.07FU	100	100	Baso	Agaricomycetes	Russulales	Russulaceae	<i>Lactarius</i>
58	<i>Pochonia bulbillosa</i>	JX535180	SH192574.07FU	100	100	Asco	Sordariomycetes	Hypocreales	Clavicipitaceae	<i>Pochonia</i>
59	<i>Trichoderma hamatum</i>	X93975	SH177682.07FU	100	100	Asco	Sordariomycetes	Hypocreales	Hypocreaceae	<i>Trichoderma</i>
60	<i>Humicola</i>	KF981440	SH195345.07FU	99	99	Asco	Sordariomycetes	Sordariales	Chaetomiaceae	NA
61	<i>Mortierella</i>	KC009383		98	96	Zygo	<i>Incertae sedis</i>	Mortierellales	Mortierellaceae	<i>Mortierella</i>
62	Hyaloscyphaceae	AB476538	SH196230.07FU	98	97	Asco	Leotiomycetes	Helotiales	NA	NA
64	<i>Pezizomycotina</i>	KF359573	SH217842.07FU	100	100	Asco	Eurotiomycetes	Chaetothyriales	NA	NA
66	<i>Aspergillus versicolor</i>	LN482531	SH186265.07FU	100	100	Asco	Eurotiomycetes	Eurotiales	Trichocomaceae	<i>Aspergillus</i>
67	<i>Russula cyanoxantha</i>	KF432956	SH186707.07FU	100	100	Baso	Agaricomycetes	Russulales	Russulaceae	<i>Russula</i>
69	<i>Oidiodendron</i>	JX456904	SH216990.07FU	99	99	Asco	Leotiomycetes	<i>Incertae sedis</i>	Myxotrichaceae	<i>Oidiodendron</i>
71	<i>Penicillium arianeae</i>	KC773833	SH005531.07FU	100	100	Asco	Eurotiomycetes	Eurotiales	Trichocomaceae	NA
72	<i>Volutella</i>	JX507700	SH217585.07FU	100	100	Asco	Sordariomycetes	Hypocreales	Nectriaceae	NA
73	<i>Trichosporon moniliiforme</i>	NR_073240	SH196643.07FU	100	100	Baso	Tremellomycetes	Trichosporonales	Trichosporonaceae	<i>Trichosporon</i>
77	<i>Tremella fibulifera</i>	KP986518		93	89	Baso	NA	NA	NA	NA
81	<i>Luellia recondita</i>	JF519380	SH179954.07FU	100	100	Baso	Agaricomycetes	Trechisporales	Hydnodontaceae	<i>Luellia</i>
83	<i>Chaetosphaeria myriocarpa</i>	AF178552	SH198584.07FU	97	97	Asco	Sordariomycetes	Chaetosphaeriales	Chaetosphaeriaceae	<i>Chaetosphaeria</i>
85	<i>Microbotryomycetes</i>	HM036653	SH180664.07FU	99	99	Baso	<i>Microbotryomycetes</i>	NA	NA	NA

APPENDICES

OTU	Reference sequence ^a				Phylogeny ^b					
	Accession ^c	SH code ^d	Q ^e	Id ^f	Phyl ^g	Class	Order	Family	Genus	
86	<i>Cladosporium cladosporioides</i>	LN482458	SH216250.07FU	100	100	Asco	Dothideomycetes	Capnodiales	Davidiellaceae	NA
88	<i>Cladophialophora chaetospora</i>	KF359558	SH213266.07FU	97	97	Asco	Eurotiomycetes	Chaetothyriales	Herpotrichiellaceae	<i>Cladophialophora</i>
91	<i>Exophiala</i>	HM439556	SH197643.07FU	100	100	Asco	Eurotiomycetes	Chaetothyriales	Herpotrichiellaceae	<i>Exophiala</i>
94	<i>Helotiales</i>	HQ021923	SH201613.07FU	99	99	Asco	Leotiomycetes	Helotiales	NA	NA
96	<i>Bionectria ochroleuca</i>	JX967106	SH182678.07FU	100	100	Asco	Sordariomycetes	Hypocreales	Bionectriaceae	NA
98	<i>Fungi</i>	KT194869		99	98	NA	NA	NA	NA	NA
103	<i>Trechispora araneosa</i>	AF347084		99	99	Baso	Agaricomycetes	Trechisporales	Hydnodontaceae	<i>Trechispora</i>
108	<i>Chytridiomycota</i>	EF619656	SH462789.07FU	98	95	NA	NA	NA	NA	NA
111	<i>Capronia fungicola</i>	AF050246	SH015749.07FU	97	94	Asco	Eurotiomycetes	Chaetothyriales	Herpotrichiellaceae	NA
112	<i>Mortierella gemmifera</i>	JX976121	SH185196.07FU	100	100	Zygo	<i>Incertae sedis</i>	Mortierellales	Mortierellaceae	<i>Mortierella</i>
113	<i>Capnodiales</i>	KF617528	SH472617.07FU	98	98	Asco	NA	NA	NA	NA
114	<i>Fungi</i>	JX675128	SH216421.07FU	95	93	Chyt	NA	NA	NA	NA
121	<i>Saccharomycetales</i>	FN610974	SH180919.07FU	97	95	Asco	Saccharomycetes	NA	NA	NA
128	<i>Helotiales</i>	HQ850140	SH215245.07FU	98	97	Asco	Leotiomycetes	NA	NA	NA
130	<i>Lycoperdon pyriforme</i>	DQ112557	SH175879.07FU	100	100	Baso	Agaricomycetes	Agaricales	Agaricaceae	<i>Lycoperdon</i>
131	<i>Lactarius quietus</i>	UDB015797	SH220118.07FU	100	100	Baso	Agaricomycetes	Russulales	Russulaceae	<i>Lactarius</i>
135	<i>Helotiales</i>	AY969487	SH195228.07FU	100	100	Asco	Leotiomycetes	Helotiales	Hyaloscyphaceae	NA
138	<i>Dermateaceae</i>	FN610995	SH014516.07FU	99	99	Asco	Leotiomycetes	Helotiales	NA	NA
140	<i>Exophiala moniliae</i>	HE605213	SH199199.07FU	100	100	Asco	Eurotiomycetes	Chaetothyriales	Herpotrichiellaceae	<i>Exophiala</i>
141	<i>Rozellomycota</i>	HM069428	SH025237.07FU	99	99	Roz	NA	NA	NA	NA
153	<i>Rozellomycota</i>	HM069429	SH025236.07FU	98	97	Roz	NA	NA	NA	NA
154	<i>Rozellomycota</i>	JQ666484	SH020528.07FU	98	96	Roz	NA	NA	NA	NA
157	<i>Helotiales</i>	AY394669	SH025727.07FU	95	95	Asco	Leotiomycetes	NA	NA	NA

APPENDICES

OTU	Reference sequence ^a				Phylogeny ^b					
		Accession ^c	SH code ^d	Q ^e	Id ^f	Phyl ^g	Class	Order	Family	Genus
161	<i>Crocicreas</i>	AY969794		99	99	Asco	Leotiomycetes	Helotiales	Helotiaceae	<i>Crocicreas</i>
177	<i>Ilyonectria crassa</i>	KJ475469	SH202967.07FU	100	100	Asco	Sordariomycetes	Hypocreales	<i>Incertae sedis</i>	<i>Ilyonectria</i>
185	Pleosporales	GU083188	SH200451.07FU	98	96	Asco	Dothideomycetes	Pleosporales	NA	NA
187	<i>Cenococcum geophilum</i>	AM087244	SH199613.07FU	100	100	Asco	Dothideomycetes	Hysteriales	Gloniaceae	<i>Cenococcum</i>
188	<i>Penicillium corylophilum</i>	KF170363	SH207150.07FU	99	99	Asco	Eurotiomycetes	Eurotiales	Trichocomaceae	<i>Penicillium</i>
190	<i>Glomeromycetes</i>	JF300543	SH462390.07FU	90	82	Glom	Glomeromycetes	NA	NA	NA
198	<i>Cladophialophora</i>	HQ211891	SH193233.07FU	97	95	Asco	Eurotiomycetes	Chaetothyriales	Herpotrichiellaceae	<i>Cladophialophora</i>
199	<i>Xenasmatella</i>	JQ272394	SH026877.07FU	100	100	Baso	Agaricomycetes	Polyporales	<i>Incertae sedis</i>	<i>Phlebiella</i>
256	Hypocreales	JF449629	SH203174.07FU	100	100	Asco	Sordariomycetes	Hypocreales	NA	NA
265	Helotiales	HM044632	SH013010.07FU	95	95	Asco	Leotiomycetes	Helotiales	NA	NA
302	<i>Mortierella parvispora</i>	AB476418	SH193938.07FU	99	99	Zygo	<i>Incertae sedis</i>	Mortierellales	Mortierellaceae	<i>Mortierella</i>
304	<i>Rhodotorula diffluens</i>	NR_073289	SH213958.07FU	94	90	Baso	Microbotryomycetes	Sporidiobolales	<i>Incertae sedis</i>	NA
350	<i>Mucor</i>	JQ676211	SH188380.07FU	100	100	Zygo	<i>Incertae sedis</i>	Mucorales	Mucoraceae	<i>Mucor</i>

^a Reference sequences based on 'massBLASter' of the UNITE database including sequences from the International Nucleotide Sequence Database (GenBank, EMBL, DDBJ) and environmental samples (isolated from soil, ectomycorrhizal roots, orchids etc.) in UNITE.

^b Phylogeny is based on the dynamic UNITE database (v7, release 01.08.2015) and was done with a bayesian classifier implied with MOTUHR based on the best hit of consensus taxonomy after 100 bootstrapped assignments (implementation of Wang *et al.* 2007). 'NA' (not applicable) indicates no further affiliation possible based on consensus taxonomy.

^c Accession number of reference sequence applicable in International Nucleotide Sequence Database.

^d SH code provided by UNITE considering species hypothesis (comprise any species level group of individuals sharing a given set of observed characteristics).

^e Query [%] of the BLAST alignment calculated with the number of mismatches over a 355 nt long input sequence and the corresponding section of the reference sequence.

^f Maximum sequence identity [%] over the BLAST alignment.

^g Fungal phyla using the following abbreviations: 'Asco', Ascomycota; 'Baso', Basidiomycota; 'Chyt', Chytridiomycota; 'Glom', Glomeromycota; 'Roz', Rozellomycota; 'Zygo', Zygomycota.

Table A 14 Labelled bacterial taxa in the treatments with methanol.

Relative abundances are shown for all fractions (H, heavy; M, middle; L, light) in [¹²C]- and [¹³C]-methanol treatments. Black faces indicate values that were used for calculating 'labelling proportions' ('LP') as indicators of relative importance. Bold faces indicate 'LP' > 5 %. This table has been published in Morawe *et al.* 2017.

Phylogenetic affiliation ^a	Labelled taxa	Relative abundance [%]						LP [%]	
		¹² C			¹³ C			H	M
		H	M	L	H	M	L	H	M
Acidobacteria									
<i>Acidobacteriaceae</i> ^c	OTU 542	0.0	0.2	0.2	0.7	0.3	0.4	1.3	
<i>Acidobacterium</i> ^d	OTU 545	0.0	0.9	0.7	0.5	0.0	0.1	0.9	
Actinobacteria									
<i>Acidimicrobiaceae</i> ^c	OTU 652	0.0	0.2	0.7	0.5	2.0	1.8		12.3
<i>Kineosporiaceae</i> ^c	OTU 703	0.9	2.8	1.7	0.7	4.3	1.3		26.2
Armatimonadetes									
<i>Fimbriimonadaceae</i> ^c	OTU 592	0.0	0.5	0.1	0.0	1.2	0.8		7.4
Chlamydiae									
<i>Parachlamydiaceae</i> ^c	OTU 108	0.0	0.0	0.0	0.5	0.0	0.0	0.9	
Firmicutes									
<i>Bacillus</i> ^d	OTU 202	0.0	0.0	0.2	0.5	0.3	0.0	0.9	
<i>Parcubacteria</i> ^{b,e}	OTU 1155	0.0	0.2	0.0	1.0	0.0	0.1	1.7	
Planctomycetes									
<i>Planctomycetales</i> ^b	OTU 836	0.0	0.0	0.7	0.2	0.5	0.0		3.3
<i>Planctomycetaceae</i> ^c	OTU 968	0.0	0.0	0.2	0.0	0.5	0.9		3.3
Alphaproteobacteria									
<i>Methylovirgula</i> ^d	OTU 438	3.5	0.5	2.5	52.5	3.7	1.8	91.1	22.1
<i>Sphingomonas</i> ^d	OTU 449	0.0	0.0	0.5	0.5	0.1	0.5	0.9	
<i>Acetobacteraceae</i> ^c	OTU 467	0.0	0.5	0.2	0.0	0.8	0.6		4.9
Betaproteobacteria									
<i>Methylophilaceae</i> ^c	OTU 360	0.0	0.0	0.0	0.7	0.0	0.0	1.3	
Verrucomicrobia									
<i>Spartobacteria</i> ^b	OTU 6	0.0	0.9	0.7	0.7	0.4	0.7	1.3	
<i>Verrucomicrobiales</i> ^b	OTU 18	1.8	2.5	1.8	0.7	3.4	1.3		20.5
Percentage of labelled taxa to total fraction [%]					58	17			

^a Phylogenetic affiliation was done with BLASTn (November 2015) and is based on the next cultivated hit for each OTU (for further information see Table A 12)

^b Sequence identity of next cultured hit < 90 %, phylogenetic affiliation up to order level

^c Sequence identity of next cultured hit < 95 %, phylogenetic affiliation up to family level

^d Sequence identity of next cultured hit ≥ 95 %, phylogenetic affiliation up to genus level

^e known as "Candidate phylum OD1"

Table A 15 Labelled bacterial taxa in the treatments with acetate.

Relative abundances are shown for all fractions (H, heavy; M, middle; L, light) in [¹²C]- and [¹³C]-acetate treatments. Black faces indicate values that were used for calculating 'labelling proportions' ('LP') as indicators of relative importance. Bold faces indicate 'LP' > 5 %.

Phylogenetic affiliation ^a	Labelled OTU	Relative abundance [%]						LP [%]	
		¹² C			¹³ C			H	M
		H	M	L	H	M	L	H	M
Acidobacteria									
<i>Solibacteraceae</i> ^c	OTU 528	0.0	0.4	1.0	0.0	0.9	0.1		1.3
<i>Acidobacterium</i> ^d	OTU 545	0.0	0.2	1.3	1.1	0.9	1.8		1.3
Actinobacteria									
<i>Conexibacteraceae</i> ^c	OTU 132	0.0	1.1	0.2	0.0	2.0	0.4		2.6
<i>Gaiellaceae</i> ^c	OTU 142	0.0	0.4	0.1	0.0	0.6	0.0		0.8
<i>Acidimicrobiaceae</i> ^c	OTU 656	0.0	0.4	0.0	0.0	0.5	0.2		0.7
<i>Kineosporiaceae</i> ^c	OTU 703	6.5	7.8	2.0	3.3	9.2	2.7		12.2
<i>Leifsonia</i> ^d	OTU 721	0.0	0.0	0.0	1.1	0.2	0.6	1.9	
<i>Mycobacterium</i> ^d	OTU 750	0.0	0.2	0.9	0.0	2.0	0.1		2.6
<i>Corynebacterium</i> ^d	OTU 752	0.0	0.0	0.0	6.7	0.0	0.0	11.5	
Bacteroidetes									
<i>Chtiniophagaceae</i> ^c	OTU 1018	0.0	0.2	0.0	2.2	0.0	0.1	3.8	
Firmicutes									
<i>Thermoanaerobacterales</i> ^b	OTU 615	0.0	1.0	0.2	1.1	0.9	0.2	1.9	
Parcubacteria ^{b,e}	OTU 1136	9.7	2.3	13.9	11.1	2.6	15.9		3.4
	OTU 1158	0.0	0.0	0.2	1.1	0.3	1.0	1.9	
Planctomycetes									
<i>Tepidisphaeraceae</i> ^c	OTU 796	0.0	0.0	0.8	0.0	0.7	0.1		0.9
<i>Phycisphaerae</i> ^b	OTU 800	0.0	0.0	0.0	3.3	0.0	0.0	5.8	
<i>Planctomycetaceae</i> ^c	OTU 923	0.0	0.6	0.0	0.0	0.9	0.1		1.1
<i>Planctomycetaceae</i> ^c	OTU 939	0.0	3.6	3.5	1.1	1.3	0.7	1.9	
Alphaproteobacteria									
<i>Caulobacter</i> ^d	OTU 431	0.0	2.5	3.4	0.0	2.9	0.1		3.9
<i>Methylovirgula</i> ^d	OTU 438	3.2	3.8	3.8	1.1	7.7	3.2		10.3
<i>Sphingomonas</i> ^d	OTU 449	0.0	0.2	1.4	7.8	1.0	0.1	13.5	1.4
<i>Acetobacteraceae</i> ^c	OTU 467	0.0	1.1	2.3	0.0	5.8	0.0		7.8
<i>Rhodospirillaceae</i> ^c	OTU 479	0.0	0.0	0.0	0.0	0.7	0.0		0.9
Betaproteobacteria									
<i>Burkholderia</i> ^d	OTU 361	0.0	0.0	0.2	2.2	2.2	0.0	3.8	3.0
Gammaproteobacteria									
<i>Rhodanobacter</i> ^d	OTU 300	9.7	21.4	15.3	23.3	32.2	23.0	40.4	42.9
Verrucomicrobia									
<i>Spartobacteria</i> ^b	OTU 6	0.0	1.0	2.3	7.8	2.3	3.1	13.5	3.1
Percentage of labelled taxa to total fraction [%]					58	75			

^a Phylogenetic affiliation was done with BLASTn (November 2015) and is based on the next cultivated hit for each OTU (for further information see Table A 12)

^b Sequence identity of next cultured hit < 90 %, phylogenetic affiliation up to order level

^c Sequence identity of next cultured hit < 95 %, phylogenetic affiliation up to family level

^d Sequence identity of next cultured hit ≥ 95 %, phylogenetic affiliation up to genus level

^e known as "Candidate phylum OD1"

Table A 16 Labelled bacterial taxa in the treatments with glucose.

Relative abundances are shown for all fractions (H, heavy; M, middle; L, light) in [¹²C]- and [¹³C]-glucose treatments. Black faces indicate values that were used for calculating 'labelling proportions' ('LP') as indicators of relative importance. Bold faces indicate 'LP' > 5 %.

Phylogenetic affiliation ^a	Labelled OTU	Relative abundance [%]						LP [%]	
		¹² C			¹³ C			H	M
		H	M	L	H	M	L	H	M
Actinobacteria									
<i>Leifsonia</i> ^d	OTU 721	0.0	0.0	0.2	2.7	0.3	0.0	4.8	
Cand. Saccharibacteria ^{b,e}	OTU 1116	0.6	0.0	0.2	0.0	0.9	0.0		1.2
Planctomycetes									
<i>Planctomycetales</i> ^b	OTU 840	0.0	0.0	0.2	0.3	0.9	0.2		1.2
Alphaproteobacteria									
<i>Methylovirgula</i> ^d	OTU 438	1.7	3.1	2.7	5.3	2.9	2.2	9.3	
<i>Sphingomonas</i> ^d	OTU 449	0.8	0.0	0.2	0.8	1.6	0.7		2.1
<i>Acetobacteraceae</i> ^c	OTU 467	0.1	0.2	0.5	0.0	0.6	0.0		0.8
Betaproteobacteria									
<i>Burkholderia</i> ^d	OTU 361	0.7	1.1	1.7	48.6	3.7	0.4	84.8	4.7
Gammaproteobacteria									
<i>Sinobacteraceae</i> ^c	OTU 278	0.0	0.0	0.0	0.0	0.6	0.0		0.8
<i>Rhodanobacter</i> ^d	OTU 300	20.5	42.6	43.9	19.6	68.9	45.7		88.0
Verrucomicrobia									
<i>Spartobacteria</i> ^b	OTU 9	0.0	0.0	0.1	0.6	0.0	0.0	1.1	
<i>Verrucomicrobiales</i> ^b	OTU 18	2.1	0.2	1.0	0.5	1.0	0.7		1.3
Percentage of labelled taxa to total fraction [%]					57	78			

^a Phylogenetic affiliation was done with BLASTn (November 2015) and is based on the next cultivated hit for each OTU (for further information see Table A 12)

^b Sequence identity of next cultured hit < 90 %, phylogenetic affiliation up to order level

^c Sequence identity of next cultured hit < 95 %, phylogenetic affiliation up to family level

^d Sequence identity of next cultured hit ≥ 95 %, phylogenetic affiliation up to genus level

^e known as "Candidate division TM7"

Table A 17 Labelled bacterial taxa in the treatments with xylose.

Relative abundances are shown for all fractions (H, heavy; M, middle; L, light) in [¹²C]- and [¹³C]-xylose treatments. Black faces indicate values that were used for calculating 'labelling proportions' ('LP') as indicators of relative importance. Bold faces indicate 'LP' > 5 %.

Phylogenetic affiliation ^a	Labelled OTU	Relative abundance [%]						LP [%]	
		¹² C			¹³ C			H	M
		H	M	L	H	M	L	H	M
Acidobacteria									
<i>Solibacteraceae</i> ^c	OTU 528	0.0	1.0	1.9	0.0	1.4	0.5		2.9
<i>Acidobacterium</i> ^d	OTU 545	0.0	0.6	2.6	0.0	2.3	1.1		5.0
Actinobacteria									
<i>Actinospica</i> ^d	OTU 758	0.0	0.0	0.0	0.6	0.0	0.0	0.7	
<i>Acidimicrobiaceae</i> ^c	OTU 654	0.0	0.2	0.1	0.0	0.6	0.0		1.4
<i>Acidimicrobiales</i> ^b	OTU 668	0.0	0.0	0.1	1.3	0.5	0.0	1.4	1.1
<i>Leifsonia</i> ^d	OTU 721	0.0	0.0	0.1	5.1	0.0	0.0	5.8	
<i>Mycobacterium</i> ^d	OTU 750	0.0	0.2	0.3	0.0	0.5	0.3		1.1
Bacteroidetes									
<i>Ferruginibacter</i> ^d	OTU 1014	0.0	0.0	1.9	0.0	1.0	3.6		2.0
<i>Mucilaginibacter</i> ^d	OTU 1073	2.9	0.5	28.6	1.9	13.3	18.4		28.4
Planctomycetes									
<i>Planctomycetales</i> ^b	OTU 836	1.5	0.6	0.3	0.0	1.3	0.5		2.7
<i>Planctomycetales</i> ^b	OTU 857	1.5	1.9	0.3	0.0	2.6	1.9		5.6
Alphaproteobacteria									
<i>Caulobacter</i> ^d	OTU 431	0.0	1.7	0.3	2.5	0.3	0.3	2.9	
<i>Methylovirgula</i> ^d	OTU 438	5.9	6.1	5.6	15.9	7.7	3.6	18.0	16.5
<i>Sphingomonas</i> ^d	OTU 449	0.0	0.0	0.0	0.0	1.2	0.0		2.5
<i>Rhodospirillaceae</i> ^c	OTU 460	0.0	0.6	0.3	0.0	1.7	0.7		3.6
<i>Rhodospirillaceae</i> ^c	OTU 479	0.0	0.0	0.0	0.6	0.0	0.0	0.7	
Betaproteobacteria									
<i>Burkholderia</i> ^d	OTU 361	0.0	1.4	1.5	62.4	0.0	0.0	70.5	
Gammaproteobacteria									
<i>Rhodanobacter</i> ^d	OTU 300	2.9	4.6	5.7	0.0	12.7	3.6		27.1
Percentage of labelled taxa to total fraction [%]					89	47			

^a Phylogenetic affiliation was done with BLASTn (November 2015) and is based on the next cultivated hit for each OTU (for further information see Table A 12)

^b Sequence identity of next cultured hit < 90 %, phylogenetic affiliation up to order level

^c Sequence identity of next cultured hit < 95 %, phylogenetic affiliation up to family level

^d Sequence identity of next cultured hit ≥ 95 %, phylogenetic affiliation up to genus level

Table A 18 Labelled bacterial taxa in the treatments with vanillic acid.

Relative abundances are shown for all fractions (H, heavy; M, middle; L, light) in [¹²C]- and [¹³C]-vanillic acid treatments. Black faces indicate values that were used for calculating 'labelling proportions' ('LP') as indicators of relative importance. Bold faces indicate 'LP' > 5 %.

Phylogenetic affiliation ^a	Labelled OTU	Relative abundance [%]						LP [%]	
		¹² C			¹³ C			H	M
		H	M	L	H	M	L	H	M
Actinobacteria									
<i>Conexibacteraceae</i> ^c	OTU 132	0.0	2.8	0.8	0.2	4.2	0.6		9.3
<i>Acidimicrobiaceae</i> ^c	OTU 652	0.0	2.1	0.8	0.0	3.0	0.7		6.7
<i>Acidimicrobiaceae</i> ^c	OTU 654	0.0	0.1	0.0	0.0	2.4	0.5		5.4
<i>Kineosporiaceae</i> ^c	OTU 703	0.0	10.8	3.5	0.0	12.9	3.7		28.8
<i>Pseudonocardia</i> ^d	OTU 723	0.0	0.6	0.0	0.0	1.1	0.2		2.4
<i>Thermomonosporaceae</i> ^{c,e}	OTU 816	0.0	0.0	0.0	0.0	1.4	0.0		3.2
Planctomycetes									
<i>Tepidisphaeraceae</i> ^c	OTU 796	0.0	0.2	2.4	0.0	0.6	1.4		1.4
<i>Planctomycetales</i> ^b	OTU 844	0.0	0.4	0.0	0.0	1.1	0.0		2.4
<i>Planctomycetaceae</i> ^c	OTU 904	0.0	0.0	0.0	0.0	0.5	0.0		1.2
<i>Planctomycetales</i> ^b	OTU 927	0.0	0.4	0.9	0.0	3.3	0.3		7.3
<i>Planctomycetales</i> ^b	OTU 945	0.0	0.4	0.2	0.0	0.5	0.2		1.2
Alphaproteobacteria									
<i>Caulobacter</i> ^d	OTU 431	0.0	0.5	0.9	0.7	0.4	0.3	0.8	
<i>Methylovirgula</i> ^d	OTU 438	2.6	4.7	6.8	0.0	11.1	10.3		24.8
<i>Sphingomonas</i> ^d	OTU 449	0.0	0.2	0.0	1.5	1.2	0.0	1.5	2.8
Betaproteobacteria									
<i>Burkholderia</i> ^d	OTU 361	18.4	20.2	14.6	96.7	1.2	0.1	97.7	
Gammaproteobacteria									
<i>Steroidobacter</i> ^d	OTU 280	0.0	0.2	0.5	0.0	1.4	1.8		3.2
Percentage of labelled taxa to total fraction [%]					99	45			

^a Phylogenetic affiliation was done with BLASTn (November 2015) and is based on the next cultivated hit for each OTU (for further information see Table A 12)

^b Sequence identity of next cultured hit < 90 %, phylogenetic affiliation up to order level

^c Sequence identity of next cultured hit < 95 %, phylogenetic affiliation up to family level

^d Sequence identity of next cultured hit ≥ 95 %, phylogenetic affiliation up to genus level

^e Query of next cultured hit was only 70 % with BLASTn analysis

Table A 19 Labelled bacterial taxa in the treatments with CO₂ and additional methanol.

Relative abundances are shown for all fractions (H, heavy; M, middle; L, light) in [¹²C]- and [¹³C]-CO₂ and additional methanol treatments. Black faces indicate values that were used for calculating 'labelling proportions' ('LP') as indicators of relative importance. Bold faces indicate 'LP' > 5 %.

Phylogenetic affiliation ^a	Labelled OTU	Relative abundance [%]						LP [%]	
		¹² C			¹³ C			H	M
		H	M	L	H	M	L	H	M
Actinobacteria									
<i>Acidimicrobiaceae</i> ^c	OTU 652	0.0	5.8	2.4	0.0	7.4	0.8		12.3
<i>Acidimicrobiaceae</i> ^c	OTU 656	0.0	0.3	0.3	0.0	0.9	0.2		1.4
<i>Kineosporiaceae</i> ^c	OTU 703	0.0	27.7	5.9	14.3	21.2	4.2	16.7	
<i>Leifsonia</i> ^d	OTU 721	0.0	0.3	0.0	42.9	0.4	0.0	50.0	
Bacteroidetes									
<i>Mucilaginibacter</i> ^d	OTU 1073	0.0	1.7	11.5	0.0	2.6	7.6		4.3
Planctomycetes									
<i>Planctomycetaceae</i> ^c	OTU 885	0.0	6.8	4.5	14.3	6.1	4.3	16.7	
<i>Planctomycetaceae</i> ^c	OTU 951	0.0	0.0	0.0	14.3	0.0	0.5	16.7	
<i>Planctomycetaceae</i> ^c	OTU 968	0.0	0.0	0.3	0.0	0.9	1.2		1.4
Alphaproteobacteria									
<i>Caulobacter</i> ^d	OTU 431	0.0	3.1	0.5	0.0	4.3	0.3		7.2
<i>Sphingomonas</i> ^d	OTU 449	0.0	0.7	0.0	0.0	0.9	0.2		1.4
<i>Acetobacteraceae</i> ^c	OTU 467	0.0	2.1	0.3	0.0	2.6	0.8		4.3
Gammaproteobacteria									
<i>Rhodanobacter</i> ^d	OTU 300	20.0	13.4	34.6	14.3	39.0	40.8		65.2
Verrucomicrobia									
<i>Verrucomicrobiales</i> ^b	OTU 18	0.0	0.0	3.6	0.0	1.3	1.9		2.2
Percentage of labelled taxa to total fraction [%]					86	60			

^a Phylogenetic affiliation was done with BLASTn (November 2015) and is based on the next cultivated hit for each OTU (for further information see Table A 12)

^b Sequence identity of next cultured hit < 90 %, phylogenetic affiliation up to order level

^c Sequence identity of next cultured hit < 95 %, phylogenetic affiliation up to family level

^d Sequence identity of next cultured hit ≥ 95 %, phylogenetic affiliation up to genus level

Table A 20 Labelled bacterial taxa in the treatments with CO₂.

Relative abundances are shown for all fractions (H, heavy; M, middle; L, light) in [¹²C]- and [¹³C]-CO₂ treatments. Black faces indicate values that were used for calculating 'labelling proportions' ('LP') as indicators of relative importance. Bold faces indicate 'LP' > 5 %.

Phylogenetic affiliation ^a	Labelled OTU	Relative abundance [%]						LP [%]	
		¹² C			¹³ C			H	M
		H	M	L	H	M	L	H	M
Acidobacteria									
Acidobacterium ^d	OTU 545	0.6	0.5	0.8	1.0	0.7	2.7		4.3
Actinobacteria									
Conexibacteraceae ^c	OTU 132	1.4	7.3	2.4	1.9	4.9	1.3	3.4	
Gaiellaceae ^c	OTU 142	0.0	0.1	0.0	0.0	0.7	0.0		4.3
Acidimicrobiaceae ^c	OTU 652	1.7	4.4	2.9	2.7	6.2	2.7	4.7	39.3
Acidimicrobiaceae ^c	OTU 656	1.4	1.3	0.5	0.1	1.9	0.3		12.1
Bacteroidetes									
Ferruginibacter ^d	OTU 1014	4.9	0.3	2.0	6.2	0.0	2.4	10.9	
Mucilaginibacter ^d	OTU 1073	12.3	2.4	13.5	34.8	3.7	15.2	61.1	23.6
Chlamydiae									
Parachlamydia ^d	OTU 93	0.1	0.0	0.1	1.0	0.0	0.0	1.8	
Firmicutes									
Bacillus ^d	OTU 202	0.5	0.0	0.4	1.0	0.1	0.6	1.8	
Parcubacteria ^{b,e}	OTU 1140	0.0	0.0	0.1	0.6	0.1	0.1	1.0	
Planctomycetes									
Planctomycetales ^b	OTU 945	0.0	0.3	0.1	0.1	0.6	0.6		3.6
Planctomycetaceae ^c	OTU 968	0.3	0.5	0.8	1.6	0.1	0.1	2.8	
Alphaproteobacteria									
Caulobacter ^d	OTU 431	0.4	0.4	0.3	0.4	0.9	0.4		5.7
Gammaproteobacteria									
Sinobacteraceae ^c	OTU 278	0.4	0.1	0.4	0.7	0.1	0.1	1.3	
Alkanindiges ^d	OTU 379	0.4	0.3	0.3	0.6	0.1	0.0	1.0	
Verrucomicrobia									
Spartobacteria ^b	OTU 6	0.9	0.3	1.0	1.3	0.1	0.0	2.3	
Spartobacteria ^b	OTU 17	0.0	0.0	0.0	0.6	0.0	0.0	1.0	
Verrucomicrobiales ^b	OTU 18	2.1	0.5	3.1	3.8	1.1	1.7	6.7	7.1
Percentage of labelled taxa to total fraction [%]					57	16			

^a Phylogenetic affiliation was done with BLASTn (November 2015) and is based on the next cultivated hit for each OTU (for further information see Table A 12)

^b Sequence identity of next cultured hit < 90 %, phylogenetic affiliation up to order level

^c Sequence identity of next cultured hit < 95 %, phylogenetic affiliation up to family level

^d Sequence identity of next cultured hit ≥ 95 %, phylogenetic affiliation up to genus level

^e known as "Candidate phylum OD1"

Table A 21 Labelled bacterial taxa in the treatments with methanol at *in situ* pH.

Relative abundances are shown for all fractions (H, heavy; M, middle; L, light) in [¹²C]- and [¹³C]-methanol treatments at *in situ* pH of the pH shift SIP experiment. Black faces indicate values that were used for calculating 'labelling proportions' ('LP') as indicators of relative importance. Bold faces indicate 'LP' > 5 %. This table has been published in Morawe *et al.* 2017.

Phylogenetic affiliation ^a	Labelled OTU	Relative abundance [%]						LP [%]	
		¹² C			¹³ C			H	M
		H	M	L	H	M	L	H	M
Actinobacteria									
<i>Leifsonia</i> ^d	OTU 721	0.4	0.54	2.5	10.8	7.0	1.2	45.0	13.9
Bacteroidetes									
<i>Chitinophaga</i> ^d	OTU 1020	3.5	11.5	1.7	5.3	9.2	2.1	22.3	
<i>Sphingobacteriales</i> ^b	OTU 1098	0.0	0.5	0.5	0.5	0.1	0.2	2.2	
Firmicutes									
<i>Paenibacillus</i> ^d	OTU 206	0.2	0.4	0.8	0.6	0.2	0.0	2.6	
Alphaproteobacteria									
<i>Methylovirgula</i> ^d	OTU 438	1.0	0.4	3.1	6.7	42.3	3.5	27.9	83.5
<i>Sphingomonas</i> ^d	OTU 449	0.2	0.0	1.7	0.7	0.6	3.0		1.2
Gammaproteobacteria									
<i>Rhodanobacter</i> ^{d,e}	OTU 343	0.2	0.0	0.2	0.1	0.7	0.7		1.4
Percentage of labelled taxa to total fraction [%]					24	51			

^a Phylogenetic affiliation was done with BLASTn (November 2015) and is based on the next cultivated hit for each OTU (for further information see Table A 12)

^b Sequence identity of next cultured hit < 90 %, phylogenetic affiliation up to order level

^d Sequence identity of next cultured hit ≥ 95 %, phylogenetic affiliation up to genus level

^e Query of next cultured hit was only 72 % with BLASTn analysis

Table A 22 Labelled bacterial taxa in the treatments with methanol at pH 7.

Relative abundances are shown for all fractions (H, heavy; M, middle; L, light) in [¹²C]- and [¹³C]-methanol treatments at pH 7 of the pH shift SIP experiment. Black faces indicate values that were used for calculating 'labelling proportions' ('LP') as indicators of relative importance. Bold faces indicate 'LP' > 5 %. This table has been published in Morawe *et al.* 2017.

Phylogenetic affiliation ^a	Labelled OTU	Relative abundance [%]						LP [%]	
		¹² C			¹³ C			H	M
		H	M	L	H	M	L	H	M
Actinobacteria									
<i>Leifsonia</i> ^d	OTU 721	1.0	1.7	2.7	8.5	9.3	2.9	19.7	19.4
Bacteroidetes									
<i>Chryseobacterium</i> ^d	OTU 1045	8.5	11.6	5.0	32.5	23.1	23.5	75.1	48.1
<i>Sphingobacterium</i> ^d	OTU 1078	1.7	0.4	0.5	0.9	1.0	0.8		2.1
<i>Sphingobacteriaceae</i> ^c	OTU 1094	0.3	0.6	0.5	0.5	0.6	0.1	1.3	
<i>Cytophaga</i> ^d	OTU 1108	0.1	0.4	0.4	0.3	0.5	0.1		1.1
Alphaproteobacteria									
<i>Caulobacter</i> ^d	OTU 431	0.8	0.3	1.6	1.0	0.1	0.6	2.3	
<i>Paracoccus</i> ^d	OTU 450	0.0	0.0	0.0	0.1	0.8	0.0		1.6
Betaproteobacteria									
<i>Methylophilus</i> ^d	OTU 358	0.6	0.2	0.5	0.4	9.8	0.0		20.4
Verrucomicrobia									
<i>Terrimicrobium</i> ^d	OTU 54	0.3	0.1	0.6	0.7	3.5	0.0	1.7	7.2
Percentage of labelled taxa to total fraction [%]					43	48			

^a Phylogenetic affiliation was done with BLASTn (November 2015) and is based on the next cultivated hit for each OTU (for further information see Table A 12)

^c Sequence identity of next cultured hit < 95 %, phylogenetic affiliation up to family level

^d Sequence identity of next cultured hit ≥ 95 %, phylogenetic affiliation up to genus level

APPENDICES

Table A 23 Labelled methylotrophic taxa in the treatments with methanol.

Relative abundances are shown for all fractions (H, heavy; M, middle; L, light) in [¹²C]- and [¹³C]-methanol treatments. Black faces indicate values that were used for calculating 'labelling proportions' ('LP') as indicators of relative importance. Bold faces indicate 'LP' > 5 %. This table has been published in Morawe *et al.* 2017.

Phylogenetic affiliation ^a	Labelled OTU	Relative abundance [%]						LP [%]	
		¹² C			¹³ C			H	M
		H	M	L	H	M	L	H	M
<i>Methylobacterium</i>	OTU 40	0.2	35.3	7.5	24.9	32.4	3.1	25.6	
	OTU 58	0.0	0.0	0.0	0.0	1.5	0.0		3.6
	OTU 79	0.0	0.0	1.9	0.0	0.6	0.0		1.4
	OTU 107	0.0	0.8	0.0	0.0	1.2	0.0		2.9
	OTU 108	0.0	0.2	0.0	0.6	0.9	0.0	0.6	2.1
	OTU 153	0.0	0.0	1.9	0.0	0.9	0.0		2.1
<i>ambiguous^b</i>	OTU 0	0.0	0.0	0.0	0.6	0.0	0.0	0.6	
	OTU 2	0.0	0.0	0.0	0.6	0.0	0.0	0.6	
	OTU 9	0.0	0.0	0.0	0.2	1.5	0.0		3.6
	OTU 222	0.0	2.1	1.9	1.6	0.6	0.0	1.7	
<i>Hyphomicrobium</i>	OTU 185	0.4	10.6	47.2	30.2	20.2	11.6	31.0	47.1
	OTU 202	0.2	0.0	1.9	0.0	2.1	0.0		5.0
<i>ambiguous^b</i>	OTU 177	0.0	0.4	0.0	0.0	0.6	0.0		1.4
	OTU 197	0.0	0.2	0.0	0.0	0.9	0.0		2.1
	OTU 210	0.0	1.3	30.2	25.4	4.0	0.0	26.0	9.3
	OTU 289	0.0	0.0	0.0	0.0	0.9	0.0		2.1
	OTU 316	0.0	0.0	0.0	0.0	0.9	0.0		2.1
<i>Methylorhabdus</i>	OTU 190	0.0	0.0	0.0	2.2	0.0	0.0	2.3	
<i>ambiguous^b</i>	OTU 18	0.0	0.0	0.0	1.8	0.0	0.0	1.9	
<i>Beijerinckiaceae</i>	OTU 144	0.2	0.0	0.0	9.5	2.8	0.8	9.7	6.4
	OTU 152	0.0	0.0	0.0	0.4	0.6	0.0		1.4
	OTU 374	0.0	0.0	0.0	0.0	0.6	0.0		1.4
<i>ambiguous^b</i>	OTU 352	0.0	0.0	0.0	0.0	0.9	0.0		2.1
not classified	OTU 275	0.0	0.0	0.0	0.0	1.5	0.0		3.6
Percentage of labelled taxa to total fraction [%]					97	43			

^a Phylogenetic affiliation was done with BLASTn (Dezember 2015) and confirmed by positioning in phylogenetic tree (for further information see Figure A 12)

^b Sequence identity with BLASTn < 90 % as well as ambiguous position in phylogenetic tree

Table A 24 Labelled methylotrophic taxa in the treatments with acetate.

Relative abundances are shown for all fractions (H, heavy; M, middle; L, light) in [¹²C]- and [¹³C]-acetate treatments. Black faces indicate values that were used for calculating 'labelling proportions' ('LP') as indicators of relative importance. Bold faces indicate 'LP' > 5 %.

Phylogenetic affiliation ^a	Labelled OTU	Relative abundance [%]						LP [%]	
		¹² C			¹³ C			H	M
		H	M	L	H	M	L	H	M
<i>Methylobacterium</i>									
<i>ambiguous^b</i>	OTU 108	0.1	0.1	3.3	0.0	1.0	1.3		7.3
	OTU 9	0.0	0.0	0.0	12.0	0.0	0.1	12.1	
	OTU 13	0.0	0.0	0.0	1.5	0.0	0.0	1.5	
	OTU 222	0.0	0.0	0.3	0.2	0.8	0.1		5.3
<i>Hyphomicrobium</i>									
<i>ambiguous^b</i>	OTU 185	0.6	7.3	36.9	50.0	11.6	30.7	50.8	82.1
	OTU 10	0.0	0.0	0.0	0.7	0.0	0.0	0.7	
	OTU 172	0.0	0.0	2.2	0.1	0.8	1.2		5.3
	OTU 236	0.0	0.0	1.4	22.6	0.0	0.9	23.0	
	OTU 298	0.0	0.1	0.3	4.4	0.0	3.6	4.5	
	OTU 301	0.0	0.0	0.1	0.5	0.0	0.5	0.5	
<i>Beijerinckiaceae</i>									
<i>ambiguous^b</i>	OTU 340	0.0	0.7	0.3	6.8	0.7	0.6	6.9	
Percentage of labelled taxa to total fraction [%]					99	14			

^a Phylogenetic affiliation was done with BLASTn (Dezember 2015) and confirmed by positioning in phylogenetic tree (for further information see Figure A 12)

^b Sequence identity with BLASTn < 90 % as well as ambiguous position in phylogenetic tree

Table A 25 Labelled methylotrophic taxa in the treatments with glucose.

Relative abundances are shown for all fractions (H, heavy; M, middle; L, light) in [¹²C]- and [¹³C]-glucose treatments. Black faces indicate values that were used for calculating 'labelling proportions' ('LP') as indicators of relative importance. Bold faces indicate 'LP' > 5 %.

Phylogenetic affiliation ^a	Labelled OTU	Relative abundance [%]						LP [%]	
		¹² C			¹³ C			H	M
		H	M	L	H	M	L	H	M
<i>Methylobacterium</i>	OTU 55	0.1	0.0	17.6	0.0	13.5	14.7		36.3
	OTU 76	0.0	0.0	0.5	0.0	2.2	0.0		5.8
	OTU 105	0.0	0.0	0.3	0.0	1.4	0.2		3.8
<i>Hyphomicrobium</i>	OTU 185	0.3	0.7	14.4	0.0	3.9	23.4		10.5
<i>ambiguous^b</i>	OTU 172	0.0	0.0	8.4	0.0	11.3	0.3		30.5
	OTU 177	0.0	0.0	0.0	0.0	1.5	0.0		4.1
	OTU 236	0.0	0.0	6.0	0.0	0.8	6.1		2.0
<i>Methylocystaceae</i>	OTU 137	0.0	0.0	0.0	47.4	0.0	0.0	47.5	
<i>Beijerinckiaceae</i>	OTU 338	0.0	0.3	0.4	0.0	1.0	0.9		2.6
<i>ambiguous^b</i>	OTU 340	0.0	0.3	0.6	52.3	1.1	0.6	52.5	2.9
Percentage of labelled taxa to total fraction [%]					100	37			

^a Phylogenetic affiliation was done with BLASTn (Dezember 2015) and confirmed by positioning in phylogenetic tree (for further information see Figure A 12)

^b Sequence identity with BLASTn < 90 % as well as ambiguous position in phylogenetic tree

APPENDICES

Table A 26 Labelled methylotrophic taxa in the treatments with xylose.

Relative abundances are shown for all fractions (H, heavy; M, middle; L, light) in [¹²C]- and [¹³C]-xylose treatments. Black faces indicate values that were used for calculating 'labelling proportions' ('LP') as indicators of relative importance. Bold faces indicate 'LP' > 5 %.

Phylogenetic affiliation ^a	Labelled OTU	Relative abundance [%]						LP [%]	
		¹² C			¹³ C			H	M
		H	M	L	H	M	L	H	M
<i>Methylobacterium</i>	OTU 55	0.0	12.3	5.0	97.4	5.8	0.4	98.5	
	OTU 79	0.0	0.7	0.1	0.8	0.0	0.0	0.8	
	OTU 269	0.0	0.0	0.0	0.0	0.6	0.0		1.4
	OTU 303	0.0	0.4	0.0	0.0	2.6	0.1		5.6
<i>ambiguous^b</i>	OTU 222	0.0	0.6	0.1	0.0	2.6	0.0		5.6
<i>Hyphomicrobium</i>	OTU 185	0.6	13.3	9.1	0.2	23.0	8.0		50.0
	OTU 202	0.0	1.7	0.0	0.0	2.6	0.7		5.6
	OTU 271	0.0	0.4	2.1	0.0	0.6	0.0		1.4
	OTU 172	0.0	2.5	19.6	0.0	3.6	23.0		7.9
	OTU 197	0.0	0.3	0.0	0.0	1.9	0.0		4.2
	OTU 210	0.1	0.3	1.5	0.0	2.8	0.4		6.1
	OTU 214	0.0	0.3	0.1	0.0	1.7	0.2		3.7
	OTU 236	0.0	2.4	4.3	0.7	0.6	5.5	0.7	
	OTU 297	0.0	0.0	0.0	0.0	0.6	0.0		1.4
	OTU 301	0.0	0.1	0.0	0.0	1.1	0.7		2.3
<i>Beijerinckiaceae</i>	OTU 144	0.0	0.1	0.3	0.0	0.9	0.8		1.9
<i>not classified</i>	OTU 249	0.0	0.0	0.0	0.0	1.3	0.1		2.8
Percentage of labelled taxa to total fraction [%]					99	45			

^a Phylogenetic affiliation was done with BLASTn (Dezember 2015) and confirmed by positioning in phylogenetic tree (for further information see Figure A 12)

^b Sequence identity with BLASTn < 90 % as well as ambiguous position in phylogenetic tree

APPENDICES

Table A 27 Labelled methylotrophic taxa in the treatments with vanillic acid.

Relative abundances are shown for all fractions (H, heavy; M, middle; L, light) in [¹²C]- and [¹³C]-vanillic acid treatments. Black faces indicate values that were used for calculating 'labelling proportions' ('LP') as indicators of relative importance. Bold faces indicate 'LP' > 5 %.

Phylogenetic affiliation ^a	Labelled OTU	Relative abundance [%]						LP [%]	
		¹² C			¹³ C			H	M
		H	M	L	H	M	L	H	M
<i>Methylobacterium</i>	OTU 40	0.0	10.5	2.2	0.2	19.1	4.0		26.1
	OTU 55	0.0	7.1	0.1	0.0	15.2	1.9		20.8
	OTU 76	0.0	0.0	0.1	0.0	1.2	0.0		1.7
	OTU 78	0.0	1.9	0.2	0.0	4.0	0.4		5.5
	OTU 80	0.0	0.0	0.0	0.0	0.7	0.0		1.0
	OTU 107	0.0	0.5	0.2	0.0	2.1	0.1		2.9
	OTU 110	0.0	0.1	0.0	0.0	1.7	0.0		2.4
	<i>Hyphomicrobium</i> <i>ambiguous</i> ^b	OTU 185	0.0	10.9	10.0	6.0	15.6	5.2	6.2
OTU 172		0.0	4.5	7.0	0.1	7.4	0.9		10.1
OTU 177		0.0	0.3	0.4	0.0	1.2	0.0		1.7
OTU 210		0.0	2.2	2.3	59.9	0.5	2.4	61.5	
OTU 214		0.0	0.4	0.1	0.0	0.6	0.6		0.9
OTU 298		0.1	2.7	0.0	27.6	2.1	0.9	28.3	
<i>Methylorhabdus</i> <i>ambiguous</i> ^b		OTU 27	0.0	0.0	0.0	1.2	0.0	0.0	1.2
	<i>Beijerinckiaceae</i> <i>ambiguous</i> ^b	OTU 144	0.0	0.8	2.5	0.0	1.6	1.8	
OTU 152		0.0	0.4	0.0	0.0	0.6	0.0		0.9
OTU 338		0.0	0.0	0.0	0.5	2.0	0.0		2.7
OTU 340		0.0	0.2	0.0	2.7	0.1	0.0	2.8	
Percentage of labelled taxa to total fraction [%]					97	73			

^a Phylogenetic affiliation was done with BLASTn (Dezember 2015) and confirmed by positioning in phylogenetic tree (for further information see Figure A 12)

^b Sequence identity with BLASTn < 90 % as well as ambiguous position in phylogenetic tree

Table A 28 Labelled methylotrophic taxa in the treatments with CO₂ and additional methanol.

Relative abundances are shown for all fractions (H, heavy; M, middle; L, light) in [¹²C]- and [¹³C]-CO₂ and additional methanol treatments. Black faces indicate values that were used for calculating 'labelling proportions' ('LP') as indicators of relative importance. Bold faces indicate 'LP' > 5 %.

Phylogenetic affiliation ^a	Labelled OTU	Relative abundance [%]						LP [%]	
		¹² C			¹³ C			H	M
		H	M	L	H	M	L	H	M
<i>Methylobacterium</i>	OTU 35	0.0	0.0	0.0	0.0	8.4	0.2		14.3
	OTU 40	0.0	37.8	15.2	0.0	45.0	24.7		76.9
	OTU 153	0.0	0.0	0.0	0.0	0.6	0.1		1.0
<i>ambiguous^b</i>	OTU 299	0.0	0.0	0.0	0.0	0.7	0.0		1.2
<i>Hyphomicrobium</i>	OTU 185	0.0	0.0	15.4	0.0	1.8	19.5		3.2
	OTU 309	0.0	0.0	0.2	58.3	0.0	0.0	58.3	
<i>ambiguous^b</i>	OTU 313	0.0	0.0	0.0	0.9	0.0	0.0	0.9	
<i>Beijerinckiaceae</i>	OTU 144	0.0	0.0	0.0	0.0	0.6	2.4		1.0
<i>ambiguous^b</i>	OTU 338	0.0	0.0	0.6	0.0	1.4	1.6		2.4
	OTU 349	0.0	0.0	0.0	40.8	0.0	0.0	40.8	
Percentage of labelled taxa to total fraction [%]					100	58			

^a Phylogenetic affiliation was done with BLASTn (Dezember 2015) and confirmed by positioning in phylogenetic tree (for further information see Figure A 12)

^b Sequence identity with BLASTn < 90 % as well as ambiguous position in phylogenetic tree

Table A 29 Labelled methylotrophic taxa in the treatments with carbon dioxide.

Relative abundances are shown for all fractions (H, heavy; M, middle; L, light) in [¹²C]- and [¹³C]-CO₂ treatments. Black faces indicate values that were used for calculating 'labelling proportions' ('LP') as indicators of relative importance. Bold faces indicate 'LP' > 5 %.

Phylogenetic affiliation ^a	Labelled OTU	Relative abundance [%]						LP [%]	
		¹² C			¹³ C			H	M
		H	M	L	H	M	L		
<i>Methylobacterium</i>	OTU 55	0.0	55.1	12.7	0.0	78.7	5.9		91.7
	OTU 78	0.0	0.8	1.9	0.0	2.1	2.0		2.4
	OTU 110	0.0	0.4	0.9	0.0	0.8	0.2		1.0
<i>Hyphomicrobium</i> <i>ambiguous</i> ^b	OTU 214	0.0	0.2	5.4	0.2	2.1	0.9		2.4
	OTU 236	0.0	0.2	3.0	0.0	1.3	1.1		1.5
	OTU 286	0.0	0.0	0.6	97.7	0.0	0.7	97.9	
<i>Beijerinckiaceae</i> <i>ambiguous</i> ^b	OTU 340	0.0	0.0	0.2	2.1	0.8	0.9	2.1	1.0
Percentage of labelled taxa to total fraction [%]					100	86			

^a Phylogenetic affiliation was done with BLASTn (Dezember 2015) and confirmed by positioning in phylogenetic tree (for further information see Figure A 12)

^b Sequence identity with BLASTn < 90 % as well as ambiguous position in phylogenetic tree

Table A 30 Labelled methylotrophic taxa in the treatments with methanol at *in situ* pH.

Relative abundances are shown for all fractions (H, heavy; M, middle; L, light) in [¹²C]- and [¹³C]-methanol treatments at *in situ* pH of the pH shift SIP experiment. Black faces indicate values that were used for calculating 'labelling proportions' ('LP') as indicators of relative importance. Bold faces indicate 'LP' > 5 %. This table has been published in Morawe *et al.* 2017.

Phylogenetic affiliation ^a	Labelled OTU	Relative abundance [%]						LP [%]		
		¹² C			¹³ C			H	M	
		H	M	L	H	M	L	H	M	
<i>Methylobacterium</i>	OTU 7	0.0	0.1	0.0	0.0	1.1	0.0		1.3	
	OTU 55	1.1	1.3	0.9	2.1	0.1	0.7	2.7		
<i>ambiguous^b</i>	OTU 0	0.0	0.0	0.2	0.2	1.9	0.1		2.2	
<i>Hyphomicrobium</i>	OTU 185	0.6	0.4	1.9	9.9	3.7	7.4	12.2	4.3	
	OTU 186	0.0	0.0	0.1	0.7	0.2	0.4	0.9		
	OTU 243	0.0	0.0	1.6	0.2	11.7	0.1		13.7	
	OTU 257	0.3	0.5	2.0	7.4	0.2	0.8	9.1		
	OTU 308	0.0	0.0	0.6	0.5	0.0	0.7	0.7		
<i>ambiguous^b</i>	OTU 309	0.1	0.0	0.5	5.3	0.0	0.1	6.5		
	OTU 172	0.1	0.2	8.2	8.7	0.0	2.8	10.8		
	OTU 210	0.1	2.6	6.2	3.0	19.9	5.5	3.7	23.1	
	OTU 214	0.5	0.2	2.2	3.5	1.6	3.2	4.4	1.9	
	OTU 236	1.6	19.5	46.0	22.1	31.7	25.4	27.3	36.9	
	OTU 266	0.4	0.0	1.4	1.4	0.1	0.3	1.7		
	OTU 310	0.0	0.1	0.2	0.1	0.5	0.3		0.6	
<i>Methylorhabdus</i>										
<i>ambiguous^b</i>	OTU 18	0.0	0.8	2.4	8.0	8.2	0.0	10.0	9.6	
<i>Beijerinckiaceae</i>										
<i>ambiguous^b</i>	OTU 144	0.0	0.0	1.3	1.0	0.0	0.2	1.2		
	OTU 337	0.0	0.0	0.1	1.5	0.1	0.0	1.8		
	OTU 338	0.1	0.1	0.3	4.1	0.0	0.3	5.1		
	OTU 340	0.1	0.7	2.3	1.5	3.8	0.6	1.9	4.5	
	OTU 349	0.1	0.6	2.9	0.5	1.7	1.4		2.0	
Percentage of labelled taxa to total fraction [%]					81	86				

^a Phylogenetic affiliation was done with BLASTn (Dezember 2015) and confirmed by positioning in phylogenetic tree (for further information see Figure A 12)

^b Sequence identity with BLASTn < 90 % as well as ambiguous position in phylogenetic tree

Table A 31 Labelled methylotrophic taxa in the treatments with methanol at pH 7.

Relative abundances are shown for all fractions (H, heavy; M, middle; L, light) in [¹²C]- and [¹³C]-methanol treatments at pH 7 of the pH shift SIP experiment. Black faces indicate values that were used for calculating 'labelling proportions' ('LP') as indicators of relative importance. Bold faces indicate 'LP' > 5 %. This table has been published in Morawe *et al.* 2017.

Phylogenetic affiliation ^a	Labelled OTU	Relative abundance [%]						LP [%]	
		¹² C			¹³ C			H	M
		H	M	L	H	M	L	H	M
<i>Methylobacterium</i>	OTU 55	27.0	37.4	25.8	72.0	39.7	9.0	95.4	80.1
	OTU 107	0.1	0.2	0.4	0.1	0.6	0.0		1.2
<i>ambiguous^b</i>	OTU 141	0.0	0.7	1.0	3.5	1.3	0.4	4.6	2.7
<i>Hyphomicrobium</i>	OTU 185	1.4	1.9	5.8	0.9	7.3	12.7		14.7
	OTU 213	0.0	0.3	0.4	0.0	0.7	0.2		1.3
Percentage of labelled taxa to total fraction [%]					75	50			

^a Phylogenetic affiliation was done with BLASTn (Dezember 2015) and confirmed by positioning in phylogenetic tree (for further information see Figure A 12)

^b Sequence identity with BLASTn < 90 % as well as ambiguous position in phylogenetic tree

Table A 32 Labelled fungal taxa in the treatments with methanol.

Relative abundances are shown for all fractions (H, heavy; M, middle; L, light) in [¹²C]- and [¹³C]-methanol treatments. Black faces indicate values that were used for calculating 'labelling proportions' ('LP') as indicators of relative importance. Bold faces indicate 'LP' > 5 %. This table has been published in Morawe *et al.* 2017.

Phylogenetic affiliation ^a	Labelled OTU	Relative abundance [%]						LP [%]		
		¹² C			¹³ C			H	M	
		H	M	L	H	M	L			
Ascomycota										
<i>Saccharomyces</i>	OTU 2	0.0	14.2	5.2	7.6	8.6	5.1	9.9		
<i>Oidiodendron</i>	OTU 9	0.0	0.7	1.0	0.6	0.0	0.4	0.8		
<i>Penicillium</i>	OTU 10	0.0	1.1	3.2	14.7	0.8	4.1	19.2		
<i>Paecilomyces</i>	OTU 14	0.0	0.1	0.4	2.5	0.0	0.1	3.3		
<i>Bionectria</i>	OTU 24	0.0	0.4	0.7	0.0	0.7	1.2		4.3	
<i>Oidiodendron</i>	OTU 32	4.1	0.3	0.9	5.4	0.1	1.0	7.1		
<i>Geomyces</i>	OTU 55	0.0	0.3	0.8	0.1	0.6	0.3		3.5	
<i>Hyaloscyphaceae</i>	OTU 135	0.0	0.1	0.1	0.0	1.1	0.1		7.0	
<i>Penicillium</i>	OTU 188	0.0	0.0	0.0	2.9	0.0	0.0	3.8		
Basidiomycota										
<i>Leucosporidiales</i>	OTU 15	0.0	4.4	2.6	1.2	3.3	2.4	1.6		
<i>Syzygospora</i>	OTU 22	0.0	2.5	1.7	0.5	2.9	1.4	0.7	18.3	
<i>Laccaria</i>	OTU 27	0.5	0.9	0.3	0.6	1.3	0.3		8.3	
<i>Cortinarius</i>	OTU 44	0.0	0.0	0.1	0.8	0.4	0.1	1.1		
<i>Cryptococcus</i>	OTU 46	0.0	0.0	0.0	23.6	0.0	0.0	30.9		
Glomeromycota										
<i>Glomeromyces</i>	OTU 25	0.0	0.8	0.4	3.4	0.3	0.2	4.5		
Rozellomycota										
	OTU 29	0.0	0.4	1.1	2.2	0.1	1.5	2.9		
	OTU 38	0.8	1.2	0.7	2.0	0.5	0.3	2.6		
	OTU 153	0.0	0.0	0.0	2.3	0.1	0.0	3.0		
Zygomycota										
<i>Mortierella</i>	OTU 5	2.8	5.0	4.6	5.1	5.7	5.8	6.7	35.7	
<i>Mortierella</i>	OTU 33	0.0	0.6	1.3	1.1	0.7	1.0	1.4	4.3	
<i>Mortierella</i>	OTU 53	0.0	0.5	0.3	0.0	0.6	0.1		3.9	
<i>Mortierella</i>	OTU 112	0.0	0.8	0.6	0.4	2.4	0.4	0.5	14.8	
Percentage of labelled taxa to total fraction [%]					77	16				

^a Phylogenetic affiliation is based on the dynamic UNITE database (v7, release 01.08.2015) and was done with a bayesian classifier implied with MOTUHR based on the best hit of consensus taxonomy after 100 bootstrapped assignments (for further reference sequences based on 'massBLASTer' of UNITE see Table A 13)

Table A 33 Labelled fungal taxa in the treatments with acetate.

Relative abundances are shown for all fractions (H, heavy; M, middle; L, light) in [¹²C]- and [¹³C]-acetate treatments. Black faces indicate values that were used for calculating 'labelling proportions' ('LP') as indicators of relative importance. Bold faces indicate 'LP' > 5 %.

Phylogenetic affiliation ^a	Labelled OTU	Relative abundance [%]						LP [%]	
		¹² C			¹³ C			H	M
		H	M	L	H	M	L		
Ascomycota									
<i>Oidiodendron</i>	OTU 9	0.2	0.0	2.0	6.4	0.0	0.1	13.7	
<i>Elaphocordyceps</i>	OTU 16	0.0	1.3	2.0	2.4	0.0	0.4	5.2	
Basidiomycota									
<i>Trichosporon</i>	OTU 1	47.3	56.5	61.8	45.7	96.1	49.6		100.0
<i>Laccaria</i>	OTU 27	0.0	0.1	0.1	1.1	0.0	0.1	2.3	
<i>Trechispora</i>	OTU 30	0.0	0.1	0.3	3.4	0.0	0.3	7.3	
<i>Inocybe</i>	OTU 31	0.0	0.8	0.1	6.9	0.2	0.1	14.7	
<i>Mycena</i>	OTU 37	0.0	0.1	0.1	0.9	0.0	0.1	2.0	
<i>Tomentella</i>	OTU 49	0.0	1.9	0.1	4.2	0.0	0.0	8.9	
<i>Trichosporon</i>	OTU 73	0.0	0.6	0.2	4.5	0.6	0.2	9.6	
Chytridiomycota	OTU 114	0.0	0.0	0.1	6.4	0.0	0.0	13.6	
Rozellomycota	OTU 141	0.0	0.0	0.1	4.2	0.0	0.0	9.0	
Zygomycota									
<i>Mortierella</i>	OTU 4	1.4	1.8	0.2	1.6	0.0	1.3	3.4	
<i>Mortierella</i>	OTU 23	0.0	0.2	0.1	2.6	0.0	0.5	5.6	
<i>Mortierella</i>	OTU 42	0.6	1.1	0.3	0.9	0.1	0.9	1.8	
<i>Mortierella</i>	OTU 50	0.6	0.3	0.0	0.7	0.0	0.0	1.5	
<i>Mucor</i>	OTU 350	0.0	0.0	0.0	0.6	0.0	0.0	1.4	
Percentage of labelled taxa to total fraction [%]					47	96			

^a Phylogenetic affiliation is based on the dynamic UNITE database (v7, release 01.08.2015) and was done with a bayesian classifier implied with MOTUHR based on the best hit of consensus taxonomy after 100 bootstrapped assignments (for further reference sequences based on 'massBLASter' of UNITE see Table A 13)

Table A 34 Labelled fungal taxa in the treatments with glucose.

Relative abundances are shown for all fractions (H, heavy; M, middle; L, light) in [¹²C]- and [¹³C]-glucose treatments. Black faces indicate values that were used for calculating 'labelling proportions' ('LP') as indicators of relative importance. Bold faces indicate 'LP' > 5 %.

Phylogenetic affiliation ^a	Labelled OTU	Relative abundance [%]						LP [%]	
		¹² C			¹³ C			H	M
		H	M	L	H	M	L		
Ascomycota									
<i>Paecilomyces</i>	OTU 14	0.0	0.4	1.4	3.8	0.7	0.1	4.1	0.8
<i>Cenococcum</i>	OTU 187	0.0	0.0	0.0	0.9	0.0	0.1	0.9	
<i>Cladophialophora</i>	OTU 198	0.0	0.0	0.1	0.8	0.0	0.1	0.9	
Basidiomycota									
<i>Trichosporon</i>	OTU 1	58.6	76.3	82.7	86.0	93.8	64.1	92.3	99.2
<i>Tomentella</i>	OTU 11	0.0	0.9	0.2	0.6	0.0	1.2	0.7	
<i>Cryptococcus</i>	OTU 13	0.0	1.2	0.2	1.0	0.4	0.6	1.1	
Percentage of labelled taxa to total fraction [%]					93	95			

^a Phylogenetic affiliation is based on the dynamic UNITE database (v7, release 01.08.2015) and was done with a bayesian classifier implied with MOTUHR based on the best hit of consensus taxonomy after 100 bootstrapped assignments (for further reference sequences based on 'massBLASter' of UNITE see Table A 13)

Table A 35 Labelled fungal taxa in the treatments with xylose.

Relative abundances are shown for all fractions (H, heavy; M, middle; L, light) in [¹²C]- and [¹³C]-xylose treatments. Black faces indicate values that were used for calculating 'labelling proportions' ('LP') as indicators of relative importance. Bold faces indicate 'LP' > 5 %.

Phylogenetic affiliation ^a	Labelled OTU	Relative abundance [%]						LP [%]	
		¹² C			¹³ C			H	M
		H	M	L	H	M	L		
Ascomycota									
<i>Oidiodendron</i>	OTU 9	0.3	1.7	1.0	0.7	0.0	0.6	0.7	
<i>Pochonia</i>	OTU 58	0.5	0.1	0.4	1.7	0.3	0.1	1.8	
<i>Davidiellaceae</i>	OTU 86	0.0	0.0	0.0	0.5	0.0	0.0	0.6	
<i>Saccharomyces</i>	OTU 121	0.0	0.0	0.1	1.4	0.0	0.1	1.5	
Basidiomycota									
<i>Trichosporon</i>	OTU 1	71.2	80.4	86.9	91.1	98.9	73.1	95.4	100.0
Percentage of labelled taxa to total fraction [%]					96	99			

^a Phylogenetic affiliation is based on the dynamic UNITE database (v7, release 01.08.2015) and was done with a bayesian classifier implied with MOTUHR based on the best hit of consensus taxonomy after 100 bootstrapped assignments (for further reference sequences based on 'massBLASter' of UNITE see Table A 13)

APPENDICES

Table A 36 Labelled fungal taxa in the treatments with vanillic acid.

Relative abundances are shown for all fractions (H, heavy; M, middle; L, light) in [¹²C]- and [¹³C]-vanillic acid treatments. Black faces indicate values that were used for calculating 'labelling proportions' ('LP') as indicators of relative importance. Bold faces indicate 'LP' > 5 %.

Phylogenetic affiliation ^a	Labelled OTU	Relative abundance [%]						LP [%]		
		¹² C			¹³ C			H	M	
		H	M	L	H	M	L			
Ascomycota										
<i>Saccharomyces</i>	OTU 2	0.0	6.7	5.6	13.1	0.7	9.3	14.0		
<i>Trichoderma</i>	OTU 8	0.0	2.0	1.8	0.8	0.1	2.5	0.8		
<i>Oidiodendron</i>	OTU 9	0.0	0.4	8.4	1.5	0.1	0.9	1.6		
<i>Nectria</i>	OTU 18	4.0	0.8	1.0	13.1	30.9	0.8	14.0	35.3	
<i>Oidiodendron</i>	OTU 32	0.0	1.1	1.0	9.6	0.0	1.1	10.3		
<i>Leptodontidium</i>	OTU 39	0.0	0.1	0.6	6.9	4.6	0.6	7.3	5.2	
<i>Penicillium</i>	OTU 51	0.0	0.0	0.4	4.3	0.0	0.1	4.6		
<i>Nectriaceae</i>	OTU 72	0.0	0.1	0.0	0.0	3.0	0.0		3.5	
<i>Cladophialophora</i>	OTU 88	0.0	0.1	0.1	0.3	1.4	0.8		1.6	
<i>Exophiala</i>	OTU 91	0.0	0.3	0.0	0.0	3.9	0.4		4.4	
<i>Bionectriaceae</i>	OTU 96	0.0	0.4	0.0	0.0	4.7	0.1		5.4	
<i>Herpotrichiellaceae</i>	OTU 111	0.0	0.6	0.2	0.0	2.5	0.1		2.8	
<i>Exophiala</i>	OTU 140	0.0	0.1	0.2	0.0	2.7	0.1		3.1	
<i>Leotiomyces</i>	OTU 157	0.0	0.3	0.1	0.0	0.7	0.4		0.8	
<i>Ilyonectria</i>	OTU 177	0.0	0.0	0.0	0.0	1.2	0.1		1.4	
Basidiomycota										
<i>Trichosporon</i>	OTU 1	0.0	0.6	2.9	5.3	0.1	3.1	5.6		
<i>Cryptococcus</i>	OTU 6	0.0	3.1	3.3	0.0	30.4	12.8		34.7	
<i>Ganoderma</i>	OTU 7	0.0	4.1	3.8	9.2	0.4	4.2	9.9		
<i>Tomentella</i>	OTU 11	0.0	1.8	1.1	6.2	0.4	1.0	6.7		
<i>Cryptococcus</i>	OTU 28	0.0	0.2	0.4	0.0	0.7	1.6		0.8	
<i>Trechispora</i>	OTU 103	0.0	0.0	0.0	3.4	0.0	0.2	3.6		
<i>Sporidiobolales</i>	OTU 304	0.0	0.1	0.1	0.0	0.8	0.0		0.9	
Glomeromycota										
<i>Glomeromycetes</i>	OTU 26	0.0	0.2	0.1	2.5	0.0	0.1	2.7		
<i>Glomeromycetes</i>	OTU 190	0.0	0.0	0.0	2.1	0.0	0.0	2.2		
Zygomycota										
<i>Mortierella</i>	OTU 5	7.0	4.4	1.3	8.8	0.9	2.0	9.4		
<i>Mortierella</i>	OTU 50	1.0	0.1	0.2	2.2	0.1	0.2	2.3		
<i>Mortierella</i>	OTU 53	3.9	0.5	0.0	4.6	0.0	0.1	4.9		
Percentage of labelled taxa to total fraction [%]					93	88				

^a Phylogenetic affiliation is based on the dynamic UNITE database (v7, release 01.08.2015) and was done with a bayesian classifier implied with MOTUHR based on the best hit of consensus taxonomy after 100 bootstrapped assignments (for further reference sequences based on 'massBLASter' of UNITE see Table A 13)

APPENDICES

Table A 37 Labelled fungal taxa in the treatments with CO₂ and additional methanol.

Relative abundances are shown for all fractions (H, heavy; M, middle; L, light) in [¹²C]- and [¹³C]-CO₂ and additional methanol treatments. Black faces indicate values that were used for calculating 'labelling proportions' ('LP') as indicators of relative importance. Bold faces indicate 'LP' > 5 %.

Phylogenetic affiliation ^a	Labelled OTU	Relative abundance [%]						LP [%]		
		¹² C			¹³ C			H	M	
		H	M	L	H	M	L	H	M	
Ascomycota										
<i>Saccharomycetes</i>	OTU 2	0.0	7.2	6.0	6.1	10.2	6.9	7.3	21.6	
<i>Trichoderma</i>	OTU 8	0.1	1.4	5.0	4.3	2.8	5.3	5.1	6.0	
<i>Oidiodendron</i>	OTU 9	0.0	4.1	1.0	1.5	0.9	0.4	1.8		
<i>Penicillium</i>	OTU 10	0.0	2.2	4.2	2.1	4.1	2.8	2.5	8.7	
<i>Elaphocordyceps</i>	OTU 16	0.0	0.5	0.4	3.0	0.8	0.6	3.6	1.7	
<i>Oidiodendron</i>	OTU 17	0.0	1.0	0.7	2.5	0.6	0.6	3.0		
<i>Elaphomyces</i>	OTU 20	0.0	1.4	0.4	0.0	2.0	0.7		4.2	
<i>Dermateaceae</i>	OTU 21	0.0	1.1	2.2	6.7	2.3	2.4	8.1	5.0	
<i>Bionectria</i>	OTU 24	0.0	0.1	0.5	3.4	0.8	0.5	4.1	1.6	
<i>Volutella</i>	OTU 35	0.0	0.3	0.8	0.0	0.6	1.1		1.3	
<i>Leptodontidium</i>	OTU 39	0.0	0.9	0.7	0.0	1.2	0.4		2.5	
<i>Chaunopycnis</i>	OTU 40	0.0	0.1	0.1	1.5	0.4	0.4	1.8		
<i>Penicillium</i>	OTU 51	0.0	0.7	0.3	0.8	0.0	0.0	0.9		
<i>Helotiales</i>	OTU 62	0.0	0.3	0.5	8.7	0.9	0.1	10.4	1.9	
<i>Aspergillus</i>	OTU 66	0.0	0.1	0.1	0.0	0.8	1.1		1.6	
<i>Oidiodendron</i>	OTU 69	0.0	0.0	0.3	0.0	1.6	0.8		3.4	
<i>Trichocomaceae</i>	OTU 71	0.0	0.1	0.4	0.0	0.6	0.6		1.2	
<i>Chaetosphaeria</i>	OTU 83	0.0	0.4	0.1	0.0	0.9	0.9		1.9	
<i>Helotiales</i>	OTU 94	0.0	0.5	0.1	4.1	0.3	0.1	4.9		
<i>Bionectriaceae</i>	OTU 96	0.0	0.0	0.2	0.0	0.6	0.4		1.2	
<i>Leotiomyces</i>	OTU 128	0.0	0.1	0.1	1.0	0.1	0.3	1.2		
<i>Helotiales</i>	OTU 138	0.0	0.0	0.1	0.0	0.6	0.1		1.3	
<i>Crocicreas</i>	OTU 161	0.0	0.3	0.1	0.0	0.6	0.1		1.2	
<i>Pleosporales</i>	OTU 185	0.0	0.0	0.1	2.8	0.0	0.0	3.4		
Basidiomycota										
<i>Trichosporon</i>	OTU 1	0.1	4.6	4.5	3.5	2.3	2.8	4.2		
<i>Ganoderma</i>	OTU 7	0.1	3.1	3.0	4.9	4.1	4.9	5.8	8.7	
<i>Agaricomycetes</i>	OTU 12	0.0	6.2	8.1	7.4	1.1	1.0	8.8		
<i>Leucosporidiales</i>	OTU 15	0.0	0.3	0.9	0.6	0.6	3.3	0.7		
<i>Cryptococcus</i>	OTU 28	0.0	1.4	0.6	0.0	2.3	1.4		4.8	
<i>Trechispora</i>	OTU 30	0.0	0.0	0.4	0.0	1.0	0.4		2.2	
<i>Inocybe</i>	OTU 31	0.0	1.1	0.6	5.5	0.5	0.1	6.6		
<i>Cortinarius</i>	OTU 44	0.0	0.2	0.4	0.0	1.7	0.3		3.5	
<i>Basidiomycota</i>	OTU 45	0.0	0.1	0.4	0.0	0.8	0.7		1.7	
<i>Lactarius</i>	OTU 57	0.0	0.0	0.3	0.0	1.4	0.6		3.1	
<i>Microbotryomycetes</i>	OTU 85	0.0	0.3	0.3	0.0	0.7	0.4		1.5	
Rozellomycota	OTU 38	0.0	0.3	0.4	0.0	0.9	0.8		1.9	
Zygomycota										
<i>Mortierella</i>	OTU 19	0.0	1.0	1.0	3.0	1.4	1.5	3.6		
<i>Mortierella</i>	OTU 23	0.0	1.0	0.7	0.0	1.7	0.8		3.5	
<i>Mortierella</i>	OTU 33	0.0	0.6	0.4	4.1	0.5	0.8	4.9		
<i>Mortierella</i>	OTU 61	0.0	0.1	0.1	0.0	1.4	0.2		2.9	
not affiliated	OTU 108	0.0	0.0	0.0	6.1	0.0	0.0	7.2		
Percentage of labelled taxa to total fraction [%]					84	47				

^a Phylogenetic affiliation is based on the dynamic UNITE database (v7, release 01.08.2015) and was done with a bayesian classifier implied with MOTUHR based on the best hit of consensus taxonomy after 100 bootstrapped assignments (for further reference sequences based on 'massBLASter' of UNITE see Table A 13)

APPENDICES

Table A 38 Labelled fungal taxa in the treatments with CO₂.

Relative abundances are shown for all fractions (H, heavy; M, middle; L, light) in [¹²C]- and [¹³C]-CO₂ treatments. Black faces indicate values that were used for calculating 'labelling proportions' ('LP') as indicators of relative importance. Bold faces indicate 'LP' > 5 %.

Phylogenetic affiliation ^a	Labelled OTU	Relative abundance [%]						LP [%]		
		¹² C			¹³ C			H	M	
		H	M	L	H	M	L			
Ascomycota										
<i>Saccharomycetes</i>	OTU 2	0.0	5.2	7.0	0.0	14.0	8.6		43.0	
<i>Trichoderma</i>	OTU 8	0.0	2.4	4.0	5.4	3.5	3.3	6.0	10.8	
<i>Oidiodendron</i>	OTU 9	1.7	0.4	7.0	3.5	0.4	2.2	3.9		
<i>Elaphocordyceps</i>	OTU 16	2.2	0.2	0.8	3.4	0.6	0.4	3.7	1.8	
<i>Oidiodendron</i>	OTU 17	0.0	0.4	1.4	9.1	1.1	0.9	10.1	3.3	
<i>Oidiodendron</i>	OTU 32	0.0	0.2	1.2	0.0	0.8	1.3		2.4	
<i>Volutella</i>	OTU 35	0.0	0.8	0.7	8.1	0.4	0.5	9.0		
<i>Bulgaria</i>	OTU 41	0.0	0.3	0.0	13.8	0.1	0.1	15.4		
<i>Penicillium</i>	OTU 51	0.1	0.0	0.8	0.7	0.0	0.1	0.8		
<i>Geomyces</i>	OTU 55	0.0	0.8	0.6	0.5	0.4	0.4	0.6		
<i>Pochonia</i>	OTU 58	0.0	0.1	0.2	1.1	0.4	0.3	1.3		
<i>Hypocreales</i>	OTU 256	0.0	0.0	0.0	1.5	0.0	0.0	1.7		
Basidiomycota										
<i>Agaricomycetes</i>	OTU 12	0.0	1.1	2.1	0.0	3.7	2.2		11.3	
<i>Cryptococcus</i>	OTU 28	0.0	0.1	0.6	0.0	2.4	1.4		7.3	
<i>Inocybe</i>	OTU 31	0.0	0.8	0.0	3.8	1.1	0.4	4.2	3.3	
<i>Cortinarius</i>	OTU 44	0.0	0.4	0.0	0.0	1.5	0.5		4.6	
<i>Agaricomycetes</i>	OTU 56	0.0	0.0	0.2	11.6	0.1	0.6	12.9		
<i>Lactarius</i>	OTU 57	0.0	0.3	0.6	4.1	0.8	1.1	4.6		
<i>Russula</i>	OTU 67	0.0	0.2	0.2	1.1	0.1	0.0	1.3		
<i>Luellia</i>	OTU 81	0.0	0.0	0.0	0.0	0.5	0.1		1.5	
<i>Lactarius</i>	OTU 131	0.0	0.1	0.4	3.4	0.0	0.1	3.7		
Glomeromycota										
<i>Glomeromycetes</i>	OTU 26	0.0	0.1	0.1	0.0	0.5	0.1		1.5	
Rozellomycota										
	OTU 29	0.0	1.2	1.8	0.0	1.4	1.1		4.4	
	OTU 38	0.0	0.3	0.4	0.0	0.8	0.5		2.4	
Zygomycota										
<i>Mortierella</i>	OTU 4	0.0	4.1	1.8	2.7	3.3	3.5	3.0		
<i>Mortierella</i>	OTU 5	0.0	7.7	2.1	6.1	5.8	2.4	6.8		
<i>Mortierella</i>	OTU 23	0.0	0.7	0.6	2.6	0.4	0.4	2.8		
<i>Mortierella</i>	OTU 33	0.0	0.1	0.4	0.0	0.7	0.7		2.2	
<i>Mortierella</i>	OTU 302	0.0	0.0	0.0	0.7	0.0	0.0	0.8		
not affiliated	OTU 98	0.0	0.0	0.0	6.7	0.0	0.0	7.5		
Percentage of labelled taxa to total fraction [%]					90	33				

^a Phylogenetic affiliation is based on the dynamic UNITE database (v7, release 01.08.2015) and was done with a bayesian classifier implied with MOTUHR based on the best hit of consensus taxonomy after 100 bootstrapped assignments (for further reference sequences based on 'massBLASTER' of UNITE see Table A 13)

Table A 39 Labelled fungal taxa in the treatments with methanol at *in situ* pH.

Relative abundances are shown for all fractions (H, heavy; M, middle; L, light) in [¹²C]- and [¹³C]-methanol treatments at *in situ* pH of the pH shift SIP experiment. Black faces indicate values that were used for calculating 'labelling proportions' ('LP') as indicators of relative importance. Bold faces indicate 'LP' > 5 %. This table has been published in Morawe *et al.* 2017.

Phylogenetic affiliation ^a	Labelled OTU	Relative abundance [%]						LP [%]		
		¹² C			¹³ C			H	M	
		H	M	L	H	M	L	H	M	
Ascomycota										
<i>Bionectria</i>	OTU 24	1.3	1.0	0.6	1.8	0.8	1.4	3.8		
<i>Chaunopycnis</i>	OTU 40	0.2	0.3	0.8	0.8	0.6	1.0	1.7		
<i>Clavicipitaceae</i>	OTU 48	0.3	0.2	1.3	0.7	0.3	0.8	1.4		
<i>Penicillium</i>	OTU 51	0.3	0.4	0.5	0.6	0.1	1.4	1.2		
<i>Trichoderma</i>	OTU 59	0.3	0.0	1.0	0.7	0.5	1.3	1.4		
<i>Chaetomiaceae</i>	OTU 60	0.6	0.4	1.9	1.3	1.2	3.1	2.7	6.9	
<i>Trichocomaceae</i>	OTU 71	0.0	0.3	0.2	0.1	0.6	0.8		3.3	
<i>Ascomycota</i>	OTU 113	0.4	0.6	0.6	0.6	0.4	0.1	1.3		
<i>Helotiales</i>	OTU 265	0.0	0.0	0.0	0.0	0.8	0.0		4.5	
Basidiomycota										
<i>Ganoderma</i>	OTU 7	2.0	2.7	3.4	2.9	3.3	2.0	5.9	19.5	
<i>Tomentella</i>	OTU 11	0.1	0.3	0.5	0.4	0.6	0.0		3.7	
<i>Agaricomycetes</i>	OTU 12	0.5	0.5	1.0	2.4	1.5	1.1	5.1	8.5	
<i>Cryptococcus</i>	OTU 13	1.3	0.8	1.2	1.9	1.2	0.6	3.9	6.9	
<i>Leucosporidiales</i>	OTU 15	1.1	3.0	1.4	3.9	2.8	1.5	8.1		
<i>Laccaria</i>	OTU 27	0.7	1.4	0.8	1.0	1.0	0.6	2.0		
<i>Trechispora</i>	OTU 30	1.6	2.0	2.1	2.9	1.8	2.0	5.9		
<i>Mycena</i>	OTU 37	0.1	0.1	0.0	0.7	0.1	0.1	1.4		
<i>Basidiomycota</i>	OTU 45	0.5	1.0	0.1	0.8	0.1	0.5	1.7		
<i>Microbotryomycetes</i>	OTU 85	0.0	0.2	0.3	0.6	0.2	0.1	1.2		
<i>Lycoperdon</i>	OTU 130	0.2	0.1	0.3	0.6	0.6	0.4	1.2	3.3	
<i>Phlebiella</i>	OTU 199	0.1	0.1	0.1	0.6	0.4	0.1	1.2		
Rozellomycota	OTU 38	0.6	1.2	0.3	1.6	1.0	0.6	3.3		
Zygomycota										
<i>Mortierella</i>	OTU 4	6.5	11.8	9.5	14.8	11.7	6.7	30.6		
<i>Mortierella</i>	OTU 5	3.4	3.2	2.3	3.6	3.9	1.8	7.5	22.8	
<i>Mortierella</i>	OTU 19	0.7	0.9	1.0	1.6	1.4	1.2	3.3	8.1	
<i>Mortierella</i>	OTU 23	0.5	0.1	0.1	0.8	0.3	0.2	1.6		
<i>Mortierella</i>	OTU 33	0.4	0.5	0.1	1.3	1.1	0.7	2.6	6.5	
<i>Mortierella</i>	OTU 50	0.6	0.5	0.5	0.6	1.0	0.2		6.1	
Percentage of labelled taxa to total fraction [%]					48	17				

^a Phylogenetic affiliation is based on the dynamic UNITE database (v7, release 01.08.2015) and was done with a bayesian classifier implied with MOTUHR based on the best hit of consensus taxonomy after 100 bootstrapped assignments (for further reference sequences based on 'massBLASTER' of UNITE see Table A 13)

Table A 40 Labelled fungal taxa in the treatments with methanol at pH 7.

Relative abundances are shown for all fractions (H, heavy; M, middle; L, light) in [¹²C]- and [¹³C]-methanol treatments at pH 7 of the pH shift SIP experiment. Black faces indicate values that were used for calculating 'labelling proportions' ('LP') as indicators of relative importance. Bold faces indicate 'LP' > 5 %. This table has been published in Morawe *et al.* 2017.

Phylogenetic affiliation ^a	Labelled OTU	Relative abundance [%]						LP [%]	
		¹² C			¹³ C			H	M
		H	M	L	H	M	L		
Ascomycota									
<i>Saccharomycetes</i>	OTU 2	1.3	0.6	0.3	1.9	0.4	0.2	3.0	
<i>Paecilomyces</i>	OTU 14	1.6	1.0	1.0	2.7	6.6	4.8	4.2	13.5
<i>Bionectria</i>	OTU 24	1.3	1.0	0.6	1.8	1.1	2.7	2.8	
<i>Chaetothyriales</i>	OTU 64	0.0	0.1	0.0	0.1	0.6	0.0		1.3
Basidiomycota									
<i>Trichosporon</i>	OTU 1	32.4	29.9	21.0	46.4	34.7	20.1	72.7	71.0
<i>Cryptococcus</i>	OTU 6	0.9	0.9	0.2	2.3	1.6	1.5	3.6	3.3
<i>Ganoderma</i>	OTU 7	2.0	2.7	3.4	2.1	3.5	1.3		7.3
<i>Leucosporidiales</i>	OTU 15	1.1	3.0	1.4	2.0	2.2	0.2	3.1	
<i>Syzygospora</i>	OTU 22	1.4	0.1	0.1	1.9	0.8	0.6	3.0	1.7
<i>Trichosporon</i>	OTU 73	0.4	0.1	0.0	1.8	0.5	0.7	2.9	
<i>Basidiomycota</i>	OTU 77	1.0	0.4	0.1	1.4	0.5	0.3	2.2	
Rozellomycota	OTU 154	0.2	0.0	0.0	0.9	0.2	0.2	1.4	
Zygomycota									
<i>Mortierella</i>	OTU 23	0.5	0.1	0.1	0.7	1.0	0.1	1.1	2.0
Percentage of labelled taxa to total fraction [%]					64	49			

^a Phylogenetic affiliation is based on the dynamic UNITE database (v7, release 01.08.2015) and was done with a bayesian classifier implied with MOTUHR based on the best hit of consensus taxonomy after 100 bootstrapped assignments (for further reference sequences based on 'massBLASter' of UNITE see Table A 13)

Table A 41 Calculated ratios based on quantified gene numbers of *mxoF* and 16S rRNA genes in different soil ecosystem types in situ and after methanol supplementation.

Average ratios are calculated on the basis of determined gene copy numbers ng⁻¹ of duplicates for each treatment (i.e., *t*₀, no treatment = *in situ*; '–', unsupplemented control; '+', methanol supplementation, 4x 5mM).

Ratio <i>mxoF</i> / 16S rRNA			Ratio <i>mxoF</i> / 16S rRNA		
Canola			Syringa		
<i>t</i> ₀	(98.39 ± 4.92)	x 10 ⁻⁸	<i>t</i> ₀	(76.58 ± 3.83)	x 10 ⁻⁹
–	(39.18 ± 63.89)	x 10 ⁻⁶	–	(80.74 ± 38.03)	x 10 ⁻⁸
+	(58.30 ± 55.80)	x 10 ⁻⁸	+	(16.75 ± 5.10)	x 10 ⁻⁷
Meadow 1			Meadow 2		
<i>t</i> ₀	(13.00 ± 0.65)	x 10 ⁻⁸	<i>t</i> ₀	(65.28 ± 3.26)	x 10 ⁻¹¹
–	(53.61 ± 18.10)	x 10 ⁻⁸	–	(14.20 ± 5.65)	x 10 ⁻⁶
+	(70.71 ± 13.47)	x 10 ⁻⁸	+	(16.90 ± 19.61)	x 10 ⁻⁸
Herbs			Blueberry		
<i>t</i> ₀	(24.53 ± 1.23)	x 10 ⁻⁹	<i>t</i> ₀	(71.40 ± 0.04)	x 10 ⁻¹³
–	(10.84 ± 1.15)	x 10 ⁻¹⁰	–	(50.33 ± 0.78)	x 10 ⁻⁸
+	(55.55 ± 12.86)	x 10 ⁻¹¹	+	(44.96 ± 0.70)	x 10 ⁻¹⁰
Mixed Forest			Pine		
<i>t</i> ₀	(96.50 ± 4.82)	x 10 ⁻⁹	<i>t</i> ₀	(44.79 ± 2.24)	x 10 ⁻⁹
–	(10.28 ± 4.10)	x 10 ⁻⁹	–	(71.54 ± 123.83)	x 10 ⁻¹¹
+	(97.43 ± 71.71)	x 10 ⁻¹⁰	+	(13.27 ± 22.21)	x 10 ⁻⁶
Beech			Birch		
<i>t</i> ₀	(35.70 ± 1.78)	x 10 ⁻¹¹	<i>t</i> ₀	(57.26 ± 2.86)	x 10 ⁻¹¹
–	(13.43 ± 3.00)	x 10 ⁻¹¹	–	(10.16 ± 5.08)	x 10 ⁻⁶
+	(39.77 ± 0.34)	x 10 ⁻¹¹	+	(41.16 ± 27.63)	x 10 ⁻⁶

APPENDICES

Table A 42 Relative abundance of bacterial taxa (16S rRNA gene sequences) of the methanol/chloromethane SIP experiment.

Data derived from combined ILLUMINA sequencing data sets of [¹²C]- and [¹³C]-isotopologue treatments. Only taxa with a relative abundance ≥ 1% are listed, abundance < 1% is indicated by *, no presence is indicated by -. Percentages are always related to analysed datasets of 16S rRNA gene sequence of amplicon libraries.

		treatment							
		t ₀	¹² MeOH	¹³ MeOH		¹² MeOH & ¹² CH ₃ Cl	¹² MeOH & ¹³ CH ₃ Cl	¹³ MeOH & ¹² CH ₃ Cl	
number of sequences combined data sets & singletons removed		28936	30854	29404	28958	34490	25383	39626	39403
Phylogenetic affiliation ^a		Relative abundance [%]							
Acidobacteria									
<i>Acetobacteraceae</i>	OTU 5	1.83	2.12	1.45	2.10	1.77	1.87	1.62	5.83
Actinobacteria		42.23	33.58	29.47	47.73	52.31	48.89	44.82	58.27
<i>Actinomycetales</i>	OTU 6	7.34	5.30	4.87	8.05	9.67	7.73	8.29	6.85
<i>Conexibacteraceae</i>	OTU 23	2.98	1.93	2.20	4.05	3.99	4.02	3.08	6.80
<i>Microbacteriaceae</i>	OTU 61	*	*	*	*	*	*	*	7.34
<i>Pseudonocardiaceae</i>	OTU 85	2.71	3.96	2.54	4.02	4.49	4.11	3.54	19.78
<i>Streptomycetaceae</i>	OTU 104	28.77	22.08	19.63	31.27	33.69	32.57	29.39	17.51
Bacteroidetes		2.27	1.41	*	*	*	*	*	*
<i>Chitinophagaceae</i>	OTU 18	1.06	*	*	*	*	*	*	*
<i>Cytophagaceae</i>	OTU 26	*	*	*	*	-	-	*	*
<i>Sphingobacteriaceae</i>	OTU 100	1.16	*	*	*	*	*	*	*
“Cand. Saccharibacteria”	OTU 108	*	*	*	1.05	*	*	*	*

APPENDICES

Phylogenetic affiliation ^a		treatment							
		t ₀	¹² MeOH	¹³ MeOH			¹² MeOH & ¹² CH ₃ Cl	¹² MeOH & ¹³ CH ₃ Cl	¹³ MeOH & ¹² CH ₃ Cl
					¹² CH ₃ Cl	¹³ CH ₃ Cl			
		Relative abundance [%]							
Firmicutes		*	*	*	*	*	*	*	*
<i>Bacillaceae</i>	OTU 11								
Planctomycetes		8.54	17.03	11.99	13.53	8.68	10.61	7.36	8.02
<i>Gemmataceae</i>	OTU 42	2.19	2.52	1.42	1.95	1.46	1.58	1.31	3.83
<i>Isosphaeraceae</i>	OTU 53	6.35	14.51	10.57	11.58	7.22	9.03	6.06	4.18
Proteobacteria		36.59	36.21	51.06	29.02	30.85	31.84	40.21	36.59
Alphaproteobacteria		24.65	23.79	47.15	23.05	24.70	23.97	33.61	20.23
<i>Acetobacteraceae</i>	OTU 3	1.83	2.12	1.45	2.10	1.77	1.87	1.62	8.57
<i>Beijerinckiaceae</i>	OTU 12	17.63	16.52	41.26	16.49	18.58	17.62	28.70	9.31
<i>Hyphomicrobiaceae</i>	OTU 49	4.01	4.23	3.50	3.49	3.46	3.59	2.60	1.75
<i>Methylocysteceae</i>	OTU 60	1.18	*	*	*	*	*	*	*
Gammaproteobacteria		11.94	12.41	3.91	5.98	6.15	7.87	6.60	5.14
<i>Chromatiaceae</i>	OTU 19	1.44	1.88	1.16	1.02	*	1.14	*	*
<i>Enterobacteriaceae</i>	OTU 33	*	-	*	*	*	1.45	*	1.65
<i>Xanthomonadaceae</i>	OTU 116	10.50	10.53	2.74	4.94	5.10	5.28	5.80	3.17
taxa < 1%		7.86	8.05	4.77	5.67	4.78	5.29	4.27	1.53

^a Phylogenetic affiliation was based on greengenes

APPENDICES

Table A 43 Relative abundance of methylotrophic taxa (*mxoF/xoxF*-type MDH gene sequences) of the methanol/chloromethane SIP experiment.

Data derived from combined ILLUMINA sequencing data sets of [¹²C]- and [¹³C]-isotopologue treatments. All detected phylotypes are listed, no presence is indicated by -. All *mxoF* gene sequence phylotypes are indicated by '*mxoF*', the residual phylotypes are *xoxF* gene sequences and not further indicated. Percentages are always related to filtered datasets of *mxoF/xoxF*-type MDH gene sequence of amplicon libraries.

	treatment							
	t ₀	¹² MeOH	¹³ MeOH	¹² CH ₃ Cl	¹³ CH ₃ Cl	¹² MeOH & ¹² CH ₃ Cl	¹² MeOH & ¹³ CH ₃ Cl	¹³ MeOH & ¹² CH ₃ Cl
number of sequences								
combined data sets & singletons removed	16701	13112	9243	19472	9857	11737	14055	11057
Phylogenetic affiliation ^a	Relative abundance [%]							
<i>Alphaproteobacteria</i>	95.98	97.97	97.15	97.52	96.63	96.56	97.05	97.64
<i>Bradyrhizobiaceae</i>	74.71	79.76	63.32	75.82	72.19	70.03	73.75	73.81
OTU 19	1.98	1.38	1.47	1.71	1.60	2.06	1.16	1.50
OTU 24	38.04	47.73	34.84	38.67	34.18	29.41	42.55	37.42
OTU 25	32.58	27.54	24.38	33.31	34.42	36.72	27.44	32.38
OTU 1	2.11	3.10	2.64	2.14	1.99	1.84	2.60	2.51
<i>Hyphomicrobiaceae</i>	7.63	5.30	14.72	7.24	9.55	11.68	9.99	9.25
OTU 2	0.57	0.53	3.88	0.75	1.31	1.85	1.75	1.85
OTU 9	0.28	0.18	0.10	0.09	0.27	0.21	0.09	0.07
OTU 10	0.13	0.05	0.11	0.03	0.08	0.08	0.06	0.07
OTU 21	2.81	2.05	8.00	2.56	3.91	5.15	4.90	4.37
OTU 22	3.18	1.82	2.08	3.10	3.16	3.24	2.58	2.23
<i>mxoF</i> OTU 20	0.66	0.67	0.56	0.71	0.82	1.15	0.61	0.65
<i>Methylobacteriaceae</i>	0.06	0.37	4.05	0.07	0.12	0.05	0.11	0.37
<i> Beijerinckiaceae</i>	0.92	0.76	1.60	0.85	1.06	1.04	1.22	1.22
OTU 5	0.26	0.27	0.23	0.33	0.39	0.44	0.43	0.37
OTU 6	0.30	0.26	0.32	0.29	0.29	0.32	0.36	0.30
OTU 11	0.02	0.02	0.23	0.04	0.02	0.03	0.04	0.14
OTU 12	0.25	0.12	0.11	0.14	0.14	0.12	0.16	0.19
OTU 16	-	-	0.05	-	-	0.01	-	0.02

APPENDICES

	<i>mxoF</i> OTU 4	0.04	0.02	0.13	0.02	0.07	-	0.04	0.04
	<i>mxoF</i> OTU 8	0.01	0.05	0.06	0.03	0.08	0.07	0.08	0.09
	<i>mxoF</i> OTU 15	0.04	0.02	0.47	0.01	0.06	0.04	0.12	0.08
<i>Rhizobiaceae</i>	OTU 17	12.52	11.44	9.55	13.43	13.53	13.62	11.71	12.57
<i>Acetobacteraceae</i>	OTU 14	0.13	0.34	3.91	0.11	0.18	0.14	0.27	0.42
<i>Betaproteobacteria</i>		4.02	2.03	2.85	2.48	3.37	3.44	2.95	2.36
	OTU 7	0.20	0.02	0.08	0.15	0.13	0.09	0.11	0.10
	OTU 13	-	0.03	-	0.01	-	0.02	0.01	0.02
<i>Burkholderiaceae</i>		3.83	1.98	2.77	2.32	3.24	3.33	2.83	2.24
	OTU 18	0.91	0.69	0.75	0.60	1.13	0.93	0.73	0.79
	OTU 23	2.92	1.28	2.02	1.72	2.11	2.40	2.10	1.46

^a Phylogenetic affiliation was done by positioning in phylogenetic tree based on *mxoF* and *xoxF* reference sequences (see Figure A 12)

APPENDICES

Table A 44 Relative abundance of methylophilic taxa (*cmuA* gene sequences) of the methanol/chloromethane SIP experiment.

Data derived from combined ILLUMINA sequencing data sets of [¹²C]- and [¹³C]-isotopologue treatments. All detected phylotypes are listed, no presence is indicated by -. Percentages are always related to filtered datasets of *cmuA* gene sequence of amplicon libraries.

	treatment							
	t ₀	¹² MeOH	¹³ MeOH	¹² CH ₃ Cl	¹³ CH ₃ Cl	¹² MeOH & ¹² CH ₃ Cl	¹² MeOH & ¹³ CH ₃ Cl	¹³ MeOH & ¹² CH ₃ Cl
number of sequences combined data sets & singletons removed	2345	2289	3072	2719	3719	3262	5160	5724
Phylogenetic affiliation ^a	Relative abundance [%]							
<i>Alphaproteobacteria</i>	99.91	99.96	99.84	99.93	99.97	100.00	100.00	100.00
OTU 1	-	-	-	11.84	5.94	0.18	0.17	0.24
<i>Methylobacteriaceae</i>	98.12	96.59	98.99	83.08	92.69	94.94	99.28	97.82
OTU 2	75.57	67.93	66.89	51.05	62.54	74.03	75.23	72.24
OTU 3	15.39	23.59	24.51	24.09	23.39	17.14	19.09	21.59
OTU 4	4.09	4.37	6.38	7.21	5.81	3.28	4.55	3.91
OTU 5	1.71	0.70	1.20	0.74	0.94	0.46	0.41	0.03
OTU 8	1.36	-	-	-	-	0.03	-	0.03
<i>Hyphomicrobiaceae</i>								
OTU 6	1.79	3.36	0.85	5.00	1.34	4.87	0.54	1.94
<i>Firmicutes</i>								
OTU 7	0.09	0.04	0.16	0.07	0.03	-	-	-

^a Phylogenetic affiliation was done phylogenetic tree positioning based on *cmuA* reference sequences (Figure A 15)

APPENDICES

Table A 45 Phylogenetic affiliation of bacterial taxa (16S rRNA gene sequences) of the methanol/chloromethane SIP experiment.

Listed are closest related sequences including cultured and environmental hits (closest related sequences are in grey bold if they are identical with the closest cultured related sequence). BLASTn analyses are based on OTU sequence lengths of 374 – 383 bp for OTUs 6 to 85 and 213 bp for OTU 108.

OTU	closest cultured related sequence ^a				closest related sequence ^b (environmental samples included)					
	Q ^d	Id ^e	Accession ^c	Phylum Class Order	Family	Q ^d	Id ^e	Accession ^c		
6	<i>Kineosporia</i> sp.	100	95	KR184502	Actinobacteria Actinobacteria Actinomycetales	Kineosporiaceae	Uncult. <i>Actinobacterium</i>	100	99	FJ661564
12	<i>Methylovirgula ligni</i>	100	99	FM252035	Proteobacteria Alphaproteobacteria Rhizobiales	Beijerinckiaceae	Uncult. <i>Alphaproteobacterium</i>	100	99	AM992784
61	<i>Gryllotalpicola daejeonensis</i>	100	99	NR_109315	Actinobacteria Actinobacteria Actinomycetales	Microbacteriaceae	<i>Gryllotalpicola daejeonensis</i>	100	99	NR_109315
85	<i>Pseudonocardia hispaniensis</i>	100	98	NR_108504	Actinobacteria Actinobacteria Actinomycetales	Pseudonocardiaceae	Uncult. <i>Actinobacterium</i>	100	99	JX100061
108	" <i>Candidatus Saccharimonas aalborgensis</i> "	100	91	CP005957	Candidatus Saccharibacteria <i>Candidatus Saccharimonas</i>	n.a.	Uncult. <i>Bacterium</i>	100	99	JQ366126

^a Closest cultured sequences includes validly published names of bacterial species with known strains. No Candidates are listed here with the exception for the candidates' phyla *Saccharibacteria* (OTU 108).

^b Closest related sequences includes uncultured hits and are affiliated at least to phylum level using NCBI and SILVA SSU databases.

^c Query values of sequences [%].

^d Maximum sequence identity [%] in BLASTn.

^e Accession number of closest sequence hit.

^f n.a. – no further details available

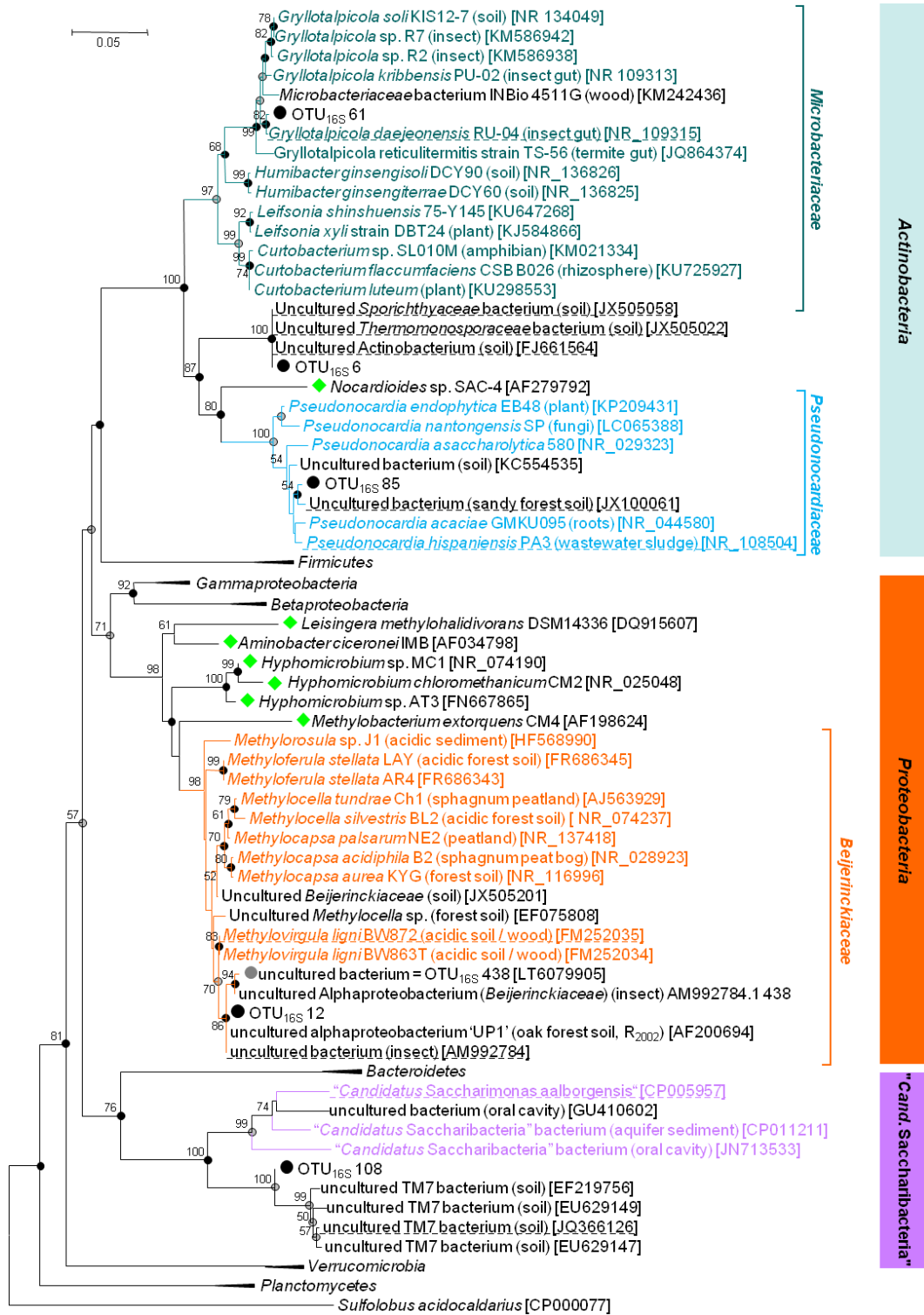


Figure A 13 Phylogenetic tree of all labelled bacterial phylotypes obtained in the methanol/chloromethane SIP experiment.

The neighbour joining tree shows all labelled phylotypes (●) and is based on 69 nucleotide sequences in total. The tree focuses on *Actinobacteria* (*Microbacteriaceae*, *Pseudonocardiaceae*), *Beijeirnckiaceae* and the "Candidatus *Saccharibacteria*" (also known as "TM7"). The partial 16S rRNA sequence from the archaeal species *S. acidocaldarius* served as outgroup and phyla that are not related with the labelled phylotypes are condensed. Bootstrap values were calculated from 1000 replicates and are shown for values ≥ 50. Dots at the nodes indicate congruent nodes with trees based on the maximum likelihood and maximum parsimony method (●, true for both phylogenetic trees; ●, only true for one phylogenetic tree). The tree includes sequences from the next hit of the

BLAST analysis of each phylotype (dashed underlined), known CH₃Cl-utilizing strains (◆), and a phylotype (OTU_{16S} 438, ●) identified as an important methylotroph in the previous substrate SIP experiment (see 3.7.1.1). If known the isolation origin of a sequence is given in brackets. Accession numbers are given in squared brackets. The bar indicates 0.05 change per nucleotide.

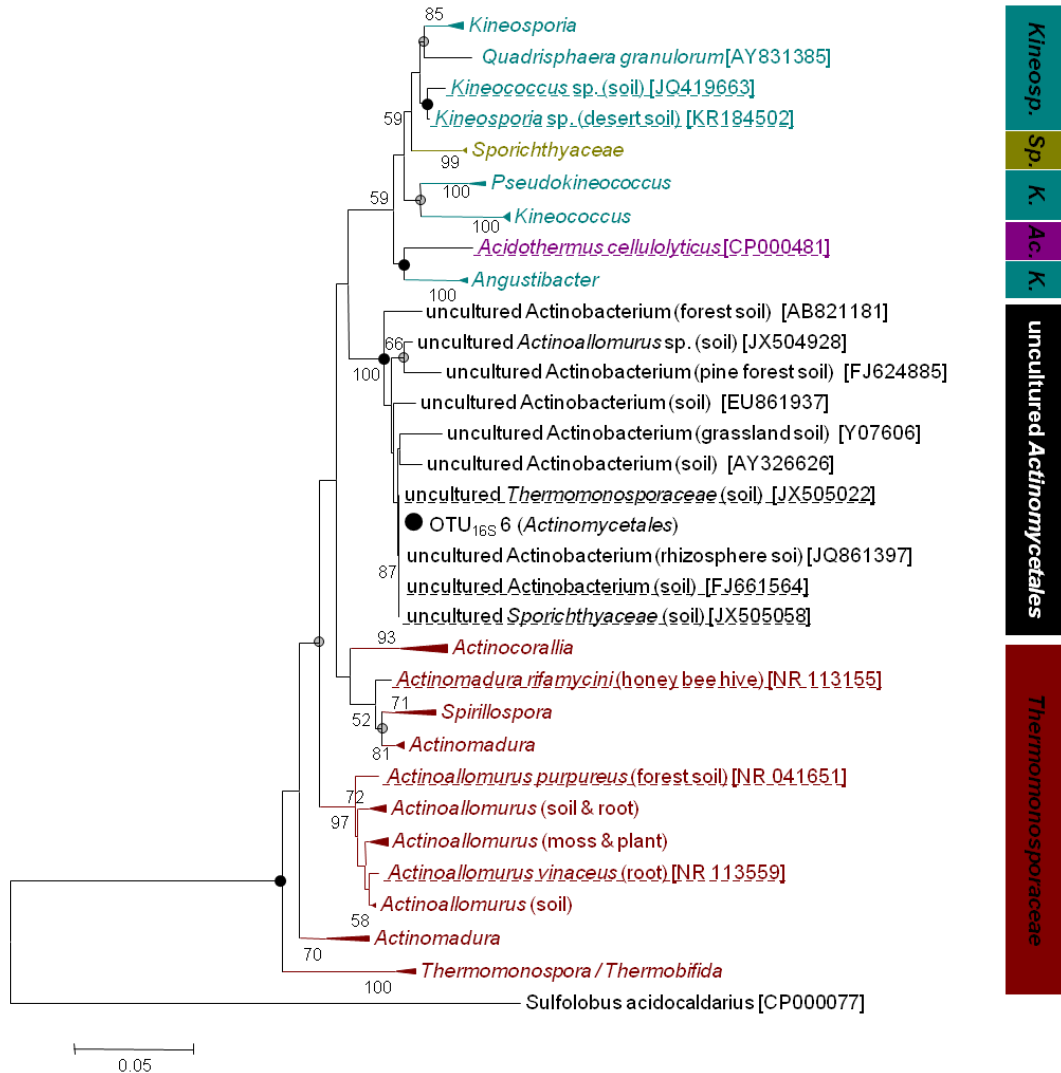


Figure A 14 Phylogenetic affiliation of the putative CH₃Cl-utilizing taxon (OTU_{16S} 6) within the *Actinomycetales*.

OTU_{16S} 6 (●) that was labelled in the approach with solely supplemented [¹³C]-CH₃Cl is clearly affiliated to a clade of uncultured *Actinomycetales* that cluster in between known genera. The neighbour joining tree is based on 52 nucleotide sequences in total. Sequences affiliated to the same genus are condensed if possible. The partial 16S rRNA sequence from the archaeal species *S. acidocaldarius* served as outgroup. Bootstrap values were calculated from 100 replicates and are shown for values ≥ 50. Dots at the nodes indicate congruent nodes with trees based on the maximum likelihood and maximum parsimony method (●, true for both phylogenetic trees; ●, only true for one phylogenetic tree). The tree includes sequences from the next hits of the BLAST analysis (dashed underlined), several sequences from uncultured *Actinobacteria*, and type species of four families of the *Actinomycetales* (i.e., *Kineosporiaceae*, *Thermomonosporaceae*, *Sporichthyaceae*, and *Acidothermaceae*). If known the isolation origin of a sequence is given in brackets. Accession numbers are given in squared brackets. The bar indicates 0.05 change per nucleotide.

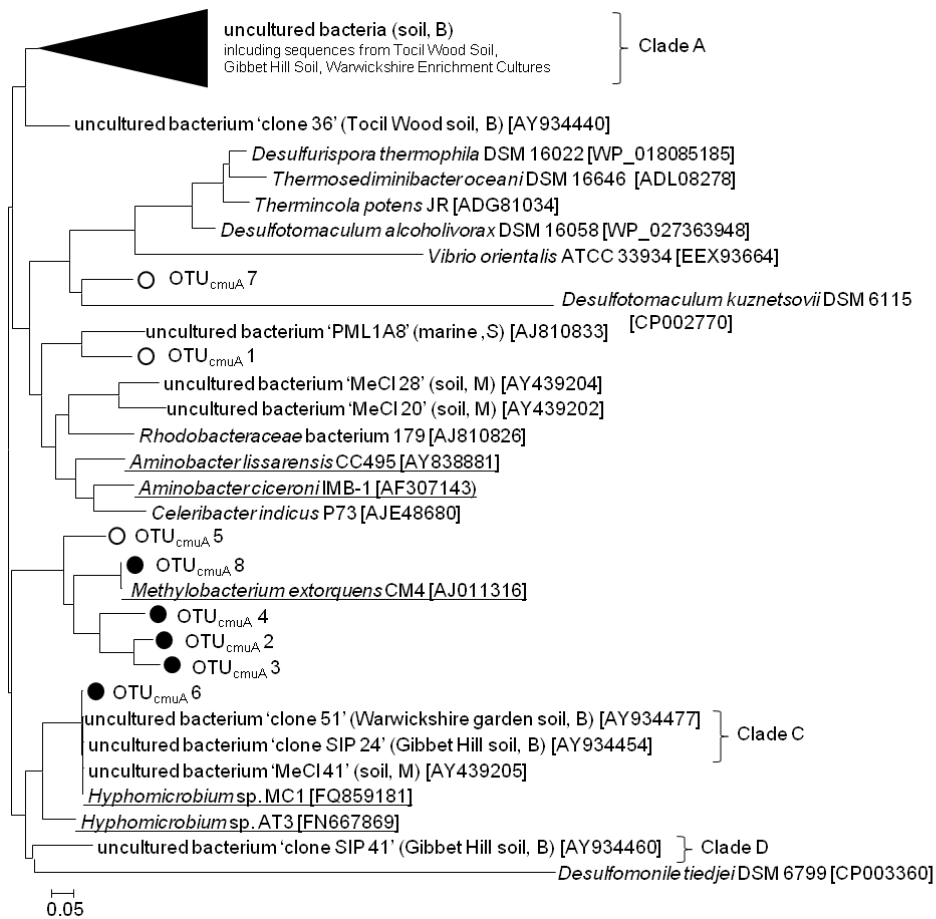


Figure A 15 Phylogenetic tree of all $cmuA$ phylotypes detected in the methanol/chloromethane SIP experiment.

The maximum likelihood tree shows the phylogenetic affiliation of all detected $cmuA$ phylotypes (OTU $_{cmuA}$ 1 to 8) and is based on nucleotide sequence alignments. Bootstrap values were calculated from 1000 replicates. Detected phylotypes are indicated with a circle (○); labelled phylotypes are highlighted with a filled circle (●). The tree includes sequences from known CH_3Cl -utilizing strains (underlined), strains known to harbour $cmuA$ sequences in their genome, and sequences from uncultured microorganisms obtained in studies focussing on CH_3Cl -utilizing microorganisms in soil and marine environments (M, Miller *et al.*, 2004; B, Borodina *et al.*, 2005; S, Schäfer *et al.*, 2005). Sequences from the study of Borodina and colleagues were additionally categorized in clades according to Borodina *et al.*, 2005. If known the isolation origin of a sequence is given in brackets. Accession numbers are given in squared brackets. The bar indicates 0.05 change per nucleotide.

Table A 46 Labelled bacterial taxa in all treatments of the methanol/chloromethane SIP experiment.

Black faces indicate values that were used for calculating 'labelling proportions' ('LP') as indicators of relative importance. Bold faces indicate 'LPs' > 5 %. Grey background indicates the abundance regardless of labelling.

treatment	Phylogenetic affiliation ^a	Labelled OTU	Relative abundance [%]						LP [%]
			¹² C-control			¹³ C-treatm.			H
			H	M	L	H	M	L	
¹³MeOH									
	<i>Alphaproteobacteria</i>								
	<i>Methylovirgula</i> ^c	OTU 12	14.24	12.47	16.20	59.35	21.61	18.22	100.0
Percentage of the labelled taxon to total fraction [%]						59			
¹³CH₃Cl									
	<i>Alphaproteobacteria</i>								
	<i>Methylovirgula</i> ^c	OTU 12	16.93	11.31	20.20	27.93	13.13	17.57	68.4
	<i>Actinobacteria</i>								
	<i>Actinomycetales</i> ^{c,d}	OTU 6	7.38	10.72	3.79	12.91	13.75	5.12	31.6
Percentage of labelled taxa to total fraction [%]						41			
¹³CH₃Cl & ¹²MeOH									
	<i>Alphaproteobacteria</i>								
	<i>Methylovirgula</i> ^c	OTU 12	17.39	11.39	21.35	31.15	28.44	14.77	95.9
	<i>Candidatus</i>	OTU 108	0.99	0.14	0.34	1.32	0.11	0.56	4.1
Percentage of labelled taxa to total fraction [%]						32			
¹³MeOH & ¹²CH₃Cl									
	<i>Actinobacteria</i>								
	<i>Gryllotalpicola</i> ^c	OTU 61	0.52	0.27	0.57	30.01	0.76	0.64	85.0
	<i>Pseudonocardia</i> ^c	OTU 85	3.39	3.41	4.72	5.30	4.06	4.35	15.0
	<i>Alphaproteobacteria</i> ^f								
	<i>Methylovirgula</i> ^{c,f}	OTU 12	17.39	11.39	21.35	13.52	15.96	18.96	
Percentage of labelled taxa to total fraction [%]						35			

^a Phylogenetic affiliation was done with BLASTn (September 2016) and is based on the next cultivated hit for each OTU (for further information see Table A 45)

^b Sequence identity of next cultured hit < 90 %, phylogenetic affiliation up to order level

^c Sequence identity of next cultured hit ≥ 95 %, phylogenetic affiliation up to genus level

^d ambiguous phylogenetic affiliation on family level with phylogenetic tree (Figure A 14)

^e known as "Candidate division TM7"

^f not identified as labelled in the treatment with [¹³C₁]-methanol and CH₃Cl; relative abundance is shown to demonstrate the presence in this approach

APPENDICES

Table A 47 Labelled methylotrophic taxa (*mxoF/xoxF*-type MDH gene sequences) in all treatments of the methanol/chloromethane SIP experiment.

Black faces indicate values that were used for calculating 'labelling proportions' ('LP') as indicators of relative importance. Bold faces indicate 'LPs' > 5 %. Grey background indicates the abundance regardless of labelling.

treatment	Phylogenetic affiliation ^a	Labelled OTU	Relative abundance [%]						LP [%]	
			¹² C-control			¹³ C-treatm.			H	M
			H	M	L	H	M	L		
MeOH										
	<i>Alphaproteobacteria</i>									
	<i>Hyphomicrobium</i>	OTU 2	0.29	0.52	1.18	4.60	5.87	1.16	11.1	23.9
	<i>Hyphomicrobium</i>	OTU 21	1.98	1.66	2.78	8.47	11.19	4.09	20.5	45.6
	<i>Methylobacterium</i>	OTU 3	0.57	0.22	0.08	12.68	2.21	0.03	30.6	9.0
	<i>Methylocella</i>	OTU 11	0.00	0.06	0.04	0.78	0.08	0.00	1.9	
	<i>Methyloligni/-ferula</i>	OTU 15	0.01	0.03	0.00	1.78	0.03	0.03	4.3	
	<i>Acidiphilum</i>	OTU 14	0.32	0.36	0.38	11.47	2.56	0.09	27.7	10.5
	<i>Betaproteobacteria</i>									
	<i>Burkholderia</i>	OTU 23	1.01	1.96	1.07	1.61	2.70	1.56	3.9	11.0
Percentage of labelled taxa to total fraction [%]						41	25			
CH₃Cl										
	<i>Alphaproteobacteria</i>									
	<i>Bradyrhizobium</i>	OTU 25	36.27	30.52	31.06	47.32	29.99	29.92	60.2	
	<i>Bradyrhizobium</i>	OTU 1	1.86	2.08	2.70	0.59	2.94	2.04		65.6
	<i>Hyphomicrobium</i>	OTU 2	0.55	0.53	1.36	2.56	0.34	1.36	3.3	
	<i>Hyphomicrobium</i>	OTU 21	2.45	1.84	3.56	6.23	1.91	4.19	7.9	
	<i>Hyphomicrobium</i>	OTU 20	0.80	0.31	0.98	1.14	0.43	0.97	1.5	
	<i>Sinorhizobium</i>	OTU 17	14.56	12.74	12.17	17.90	12.79	11.32	22.8	
	<i>Betaproteobacteria</i>									
	<i>Burkholderia</i>	OTU 18	0.29	1.19	0.52	1.46	1.54	0.52	1.9	34.4
	<i>Burkholderia</i>	OTU 23	1.35	2.66	1.36	2.01	2.74	1.60	2.6	
Percentage of labelled taxa to total fraction [%]						79	4			
¹³CH₃Cl & ¹²MeOH										
	<i>Alphaproteobacteria</i>									
	<i>Bradyrhizobium</i>	OTU 24	3.39	40.93	41.89	42.93	41.23	43.72	95.0	
	<i>Bradyrhizobium</i>	OTU 1	0.35	2.88	2.27	2.28	2.99	2.47	5.0	
Percentage of labelled taxa to total fraction [%]						45				
¹³MeOH & ¹²CH₃Cl										
	<i>Alphaproteobacteria</i>									
	<i>Bradyrhizobium</i>	OTU 19	3.20	1.94	1.23	1.39	2.07	1.08	2.2	3.8
	<i>Bradyrhizobium</i>	OTU 25	52.49	28.26	30.26	40.29	31.08	29.31	62.4	57.2
	<i>Bradyrhizobium</i>	OTU 1	0.35	2.88	2.27	2.21	2.97	2.26	3.4	
	<i>Hyphomicrobium</i>	OTU 2	3.01	0.79	1.69	1.59	1.76	2.07	2.5	3.2
	<i>Hyphomicrobium</i>	OTU 21	7.26	2.85	5.15	4.29	3.93	4.78	6.6	7.2
	<i>Methylobacterium</i>	OTU 3	0.00	0.06	0.09	0.29	0.81	0.04		1.5
	<i>Sinorhizobium</i>	OTU 17	18.66	12.08	10.68	14.22	12.64	11.64	22.0	23.3
	<i>Acidiphilum</i>	OTU 14	0.00	0.26	0.15	0.37	0.68	0.22		1.3
	<i>Betaproteobacteria</i>									
	<i>Burkholderia</i>	OTU 18	1.08	1.15	0.65	0.53	1.36	0.43	0.8	2.5
Percentage of labelled taxa to total fraction [%]						65	54			

^a Phylogenetic affiliation was done by positioning in phylogenetic tree (see Figure A 12)

APPENDICES

Table A 48 Labelled methylotrophic taxa (*cmuA* gene sequences) in all treatments of the methanol/chloromethane SIP experiment.

Black faces indicate values that were used for calculating 'labelling proportions' ('LP') as indicators of relative importance. Bold faces indicate 'LPs' > 5 %.

treatment	Phylogenetic affiliation ^a	Labelled OTU	Relative abundance [%]						LP [%]	
			¹² C-control			¹³ C-treatm.			H	M
			H	M	L	H	M	L	H	M
MeOH										
	<i>Methylobacteriaceae</i>	OTU 2	34.96	69.12	70.33	64.05	67.32	71.40	65.3	
		OTU 3	3.25	25.96	23.82	26.62	25.95	14.42	27.1	
		OTU 4	2.44	3.42	5.28	7.42	6.62	3.20	7.6	100.0
Percentage of labelled taxa to total fraction [%]						98	7			
CH₃Cl										
	<i>Methylobacteriaceae</i>	OTU 2	11.89	49.40	56.82	63.76	59.44	63.64	100.0	
Percentage of the labelled taxon to total fraction [%]						64				
¹³CH₃Cl & ¹²MeOH										
	<i>Methylobacteriaceae</i>	OTU 2	51.84	74.08	80.07	83.75	77.10	56.53	100.0	
Percentage of the labelled taxon to total fraction [%]						84				
¹³MeOH & ¹²CH₃Cl										
	<i>Methylobacteriaceae</i>	OTU 3	13.88	19.64	16.37	18.24	24.96	18.40	31.8	83.6
		OTU 4	1.95	4.22	3.02	3.26	4.91	2.93	5.7	16.4
		OTU 8	0.22	0.00	0.00	0.65	0.00	0.00	1.1	
	<i>Hyphomicrobiaceae</i>	OTU 6	31.67	1.08	0.06	35.18	0.11	0.00	61.4	
Percentage of labelled taxa to total fraction [%]						57	30			

^a Phylogenetic affiliation was done by positioning in phylogenetic tree (see Figure A 15)

9. (EIDESSTATTLICHE) VERSICHERUNGEN UND ERKLÄRUNGEN

(§ 5 Nr. 4 PromO)

Hiermit erkläre ich, dass keine Tatsachen vorliegen, die mich nach den gesetzlichen Bestimmungen über die Führung akademischer Grade zur Führung eines Doktorgrades unwürdig erscheinen lassen.

(§ 8 S. 2 Nr. 5 PromO)

Hiermit erkläre ich mich damit einverstanden, dass die elektronische Fassung meiner Dissertation unter Wahrung meiner Urheberrechte und des Datenschutzes einer gesonderten Überprüfung hinsichtlich der eigenständigen Anfertigung der Dissertation unterzogen werden kann.

(§ 8 S. 2 Nr. 7 PromO)

Hiermit erkläre ich eidesstattlich, dass ich die Dissertation selbständig verfasst und keine anderen als die von mir angegebenen Quellen und Hilfsmittel benutzt habe.

(§ 8 S. 2 Nr. 8 PromO)

Ich habe die Dissertation nicht bereits zur Erlangung eines akademischen Grades anderweitig eingereicht und habe auch nicht bereits diese oder eine gleichartige Doktorprüfung endgültig nicht bestanden.

(§ 8 S. 2 Nr. 9 PromO)

Hiermit erkläre ich, dass ich keine Hilfe von gewerblichen Promotionsberatern bzw. Promotionsvermittlern in Anspruch genommen habe und auch künftig nicht nehmen werde.

Bayreuth, 12.12.2017, M. Morawe

Ort, Datum, Unterschrift